UNIVERSITY COLLEGE LONDON
Department of Anatomy and Developmental Biology
Neurodegeneration Research Group

An Ultrastructural and Molecular Analysis of Neuronal Degeneration in Huntington's Disease

A thesis submitted for the degree of Doctor of Philosophy by

Lee-Jay Bannister

October 2003

ProQuest LLC
789 East Eisenhower Parkway
P.O. Box 1346
Ann Arbor, MI 48106-1346

Abstract

HUNTINGTON'S disease (HD) is an inherited, progressive, neurodegenerative disorder for which there is no effective treatment. It is one of nine disorders known to be caused by the expansion of a genomic CAG repeat sequence, producing a protein with an expanded array of polyglutamine residues. The mechanisms underlying the degeneration and death of neurons in HD remain unclear; and are the subjects of this investigation.

Several animal models have been generated to investigate the pathogenic mechanisms underlying HD, of which this thesis uses two: the Bates R6/2 mouse, which has the affected region of the human gene inserted into its genome; and the Shelbourne *Hdh* 'knock-in' mice, in which the CAG repeat sequence of the murine huntingtin gene homologue has been expanded into the pathogenic range.

Ultrastructural analyses have been undertaken on the CNS from each of the mouse models, detailing the subcellular changes that occur. This has been furthered by analyses of the molecular machinery of apoptosis in an attempt to identify factors involved in neurodegeneration.

Affected neurons in each of the HD models, and in aged wild-type mice, exhibit very similar morphologies: a condensation of cytoplasm and nucleoplasm, disturbances in the nuclear membrane, dilation and disruption of cell organelles and increased autophagic activity. These morphologic changes do not correlate with those reported to occur during apoptosis. Furthermore, molecular analyses reveal the involvement of none of the components of apoptosis.

In relating each of the mice, it is clear that neurodegenerative changes do not correlate with phenotypic changes; rather the early and most pronounced symptoms of HD are a result of neuronal dysfunction. It is also concluded that the increased autophagic activity and cell condensation occur in adult neurons under stress and thus may be indicative of a common process by which adult neurons die.

In loving memory

Ella Rhoda Bell

Acknowledgements

THERE are many I need to thank for getting me to and through my PhD. Most directly, I must thank my supervisor, Stephen W. Davies, for giving me a place in his research group. I must also thank him for granting me extra funding so I could stay on after my official time was up and study the mice so generously provided by Peggy Shelbourne. Likewise, I thank John Scholes, my second supervisor, for volunteering his animals and his mad-scientist skills with his ludicrously old-fashioned X-ray machine. Further thanks for material are extended to the Gillian Bates Group, home to the R6/2s; and to Hannah Mitchison for allowing me a brief foray into the world of Batten's disease through her *cln3* knockout mice. Without doubt, my greatest thanks for help with my PhD go to Mark Turmaine, who not only was always willing to lend a technical hand, but who also provided his unmatched ultrastructural knowledge, his ideas, his support and his keen insight.

I thank Rushee Jolly for teaching me westerns, for proof-reading my introduction and for also ordering the 'beef' in California. My thanks to Barbara Cozens, for always being on hand to help with histology, microscopes and the odd crossword or two. I should also thank the BSc students who have passed through the lab in my time, as helping them was always a pleasure. My warmest thanks have to go to Elizabeth Slavik-Smith, as without her friendship and support I doubt I would have survived until the end. I wish Rush and Liz the best of luck in getting their PhDs finished and getting to wherever they hope to be.

Outside work I must thank those who helped get me where I am. Above all, my parents, for spending so much time with me in those important years: my mother, Christine, for teaching me to read (backwards, of course) and for teaching me all the maths I've long since forgotten; and my father, Graham, for inspiring me with the practical world, giving me a desire to find out how things work (by breaking them, of course).

It would be impossible to thank all those teachers who have inspired me over the years, but I should make a point of thanking Ken Russell, for getting me into Cambridge. On which note I should thank James Follett, for turning a molecular biologist into a neuroscientist. His reasoning may have been questionable: "nothing in the third term *and* two reading weeks, mate", but I'm glad he convinced me.

And so to London, where I thank those with whom I've lived for putting up with me. I also thank those friends who gave me places to stay when fire drove me out of my own home: Stephan Geuorguiev & Kate Hamilton, Lorna McCune & Peter Sandbach and Sandy Morales. My sincerest thanks to my current housemates, David Blundell & Sarah Ryder who not only rescued me from homelessness, but have been providing me with support (and good food!) whilst I've been writing all this.

Finally, I should mention those whom I haven't had a reason to thank yet, but without whom life just wouldn't be the same: Birte Hacker for her grace; Israel Butler for his constancy; Simon Coles for his generosity; Robin Kemp for his lifelong friendship; Claudia Huber for being so entertaining; Robert Smith for his laconic wit; Amanda Neale for her Mandyism and Faye Edwards for keeping me under control with her cello bow.

It's a sign of mediocrity when you demonstrate gratitude with moderation.

~ Roberto Benigni

It's all in the mind, you know.

~ Spike Milligan

Contents

List of Figures

Introduction

Materials and Methods

Results

Discussion

Guide to Abbreviations

AD	Alzheimer's disease
AIF	apoptosis initiation factor
ALS	amyotrophic lateral sclerosis
AP2	adaptor protein 2
Apaf-1	apoptotic protease activating factor 1
Asp	aspartic acid
Aß	ß-amyloid
AV	autophagic vacuole
BDNF	brain-derived neurotrophic factor
C / CN	caudate nucleus
(I)CAD	(inhibitor of) caspase-activated DNase
CAG	DNA sequence coding for *glutamine*
CARD	caspase activation & recruitment domain
CB	Cajal body
CBD	corticobasal degeneration
CBP	CRE (cyclic-AMP response element) binding protein
CJD	Creutzfeldt-Jakob disease
CMV	cytomegalovirus
CNS	central nervous system
CVT	cytosol to vacuole targeting vesicles
cx	cortex
cyt c	cytochrome c
DCD	dark cell degeneration
DD	death domain
DED	death effector domain
DFF	DNA fragmentation factor
DIABLO	direct IAP binding protein with low pI
DISC	death-inducing signalling complex
DLBD	dementia with Lewy body disease
DM1 (2)	myotonic dystrophy type 1 (type 2)
DMPK	dystrophia myotonica-protein kinase
DNA-PK	DNA-dependent protein kinase
DRPLA	dentatorubralpallidoluysian atrophy
EM	electron microscopy
EPM1	Progressive myoclonus epilepsy
ER	endoplasmic reticulum
FMR(P)	fragile X mental retardation (protein)
FRAXA	Fragile X syndrome
FRAXE	Fragile XE disorder
GAPDH	glyceraldehyde-3-phosphate dehydrogenase
GP	globus pallidus
HAP1	Huntingtin-associated protein 1
HAP40	Huntingtin-associated protein 40
HD	Huntington's disease

Hdh	Huntington's disease homologue
HDL2	Huntington's disease-like 2
HIP1	Huntingtin-interacting protein 1
HIP2	Huntingtin-interacting protein 2
hnRNP	heterogeneous nuclear ribonuclear protein
HSP	heat-shock protein
htt	huntingtin
IAP	inhibitor of apoptosis protein
IL-1ß	interleukin-1ß
IT15	Interesting transcript 15 – the HD gene
kb	kilobases
kDa	kiloDaltons
LM	light microscopy
LV	lateral ventricle
MJD	Machado-Joseph disease
MND	motor neuron disease
MVB	multivesicular body
NII	neuronal intranuclear inclusion
NMDA	N-methyl D-aspartate (glutamate receptor)
NuMA	nuclear matrix associated protein
P	putamen
PARP	poly-ADP ribose polymerase
PD	Parkinson's disease
PHF	paired-helical filaments
polyQ	polyglutamine
pRb	retinoblastoma protein
PS	phosphatidylserine
PSD-95	post-synaptic density 95
Q	single letter code for *glutamine*
RFLP	restriction fragment length polymorphism
SBMA	spinobulbar muscular atrophy
SCA	spinocerebellar ataxia
Smac	second mitochondria-derived activator of apoptosis
snRNP	small nuclear ribonuclear protein
SREBP	sterol regulatory element-binding proteins
TBP	TATA-binding protein
TSE	transmissible spongiform encephalopathies
tTG	tissue transglutaminase
TUNEL	terminal transferase-mediated nick-end labelling
UPS	ubiquitin-proteasome system
UTR	untranslated region
VDAC	voltage-dependent anion channel (*aka* porin)
YAC	yeast artificial chromosome
ZNF9	zinc finger protein 9

Introduction

1.1 *Huntington's Disease*

1.1.1 *Huntington's Disease*

HUNTINGTON'S disease is an inherited, progressive neurodegenerative disorder. The disorder was originally termed *Huntington's Chorea*, after the dancing movements exhibited by sufferers, but the discovery of a juvenile form which lacks chorea, and the fact that adult symptoms include far more than just chorea led to the renaming. Other motor abnormalities exhibited by Huntington's disease (HD) patients include athetosis (slower writhing movements of the limbs), bradykinesia (slowing of voluntary movements, similar to Parkinson's disease), myoclonus (sudden jerking movements), dystonia (strange posture due to muscle spasms), and oculomotor apraxia (difficulty in making rapid eye movements).

Patients also experience cognitive decline and psychiatric symptoms, which may begin up to ten years prior to onset of motor symptoms. Such symptoms usually begin with personality changes, a lack of interest in life and increased irritability; followed by behavioural changes, including social disinhibition and a tendency to act impulsively and violently. Psychiatric symptoms may also include affective disorder and schizophrenia, with some patients occasionally experiencing seizures and convulsions (for a comprehensive review of the clinical profile of HD, see *Huntington's Disease* P.S. Harper, Saunders Press).

Severe weight-loss is also associated with the disorder and in the past has been attributed to the dysphagia also seen. However, it has since been shown that weight loss cannot be attributed to diet, rather that HD patients have a higher resting energy expenditure, possibly due to the increased motor activity (Pratley *et al.* 2000; Morales *et al.* 1989).

The juvenile form of HD lacks chorea and presents more like Parkinson's disease (PD) with the bias of symptoms towards bradykinesia and psychiatric abnormalities, whilst the late-onset form tends more towards a pure movement

disorder. The distinction between the two is somewhat arbitrary with onset below 20 years of age generally considered juvenile presentation.

1.1.2 Prevalence and Progression

Globally, HD has a prevalence of approximately 10 per 100,000 but varies widely. The lowest incidence is found among the Japanese and Chinese with prevalence around 0.5 per 100,000 (Nakashima *et al.* 1996; Chang *et al.* 1994) whilst the highest prevalence, 700 per 100,000, is found near Lake Maracaibo in Venezuela (Jenkins and Conneally 1989). The figures for the UK and the USA are approximately 8 and 5 per 100,000 respectively Juvenile HD accounts for approximately 6% of Huntington's cases. The reason for the global variation is explained further in *1.3.3.*

The mean age of onset of symptoms is approximately 40 years, which is followed by a progressive deterioration with death occurring 10 to 17 years after onset. Death normally occurs as a result of secondary complications from the disease, the commonest being pneumonia and cardiovascular disease.

1.1.3 Gross Pathology

Post-mortem examination of an end-stage HD brain reveals massive enlargement of the lateral ventricle due to atrophy of the caudate and putamen – as a result of abundant cell loss – and to a lesser extent thinning of the cortex (see figure 1). During the course of the disease there is also cell loss and shrinkage in the globus pallidus, hippocampus and thalamus. There is also a progressive decrease in size and weight of various parts of the brain. Interestingly, patients show up to a thirty percent reduction in weight of the cortex, hippocampus and thalamus before pathology is visible to gross examination (de la Monte *et al.* 1988).

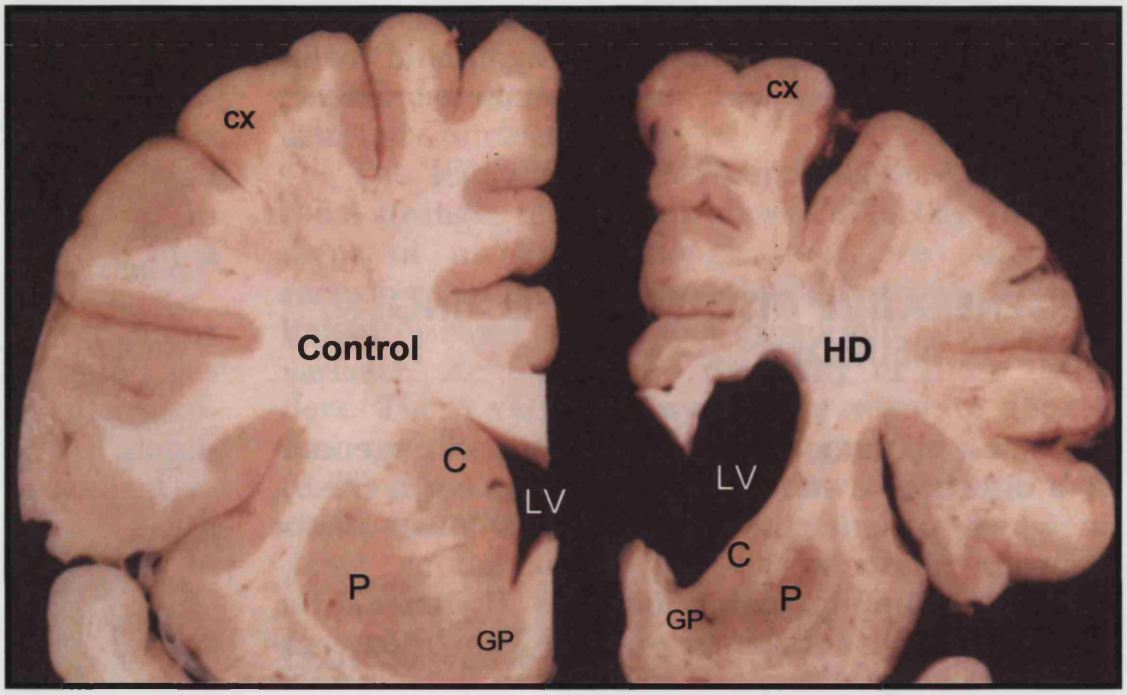

Figure 1 A comparison of normal and HD post-mortem brains. Coronal sections through the basal ganglia. Note the enlargement of the lateral ventricle (LV) due to shrinkage of the caudate nucleus (C) putamen (P) and globus pallidus (GP). Note also the thinning of the cortex (cx).

Taken from *Pathological Basis of Disease* Saunders Press, 5th Ed.

Vonsatell (Vonsattel *et al.* 1985) devised a classification system for disease severity based on macroscopic and microscopic post-mortem observations. His system is based on five grades of pathology. Grade 0 includes those with psychiatric symptoms but no observable gross pathological changes. In some Grade 0 brains astrocytosis can be detected. As with Grade 0, Grade 1 brains show no macroscopic changes, but histologically a large proportion of the striatal medium spiny projection neurons can be found to have been lost. Throughout Grades 2 to 4 there is further loss of the striatal neurons with shrinkage of the areas already mentioned. By Grade 4 95% of the striatal projection neurons are lost, figure 1 contains an example of such a brain. The majority of HD patients are Grades 3 or 4 at time of death.

The initial pathology is confined to the medium spiny neurons of the caudate nucleus (CN), spreading from the medial paraventricular parts to the tail of the CN, and thence to the dorsal putamen and its medium spiny neurons (Vonsattel and DiFiglia 1998). It seems somewhat counterintuitive that the initial damage should be in the basal ganglia and yet the initial symptoms are typically psychiatric. However, one group has developed a technique for detecting HD in presymptomatic patients by testing motor skills (Smith *et al.* 2000). Through accurate measurements of movements during reaching tasks they are able to detect abnormalities in HD gene carriers up to seven years before predicted onset of 'classical' symptoms.

The most striking pathological changes are found in cases of juvenile HD, with neuronal loss spreading beyond the regions affected in adult HD, such as the Purkinje cells of the cerebellum. Along with increased severity of symptoms and a faster rate of decline, this suggests juvenile HD is a more aggressive form of the adult disease (Myers *et al.* 1988)

1.2 *The History of Chorea*

1.2.1 The History of Chorea

HUNTINGTON'S disease was originally one of many disorders bounded together under the title of "Dancing Manias", or what would become known as *choreas*. The earliest descriptions of what may have been choreas include ancient Egyptian papyri and the Bible. In fact, it seems that the ancient Egyptians were even partially aware of the causative element of the diseases, ascribing the symptoms to brain dysfunction (Edwin Smith papyrus, 3000BC). Considering the ancient Egyptians regarded the brain as an organ of little importance it is even more surprising that they would have made this conclusion. Of course, this suggestion was lost and it was not until the early sixteenth century that the nature of the diseases came to be investigated again.

There are reports of dancing manias throughout the middle ages. At the time the symptoms were attributed to the work of the Devil. It was believed affected individuals were possessed, or being punished by God for some unknown transgression. Paracelsus (1493 – 1541) contradicted this general belief stating they are not due to "ghostly beings or spirits" but the "result of some fault in the affected person's personality". Of course, contradicting the Church was not a healthy idea at the time and he was denounced as the "Luther of Medicine".

It was Paracelsus who introduced the term chorea - from the Latin *chorea,* a dance (in a ring). He also subdivided choreas into three types: "*chorea imaginative aestimative*" arising from the 'imagination'; "*chorea lasciva*" arising from 'sensual desires' and "*chorea naturalis coatta*", arising form an organic basis. The latter classification may have been based on his work with Huntington's disease patients.

John Elliotson (1791 – 1868) provided us with the first definite mention of heredity in causation of adult chorea in 1832 (Elliotson 1832). The Professor of Medicine at University College London states that when chorea:

> "...occurs in adults it is frequently connected with paralysis or idiotism and will perhaps never be cured. It appears to arise for the most part from something in the original constitution of the body, for I have often seen it hereditary."

1.2.2 George Huntington (1850 – 1916)

George Sumner Huntington was born on April 9th 1850 in East Hampton, Long Island. He was the son and grandson of physicians and graduated from the College of Physicians and Surgeons himself in 1871. A year after his graduation he gave a lecture entitled "On Chorea" to the *Meigs and Mason Academy of Medicine*, the subject matter for this talk he subsequently published in the Philadelphia–based *Medical and Surgical Reporter* (Huntington 1872) (figure 3, see 6.1 *for transcript*). Both the lecture and the paper dealt with what he called the "hereditary chorea", his work on which he described in a very anecdotal way, as a reminiscence of his childhood in Long Island. He recalled patients and their families from his father's surgery:

> "...It is spoken of by those in whose veins the seeds of the disease are known to exist, with a kind of horror, and not at all alluded to except through dire necessity, when it is mentioned only as 'that' disorder."

Huntington notes three essential features, or 'peculiarities' in this disease:

> Its hereditary nature
>
> A tendency to insanity and suicide
>
> Its manifesting itself as a grave disease only in adult life

Even today, George Huntington is still commended for the detailed yet succinct nature of his account, and it is fitting that such an excellent description earned the labelling of the disease with his name.

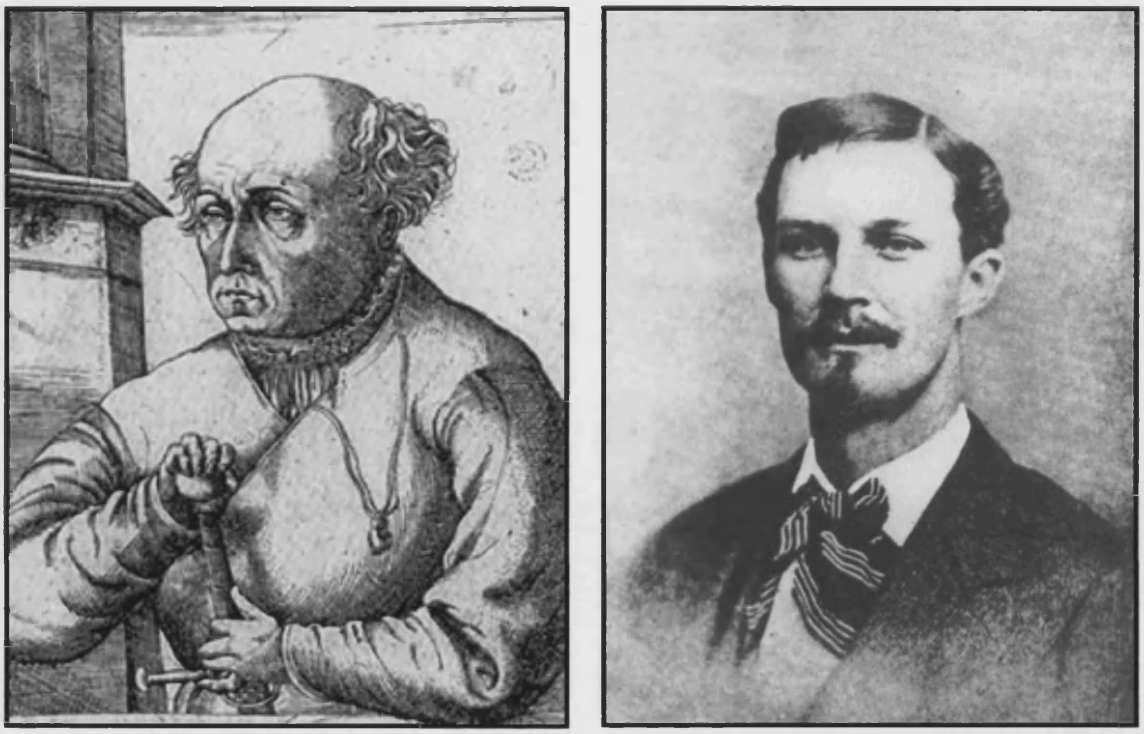

Figure 2 *Left*: Paracelsus (Aureolus Philippus Theophrastus Bombastus von Hohenheim). *Right*: George Sumner Huntington. Taken around the time he wrote *On Chorea*.

MEDICAL AND SURGICAL REPORTER.

No. 789.] PHILADELPHIA, APRIL 13, 1872. [Vol. XXVI.—No. 15.

ORIGINAL DEPARTMENT.

Communications.

ON CHOREA.

By George Huntington, M. D.,
Of Pomeroy, Ohio.

Essay read before the Meigs and Mason Academy of Medicine at Middleport, Ohio, February 13, 1872

Chorea is essentially a disease of the nervous system. The name "chorea" is given to the disease on account of the *dancing* propensities of those who are affected by it, and it is a very appropriate designation. The disease, as it is commonly seen, is by no means a dangerous or serious affection, however distressing it may be to the one suffering from it, or to his friends. Its most marked and characteristic feature is a clonic spasm affecting the voluntary muscles. There is no loss of sense or of volition attending these contractions, as there is in epilepsy; the will is there, but its power to perform is deficient, the desired movements are after a manner performed, but there seems to exist some hidden power, something that is playing tricks, as it were, upon the will, and in a measure thwarting and perverting its designs; and after the will has ceased to exert its power in any given direction, taking things into its own hands, and keeping the poor victim in a continual jigger as long as he remains awake, generally, though not always, granting a respite during sleep. The disease commonly begins by slight twitchings in the muscles of the face, which gradually increase in violence and variety. The eyelids are kept winking, the brows are corrugated, and then elevated, the nose is screwed first to the one side and then to the other, and the mouth is drawn in various directions, giving the patient the most ludicrous appearance imaginable. The upper extremities may be the first affected, or both simultaneously. All the voluntary muscles are liable to be affected, those of the face rarely being exempted.

If the patient attempt to protrude the tongue it is accomplished with a great deal of difficulty and uncertainty. The hands are kept rolling—first the palms upward, and then the backs. The shoulders are shrugged, and the feet and legs kept in perpetual motion; the toes are turned in, and then everted; one foot is thrown across the other, and then suddenly withdrawn, and, in short, every conceivable attitude and expression is assumed, and so varied and irregular are the motions gone through with, that a complete description of them would be impossible. Sometimes the muscles of the lower extremities are not affected, and I believe they never are *alone* involved. In cases of death from chorea, all the muscles of the body seem to have been affected, and the time required for recovery and degree of success in treatment seem to depend greatly upon the amount of muscular involvement. Romberg refers to two cases in which the muscles of *respiration were affected*.

The disease is generally confined to childhood, being most frequent between the ages of eight and fourteen years, and occurring oftener in girls than in boys. Dufosse and Rufz refer to 429 cases; 130 occurring in boys and 299 in girls. Watson mentions a collection of 1,029 cases, of whom 733 were *females*, giving a proportion of nearly 5 to 2. Dr. Watson also remarks upon the disease being most frequent among children of *dark* complexion, while the two authorities just alluded to, Dufosse and Rufz, give as their opinion that it is most frequent in children of *light* hair. In every case visiting the clinics

Figure 3 The front page from George Huntington's paper "On Chorea", April 1872

1.2.3 Tracing the Origins of Huntington's Disease

The dominant hereditary nature of Huntington's disease allows for genealogical studies to be carried out with comparative ease. The well-known genealogical studies were conducted before the locus of the affected gene had been pinpointed (see 1.3), that is to say, before precise genetic testing for Huntington's disease existed. What has become clear since then is that in a surprising number of cases, HD arises as the result of new mutation. However, at the time genealogies were being elucidated it was believed that very few new mutations occurred. Stevens (1976) estimated that in his study one percent of affected individuals resulted from new mutations. Family histories can be very difficult to obtain, especially if there has been an attempt to conceal the disease, and so it was very easy for those spending their time tracing the timeline to dismiss negative family histories, especially when they could always question paternity.

The first of such studies began in the US, fittingly with the descendants and ancestors of the patients of Drs Huntington. The origins of the mutations passed through this genetic line have been traced back as far as seventeenth century Britain. This was a time of great religious persecution and oppression, meaning that anyone behaving "abnormally" was not well-regarded. Many Britons, especially those under such persecution emigrated, with America a popular choice of new homeland. The emigrants of this time included three men: Jeffers, Nicolas (Nichols) and Wilkes (Wilkie), as well as one Simon Huntington, all of whom left within three years of each other from East Anglia. It is something of an historical twist of fate that the three earliest known affected individuals and the ancestor of the man whose name the disease know bears should follow the same journey (Critchley 1973).

It is possible that these three men fled to America to escape 'family burdens' at home. If their family had a history of the disease and had been persecuted for dancing the "Devil's dance", perhaps they believed they could escape such persecution by fleeing. Alternatively, they may have been sent to New England because of their family history. Either way, the views concerning 'unnatural behaviour' were not limited to England.

~

The seventeenth century saw a great fear of witchcraft: the first anti-witchcraft laws were passed in 1642 in New England, and fear continued to grow culminating in the Salem witch hunts of 1692. The appropriate punishment for a witch/warlock was death. It was believed that a witch's power was contained in the blood, hence the appropriate means of execution became burning alive. Seven of the female descendents of the three men were regarded as witches. Of the men themselves, it is known that each one had problems with the law. Their sociopathic traits, combined the labelling of their female descendents as witches suggests they had been suffering from Huntington's Disease (Maltsberger 1961).

Similar genealogical studies have since been carried out across the globe and have been used to suggest a spread of the HD mutation around the world from a source or sources somewhere in Northwest Europe, in particular France, Germany and/or Holland. Whilst it seems the genealogical history of the New England patients is true, at least in part, it is doubtful as to whether the stories of the rest of the world hold up to test. Odd cases in more remote parts have been put down to 'actions' of colonial seamen. But it is more likely that these cases, and many others arose independently as a result of new mutation.

Since the discovery of the affected locus genetic screening has been possible. Studies since have indicated that there is a higher number of new mutations responsible than at first thought. Two such studies (Nance *et al.* 1996; Siesling *et al.* 2000) have yielded similar results from different groups of patients. Ignoring patients with unknown or suspect histories, Siesling *et al.* found eight out of 126 patients with an HD gene in the disease range had negative family histories (6.3%). The Nance group suggest between 4.5 and 7.5% of cases occur with a negative family history. Generally such patients have fewer CAG repeats (see 1.3.3) and a lower age of onset supporting the idea of a recent expansion. Such a high number of novel mutations casts doubt on the reliability of the genealogical data. Whilst it is unlikely that the East Anglia to Eastern America data are all coincidence, many other appearances of the disease may have been spontaneous.

1.3 The Genetic Basis

1.3.1 The Venezuela Search

A NUMBER of investigators examined Huntington's disease pedigrees in search of a marker linked to the disease; a difficult task given the late age of onset of the disorder. Initial investigations used classical antigen and enzyme polymorphisms in attempts to find a correlate with HD (Pericak-Vance 1979; Volkers 1980). Whilst they were unsuccessful in finding a marker, they did exclude approximately 20% of the genome as possible locations for the HD gene.

The identification of stretches of DNA which show high variability between individuals: restriction fragment length polymorphisms (RFLP), allowed for a more detailed exploration of the genome, including those parts which do not code for proteins. However, even with this technique, the success of any study depends largely on the quantity and quality of pedigree material available.

The *Huntington's Disease Collaborative Research Group* were successful in identifying the locus, and later the gene, primarily because they had access to such a large pedigree. Along the shores of Lake Maracaibo, Venezuela lives the largest known concentration of HD carriers, some 3000 since the early nineteenth century, all interrelated and, it would appear, stemming from one common ancestor. Nancy Wexler and colleagues obtained pedigree information, blood samples, and neurological diagnoses from these inhabitants. Given the late onset, it is difficult to identify all HD carriers, and some patients were examined over three years to confirm the presence of HD. From the blood samples, James Gusella *et al.* established Epstein-Barr virus-transformed lymphoblastoid cell lines, so as to provide a permanent source of genetic material. In the RFLP analysis a number of DNA probes were used to label fragments on the Southern blots, but only one suggested a polymorphism inherited with HD: the G8 probe. In fact, the G8 locus and the HD gene are very close together indeed, 0-10 centiMorgans (99% confidence) (Gusella *et al.* 1983).

~

Using a Southern blot analysis of human-mouse somatic cell hybrids, Gusella *et al.* showed that the probe corresponds to a region of chromosome 4. Furthermore, other probes used in the initial RFLP analysis corresponded to different regions on chromosome 4, with varying degrees of co-segregation, thus allowing a substantial portion of chromosome 4 to be eliminated as a locus for the HD gene.

Not only did a marker for HD now exist, facilitating pre-symptomatic genetic testing, but the possible location of the gene had been narrowed to a relatively small portion of the genome. Over the next ten years the locus was steadily refined until the candidate region reached 500kb, whereupon exon amplification was used to identify coding sequences and thus the gene (Huntington's Disease Collaborative Research Group 1993).

1.3.2 Huntingtin

The affected gene, IT15 (Interesting Transcript 15), spans approximately 210kb within the 4p16.3 locus. Its 67 exons code for a protein 348kDa in size, named huntingtin (htt). The function of normal htt remains unclear. Huntingtin mRNA is expressed throughout the foetal and adult body, in peripheral tissues as well as the brain (Ambrose *et al.* 1994); and exists in two forms originating from the one gene, a 10.3kb and a 13.7kb transcript resulting from differential 3' polyadenylation (Lin *et al.* 1993). It is suggested that this is a form of regulation of expression. Both transcripts are present in most tissues, although the 13.7kb form is more abundant in brain (Lin *et al.* 2001; Strong *et al.* 1993).

Studies investigating the protein rather than the mRNA have yielded similar results: huntingtin is expressed in most tissues - and at higher levels in the brain, which is perhaps due to the predominance of the highly polyadenylated transcript, which persists for longer. Only one study has suggested an hetrogenous expression of protein within the brain. Ferrante *et al.* state they found a greater expression in the medium spiny neurons of the striatum, which would provide a possible explanation for selective degeneration, but the data have not been replicated (Ferrante *et al.* 1997).

Cell fractionation experiments indicate that the protein is cytoplasmic and, as revealed by immunostaining, is found throughout the cell bodies, dendrites, axons and terminals of neurons (DiFiglia *et al.* 1995). Immunofluorescence studies have shown that htt co-localises with the *transferrin* receptor, coated vesicles and the multivesicular bodies associated with the endosome-lysosome pathway. For these reasons it has been suggested that htt may have a role in vesicle trafficking in the secretory and endocytic pathways (DiFiglia *et al.* 1995; Sapp *et al.* 1997; Velier *et al.* 1998).

Whatever the role of normal huntingtin, it is of great importance. Identification of the murine homologue of huntingtin, *Hdh* (Barnes *et al.* 1994) allowed for manipulative experiments to be performed on the native mouse gene. Homozygous knockout of *Hdh* is lethal in the early embryonic stage, during gastrulation, before the onset of neurolation (Nasir *et al.* 1995; Duyao *et al.* 1995)[*]. Heterozygous knockout has no distinguishable effect. Likewise, in humans loss of one htt allele does not produce HD pathology. There exists a disorder, Wolf-Hirschhorn syndrome, which is caused by a large deletion of the tip of chromosome 4, including IT15. Whilst individuals with Wolf-Hirschhorn exhibit a number of abnormalities they do not exhibit HD-like neuropathology (Gottfried *et al.* 1981).

Such embryonic lethality suggests that htt has a crucial role in development, a role which seems unaffected by the loss of one allele or the presence of a mutant form of the gene. Furthermore, the generation of mice homozygous for *Hdh* containing an expanded polyglutamine tract (see 1.3.3) has shown that the HD-causing mutation does not affect the normal function of the protein (White *et al.* 1997). The existence of humans homozygous for the HD mutation in Venezuela supports the case for this being true in human HD. Therefore, the dominant effects of mutant htt act not through loss of the normal function of the gene product

[*] It should be noted the Nasir *et al.* study was not a complete inactivation of the Hdh gene as in the Duyao *et al.* study, rather a disruption – precisely, a premature termination. Exons 1-4 were still expressed. However, this was sufficient to cause embryonic lethality.

1.3.3 The Polyglutamine Tract

In cloning the gene, the aetiology of HD immediately became apparent. Contained within exon 1 of htt is a stretch of nucleotide repeats. The codon CAG, coding for the amino acid glutamine, is repeated many times. The exact number varies widely from as few as 6 to as many as 250 times. However, patients with HD always have a larger number. There is a threshold, somewhere between 34 and 37 repeats, at which the disease appears. Most normal individuals have between 11 and 35 CAG repeats, with most HD patients having greater that 35. In the original 75 Venezuelan families studied, 98% of unaffected individuals had fewer than 24 CAG repeats, whilst 100% of HD patients had greater than 42 (Huntington's Disease Collaborative Research Group 1993). However, there is a 'grey area' between 35 and 40 repeats. There are cases of HD in patients with 36 repeats, and yet there are also apparently healthy elderly individuals with 36-39 repeats. There has yet to be a case of HD with fewer that 36 repeats (Rubinsztein *et al.* 1996).

There is an inverse correlation between age of onset (and severity of symptoms) and CAG repeat length (figure 4). However, patients with identical repeat lengths can differ in their ages at onset. It seems there are a number of modifiers which can either delay or promote onset of the disease. One such factor was found in 1998. Vuillaume *et al.* demonstrated that the presence of a glutamic acid polymorphism adjacent to the CAG repeat reduces the age at onset (Vuillaume *et al.* 1998). Current estimates suggest that CAG repeat length alone accounts for up to 74% of factors determining age at onset in HD (MacDonald *et al.* 1999). Furthermore, the fewer the number of repeats the less they determine age of onset. Figure 5 represents the same data used for figure 4 but with the variance at each repeat length added into the graphic. It is evident that as repeat size increases, variance is reduced. Also added is the number of individuals in these studies at each repeat length. Less than 10% of HD cases have a repeat size greater than 60, when this fraction of the sample is removed from the calculation, CAG repeat length accounts for less than half of the variability in age of onset (Myers *et al.* 1998). It is reasonable to assume that as CAG length increases the effects of the expanded polyglutamine

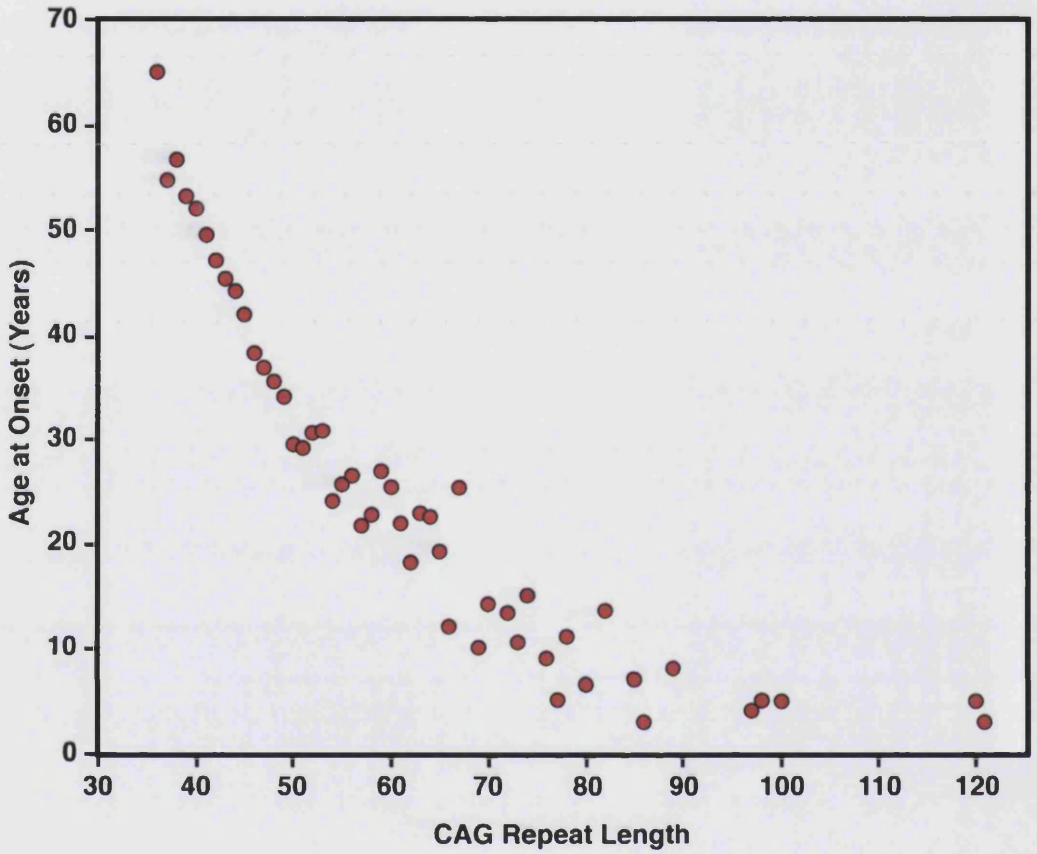

Figure 4 Relationship between CAG repeat sequence length and age at onset of HD symptoms. Data compiled form several published studies. There is an inverse correlation between the number of CAG codons and age at onset.

Adapted from J.F. Gusella *et al. Huntington's Disease* in Cold Spring Harbor Symposia on Quantitative Biology, Volume LXI: *Function & Dysfunction of the Nervous System* Cold Spring Harbor Laboratory Press 1996

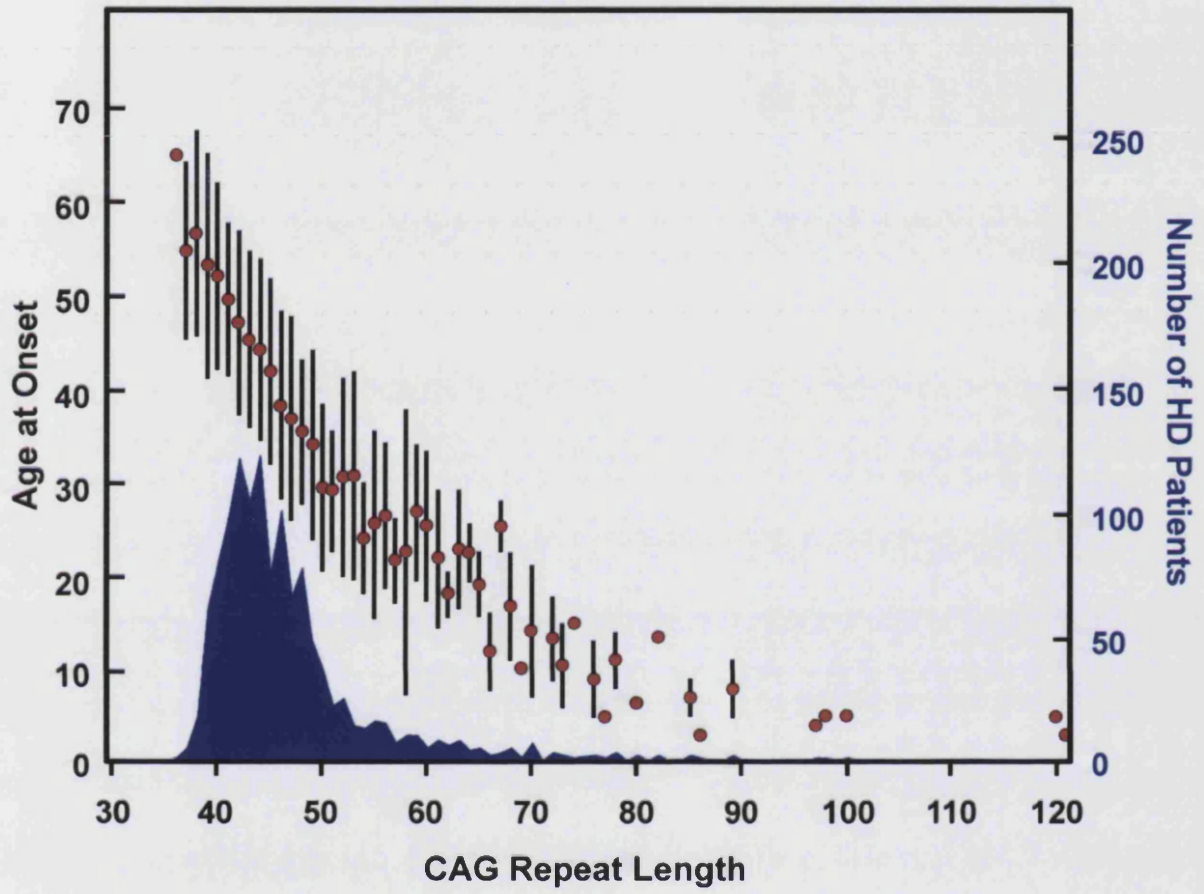

Figure 5 There is a greater variation among ages at onset with lower repeat sizes. As repeat size increases the effects of any modifiers are negated, thus repeat size alone becomes the major determining factor. The blue area indicates the number of HD individuals at any given repeat size. More than 90% of cases are below 60 repeats.

Adapted from J.F. Gusella *et al. Huntington's Disease* in Cold Spring Harbor Symposia on Quantitative Biology, Volume LXI: *Function & Dysfunction of the Nervous System* Cold Spring Harbor Laboratory Press 1996

tract alone become greater thus negating the actions of any modifiers (Stine *et al.* 1993; Brinkman *et al.* 1997).

1.3.4 Instability and Anticipation

Not only is there a variation between individuals within a particular generation, repeat lengths also vary from generation to generation. The polyglutamine tract exhibits intergenerational instability, undergoing both expansions and contractions. However, there is a general tendency for the size to increase (Gusella *et al.* 1993). This phenomenon is called *anticipation*, and is influenced both by the sex of transmitting parent and the original length of the repeat. When transmitted from mother to child the repeat length expands or contracts by around 4 CAG repeats, with a mild bias towards expansion. In the case of paternal transmission the tendency for expansion is very much greater than that for contraction (Zuhlke *et al.* 1993). The degree of expansion is also size-dependent, with the largest increases occurring during vertical transmission from males with the largest repeat length. It has been known for repeat length to double from around Q100 to Q200 in this scenario (Ranen *et al.* 1995; Trottier *et al.* 1995).

Marcy MacDonald *et al.* took four sets of monozygotic twins and measured their repeat lengths; they were identical for each pair (MacDonald *et al.* 1993). They also measured repeat lengths in the same individual using brain, blood and lymphoblast DNA and found no variation. These results suggest that expansion occurs during gametogenesis, or very early on in embryonic life. In support of this, they analysed the repeats in sperm from HD patients and found a remarkable amount of variation. The apparent startling instability during spermatogenesis explains why paternal transmission of the faulty gene tends so greatly towards an increase. It also explains why in all documented cases of new expansions – that is, patients with no previous family history of HD – the father has been found to have an intermediate length repeat. In these cases, during spermatogenesis a repeat length just below the threshold for disease is expanded into the disease range and an apparently 'sporadic' case emerges.

This also explains the global variation in the prevalence of HD: African and Asian populations have fewer repeats, thus it is less likely for an expansion above threshold level to occur. Furthermore, as expansion is size-dependent, it is likely that any expansions that do occur will be of fewer repeats than those seen in European or American individuals.

One group (Telenius *et al.* 1994) reported mosaicism in all tissues found during a human post-mortem study, with the strongest variations found in brain and sperm. Within the brain the greatest variation was found in the basal ganglia, the focus for HD degeneration. These results have yet to be replicated and subsequent human studies have found limited mosaicism in the somatic tissues of HD patients (Benitez *et al.* 1995; De Rooij *et al.* 1995; Giovannone *et al.* 1997). However, evidence of somatic instability has been found in the mouse models of the disease. Both in the exon1 transgenic mice, and the *Hdh* knock-in mice (see 2.1 *and* 2.2) there exists somatic instability which mirrors the Telenius results: the greatest variation being found in the striatum. Certainly in the mouse models at least, somatic instability may play a role in the selective neurodegeneration (Kennedy and Shelbourne 2000; Mangiarini *et al.* 1997).

Later work on model mice added to this tale with the suggestion that the gender of the embryo contributes to polyQ variation. In the R6 mouse models (see 2.1) expansions are also predominantly through the paternal line, but there is a skewed variation between male and female progeny from the one father (Kovtun *et al.* 2000). Furthermore, the repeat distribution in the progeny does not reflect the repeat distribution in the sperm of the father. Expansion does occur during spermatogenesis, but it seems male offspring may then undergo further expansion of the CAG repeat. Due to the variation in the sperm repeat lengths to begin with, such an analysis is only possible with very large numbers of offspring. As a result we do not know if this is true for human transmission.

1.4 The Repeat Expansion Diseases

1.4.1 Polyglutamine Repeat Diseases

HUNTINGTON'S disease is but one of a number of disorders caused by expansion of repetitive stretches of DNA (see figure 6). In the case of HD and (currently) nine other disorders the repeated sequence is CAG, which codes for the amino acid glutamine. In each disease the $[CAG]_n$ sequence is found within a different protein, and yet the effect is similar: the formation of aggregates and degeneration of a specific population of neurons. Each of the proteins shows no homology to the others outside of the polyglutamine tract, and yet the thresholds for the dominantly inherited diseases are similar: 30 to 40 glutamines[*].

The fact that the native protein has little effect on the pathology supports the notion that the polyQ region confers a novel property on the protein: the toxic gain-of-function. Furthermore, in animal models, overexpression of polyQ tracts in proteins not previously associated with disease, or the insertion of an elongated polyQ tract into proteins normally free from them produces neurological disorders concomitant with polyQ aggregates (Lin *et al.* 1999; Satyal *et al.* 2000; Warrick *et al.* 1998).

Each of the polyQ diseases also exhibits the properties explained earlier, including: somatic and germline instability tending towards exapansion; anticipation is greatest on paternal transmission; and increased repeat length is associated with a decreased age of onset, together with increased severity of symptoms. There is, however, a variation in the populations of neurons affected. There is no explanation as to why neurons in particular are affected in polyglutamine expansion disease, especially as the patterns of expression include many non-neural tissues. Perhaps the novel property gained by expansion interacts with substrates found only in neurons. On the other hand it could be that the neuron is simply less able to deal with the

[*] SCA6 in the exception, with a disease threshold slightly lower than the polyglutamine repeat disorders. SCA6 patients tend to have between 20 and 30 CAG repeats.

mutant protein. It would appear that extended polyglutamine tracts cause neurodegenerative disease, whilst the protein context confers the regional specificity. The functions of some of the disease-affected gene products are known (see figure 6), and in one case at least can explain some of the symptoms. The affected protein in spinal and bulbar muscular atrophy (SBMA) is the androgen receptor. Whilst the primary pathology in SBMA is motor neuron degeneration, androgen insensitivity is also seen, most ostensibly seen as breast development. In this case, loss of function plays a small part in the disease as SBMA is X-linked. It may well be that loss of function has a phenotypic role in some of the other disorders, but it is clear that the overriding cause of pathology, and thus the most important area of study, is the gain of function conferred upon the mutant protein.

1.4.2 Non-Coding Repeat Expansion Diseases

There are (currently) nine known neurodegerenative diseases cause by expansions of repeat sequences that are not located in coding segments of the gene. Only one of these disorders is caused by polyglutamine, and three are caused by repeats of sequences greater than three nucleotides (see figure 6). These diseases tend to have large and variable expansions, with a much larger threshold for disease. At the extreme, the pathogenic threshold for SCA10 requires 750 repeats of the sequence ATTCT. Progressive myoclonic epilepsy type 1 (EPM1) has a threshold similar to the expressed polyQ diseases – 30 – but it must be taken into account that the repeated sequence is twelve amino acids in length (CCCCGCCCCGCG) and the normal population has only 2 or 3 repeats. Each of these diseases results in multiple tissue dysfunction and degeneration. The specific pathology varies from diseases to disease, and is dependent on the particular nucleotide sequence, its location within the gene, and the function of the normal protein.

In the cases of Fragile X syndrome and Freidreich's ataxia, the expansion of the non-coding sequence leads to a reduction or loss of the normal protein. Both types

Disease	Gene	Locus	Repeat	Coding	Normal repeat length	Expanded repeat length
HD	Huntingtin	4p16.3	CAG	PolyQ	6-35	36-121
SCA1	SCA1/ATX-1	6p23	CAG	PolyQ	6-38	39-83
SCA2	SCA2	12q24	CAG	PolyQ	14-31	32-77
SCA3	MJD	14q21	CAG	PolyQ	12-40	54-86
SCA6	CACNA1A	19p13	CAG	PolyQ	4-19	20-30
SCA7	SCA7	3p21.1-p12	CAG	PolyQ	4-35	37-200
SCA17	TBP	6q27	CAG	PolyQ	29-42	47-63
DRPLA	Atrophin-1	12p13.31	CAG	PolyQ	3-35	49-88
SBMA	Androgen receptor	Xq11-12	CAG	PolyQ	9-36	38-62
HDL2	Junctophilin-3	16q23	CTG	PolyL/PolyA	7-26	44-57
SCA12	PPP2R2B	5q31-33	CAG	5' UTR	7-28	66-78
SCA8	SCA8	13q21	CTG	UTR	16-91	107-127
SCA10	SCA10	22q13	ATTCT	Intron	10-22	750-4500
EPM1	Crystatin B	21q22.3	CCCCGCCCCGCG	5' flanking	2-3	30-75
DM1	DMPK	19q13.3	CTG	3' UTR	4-37	50-4000
DM2	ZNF9	3q21	CCTG	Intron	≤26	75-11,000
Friedreich's ataxia	Frataxin	9q13	GAA	Intron	8-22	120-1700
FRAXA	FMR1	Xq27.3	CGG	5' UTR	6-54	>230
FRAXE	FMR2	Xq28	GCC	Promoter	6-25	>200

Figure 6 The repeat expansion disorders (see pp. 13-14 for abbreviations)

of Fragile X syndrome (FRAXA and FRAXE) involve an expansion of an untranslated trinucleotide sequence which results in hypermethylation and silencing of the gene (Fu *et al.* 1991; Knight *et al.* 1993; Verkerk *et al.* 1991). However, in Freidreich's ataxia the disease arises from a $[GAA.TTC]_n$ expansion within intron 1 of the gene (Frataxin). This expansion gives rise to "sticky DNA" which inhibits transcription by sequestering RNA polymerases within the complex DNA structure (Sakamoto *et al.* 2001). As these disorders result in the reduction or loss of normal protein function they are inherited in a recessive manner. However, there is another group of disorders all of which exhibit a dominant inheritance pattern in spite of the expansions being in untranslated regions.

Myotonic dystrophy (types 1 and 2), SCA8, SCA10, SCA12 and EMP1 involve a variety of nucleotide repeats, each in a transcribed but untranslated region of the associated gene. The pattern emerging is that novel gain-of-function properties are not confined to proteins, rather mRNA molecules can act in a similar manner to the polyglutamine-containing proteins discussed earlier. Of these disorders, the greatest amount of work has been the investigating of myotonic dystrophy. DM1 results from an expansion of a CTG region in the 3' UTR of the *DMPK* (dystrophia myotonica-protein kinase) gene (Brook *et al.* 1992). Whilst not translated, the CTG region is transcribed and the $[CUG]_n$-containing mRNA product is seen to accumulate in nuclear foci. This alone would result in a loss of the DMPK protein and a recessively inherited disease, but it has also been shown that these foci alter the regulation of a number of CUG-binding proteins such as CUG-BP1, CUG-BP2 (Timchenko *et al.* 1996a; Timchenko *et al.* 1996b) and muscleblind (Miller *et al.* 2000). These nuclear factors are thought to interact aberrantly with the CUG tract when it reaches a certain length due to the extended CUG repeat sequence forming RNA hairpins which bind such factors (Miller *et al.* 2000). As a result of the sequestration, the RNA splicing of several other genes is affected, including cardiac troponin T (Philips *et al.* 1998) and the insulin receptor (Savkur *et al.* 2001), which may explain the cardiac defects and propensity for diabetes seem in DM1 patients. The CCTG repeat in DM2 also produces foci of mRNA which also bind muscleblind (Mankodi *et al.* 2001), which may explain the similar phenotypes from two very different affected genes.

1.4.2 Huntington's Disease-Like 2

Huntington's Disease-Like 2 (HDL2) is a recently characterised disorder that has a very similar clinical presentation to HD, and likewise, is an autosomal dominant condition (Margolis *et al.* 2001). However, it arises from a different expansion in a different gene: a CTG repeat sequence, within the *JPH3* gene. *JPH3* codes for Junctophilin-3, a protein involved in the formation of junctional membrane structures, anchoring the plasma membrane to the endoplasmic reticulum. HDL2 has a similar repeat threshold to HD (6-27 repeats in unaffected individuals and 50-60 in disease patients) and the repeat expansion is located within a translated region, but the genetics are more complicated than the other disorders. The $[CTG]_n$ sequence is located in a variably spliced exon of the gene and, depending on splicing, the sequence can be translated or not translated. It is also read in more than one reading frame, producing either a polyleucine or polyalanine polypeptide chain (Holmes *et al.* 2001).

Given the similarity to HD, it may be that the pathology results merely from the accumulation of the polyL/polyA-containing protein. However, we currently cannot rule out the possibility that HDL2 represents a mix of pathogenic mechanisms involving toxic RNA effects as well as toxic protein effects.

1.4.4 A Unified Pathogenesis?

It is possible that many codon repeat sequences, translated or not, can cause disease once a threshold has been reached. The variety of sequences seen in the non-coding repeat expansion disease suggests this might be the case. In these disorders the number of repeats required to cause pathogenesis also varies widely, from 50 (DM1) to 750 (SCA10), which stands in contrast to the limited range seen in the polyglutamine diseases. The high number of diseases involving CAG repeats may reflect a particular property seen at its highest in glutamine, thus requiring the fewest repeats for pathogenesis.

1.5 *Degradation, Aggregation and Inclusion Formation*

1.5.1 Chaperones

DURING protein synthesis, RNA transcripts are translated to yield a linear array of peptides. The polypeptide chain forms the primary structure of the protein, which then forms structural motifs producing the secondary structure. Such motifs include α-helices and β-sheets, which tend to form unaided and in approximately the correct spatial relationship. However, at this stage the structure is unusually open and flexible: the *molten globule*. Conversion to the correct tertiary structure normally requires the aid of *molecular chaperones* to adjust incorrectly folded side-chains (Ptitsyn 1991; Christensen and Pain 1991).

Molecular chaperones were first identified in *E. coli* as proteins whose expression is greatly increased following mild heat shock, hence they were termed heat shock proteins: *hsp60* and *hsp70*. Upon exposure to high temperatures proteins can become denatured, that is the (quaternary and) tertiary structure is altered and protein functionality is lost. The purpose of the *hsps* was believed to be in aiding the refolding of proteins to the correct confirmation (Visick and Clarke 1995). It is now apparent that they have a more constitutive role in protein folding (Craig *et al.* 1993; Agashe and Hartl 2000).

Eukaryotic cells have families of chaperones related to the bacterial heat shock proteins, with different family members particular to cell organelles. During protein synthesis the polypeptide chain is exposed to the cytosol and the possibility exists that certain residues will interact with cell components. The chaperones have an affinity for exposed hydrophobic residues on incompletely folded proteins. The term *chaperone* came into use as it was believed the components became bound to hydrophobic residues to prevent unwanted, or premature reactions. It now seems that the chaperones play a more intimate role with nascent proteins, manipulating certain regions likely to be incorrectly folded such that the protein is more likely to

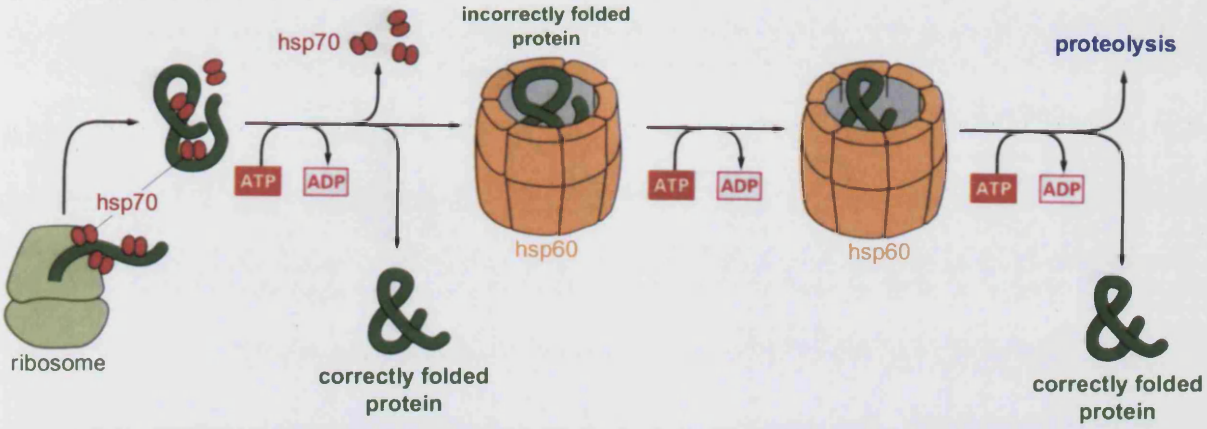

Figure 7 Chaperone-mediated protein folding. As the polypeptide chain emerges form the ribosome members of the *hsp70* family bind to strings of hydrophobic residues preventing interaction with cytosolic components. If the protein remains incorrectly folded, or a previously folded protein loses tertiary structure, the *hsp60* family, forming large barrel-like structures, isolates the protein from the cytosol until the protein is either refolded correctly or degraded by the proteasome (see 1.5.2).

Adapted from *Molecular Biology of the Cell* (3rd Ed.) Garland Press

achieve the correct conformation (Rassow and Pfanner 1996; Becker and Craig 1994). Figure 7 illustrates the different roles of the hsp60-like and hsp70-like families of chaperones.

1.5.2 The Ubiquitin-Proteasome System

In order to maintain homeostasis, a dynamic equilibrium is necessary balancing anabolism and catabolism. Cellular components are continually made and broken down, the balance between these two is altered as circumstances demand. In both cases, accurate control over the specificity and rates of reaction are needed. At the centre of the degradation of cellular components is the *ubiquitin proteasome system* (UPS). Selective proteolysis by the UPS occurs in two steps: firstly, the tagging of the target substrate by the covalent attachment of a 76-residue molecule, ubiquitin; secondly the degradation of the tagged protein by the proteasome complex with subsequent release of polypeptides and reusable ubiquitin (see figure 8).

Ubiquitination of the target protein is mediated by a series of enzymes. The ubiquitin-activating enzyme (E1) firstly activates ubiquitin by forming a high energy thiol ester intermediate (E1-S~ubiquitin). The activated ubiquitin is transferred via a second intermediate with one of many ubiquitin-conjugating enzymes (E2) to a protein substrate bound to a third enzyme, a member of the large ubiquitin-protein ligase family (E3) which catalyses the transfer (Hershko 1983). Ubiquitin preferentially binds at lysine residues and ubiquitin itself contains an internal lysine residue, thus successive addition to a target protein yields a polyubiquitin chain.

The polyubiquitin chain is recognised by the 26S proteasome complex, a multicatalytic protease that degrades proteins to small peptides. It is comprised of two structures, the 20S core particle and the 19S regulatory particle, which form a large barrel-shaped structure isolating the proteolytic subunits from the cytosol (see figure 9). The 20S unit contains four stacked rings, 2 outer α-rings and 2 inner β-rings,

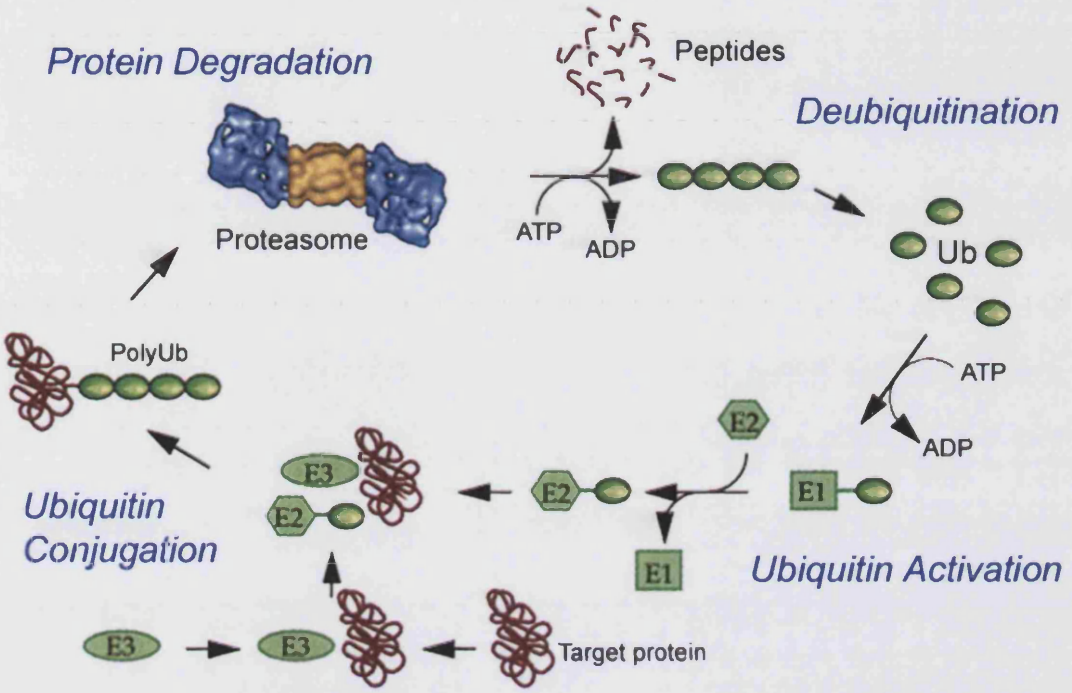

Figure 8 The ubiquitin-proteasome pathway. Free ubiquitin is activated by the enzyme E1 and transferred via an E2 enzyme to proteins recognised by a member of the E3 family. Further ubiquitin is added forming a polyubiquitin chain which is recognised by the proteasome. The proteasome unfolds the protein and degrades the polypeptide chain releasing peptides and free ubiquitin.

Image adapted from the MRC Human Genetics Unit website

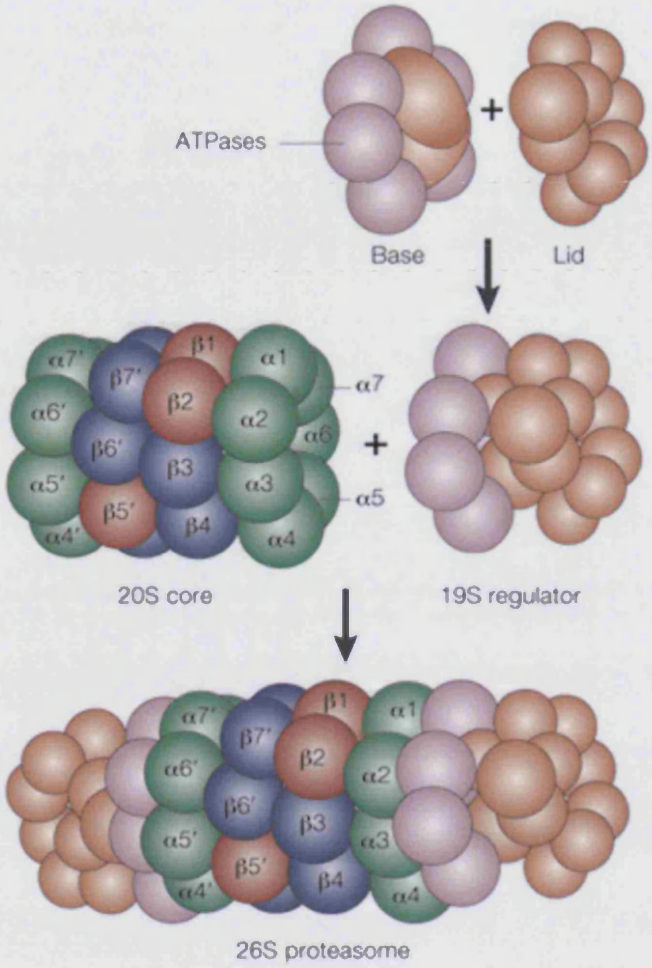

Figure 9 Structure of the proteasome. The 19S regulatory unit of the proteasome is composed of a 'lid' recognising target proteins and a 'base' controlling entry into the catalytic core of the complex. The 20S core unit contains four stacked rings 2 outer (α) and 2 inner (β) rings, each composed of seven subunits. Catalytic activity is localised to subunits β1, β2 and β5 – yielding six proteolytic sites in total (red).

Taken from Kloetzel 2001

each (in eukaryotes) composed of seven subunits. The catalytic activity is localised to three of the β-ring subunits. The 19S unit caps either end of the 20S unit and regulates the entry of proteins into the proteolytic unit. It recognises polyubiquitinated proteins, and other substrates for the proteasome, and unfolds them for insertion into the 20S. The 19S is also responsible for opening the 20S, therefore restricting access to the catabolic subunits when no recognition unit is in place. The unfolding of proteins and opening of the 20S require energy and the 19S contains six different ATPase subunits (Zwickl *et al.* 1999).

Specificity in the system is determined by the ubiquitin-protein ligase family members and other ancillary proteins. In some cases either the E3 or the protein must be modified in some way before recognition occurs, phosphorylation or binding to other proteins, for example. Phosphorylation can have opposite effects (preventing UPS recognition or enabling it) depending on the substrate, such that the activity of a single kinase can increase the presence of some proteins, whilst causing the loss of others. This provides another level of control of the turnover rates of different proteins (Glickman and Ciechanover 2002).

Quite surprisingly, it is estimated that between 30% and 50% of polypeptide chains are degraded cotranslationally (Turner and Varshavsky 2000; Schubert *et al.* 2000). It is suggested that the these nascent proteins contain errors in either coding or folding. As discussed, wrongly folding proteins are recognised by the molecular chaperones, but it is possible that the 19S unit interacts directly with these proteins. The proteasome itself can, *in vitro* at least, function as a chaperone. The 19S has been shown to bind certain unfolded proteins, accelerate their refolding and then release them in their native forms (Strickland *et al.* 2000; Braun *et al.* 1999). Increasingly, it seems that chaperones and the proteasome are linked in function. Not only does the 19S possess intrinsic chaperone properties, but chaperones have been shown to copurify with the proteasome.(Montel *et al.* 1999; Wagner and Margolis 1995) and in yeast, overexpression of Hsp70 can suppress growth defects associated with mutant 20S subunits (Ohba 1997). It is probable that when chaperones fail to restore the tertiary structure of a misfolded protein they shuttle them to the proteasome for

degredation, thereby limiting the effects of any inappropriate properties the misfolded protein may possess.

1.5.3 The Neuronal Intranuclear Inclusion

When the Huntington's disease gene was characterised in 1993 (Huntington's Disease Collaborative Research Group 1993) the polyglutamine repeat aetiology became apparent. Whilst it seems clear that pathology arises from a dominant gain of function (see 1.3) the exact novel physical property underlying this change remains elusive.
Given the extensive cellular machinery that exists to deal with misfolded or incorrectly translated proteins, it is reasonable to assume that cells expressing mutant or abnormal protein would mount a response against their effects. In studying the degradation of abnormal proteins in neurological disease, Ii *et al.* (1997) examined structures known to be ubiquitinated in neurological disease (AD, PD) and the elderly. They found colocalisation of proteasome components in certain structures but not in others. For example, in Alzheimer's disease both the dystrophic neurites and neurofibrillary tangle are ubiquitinated, but the proteasome is only found the former. Davies *et al.* (Davies *et al.* 1997) conducted similar studies on transgenic mouse models of Huntington's disease (see 2.1). Using antibodies raised against the N-terminal of huntingtin, they examined three lines of mice transgenic for exon 1 of the human *htt* gene with an expanded polyglutamine repeat. In control brains the distribution was similar to that seen in adult human brains with labelling of the entire grey matter, localised to the cytoplasm of neurons along with the axons and dendrites. In the transgenic mice, however, in addition to the staining seen in the control a 'densely stained circular inclusion' is seen within neuronal nuclei. The Davies *et al.* study also used anti-ubiquitin antibodies and found the newly named *neuronal intranuclear inclusion* (NII) also stained for ubiquitin (see figure 10). Subsequent analysis has also revealed many other components of the pathways discussed in *1.5.1* and *1.5.2* colocalise to the NII in mouse and cell culture as well human tissue, including

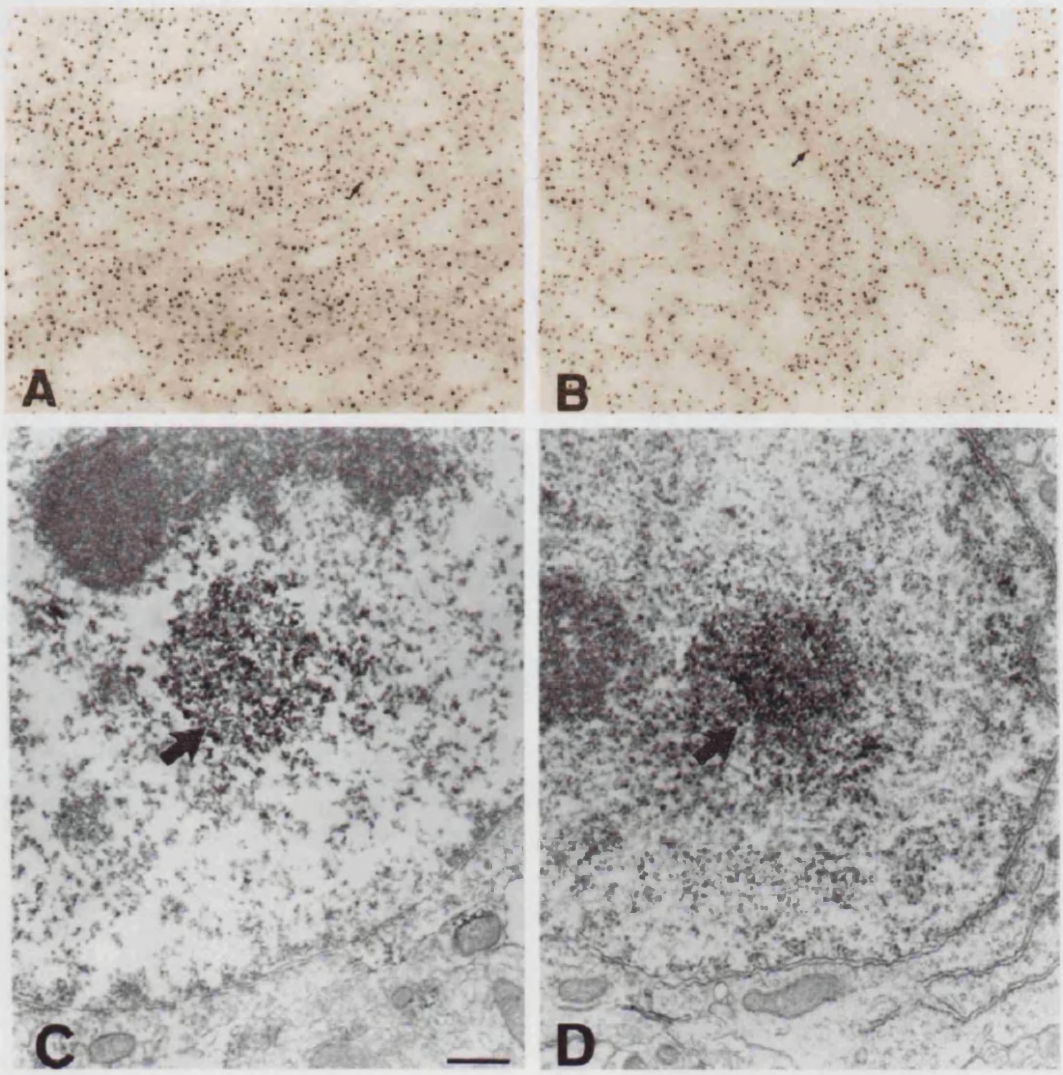

Figure 10 Huntingtin (A,C) and ubiquitin (B,D) immunoreactivity in the striatum of the R6/2 mouse (see 2.1). Nuclear inclusion are evident throughout the striatum (A,B). DAB reaction product is seen together with a discreet structure an the electron microscope level (C,D). Scale bar for (C) and (D) 500nm.

Adapted from Davies *et al.* 1997

chaperones Hsp70, Hsp40, BiP & HDJ-2 and proteasome components 20S, 19S & 11S (Waelter *et al.* 2001; Davies *et al.* 1999). These results suggest that the neuron attempts to contain the mutant protein via the chaperone response and as the protein cannot be folded correctly it is degraded, or at least an attempt is made, by the proteasome. Why the mutant protein, together with the chaperone/UPS components, forms inclusions is another unresolved issue. However, they now appear to be the hallmark of Huntington's disease.

Since their discovery in transgenic mice, neuronal intranculear inclusions have been identified also in human HD post-mortem tissue (Becher *et al.* 1998; DiFiglia *et al.* 1997). It has also become apparent that, although not named as such, the NII was discovered in human HD biopsy tissue in 1979 by Roizin *et al.* (Roizin *et al.* 1979). Furthermore, studies on human HD show that not only is the mutation localised to exon 1 but that the huntingtin that forms the inclusions is a truncated form from the N-terminus. It is probable that the neuron makes an attempt at proteolysis but cannot degrade the polyglutamine, thus leaving the N-terminal truncated forms to aggregate.

1.5.4 Neurite Inclusions

The Neuronal Intranuclear Inclusion is not the only aggregate seen in Huntington's disease. With techniques similar to those used in the identification of the NII, one can identify intensely staining structures outside the neuronal nucleus. In human biopsy material as well as the mouse models it is apparent that dystrophic neurites also contain inclusions composed of ubiquitinated N-terminal huntingtin (DiFiglia *et al.* 1997). In cell culture models of HD, aggregation of mutant huntingtin occurs both in the nucleus and the cytoplasm (Cooper *et al.* 1998) and is probable that such cytoplasmic aggregation underlies the neuritic degeneration.

1.5.5 Aggregation

The mechanism by which mutant huntingtin, together with the many components also recruited, form inclusions remains unclear. The late Max Perutz postulated that the expansion of a polyglutamine stretch beyond a certain length would lead to a phase change from random coils to hydrogen-bonded hairpins. These would naturally tend to associate with each other and form highly stable β-sheets: the *polar zipper* model (Perutz 1996). *In vitro,* N-terminal huntingtin with expanded polyglutamine stretches can indeed form aggregates[*] rather like the beta-amyloid fibrils seen in Alzheimer's disease (Scherzinger *et al.* 1997).

A second model states that aggregation results from the activity of tissue transglutaminase (tTG). It has been shown in cell culture that protein polyglutamine stretches are substrates for tTG, with longer stretches resulting in greater tTG activity. Furthermore, the addition of tTG inhibitors reduces the degree of aggregate formation. As a result it has been suggested that it is this activity that leads to the formation of aggregates via the creation of isopeptide bonds which crosslink polyQ-containing proteins (Kahlem *et al.* 1998). There is some support for this occuring *in vivo* as elevated tTG levels and activity can be found in HD brains (Karpuj *et al.* 2002), however the areas of increased tTG activity do not correlate well the the distribution of NIIs (Vonsattel and DiFiglia 1998) and increasing tTG levels does not affect aggregate formation (Chun *et al.* 2001).

Wyttenback *et al.* treated transfected cells with heat shock and lactacystin (a proteasome inhibitor) and found that both increased the amount of htt exon 1 found in the inclusions (Wyttenbach *et al.* 2000). They suggest that inclusions form when the chaperone/proteasome system cannot cope with the mutant protein. This can be interpreted as the chaperone/proteasome system binding to the mutant protein preventing β-sheet formation and/or transglutamination.

[*] Under very non-physiological conditions.

1.5.6 Inclusions and Disease

The discovery of the NII and neurite inclusions in Huntington's disease means that HD joins a growing number of neurological diseases associated with the formation of aggregates. There are a number of different structures, some characteristic of a particular disorder, others occurring in many diseases, each with a different protein constitution (see figure 11). What is clear is that aggregation is a common event in many diseases involving many proteins, which suggests that either cells are particularly vulnerable to the accumulation of protein, or that a cellular response exists which purposefully aggregates harmful protein. There is evidence to suggest that formation of the inclusion is beneficial to the cell (see 1.6.3), providing support for the evolution of a cellular response to aggregate harmful protein.

Whether the neuronal intranuclear inclusion is the underlying cause of pathology in HD, or whether it is simply a symptom of the mutant protein load remains under debate.

Inclusions	Disease	Components	Cell Type
cytoplasmic			
Ballooned neurons	Pick's, CBD, AD, CJD, ALS	Neurofilaments	Neurons
Dystrophic neurites	AD, PD, DLBD, MND, CBD	α-synuclein, proteasomes	Neurites
Granulovascular bodies	AD, normal ageing	Neurofiliaments and tau	Neurons (vacuoles)
Lewy bodies	PD, DLBD	α-synuclein, α-crystallin, proteasome	Neurons
Lewy body-like	ALS	Neurofilaments	Motorneurons
Neurofibrillary tangles	AD	Paired helical filaments, HSPs	Perikarya
Pick bodies	Pick's disease	PHF with tau	Neurons
Rosenthal fibres	Alexander's disease	α-crystallin, intermediate filaments	Astrocytes
Endosomal/lysosomal			
Lysosome-related structures	TSE, AD	Prion protein, HSP70	Neurons
Bunina bodies	ALS	Vimentin, HSP70	Neurons
nuclear			
Intranuclear inclusion	CAG repeat diseases	Gene products, HSPs, proteasome, α-synuclein	Neurons

Figure 11 The variety of inclusions seen in neurological disease (see pp 13-14 for abbreviations)

1.6 *The Nature of the Inclusion*

1.6.1 *The Neurotoxic Nature of Inclusions*

IN adult HD brains, NIIs are found in the striatum and cortex, but rarely in the hippocampus, red nucleus and cerebellum, which correlates well with the degeneration seen in adult HD (Becher *et al.* 1998; Sieradzan and Mann 2001). Furthermore, in the juvenile form of HD the cerebellum also degenerates and in this case, inclusions are found in the cerebellar Purkinje cells. Whilst one cannot rule out the possibility that the inclusion is merely another symptom of degeneration, these data have led many to suggest a causal relationship between inclusion formation and neuronal degeneration

Various N-terminal fragments of mutant huntingtin have been shown to form aggregates *in vitro* and *in vivo*. In general, the propensity for aggregation increases with increasing polyglutamine length and decreasing non-glutamine content (Martindale *et al.* 1998; Li and Li 1998). This suggests that polyglutamine stretches tend to aggregate naturally, arguing against a cellular mechanism for aggregation. In this case, the variation in inclusion distribution may arise from the ability of the cell to degrade the protein before it aggregates. In a Drosophila model of HD, aggregation has been limited through the expression of an artificial huntingtin-binding polypeptide. Inclusion appearance was limited as were both neuronal degeneration and death (Kazantsev *et al.* 2002) further suggesting a relationship between the formation of inclusions and degeneration.

Bucciantini *et al.* expanded the issue of aggregate formation by showing that many proteins are capable of aggregating into defined structures, and that these structures have an inherent toxicity (Bucciantini *et al.* 2002). Under certain conditions Bucciantini *et al.* caused two proteins not previously associated with disease to aggregate; the SH3 domain from bovine phosphotidyl-inositol-3'-kinase and the N-terminal of *E. coli* HypF protein. The addition of these aggregates (at certain stages of

aggregation) to cell culture media proved cytotoxic whereas the native proteins did not, suggesting that protein aggregates in general are toxic to cells.

1.6.2 The Toxic Fragment Hypothesis

Huntingtin was the first neuronal protein to be shown to be a caspase substrate (Goldberg *et al.* 1996). It has since been established that the protein contains cleavage sites for caspases 2, 3 and 6 (see 1.7.4). Caspase neoepitopes[•] have been detected in both normal and HD brains (Wellington *et al.* 2002). Other proteases are presumed to cleave huntingtin as multiple fragments of N- and C-termini have been detected with varying amounts according to region and HD status (Mende-Mueller *et al.* 2001), however the studies referenced in *1.6.2* were able to prevent aggregate formation by preventing the cleavage of huntingtin using caspase inhibitors. Likewise, Wellington *et al.* have generated yeast artificial chromosome mouse models of HD, including a model with huntingtin lacking caspase 3 and 6 cleavage sites. In these mice, aggregate formation and toxicity is also reduced (Wellington *et al.* 2000). The R6/2 mouse model (see 2.1) is widely used as it exhibits the most aggressive phenotype. In this model huntingtin is already in a truncated form.

The *toxic fragment hypothesis* centres around the cleavage of huntingtin as the key event. The N-terminus alone is sufficient to cause neurodegeneration (Mangiarini *et al.* 1996), and proteins with fewer nonglutamine residues flanking the repeat sequence are of greater toxicity (Martindale *et al.* 1998). The generation of N-terminal fragments is believed to bring about the entry of the cell into a vicious circle. Caspase cleavage of htt generates the N-terminal fragments, the inherent toxicity of which causes apoptotic caspase activation, which in turn causes more htt cleavage (Hackam *et al.* 1998; Cooper *et al.* 1998; Saudou *et al.* 1998). There is little doubt

[•] Epitopes produced only when a protein is cleaved at a particular site, in this case the caspase cleavage sites

that the N-terminal fragment is more toxic that full length mutant protein, but whether this vicious circle exists *in vivo* remains to be seen.

1.6.3 The Neuroprotective Nature of Inclusions

It is clear that the accumulation of mutant N-terminal huntingtin leads to dysfunction and death, but some argue that the aggregate ameliorates this effect. The studies listed above prevent aggregate formation by preventing cleavage of huntingtin. According to the toxic fragment hypothesis, this alone will reduce toxicity. Furthermore, suppression of NII formation between the stages of cleavage and aggregation proves more toxic to cultured cells transfected with mutant htt (Saudou *et al.* 1998).

Nuclear inclusions also form in SCA1. The mutant protein, ataxin 1, contains a self-association region which promotes aggregation on top of the polyglutamine effects. Transgenic mice have been generated with a deletion in this region (Klement *et al.* 1998). Whilst aggregation is significantly reduced, and NIIs are not observed, degeneration of the Purkinje cells still occurs.

Closer analysis of inclusions in human post-mortem brain has found that distribution in terms of cell type, rather than region, does not correlate with HD pathology. NIIs are more frequent in the cortex yet most degeneration occurs in the striatum (Gutekunst *et al.* 1999). Furthermore, NIIs are found in striatal interneurons, which are completely spared in HD (Kuemmerle *et al.* 1999). Many of the studies purporting a link between aggregate formation and cell death *in vitro* relate amount of apoptotic activity to amount of aggregate formation, but one study analysing sensitivity to apoptotic stimuli in N-htt transfected cells compared distribution of NIIs to caspase activity. Whilst in general the mutant htt tranfected cells were more susceptible to apoptosis, there was no correlation between NII formation and such apoptotic sensitivity (Chun *et al.* 2002).

The Bucciantini *et al.* study mentioned in *1.6.1* (Bucciantini *et al.* 2002) shows that under the right conditions many proteins can form aggregates. In the case of the Hyp-F-N induced aggregation, the structure changed over time. Within minutes of being placed in a pH5.5 solution the protein formed amorphous aggregates with β-sheet properties. Over time, up to 20 days, these structures organised themselves into protofibrils and then fibrils in a manner similar to β-amyloid (Walsh *et al.* 1999). Extracts taken at later times and added to cell culture media prove less and less toxic. As the protein changes from amorphous aggregate to regular fibrillar structure toxicity lessens. A similar pattern has been shown for β-amyloid itself and α-synuclein; the prefibrillar structures are more cytotoxic in both cultured cells and transgenic mice (Conway *et al.* 2000; Hartley *et al.* 1999; Pillot *et al.* 1999).

The toxicity of prefibrillar structures is likely to arise as hydrophobic sidechains, and other regions, are much more exposed. In other words, the fully formed fibrils are less likely to cause abnormal protein-protein interactions. This would imply that the NII is rather a benign structure. Given the apparent toxic nature of the polyglutamine-containing fragments, such aggregation as is observed can be considered a beneficial effect.

1.6.4 Interactions

Huntingtin has been shown to interact with a large number of other proteins. Many of these have also been shown to vary according to polyglutmaine length. One can therefore conclude that mutant htt interacts abnormally with cellular proteins. Huntingtin interacting proteins include:

Glyceraldehyde-3-phosphate dehyrogenase (GAPDH)
Calmodulin
Huntingtin-inteacting protein 1 (HIP1)
Huntingtin-interacting protein 2 (HIP2)

Huntingtin-associated protein 1 (HAP1)
Huntingtin-associated protein 40 (HAP40)
WW domain proteins
Cystathionine β-synthase
SH3-containing Grb-like protein 3 (SH3GL3)

GAPDH has been shown to interact directly with the polyQ tract and interacts more strongly with smaller fragments (Burke *et al.* 1996). It has been suggested that this interaction results in impaired glycolysis in HD, perhaps underlying some of the dysfunction. However, studies on human HD post-mortem tissue have found normal GAPDH activity (Kish *et al.* 1998).

Huntingtin from HD brains has been shown to bind calmodulin in the presence of calcium more avidly than wild-type huntingtin (Bao *et al.* 1996). Calmodulin is small regulatory protein which binds calcium. With calcium bound it interacts with many target proteins, with either inhibitory or stimulatory roles, thus providing a multi-target mediator in calcium signalling. Once again, this preferential interaction with expanded huntingtin may have some bearing on cell dysfunction.

Huntingtin-interacting protein1 (HIP1) was identified through its altered interaction with mutant htt. The interaction with htt becomes weaker as polyglutamine length increases. Its function was unknown at the time, but overexpression resulted in caspase 3-mediated cell death (Hackam *et al.* 2000). HIP1 contains a death effector domain (DED) (see 1.7.5) the overexpression of which alone is sufficient to induce the caspase 3-mediated cell death seen. If the DED is mutated out of HIP1 the toxicity is eliminated entirely (Hackam *et al.* 2000). Thus, the greater the polyglutamine length the more free HIP1 (and DEDs) there is. It has since been shown that HIP1 is involved in clathrin-mediated endocytosis. It is found to be enriched on coated vesicles where it binds to adapter protein 2 (AP2) and the clathrin heavy chain. Furthermore, expression of truncated HIP1 blocks clathrin-mediated endocytosis (Metzler *et al.* 2001). Its interaction with huntingtin is therefore very interesting given the suggested roles of htt in vesicle trafficking.

~

Huntingtin-interacting protein 2 (HIP2) has been identified as the ubiquitin-conjugating enzyme hE2-25K (a member of the E2 family; see 1.5.2). HIP2 in expressed throughout the body, but a slightly larger version is expressed in brain, most probably resulting from alternate splicing. The interaction of HIP2 with huntingtin does not vary with polyglutamine length, casting doubt on this interaction underlying the ubiquitination of mutant htt, or the interaction being part of a chaperone response, nevertheless it may have an ancillary role in the processing of mutant huntingtin (Kalchman *et al.* 1996).

Huntingtin-associate protein 1 (HAP1) is another huntingtin interacting protein with a role in vesicle function. It is predominantly a membrane-associated protein enriched, much like huntingtin, on synaptic vesicles (Li *et al.* 1995). It has also been suggested that HAP1, in its two isoforms, is involved in the formation of the stigmoid body through self-association (Li *et al.* 1998) Mice have been generated with disruption to the HAP1 gene. These mice die in the early postnatal period due to depressed feeding behaviour. With the exception of starvation-associated changes, there appears to be little change on post-mortem examination (Chan *et al.* 2002). The interaction of HAP1 with huntingtin is the reverse situation to HIP1, namely as polyglutamine length increases as does the affinity with HAP1. It is possible that the self-associative nature of HAP1 aids the aggregation of huntingtin. Furthermore, as disruption of HAP1 can produce profound behavioural changes in the absence of gross pathology, it is possible that the sequestration of HAP1 by mutant huntingtin is the cause of some of the psychological changes seen in HD.

Huntingtin-associated protein 40 (HAP40) is so called as it is a 40kDa protein which interacts with normal huntingtin. HAP40 is encoded within intron 22 of the Factor VIII gene. Normal huntingtin appears to anchor HAP40 to the cytoplasm of a cell, without this normal action, HAP40 is actively translocated to the nucleus (Peters *et al.* 2002). The implications of this are unclear, but it may indicate a role in the normal function of huntingtin which is disrupted in the disease state.

The WW domain proteins consist of three proteins that interact with huntingtin N-terminus, both wild type and mutant, via the same region: the WW domain. These proteins, HYPA, HYPB and HYPC interact with the proline-rich region

adjacent to the polyglutamine region of huntingtin. The interaction is enhanced as the polyglutamine tract lengthens (Faber *et al.* 1998). HYPA is known to be involved in spliceosome function, and HYPC has since been shown to have a similar function. HYPB has also been identified as a transcription factor, thus it is suggested that altered mRNA production and maturation may play a role in HD pathogenesis (Passani *et al.* 2000).

Cystathionine β-synthase binds to huntingtin but no other polyglutamine-containing proteins. Furthermore, this interaction is independent of polyglutamine length, suggesting an interaction with a region outside of the N-terminus (Boutell *et al.* 1998). Cystathionine β-synthase is a key enzyme in the conversion of methionine to cysteine. The condition homocysteinuria is an autosomal recessive disorder resulting from the absence of cystathionine β-synthase, which leads to a build-up of homocystein, one of the substrates of the enzyme. Symptoms include severe mental retardation, seizures and psychiatric disorders. Two oxidation products of homocysteine, homocysteate and homocysteine sulphate, are potent NMDA receptor agonists. It is suggested that an accumulation of huntingtin may hinder the normal function of the enzyme resulting in a build-up of the homocystein oxidation products and promotion of excitotoxic damage (see 1.8.1).

SH3-containing Grb-like protein 3 (SH3GL3) preferentially binds the N-terminal fragment of huntingtin with an expanded polyglutamine tract. Furthermore, transfection of mutant htt-expressing cells with SH3GL3 promotes aggregate formation (Sittler *et al.* 1998). SH3GL3 is preferentially expressed in brain and testis, hence it may have an effect on inclusion formation *in vivo*. There is a further link between huntingtin and vesicle function as SH3GL3 plays a major role in the regulation of the exo/endocytic cycle of synaptic vesicles (McPherson 1999).

As has been established, huntingtin interacts with a variety of proteins, and in some cases there is a preferential interaction with mutant huntingtin. In the course of Huntington's disease, with both free huntingtin and the NII-contained htt it would be foolish to believe that events are limited to the direct effects of the huntingtin mutation *per se*.

1.7 *Apoptosis*

1.7.1 *The Physiological Role of Apoptosis*

APOPTOSIS, the Greek word describing the "falling off" of leaves from a tree, was used in 1972 by Kerr, Wyllie and Currie to describe a "mechanism of controlled cell deletion, which appears to play a complimentary but opposite role to mitosis in the regulation of animal cell populations" (Kerr *et al.* 1972).

Apoptosis is a fundamentally important process in all multicellular organisms, essential for the development and, in vertebrates at least, the maintenance of the organism. During metazoan development numerous structures are formed which are removed by apoptosis at a later stage (Jacobson *et al.* 1997). This affords a greater degree of flexibility as primordial structures can be remoulded or removed for different functions at later stages in life, or sex. For example, the Müllerian duct which forms the uterus and oviduct in females is removed apoptotically in males. On the other hand, the Wolffian duct which forms the male reproductive organs is removed in females. Likewise, there are many structures which form during development that are evolutionary hold-overs, structures which produce functioning tissues in lower organisms but which are no longer needed, these too need deleting. The apoptotic pathways also act as a check mechanism for the developing organism, correcting many errors which may occur. For example, Drosophila dosed with extra *bicoid (bcd)*, a morphogen, initially develop severely mispatterned anterior regions, but the apoptotic checking means these develop into relatively normal adults (Namba *et al.* 1997).

The ability to induce rapid and selective suicide in supernumerary, misplaced or dysfunctional cells is thus of vital importance to the development and survival of the organism. This is further exemplified by the large number of diseases which result from a dysregulation of apoptosis with consequences including tumorigenesis, autoimmunity, neurodegenerative disease, hematopoietic deficiencies and infertility

1.7.2 Identifying the Apoptotic Machinery

The initial work on the molecular machinery underlying apoptosis was carried out on the nematode worm *C. elegans,* which is particularly useful for such development studies as its developmental programme never varies. The fate of each cell in the development of the *C. elegans* adult worm has been mapped from start to finish. Sulston and Horvitz noted that during development 131 of the 1090 somatic cells of *C. elegans* are removed apoptotically (Sulston and Horvitz 1977). Genetic screens for mutants defective in this development revealed a number of genes responsible for the regulation and execution of apoptosis. The four crucial genes for *C. elegans* cellular demise are *egl-1, ced-3, ced-4* and *ced-9.* Loss of function of either *egl-1, ced-3* or *ced-4* results in survival of all 131 cells which are normally removed. In contrast, loss of *ced-9* function results in massive, lethal, cell death early in development. As over-expression of *ced-9* leads to survival of the 131 cells, it is clear that *ced-9* is a suppressor of apoptosis (Horvitz *et al.* 1983). These proteins are highly conserved throughout evolution, illustrating the importance of the apoptotic machinery, and each of the *C. elegans* death proteins has a homologue in human apoptosis.

1.7.3 The Morphology of Apoptosis

The original definition of apoptosis by Kerr, Wyllie and Currie in 1972 was based on morphological descriptions alone. It was defined as occurring in two discrete stages. Firstly, the dying cell undergoes nuclear and cytoplasmic condensation and fragments into membrane-enclosed, ultrastructually well-preserved fragments (apoptotic bodies). The second stage involves the engulfment of the apoptotic remnants by other cells where they are degraded (illustrated in figure 12) (Kerr *et al.* 1972).

The earliest changes identified in the original work involve the condensation and aggregation of nuclear chromatin beneath the nuclear envelope. This is followed by shrinkage, both nuclear and cytoplasmic, and nuclear fragmentation (figure 13,A).

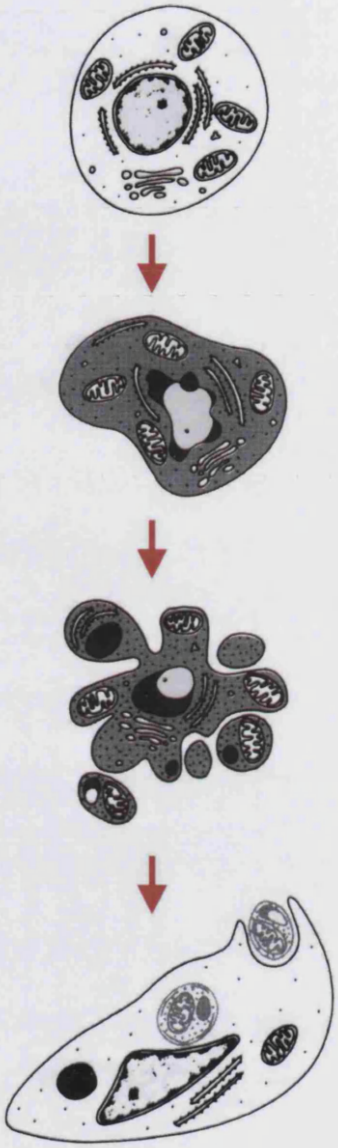

Figure 12 An illustrative summary of apoptosis. The dying cell undergoes a series of changes beginning with nuclear and cytoplasmic condensation. Chromatin condenses whilst the nuclear membrane initially remains intact. The plasma membrane "blebs" eventually leading to fragmentation of the cell into membrane-bound, ultrastructurally well-preserved fragments (apoptotic bodies). These apoptotic remnants are engulfed by other cells whereupon they are degraded lysosomally.

Image adapted from Kerr & Harman: *Definition and Incidence of Apoptosis: An Historical Perspective* – In *Apoptosis: The Molecular Basis of Cell Death* Cold Spring Harbor Press

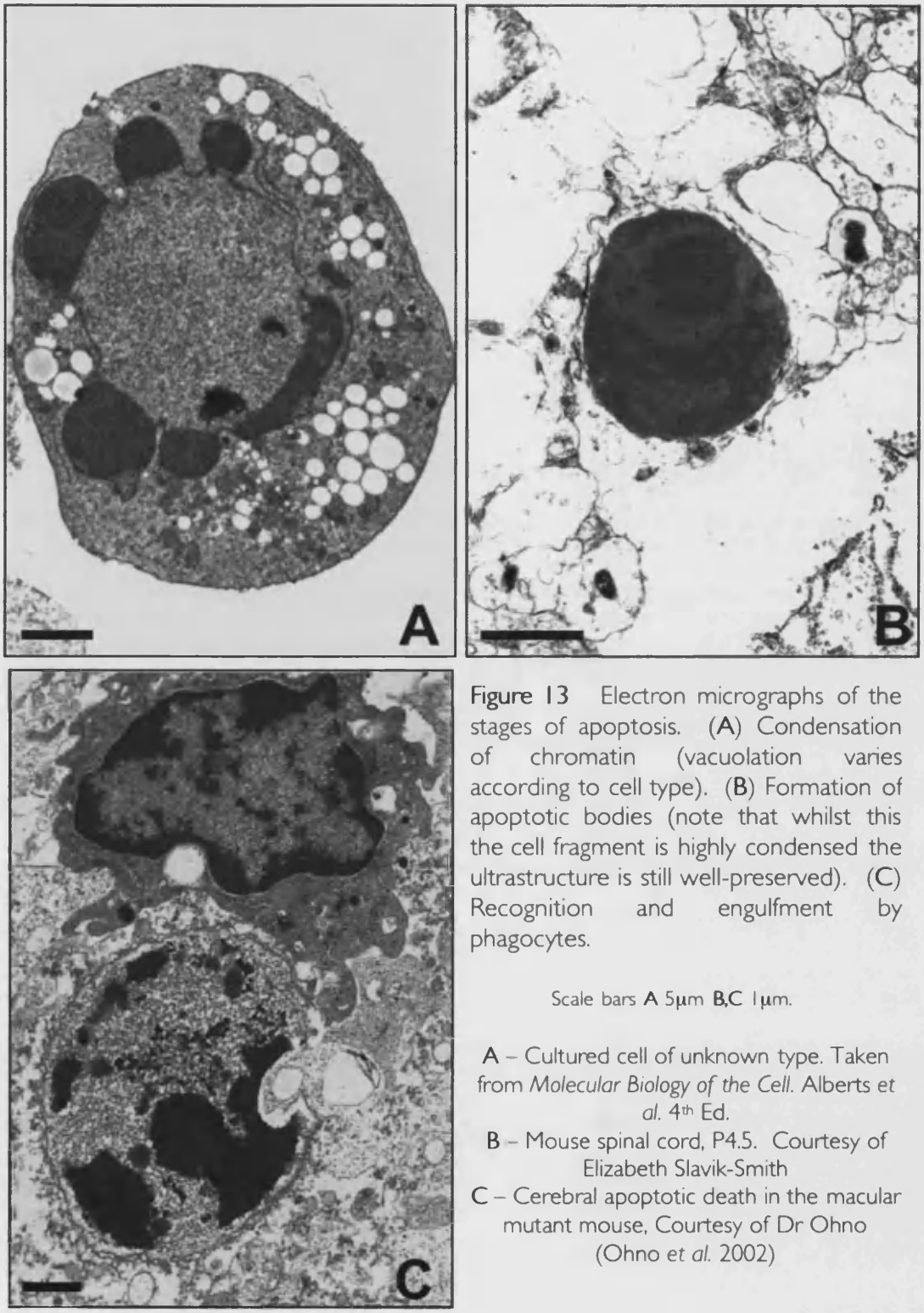

Figure 13 Electron micrographs of the stages of apoptosis. (A) Condensation of chromatin (vacuolation varies according to cell type). (B) Formation of apoptotic bodies (note that whilst this the cell fragment is highly condensed the ultrastructure is still well-preserved). (C) Recognition and engulfment by phagocytes.

Scale bars A 5μm B,C 1μm.

A – Cultured cell of unknown type. Taken from *Molecular Biology of the Cell.* Alberts *et al.* 4th Ed.
B – Mouse spinal cord, P4.5. Courtesy of Elizabeth Slavik-Smith
C – Cerebral apoptotic death in the macular mutant mouse, Courtesy of Dr Ohno (Ohno *et al.* 2002)

The cell surface also undergoes changes in the form of the development of protuberances, a process since labeled "blebbing", which eventually separate off forming apoptotic bodies. The bodies themselves are of greatly varying size, though all compact, and are structurally well-preserved containing closely packed organelles which may themselves be condensed, but which are believed to be chemically and structurally intact (figure 13,B).

In all of the tissues studied in the original work, the majority of apoptotic bodies were found within the cytoplasm of intact cells, suggesting they are very rapidly phagocytosed. It was postulated (and has since been proven) that this results from changes to the cell surface of the apoptotic cell which are recognised and contacted by phagocytic cells (figure 13,C). Once phagocytosed, the bodies begin to degrade in a process that is "ultrastructurally very similar to ischemic coagulative necrosis and *in vitro* autolysis" (Kerr *et al.* 1972). In essence, the bodies begin to lose their structural integrity and it was suggested that this results merely from their inability to maintain homeostasis within the phagocytosing cell. The bodies are then further degraded by lysosomal enzymes from the engulfing cell and are rapidly reduced to electron-dense lysosomal bodies.

The apoptotic journey is over fairly quickly. The entire process, from the initial changes in chromatin and cell condensation through to the complete degradation of apoptotic bodies within phagosomes, was said to be completed within twenty-four hours (Kerr *et al.* 1972). No work has yet contradicted this statement.

Since 1972 the field of apoptosis research has continued to expand. The identification of the genetics and proteins involved in apoptosis led to an explosion of interest in programmed cell death, and as a result the number of publications on apoptosis each year has risen almost exponentially since the early nineties (figure 14).

The field of apoptosis research is now phenomenally large, which brings with it both complication and confusion. To describe all the known apoptotic processes and cellular machinery would make this discourse too large and confusing; therefore an overview of the key elements will be presented here and a discussion of some of the confusions and errors that have arisen in the field can be found in chapter 5.

~

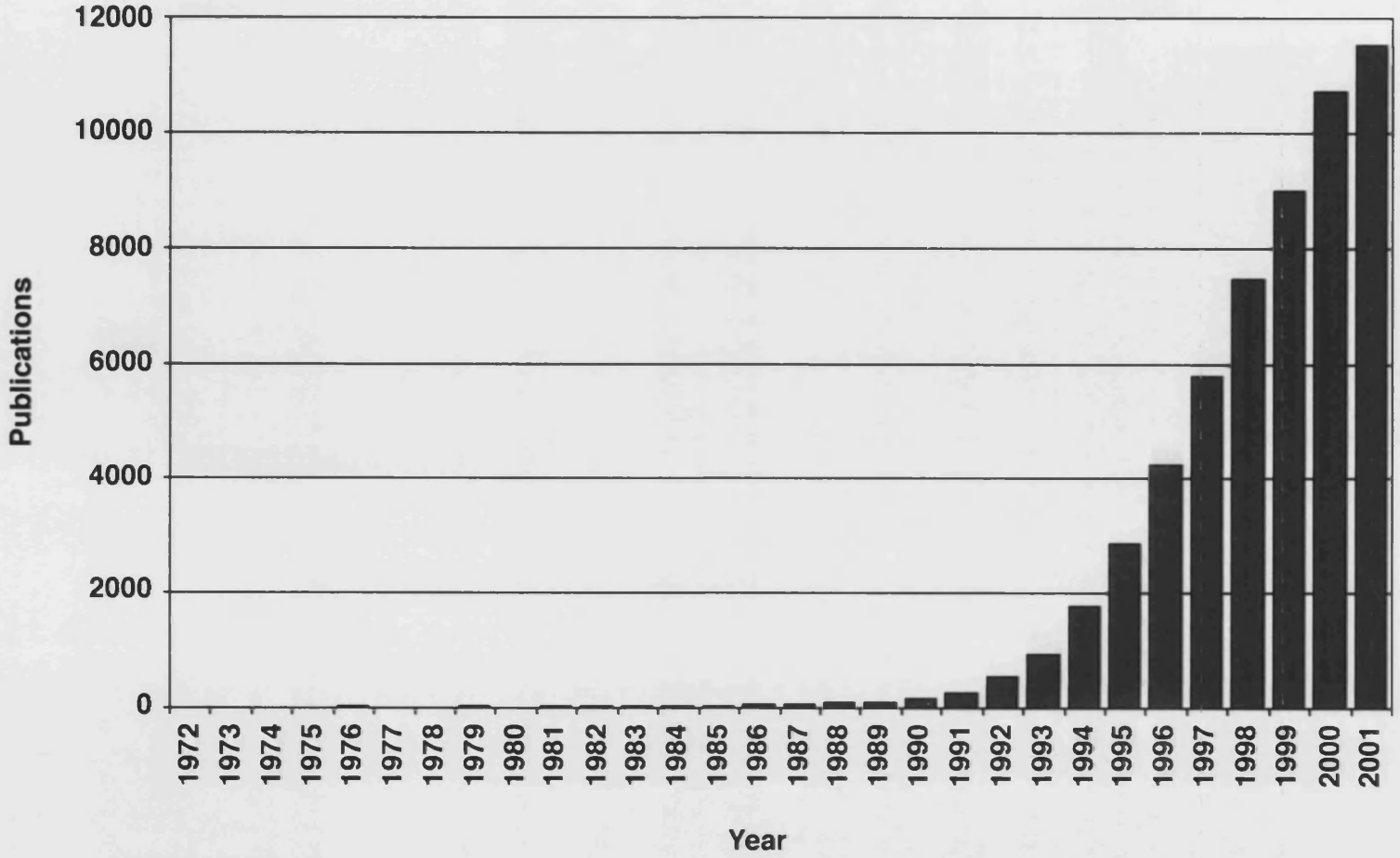

Figure 14 The number of publications on apoptosis each year since 1972, the year in which the term was coined. The identification of the molecular mechanisms throughout the early nineties led to an explosion of work in the field.

Data gathered from Pubmed searches using "apopt*" OR "program* cell death" as terms.

Thirty years after its denomination we have a far greater understanding of apoptosis, particularly the molecular mechanisms behind the process. Today we divide the process into three broad stages: the *initiation phase*, the *execution phase* and the *degradation phase*. Each involves what is generally considered the most important family of proteins in cell death, the caspases.

1.7.4 Caspases

The caspases are a family of homologous proteases highly conserved throughout evolution. Each and every caspase possesses an active-site cysteine and cleaves substrates after aspartic acid (Asp) residues. Beyond this, the specificity of each protease is determined by the four amino acids to the N-terminal side of the Asp-Xxx cleavage site (Nicholson and Thornberry 1997; Thornberry *et al.* 1997). The caspases cleave a restricted set of target proteins, usually at very few positions, making them "surgical tools" rather than general proteases. Around one hundred substrates have so far been identified, and more are continually being found. It is unlikely that all of these are involved in the death pathway, rather there are many 'bystanders' cleaved for no specific purpose other than general degradation of cellular components. In the majority of cases caspase cleavage of a protein causes its inactivation, but there are cases whereby caspase cleavage activates proteins, either directly, by cleaving off a regulatory domain of the target protein, or indirectly, by inactivating a repressing regulatory subunit (Nicholson 1999; Earnshaw *et al.* 1999).

Like many enzymes, caspases are synthesised as inactive precursors (zymogens), the procaspase precursor being composed of three domains: an N-terminal pro-domain, a p20 domain and p10 domain (figure 15). Activation of the enzyme can occur in three ways. Most commonly, they are activated by another caspase. The two cleavage sites between each of the three domains are Asp-Xxx sites, thus making caspases themselves targets for caspase-mediated proteolysis. Hence the term, *caspase cascade*; activation of any of the

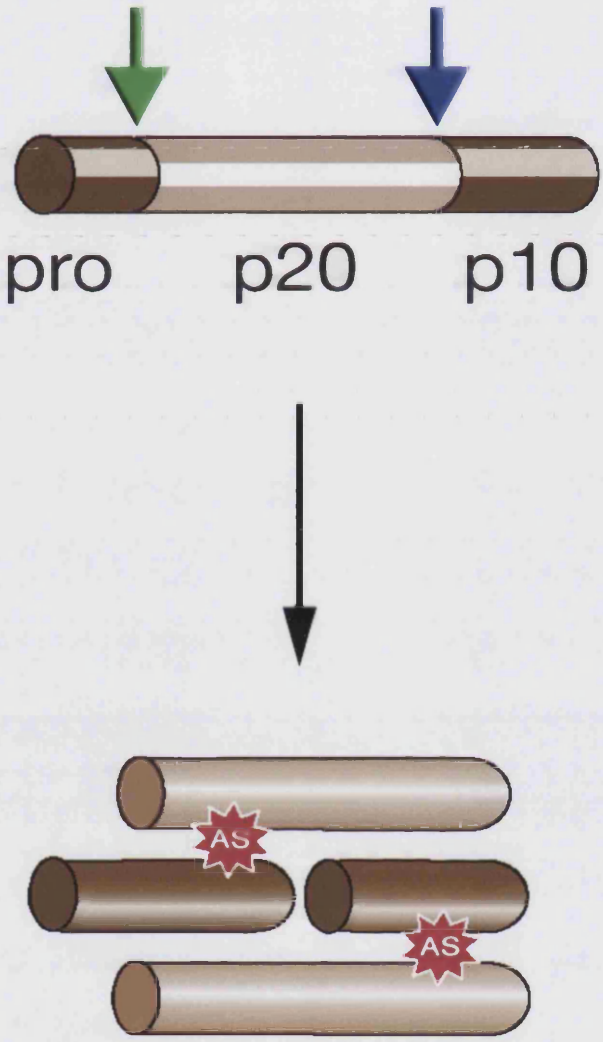

Figure 15 Caspases are synthesised as inactive zymogens consisting of three domains: p10 domain, p20 domain and a prodomain of varying length (long for upstream caspases, short for downstream). Activation occurs through cleavage – by either another active caspase or induced proximity with another procaspase – between the p10 and p20 domains (blue arrow) and usually also between the p20 and prodomains (green arrow). The active enzyme is a heterotetramer of two p20 and two p10 domains containing two active sites (AS). The exception is caspase-9 which is activated by the formation of a holoenzyme with Apaf-1 and cytochrome c.

caspases results in cleavage and activation of others in a self-propagating manner. The mature caspase enzyme is a heterotetramer consisting of two p20 and two p10 domains, thereby yielding two active sites (figure 15).

The procaspase zymogens are not completely enzymatically inactive, rather they are of limited efficacy. The second method of activation utilises this fact, and is described in *1.7.5* in terms of Fas-mediated activation of apoptosis. By recruiting procaspases into limited regions – *induced proximity* – the reduced autocatalytic properties of the zymogens are sufficient to cause cleavage and activation.

The third method of activation does not involve cleavage at all. In the case of procaspase-9, association with the regulatory subunits of apoptosome (Apaf-1 and cytochrome c) alters the protein confirmation in such a way as to confer full efficacy on the active site, making it a holoenzyme (Rodriguez and Lazebnik 1999). Indeed, proteolytic cleavage of procaspase-9 yields only a minor increase in catalytic activity (Stennicke *et al.* 1999).

Generally, caspases activated via their association with other units are the upstream caspases (such as caspase-9, caspase-2, caspase-8 and caspase-10) and have long prodomains to accommodate the various elements underlying the interactions, such as the DED and CARD described in *1.7.5*, whereas the downstream caspases (including caspase-3, caspase-6 and caspase-7) have short prodomains and are activated by proteolysis.

1.7.5 Initiation

The initiation of apoptosis can be divided into two pathways: intrinsically- and extrinsically-signalled apoptosis. Intrinsic activation can result from a number of factors, including DNA damage, serum starvation and the actions of some steroid hormones and drugs (chemotherapy). In the case of hormones, serum starvation and some drugs, apoptosis is initiated via the alteration of gene expression, tipping the balance of pro- and anti-apoptotic factors in favour of the former (see 1.7.6). DNA

damage, of chemical, physical, drug-induced or spontaneous origin leads to the activation of the protein p53. Activation of p53 leads to the release of cytochrome c from the mitochondria, although the exact mechanism remains unclear. p53 is a transcription factor and thus is was suggested that p53 activation leads to upregulated expression of pro-apoptotic factors, in particular the protein Bax (see 1.7.6). However, it has since been demonstrated that the Bax-activation properties of p53 are independent of the nuclear localisation and transcriptional regulation domains of the protein. It appears there is a transcription-independent mechanism by which p53 causes the relocalisation of Bax to the mitochondria (Goldstein *et al.* 2000; Schuler *et al.* 2000). The mechanisms of Bax action are discussed in *1.7.6* , the result being the release of factors including cytochrome c and AIF (apoptosis initiation factor) from the mitochondria. In the cytosol, cytochrome c forms a complex with Apaf-1 (apoptosis protease activating factor-1) and procaspase-9, known as the 'apoptosome', which functions as a multisubstrate protease initiating the caspase activation cascade and moving the cell into the execution phase of apoptotic death.

In physiologic cell death, such as described in *1.7.1* the apoptosis programme is activated extrinsically, via cell surface receptors. All cells require trophic support in order to survive. In the case of developing neurons, trophic support is derived from their targets. Only those neurons which make correct synaptic contacts with their targets will survive: the *neurotrophin hypothesis.* Those neurons which lose out in the competition for target-derived trophin support die by apoptosis. In this case, loss of trophic support leads to an increase in levels of the transcription factor c-Jun and its N-terminal kinase JNK. Phosphorylated c-Jun upregulates the transcription of many target genes, including the pro-apoptotic members of the Bcl-2 family. Interestingly, the neurotrophin hypothesis applies mainly to development alone. The addition of neurotrophins to fully differentiated, adult neurons can in fact induce apoptosis. Likewise, apoptosis can be activated extrinsically by the binding of ligands to 'death receptors'. For example, as part of the immune response T-lymphocytes and Natural Killer (NK) cells can induce the death of an infected cell through Fas-mediated apoptosis (figure 16). The Fas receptor (otherwise known as CD95) is a surface protein of the TNF family (tumor necrosis factor) expressed by most mammalian cells.

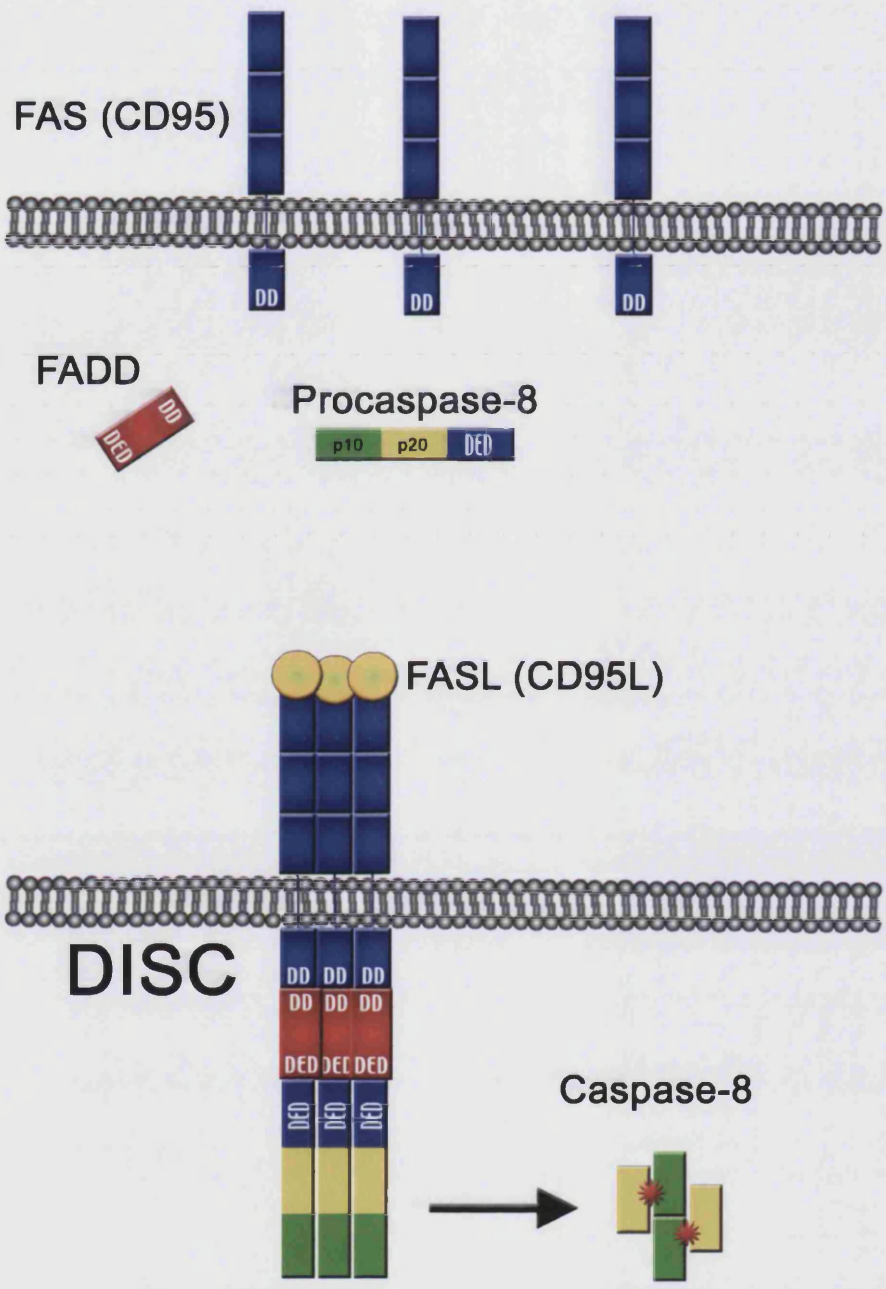

Figure 16 Formation of a DISC (death inducing signalling complex) involving the Fas (CD95) receptor. Ligation with FasL causes clustering of the receptor, the cytoplasmic domain of which contains a Death Domain (DD) which interacts with the adaptor molecule FADD (Fas-associated death domain protein). FADD contains a Death Effector Domain (DED) through which it interacts with the DED of procaspase-8. The induced proximity of procaspase-8 proteins causes autocatalytic actibation and release of the mature enzyme.

The cytoplasmic portion of the receptor, and indeed all of the 'death receptors', contains a 'death domain' (DD) through which the receptor interacts with a number of other cytoplasmic proteins. The receptor ligand, FasL, (CD95L) is expressed predominantly on the surface of activated T-lymphocytes and NK cells as a trimer. The binding of FasL to the Fas receptor brings many Fas receptors into close proximity, resulting from both the trimeric nature of the ligand and the expression of a number of FasL proteins locally on the surface of the T-/NK cell. The complex which is formed is known as the death-inducing signaling complex (DISC). Through the DDs of the death receptors a number of other DD-containing proteins are also recruited to the DISC, including the adaptor molecules FADD (Fas-associated death domain), RIP (receptor interacting protein) and RAIDD (RIP-associated ICH-1/CED-3 homologous protein with a death domain). RIP and RAIDD appear to stabilise each other's localisation to the DISC, and the latter contains a CARD (caspase activation and recruitment domain) which recruits procaspase-2 into the complex. Similarly, FADD contains a DED (death effector domain) which recruits the DED-containing procaspase-8. The result is an activation of caspase-8 and/or caspase-2 and, once again, entry into the caspase cascade.

1.7.6 Regulation

Given the autocatalytic properties of the procaspases and the cascade nature of the apoptotic executioners, it should be no surprise to learn that there is a large and ever-growing array of proteins involved in the regulation of apoptotic activation and execution, the more important of which are summarised in figure 17.

The Bcl-2 family of proteins play a crucial role is the initiation and transduction of apoptotic signaling. The family is divided into three groups according to the repetition of Bcl-2 homology domains (BH-domains). Group I proteins, including Bcl-2 (the mammalian homologue of *ced9* [see 1.7.2]) and Bcl-xl possess 4 BH domains and are anti-apoptotic; groups II and III are both pro-apoptotic and possess 3 BH domains (Bax and Bak) and 1 BH domain (Bid and Bad) respectively. The major anti-apoptotic

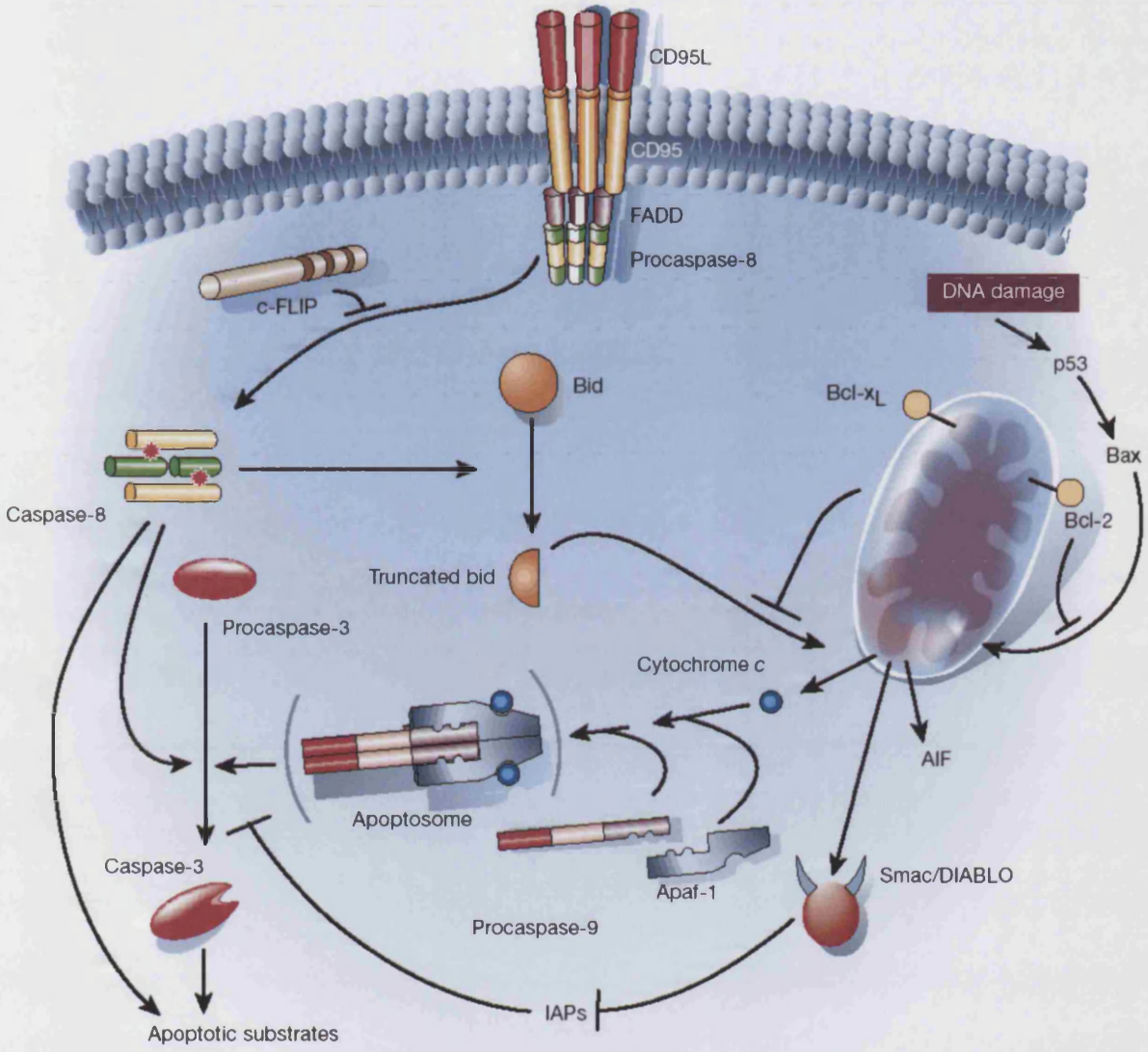

Figure 17 Summary of the initiation and regulation of apoptosis. Initiation occurs either intrinsically - for example DNA damage leading to p53 activation - or extrinsiclally, - ligation of receptors such as CD95. Both pathways lead to release of cytochrome c, AIF (apoptosis initiation factor) and regulatory proteins such as Smac/DIABLO from mitochondria. Once activated (directly in extrinsically-signalled, via apoptosome formation for intrinsically-signalled apoptosis), caspases enter into a self-perpetuating cascade of activating each other as well as cleaving the many death substrates.

Taken from Hengartner 2000

proteins, Bcl-2 and Bcl-x_l are localized to the mitochondrial outer membrane and the endoplasmic reticulum. It has been shown that over-expression of Bcl-2 alone can support the survival of sympathetic neurons following NGF withdrawal (Garcia *et al.* 1992), whilst transgenic mice over-expressing Bcl-2 are protected against neuronal death during development (Martinou *et al.* 1994). The expression of Bcl-2 is high in the central nervous system during development and is subsequently down-regulated after birth. In contrast, Bcl-2 expression in the peripheral nervous system is maintained throughout life (Merry and Korsmeyer 1997). Bcl-2 knockout mice develop normally, but show subsequent loss of motor, sensory and sympathetic neurons after birth (Veis *et al.* 1993; Michaelidis *et al.* 1996) suggesting that Bcl-2 is crucial for cell survival. Bcl-x_l is expressed during development also, but in contrast to Bcl-2 expression continues into adulthood.

Many members of the Bcl family can dimerise, but they can also form heterodimers with either pro- or anti-apoptotic results. The key function of this family of proteins appears to be in regulating the release of apoptotic initiating factors, in particular the release of cytochrome c from the mitochondria. It is not fully known how cytochrome c manages to cross the mitochondrial outer membrane, but it is clear that the Bcl-2 family is involved. Addition of pro-apoptotic family members to isolated mitochondria induces cytochrome c release, whilst addition of anti-apoptotic members prevents it. There are three models for the action of the Bcl-2 family: channel formation by protein members; channel formation induced by protein members; and membrane rupture. In support of the first notion, Bcl-2 proteins have been shown to oligomerise and form channels in synthetic bilayers. However, Bcl-2 proteins have been shown to interact with a large number of other proteins, and it may be that *in vivo* the Bcl-2 oligomers recruit proteins which generate a pore. Such interactions may also support the third idea, that the Bcl-2 family disturbs homeostasis and causes disintegration of at least part of the mitochondria. Indeed, Bcl-2 proteins have been shown to interact with the mitochondrial proteins voltage-dependent anion channel (VDAC) and adenosine nucleotide transporter (ANT) thus they may upset mitochondrial homeostasis.

~

The heat shock proteins (see 1.5.1) have also been implicated in the regulation of apoptosis. A pool of Hsp27 spins down with mitochondria in heat-treated cells (Samali *et al.* 2001) and *in vitro* studies have shown an interaction between Hsp27 and cytochrome c (Bruey *et al.* 2000; Concannon *et al.* 2001). It may be that one role of heat shock proteins is to restrict the activation of apoptosis. Furthermore, Hsp27 has been shown to interact with procaspase-3 (Concannon *et al.* 2003; Pandey *et al.* 2000a) which may suggest a role in preventing caspase activation. Indeed, Hsp70 and Hsp90 have been reported in inhibit apoptosis by preventing caspase activation. Hsp70 interacts with Apaf-1 preventing the recruitment of procaspase-9, and similarly Hsp90 inhibits Apaf-1 oligomerisation, thus preventing formation of the apoptosome (Beere *et al.* 2000; Pandey *et al.* 2000b).

Two further proteins have been identified which have an antagonistic action on apoptosis initiation through death receptor pathways. Usurpin contains a DED homologue which competes with procaspase-8 for recruitment into the death inducing signaling complex (Rasper *et al.* 1998). Similarly, the protein cFLIP (cellular FLICE [FADD-like interleukin-1 converting enzyme] inhibitory protein) also contains a DED homolgoue, reducing or preventing caspase-8 activation via the DISC (Scaffidi *et al.* 1999).

Caspase activation is further inhibited by the inhibitor-of-apoptosis proteins (IAPs), a family of eight (in mammals) proteins which appear to have a number of constitutive roles including the regulation of cell cycle progression and the modulation of receptor-mediated signal transduction. IAPs contain a RING finger domain similar to E3 proteins (see 1.5.2) and thus it has also been suggested that IAPs possess ubiquitin ligase activity. IAPs inhibit apoptosis via their binding to activated caspases, in particular caspases-3 -7 and -9, thereby negating their activity (Deveraux and Reed 1999). It is reasonable to assume that IAPs serve to quell inappropriately activated caspases, which can be produced spontaneously due to their auto-catalytic properties. Upon activation of apoptosis certain IAPs have been shown to be ubiquitinated and degraded, thereby removing the brake from the caspase cascade (Yang and Li 2000).

Further removal of caspase inhibition occurs upon apoptotic initiation. Upon stimulation of apoptosis the mitochondrial protein Smac (second mitochondrial-

derived activator of caspases), also known as DIABLO (direct IAP-binding protein with low pI) is proteolytically processed and released from the intermembrane space and the cytosol along with other pro-apoptotic factors such as cytochrome c and AIF. Smac/DIABLO interacts directly with multiple IAPs neutralising their caspase-interacting properties, thus removing IAP-mediated caspase inhibition (Springs *et al.* 2002; Verhagen *et al.* 2000; Chai *et al.* 2000). Interestingly, Smac/DIABLO knockout mice appear to develop normally, unlike many other apoptosis-deficient mice, and respond normally to apoptotic stimuli (Okada *et al.* 2002). This suggests a redundancy, which should not be surprising given the complexity and the ever-growing number of protein components in the system.

1.7.7 Execution

As mentioned in *1.7.4*, caspases can be divided into two groups: upstream and downstream. The downstream caspases are considered the "central executioners" of apoptosis and are activated via proteolytic cleavage by an upstream caspase. Many of the upstream events can be buffered halting apoptosis midway, but once the downstream, executioner caspases are activated, a point-of-no-return is passed. This exact moment, at which a cell becomes "committed to die" remains under debate, but just as Smac/DIABLO perpetuate the apoptotic cascade by negating the effects of the inhibitors of apoptosis, the downstream caspases cleave and inactivate those proteins which would act to repair the 'damage' caused by apoptosis.

The targets of activated caspases-3, -6 and -7 are too numerous to list in their entirety. The key events, which also illustrate the self-perpetuation principle, include the cleavage of DFF45 (DNA fragmentation factor 45) which is normally bound to DFF40. Upon cleavage of DFF45 by caspase-3 DFF40, a DNAse, is released and translocates to the nucleus whereupon it begins cleaving the chromatin. Within the nucleus resides PARP (poly-ADP ribose polymerase), the normal function of which is to repair damaged DNA. PARP is also a substrate for caspase-3, thus in apoptosis it is

cleaved and inactivated preventing it from repairing the fragmenting chromatin. Certainly, once repair proteins are inactivated there is no stopping the deconstruction of apoptosis; the 'committal' point has been passed.

Many other caspase targets are involved in DNA repair and regulation of the cell cycle, including pRb, DNA-PK and NuMA; as well as proteins involved in transcription and translation, including SREBPs, hnRNPs and snRNPs; and proteins essential to cell regulation including kinases. Furthermore, the loss of structure seen in apoptosis can be accounted for by the cleavage of structural proteins including lamin A, lamin B and G-actin by caspases.

In summary, the activation of downstream caspases leads to a series of proteolytic events causing the systematic degradation of both those molecules essential for maintenance of cell function and structure, together with those proteins responsible for the repair of such degradation.

1.7.8 Removal

The original definition of apoptosis by Kerr, Wylie and Currie included a description of the means by which apoptotic bodies are removed from the biological system. Indeed, the title of a more recent paper makes the claim that "corpse clearance defines the meaning of cell death" (Savill and Fadok 2000). Of course, clearance of the apoptotic remnants is as important as the process of degradation itself seeing as the aim is to prevent the leakage of cell contents and an inflammatory response. In some cases apoptotic bodies can simply be shed from epithelial-lined surfaces, for example figure 1 from the seminal paper illustrates the shedding of apoptotic bodies from human glandular epithelium into the lumen (Kerr *et al.* 1972). Where shedding is not possible, apoptotic bodies are seen to be taken up by other cells and digested. Whilst many cells appear to be capable of ingesting apoptotic bodies, in mammals corpse clearance is normally carried out by professional phagocytes: granulocytes and cells of the macrophage lineage (including microglia in the CNS).

Successful engulfment requires the display of so-called 'eat-me' signals on the apoptotic cell surface and the recognition of such by phagocytes (figure 18). A number of 'eat-me' signals have been identified, the most well-characterised, and perhaps the most prominent of which is the phospholipid phosphatidylserine (PS). In a healthy cell, PS is localised to the internal surface of the plasma membrane. During apoptosis decreased aminophospholipid translocase activity results in externalisation of PS and its presentation on the cell surface (Fadok *et al.* 1998a). Phagocytic cells interact with the exposed PS via PS receptors expressed on their surfaces. Likewise there are also changes in cell surface sugars which are detected by phagocyte lectins (Savill and Fadok 2000). It also appears that the ICAM-3 immunoglobulin family has a role as an 'eat-me' signal (Moffatt *et al.* 1999). Other signals require the interaction of 'bridging' molecules present in the extracellular fluid, such as C1q, a component of the complement cascade. It has been noted that C1q-null mice have defective apoptotic cell clearance (Botto *et al.* 1998). There are a number of other molecules that have been implicated in apoptotic clearance, as illustrated in figure 18, the exact nature and degree of importance of each has yet to be clarified.

Once the phagocyte receptors bind the 'eat-me' flags, a signalling complex is recruited to the plasma membrane of the phagocytic cell which causes the activated of a number of GTPases which are involved in the regulation of the actin cytoskeleton (Conradt 2001). Reorganisation of the cytoskeleton brings about the change in cell shape underlying engulfment.

The engulfed apoptotic body undergoes a series of changes involving further degradation of structure, including loss of mitochondrial integrity. Kerr and colleagues believe that apoptotic bodies are still metabolically active until they enter the phagocytosing cell. Certainly, in order to maintain plasma membrane structure – the key feature of apoptosis – there must be some activity, and in support of this mitochondria appear to be the last organelles to lose integrity. Kerr *et al.* suggest that this stage of degradation arises from the body's "inability to maintain...homeostasis within phagosomes" (Kerr *et al.* 1972). The final degradation is mediated directly by the phagocytosing host, as lysosomes fuse with the phagosomes containing apoptotic bodies releasing hydrolases into the closed environment.

~

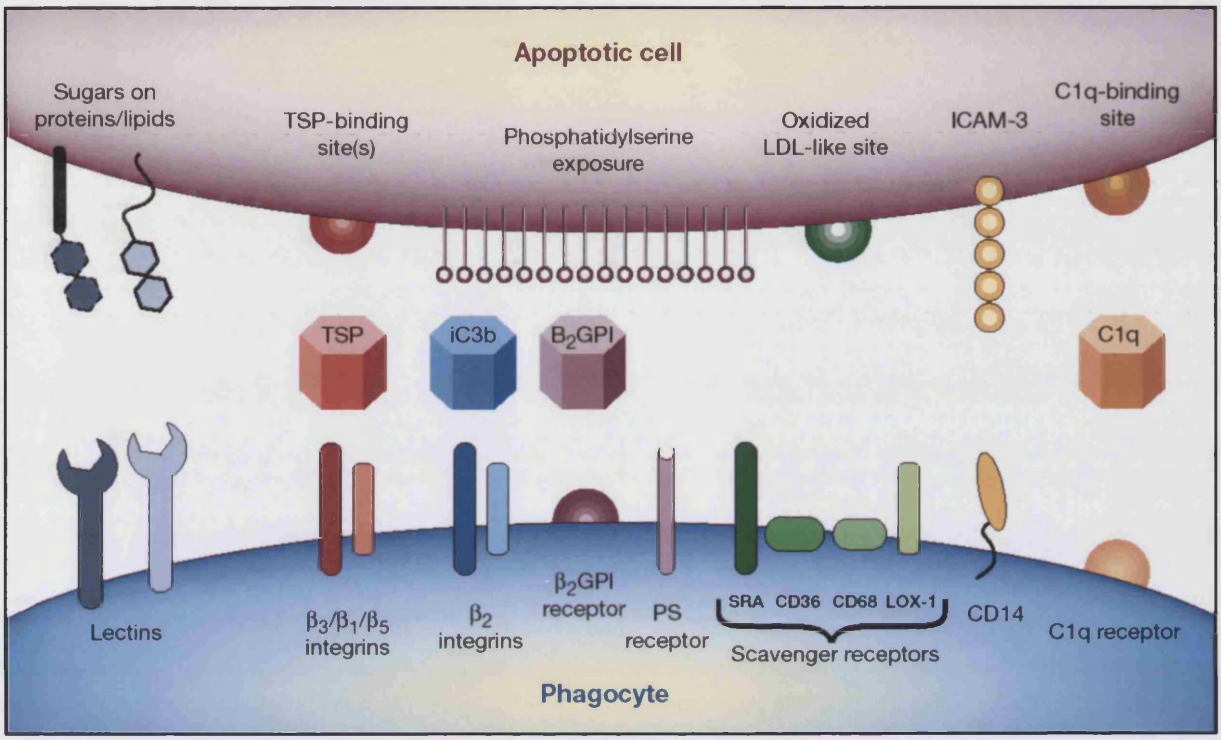

Figure 18 The recognition of apoptotic cells by phagocytes. A number of 'eat-me' signals presented on the surface of a cell undergoing apoptosis are recognised by phagocyte receptors, either directly or via serum-derived bridging molecules. TSP, thrombospondin; LDL, low-density lipoprotein; C1q, component of the compliment cascade; PS, phosphotidylserine; SRA, class A scavenger receptor.

Taken from Savill & Fadok, 2000

The relationship between apoptotic cell and phagosomes has recently been called into question. It seems the role of the phagocyte may not simply be the passive removal of 'waste'. In some cases phagocytes seem to induce apoptosis of a cell before removal. For example, the co-culturing of activated macrophages with mesangial cells induces apoptotic cell death in these cells (Duffield *et al.* 2000). Furthermore, *in vivo* the elimination of macrophages in the rat eye results in the survival of vascular epithelial cells which normally die by apoptosis during capillary regression (Diez-Roux and Lang 1997; Lang and Bishop 1993). In other cases phagocytes appear to play a role in promoting the execution of the apoptotic process. There exists a mutation in the *C. elegans ced3* gene (the caspase-3 homologue) which only partially reduces the efficacy of the enzyme. Alone, this mutation results in an average of 1.5 of the 16 cells that would die during normal development of the anterior pharynx surviving. Loss-of-function mutations in any of the seven *C. elegans* engulfment genes do not affect death of these cells on an otherwise wild-type background. However, in combination these mutations result in between 5 and 6.2 extra cells in the mature anterior pharynx (Hoeppner *et al.* 2001; Reddien *et al.* 2001). Thus engulfment can partially rescue phenotype when *ced-3* is compromised[α], suggesting that phagocytes plays a role in enhancing the execution of apoptosis, ensuring that cells committed to die complete the process. It is possible that the examples of phagocyte-induced apoptosis given above are actually cases of loss of enhancement. In the case of the rat eye vascular epithelial cells, the cells may survive as the 'apoptotic drive' is not strong enough without the macrophage enhancement. In the case of the cultured mesangial cells the macrophages had been cytokine-activated prior to co-culture. It is possible that such activation induced pathways that may normally be activated by 'eat-me' signals. Therefore, whilst the absolute toxic nature of phagocytes may be in question, in seems apparent that these cells, at least in some cases, are part of a feedback loop enhancing apoptosis.

The relationship between phagocyte and apoptotic cell deepens further. The uptake of apoptotic cells by macrophages actively suppresses the secretion of

[α] Complete inactivation of *ced-3* results in survival of all cells irrespective of engulfment.

proinflammatory cytokines such as TNFα. Thus, the apoptotic mechanism is doubly protective against inflammation: not only does it prevent the release of cell contents but also has a 'calming' effect on inflammatory cells, resetting activated macrophages (see figure 19). The effect appears to result as a side-effect of ligation of receptors associated with engulfment, in particular CD36, thrombospondin and phosphatidylserine (Fadok *et al.* 1998b; Voll *et al.* 1997).

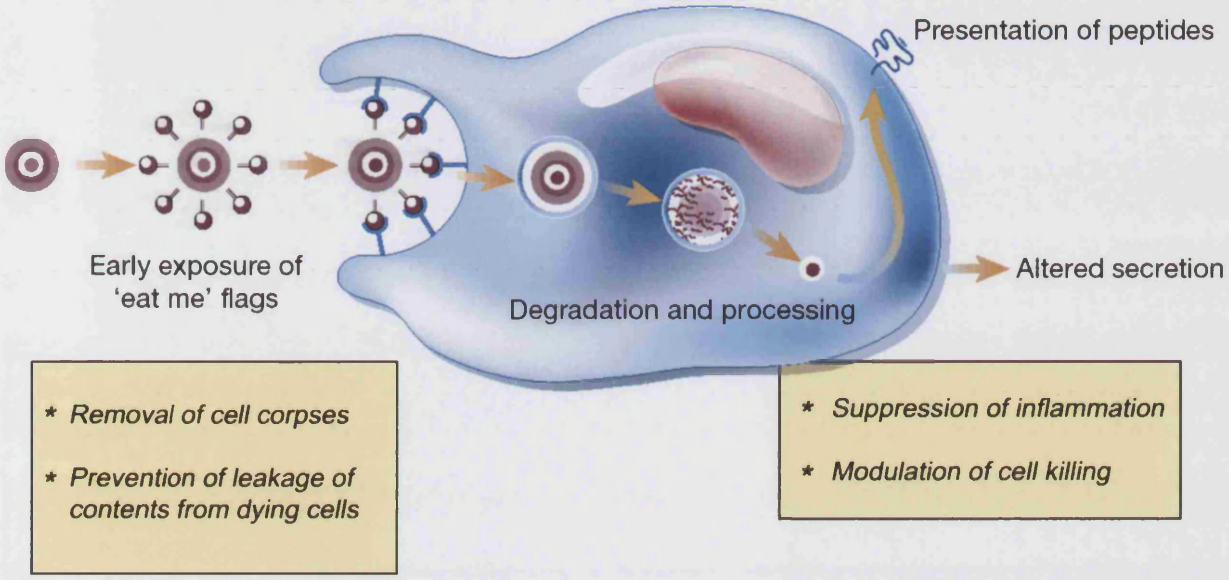

Figure 19 Summary of the relationship between phagocyte and apoptotic cell. In the early stages of apoptosis the dying cell displays various 'eat-me' signals on its surface which are recognised by phagocyte receptors triggering the engulfment and subsequent degradation of the apoptotic body. It has recently become apparent that as well as waste removal, the phagocyte functions as an enhancer of cell death. Furthermore, engulfment of an apoptotic body 'deactivates' the phagocyte, suppressing inflammation.

Adapted from Savill & Fadok 2000

1.8 *Neuronal Death in Huntington's Disease*

1.8.1 Introduction

THE cause and nature of cell death in Huntington's disease are the main areas this thesis seeks to address. Throughout the past few decades a number of theories have been put forward in attempts to answer these questions. The theory in vogue at the moment is that the accumulation of mutant huntingtin begins to exceed to neuron's ability to buffer any damaging effects, at which point apoptosis is initiated resulting in cell death. The finer points of apoptosis are discussed in *1.7*, and further discussion on its role in HD, and the evidence presented herein, can be found in *4.1*. In order to provide some introduction there follows a brief summary of the apparent evidence for an apoptotic response along with a discussion on the previous theory *de mode*: excitotoxicity.

1.8.2 Apoptosis

Human HD is dominated by cell death throughout the caudate, putamen and cortex (see 1.1.3). The cell death seen is certainly not necrotic. There is no clear imflammatory response and ultrastructurally, degenerating neurons are generally well-preserved (Vonsattel and DiFiglia 1998). Coupled with the naïve notion that death always presents as one of two extremes, this evidence alone is sufficient to convince some that neuronal death in HD is an apoptotic process.

There is a wealth of evidence to support a role for apoptotic components in the pathology of HD. In human post-mortem tissue, a subset of neurons and glia in the striatum have been shown to stain positive with TUNEL (terminal transferase-mediated d-UTP-biotin nick-end labelling) indicating the presence of double-stranded DNA breaks suggested to be the result of apoptotic DNAse activity (Dragunow *et al.*

1995; Thomas *et al.* 1995). Furthermore, one group identified the activated form of caspase-8 in the insoluble fractions of human post-mortem brain areas affected in HD (Sanchez *et al.* 1999). Using a cell model based around the expression of an ataxin3 Q79 construct, the same group showed caspase-8 recruited to the Q79 aggregate. Blocking caspase-8 recruitment and subsequent activation in this system prevented cell death. Likewise, Miyashita *et al.* identified activation of caspase-8, and subsequently, caspase-3 in an inducible cell model of polyglutamine disease (Miyashita *et al.* 1999). Subsequent work by this group found a redistribution of caspase-8 upon induction of extended glutamine expression and aggregate formation. Indeed, activated caspase-8 was only found in association with the polyQ aggregate. Immunoprecipitation experiments revealed a selective interaction between polyQ and caspase-8, however, *in vitro* binding assays show that for any polyQ length this interaction does not occur directly (U *et al.* 2001). Rather an adaptor molecule, or molecules must exist.

Conversely, it has been suggested that activation of caspase-8 occurs not as a result of recruitment to the aggregates, but as a result of loss of a function of normal huntingtin. The huntingtin-interacting protein 1 (HIP-1) was identified through its weaker interaction with mutant huntingtin compared to wild type protein (Wanker *et al.* 1997). Overexpression of HIP-1 has been shown to induce rapid caspase-3-dependent cell death (Hackam *et al.* 2000). More recently a partner to Hip-1 was identified, Hippi, which forms a complex with free Hip-1 and caspase-8. Both HIP-1 and Hippi contain proteins similar to the death-effector domain (DED) of caspase-8 (see 1.7.5) and it is believed that the interaction of these domains underlies the formation of the complex and its toxicity. As the interaction between HIP-1 and huntingtin is inversely proportional to polyQ length, in HD there is a greater amount of free HIP-1 available to dimerise with Hippi and recruit and activate caspase-8 (Gervais *et al.* 2002).

Caspase-9 enzymatic activity is induced as part of the apoptotic process, but it has also been suggested to play role in the pathogenesis of HD by one group studying CNS-derived cells. Rigamonti *et al.* identify cytochrome c release and activation of caspases -9 and -3 as part of the death process, and find that over-expression of wild-type huntingtin prevents caspase-9 and -3 activation whilst having no effect on

cytochrome c release. The implication being that the anti-apoptotic effects of wild-type huntingtin are mediated at the level between cytochrome c release and caspase-9 activation (Rigamonti *et al.* 2001). In other words, by preventing apoptosome formation.

(Li *et al.* 2000) report that in their cell culture model intranuclear mutant huntingtin increases the activity of caspase-1 which promotes cytochrome c release, leading to caspase-3 activation. Cytochrome c release is also reported by the Rigamonti group discussed earlier, and by Jana *et al.* who found that after expressing expanded polyQ in neuro2a cells for three days, isolated mitochondria contained a reduced amount of cytochrome c (Jana *et al.* 2001). Support for a role for caspase-1 *in vivo* comes from work on R6/2 mice showing that inhibition of caspase-1 (or crossing onto caspase-$1^{-/-}$ mice) seems to delay onset of symptoms and prolong survival in the R6/2 mouse model of HD (Ona *et al.* 1999). Other groups have also reported the rescue of transfected cells using anti-apoptotic compounds such as $BclX_L$ or caspase inhibitors (Hackam *et al.* 2000; Saudou *et al.* 1998).

It may not be that huntingtin directly induces apoptosis, rather that apoptosis occurs more readily. As described in *1.7*, there exists a balance between pro- and anti-apoptotic drives in the resting cell, the aggregation of mutant huntingtin, and the sequestration of those proteins with which it interacts may alter this balance in favour of the pro-apoptotic mediators. Several groups report an increased sensitivity to stressful, or apoptotic stimuli in cells transfected with mutant htt.

1.8.3 Excitotoxicity

Exictotoxicity was identified in 1957 when D.R. Lucas and J.P. Newhouse found that feeding infant mice sodium glutamate destroyed retinal neurons (Lucas and Newhouse 1957). The term, *excitotoxicity* was coined later by J.W. Olney, who identified the pattern and nature of the death; namely, that death is restricted to post-synaptic cells

and is dependent on excitatory mechanisms similar to those employed in glutamate signaling (Olney 1969; Olney *et al.* 1971).

During normal synaptic transmission levels of glutamate in the synaptic cleft rise to high levels, but only for a matter of milliseconds before re-uptake or removal by astrocytes. Accumulation of glutamate occurs in conditions when removal from the cleft is impaired, most notably in times of metabolic impairment such as occurs during ischemia. Accumulation can also occur as a result of hyperstimulation of the presynaptic neuron. Such accumulation causes as influx of calcium ions through the glutamate NMDA receptors, which, to a certain extent can be removed from the cytosol by calcium pumps at the plasma and ER membranes. Neurons also possess a calcium-sodium ion exchanger to further buffer the effects of calcium influx. If the calcium influx cannot be buffered a number of changes occur in the neuron, most notably impairment of mitochondrial function and activation of a group of calcium-dependent proteases, the calpains. Calpains are essentially inactive under basal conditions, but when bound to calcium they cleave a large variety of substrates in a manner similar, but more general, to caspases (Reverter *et al.* 2001). Inhibition of the proteolytic activity of calpains rescues neurons from glutamate-induced excitotoxic death (Brorson *et al.* 1995; Rami *et al.* 1997).

The damage caused by calcium influx includes metabolic impairment, thereby hindering the function of the calcium pumps/exchanger, thus potentiating the problem. Similar to the process of apoptosis, there is a threshold beyond which the death-signal cannot be buffered. Likewise, as the cell begins to destroy that machinery which would otherwise repair the damage being caused, a point-of-no-return is passed and death is inevitable.

Excitotoxicity has long been implicated in the pathogenesis of Huntington's disease. The earliest models of the disease were generated using the NMDA-receptor agonist quinolinic acid as the resulting pattern of cell loss was suggested to be similar to that seen in HD (Beal *et al.* 1991; Ferrante *et al.* 1993; Hantraye *et al.* 1990)[6]. The striatum receives abundant glutamatergic input from the cortex and

[6] Although criticisms of the validity of excitotoxic-lesion models of HD existed at the time (Davies & Roberts 1987).

studies have claimed that those neurons that die preferentially in HD are those that are the most sensitive to glutamate excitotoxicity. It has been shown that a greater membrane depolarization and inward current is induced by exogenous glutamate receptor agonists in medium spiny neurons compared to aspiny interneurons (Calabresi *et al.* 1998; Cepeda *et al.* 2001b). Indeed, both striatal and cortical projection neurons are highly vulnerable to NMDA-receptor agonists, whilst interneurons are relatively spared (Figueredo-Cardenas *et al.* 1994). This apparent explanation of cell specificity has made excitotoxicity an attractive explanation for cell death in HD.

The exact role, if any, mutant huntingtin plays in exitotoxicty remains under debate. As described in *1.3.2* and *1.6.4*, huntingtin appears to be associated with neuronal terminal vesicles, interacting with several exo/endocytic vesicle proteins such as HIP-1, HAP-1 and SH3GL3. It is therefore possible that mutant huntingtin interferes with the regulation of synaptic vesicle cycling, causing a build-up of excitatory neurotransmitters.

Huntingtin associates with a post-synaptic protein, PSD-95 (post-synaptic density 95) which binds NMDA receptors regulating NMDA-dependent long-term potentiation and depression. Expanded polyglutamine within htt inhibits binding to PSD-95 and increases the sensitivity of NMDA receptors (Sun *et al.* 2001). There is *in vivo* evidence for an increased sensitivity to excitotoxicity in HD. Cepada *et al.* report a greater inward current and, importantly, calcium ion influx in R6/2 striatal neurons stimulated with quinolinic acid compared to wild-type mice. They find a similar, yet smaller, increase in response in the same situation using the YAC72[§] mouse model (Cepeda *et al.* 2001a). Likewise, Zeron *et al.* found that injection of QA into the striata of the YAC72 mice produces a greater amount of medium spiny neuron death than a similar dose in control mice. They see a similar result using NMDA/AMPA on cells in culture (Zeron *et al.* 2001).

[§] A model generated in the laboratories of Michael Hayden, possessing a yeast artificial chromosome (YAC) expressing full-length huntingtin with 72 glutamine repeats (Hodgson *et al.* 1999).

Whilst these data do not show conclusively that mutant huntingtin causes cells to die via excitotoxicity, it does seem apparent that both the medium spiny neurons of the striatum are more sensitive to excitotoxicity than other cells, and that the presence of mutant huntingtin enhances this susceptibility.

1.8.4 Neurotrophins

There is also a suggested role for neurotrophins in the pathology of Huntington's disease whatever the mechanism of cell death. As described in *1.7.5* neurotrophins are vital to cell survival, particularly in the developing nervous system. It has been shown that the levels of the neurotrophin BDNF (brain-derived neurotrophic factor) are lower in the caudate and putamen of HD patients, in some cases almost half basal levels (Ferrer *et al.* 2000); a condition which has also been demonstrated in the YAC72 mouse model of HD (Zuccato *et al.* 2001). Whilst the toxicity of mutant huntingtin appears to result from a toxic gain-of-function, the laboratory of Elena Cataneo believes the loss of a beneficial property of wild type huntingtin, namely the up-regulation of BDNF transcription in cortical neurons (which is released in the striatum and required for survival of striatal neurons), makes striatal neurons more sensitive to cellular perturbation and more prone to death (Reilly 2001; Zuccato *et al.* 2001).

One of the candidate therapeutic drugs for Huntington's disease, *Riluzole* has been shown to increase life-span of the R6/2 mouse (Schiefer *et al.* 2002) though the effect in human patients appears to be transient (Seppi *et al.* 2001). The actions of Riluzole include elevation of levels of BDNF, GDNF (glial-derived neurotrophic factor) and NGF (neuronal growth factor). Whilst these increases are a result of actions on astrocytes (Mizuta *et al.* 2001) rather than the cortical neurons the increase in BDNF may offset some of the decrease which results from huntingtin mutation. It has also recently been demonstrated that dietary restriction in the R6/2 mice can prolong

survival, purportedly through upregulation of BDNF and Hsp70 in the cortex and striatum (Duan *et al.* 2003).

The evidence firmly indicates that there is a decreased level of BDNF within the striatum in Huntington's disease. Whether this has a direct effect on pathology, however, is unclear. Increasing BDNF levels does seem to slow disease progress, suggesting that BDNF depletion may indeed contribute to pathology. Local neurotrophin depletion may make certain cell populations more susceptible to injury and contribute to disease progression. Nevertheless, I believe that these effects are secondary to the toxic nature of the huntingtin mutation.

Materials and Methods

2.1 The R6 Mouse Models of Huntington's Disease

2.1.1 Generating the Model

THE first genetic model of polyglutamine disease was a spinocerebellar ataxia-1 (SCA1) mouse generated using a human SCA1 cDNA construct, expressed under a Purkinje cell-specific promoter (Burright *et al.* 1995). Mice were generated with either normal or expanded CAG repeats in the construct, those expressing an expanded repeat exhibited Purkinje degeneration. Thus, these mice not only established that human glutamine repeat-expansion diseases can be modelled in mice, but also provided evidence for the argument that expanding CAG repeat in a protein is sufficient to cause pathology.

The first polyglutamine disease models to be created were the HD mouse models generated in the laboratories of Gillian P. Bates. Originally, they attempted to generate a model using a yeast artificial chromosome (YAC) to introduce the gene. However, these proved to be too unstable and furthermore, CAG repeats appear to be highly unstable in yeast. Instead, a transgenic model was generated using a construct derived from a human HD patient.

A 1.9kb restriction enzyme fragment (Sac1-EcoR1) was taken from the five prime end of the HD gene isolated from a human patient with 130 CAG repeats. This fragment contains approximately 1kb of upstream elements, the entire of exon 1 and the first 262 base pairs of intron 1 (figure 20). This produces a protein approximately equivalent to the first ninety amino acids of normal huntingtin (CAG_{21}). To prevent the possible expression of an unspliced transcript a stop codon was generated at the beginning of intron 1 and indeed, northern and western blot analyses reveal that when the trangene is active exon 1 alone is transcribed and translated (Mangiarini *et al.* 1996).

Transgenic mice were generated by microinjection of the construct into single cells of mouse embryos (CDAxC57Bl/6 strain). Only one transgenic mouse survived: the R6 founder. It appears that the construct had integrated into five different regions

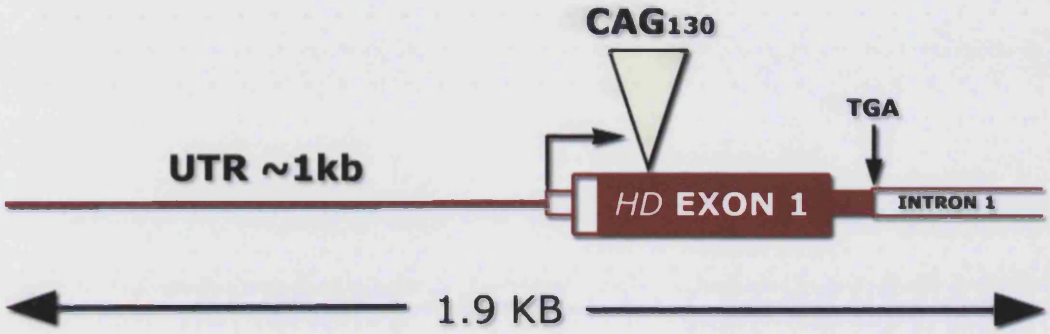

Figure 20 Genetic construct used for the generation of the transgenic R6 lines of mice. The construct, isolated from a human HD patient, is comprised of approximately 1kb of upstream untranslated sequence, exon 1 with an expanded CAG repeat sequence and the first 262bp of intron 1. There is also an in-frame mutation providing a stop codon (TGA) at the 5' end of intron 1.

of the founder genome, thus backcrosses onto wild-type C57Bl/6 yielded five different strains of mice: R6/0, R6/1, R6/2, R6/5 and R6/T (figure 21). Furthermore, as the repeat is unstable (see 1.3.4) the F1 generation of mice had variable repeat sizes, but all within region of the 130 used in the construct. Lines R6/0, R6/1, and R6/T result from a single integration, although in the R6/T line most of the 5' end of the construct has been deleted leaving a highly truncated, non-expressing transgene. Surprisingly, the R6/0 line does not express the transgene. Southern blotting indicates that the transgene has integrated adjacent to a highly repetitive region of the genome as a very large fragment is produced. It is suggested that this region somehow silences the surrounding genome. The R6/1 line possess a single copy of the transgene containing 116 glutamine repeats which is expressed in all tissues tested. These mice develop a phenotype similar to the R6/2 line but much less severe and with a later onset. The R6/5 line appears to have resulted from a four-copy integration with. The suggested arrangement is shown in figure 21, but this is speculative.

The R6/2 line resulted from a three-copy integration of the construct into the founder genome, but at some point deletions occurred at both the 5' and 3' ends of the transgene leaving a single whole functioning copy with 144 repeats and two flanking UTR remnants.

2.1.2 *Phenotype of the R6/2 Mouse*

The R6/2 line has become one of the most widely used models of Huntington's disease. Whilst the R6/1 and R6/5 lines also develop a phenotype (only in the homozygous state in the R6/5 line) the R6/2 is the most aggressive and mice pass through the spectrum of disease in a matter of weeks rather than months. Age at onset has been seen to be as low as 4 weeks, though most R6/2 mice develop overt symptoms between 9 and 11 weeks. Death usually occurs around 12 or 13 weeks of age. The cause of death is generally unknown, though most likely to be a result of complications arising from the symptoms.

~

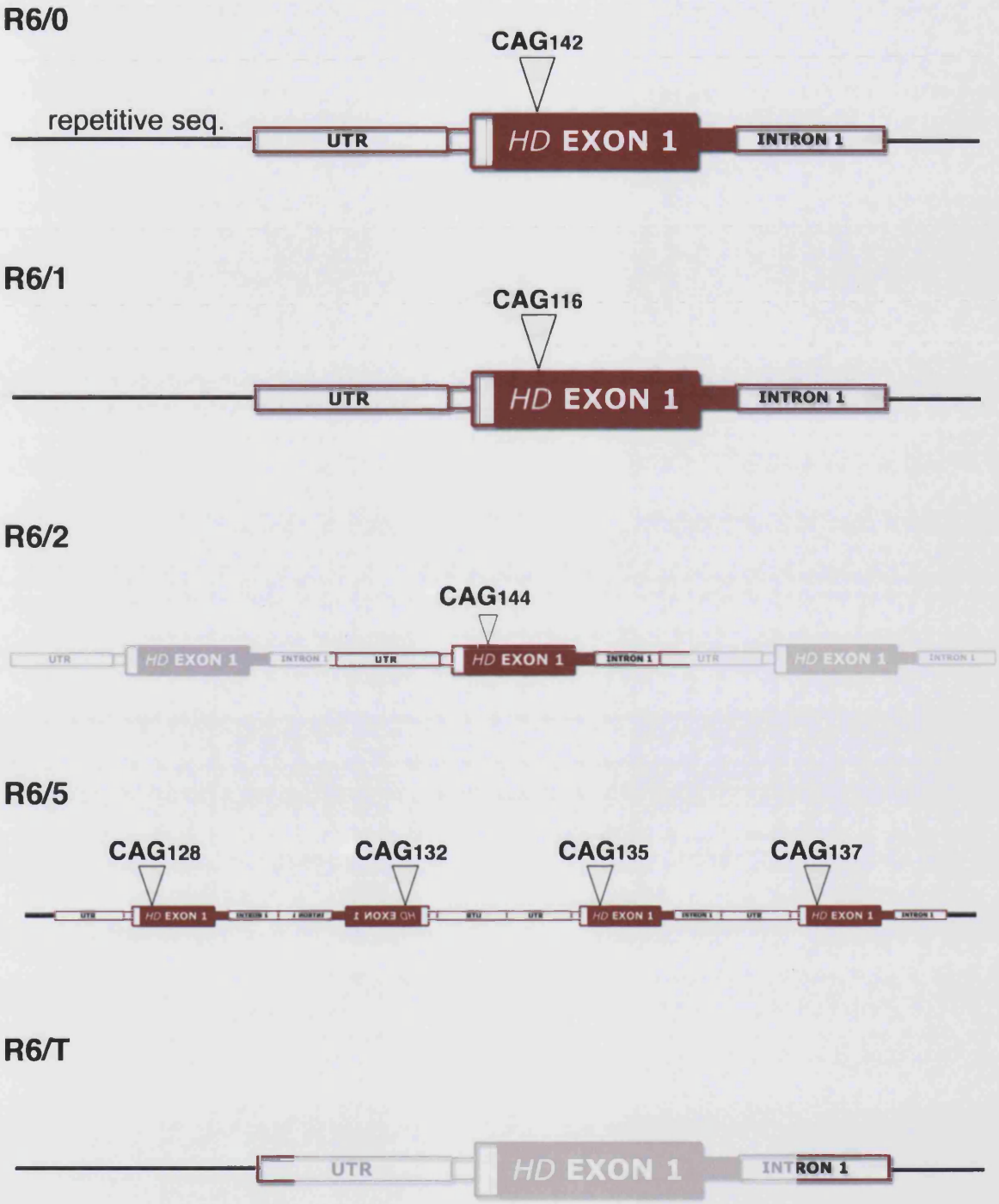

Figure 21 The genomic structures of the R6 lines of mice resulting from the five integrations of the construct into the founder mouse genome. Pale regions indicate deletions that are presumed to have occurred to generate the fragments that remain.

The mice develop a motor disorder reminiscent of HD including a resting tremor and the display of choreic movement. In some cases, a mild ataxia is also seen. One measure of disease progression in the R6/2 mouse is the degree of "clasping". When picked up by their tails mice spread their legs in an attempt at counterbalance. The R6/2 mice however, clasp their feet together. As disease progresses the ability to release this clasping posture lessens. Handling also induces epileptic seizures in late R6/2 mice, which can last for several minutes. It has been suggested that this epileptic activity may underlie the cause of death in at least some of the mice.

R6/2 females are sterile and so the line has to be maintained through the mating of heterozygous males with wild-type females, which has important implications on the stability of the repeat length (see 1.3.4). Further maintenance complications arise from the fact that males also exhibit a reduced fertility. Post-mortem analysis finds females with 'miniscule ovaries and a hair-like uterus' whilst males have small testes, seminal ducts and coagulation glands (Mangiarini *et al.* 1996).

In the presymptomatic stages, R6/2 mice are physically indistinguishable from littermate controls, but coincident with onset of symptoms, the R6/2 bodyweights plateau and then progressively decline as the disease progresses. End-stage mice have been observed weighing as little as 60% of their normal littermates, in spite of the fact that they continue to eat. Furthermore, post-mortem analysis reveals food in the stomach and faecal pellets of the gut. The situation is similar to that seen in human HD patients, as documented in *1.1.1* (Mangiarini *et al.* 1996).

2.2 *The* Hdh *Knock-In Models of Huntington's Disease*

2.2.1 *Generating the Models*

A COMMON criticism of the R6 mouse models of HD is the "unphysiological" nature of the transgenics. A foreign gene under a foreign promoter is inerted randomly into the mouse genome. It is clear from the differences between the R6/0, R6/1, R6/2 and R6/5 mice that transgene insertion point plays a pivotal role. The R6/1 mice carried (initially) 116 CAG repeats; the R6/2 a comparable 114 repeats. Whilst both express the mutant protein and exhibit a phenotype, the R6/1 disease process occurs over months, normally beyond the lifespan of the mouse, a stark contrast to the R6/2 mice, which die at around 15 weeks of age.

It seems obvious that the most apt mouse model of human HD would be the introduction of the human mutation into the mouse homologue of the human gene, *Hdh*. Such a model has been generated by the laboratory of Peggy F. Shelbourne.

As described in Shelbourne *et al.* (1999), targetting vectors were constructed such that an expanded CAG repeat of 72 to 80 units replaced the normal mouse *Hdh* repeat sequence. To identify transfected cells a neomycin resistance cassette, flanked by two *loxP* sites, was inserted into intron 1 of the gene. Transfected embryonic stem cells were used to generate two lines of mice (*Hdh4/neo* and *Hdh6/neo*), males of which were crossed with homozygous β-actin-*cre* females thereby achieving *cre*-mediated deletion of the *loxPneo* sequences. Subsequent analysis confirms removal of the *neo* cassette from all cells. Therefore, the resultant founder mice have effectively had an extended polyglutamine tract inserted into their *Hdh* genes (figure 22).

The founder mice were bred to establish two lines of mice, the *Hdh4/Q80* mice with 80 CAG repeats, and the *Hdh6/Q72* mice with 72 repeats. The mice used for generating the models were of C57BL/6 strain. Subsequently, the models have been both maintained on the C57BL/6 background and crossed onto the FVB background strain of mice. Both backgrounds, with identical mutations, have been used in this study.

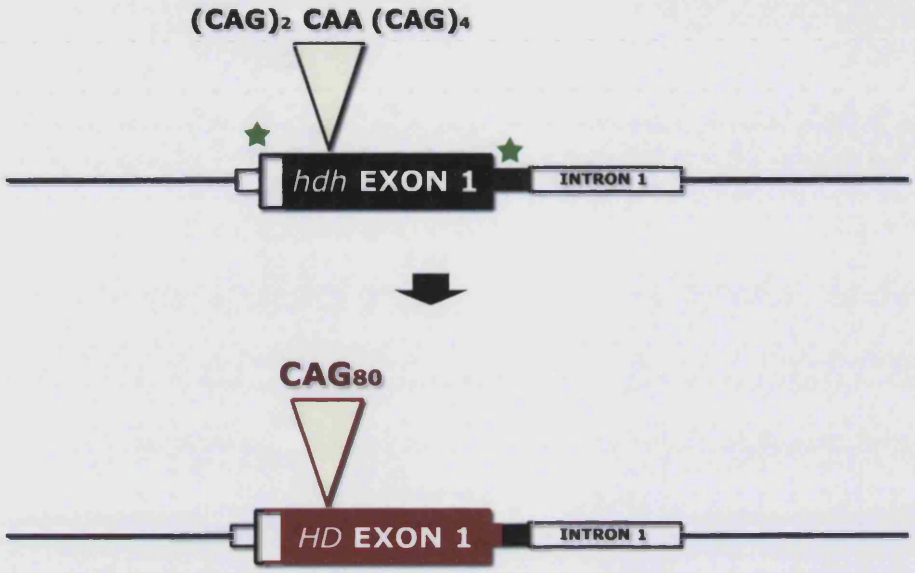

Figure 22 Generation of the *Hdh* knock-in mouse models. A restriction fragment element from the mouse huntingtin gene homologue (green stars represent restriction enzyme sites) is replaced with a construct containing an expanded (72/80) CAG repeat sequence.

2.2.2 *Phenotype of the* Hdh *Mouse*

At the genetic level, the mice mimic the human disease not only in the nature of the mutation but also in its behaviour. The mice exhibit germ-line instability, with a tendency towards anticipation, and similar sex-of-origin dependencies to the human (Shelbourne *et al.* 1999).

In the initial study mice were studied up until 18 months, during which time the *Hdh* mice showed no difference in eating or drinking behaviour and were of similar body weight to the littermate controls. In further contrast to the R6 mice, fertility also remained unaffected. The only phenotype observed in the knock-in mice is a behavioural abnormality. The mutant mice, in particular the males, exhibit a chronic aggressive behaviour. Given the lack of any other symptoms it is surprising that these behavioural changes can be seen as early as three months of age. The degree of aggressiveness is such that affected males have to be housed separately.

It is suggested that these mice mirror the early changes seen in human HD. Psychiatric symptoms present in HD patients up to a decade before the onset of motor symptoms, such symptoms include inappropriate behaviour and aggressiveness (see 1.1.1).

In a manner similar to the human disease and the R6 models, mutant huntingtin cam be seen to accumulate when immunostained at the light level. Li *et al.* report the appearance of both nuclear and neuropil aggregates in the knock-in mice. Whereas intranuclear inclusions appear in many areas, including those unaffected in HD, in the R6/2 mice, there is a preferential accumulation of NIIs in the striatum of the knock-in model. Furthermore, these NIIs appear to form in the medium spiny projection neurones, which preferentially degenerate in HD (Li *et al.* 2001). Aggregates are reportedly seen outside of the striatum in those regions to which the striatum projects; including the lateral (and to a lesser extent the medial) globus pallidus and the substania nigra, but these are neuropil aggregates rather than intranuclear inclusions, suggesting that their later appearance in these regions represents the formation of aggregates in the axons and dendrites of those cells which are affected by intranuclear inclusions. It also appears that axons containing these

aggregates degenerate in the later stages of the mouse life in the absence of any noticeable cell body death (Li *et al.* 2001). It is suggested that the context of the full-length huntingtin protein, as opposed to a truncated transgenic form, confers the pathological cell specificity seen in HD. It is certainly true that the knock-in model differs markedly from the R6 lines.

2.3 *Experimental Protocols*

2.3.1 *Perfusion of Mice*

ALL perfusions of R6/2 and *Hdh* mice used in this study were conducted by Professor Davies, under the guidelines of his personal license. Mice were first anesthetised with an overdose of sodium pentobarbitone, approximately 100 mg/kg, delivered intraperitoneally. Once the anaesthetic had taken full effect the chest cavity was exposed and an incision made into the right atrium of the heart. The animals were then perfused through the left ventricle with either 2% PLP, for tissue to be used in light microscopy, or 4% paraformaldehyde for tissue destined for the electron microscope, until a clear solution is continuously expelled form the breached right atrium. Each brain was then carefully removed from the cranium and placed in fresh fixative.

Tissue for light microscopy was fixed *in vitro* for a further six hours before being placed in a cryoprotectant solution of 30% sucrose at 4°C. Tissue for electron microscopy was placed in a solution of 4% paraformaldehyde also containing 0.2% gluteraldehyde for a minimum of 24 hours at 4°C.

2.3.2 *Preparation of Tissue for Light Microscopy*

After incubation in 30% sucrose cryoprotectant brains were removed and trimmed with a razor blade to provide planar surfaces at both extremes of the sections under study. They were then embedded in Tissue-Tek mounting medium on the stage of a Leica SM2000R sledge microtome. The tissue, and mounting medium, was frozen with powdered carbon dioxide pellets and maintained in a frozen state by use of the $CO_{2(S)}$ reservoir surrounding the stage. Coronal sections of, usually, 40mm were cut

and carefully collected using a paintbrush. Sections were deposited serially in a 'dimple tile' filled with 0.1M TRIS buffer, which was then stored at 4°C until needed.

2.3.3 Preparation of Tissue for Electron Microscopy

Following post-fixation in a 4% paraformaldehyde / 0.2% gluteraldehyde solution, brains were removed and trimmed with a razor blade to provide a planar surface at posterior extremity of the region under study. This surface was then bonded to the mounting block of a Vibratome Series 1000 using superglue (cyanoacrylate). The Vibratome reservoir was filled with 0.1M phosphate buffer and sections of 50-200mm were cut and collected into 'dimple tile' wells containing 0.1M phosphate buffer.

2.3.4 Processing for Standard Transmission Electron Microscopy

Sections were osmicated in 1% osmium tetraoxide (in 0.1M phosphate buffer) for 60 minutes at 4°C. Sections were then washed in phosphate buffer, followed by washes in 0.1M sodium acetate. They were then stained in a solution of 2% uranyl acetate (in 0.1M sodium acetate) for 45 minutes at 4°C.

Following washes in sodium acetate and distilled water, sections were then dehydrated though a graded ethanol series (35%, 50%, 70%, 90%, 100% x4); and cleared through four changes of propylene oxide (taking care not to expose the sections to the air, thereby risking osmium extraction). Sections are then incubated for 45 minutes in a solution of 50% araldite resin in propylene oxide, followed by an overnight incubation in pure araldite resin on a rotator.

The sections are then sandwiched between two sheets of Melanex and stacked beneath glass plates weighted down with brass weights. This stack is placed overnight in an oven at 60% to polymerise the araldite resin.

~

Areas of interest from each section are superglued onto blocks of solid resin and sectioned using an ultramicrotome. Once the block-face has been polished to a flat surface, semi-thin (0.5-1mm) sections are collected in a well of distilled water attached to the glass knife and transferred to slides. Once dry, these sections are counter-stained with toludine blue and viewed under the light microscope. From these semi-thin sections one can determine whether or not one is cutting enough tissue to warrant collection for electron microscopy. If not the block can be polished further. If so, sections are cut at the ultrathin level (approximately 70nm) and collected on copper-mesh grids.

Grid-mounted sections are counterstained in lead citrate for 3 minutes, washed in distilled water, and allowed to dry before being viewed in a JEOL 1010 transmission electron microscope.

2.3.5 EM-level Immunohistochemistry

Sections are incubated in primary antibody, diluted to the appropriate concentration in primary antibody buffer, for 72 hours at 4°C. Sections are then washed in buffer before being incubated in the appropriate secondary antibody, according to which species the primary antibody was raised in and the type of label to be used.

Immunohistochemically-stained sections can be visualised at EM using either the HRP-DAB reaction product as used in light sections or by using secondary antibodies conjugated to gold particles. For the processing method for the former see *2.3.6*, adapted only in that sections are not mounted onto slides.

For immunogold, primary-labelled sections are washed before being incubated in immunogold secondary antibodies, usual concentration 1:200 in phosphate buffer, overnight at 4°C. Sections are then washed and further fixed in 0.1% gluteraldehyde for 10 minutes at room temperature. Immunogold secondary antibodies conjugated to large gold particles (10nm) can be viewed without enhancement, but small particles are usually enhanced with silver staining.

Sections to be silver-enhanced are washed first in phosphate buffer then in sodium acetate, before being placed in constituted *Nanoprobes* HQ Silver Enhancement Kit in the dark for between 1 and 5 minutes. The reaction if stopped by transferring sections to acetate buffer. Sections are then washed in acetate followed by phosphate buffers and processed for EM.

Processing of immunogold sections for EM involves a shorter osmication time as the silver enhancement reaction product dissolved in the osmium solution. Sections are osmicated in 1% osmium tetraoxide (in 0.1M phosphate buffer) for only 7 minutes at 4°C; they are then washed and dehydrated as for standard tEM (see 2.3.4). Similarly, sections stained with DAB are processed in 1% osmium tetraoxide for only 30 minutes at 4°C. Neither process involves *en-bloc* staining with uranyl acetate, although individual sections can be stained in a manner similar to lead citrate staining in standard tEM processing.

2.3.6 LM-Level Immunohistochemistry Processing

Sections are incubated in primary antibody, diluted to the appropriate concentration in primary antibody buffer, for 72 hours at 4°C. They are then washed thoroughly in 0.1M TRIS before being incubated in appropriate biotinylated secondary antibody (raised against the species of primary antibody and conjugated with biotin), usually at a concentration of 1:200, for two hours at room temperature. Sections are then washed in 0.1 TRIS before being transferred into a 1:100 dilution of *VectorLabs ABC* solution for 90 minutes at room temperature. *ABC* consists of avidin, which binds biotin, including the biotin conjugated to the secondary antibody, and biotinylated horseradish peroxidase (HRP); thus forming an amplifying complex linking many HRP molecules to each biotinylated secondary antibody.

Following *ABC*, sections are washed in TRIS before being developed using a diaminobenzidine/hydrogen peroxide solution (DAB). Sections are developed in DAB for up to 30 minutes depending on the rapidity of staining development. Once

enough reaction product has been produces, cells are washed in 0.1M TRIS and mounted onto gelatinised slides.

The slide-mounted sections are allowed to air dry before being dehydrated though an ascending ethanol series (70%, 80%, 95%, 100% x2) and cleared in two changes of *Histoclear*. Slides are then coverslipped using DPX mountant, which is allowed to harden before viewing.

2.3.7 Immunofluoresence

Sections for immunofluoresence are incubated for 72 hours in primary antibody as with the other labelling protocols, however, if multiple-labelling is the aim, each primary antibody must have been raised in a different host species as this is the basis for differentiation between labels.

Following incubation in primary antibody/antibodies and washing in 0.1M TRIS, sections are incubated fluorophore-linked secondary antibody (usual concentration 1:200 in 0.1M TRIS) for two hours in the dark. Sections are then washed in 0.1M TRIS in the dark, and then if there are multiple labels, the secondary antibody labelling is repeated with each secondary. To achieve good multiple labelling each of the secondary fluorophore-linked antibodies must meet the following criteria: they must be raised in the same host species; they must be raised in a species not used to raise any of the primary antibodies; and they must be conjugated with fluorophores in such a combination as to give maximum separation of absorbance and emission spectra. For these reasons, a series of secondary antibodies all raised in donkey and conjugated to a variety of fluorophores were used.

Following secondary antibody labelling sections are washed in 0.1M TRIS and mounted onto slides. Before the sections dry, the slides are coated with *Vectashield DAPI* mounting medium, which contains the nucleic acid-counterstaining fluorophore DAPI, coverslipped and sealed with a small rim of clear nail varnish.

Sections were viewed using a *Leica* confocal microscope.

2.3.8 *TUNEL Labelling*

TUNEL (terminal transferase-mediated b-UTP nick-end labelling) incorporates biotinylated UTP molecules to the free ends of double-stranded DNA. Hence its use as a marker for double stranded DNA breakages.

Tissue is sectioned as for light immunohistochemistry and incubated in *Boeringer-Manheim* TUNEL mix for 90 minutes at 37°C. The reaction is stopped with cold 0.1M phosphate buffer and sections are washed thoroughly.

The biotin conjugated to the UTP molecules is revealed in an identical manner to staining for biotinylated secondary antibodies: incubation in *ABC* and development with DAB. Sections are them washed and mounted on gelatinised slides.

2.3.9 *Western Blotting*

In order to achieve maximum separation of proteins in the expected range, brain region homogenates (and markers) were electrophoretically separated on a 15% SDS-polyacrylamide gel. The separated proteins were then electrically blotted form the gel to PVDF membranes using cooled Bio-Rad blotting tanks overnight. Gels were stained with Coomassie Blue to confirm clean protein separation. Membranes were immunolabelled, the labelling revealed using chemiluminescence detected by exposure to photographic film.

2.3.10 *Image Analysis*

Counts of cell number, measurement of brain region cross-sectional areas and nuclear size were carried out using *Improvision*'s *OpenLab* software (v2.2.5) capturing data from a *Roper Scientific Photometrics CoolSnap* CCD camera attached to a *Leica* microscope.

~

Cross-sectional areas were calculated by drawing around the areas of interest after calibrating the software for each magnification using a captured image of a graticule. Cell counts were conducted by 'density slicing' a captured image. A number of 'regions of interest' (ROIs) are defined by the user and the properties of each ROI analysed by the software. The software then selects all regions it calculates to be similar to these ROIs. This is fine-tuned by the user until they are confident the system is selecting all it should be and no more. *OpenLab* then 'slices' the captured image creating a representation of all appropriate regions and their properties (number, area, perimeter etc.).

2.4 Methods Employed

2.4.1 Immunohistochemistry

ALL adult tissue for immunohistochemistry was prepared according to the protocols described in 2.3, sectioned at 40μm. The juvenile wild-type mice, both unadulterated and X-irradiated, were sectioned at greater thicknesses so as to maintain as much structural integrity as possible. Accurate details of section thickness cannot be given as each brain, and areas within, were sectioned in an *ad hoc* manner.

The primary antibody incubation time of 72 hours at 4°C was never varied; rather the only variable factor was antibody dilution. The ubiquitin, N-terminal huntingtin and GFAP antibodies (see 6.3) have been used previously by members of our group and have been shown to work well under these conditions at a dilution of 1:1000; therefore, this concentration was always used for these antibodies.

The antibodies to the various factors involved in apoptosis were new to the laboratory. Furthermore, given the nature of the experimental work – searching for a factor which may not be present – it was necessary to use a range of dilutions for these antibodies. Such dilutions ranged from 1:50 to 1:1000.

Likewise, the processing of primary antibody labeling, and preparation for viewing, was never varied from the protocol given in 2.3.6.

2.4.2 TUNEL

Sections for TUNEL were usually taken from brains cut for immunohistochemisty, and thus all adult sections were 40μm in thickness. The juvenile mice were sectioned at greater thicknesses in an *ad hoc* manner similar to those for immunohistochemistry.

TUNEL labeling was conducted by following the instructions provided with the kit, as described in 2.3.8. The recommended time for incubation (at 37°C) with the

constituted TUNEL mix is 90 minutes. However, during these experiments, to ensure and reaction that could take place *would* take place, incubation times were increased up to three hours.

2.4.3 X-irradiation

The juvenile mice used as positive controls had areas of apoptosis induced by X-irradiation. Dr John Scholes, of the UCL Department of Anatomy, routinely uses X-irradiation in a manner similar to radiotherapy. Indeed, the very principle of radiotherapy is that dividing cells are more susceptible to apoptosis induced by radiation damage, thus destroying more of a growing tumor than healthy post-mitotic tissue. In a similar vein, cells in the developing mouse that have not yet exited the cell cycle can persuaded to die apoptotically.

An X-irradiator, once used for medical radiography was used as a source. Pups were placed in a small, thin cardboard box with lid and the entire package placed under the field of X-irradiation. They were exposed for one minute to a middling does of radiation. Following exposure they were left for four hours, for the nuclear-led apoptotic events to exert their effects, before being perfused.

2.4.4 Western Blotting

13 week-old R6/2 and LMC brains were dissected and sections of frontal cortex, striatum and cerebellum removed. These regions were homogenised and protein content assayed. Samples were loaded such that 20µg of protein (denatured in sample buffer) from each region were run in each lane of the gel. Primary antibodies for caspase-1 were used at a dilution of 1:1000 (others, not presented here, were used at lower concentrations). Secondary (anti-rabbit) antibody was used at a

concentration of 1:15,000; a dilution found in preliminary experiments to produce the best balance between noise and signal.

2.4.5 Striatal Oligodendrocyte Counts

The counts of striatal oligodendrocytes were conducted using semi-thin (0.5 µm) sections from tissue processed according to the EM preparation documented in *2.3.4*. Semi-thin sections were taken from R6/2 mice of 4, 6, 8, 10, 12 and 17 weeks of age, and littermate control mice of 17 weeks of age. Sections were stained with toludine blue and viewed under the standard light microscope.

Oligodendrocytes were identified according to their morphology and counted manually. By using a microscope connected to the *OpenLab* imaging system one can scan through defined strips of the striatum without the possibility of overlap or separation that would undermine counts conducted when viewing the microscope image directly. Individually, oligodendrocytes are 'flagged' and counted by the computer as the entire striatum is scanned. The section is then viewed using a low power lens and the striatum outlined by the user. The cross-sectional area thus provides a means of calculating density of oligodendrocytes within each section of striatum.

To minimise effects from sampling different areas of the striatum, three sections were taken from each of seven mice through the region where the striatum is largest in cross-sectional area.

The average for each mouse was calculated and compared to each of the others using the *students t-test* (n=7).

2.4.6 *Corpus Callosum Oligodendrocyte Counts*

Counting oligodendrocytes within the corpus callosum is somewhat easier than in the striatum as one can be fairly certain that all cell somata within the region belong to oligodendrocytes.

Thionin-stained 40µm sections from R6/2 and LMC mice from 1 to 12-weeks of age (n=2 for each time-point) were viewed using the *OpenLab* software as described above, such that the corpus callosum filled the entire field of view analysed by the software. Several nuclei were defined as ROIs and density slices (see 2.3.9) were taken throughout the corpus callosum. Similar to the striatal counts, the cross-sectional area of the corpus callosum was then measured to yield densities.

It should be noted that the measurements from striatum and corpus callosum are not directly comparable as they were conducted using different sectioning methods. There will be far more cells contained within any given region of a 40µm section than there are in the corresponding 0.5µm section.

2.4.7 *F36 Longitudinal Study*

Anticipation (see 1.3.4) means that repeat sizes are gradually increasing in each subsequent generation of R6/2 mice. The original construct contained 150 CAG repeats, but current generations have repeat lengths closer to 200. Thus, in order to conduct an accurate study into the timing of inclusion and degeneration events, I decided to take a single generation of mice, the F36 generation, and take littermates (transgenic and control) at 4, 6, 8, 10 and 12 weeks of age. There is also the possibility of variation from one sibling to the next, and so I took sections for immunohistochemistry and sections for standard electron microscopy from each individual brain. Therefore, in contrast to the protocols given in 2.3, mice for this study were perfused with 4% paraformaldehyde without gluteraldehyde. Furthermore, sections for light microscopy were cut on the *Vibratome* alongside the sections for EM.

Two sections of 50μm followed by one section of 200μm were cut in series through the brain. The 200μm sections were post-fixed in 0.2% gluteraldehyde for one hour before being processed for EM as normal. The 50μm sections were processed for immunohistochemistry according to the protocol given in *2.3.6.*

2.4.8 ImmunoEM

This study has used the *DAKO* anti-ubiquitin and *Santa Cruz* anti-huntingtin n-terminus antibodies for immunocytochemical labelling at the EM level. Both of these antibodies have been thoroughly characterised and have been shown to possess sufficient affinity for their target proteins that they can be used on tissue fixed with 4% paraformaldehyde without significant loss of signal. Thus, tissue for immunoEM was taken from standard EM-fixed tissue.

Results

3.1 Degeneration in the R6/2 Mouse

3.1.1 Introduction

REGULATIONS now stipulate that R6/2 mice are to be culled no later than 13 weeks of ages. In mice of this age, symptoms are very apparent (one reason for the current restriction) and so whatever underlies the neurological dysfunction seen in HD must also be apparent at this age. For analyses of degeneration I have therefore used mice of 12 to 13 weeks of age. Previous material collected before the onset of this particular project has also been kindly made available by Mark Turmaine; this material, in the form of tissue prepared for electron microscopy, includes sections from mice up to 17 weeks old.

3.1.2 Inclusion Formation and Distribution

Davies *et al.* identified the neuronal intranuclear inclusion in the R6/2 mouse in 1997, and claimed the formation of this body 'underlies the neurological dysfunction' seen this model. As discussed in *1.5*, such aggregates are seen in all polyglutamine diseases, however the toxicity of the aggregate remains under debate. In order to address this question myself, I have analysed the distribution of inclusions and compared it to the pattern of pathology.

The inclusion can be identified at the level of light microscopy by labelling with either anti-huntingtin N-terminus (htt_n) or anti-ubiquitin antibodies (see *2.2* for details). Figure 23 is an example of the staining seen with anti-htt_n illustrating the presence of both intranuclear and neurite inclusions. Anti-ubiquitin staining yields a similar image as both ubiquitin and htt_n co-localise to the inclusion, as illustrated in figure 24.

Labelling of late-stage R6/2 mice with anti-htt_n readily highlights inclusions, visible even at low magnification. The nuclei of such mice also appear to contain non-

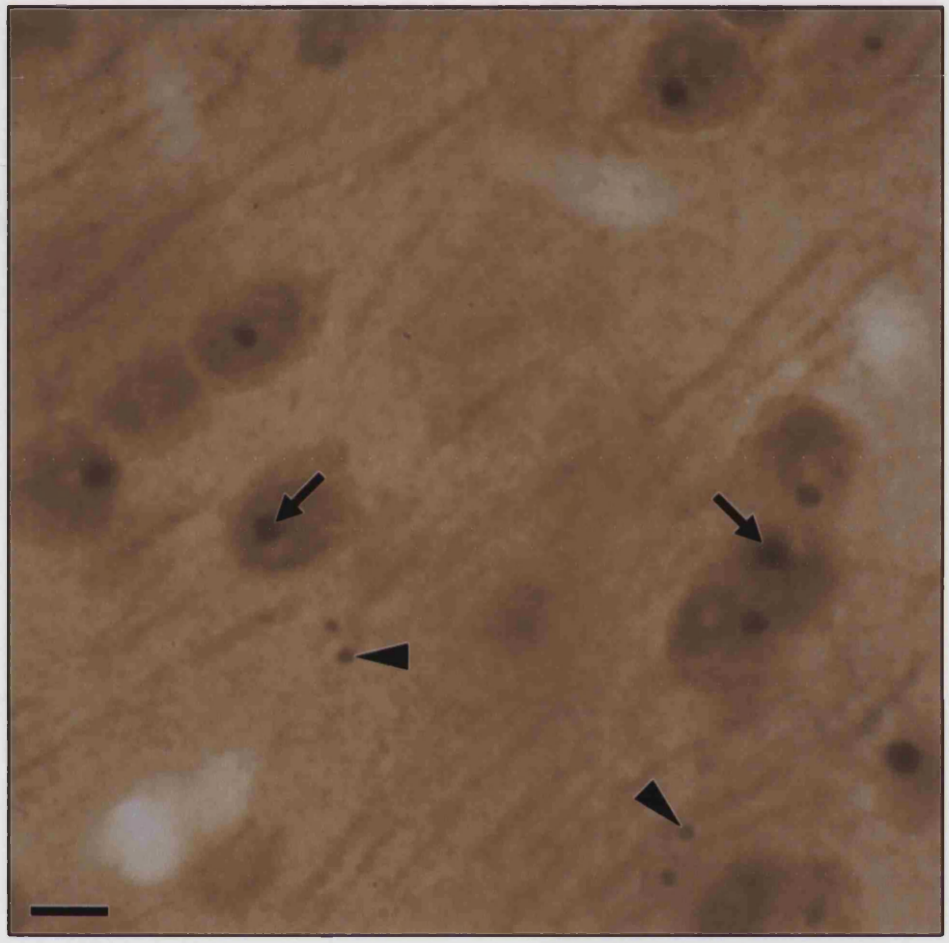

Figure 23 Cortical section from a 10 week old R6/2 mouse immunolabelled for N-terminal huntingtin. Note the dark nuclei containing inclusions (arrows) and the neuropil aggregates (arrowheads). Scale bar = 10μm

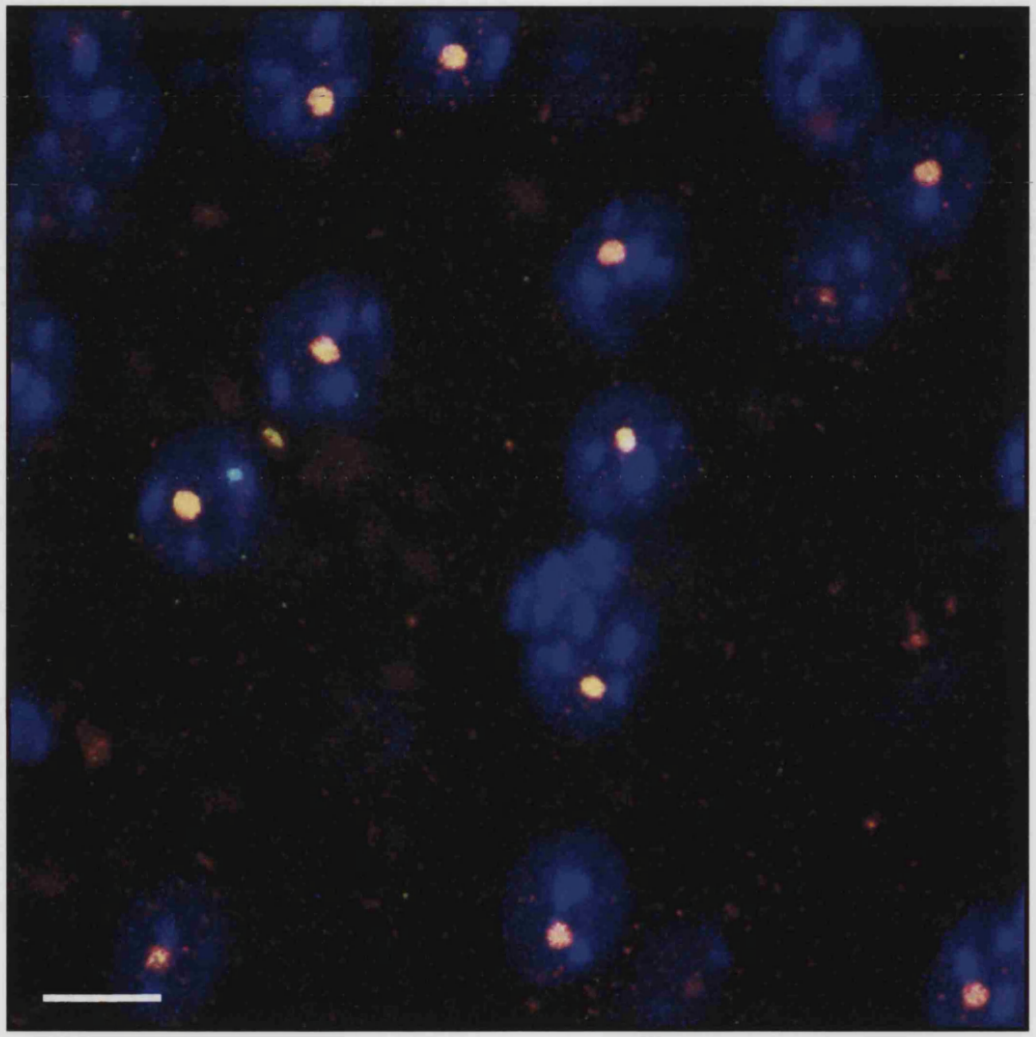

Figure 24 A confocal micrograph showing the co-localisation of ubiquitin and N-terminal huntingtin to the inclusions of striatal neurons. The nucleus is stained with DAPI (blue); ubiquitin and huntingtin are stained green and red respectively, but when co-localised in this merged image, they are shown as yellow. Scale bar = 10μm.

aggregated huntingtin, whereas in littermate controls, huntingtin is predominantly found in the cytoplasm (figure 25).

The rate at which inclusions appear varies according to cell type/brain region. It is conceivable that this variation may underlie some of the specificity seen in HD. In order to address this I have analysed the formation of inclusions and degree of degeneration in the R6/2 mice. As most change in repeat size occurs on vertical transmission this analysis was limited to one generation of mice. Transgenic and wild-type mice were culled at 4, 6, 8, 10 and 12 weeks of age. The htt_n antibody is extremely effective, so much so that tissue can be fixed for EM (4% paraformaldehyde) without significant loss of signal. Therefore, mice were perfused with 4% paraformaldehyde and vibratome sections were cut in a repeating series of four 50mm sections for immunohistochemistry followed by a single 200mm section, which was fixed further in 0.1% gluteraldehyde, for processing to the semi- and ultra-thin level. This permits a direct comparison between htt_n staining and ultrastructural appearance.

Work on previous generations of mice shows inclusions are most apparent throughout the cortex, striatum and hippocampus, therefore I chose to focus on four areas of cortex: the cingulate, motor, somatosensory and pyriform cortices; the CA1 and CA3 fields of the hippocampus, the dentate gyrus and the anterior striatum (see figure 26).

At four weeks of age, nuclear inclusions are already apparent in some areas, to wit: the somatosensory cortex, striatum and CA1 field of the hippocampus (see figures 27 and 28). These inclusions are relatively small, the largest being the CA1 inclusions. In the striatum not all cells show inclusions, suggesting that the striatum is at a threshold point around four weeks of age. Cells which do not yet possess inclusions can often be seen to contain small foci of htt_n; likewise, in the cingulate, motor and pyriform cortices, the nuclei stain rather prominently for htt_n and small foci can often be seen, yet inclusions are absent from the upper layers and rare in the deep layers of these cortices. It is interesting that the inclusions are common in the somatosensory cortex at this age and yet rare in the other cortical areas. Furthermore, within the hippocampus, the CA1 neurons possess the largest inclusions seen at this age, whilst

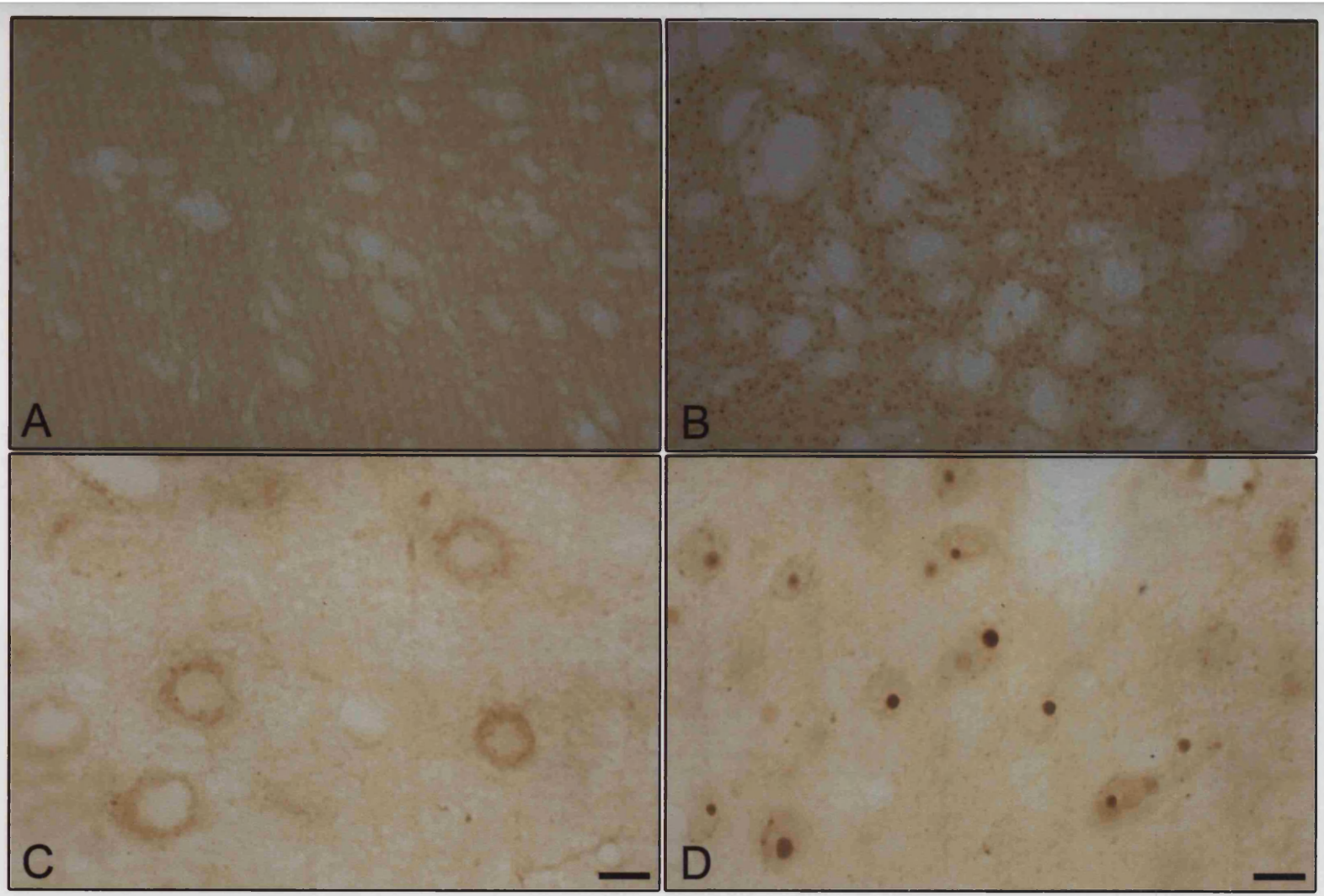

Figure 25 Striatal sections from 12 week old wild-type (A, C) and R6/2 (B, D) mice immunolabelled for N-terminal huntingtin. Scale bar 10μm (C,D)

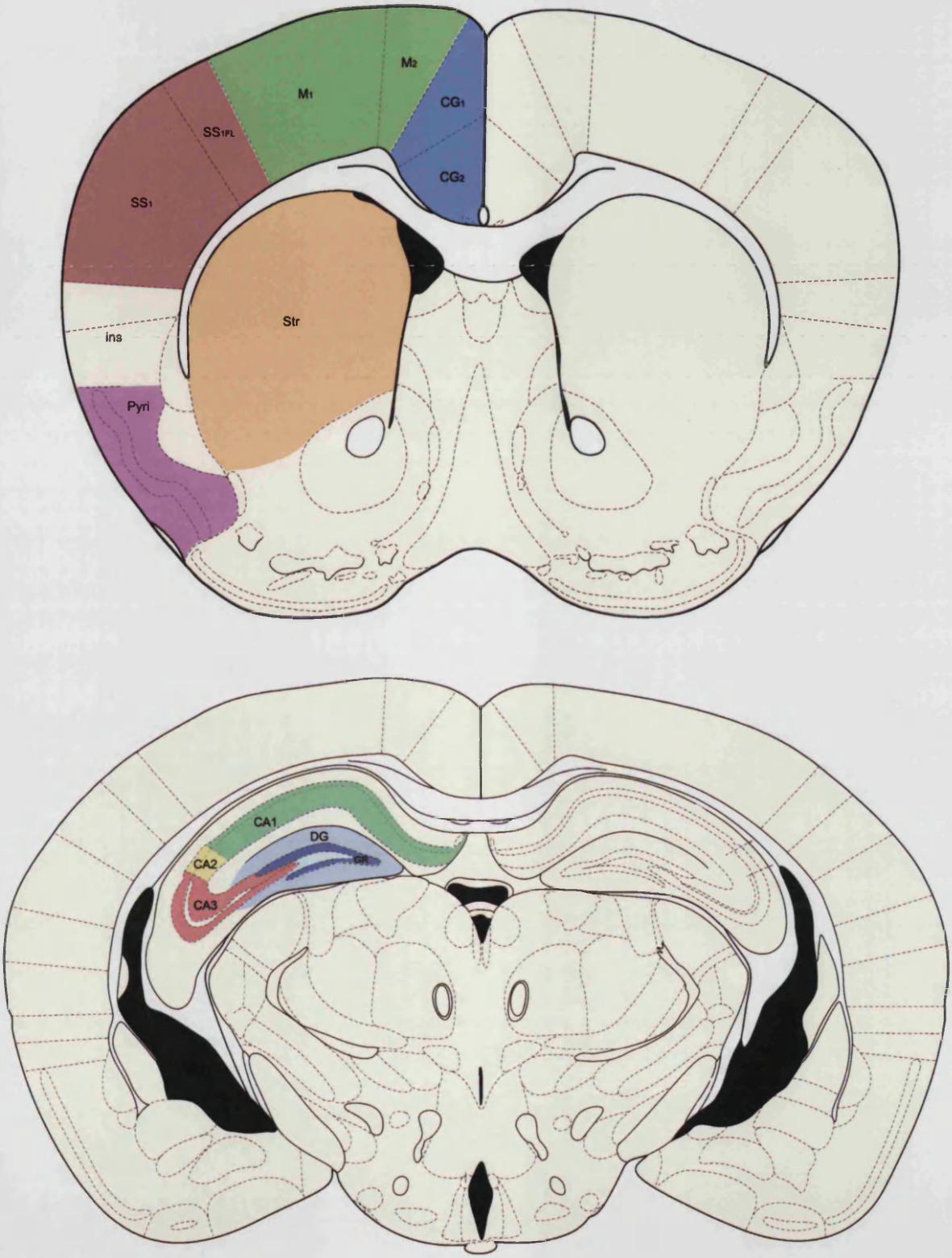

Figure 26 Topography of the mouse brain. Areas under discussion are highlighted. CG: cingulate cortex. M: motor cortex. SS: somatosensory cortex. Pyri: pyriform cortex. Str: striatum. DG: dentate gyrus (GC: granule cells). Hippocampal areas CA1, CA2 and CA3.

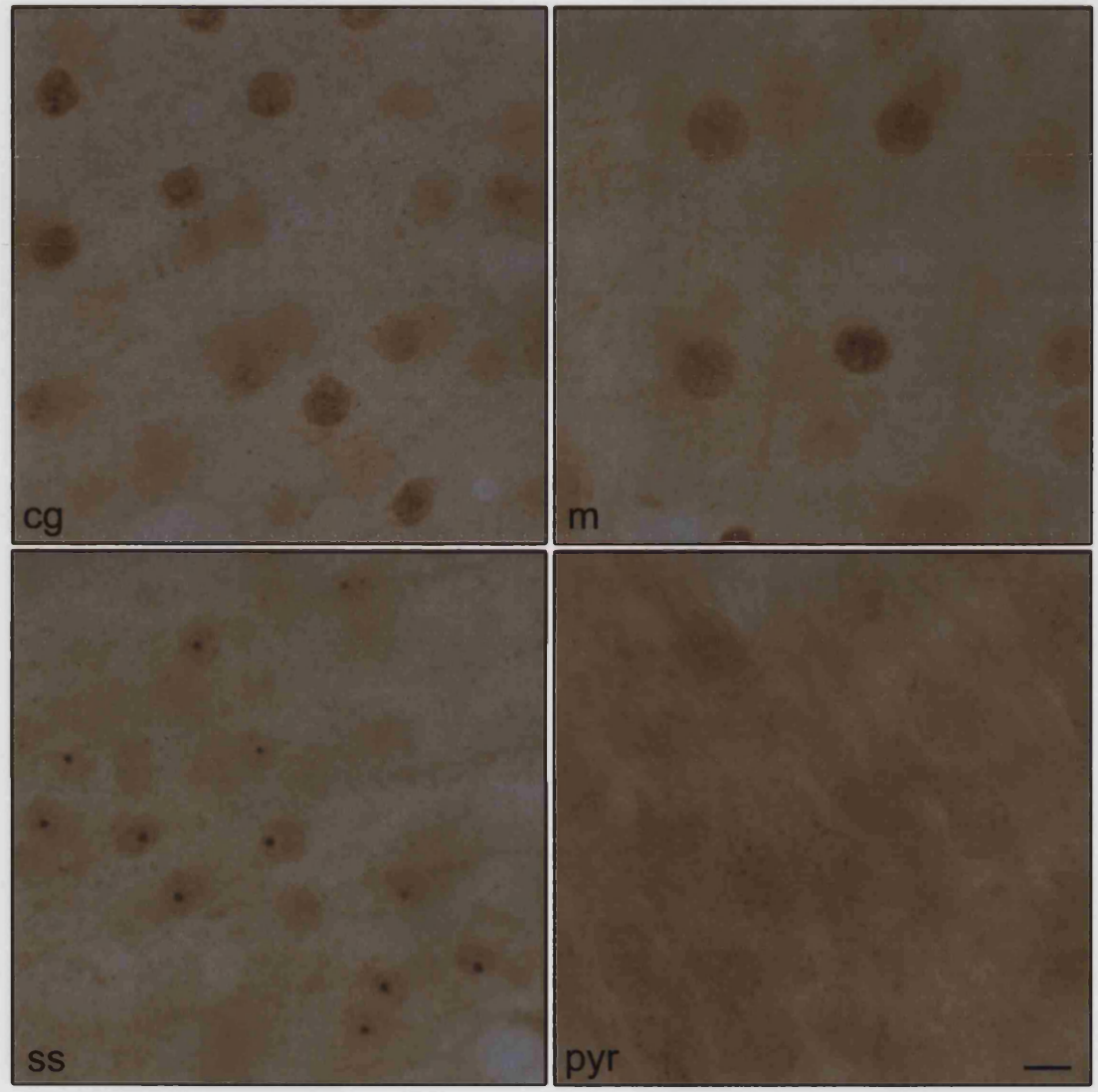

Figure 27 Sections from a 4 week old R6/2 mouse immunolabelled for N-terminal huntingtin. Cingulate cortex (cg), motor cortex (m), somatosensory cortex (ss) and pyriform cortex (pyr), Scale bar = 10μm

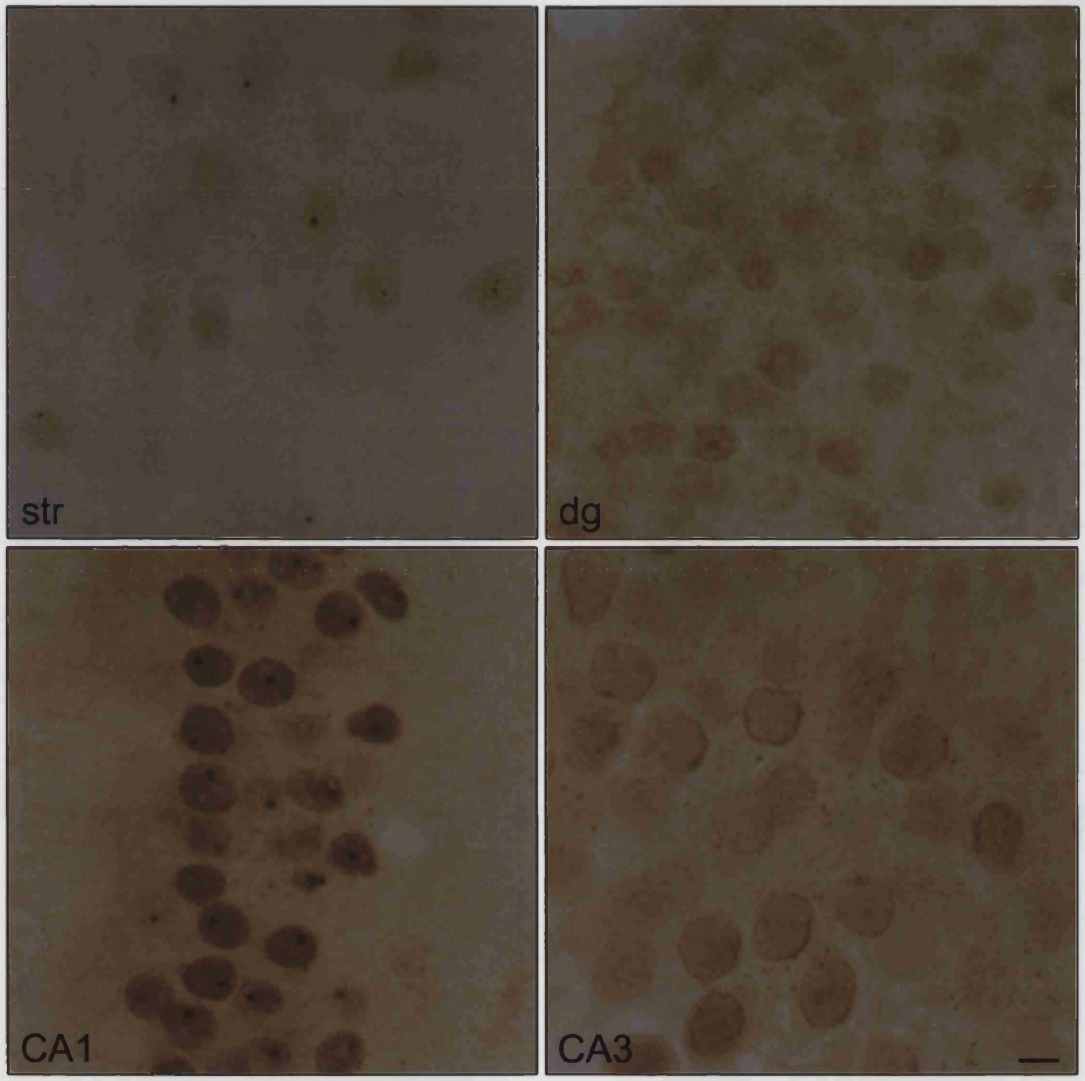

Figure 28 Sections from a 4 week old R6/2 mouse immunolabelled for N-terminal huntingtin. Striatum (str), dentate gyrus (dg), hippocampal CA1 field (CA1) and hippocampal CA3 field (CA3), Scale bar = 10μm

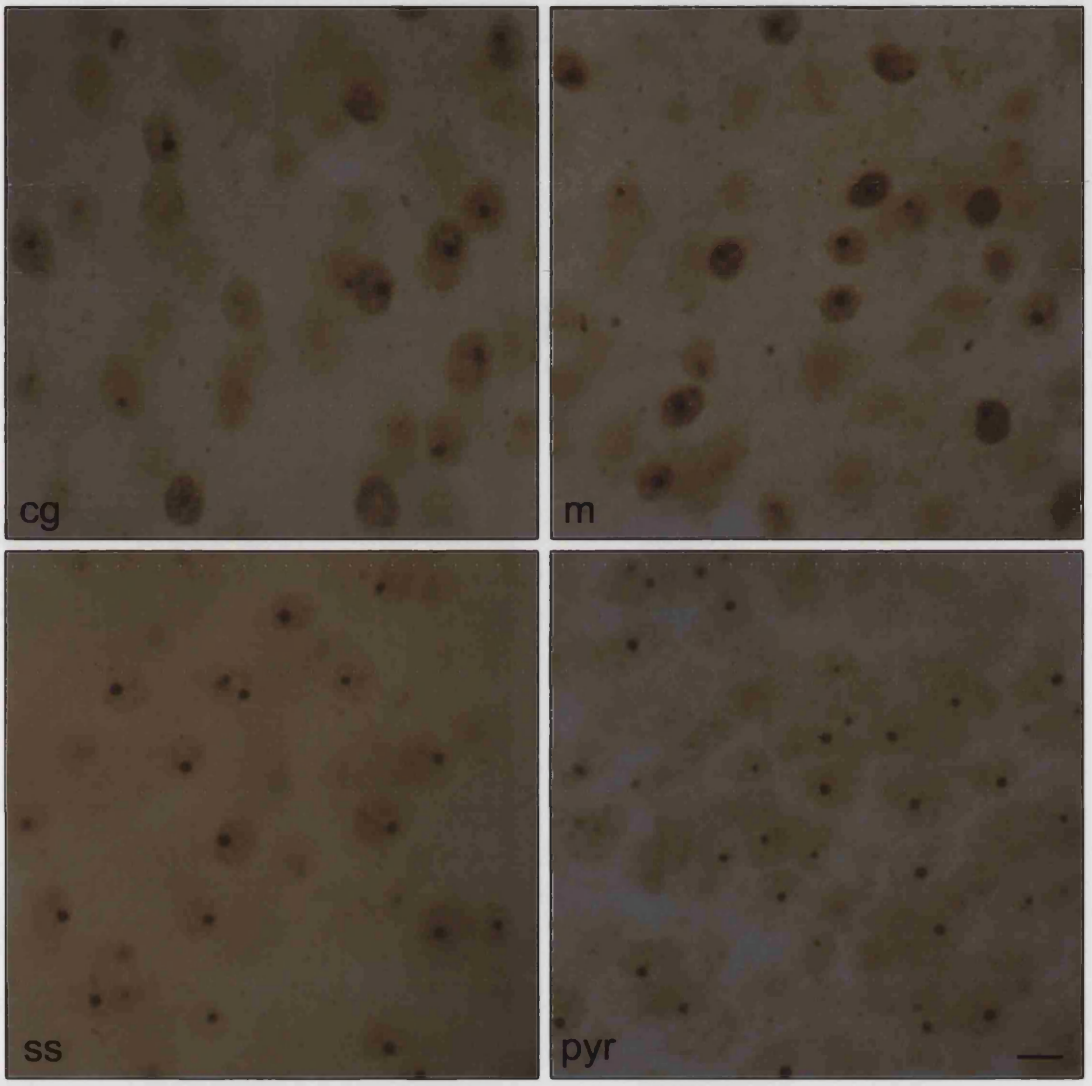

Figure 29 Sections from a 6 week old R6/2 mouse immunolabelled for N-terminal huntingtin. Cingulate cortex (cg), motor cortex (m), somatosensory cortex (ss) and pyriform cortex (pyr), Scale bar = 10μm

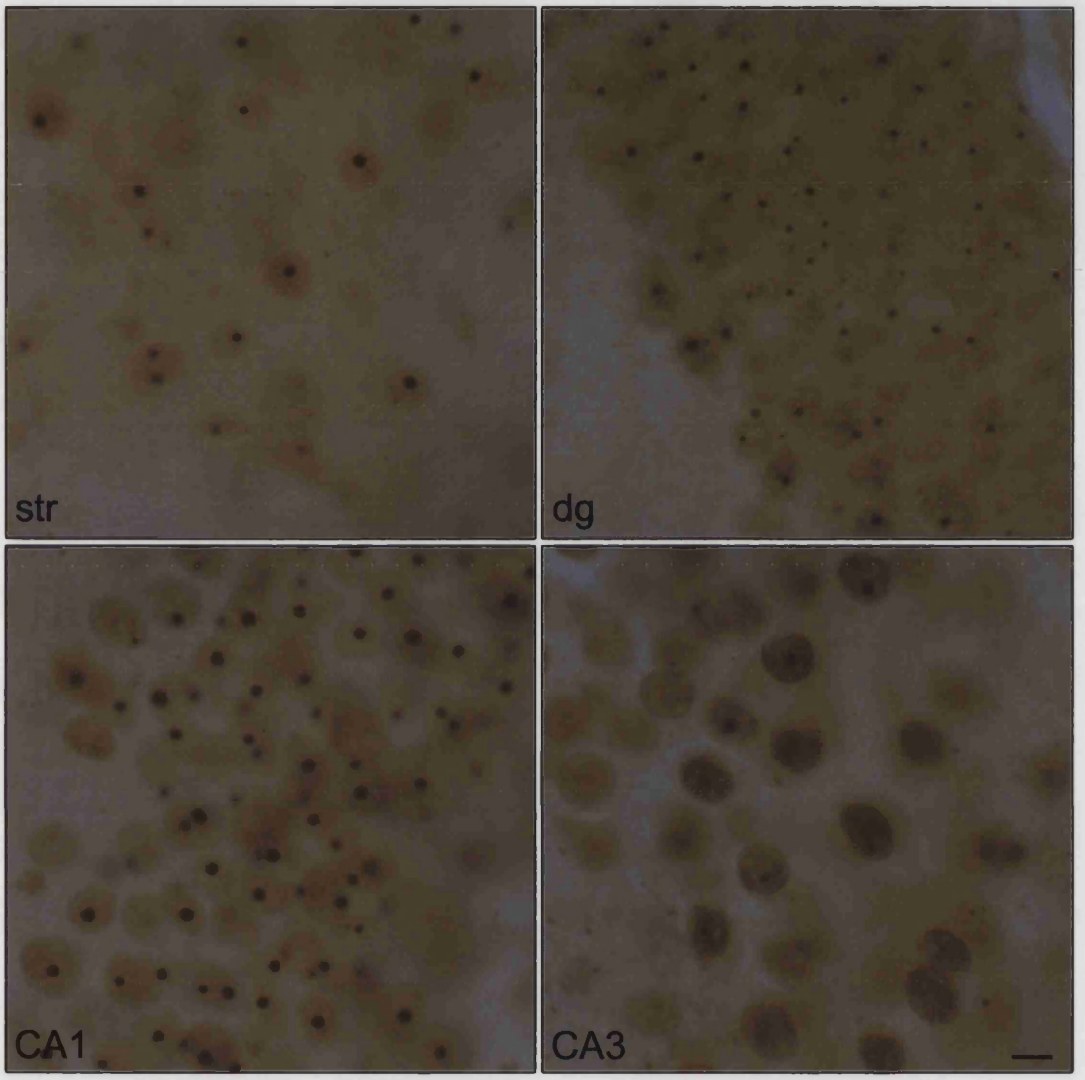

Figure 30 Sections from a 6 week old R6/2 mouse immunolabelled for N-terminal huntingtin. Striatum (str), dentate gyrus (dg), hippocampal CA1 field (CA1) and hippocampal CA3 field (CA3), Scale bar = 10μm

the CA3 cells are completely devoid of aggregates, either inclusions and foci of htt_n. Indeed, the CA3 fields seem to have very little htt_n within the nucleus, rather their staining suggests a concentration of htt_n at the cytoplasmic face of the nuclear membrane. It is likely this indicates an early stage in the evolution of inclusions in which htt_n is processed to the nucleus before aggregating into foci and then the inclusion.

At six weeks of age, inclusions are evident in all areas under study (see figures 29 and 30). The cingulate and motor cortices now resemble the somatosensory cortex and the pyriform cortex shows prominent inclusions. All neurons in the striatum show inclusions and the dentate gyrus and CA3 neurons have progressed from showing no inclusions to a widespread distribution. Furthermore, the intense staining at the nuclear periphery of the CA3 cells has disappeared, to be replaced by a pan-neuronal staining with either multiple focal aggregates or an inclusion; this furthers the notion that the perinuclear staining indicated a phase of translocation of N-terminal huntingtin to the nucleus.

By eight weeks of age, nuclear inclusions are very apparent and neurite inclusions have become evident (see figures 31 and 32). At this point, the inclusions of the pyramidal cells in the pyriform cortex, which were among the last to show inclusions, have now become among the largest inclusions of the cortex; indeed, they appear as large as the inclusions of the somatosensory cortex which were the first to appear in the cortex. Likewise, the dentate gyrus and hippocampal CA3 neurons, which were among the last to develop inclusions, now posses very evident aggregates. The largest inclusions, however, remain in the CA1 neurons.

Figure 37 is an illustration of the suggested process of inclusion formation. I have used an idealised hippocampal CA3 neuron, as in this study, beginning at week four, I see the earliest changes only in these neurons. The earliest stage, before four weeks, is an extrapolated state based on the appearance of control mouse neurons stained for htt_n. In summary, htt_n is targeted from the cytoplasm to the nucleus, which results in an accumulation at the nuclear membrane whilst proteins are being translocated. This accumulation disappears once the nucleus has been filled with htt_n. The six-week stage in figure 37 is based on the most immature cells rather than a

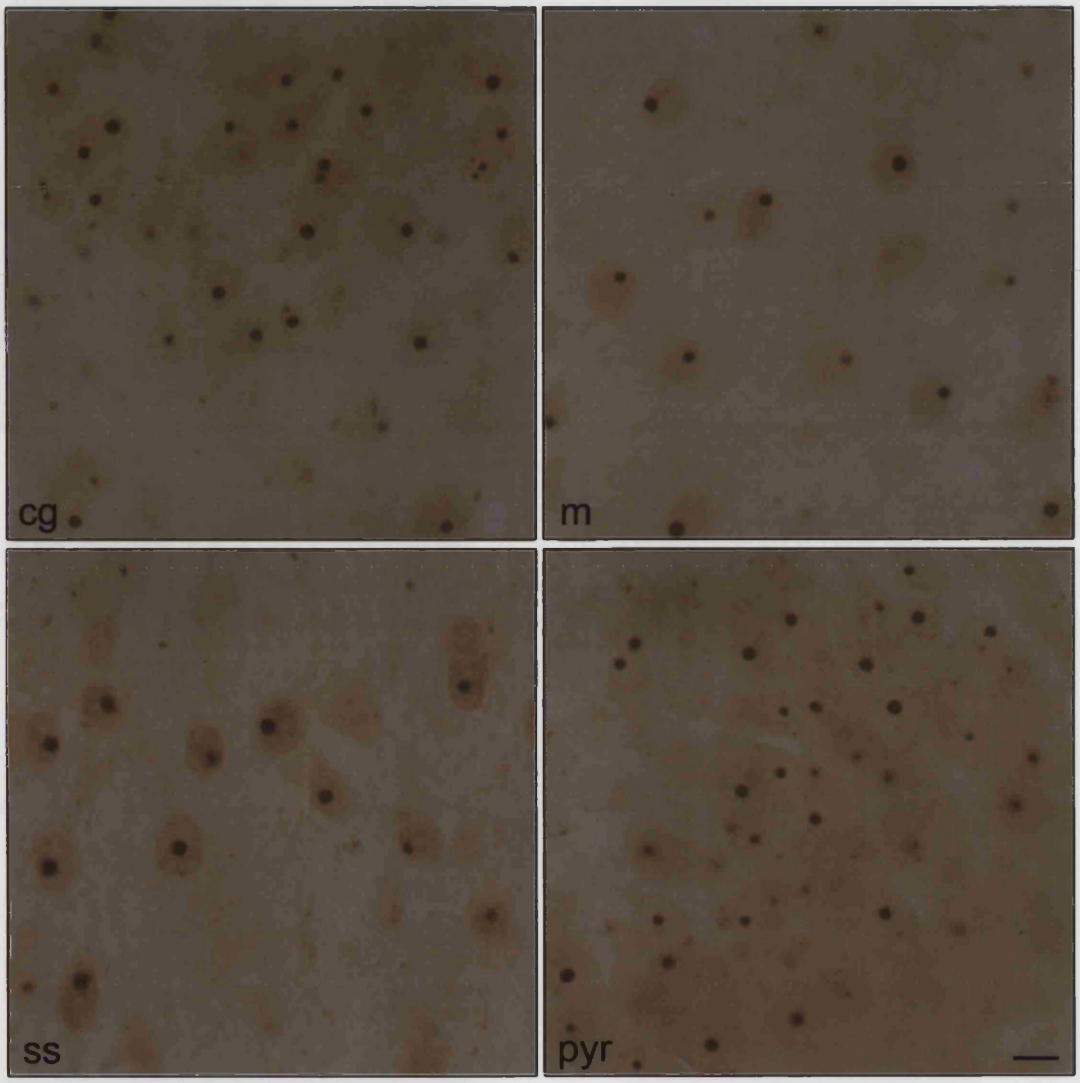

Figure 31 Sections from an 8 week old R6/2 mouse immunolabelled for N-terminal huntingtin. Cingulate cortex (cg), motor cortex (m), somatosensory cortex (ss) and pyriform cortex (pyr). Scale bar = 10μm

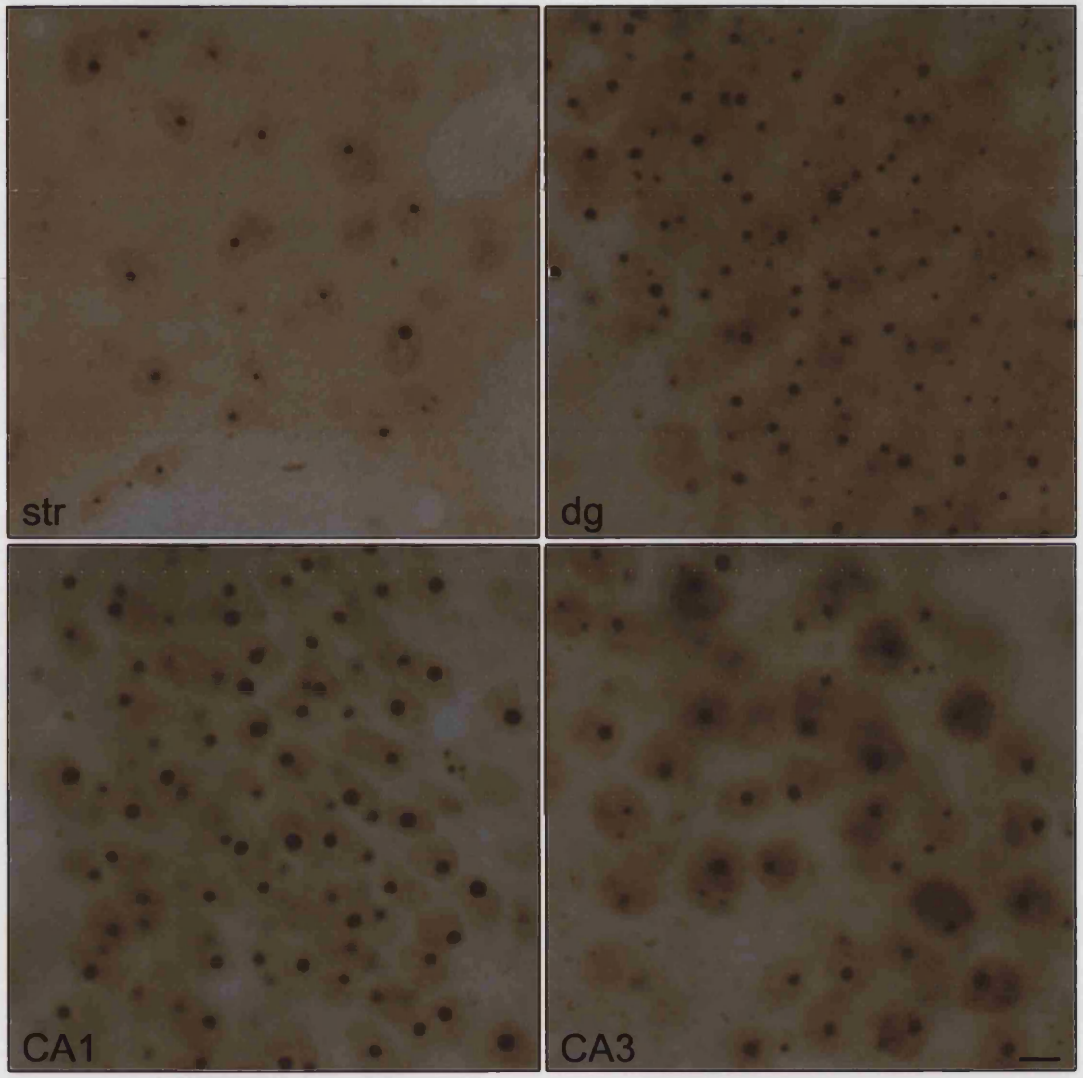

Figure 32 Sections from an 8 week old R6/2 mouse immunolabelled for N-terminal huntingtin. Striatum (str), dentate gyrus (dg), hippocampal CA1 field (CA1) and hippocampal CA3 field (CA3). Scale bar = 10μm

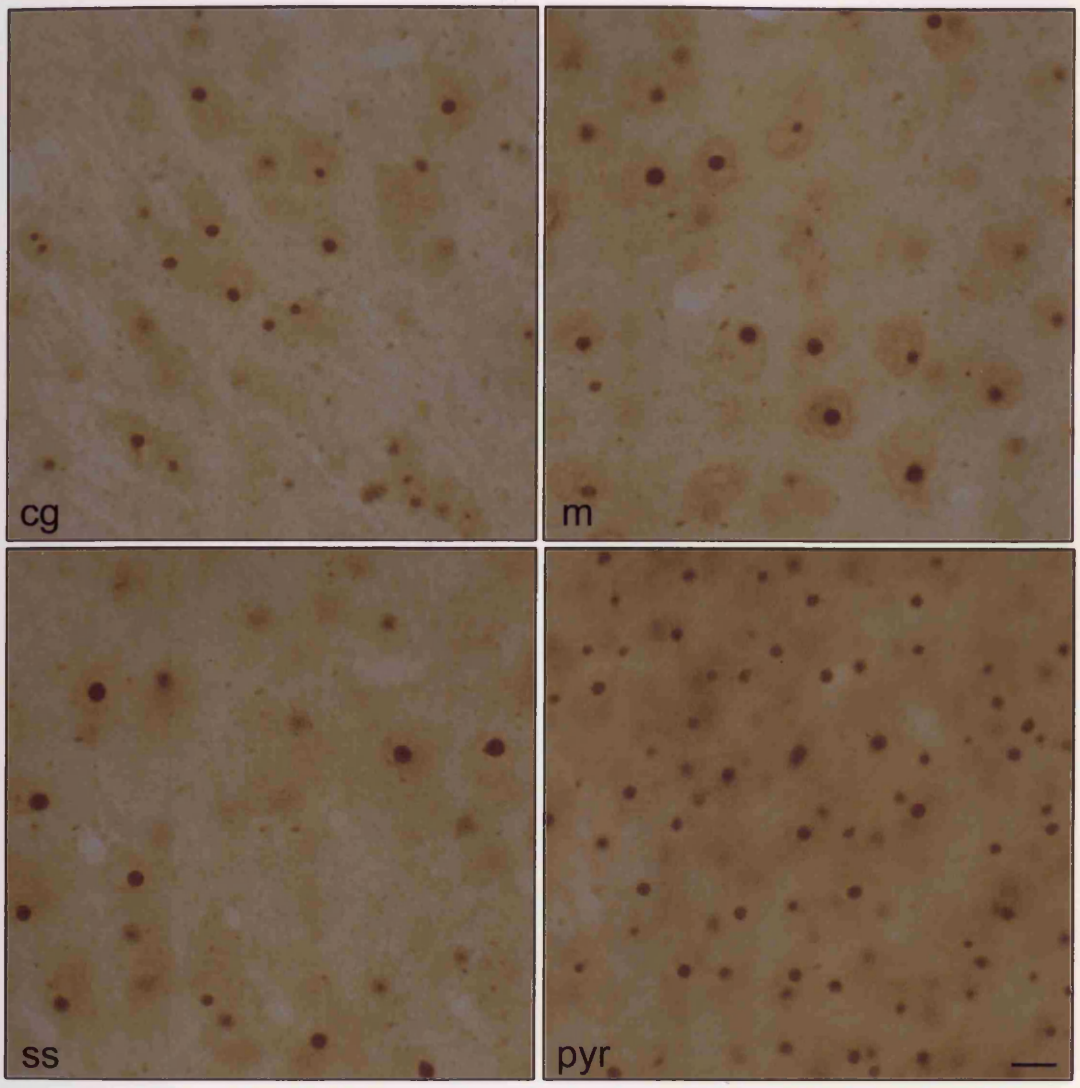

Figure 33 Sections from a 10 week old R6/2 mouse immunolabelled for N-terminal huntingtin. Cingulate cortex (cg), motor cortex (m), somatosensory cortex (ss) and pyriform cortex (pyr). Scale bar = 10μm

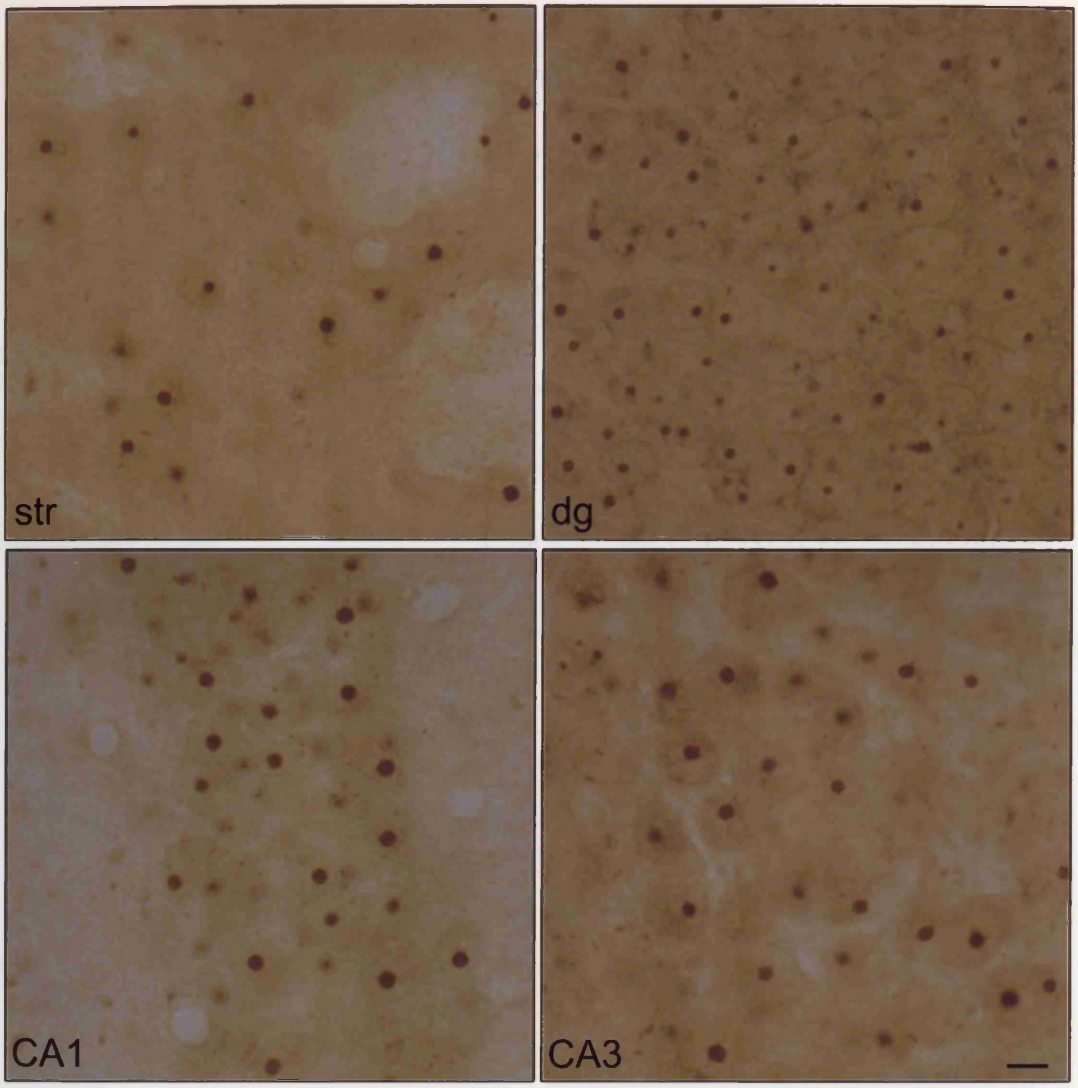

Figure 34 Sections from a 10 week old R6/2 mouse immunolabelled for N-terminal huntingtin. Striatum (str), dentate gyrus (dg), hippocampal CA1 field (CA1) and hippocampal CA3 field (CA3). Scale bar = 10μm

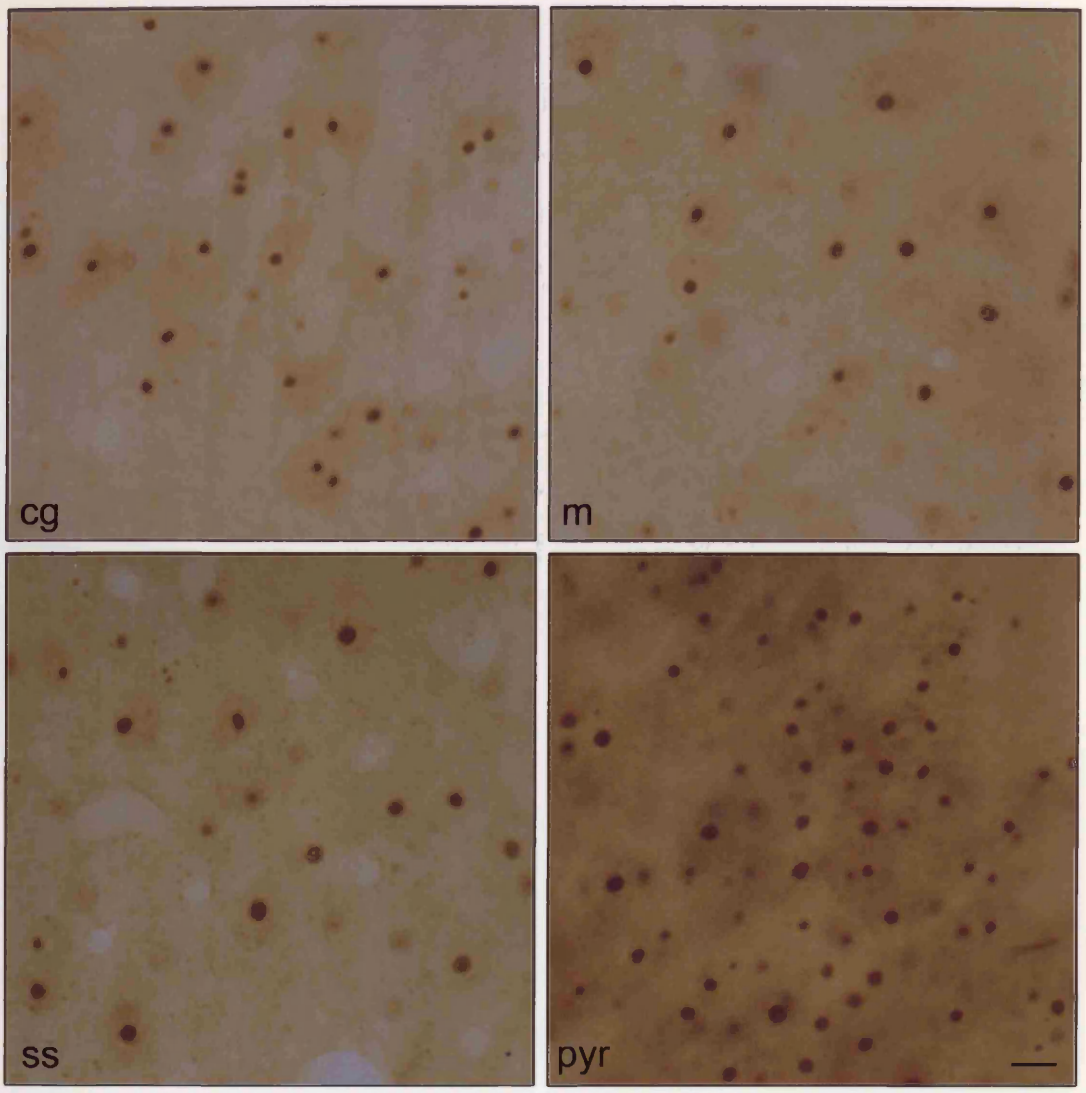

Figure 35 Sections from a 12 week old R6/2 mouse immunolabelled for N-terminal huntingtin. Cingulate cortex (cg), motor cortex (m), somatosensory cortex (ss) and pyriform cortex (pyr). Scale bar = 10μm

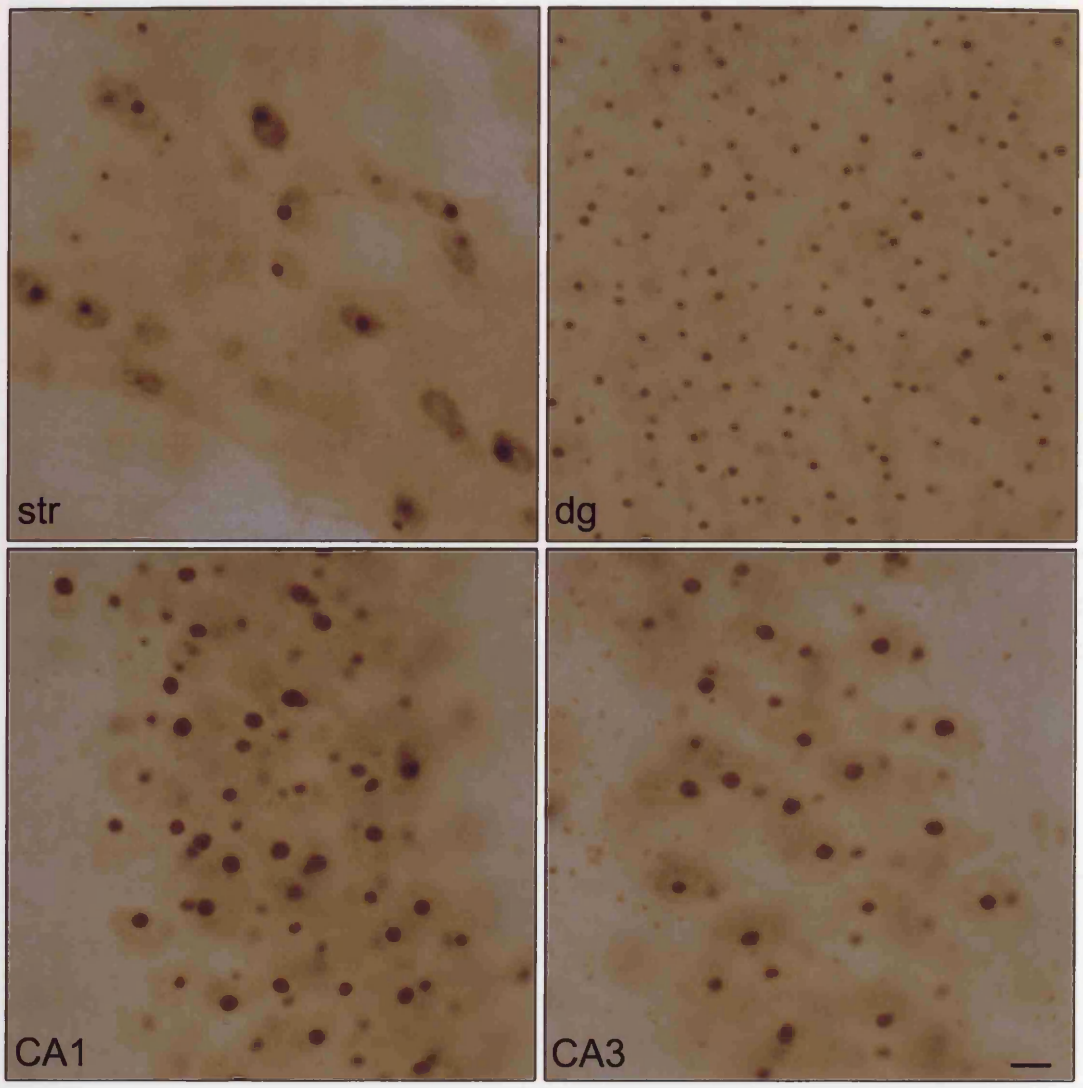

Figure 36 Sections from a 12 week old R6/2 mouse immunolabelled for N-terminal huntingtin. Striatum (str), dentate gyrus (dg), hippocampal CA1 field (CA1) and hippocampal CA3 field (CA3). Scale bar = 10μm

representative sample seen in the six week sections studied. Therefore, I interpolate that some time before six weeks the now-nuclear htt_n begins to aggregate forming multiple foci against the background of a nucleus filled with htt_n. Between six and eight weeks these foci disappear to be replaced by the familiar intranuclear inclusion. It is logical to assume that the inclusion results from the seeding effect of one of the foci. If the other foci move in and coalesce with the nascent inclusion, it is surprising that neither myself nor any of my colleagues have observed a stage of coalescence; presumably a 'raspberry-like' structure. The inclusion continues to grow between eight and ten weeks, presumably by the addition of more now-nuclear htt_n to the inclusion surface. However, growth then slows such that comparatively little occurs between ten and twelve weeks. However, whilst the NIIs slow in their growth, neurite inclusions become more apparent. It may be that as the nucleus becomes "saturated" with htt_n, the process of aggregation occurs before nuclear translocation can occur. However, the question of why non-neuronal aggregates are found in the neuronal processes and not in the soma remains a mystery.

It is shown that inclusions appear at differing ages in each brain region, and that inclusions increase in size over time. However, it appears that whilst inclusions increase in size rapidly at first, this growth reaches a threshold size at which growth rate declines considerably, or may even stop. The inclusions of the dentate gyrus are amongst the last to appear, but by eight weeks of age they seem to have reached their maximum size (*compare* figures 32, 34 and 36). Furthermore, at four weeks inclusions are present in the CA1 neurons of the hippocampus, whilst huntingtin has yet to fill the nucleus of the CA3 neurons (see figure 28). By ten weeks of age, the inclusions of the CA3 nuclei are indistinguishable from those of the CA1 cells. Indeed, between eight and ten weeks all cells appear to reach a point whereby inclusion growth slows dramatically. In terms of NII size, sections from a 10-week old R6/2 mouse are almost indistinguishable from those of a 12-week R6/2 mouse. This is an important observation when one is considering the relationship between inclusions and degeneration. Whilst inclusion growth appears to plateau, phenotype progressively worsens. It may be that the cell cannot continue to sequester mutant huntingtin to the inclusion indefinitely, thus its effects are no longer buffered and phenotype

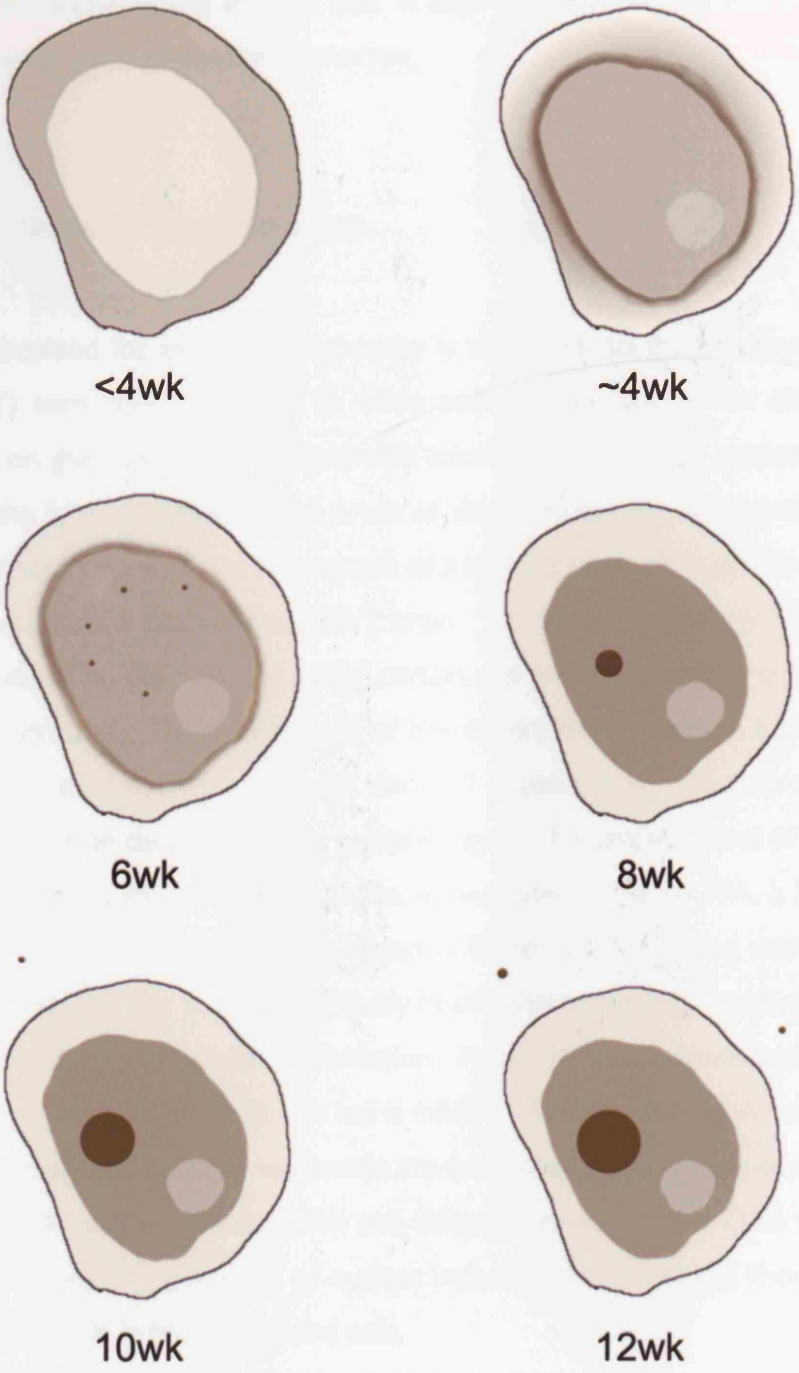

Figure 37 An illustrative summary of inclusion formation. Ages are based on the inclusion formation within a hippocampal CA3 neuron.

worsens. If true, this supports the notion that the formation of the inclusion is a beneficial response by the affected cell. It also counters the idea that the inclusion is the underlying cause of disease phenotype.

3.1.3 Patterns of Degeneration

Tissue processed for electron microscopy is taken first to the toludine blue-stained ('tol blue') semi-thin stage: 0.5 to 1mm sections are cut on an ultramicrotome, mounted on glass slides and stained with toludine blue. These sections are viewed through the light microscope and areas of degeneration are apparent even at low magnifications. Figure 38 is a micrograph of a tol blue taken through the cingulate and motor cortices of a twelve week R6/2 brain. The nuclei of healthy neurons appear pale in contrast to the neuropil, whilst certain glial and degenerating cells stain darker than the surround. This dark nature of the degenerating neurons is what led Mark Turmaine to label this type of death *dark cell degeneration*. Degenerating cells and healthy glia can be distinguished by morphology; at the simplest level of identification, dying cells show a more irregular profile, as illustrated in figure 39A, a high powered section of the cingulate cortex highlighted in figure 38. The dying neurons (arrows) are considerably darker than the relatively healthy neurons in the same area, exhibiting both nuclear and cytoplasmic condensation. Figure 39A also shows a cell in the early stages of this process (asterisk): this cell is mildly darker than the other healthy neurons and the nuclear and plasma membranes are becoming irregular in appearance. Figure 39B is a similar section labelled with anti-ubiquitin, revealed with DAB stain (yellow), clearly illustrating the presence of nuclear inclusions (red arrows), though staining is hard to distinguish in the condensed cells.

When studying the degeneration in the R6/2 mice it became clear that the cells appear completely healthy long after inclusion formation. I have documented inclusion formation at four weeks of age, but the earliest observable changes in micro-morphology do not occur before ten weeks of age. Figures 40 and 41 are tol blues though the areas studied in *3.1.2* of a ten week old R6/2. In most areas, cells appear

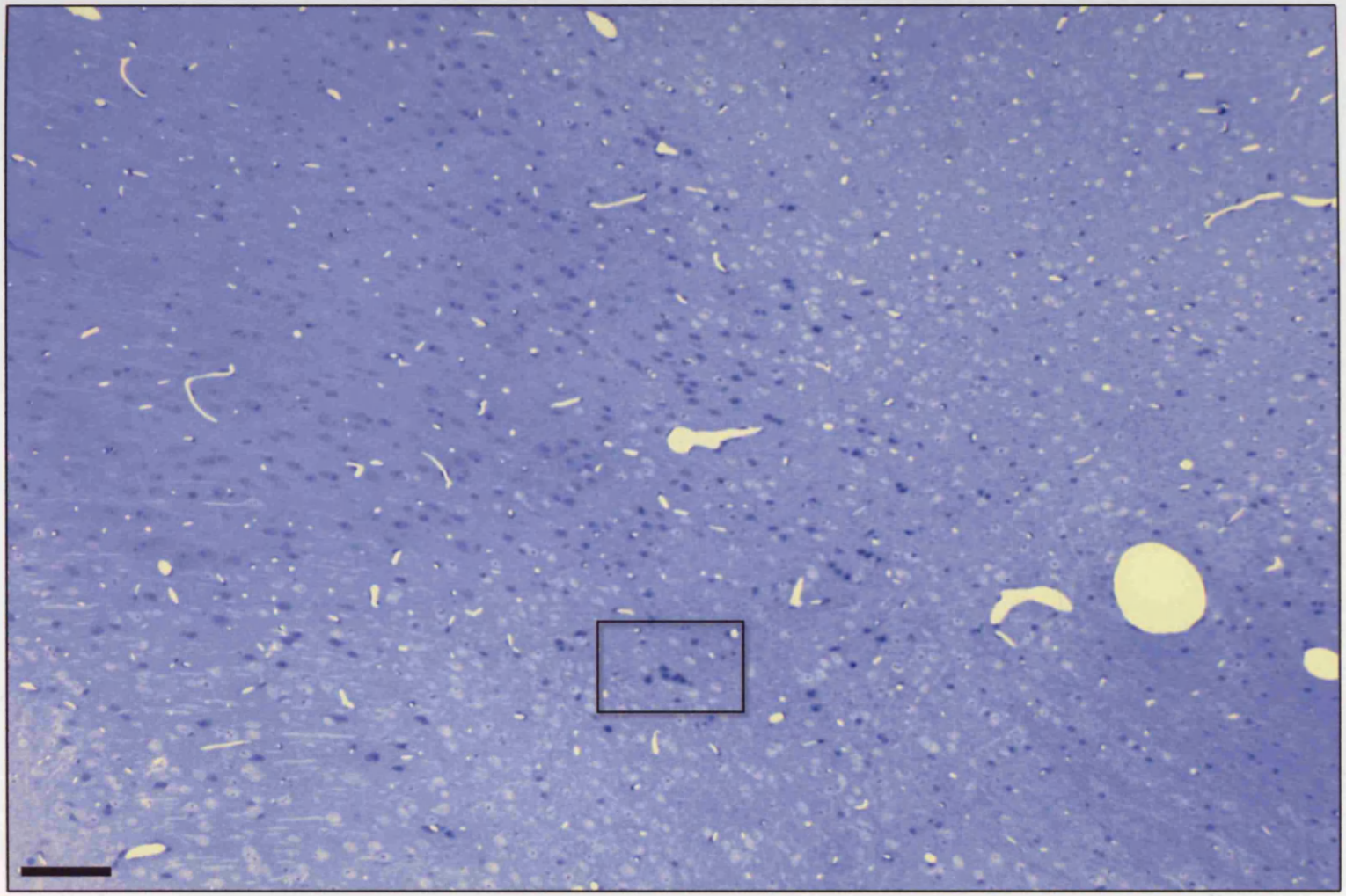

Figure 38 1µm section through the cingulate and motor cortices of a 12 week old R6/2 mouse. Degenerating neurons are identifiable by their darkened appearance. Highlighted section is magnified in figure 39. Scale bar = 100µm

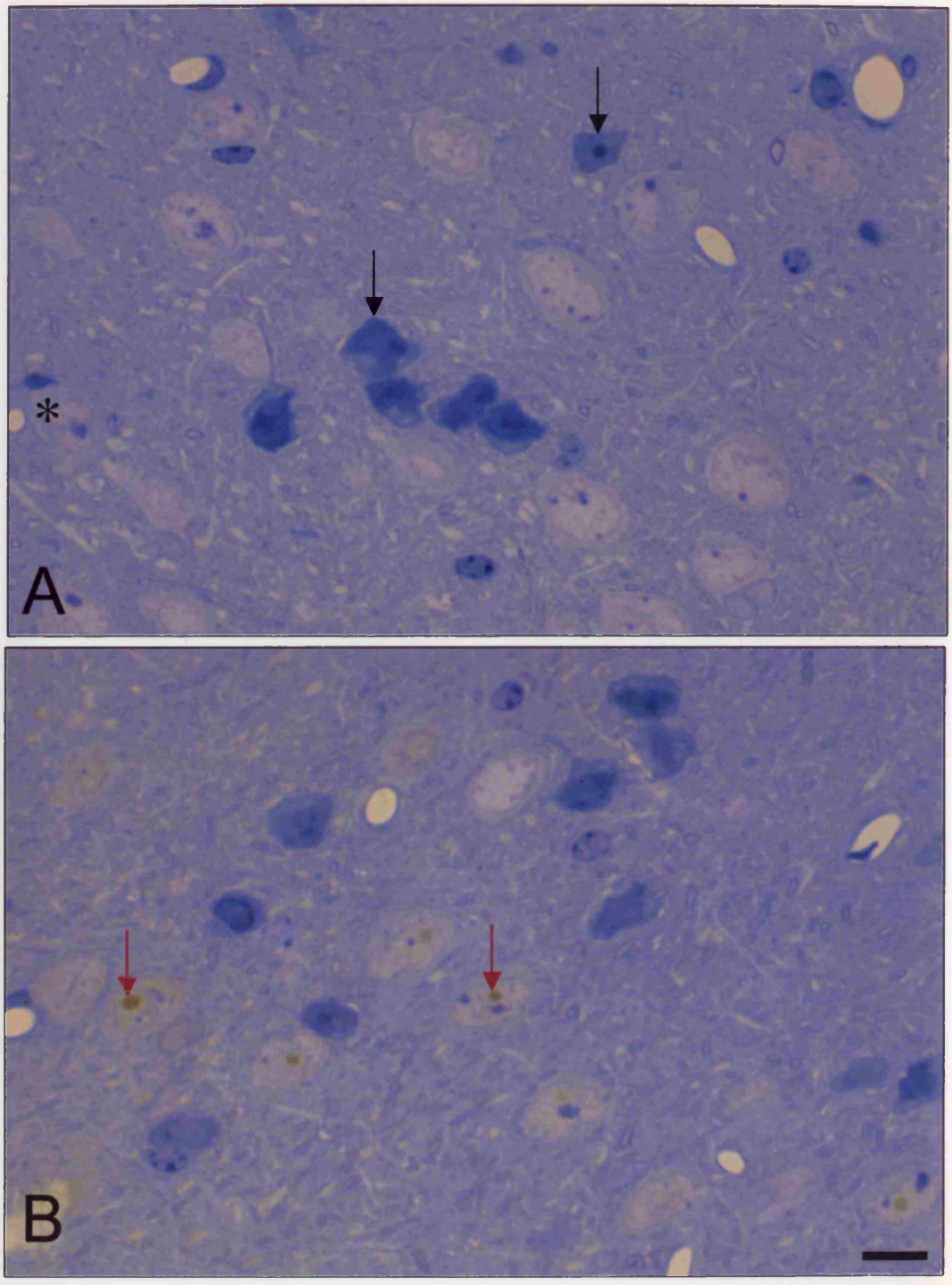

Figure 39 Toludine blue-stained semi-thin (1 µm) sections through the cingulate cortex of a 12 week old R6/2 mouse. A: unlabelled section. Degenerating neurons in early (asterisk) and late (arrows) stages. B: immunolabelled for N-terminal huntingtin. Inclusions identifiable by the presence of DAB staining (red arrows). Scale bar = 10µm

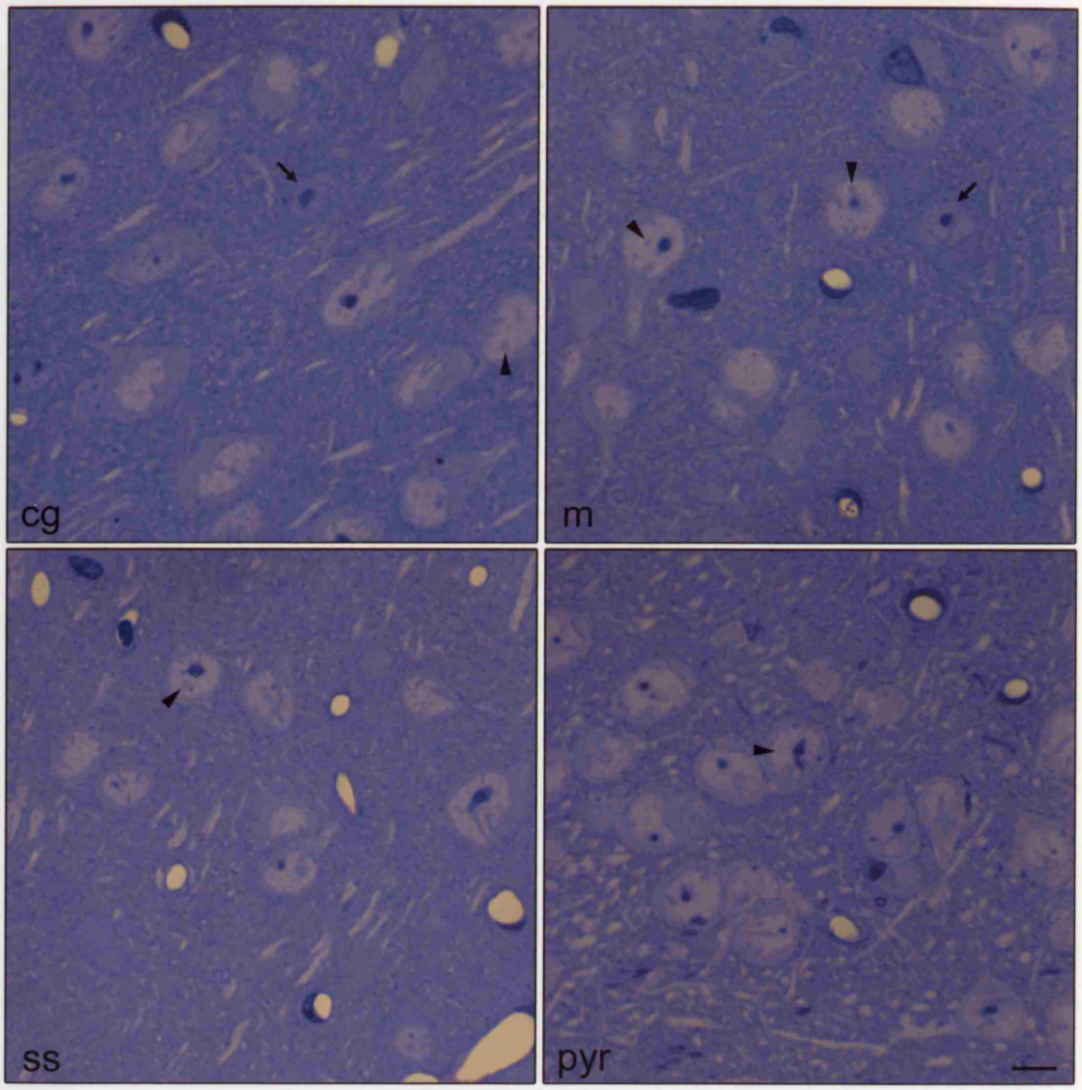

Figure 40 Toludine blue-stained semi-thin (1μm) sections through the cortical regions of a 10 week old R6/2 mouse. Cingulate cortex (cg), motor cortex (m), somatosensory cortex (ss) and pyriform cortex (pyr). Inclusions are visible in many neurons (arrowheads) and some cells show early signs of degeneration (arrows). Scale bar = 10μm

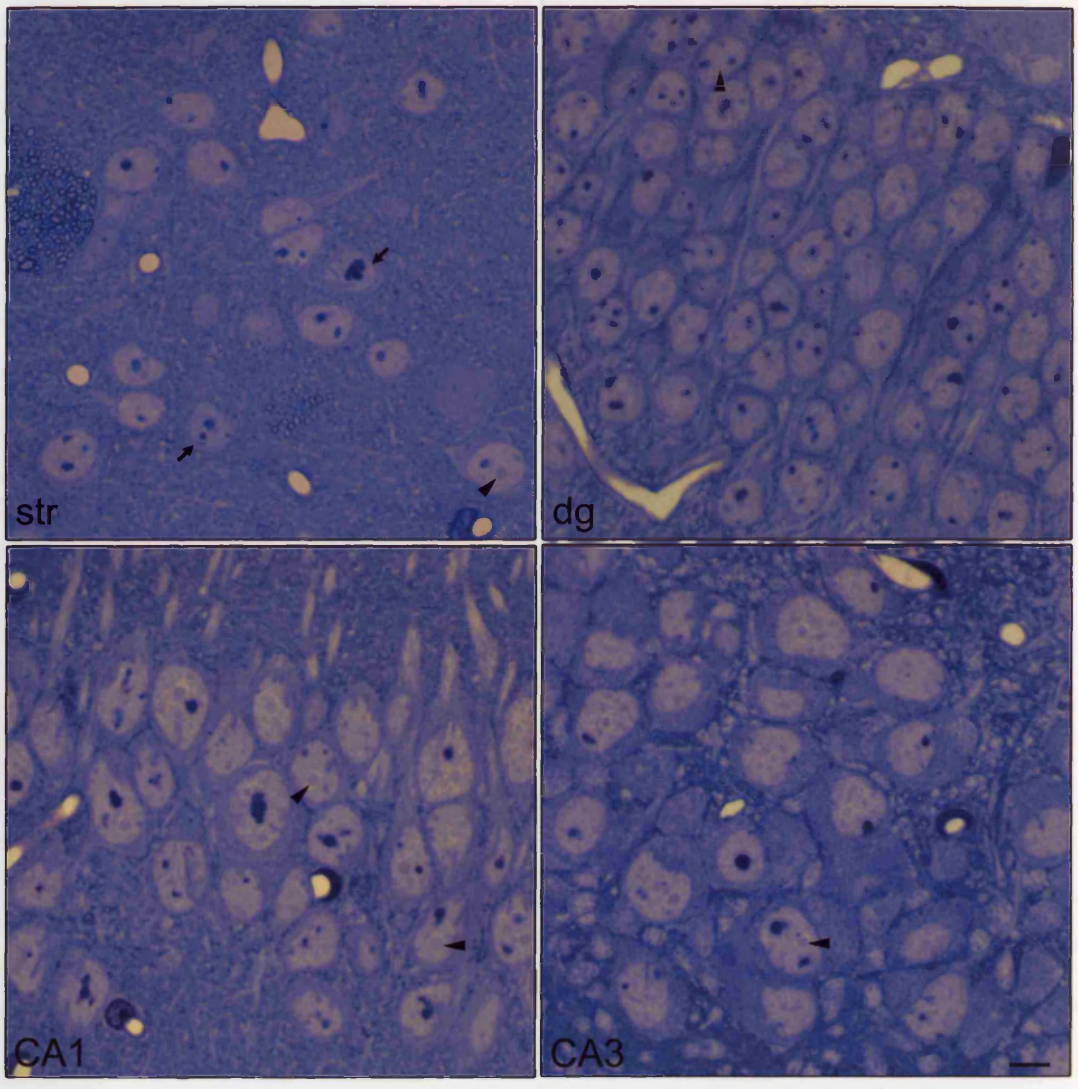

Figure 41 Toludine blue-stained semi-thin (1µm) sections through the subcortical regions of a 10 week old R6/2 mouse, Striatum (str), dentate gyrus (dg), hippocampal CA1 field (CA1) and hippocampal CA3 field (CA3),. Inclusions are visible in each region (arrowheads), but degenerative changes are only observable in striatal neurons (arrows). Scale bar = 10µm

normal, with the exception of the inclusion, which can be seen, unlabelled, at this level of examination (arrowheads). I have included micrographs of the cingulate & motor cortices and anterior striatum, which illustrate early condensation in isolated cells (arrows), but these are not representative samples. A representative sample of each area would should all neurons with large pale nuclei; rather these images represent extremes which are difficult to locate. Nevertheless, it can be said that whilst rare, these are the earliest changes seen in the R6/2 mouse.

At twelve weeks of age the situation is dramatically different, dark cells are abundant in the cingulate & motor cortices and frequent in the striatum. Rarely, they can also be found in the somatosensory cortex. Figures 42 and 43 are representative of that which is seen in these areas. Inclusions are visible unlabelled (arrowheads), and can be clearly seen within the neurons of the hippocampus and dentate gyrus in the complete absence of any degenerative changes.

3.1.4 Inclusions and Degeneration

Figure 44 presents a simplified summary of the results seen in this longitudinal study. It seems clear that the relationship between inclusion formation and degeneration is not absolutely causative. At the extreme, the largest inclusions are seen in the hippocampus, and yet within the lifespan of the R6/2 mouse, no hippocampal degeneration is seen. Within the cortex, inclusions are first apparent in the somatosensory cortex. Furthermore, the inclusions of the somatosensory cortex remain larger than those of the cingulate and motor cortices, and yet the bias of degeneration is heavily weighted towards these latter areas.

It must also be taken into account that the inclusions exist for many weeks before degeneration occurs. Indeed, there seems to be a sudden increase in the degree of degeneration in the last two weeks of the study. All cell types contain sizeable inclusions by six weeks of age, and yet the vast majority remain healthy in appearance until 10-12 weeks of age. As inclusion growth slows towards this time point, it could be that the cell loses its ability to isolate mutant htt_n to the inclusion. As

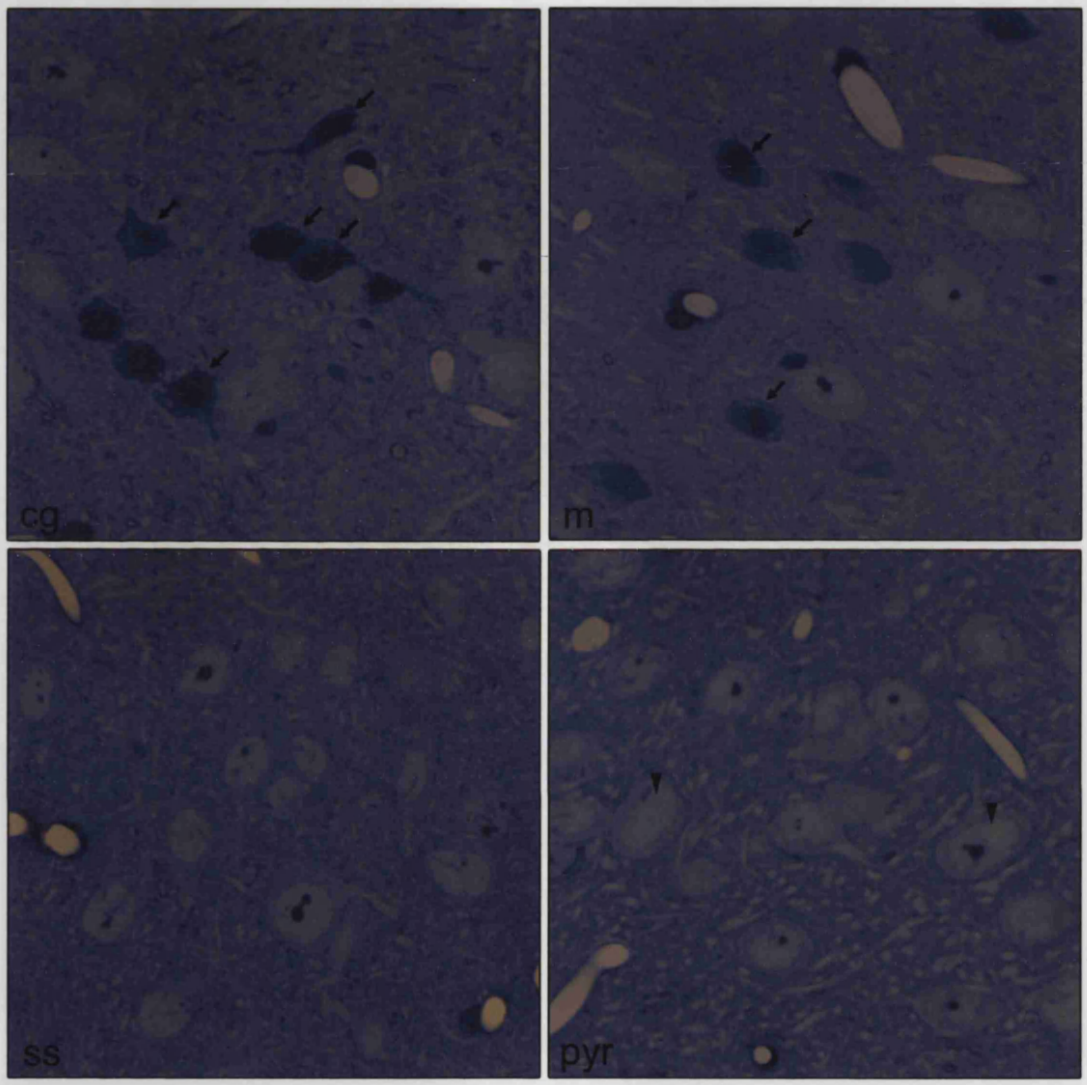

Figure 42 Toludine blue-stained semi-thin (1μm) sections through the cortical regions of a 12 week old R6/2 mouse. Cingulate cortex (cg), motor cortex (m), somatosensory cortex (ss) and pyriform cortex (pyr). The cingulate and motor cortices show degenerating neurons (arrows). Scale bar = 10μm

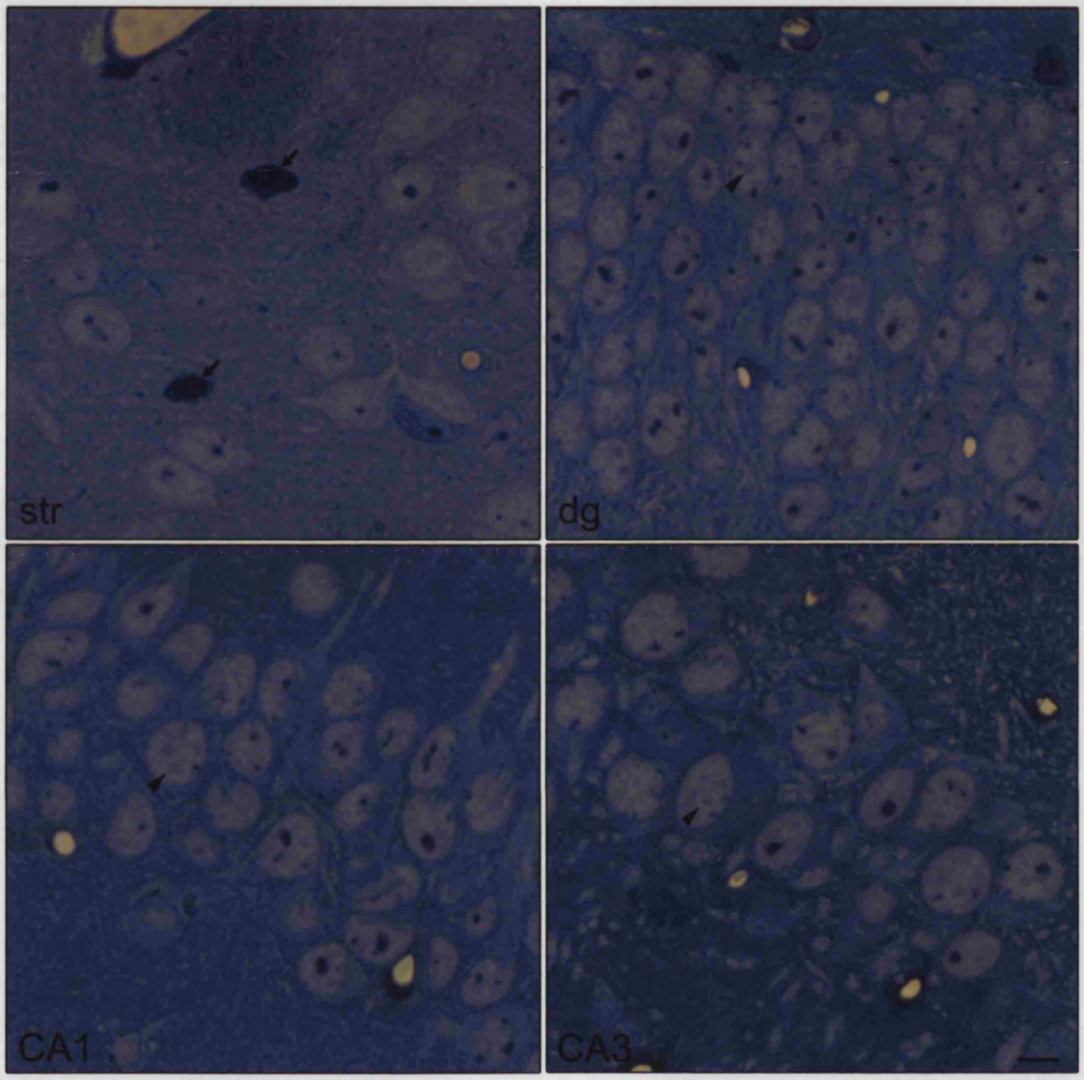

Figure 43 Toludine blue-stained semi-thin (1µm) sections through the cortical regions of a 12 week old R6/2 mouse. Striatum (str), dentate gyrus (dg), hippocampal CA1 field (CA1) and hippocampal CA3 field (CA3). Inclusions are evident in each section (arrowheads) but only the striatum exhibits degenerating neurons (arrows). Scale bar = 10µm

		Cortical area				Subcortical area			
Age (wk)		cg	m	ss	pyr	str	dg	CA1	CA3
4	Inclusions	✓	✓	✓✓	✓	✓✓	✓	✓✓	-
	Degen.	-	-	-	-	-	-	-	-
6	Inclusions	✓✓	✓✓	✓✓	✓✓	✓✓	✓✓	✓✓✓	✓✓
	Degen.	-	-	-	-	-	-	-	-
8	Inclusions	✓✓✓	✓✓✓	✓✓✓	✓✓✓	✓✓	✓✓	✓✓✓	✓✓
	Degen.	-	-	-	-	-	-	-	-
10	Inclusions	✓✓✓	✓✓✓	✓✓✓	✓✓✓	✓✓	✓✓	✓✓✓	✓✓✓
	Degen.	*	*	-	-	*	-	-	-
12	Inclusions	✓✓✓	✓✓✓	✓✓✓	✓✓✓	✓✓	✓✓	✓✓✓	✓✓✓
	Degen.	***	***	*	-	**	-	-	-

Figure 44 Table correlating inclusion formation and dark cell degeneration within cortical and subcortical areas. Inclusions refer to neuronal intranuclear inclusions and frequency & size are scored 0-3, 0 (-) representing no NII formation, 3 (✓✓✓) representing the maximum seen. Degeneration is similarly rated, 0 (-) representing no dark neurons, 3 (***) representing the maximum concentration of dark cells observed.

mentioned previously, this correlates with the increased appearance of neurite inclusions. Two possible conclusions can be drawn: that the NII is protective and the neurite aggregate is the toxic species; or that as the cell loses its ability to sequester htt_n, in either form of protective inclusion, the non-aggregated species is free to exert toxic effects.

3.1.5 The Ultrastructural Appearance of Apoptosis

The current theories on the nature of cell death in Huntington's disease are summarised in *1.8* and are discussed further, in light of this study, in *Chapter 4*. In short: the prevailing theories argue for an apoptotic mode of cell death in Huntington's disease. As apoptosis was first defined using morphological criteria (see 1.7) it seems appropriate to examine the morphological details of degeneration first.

Comparing results from the R6/2 mouse to published micrographs of 'classical apoptosis' is fraught with problems. For example, differences in preparation techniques may produce artefacts which are interpreted as real differences between accepted norms and results observed. Therefore, before beginning a detailed analysis of the ultrastructural changes of the R6/2 mouse, I sought to obtain images, prepared using identical techniques to those used for preparing R6/2 tissue, of classical apoptosis.

Apoptosis can be induced in a variety of ways, chemical or physical, and indeed, I have used X-ray induction of apoptosis in parts of this study. However, as these techniques are by definition harmful, one has no guarantee that the methods preserve the "natural" profile of death. Therefore, in order to obtain reliable ultrastructural data of classical apoptosis *in vivo*, I took what I considered to be the only viable approach: to locate developmental cell death (the original definition of apoptosis) in the mouse brain.

The overwhelming amount of developmental cell death in the mouse occurs pre-natally. Furthermore, as I wanted to prepare developmental tissue using identical methods to those used for adult R6/2 brain, sections had to be cut using a *Vibratome*.

This made it extremely difficult to prepare tissue from mice younger than 7 days old (P7). However, I successfully managed to cut several P5 and P6 brains and process the sections (200-300mm) for electron microscopy.

Not only is developmental cell death at this age rare in the mouse, but one must also take into consideration the fact that classical apoptosis is reported to be completed within a matter of hours. Thus, cells undergoing apoptosis are extremely difficult to find. P5/P6 sections were therefore first processed to the semi-thin stage and toludine blue revealed any pyknotic cells within each plane. As expected, for the majority of semi-thin sections there were no visible dying cells. However, very rarely, a darkened profile could be seen and the subsequent section was cut at the ultrathin level and viewed in the electron microscope.

Figures 45 through 48 represent the results seen in the P5/P6 wild-type mice, which correlate well with the published accounts on the appearance of apoptosis. Figures 45 and 46 illustrate the appearance of the majority of the (very few) cells seen. The cell is shrunken in size; and both the cytoplasm and nucleoplasm are condensed. In each figure the appearance of cytoplasm (and in fig. 45, nucleoplasm) in a healthy cell can be seen towards the periphery (black arrow). Chromatin (c) is seen to be condensed into large bodies, which are found against the nuclear periphery. The plasma membrane, conclusively in figure 45, has a 'scalloped' appearance, possibly corresponding to an early stage of the 'membrane blebbing' described as a feature of apoptosis. In the earlier stages, figures 45-47, the nuclear membrane is seen intact, and appears to remain so until quite late in the process.

The nucleolus in these cells appears to gradually fragment whilst the individual fragments themselves condense. Figure 47 shows an early stage of nucleolar fragmentation. The nucleolus (white arrowhead) mostly retains its traditional 'raspberry-like' structure, but the components of this structure appear considerably darker than those of the nucleolus of a healthy cell. Dissociated nucleolar fragments are also visible in figures 45 and 46 (white arrowheads) those in these cases the overall structure cannot be seen, possibly due to a greater degree of fragmentation. Certainly, by the very latest stages observed in these mice (figure 48) there is no identifiable nucleolus, however certain dark fragments are evident, distributed widely

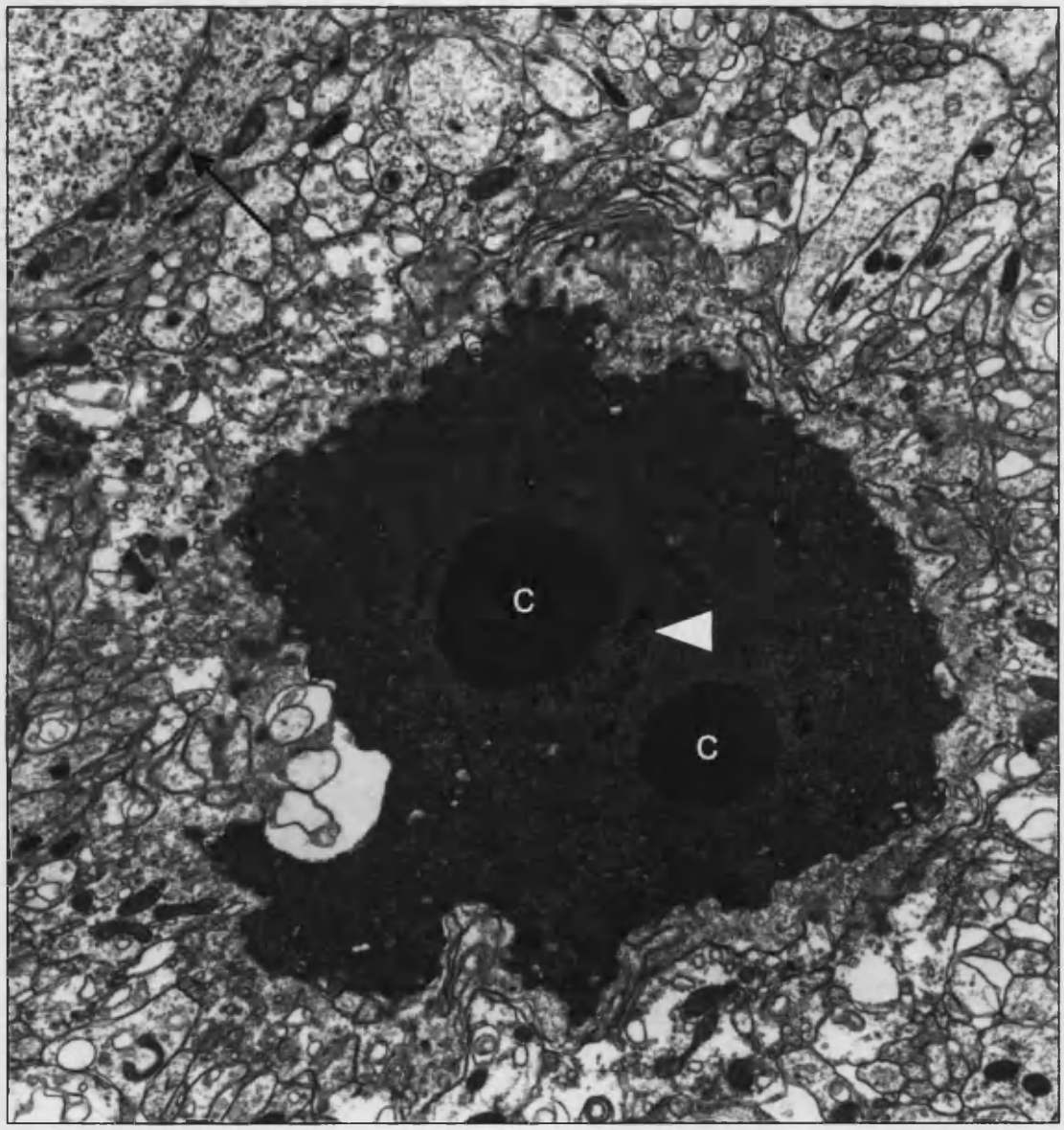

Figure 45 Electron micropgraph of an apoptotic cell in the brain of a P6 wild-type mouse. Note the ruffling of the plasma membrane, the condensation of the chromatin (C) and the loss of nucleolar structure (arrowhead). The degree of condensation of the cell is noted by comparison to the cytoplasm and nucleoplasm of a healthy cell (arrow).

Figure 46 Electron micropgraph of an apoptotic cell in the brain of a P6 wild-type mouse. Note the condensation of the chromatin (c) and the loss of nucleolar structure (white arrowheads). The degree of condensation of the cell is most notable by comparison to the cytoplasm of a healthy cell (black arrow). Autophagic activity is evidenced by the presence of autophagic vacuoles (white arrow) and multivesicular bodies (black arrowhead).

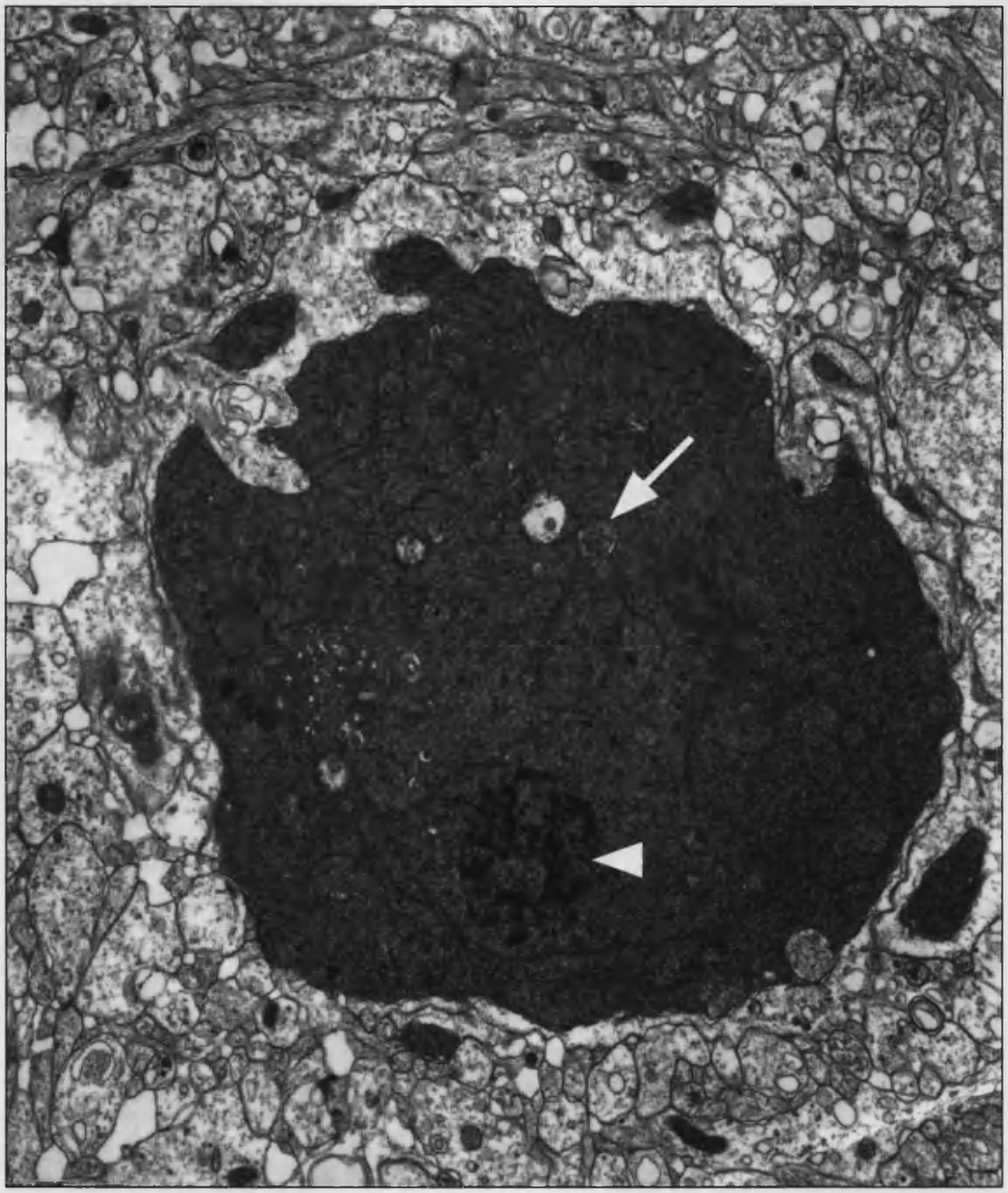

Figure 47 Electron micropgraph of an apoptotic cell in the brain of a P5 wild-type mouse. Note the loss of nucleolar structure (white arrowhead). Autophagic activity is evidenced by the presence of autophagic vacuoles (white arrow).

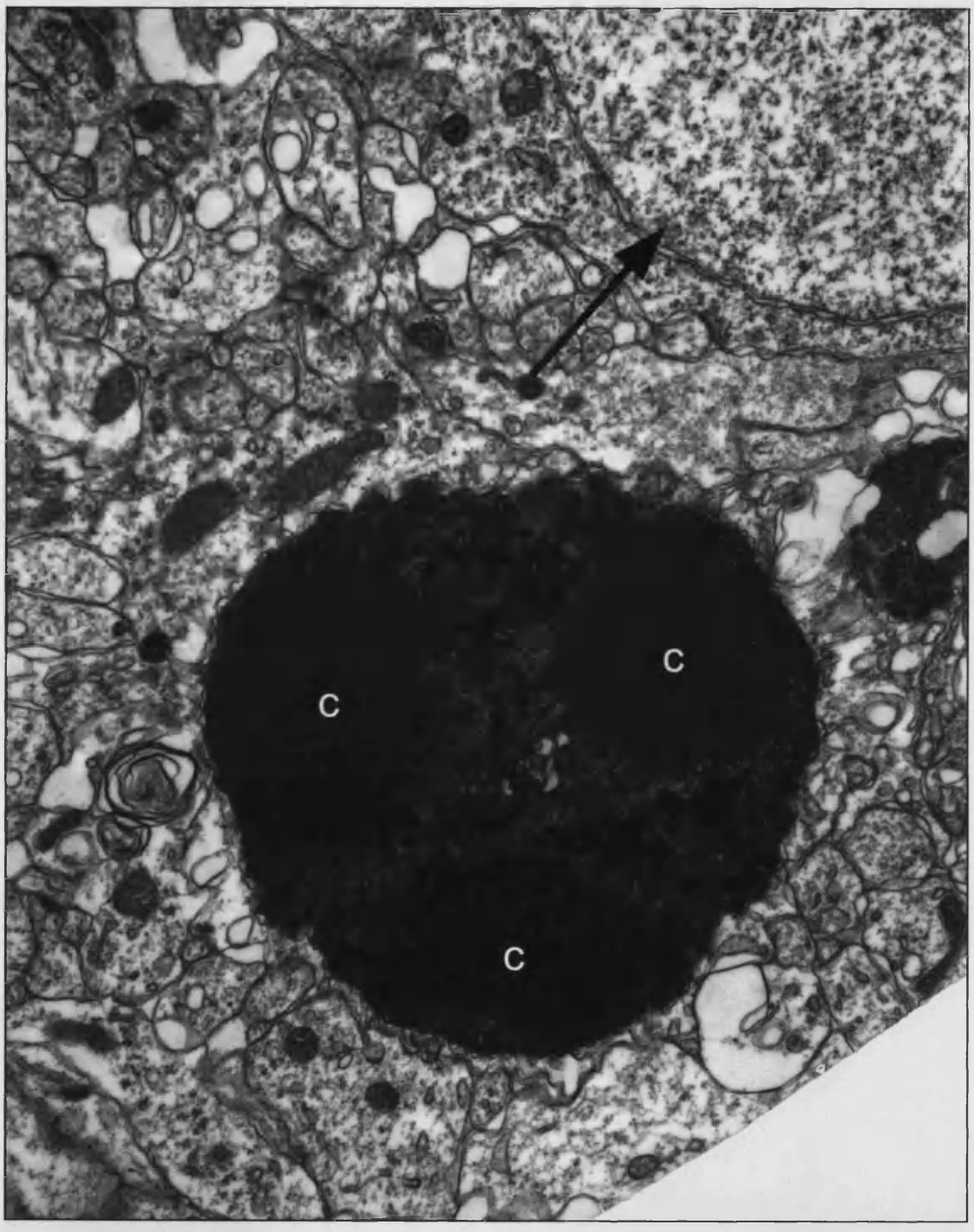

Figure 48 Electron micropgraph of an apoptotic body in the brain of a P5 wild-type mouse. Note the marginated chromatin clumps (c). The degree of codensation is noted by comparison to a healthy cell (arrow).

across the cell; even if these are nucleolar fragments it suggests a complete disintegration of the nucleolus. This latest stage also illustrates the persistence of the chromatin condensations (c) within a highly condensed structure possessing no nuclear membrane: the distinctive "apoptotic bodies" of programmed cell death. According to other reports of classical apoptosis, including the seminal paper, apoptotic bodies are said to be ultrastructurally well-preserved. However, the body in figure 48 has little identifiable internal structure. There appears to be some sort of membrane-bound organelle, or remnants thereof, in the centre of the body, but in contrast to previous reports one cannot locate any preserved mitochondria, for example.

One important feature to come out of this analysis is the evidence of autophagic activity within apoptotic cell death. In figures 46 and 47 one can see double membrane-bound structures containing other cellular constituents (white arrows); one can also identify multivesicular bodies (black arrowheads), both structures being associated with the endosome-lysosome pathway and autophagy. As discussed in *4.2*, it is becoming clear than autophagy and apoptosis are not entirely distinct processes. This evidence supports the notion that autophagic degradation of cellular components is involved in the apoptotic break-down of a doomed cell.

It is thus confirmed that apoptosis within the mouse brain produces an ultrastructural profile similar to those reported in other studies, particularly those that seek to define the nature of the process. Furthermore, as the EM preparation protocols within this study are unvaried, one can conclude that the preparation of tissue does not significantly alter the ultrastructural profile, rather that if classical apoptosis is occurring, these procedures are able to identify it.

3.1.6 The Ultrastructural Appearance of Degeneration

The most apparent ultrastructural feature of the R6/2 mouse central neurons is the intranuclear inclusion. They are visible without immunolabelling at relatively low magnifications due to their unique texture, which stands out against the background of

the nucleoplasm (figure 49, A). Needless to say, such inclusions are never found in tissue from control animals (figure 49, B). In the older mice in particular, the inclusion fills a remarkable percentage of the nuclear volume; correlating well with the immunohistochemistry presented in *3.1.2*. Figure 49, A also illustrates the second most evident feature seen in the R6/2, the invagination of the nuclear membrane (arrowhead). Within the cortex it is difficult to attribute nuclear membrane invagination to pathology as certain cortical neurons often show invaginations in control mice, however within the healthy striatum, cells exhibit a well-rounded nuclear profile (figure 49, B), thereby permitting the attribution of invagination to pathology. Figure 50 contains a striatal neuron from a 10-week R6/2 mouse exhibiting the first signs of change. The cell appears to be extremely healthy – in spite of the presence of the inclusion – with the exception of the first signs of invagination of the nuclear membrane (arrows).

As the pathological processes continue to exert their effects, the most notable change is the condensation of the cell. In section *3.1.3*, this condensation was used as the identifying characteristic of degeneration. Figure 51 contains a section of striatum in which two neurons in different stages of degeneration can be seen. Note that the NIIs seen in both are of comparable size (arrowheads) and yet the healthier cell is much larger and paler than the other. Note also that there is a greater degree of invagination of the nuclear membrane in the darker cell. Whilst this one image alone does not prove that invagination increases with time, as one can easily imagine a plane of section through a highly invaginated cell which would yield an image with a rounded nucleus, the number of sections viewed throughout this study (including those to be presented herein) allows one to say with good confidence that as the cell becomes darker, the number and severity of invaginations also increase.

Figure 52 illustrates three stages of degeneration within the R6/2 cortex. The most advanced neuron includes the apical dendrite and so appears larger, but if one takes the somata alone it is apparent that as the cell steadily darkens so too it shrinks. It should be noted that the nucleoplasm and cytoplasm darken at the same rate; however, throughout these stages the nucleus shrinks at a faster rate than the cytoplasm, such that as degeneration progresses the ratio of cytoplasm (within the

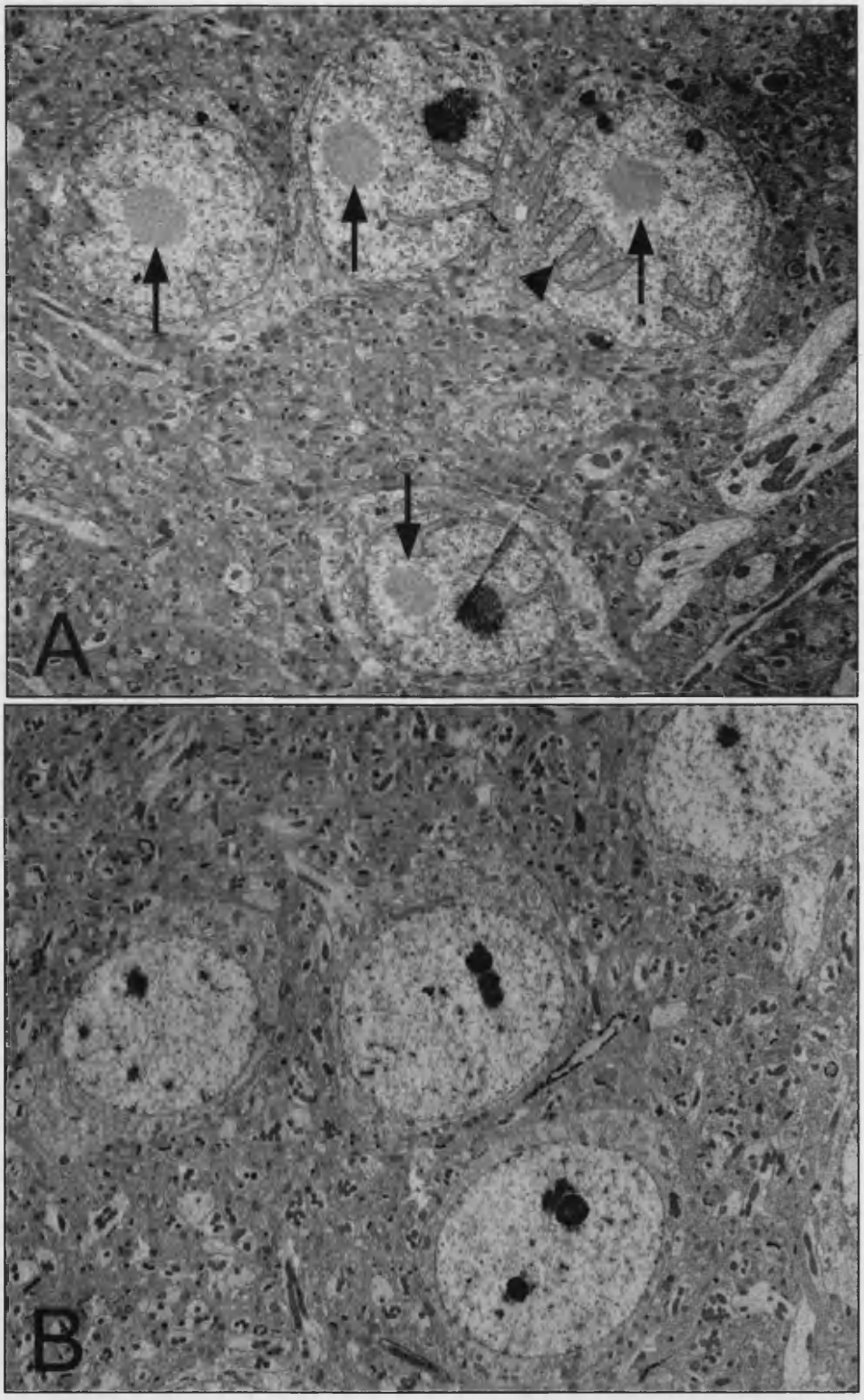

Figure 49 Electron micropgraphs of striatal neurons from a 17 week-old R6/2 mouse (A) and a 10 week-old wild-type mouse (B). Note the intranuclear inclusions (arrows) and invagination of the nuclear membrane (arrowhead) in the R6/2 neurons.

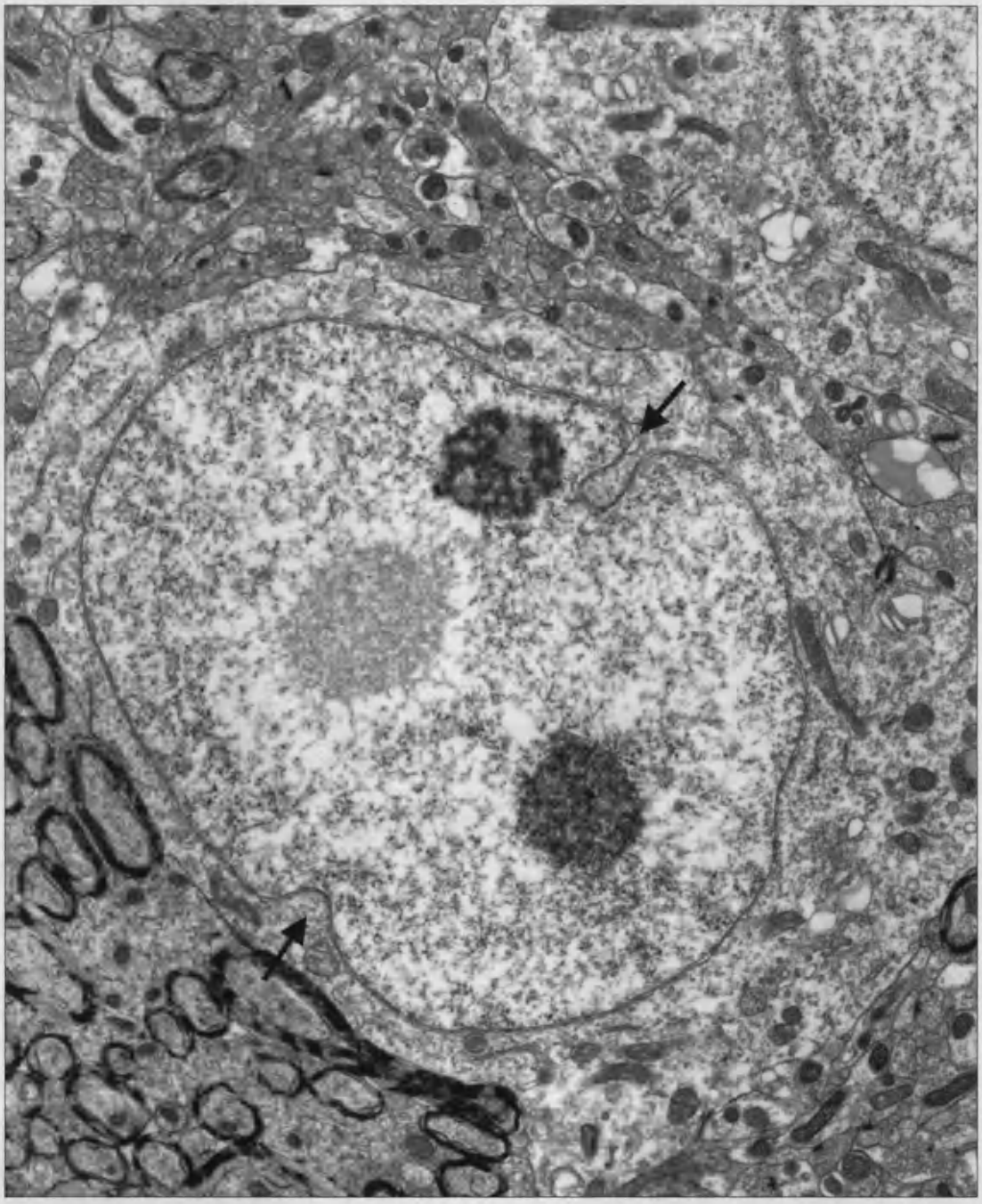

Figure 50 Electron micrograph of a striatal neurons from a 10 week-old R6/2 mouse. The first signs of pathology, invaginations of the nuclear membrane are evident (arrows).

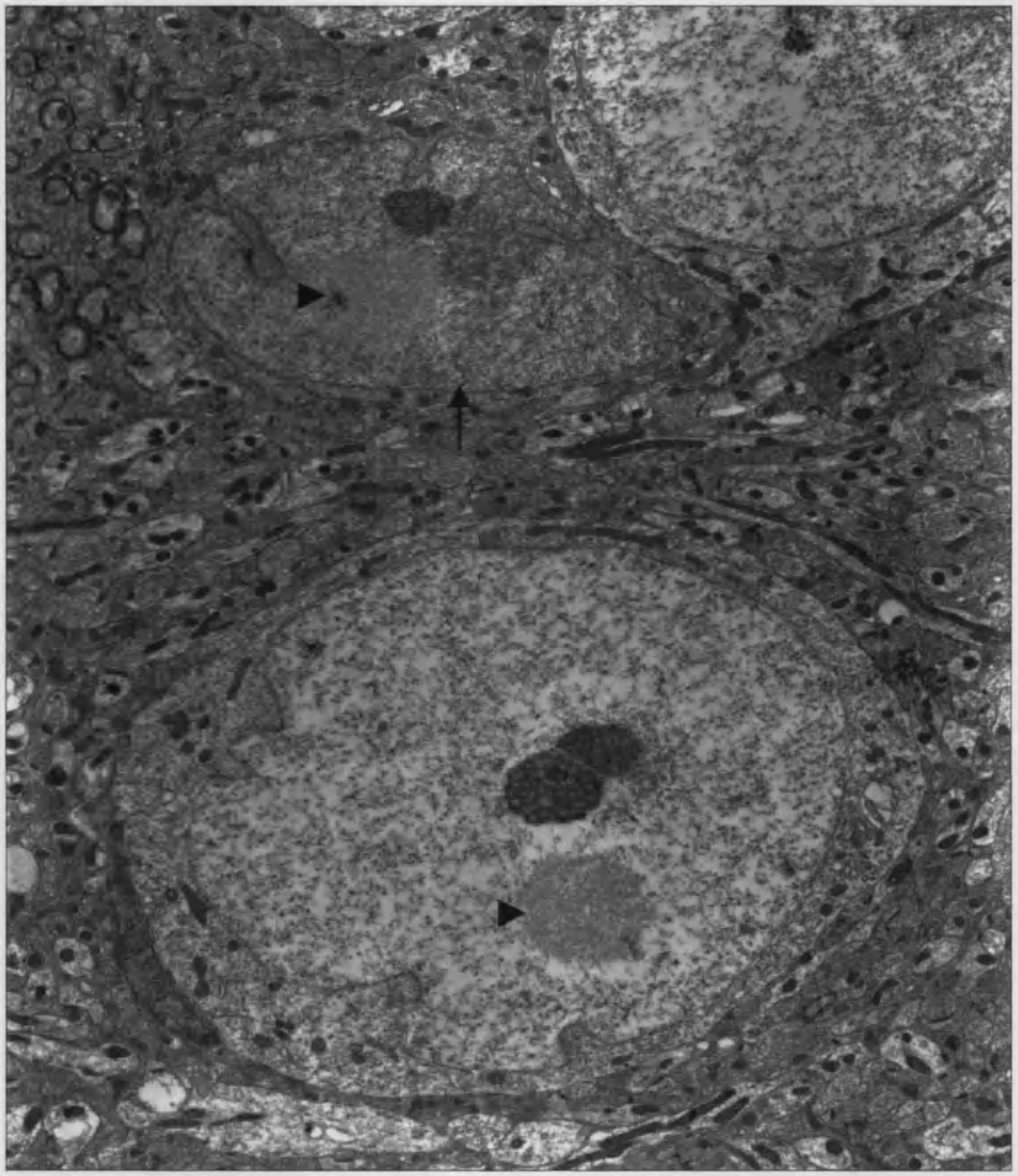

Figure 51 Electron micrograph of striatal neurons from a 12 week-old R6/2 mouse. Note the neuronal intranuclear inclusions (arrowheads) which become less distinguished as cells darken (arrow).

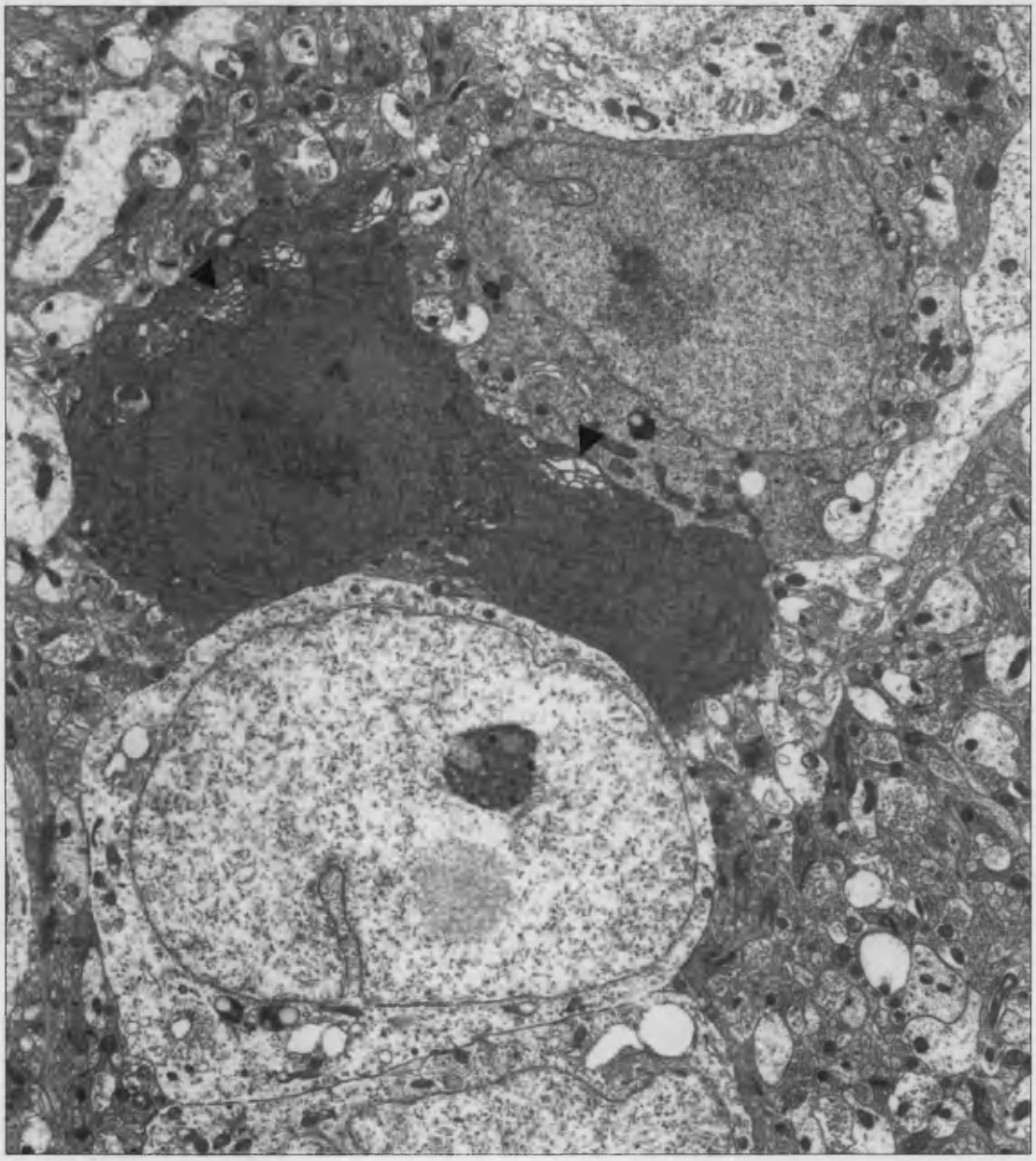

Figure 52 Electron micrograph of cortical neurons from a 12 week-old R6/2 mouse. Note the dilation of golgi / endoplasmic reticulum, most apparent in the most condensed neuron (arrowheads).

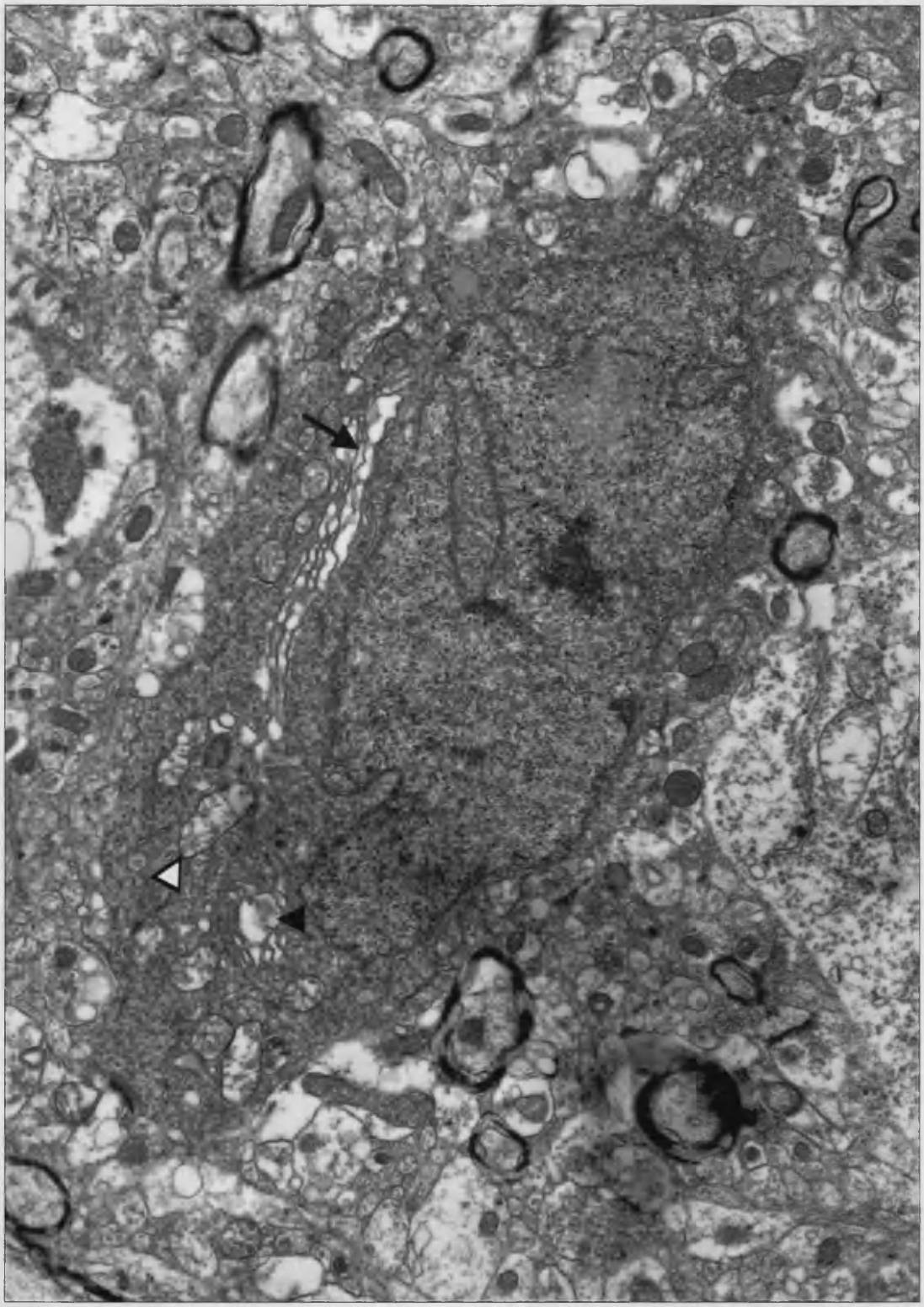

Figure 53 Electron micrograph of a cortical neuron from a 13 week-old R6/2 mouse. Note the dilation of the endoplasmic reticulum (arrow), golgi apparatus (solid arrowhead), and mitochondia (open arrowhead).

soma) to nucleoplasm is biased to favour the former. One explanation for this may be the dilation of cytoplasmic organelles, which in figure 52 is seen most clearly in the darkest cell (arrowhead).

The dilation of organelles can be seen even more strikingly in figure 53. This cortical neuron, from a 13-week R6/2 mouse, contains dilated endoplasmic reticulum (arrow), golgi apparatus (solid arrowhead) and mitochondria (white arrowheads). There is always the possibility that such dilatory changes are an artefact from perfusion and processing, however, given that it is seen as a consistent feature from each R6/2 mouse to the next this is unlikely. Furthermore, figure 54 is a high-power micrograph showing parts of two adjacent cells in the R6/2 striatum, one in the latter stages of degeneration and the other merely showing early nuclear membrane invagination. Golgi apparata (arrow) in the degenerating cell are markedly dilated; the mitochondria (arrowheads) even more so. Indeed, many of the mitochondria of the degenerating cells in both figures 53 and 54 appear not only to be dilated but also to be losing internal structural integrity. Whilst the outer membrane of the mitochondria remains intact, the inner membrane – forming the cristae – loses its defined structure and may in some cases even fragment. This is also illustrated in figure 55, where the mitochondria of the dark cell can be compared to those in the adjacent neuropil (open arrowheads). Figure 55 also illustrates another key feature of the R6/2 neuronal degeneration: the involvement of the lysosome/autophagosome and the build-up of lipofuscin.

In the previous section I mentioned the presence of autophagic profiles within cells undergoing apoptosis. Such profiles are also evident with degenerating R6/2 neurons. As discussed in 4.2, the distinction between lysosomal-based cellular turnover and autophagy is somewhat arbitrary, but breakdown of cellular components remains at the basis. There appear to be four general types of profile seen in these cells. The first is the *multi-vesicular body* (MVB), a single membrane-bound structure containing a number of small vesicles, as shown in figure 56 (solid arrowheads). The second profile is that of the classical lysosome; a single membrane-bound structure containing homogenous material, most probably resulting from the proteolysis of the contents, as illustrated in figures 56 (blue arrowhead). The relationship between these first two

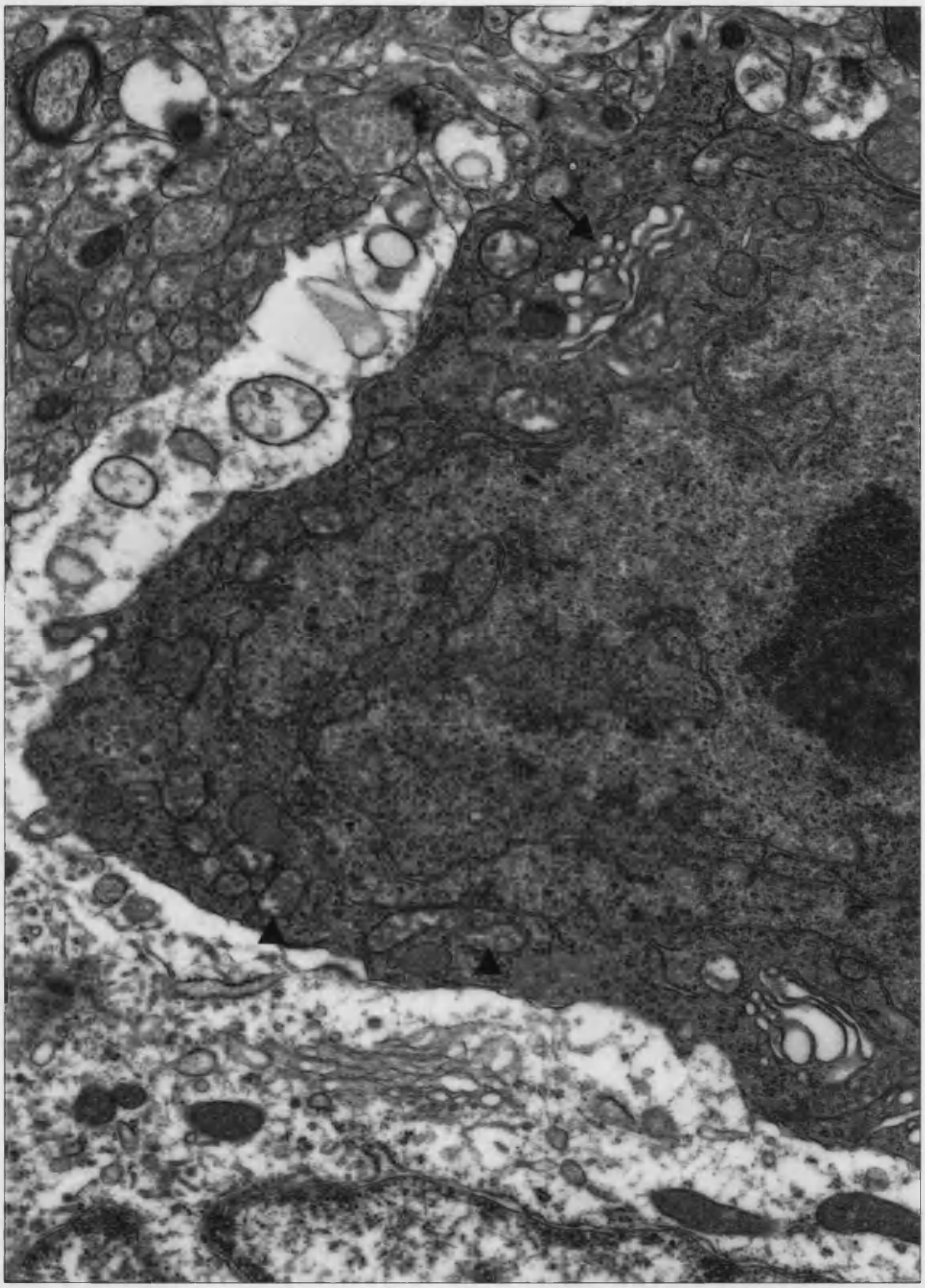

Figure 54 High-magnification electron micrograph of adjacent striatal neurons from a 13 week-old R6/2 mouse. In the dark cell, note the dilation of the golgi apparatus (arrow), and mitochondia (arrowheads).

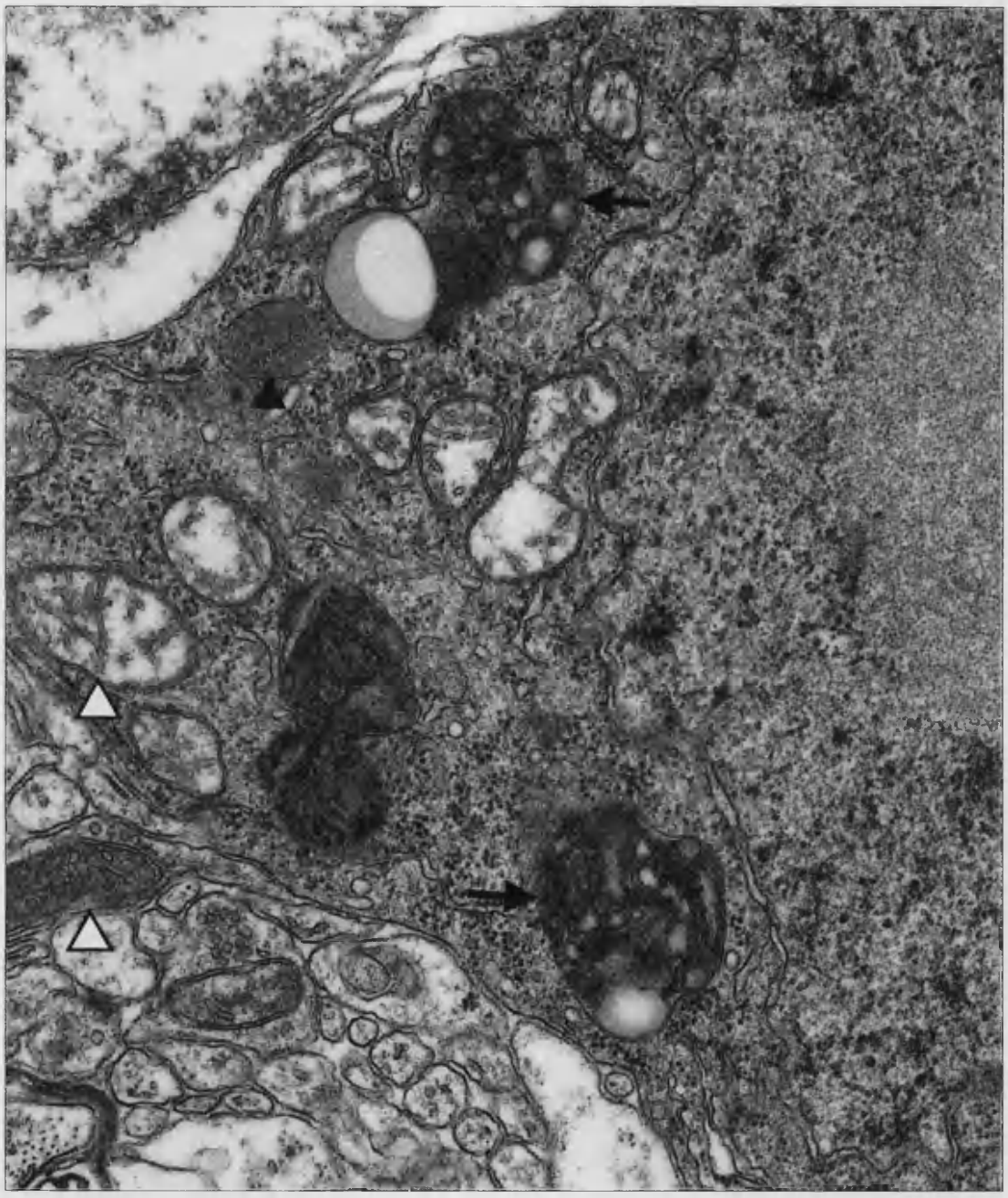

Figure 55 High-magnification electron micrograph of a cortical neuron from a 17 week-old R6/2 mouse. The dilation of mitochondria in the degenerating neuron is noted by comparison of its mitochondria with those in the neuropil (open arrowheads). Note the evidence of lysosomal activity (solid arrowhead) and the accumulation of lipofuscin (arrows)

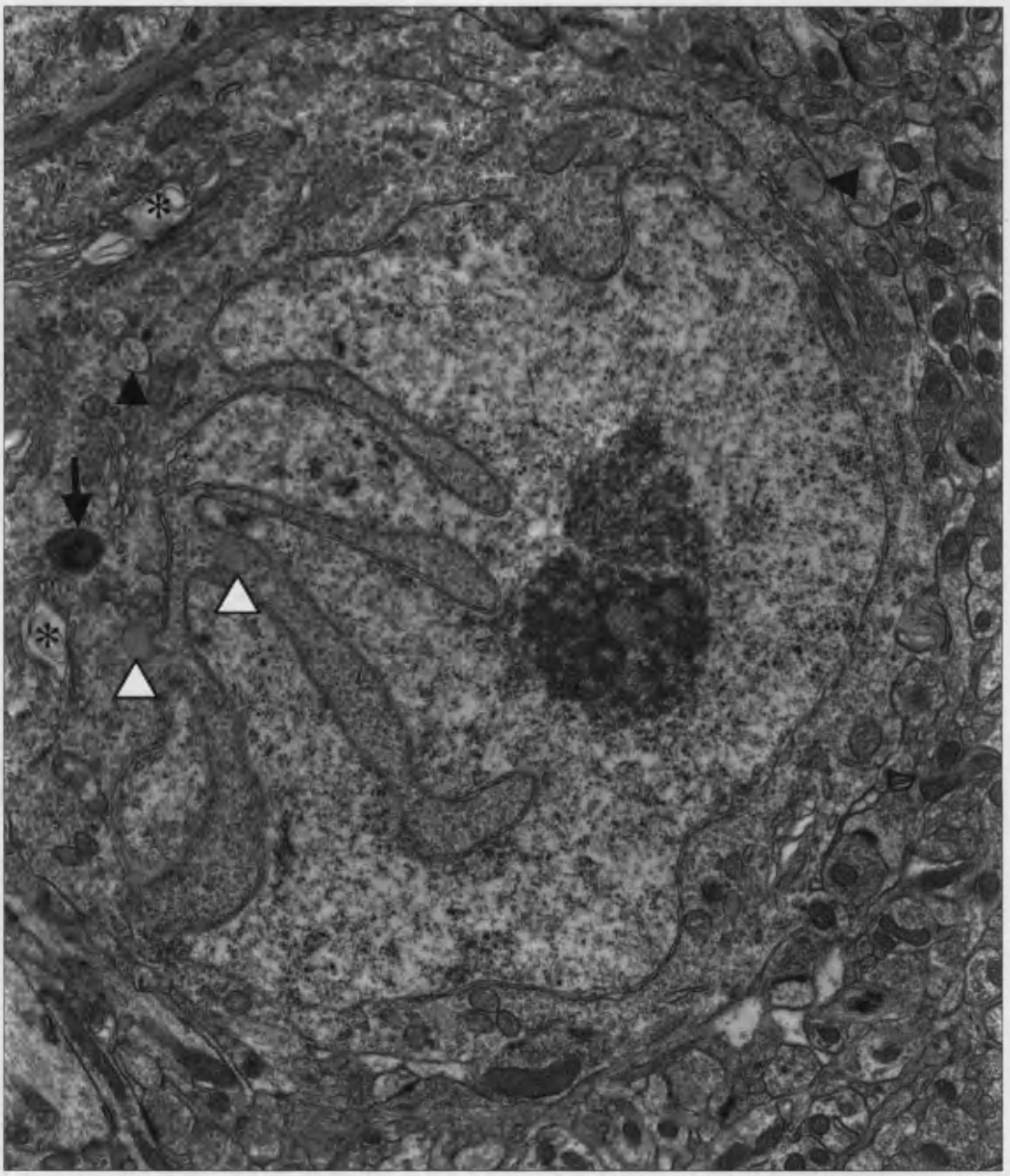

Figure 56 Electron micrograph of a cortical neuron from a 13 week-old R6/2 mouse. Autophagic processing is occuring as indicated by the presence of multivesicular bodies (solid arrowhead), autophagic vacuoles (open arrowheads), lysosomes (blue arrowhead) and accumulation of membranous material (arrow).

classes of lysomsomal/autophagic profiles and the latter two remains under debate. As will be discussed, lysosomes and MVBs exist in healthy cells; a general turnover mechanism without the specificity of the ubiquitin-proteasome system. However, the second two classes are considered more to be a part of traditional autophagy rather that constitutive lysosomal turnover.

The third profile is the autophagic vacuole, or autophagosome: a double membrane-bound structure believed to originate from the endoplasmic reticulum, visible in figure 56 (open arrowheads). Such structures often contain further layers of membrane, forming multi-lamellar bodies, though they may contain anything from homogenous cytoplasm to entire mitochondria.

The final class is the most prominent: the membrane whorl. This is a single membrane-bound structure containing an accumulation of membranous material, and variable amounts of the protein component of lipofuscin. The size and shape of each of these structures varies, as does the degree of condensation; but the defining characteristic remains the same: the laminar appearance of the membranous component, as seen in figure 56 (arrows). Clearly visible in figure 55 is the fact that the lipofuscin protein component within the autophagic whorl is contained within its own single-membrane. This raises the possibility that as the autophagic contents are processed, the membrane and protein components are isolated to distinct storage sites. How these structures are formed also remains under debate. It is clear that there is a great amount of membrane within each structure, suggesting an accumulation rather than a single processing event. Figure 57 contains examples of the early double-membrane structures (solid arrowhead) as well as the persistent membrane whorls (arrow). In support of the formation of autophagosomes from ER and Golgi, many autophagosomes are seen to form in the vicinity of a very prominent and somewhat dilated reticular network (asterisks)(see *also* figure 56, asterisks). The shape of the labelled membrane whorl is representative of many seen: a variable number of 'lobes' within a single membrane-bound structure. This suggests that the large whorls seen result from the fusion of a number of smaller autophagosomes, a processes familiar in lysosomal processing.

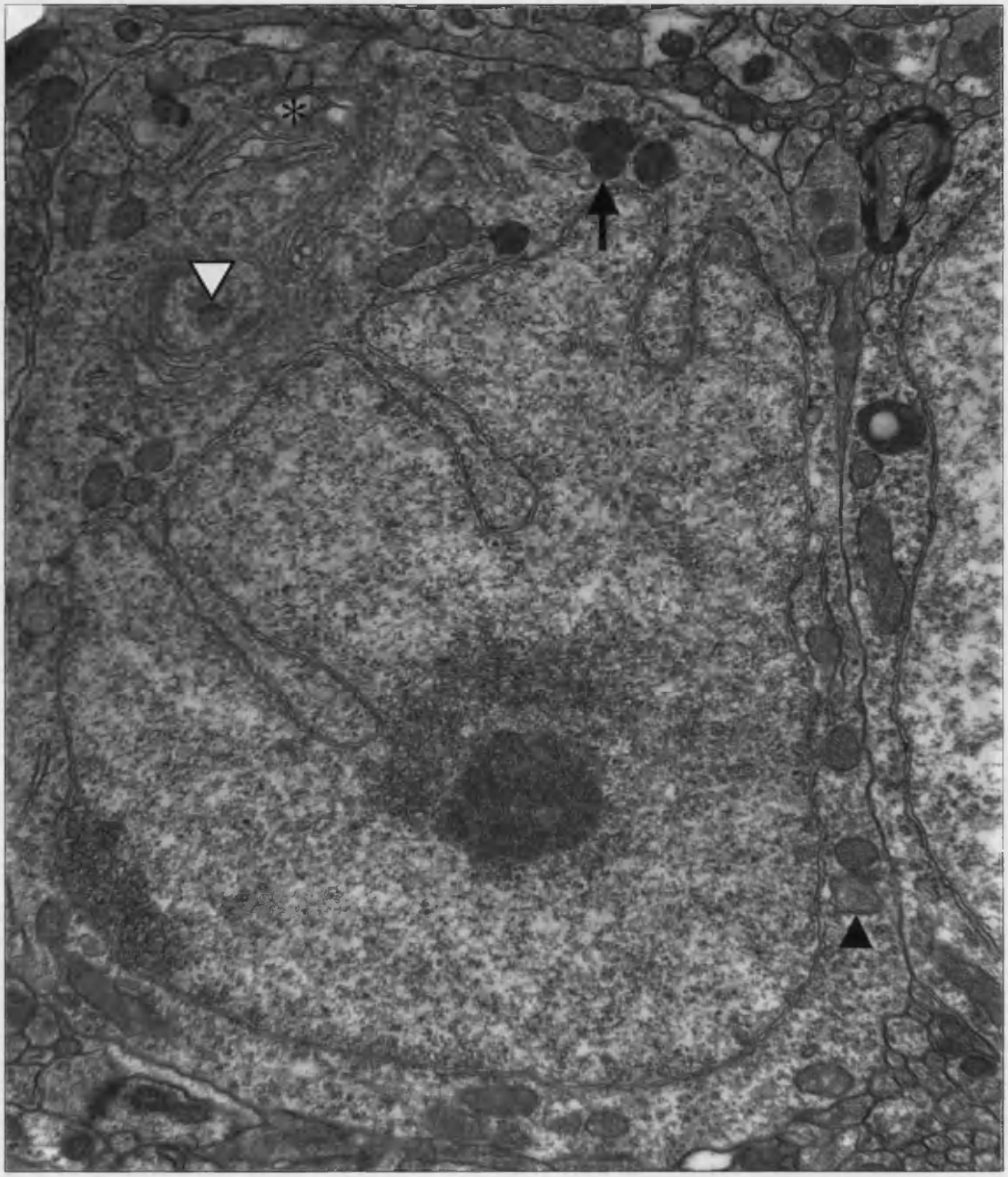

Figure 57 Electron micrograph of a cortical neuron from a 10 week-old R6/2 mouse. Autophagic vacuoles have formed (arrowheads), possibly originating from the endoplasmic reticulum and/or Golgi apparatus (asterisk). The sequestered product is degraded leaving membranous material, which, most probably, accumulates trough the fusion of product-filled autophagic vacuoles and lysosomes, yielding the multi-lobed structure seen here (arrow).

Figure 57 also acts as acts as an example of a further change seen in this form of degeneration. Whilst the nuclear membrane persists even unto the end stages (as shall be shown) following invagination, it begins to adopt a 'ruffled' appearance. In figure 57 this is most noticeable in the outer membrane of the nuclear envelope. As this occurs after onset of invagination and concomitant with nuclear shrinkage, the ruffling may simply be a consequence of these events. However, Mark Turmaine has conducted freeze-fracture analyses of the R6/2 nuclear membrane and has found an increase in the density, and presumably number, of nuclear pores (Davies *et al.* 1999). There are also reports of mutant huntingtin being associated with the nuclear membrane, therefore it is possible that htt_n disrupts cytoplasmic-nuclear transport leading to the increase in pores, membrane ruffling and invagination. Similar changes are also seen in the plasma membrane, particularly in the later stages of degneration, though this may also simply be a consequence of cell shrinkage.

One of the changes most difficult to characterise is the alteration of the nucleolus. Elizabeth Slavik-Smith is currently undertaking a detailed study of the subnuclear changes in the R6/2 mouse, including an analysis of the molecular components of each of the nuclear bodies, including the nucleolus, and her results will no doubt shed considerable light on these changes. On a gross, morphologic level, I have observed a general loss of definition of the nucleolus. Figure 58 contains examples of both wild-type and R6/2 nucleoli. There is a great degree of variation in the appearances of the wild-type nucleoli alone, but each seems more defined than their R6/2 counterparts. One can more easily identify the component regions of the nucleolus – the *fibrillar centres* (open arrowhead) surrounded by the *dense fibrillar component* (solid arrow), the *granular component* (open arrow) and the *perinucleolar cap* (solid arrowhead) – in the wild-type examples. However, the nucleolus, and often its substructure (particularly the fibrillar centres) remains evident in dark neurons even unto the most advanced stages of degeneration (F). Furthermore, the perinucleolar cap appears to be enlarged in degenerating neurons (58, D-E); though wild-type nucleoli can also show extremely large perinucleolar caps (C). Importantly, the changes seen in the nucleoli of the R6/2 certainly do not resemble those show to occur during apoptotic cell death. As illustrated in figure 47, the neuronal nucleus

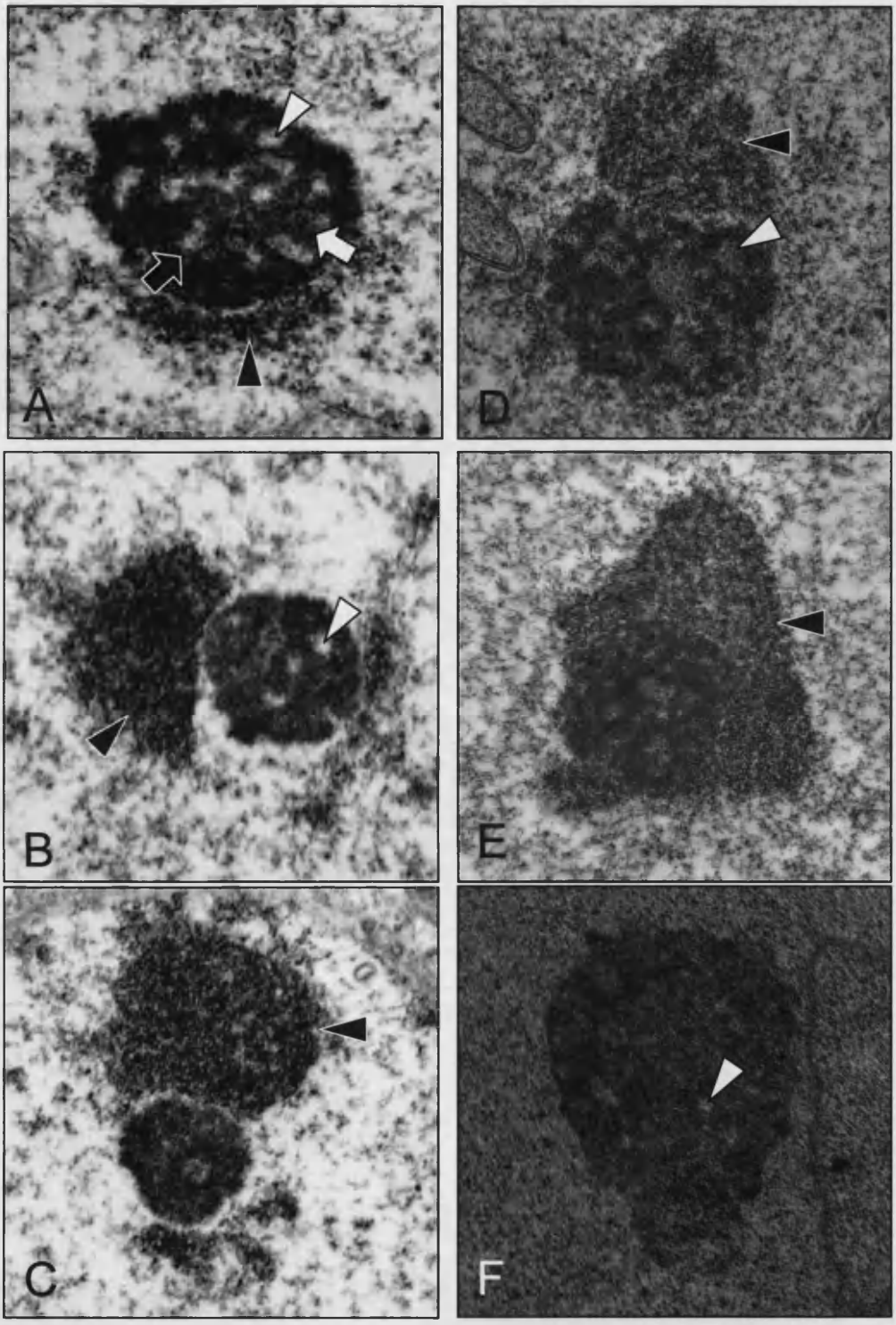

Figure 58 Nucleoli from wild-type (A-C) and R6/2 (D-F) mice. The wild-type nucleolus substructure consists of the *granular component* (open arrow), and *dense fibrillar components* (solid arrow) surrounding the *fibrillar centres* (open arrowhead). It is bordered by the *perinucleolar cap* (PNC)(solid arrowhead). R6/2 neuronal nucleoli generally show a more diffuse, less defined structure; though the components are still visible (D) even unto the darkest stages (F). The PNC often appears enlarged in the R6/2 (E), though wild-types may also possess large PNCs (C).

during apoptosis appears to condense down into its individual components before disintegrating.

One further change observed in these mice is the relocation of the Cajal body (also known as the coiled body). The Cajal body (CB) is so called as it was first identified by Ramon y Cajal. In spite of long time since its identification, its function still remains under debate. It is currently believed to be involved in snRNP maturation and/or transport (see Ogg & Lamond 2002 *for review*). Given its size (0.15 to 1.5μm in diameter), it is rarely caught within 70nm EM preparations, but can readily be identified in 5-10μm toludine blue-stained sections, as illustrated in figures 40 (ss, arrowhead) and 41 (CA3, arrowhead). The feature to note is that the CB is usually seen in association with the NII in R6/2 mice, far too frequently to be a chance occurrence. In wild-type tissue, the CB is normally nucleolar-associated or free in the nucleoplasm. The relocation to the NII is confirmed in ultra-thin sections that do happen to include the CB, such as seen in figure 59. Figure 59 indicates that the CB (arrowhead) associates with the NII (arrow) even when in close proximity to its normal partner, the nucleolus.

As previously described, the degenerating cells continue to darken as the pathological process continues. Figure 60 is a section through a 17-week R6/2 cortex showing two cells in the late stages of degeneration. Also in section is a relatively healthy cell, which shows only the presence of an NII (open arrowhead) and a mild invagination of the nuclear membrane (solid arrowhead). The differences in densities of cell content are quite striking. In the dark cell at the top of the figure the NII is still discernible (open arrowhead). Even at this level of condensation, mitochondria and Golgi apparatus are still structurally intact, although still dilated. The extent to which organelles persist is even more evident in the high magnification of the second degenerating cell: figure 61.

This cell has been sectioned towards one extreme of the nucleus (asterisk) and as a result an NII is not present. Nevertheless this section affords a relatively large sample of degenerating cytoplasm. Mitochondria are still present, and whilst dilated, given that they maintain external structure and some degree of internal structure one can presume that they are functional (open arrowhead). It is also important to note

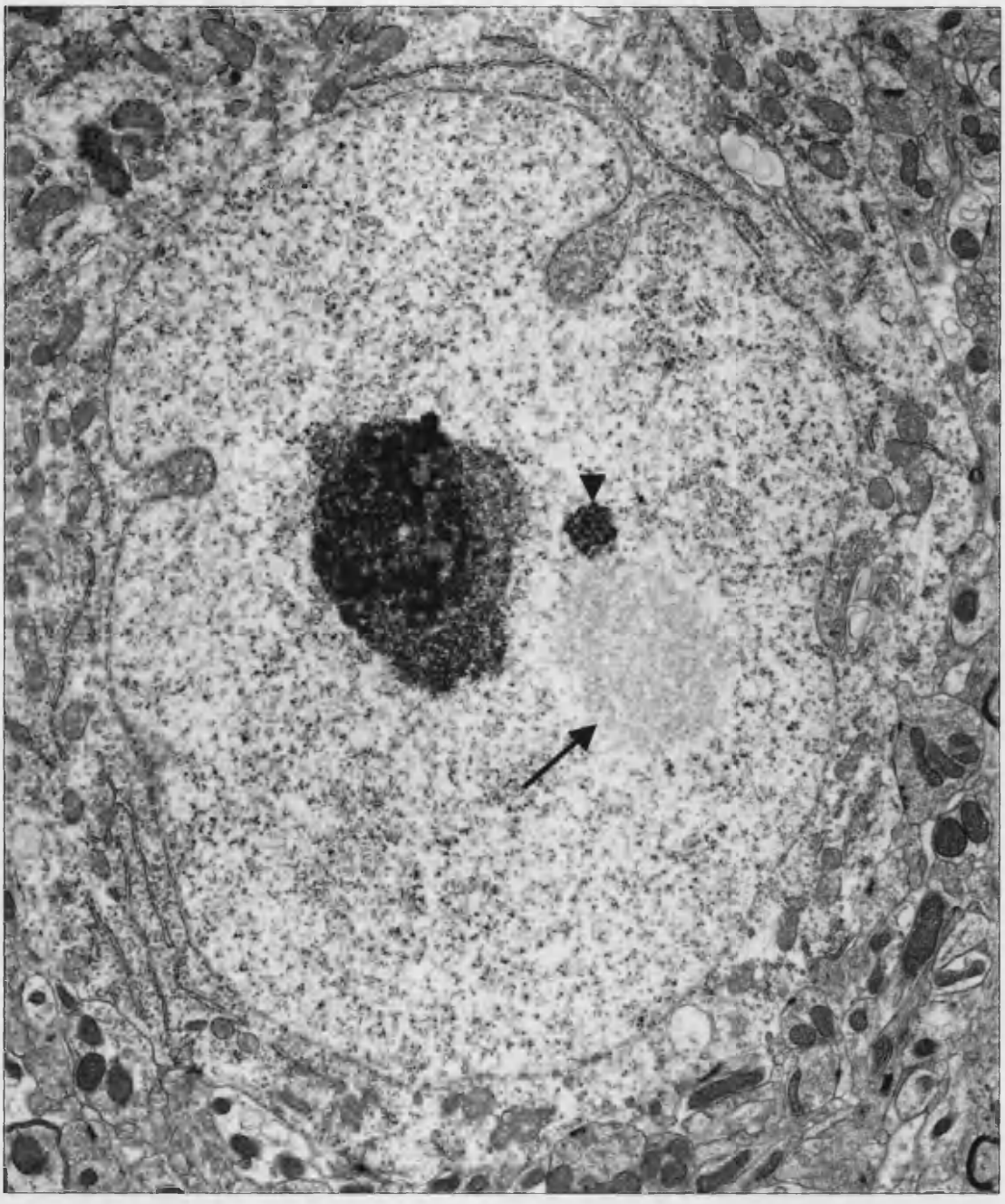

Figure 59 Electron micrograph of a cortical neuron from a 13 week-old R6/2 mouse. Even at this early stage in the degenerative process the Cajal body (arrowhead) has become associated with the intranuclear inclusion (arrow).

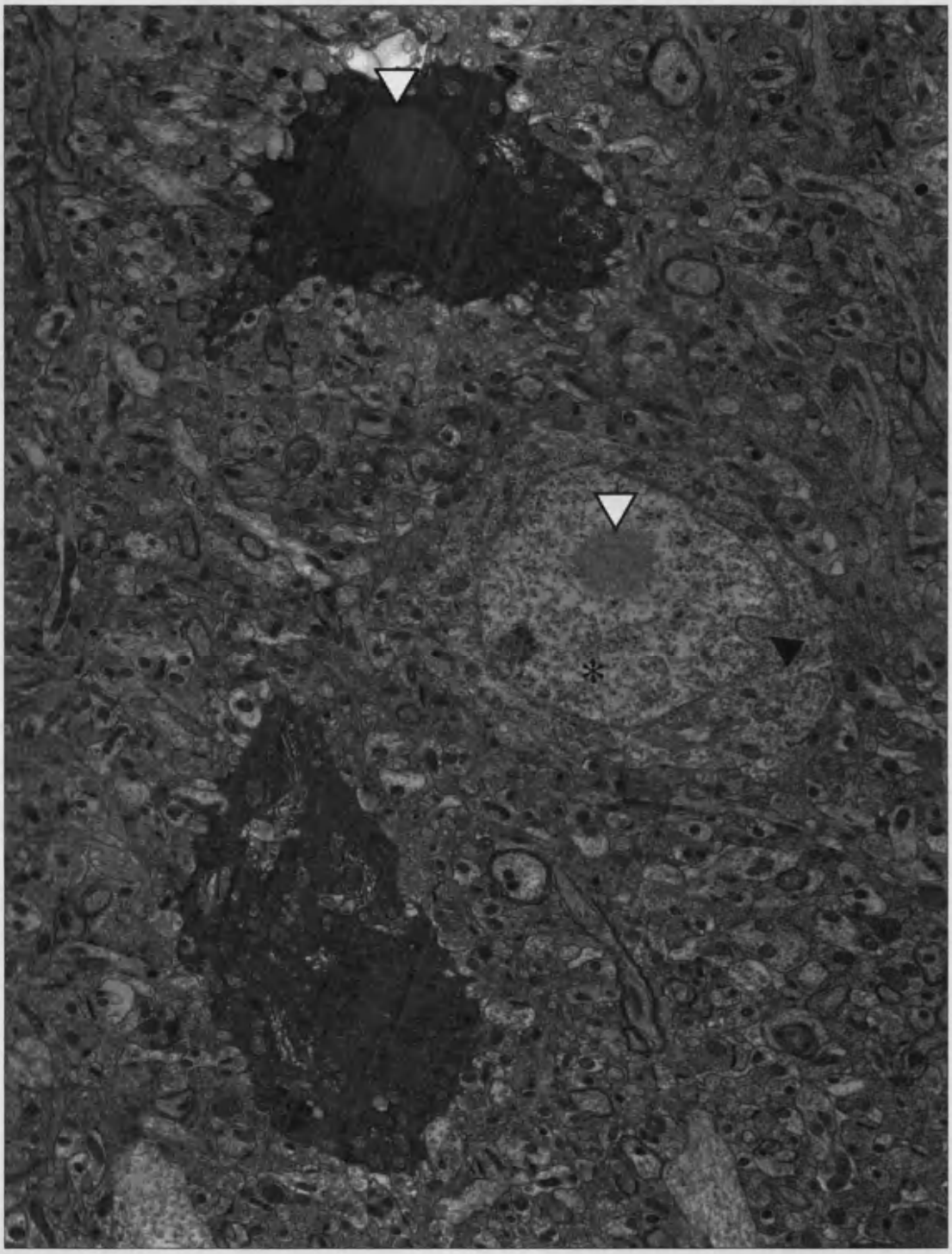

Figure 60 Electron micrograph of a section through the cortex of a 17 week-old R6/2 mouse. Two cells in the most advanced stages of dark cell degeneration are visible together with a cell showing the very earliest signs of change, including membrane invagination (solid arrowhead). Inclusions are evident at both extremes (open arrowheads).

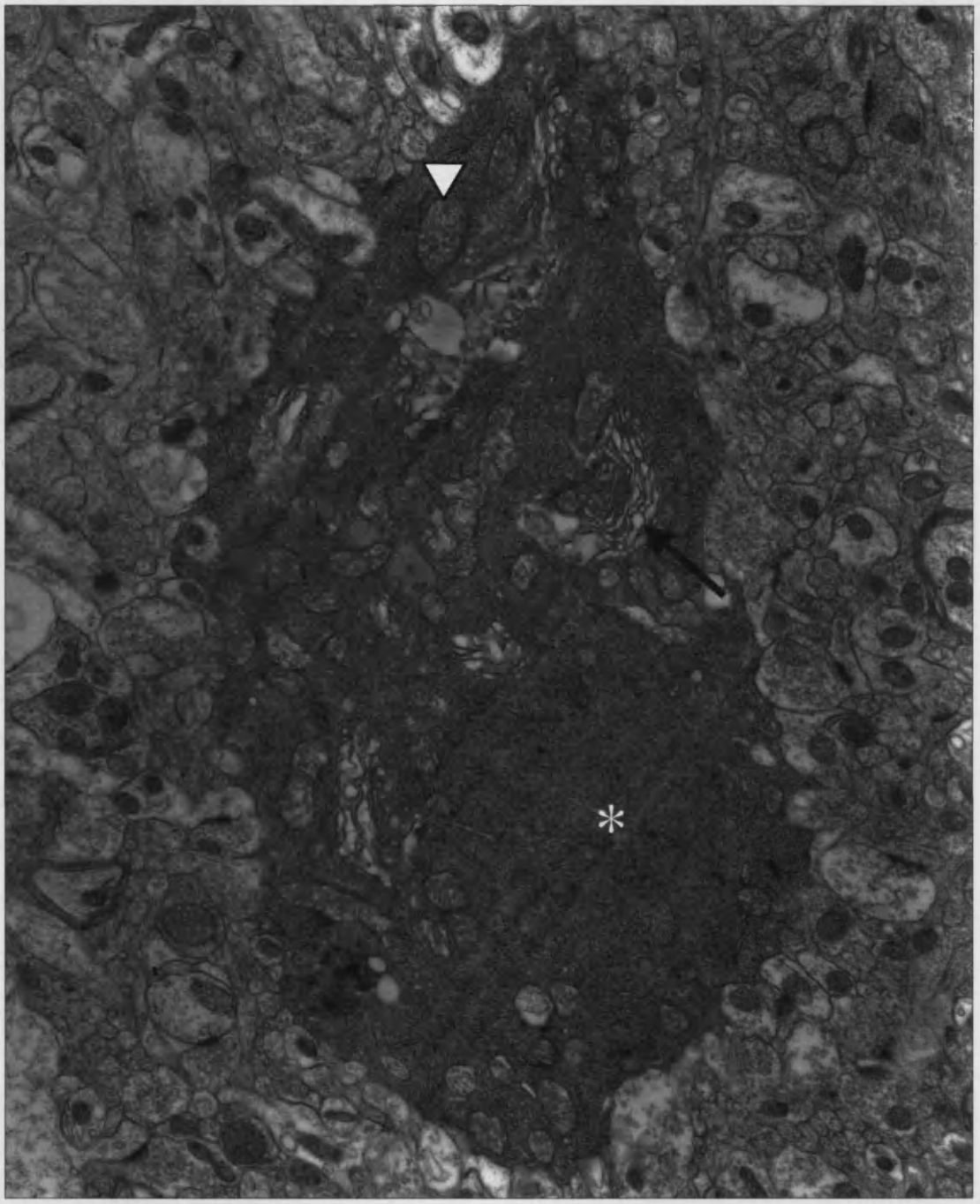

Figure 61 High-magnification electron micrograph of a cortical neuron from a 17 week-old R6/2 mouse in the end stages of degeneration. Even at this late stage, organelles are still discernible including mitochondria (open arrowhead) and Golgi apparatus (arrow). Though difficult to distinguish in this reproduction, the nucleus (asterisk) has an intact membrane.

that whilst the nuclear membrane can become extremely convoluted, it persists. The nuclear membrane is just visible in figure 61, however, as this figure indicates, it becomes increasingly difficult to trace the membrane in micrographs as the cells darken. Nevertheless, under the electron microscope one has the advantage of being able to increase magnification and roam through the section, following the membrane. Such analyses suggest that in contrast to the defined nature of apoptosis, the nuclear envelope does not disintegrate.

A further contrast, marked by its absence, is the condensation of chromatin. Figure 60 shows that even unto the darkest stages of dark cell degeneration, the nucleus remains devoid of the chromatin condensations associated with apoptosis (*cf.* figures 45, 46 & 48). In the earlier stages of degeneration one can find areas of nucleoplasm darker than the surrounding material (*for example,* see figure 55), which may indeed correspond to mild chromatin condensations, but these neither marginate nor coalesce to form the characteristic condensations of apoptosis.

There are suggestions of oligodendrocyte and astrocyte involvement in the pathology of HD (Myers *et al.* 1991; Vonsattel *et al.* 1985). Both types of glia have been said to proliferate during the disease process. Investigations into the proliferation of glial cells are reported in *3.1.9*; the question addressed here is whether these glia have a more direct role in the degeneration of R6/2 neurons. As described in *1.7*, glial cells have an active role in apoptosis; indeed, the seminal paper includes the involvement of phagocytic glia as part of the definition of apoptosis.

At the EM level, glia are often seen in close association with neurons; both in wild-type (figure 62) and R6/2 (figure 63) tissue. The majority of these glia have an ultrastructural profile corresponding to oligodendrocytes: a large ovoid nucleus with condensations of chromatin at the periphery, and a thin band of relatively dense cytoplasm. Given the association of these glia with neurons in the control tissue, one can assume that these are a feature of the normal glial-neuronal relationship, providing support for the functioning of the neuron. However, uniquely within the R6/2, glia that might otherwise me classified as oligodendrocytes sometimes present a somewhat different profile. Figure 64 contains an example of such an instance. The cortical neuron (n) is in contact with a glial cell (g) that resembles an oligodendrocyte

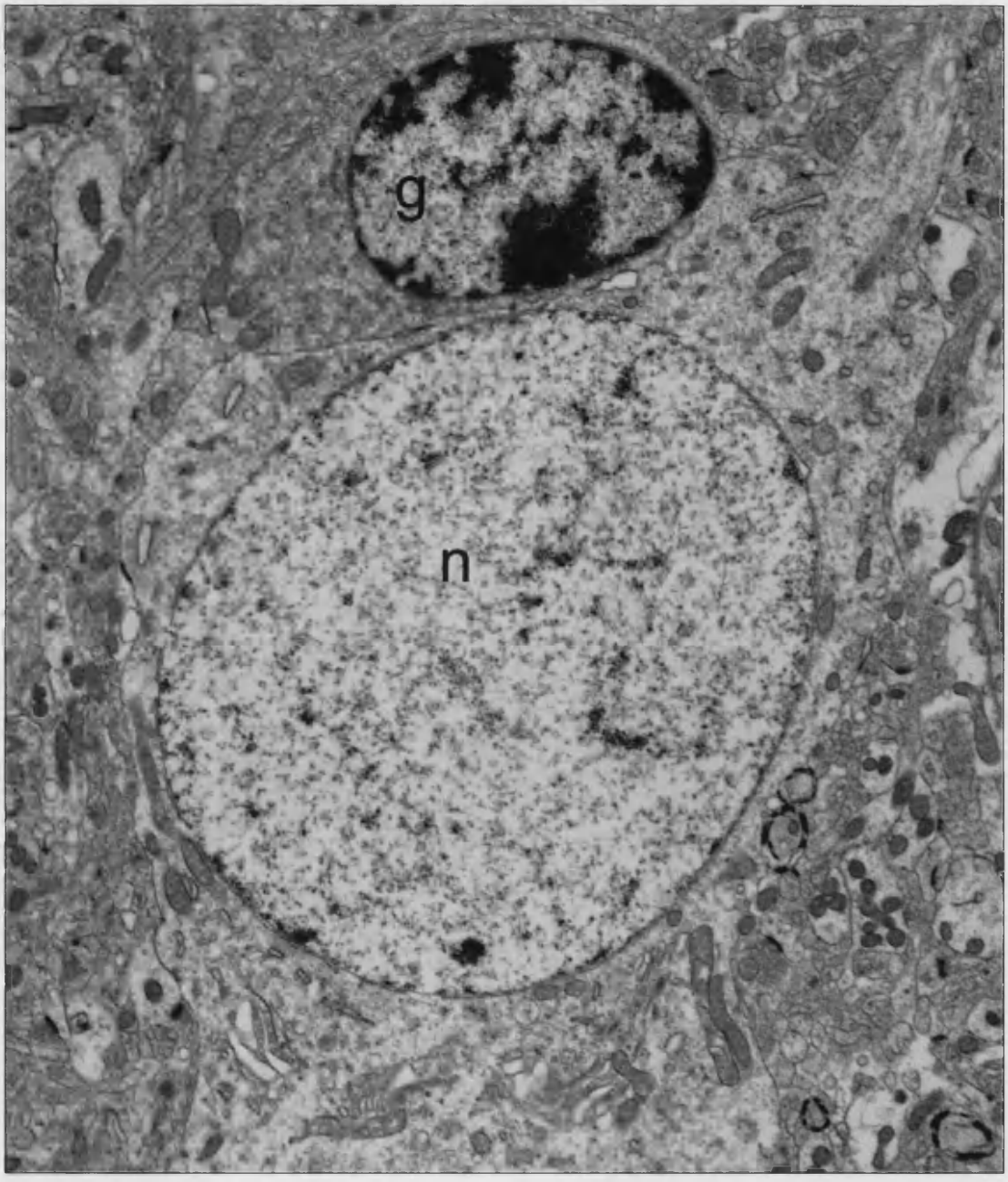

Figure 62 Electron micrograph of a striatal neuron from a 10 week-old wild-type mouse (n). A glial cell (g) is seen in close contact with the neuron. The morphological appearance of this glial cell is indicative of an oligodendrocyte.

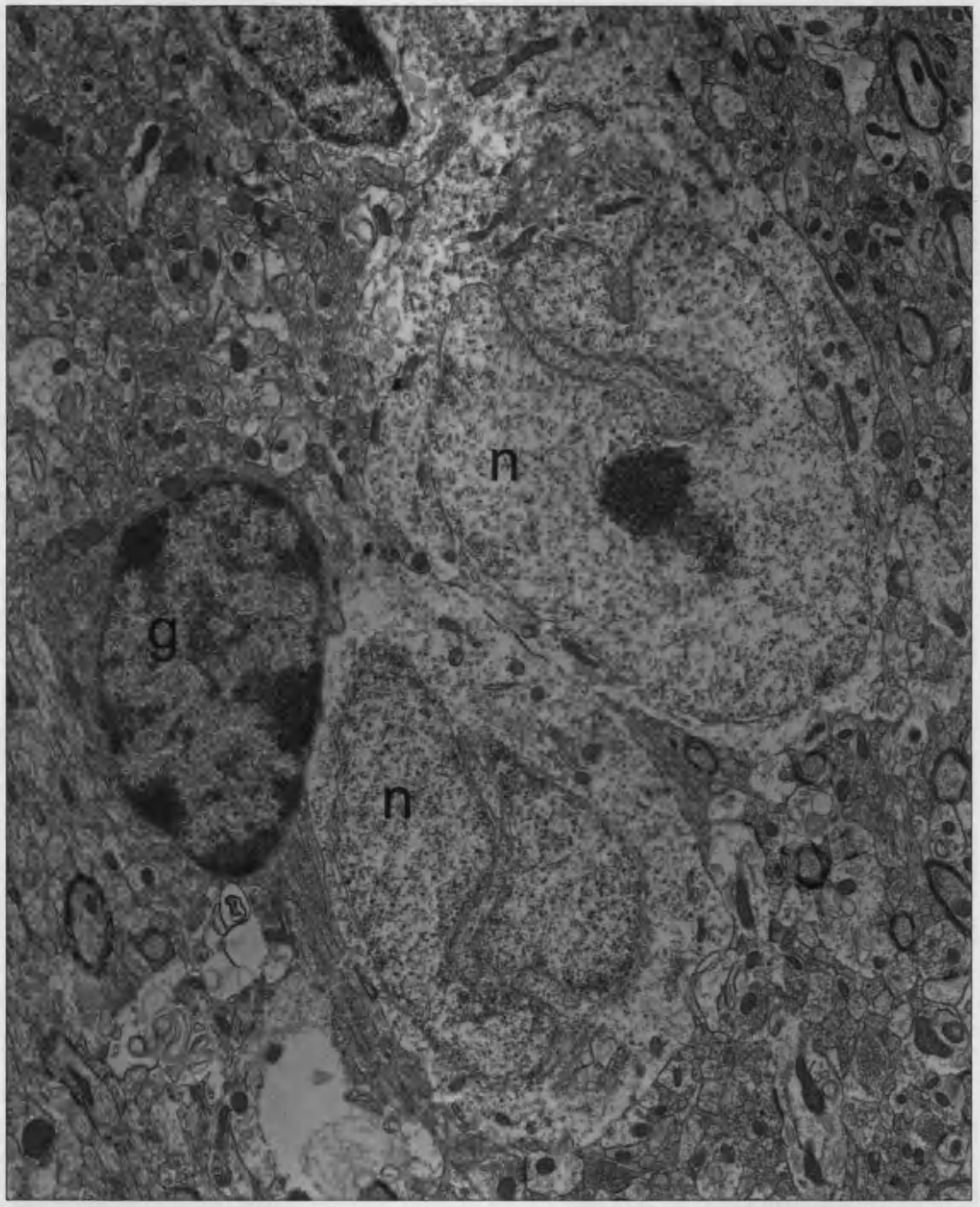

Figure 63 Electron micrograph of a striatal neurons from a 13 week-old R6/2 mouse (n). A glial cell (g) is seen in close contact with the neuron. The morphological appearance of this glial cell is indicative of an oligodendrocyte.

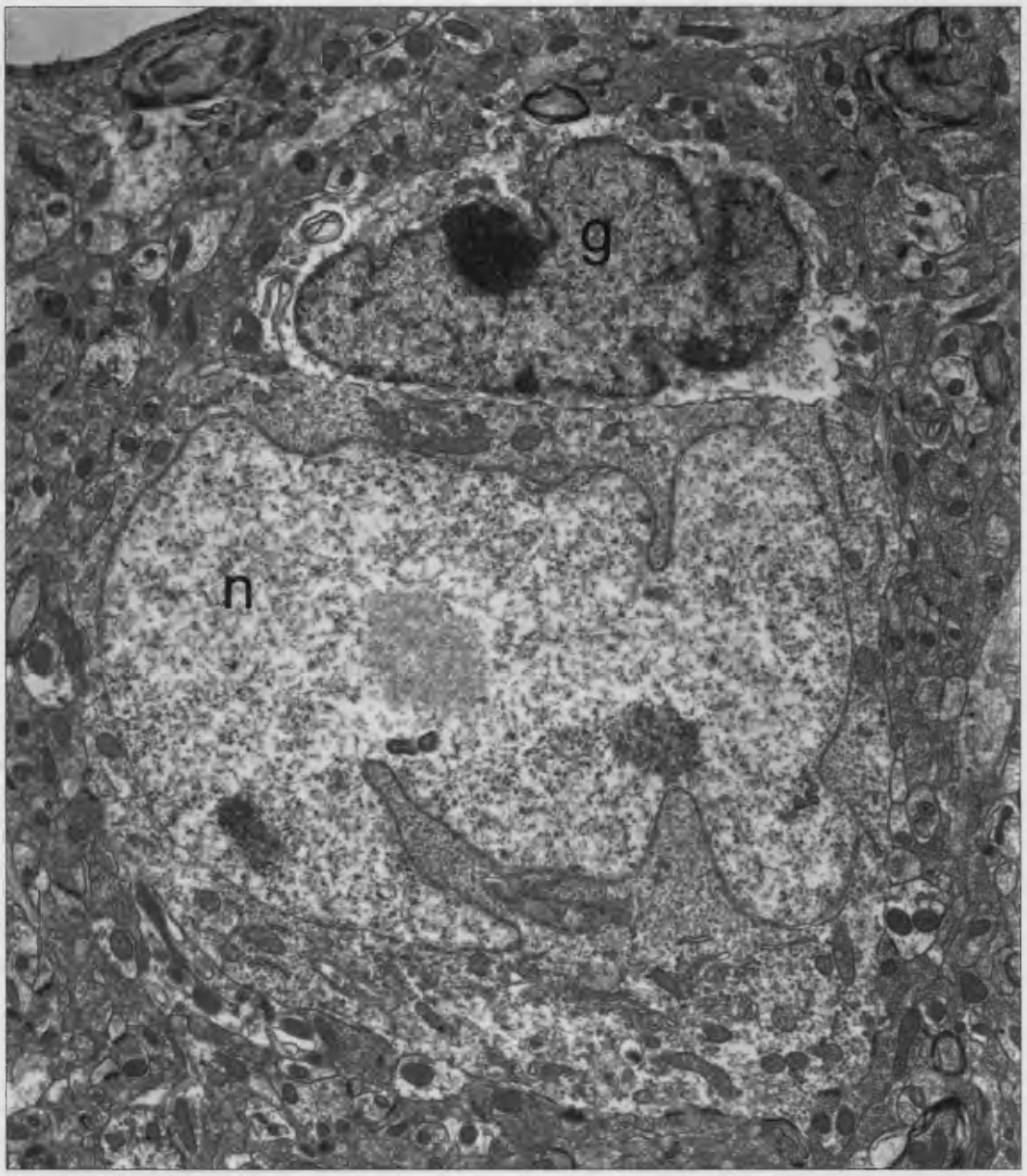

Figure 64 Electron micrograph of a cortical neuron from a 13 week-old R6/2 mouse (n). A glial cell (g) is seen in close contact with the neuron. The morphological appearance of this glial cell is unusual, thus its nature cannot easily be defined.

but for the small degree of marginated chromatin and the invaginated nucleus. Furthermore, the cytoplasm appears relatively large and pale in comparison to 'classical' oligodendrocytes. The nature of these glia remains under question. As explained below, glia within the R6/2 brain may be directly affected by the HD mutation.

Within the R6/2 one can also frequently find associations between neurons and another type of glial cell. Figure 65 contains contact between a neuron and a glial cell with an astrocytic profile: a large, spherical pale nucleus within a large, tenuous cytoplasm. Such contact between these astrocyte-like glia and neurons can be found at all stages of degneration. Figure 66 contains a neuron at a later stage of degeneration contacted by an astrocyte-like glial cell. This figure also raises another important difference between the human condition and the R6/2 model: within the glial nucleus is found a structure corresponding to the NII (arrow). As shown in *3.1.9* these aggregates appear to be glial inclusions similar to those of the neurons.

As described previously, at the light microscopy level one can identify neurite aggregates using the same anti-ubiquitin and/or anti-htt_n labelling used to highlight the intranuclear inclusions. Likewise, at the EM level, the neurite aggregates can also be identified without labelling due to their structure. Figure 67 contains an R6/2 cortical neuron in the early stages of degeneration, but it also contains a visible neurite aggregate, enlarged in the insert (arrow). Using standard electron microscopy it is impossible to establish from which cell this process originates, but given the ubiquity of NIIs within the R6/2 model, one can safely assume that the soma from which this neurite stems also contains a nucleus with an inclusion. What effects the presence of aggregates within the processes exert remains unknown. It is clear that certain cells within a population degenerate more rapidly than others and this may relate to differing pathogenicities of inclusions within the nucleus and neurite.

Whether a consequence of the somal degradation, or an effect caused by the presence of extra-nuclear aggregates, degeneration is also seen with the processes. Darkened processes can be seen in the R6/2 mouse, which most likely correspond to cytoplasmic condensation. However, within axons a different mechanism of degeneration has been seen. Figure 68 contains a section through a striatal fascicle

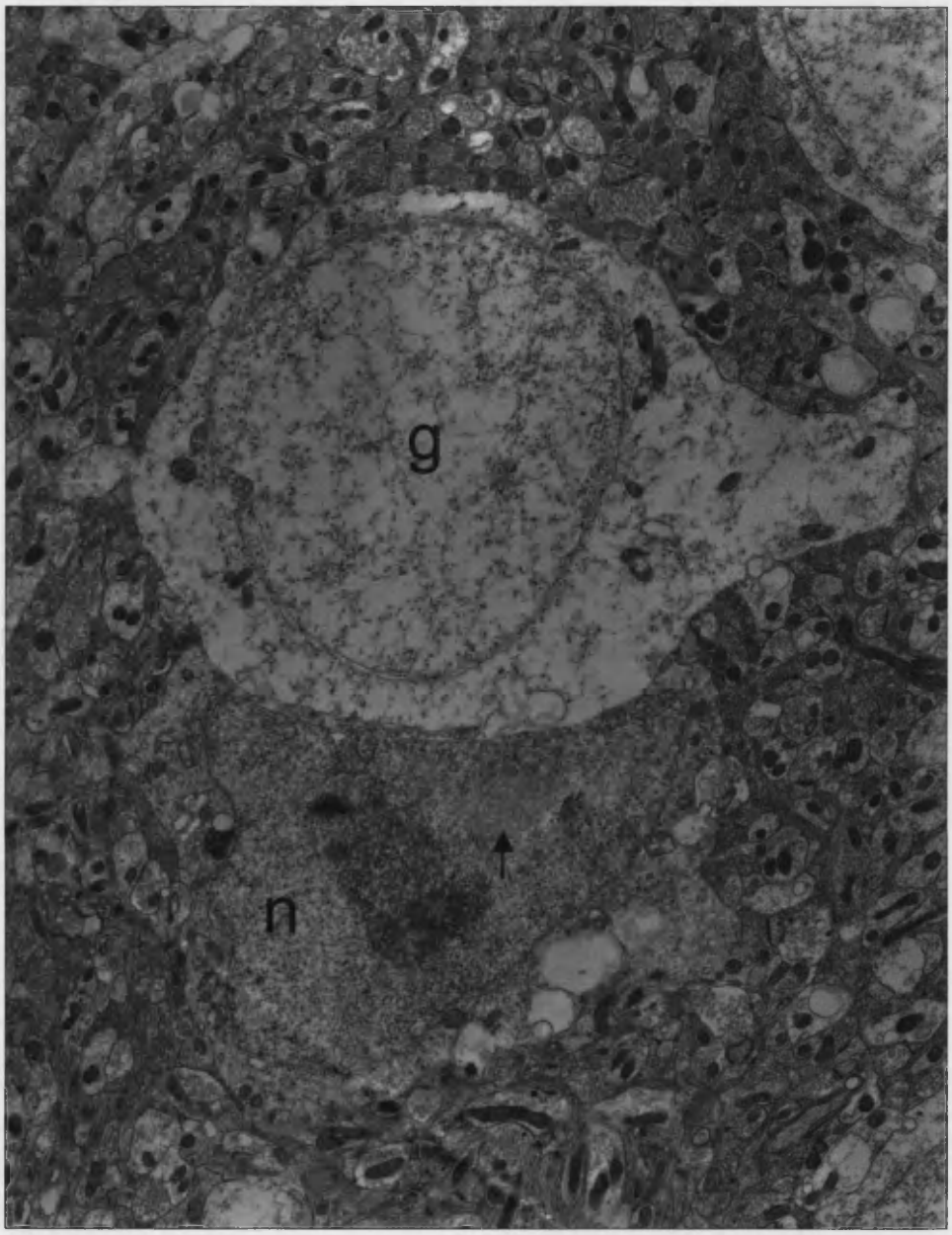

Figure 65 Electron micrograph of 17 week-old R6/2 cortex. There is a darkened cell which is most probably a neuron (n), containing an inclusion (arrow), which is closely contact by a glial cell (g). The morphological appearance of this glial cell suggests that it is an astrocyte.

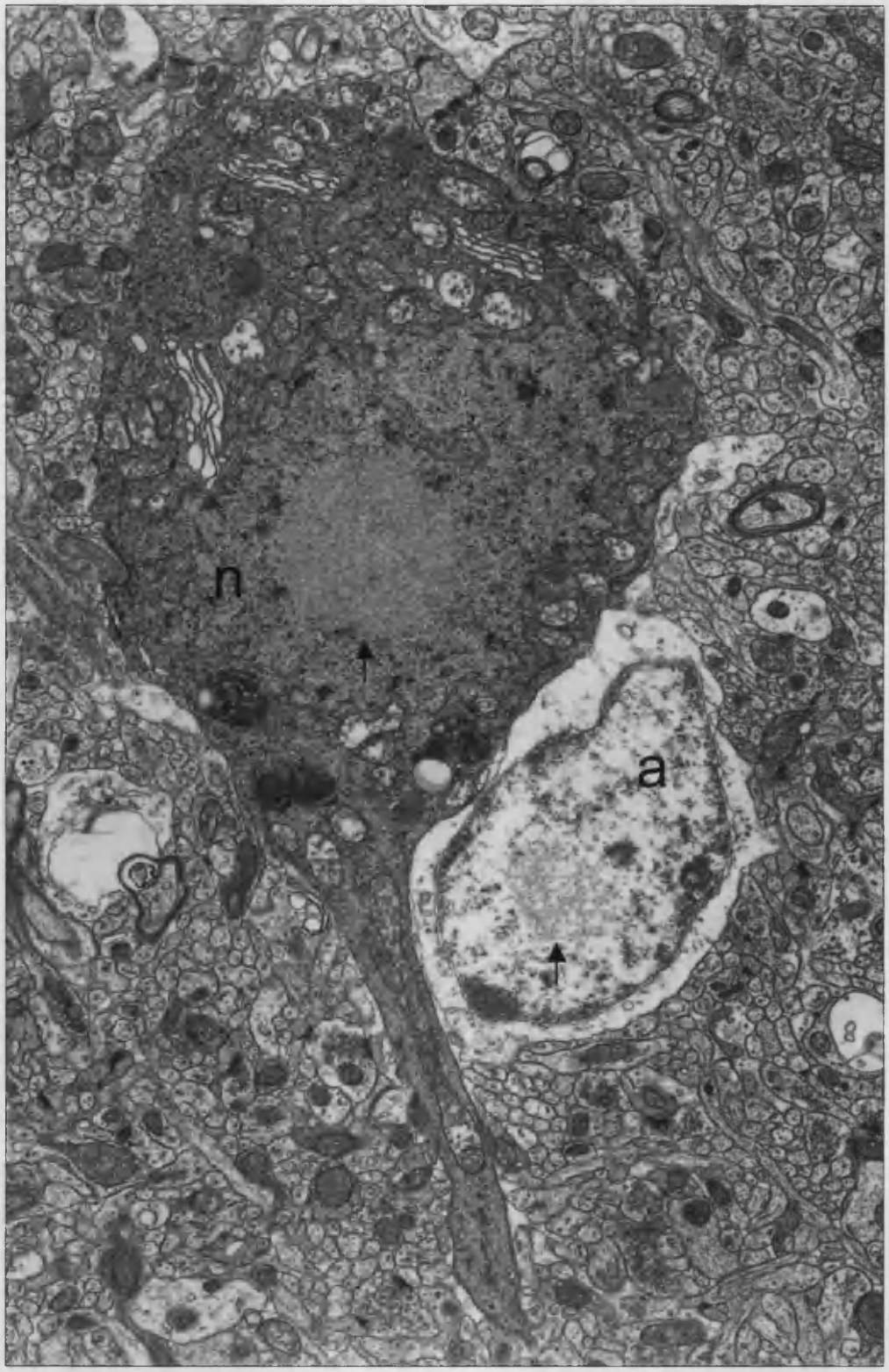

Figure 66 Electron micrograph of a degenerating 17 week-old R6/2 cortical neuron (n), which is closely contact by a glial cell of astrocytic morphology (a). Both cells contain intranuclear aggregates (arrows).

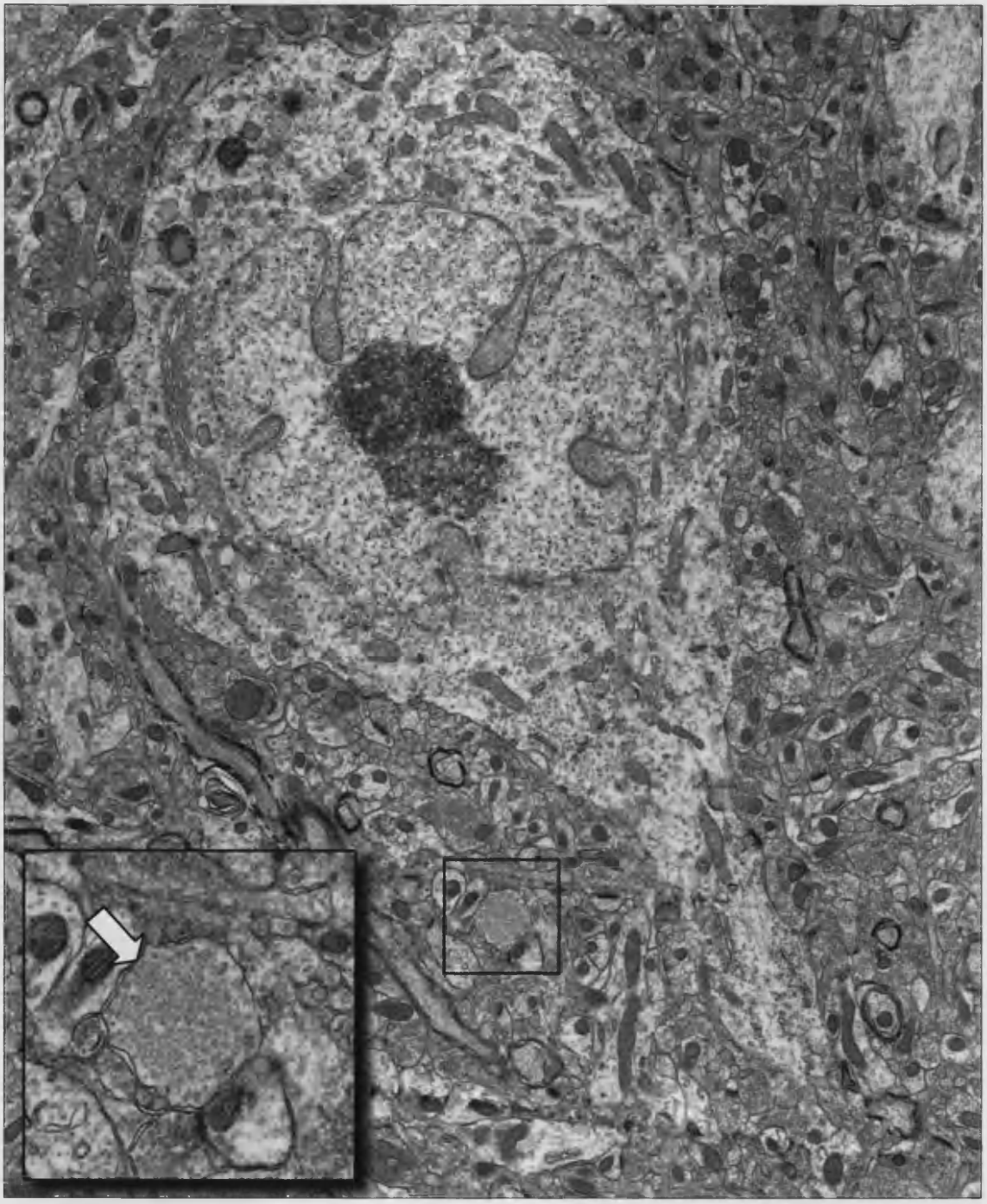

Figure 67 Electron micrograph of a cortical neuron from a 13 week-old R6/2 mouse. Within the surrounding neuropil, a neurite aggregate is found. Highlighted and enlarged in inset (open arrow).

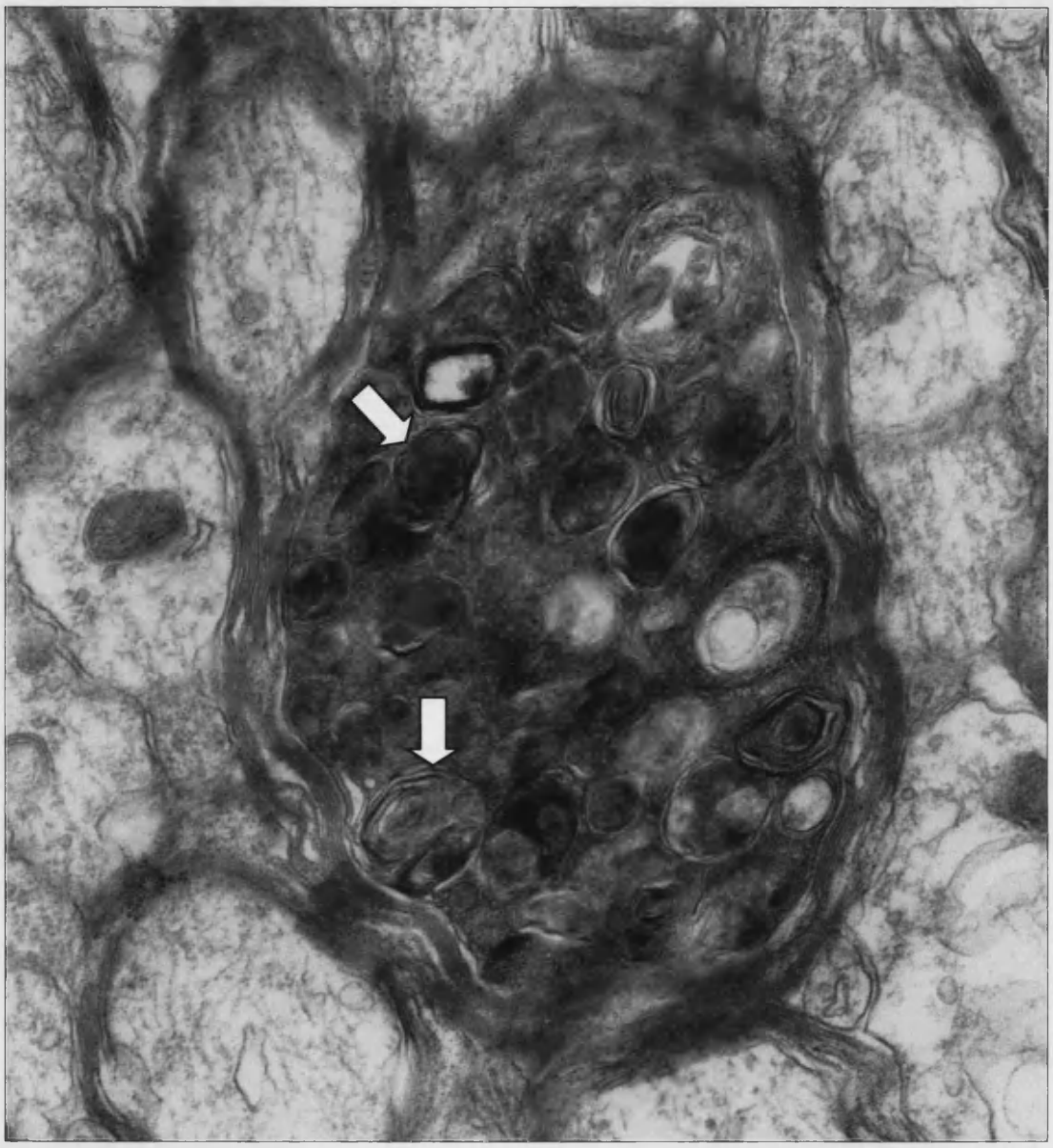

Figure 68 Electron micrograph of an axon bundle in a 17 week-old R6/2 mouse. The axon shown appears to be degenerating via autophagy; as indicated by the dominance of membrane whorls (arrows)

from an R6/2 mouse. Within the axon are numerous membrane whorls indicative of autophagic degeneration, from open, early whorls to late, darkened bodies (arrows). As seen in figure 67, the neurite aggregate occupies most of the cross-sectional area of the process; therefore, it may be that the presence of the aggregate isolates the process – distal to the aggregate – and induces an autophagic 'dismantling' of the contents. One important caveat, however, is that degeneration and the presence of an inclusion have not been seen together within a single process; thus, a causative relationship cannot be confirmed.

3.1.7 The Appearance of Inclusions

The structural elements underlying the formation of the inclusion remain under debate. As described in *1.5.5*, the prevailing theory for the formation of the inclusion is the polar zipper model, which involves the formation of ß-pleated seats. Such a mechanism of aggregation would produce fibrous structures akin to those seen in Alzheimer's and Parkinson's disease (see 4.4). However, as mentioned previously, the NII presents as a roughly spherical, homogenous structure with little discernible structure. Figure 69 contains representative examples of NIIs from a variety of R6/2 mice. There is some variation between each, but the overall appearance is of a roughly spherical, granular structure. Occasionally, within NIIs one may find structural elements that one may define as fibrous, but these are relatively rare (arrowheads).

The neurite aggregates present with a rather different ultrastructural appearance. Their shape appears to be defined by the shape of the process. A process with a large circular cross-sectional area will allow the formation of an inclusion with a roughly circular cross-section akin to those of the nucleus (figure 70). However, a process with a smaller oval cross-section will possess oval aggregates (figure 71) suggesting that the inclusion increases in size to fill the available space, supporting the suggestion earlier that the neurite aggregate may block and isolate the distal dendrite.

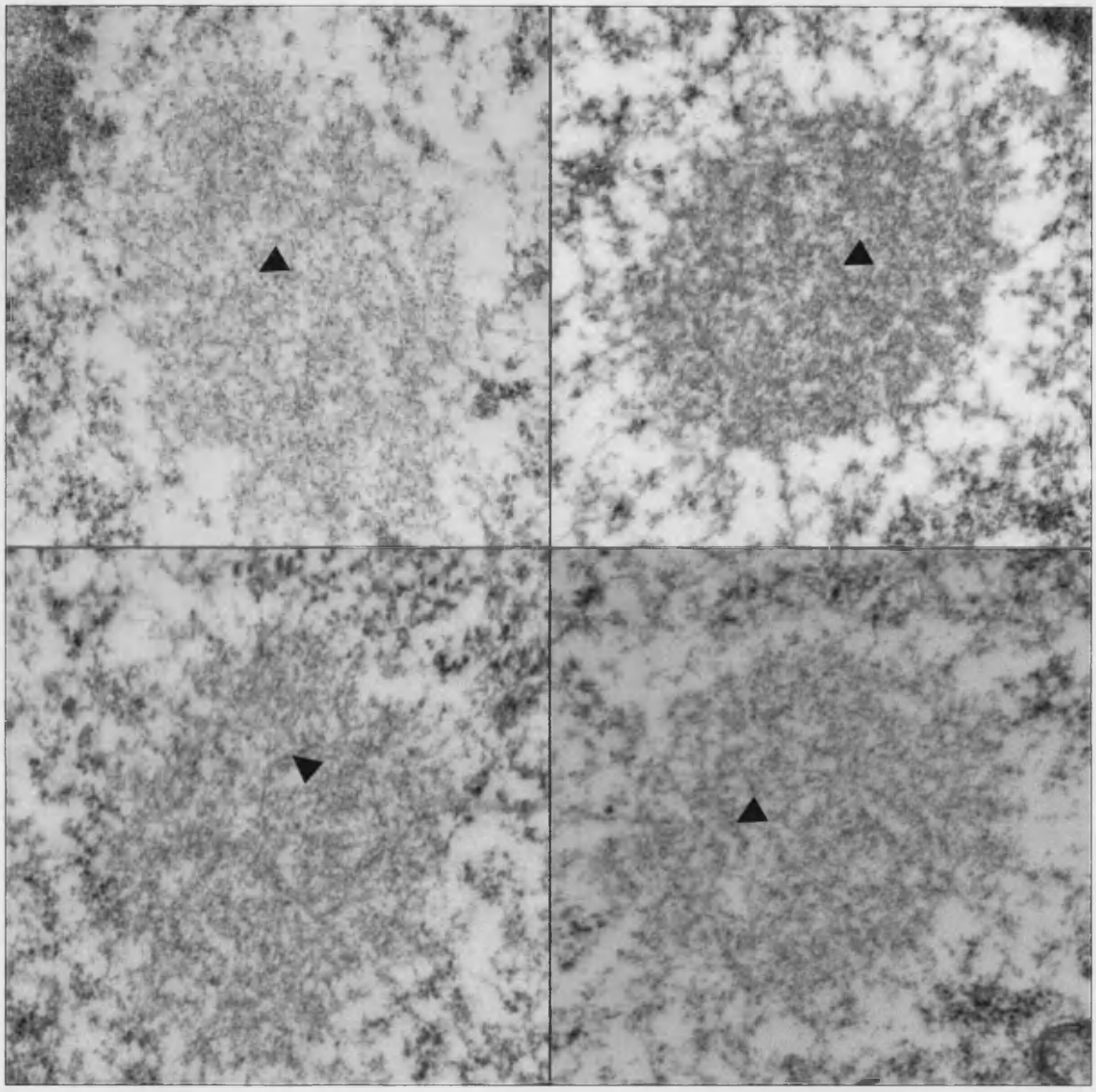

Figure 69 Electron micrograph of inclusions from R6/2 mice of varying ages. Note the dominating granular appearance of each, with occasional elements which may be interpreted as fibrous (arrowheads).

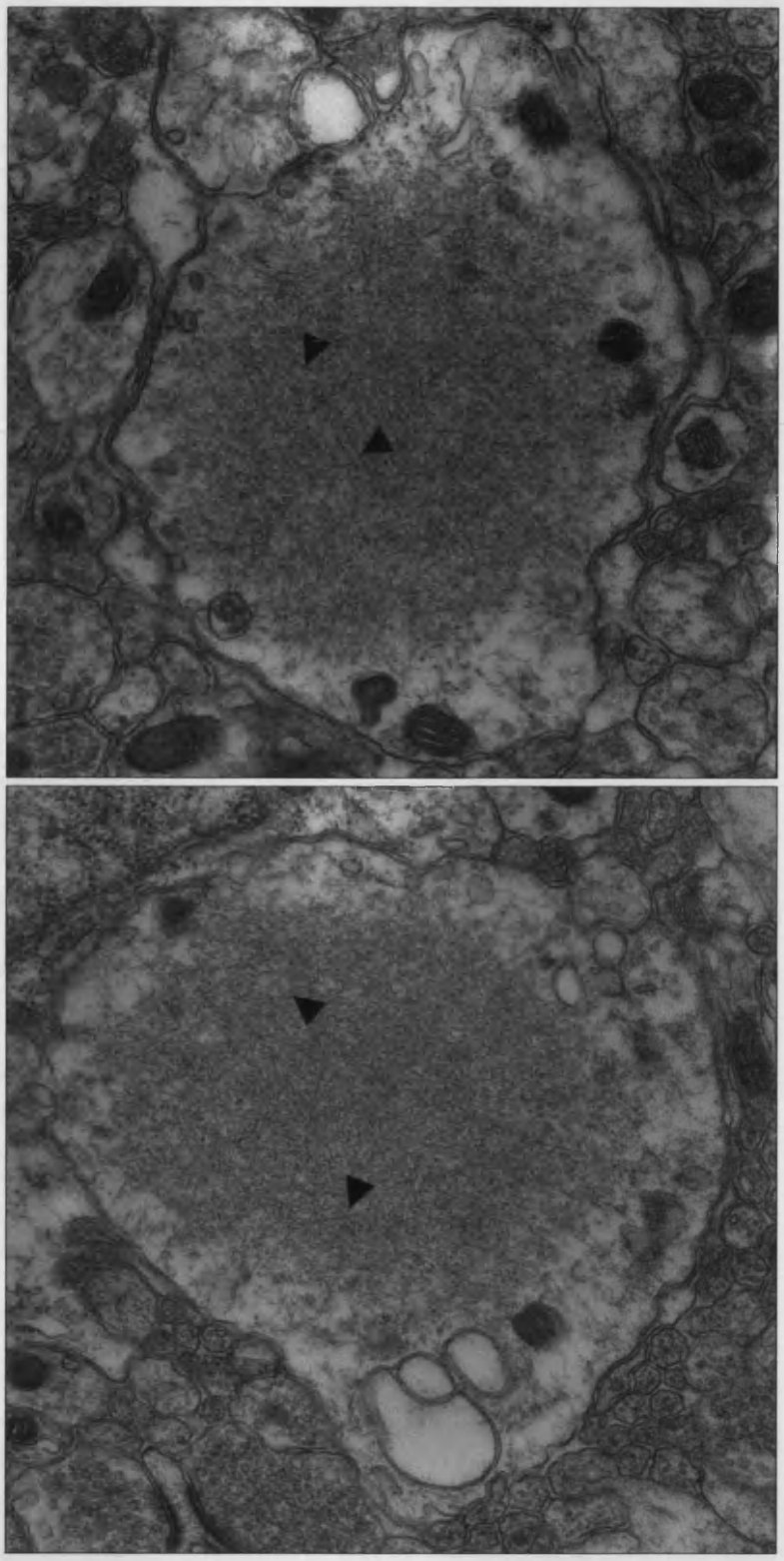

Figure 70 High-magnification electron micrograph of neurite inclusions from 17 week-old R6/2 mice. These aggregates resemble intranuclear inclusions but show more elements which may be considered fibrous (arrowheads).

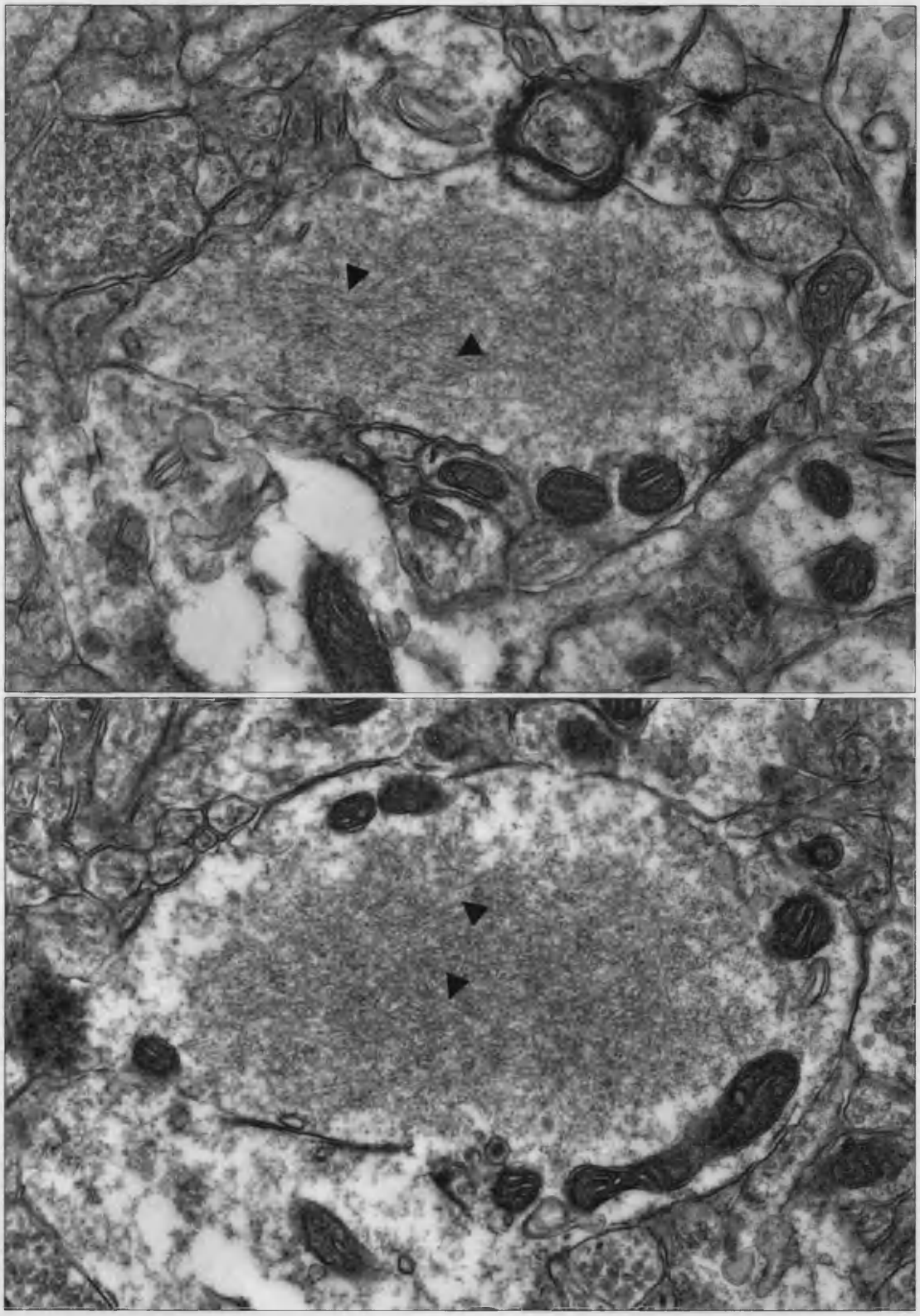

Figure 71 High-magnification electron micrograph of neurite inclusions from 17 week-old R6/2 mice. These aggregates further demonstrate the presence of elements which may be considered fibrous (arrowheads), but exhibit an oval morphology.

The important feature to note is the structure of the neurite aggregates. Figures 70 and 71 contain representative neurite inclusions within which one can identify structural elements (arrowheads). Whilst there is no regular structure to the degree of the Lewy Body of Parkinson's disease (see 4.4), many fibrous elements appear to be present within the aggregate, considerably more than seen in the neuronal intranuclear inclusion. As there is a structural difference between the neuronal inclusion and the neurite inclusion, there may also be a functional difference. The subcellular localisation of the mutant protein, and its aggregates, may have important pathological consequences. Conversely, given that fibrous elements are rare with the NII it is unlikely they are required for inclusion formation. They may develop as a secondary consequence of inclusion formation. As it has been shown that polyglutamine stretches tend toward fibrilisation, induced increases in concentration are likely to increase the likelihood of such events occuring. As discussed in *4.4*, the fewer structural elements in the NII may in fact indicate a greater rather than simpler complexity.

3.1.8 The Biochemical Profile of Degeneration

Since the identification of the molecular machinery behind apoptosis (*see 1.7*), it has become common practice to define mode of cell death through involvement of this machinery. Indeed, much of the evidence supporting an apoptotic mode of cell death in HD originates from the identification of 'markers' of apoptosis in various models. Often, the identification of only one player in the plethora of proteins involved in apoptosis has led some groups to hail apoptosis as the answer.

As shown above, whilst the neuronal intranuclear inclusion appears early on in the lifespan of the R6/2 mouse, indeed before the onset of symptoms, cellular degeneration does not occur until the last weeks of the mouse's life. Before twelve weeks of age there is little readily identifiable cellular pathology in the R6/2 mouse. The beginnings of nuclear condensation can rarely be detected in mice as young as ten

weeks, but the later pathological events are only found in mice older than twelve weeks (see previous section).

In order to be certain that markers being sought after are in areas where they would be found if present, I have limited the results presented here to the cingulate and motor cortices. I have previously shown that degeneration is most prevalent in these areas, therefore there is a greater chance of identifying activated apoptotic machinery in these areas. During my investigation I have examined all areas of the brain for evidence of apoptosis, and I can confidently say that the cortical results are representative of all areas studied. Nevertheless, in order to provide the most convincing evidence, sections through the motor and cingulate cortices are shown here.

The micrographs presented in this section are all taken from two (consecutive) generations of mice, transgenic and wild type, culled at either 12 weeks 4 days or 12 weeks 5 days of age. The degree of degeneration in the cingulate and motor cortices of the R6/2 mouse at this age is illustrated in figure 72A, a semi-thin toludine blue-stained section. Dark profiles are evident throughout the region. Figure 72B is a corresponding section of R6/2 brain labelled with anti-cleaved caspase-3 and processed for DAB.

Caspase-3 is generally considered to be the central component of the apoptotic pathway. It sits at the crux of the pathways linking the initiation events to the execution events of apoptosis. As explained in chapter *1.7* once caspase-3 is activated there is little hope of redemption for a cell.

There appears to be no staining above background in the regions one would expect to find cell death. Figure 72C is a high magnification image of the section shown in B. Some cells appear to have stained slightly darker than others, but as the littermate control section in D shows, this is part of the normal variation.

The other common marker for apoptotic cell death in the use of TUNEL which labels double-stranded DNA breaks (see *2.3.x*) such as occur as a result of DNAse activation in apoptosis. Figure 73 illustrates the staining of the cingulate/motor cortex of the R6/2 (A&C) and LMC (B&D) mice. There is no evidence of DNA

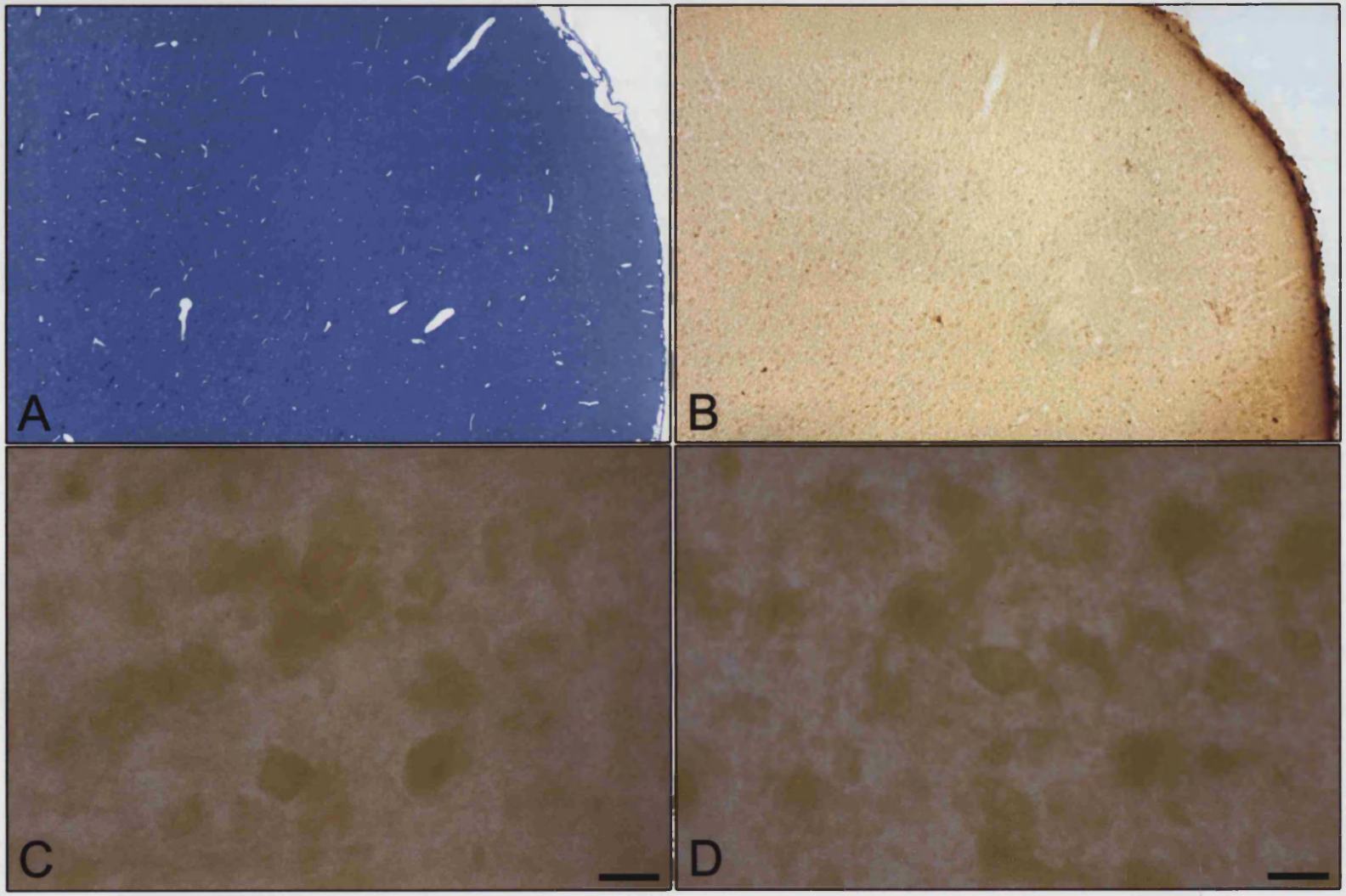

Figure 72 **A:** Toludine blue-stained semi-thin section of cingulate and motor cortices from a 12 week-old R62 mouse. **B:** Corresponding section immunolabelled for activated caspase-3. **C:** Sample high power section from B. **D:** Corresponding image from a littermate control mouse. Scale bar for C and D = 10μm

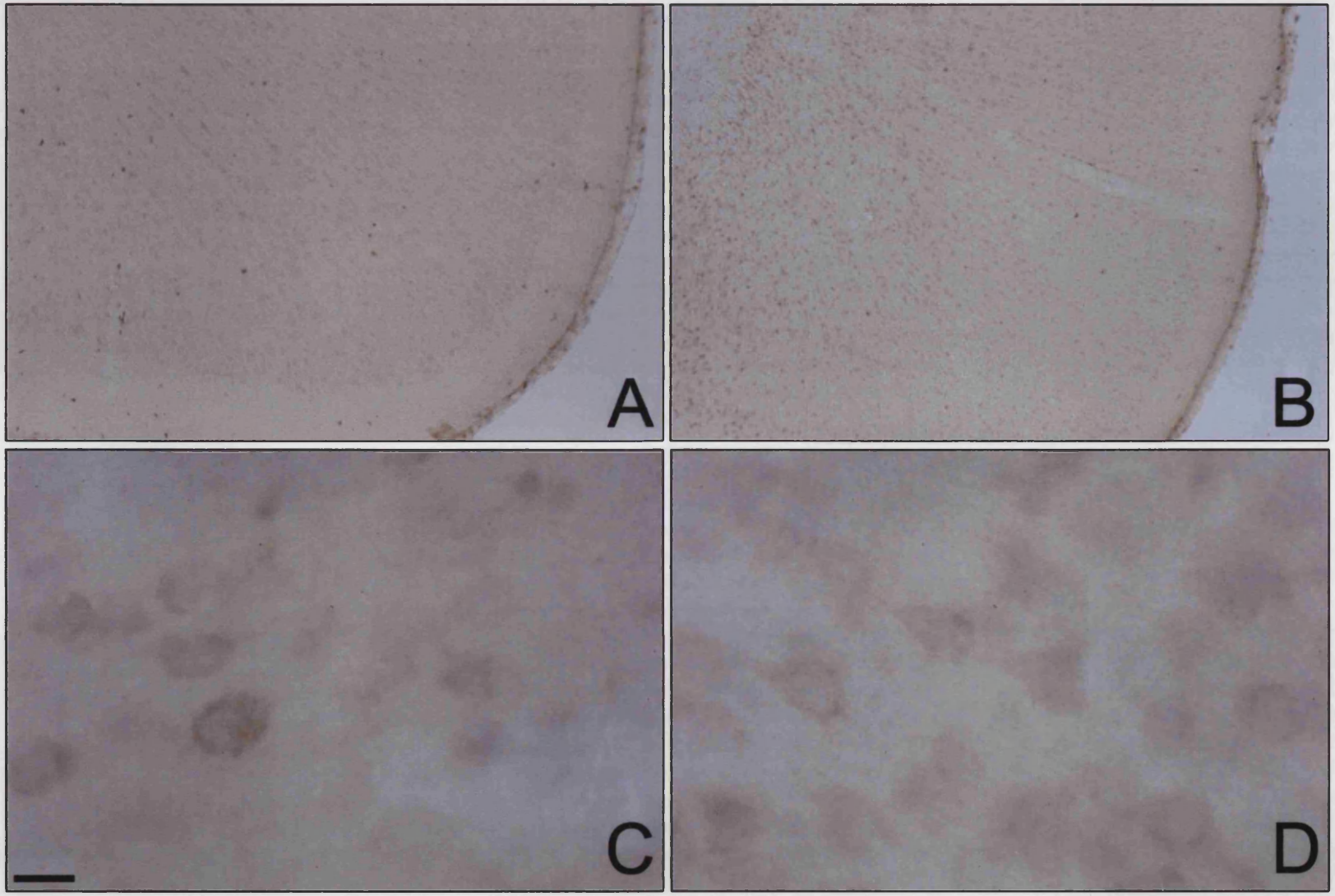

Figure 73 Corresponding sections of cingulate and motor cortices in 12 week-old R6/2 (**A**) and littermate control (**B**) mice after TUNEL processing. High magnification images of A and B presented in **C** and **D**. Scale bar for C and D = 10μm

breakage using TUNEL labelling in the R6/2 mouse. Indeed, the neuronal nuclei appear to be the clearest parts of the section.

Figures 74-77 illustrate the staining patterns obtained using the ABC-DAB method for processing labelling with other apoptotic indicators.

Apoptosis Initiation Factor (AIF) is normally localised to the mitochondrion and is released upon stimulation of apoptosis. Interpretation of the results obtained with the AIF antibody is difficult, as it appears the cytoplasm of all cells is filled with AIF. Whereas cytochrome c produces punctate staining corresponding to individual mitochondria, AIF does not. In an apoptotic cell one would expect AIF to first fill the cytoplasm and then the whole of the condensed neuron as the structural integrity of the nuclear membrane is lost. As shown in *3.1.5* the nuclear membrane of degenerating R6/2 neurons retains integrity throughout the measurable process of degeneration, therefore even if AIF is released from the mitochondria it is unlikely one would ever see it fill the neuron. It is therefore difficult to draw any conclusions about release of AIF in the degeneration of R6/2 neurons. What can be said is that there is no correlation between areas of degeneration and pattern of AIF staining. Furthermore, littermate control sections produce identical staining patterns.

Apoptosis activating factor-1 (Apaf-1) is normally found throughout the cytosol. During apoptosis it forms the apoptosome, a holoenzyme, through interaction with procaspase-9 and cytochrome c released from the mitochondria. Interestingly, the staining pattern obtained here appears to label the nuclei for Apaf-1 as well as the cytoplasm. Once again it would therefore be difficult to draw any conclusions about the involvement of such a protein given that there would be little change upon activation of apoptosis. Rather, useful results are only really obtainable from either labelling proteins which alter their subcellular distribution or from the use of antibodies raised against the active forms of the components.

The antibody used to label cleaved DFF45 (DNA fragmentation factor 45) is an example of such. DFF45, otherwise known as ICAD (inhibitor of CAD), is normally bound to DFF40/CAD (caspase activated Dnase) inhibiting its actions. During apoptosis ICAD is cleaved releasing CAD. The labelling obtained does show some faint cytoplasmic staining, with foci occasionally visible. This suggests either an

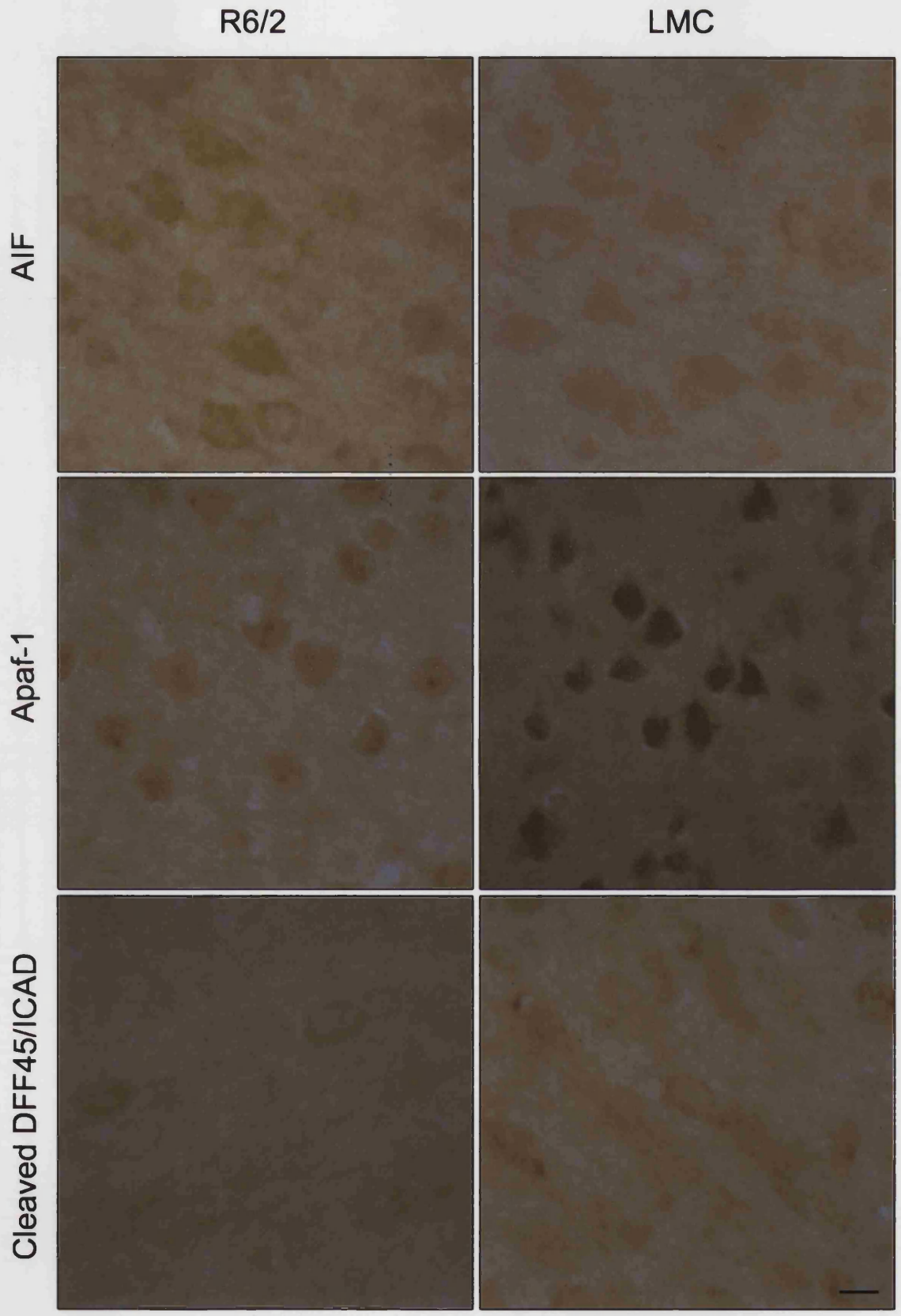

Figure 74 Sample light micrographs 13 week-old R6/2 and littermate control cingulate cortical neurons, immunolabelled as indicated.
Scale bar applies to all (10μm).

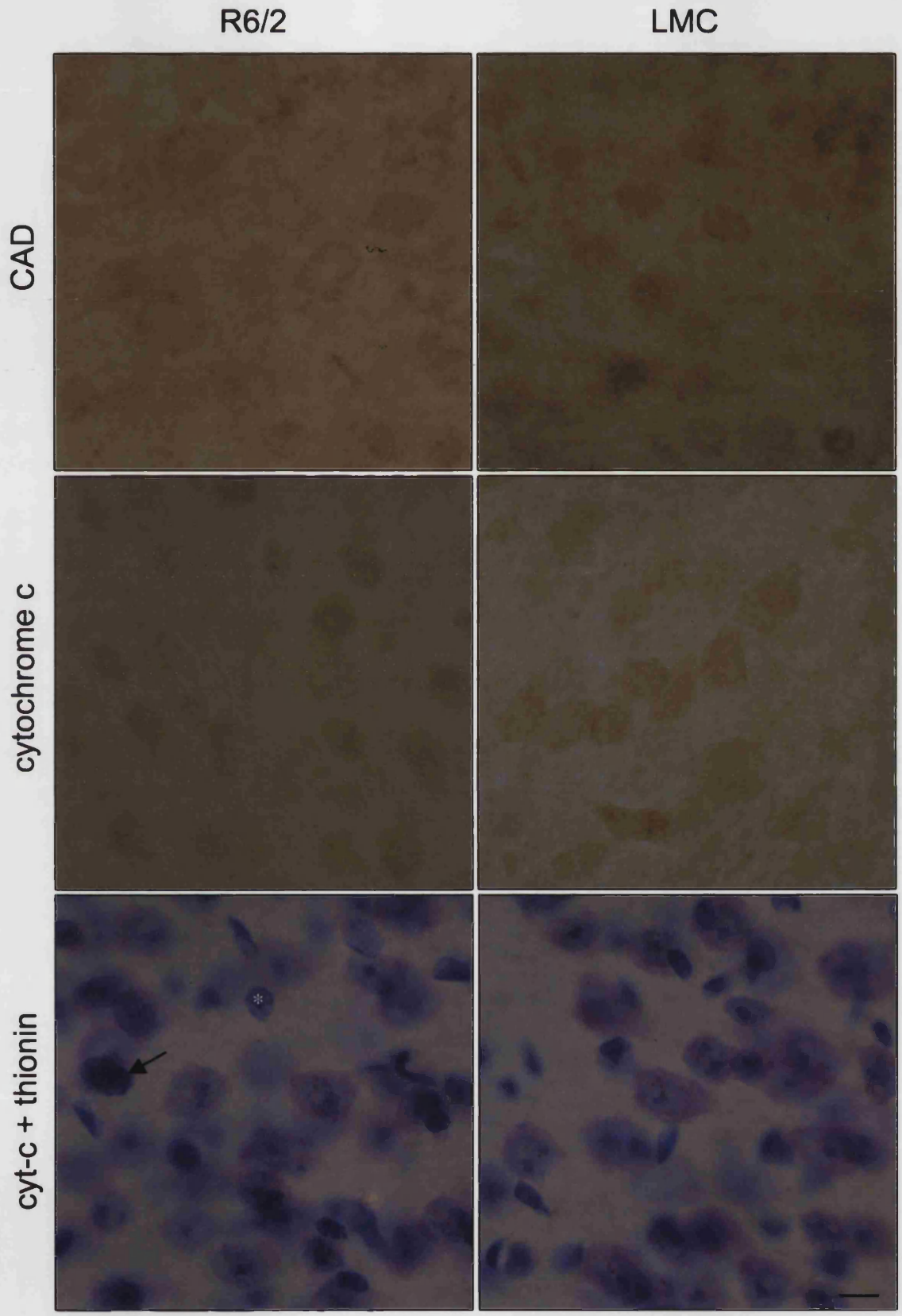

Figure 75 Sample light micrographs of 13 week-old R6/2 and littermate control cingulate cortical neurons, immunolabelled as indicated.
Scale bar applies to all (10μm).

antibody with some affinity for the uncleaved species, or some degree of tonic cleavage of ICAD. Given the mild catalytic nature of the caspase zymogen it may be that these occasional foci represent cleaved ICAD. In either case, there is no detectable difference between the R6/2 and LMC sections.

Once released from its inhibitory bondage by caspase-mediated cleavage of ICAD, CAD translocates to the nucleus whereupon it begins degrading the chromatin. If CAD is active in the degenerating cells of the R6/2 brain one would expect to see DAB staining in the nucleus. However, even in the areas of known degeneration anti-CAD labelling fills the cytoplasm leaving the nucleus at background level.

As mentioned previously, labelling for cytochrome c normally yields a punctate staining of the cytosol corresponding to individual mitochondria. During apoptosis, the apoptosome forms as a result of release of cyt c from the mitochondria to the cytoplasm. One would therefore expect to diffuse labelling of the cytosol in an apoptotic cell labelled for cyt c. However, as shown in *3.1.5* whilst there is a transient swelling of mitochondria they remain intact throughout the degenerative process. Furthermore, as the degenerating neuron persists for a relatively long time, we assume that the remaining mitochondria are functional, requiring the presence of cyt c. Therefore, the staining pattern obtained is difficult to interpret. There does appear to be some diffuse cytoplasmic labelling along with the mitochondrial foci. In order to make the result more clear, I removed the coverslips from the cyt c sections and counterstained them with thionin. This provides enough contrast to remove the background staining making the mitochondrial foci more easily identifiable. Furthermore, thionin staining also facilitates identification of condensed cells. Such an example is included in figure 75. The cell (arrow) appears darker than the surrounding neurons (and larger than the oligodendrocytes [asterisk]) but cytochrome c foci are still visible. This supports the idea put forward in *3.1.5* that the mitochondria persist in a functional state, and also suggests that cytochrome c is not released into the cytosol.

Figure 76 contains two more examples of activated caspase-3 labelling. The *New England Biolabs* antibody and CM1 (*Idun Pharmaceuticals*). Each yields a slightly different staining pattern, the CM1 producing a more punctate appearance. As with the anti-ICAD antibody it may be that the CM1 antibody has some affinity for

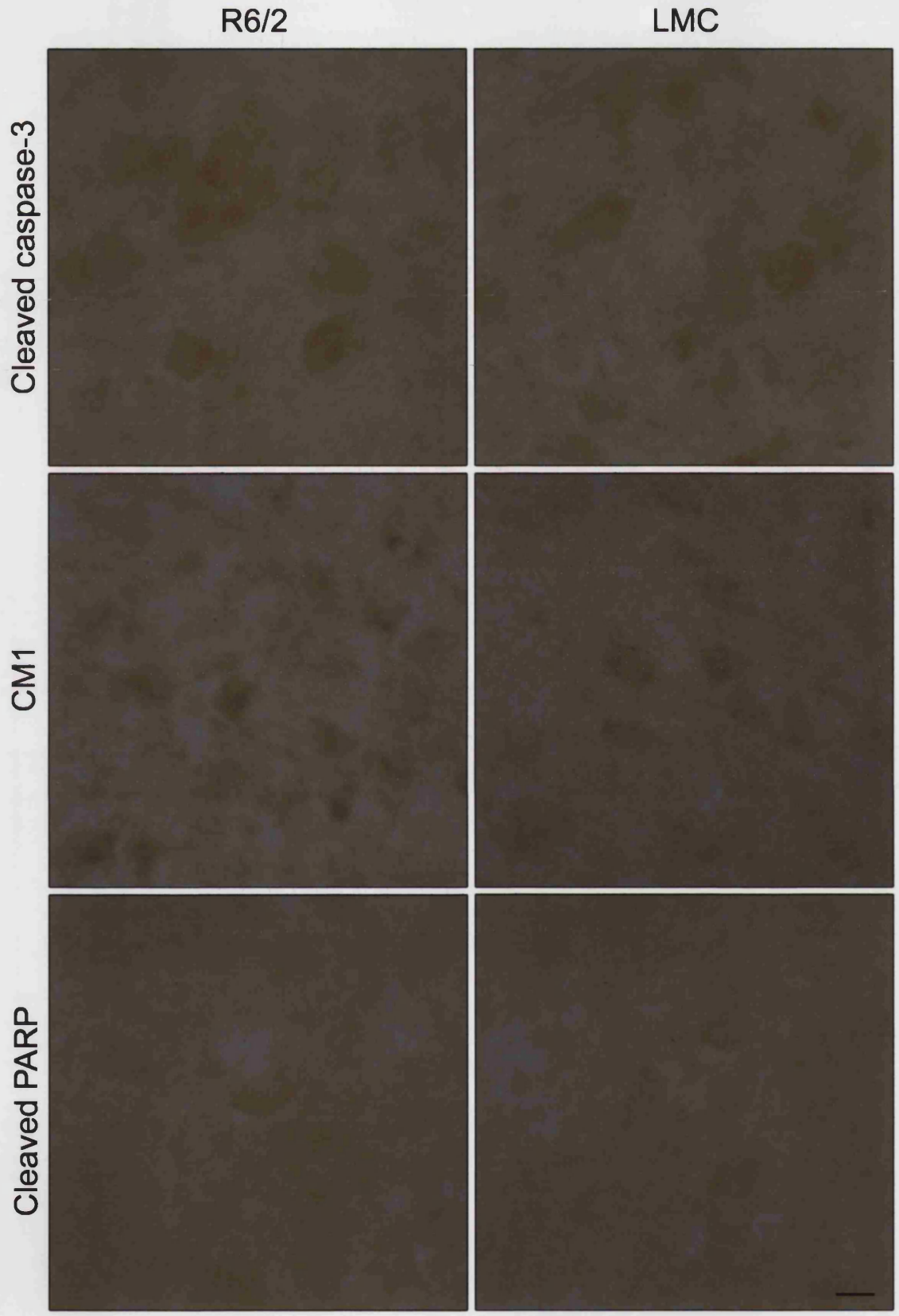

Figure 76 Sample light micrographs of 13 week-old R6/2 and littermate control cingulate cortical neurons, immunolabelled as indicated.
Scale bar applies to all (10μm).

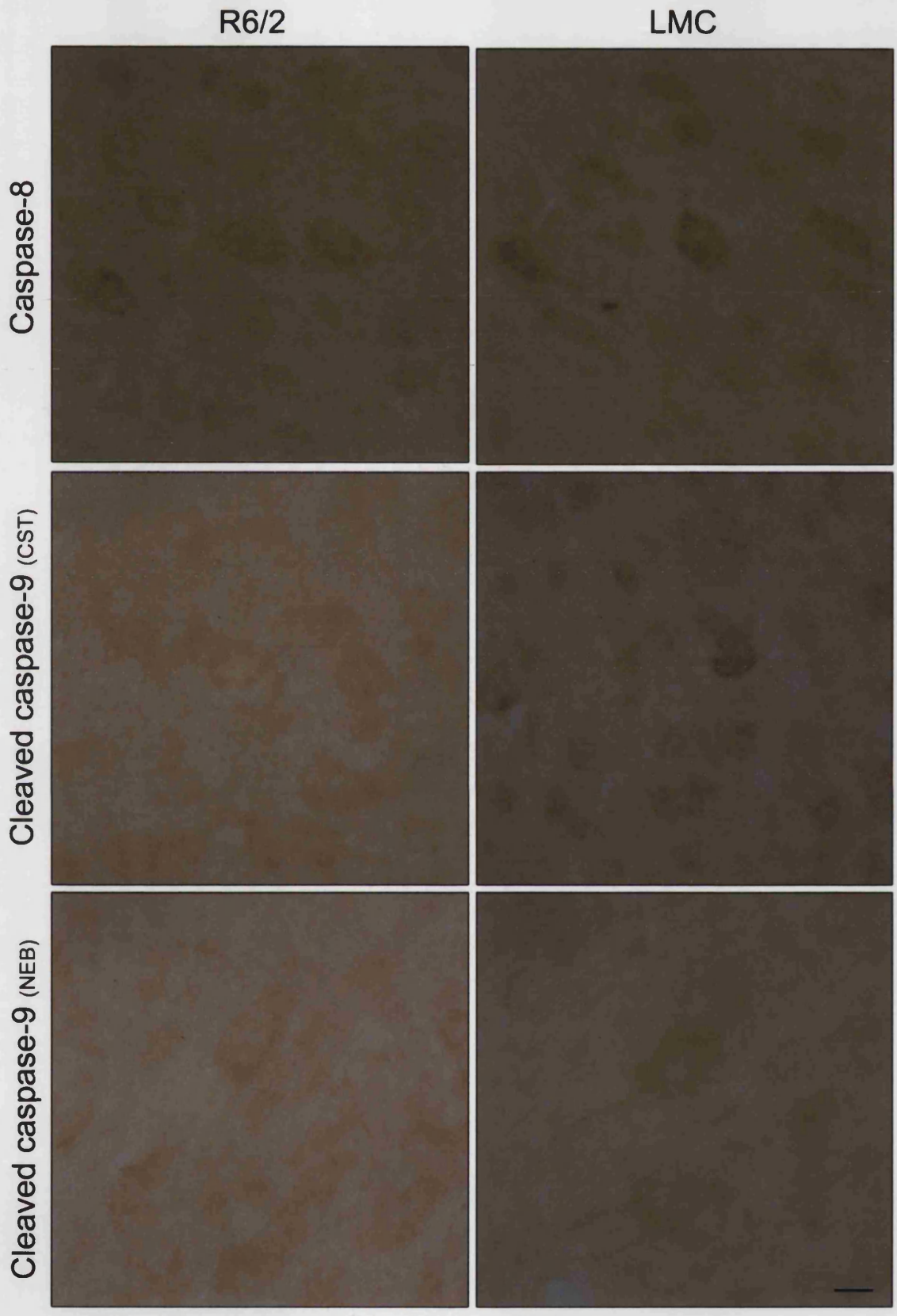

Figure 77 Sample light micrographs of 13 week-old R6/2 and littermate control cingulate cortical neurons, immunolabelled as indicated.
Scale bar applies to all (10μm).

unprocessed species, and yet neither caspase-3 antibody produces any significant staining. This suggests further that caspase-3, for many the major identifying factor of apoptotic cell death, is not activated in the degenerating R6/2 neurons.

One of the targets of activated caspase-3 is poly-ADP ribose polymerase (PARP), whose normal function is to repair DNA damage. The cleavage of PARP prevents it from repairing the breakages caused by DFF40/CAD thus reinforcing the catalytic efficacy of activated caspase 3. As no evidence for either caspase-3 activation or DFF40/CAD translocation has been found it should be unsurprising to report that there is no evidence for PARP cleavage either.

It has been suggested that caspase-8 is recruited to the neuronal intranuclear inclusion in a cellular model of polyglutamine disease (Sanchez *et al.* 1999). In the R6/2 mouse model, however, caspase 8 is seen to be localised throughout the cell, but has never been seen to colocalise with the NII.

Caspase-9 is unique among the caspases in that it does not have to be cleaved to reach maximum efficacy. Rather, as mentioned, it functions as a holoenzyme with Apaf-1 and cytochrome c. Free procaspase-9 will be cleaved during apoptosis as a result of the general self-activation of the caspase family, but is not fundamental to the apoptosis process. Nevertheless, it is interesting to find that one of the two antibodies used to label cleaved caspase 9 produces the punctate pattern reminiscent of other results. These experiments were conducted on consecutive sections, with the only altered variable between the two being the primary antibody. Therefore, it may be that the *Cell Signalling Technologies* cleaved caspase-9 antibody has a mild affinity for the non-activated form, as suggested for the cleaved ICAD and CM1 antibodies, but it may also be that this pattern is the result of some sort of general background staining, seen so prominently only as the sections are processed in DAB for a relatively long time to bring out any staining as might be present. However, without a positive control for comparison it is impossible to say whether this signal would be developed in the presence of confirmed apoptosis. Indeed, whilst the negative controls of the LMC mice provide a means of comparison for the R6/2 mice, it has yet to be shown whether these antibodies will actually recognise apoptosis if it is occurring.

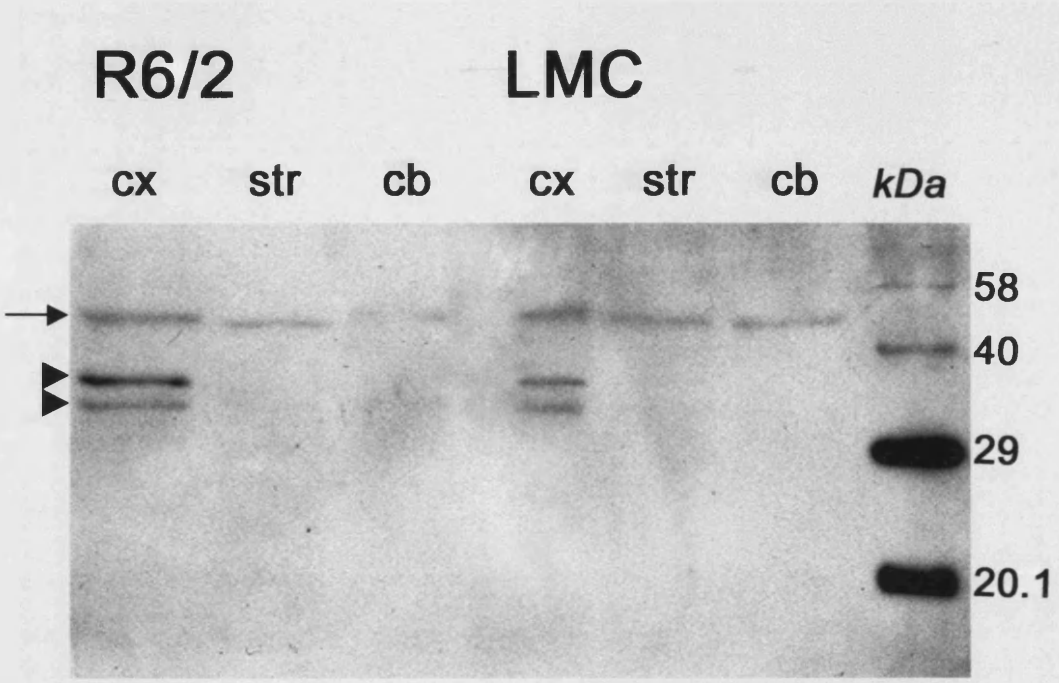

Figure 78 Western blot (chemiluminescence detection) of 13-week R6/2 and littermate control brain lysates (**cx**: cortex; **str**: striatum; **cb**: cerebellum) immunoblotted for caspase-1. The zymogen is present as a 45kDa band (arrow), precursor forms appear as intermediates (arrowheads) in the cortices of both mice. Activated caspase-1 should appear as a 20kDa band.

For the vast majority of my analyses into the involvement of the apoptosis players in dark cell degeneration, I have used immnohistochemistry, the advantage being that activity within individual cells can be identified. For caspase analyses, antibodies have been used which are engineered to recognise only the cleaved, activated form of each. As caspase-1 has been reported to be activated in R6/2 mice (Chen *et al.* 2000), it was important for me to assess the involvement of this factor myself. However, such an antibody has yet to be made against the activated form of caspase-1. Thus, in order that I might distinguish between the inactive and active forms of the enzyme I turned to western blotting. Figure 78 is an example of a blot immunolabelled for caspase-1, obtained form a gel on which lysates from 13-week old R6/2 and littermate control mice have been separated. The active form of caspase-1 should appear as a labelled band at approximately 20kDa. However, whilst the inactive forms of the protein are labelled, including, interestingly, two precursor forms in the cortex fractions from both mice, the blot is clear between 15 and 30kDa. Whilst there is the strong possibility that levels of activated caspase-1 are dwarfed by the inactive form in the greatly outnumbering non-dark cells (the very reasoning behind immunocytochemistry being my weapon of choice) my results certainly do not replicate the published reports which use identical methods to show considerable caspase-1 activation in the R6/2 mouse (*ibid.*).

As reported in *3.1.5* the identification of a positive control for morphological analysis was fraught with difficulties. At the five and six day age cells dying by developmental apoptosis in the mouse are exceptionally rare. At the semi-thin tol-blue level one may find one or two dark cells which one can then centre in on for ultra-thin EM analysis. With 40mm frozen sections one would have no guarantee that dying cells are present, and it would be almost impossible to verify this post-immunocytochemical analysis.

In order to address this question I investigated the possibility of inducing apoptosis, in as large numbers of cells as possibly, and preferably within the same tissue to act as a good positive control. John Scholes of the UCL Department of Anatomy, routinely X-irradiates rodents. Cells still in the cell cycle are more susceptible to radiation damage than post-mitotic cells (the basis for radiotherapy) and

therefore it was reasoned that in the P4-P6 mouse, whilst cells undergoing a natural apoptotic 'pruning' are rare, there may be many more in which apoptosis could be induced by X-ray damage.

The method of X-irradiation used is described in *2.4.x*. PLP-fixed tissue had to be cut at 80mm as at this age, it is very difficult to keep the tissue from disintegrating. Sections were processed for either DAB-immunocytochemistry of immunofluorescence. The latter involves fewer steps and thus yielded the greater quality tissue at the end of processing.

X-irradiation stimulated more than the death of a few more isolated, susceptible cells. There appear to be whole populations of neurons that undergo apoptosis when X-irradiated at P4/P5; particularly the sub-ventricular zone and the granule cells of the cerebellum. These areas are the last to complete cell division/maturation, and therefore posses the most cells yet to leave the cell cycle, making them the most sensitive to radiation damage. The very centres of these areas labelled with, for example, anti-activated caspase-3 and developed using the ABC-DAB system produces areas so dark that it is difficult to identify individual cells. Processing for confocal microscopy allows one to 'optically section' the sample and it is therefore easier to see individual cells amongst the cacophony of labelling. Figure 79 contains examples of apoptotic labelling in the sub-ventricular zone (A&B) and cerebellar cortex (C&D). The efficacy of the labelling is without question. Figures 79A & B are labelled for cleaved caspase-3, using the *New England Biolabs* and CM1 antibodies respectively. B is shown at high magnification such that the ultrastructure can be more easily distinguished. The cells in the plane of this optical section show pan-cellular labelling with the exception of one or more large circular regions which correspond to the condensations of chromatin formed in the generation of the apoptotic bodies, as illustrated at the EM level is figures 45-48. Figure 79C represents the labelling of cleaved DFF45/ICAD seen in the cerebellar cortex. There appears to be a distinct population of cells within the cortex that label for cleaved DFF45/ICAD, most likely the granule cells as these are the last to mature. Figure 79D shows cleavage of PARP, also within the cerebellar cortex.

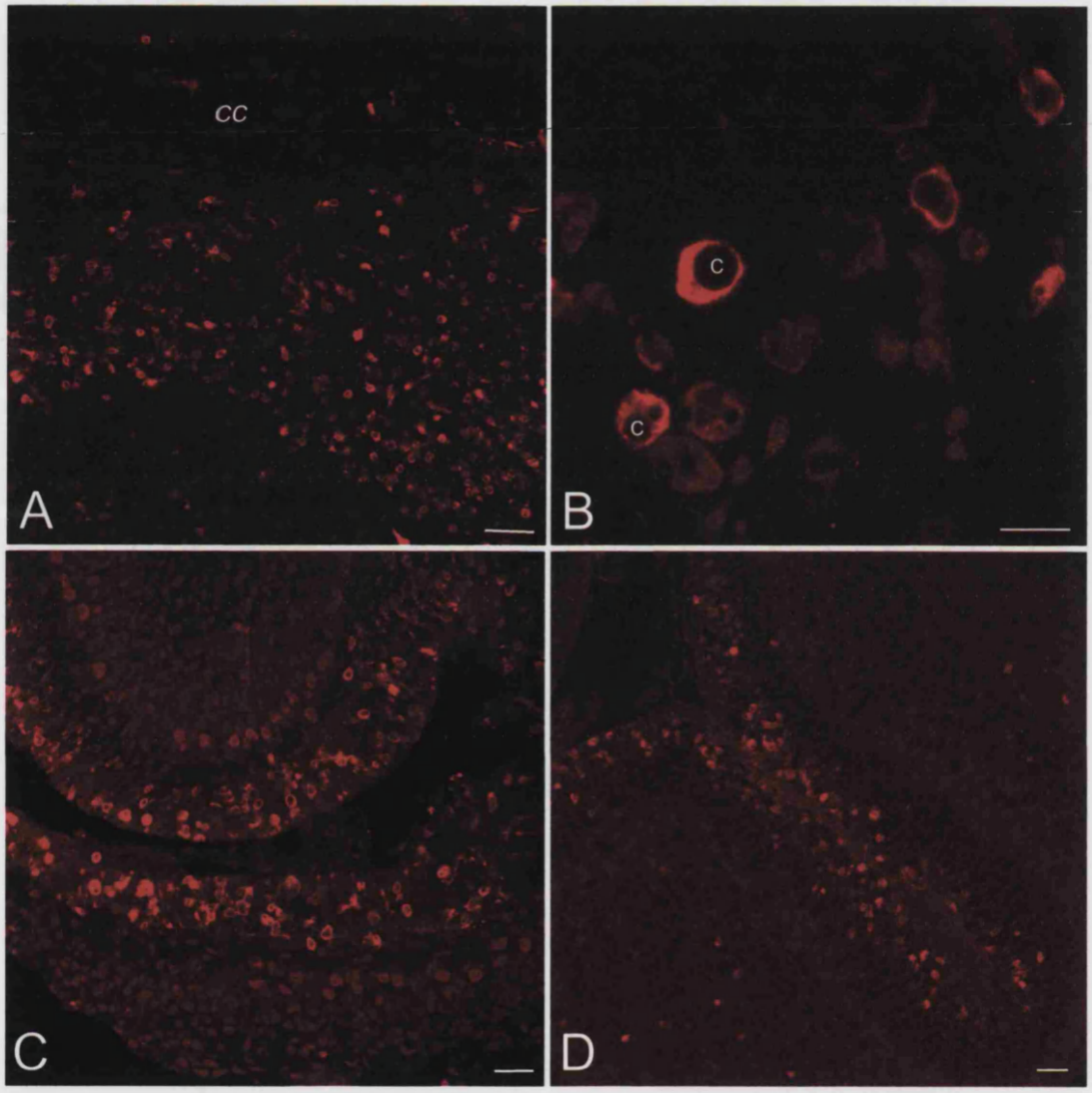

Figure 79 Confocal microscopy immunofluorescence on x-irradiated neonates. **A:** activated caspase-3 (*NEB*) in the subventricular zone (cc=corpus callosum) **B:** activated caspase-3 (CM1) shown at higher magnification (c=chromatin condensation) **C:** cleaved ICAD in the cerebellar cortex **D:** cleaved PARP in the cerebellar cortex.
Scale bars in A, C & D = 50μm; scale bar in B = 10μm

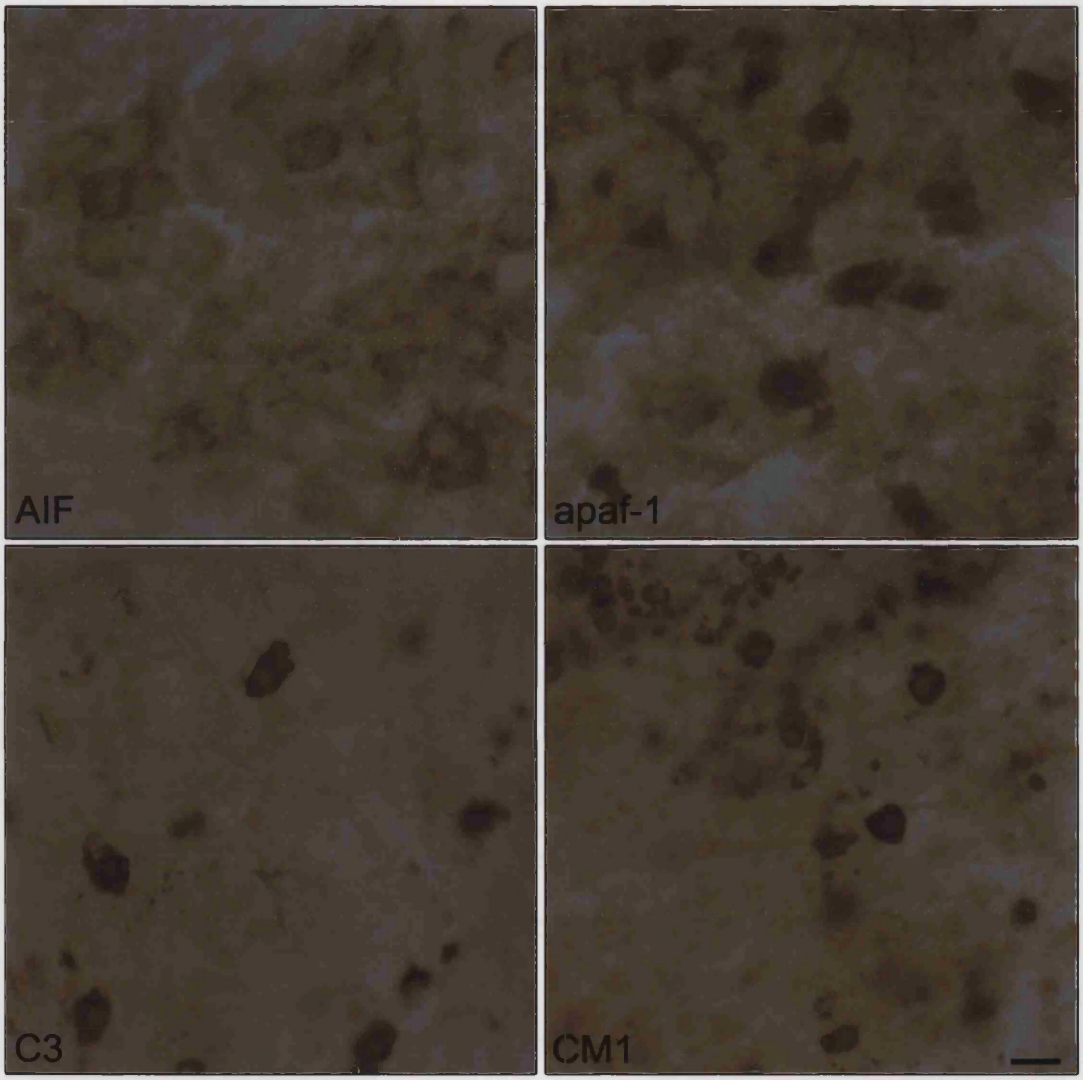

Figure 80 Cells in the subventricular zone of neonates following x-irradiation. Immunolabelled for listed factors (both **CM1** and **C3** are labelled for activated caspase-3) and processed using the ABC/DAB system. Scale bar = 10μm

Using DAB-immunocytochemistry individual cells can be identified on the periphery of these apoptosis-rich areas, and these also show morphology reminiscent of the apoptosis seen in the developing mouse in *3.1.5*. Figure 80 contains examples of cleaved caspase-3 (C3 & CM1) labelling using DAB. Though not as apparent as the optically sectioned confocal sections, circular DAB-free areas can be identified. Interesting, labelling for AIF yields no significant results, even in these areas of high apoptosis. One can find areas of darker staining, but neurons within these areas exhibit a healthy morphology with large pale nuclei, similar to the results seen in the adult R6/2 and LMC mice. Similarly, there appears to be no difference in staining for Apaf-1. Once again, there are zones within the apoptotic areas that exhibit a darker staining, but these resemble areas seen in the adult mice (*cf.* figure 74).

Unfortunately, whilst I attempted to do so several times, I did not manage to complete TUNEL labelling of X-irradiated sections due to the complexity of the procedure. By then end of processing very little remained of the sections.

Nevertheless, it can be said with a good degree of confidence that as these antibodies do label cells artificially induced into apoptosis in the P4-P6 brain they would label apoptotic cells in the adult brain if the appropriate protein species were present. Therefore, I believe it is reasonable to conclude that the negative results gathered in this study are true negative results.

3.1.9 The Role of Glia

Kerr, Wylie and Currie's original definition of apoptosis included as the second stage the engulfment of the apoptotic cell by surrounding cells. In the nervous system this normally falls under the purview of the microglia: the macrophages of the CNS. In the case of necrotic cell death the resultant inflammatory response in dominated by astrocytes.

As mentioned in *3.1.5* glial cells are often seen juxtaposed to degenerating neurons. It has also been suggested that processes from these glia penetrate the degenerating neurons (Mark Turmaine, personal communication). The question,

therefore, is what are these glia and what role do they have in the degeneration of the R6/2 neurons?

Astrocytosis occurs as part of HD (Vonsattel *et al.* 1985); there are also reports of an increase in density of oligodendrocytes (Myers *et al.* 1991). Astrocytes are identifiable at the electron microscope level, but at the light level, they need to be labelled to facilitate counting. Labelling with GFAP, produces highly variable staining patterns, not only between individual mice but between individual sections from each mouse. Attempts at quantifying astrocyte numbers therefore proved fruitless. However, since oligodendrocytes are relatively easy to identity in tol-blue sections, this issue is more easily addressed.

The increase reported by Myers *et al.* occurs before the onset of symptoms, indeed, they suggest that the increased number of oligodendrocytes may be indicative of developmental changes in HD gene carriers affecting glial numbers from birth (redrawn from original data as figure 81). Using tol-blue sections of the striatum I counted the number of oligodendrocytes at each age and also measured the total cross-sectional area of each striatal slice. As it cannot be guaranteed that each section is from an identical region of the striatum, a comparison of cross-sectional areas would not yield a reliable result, however, oligodendrocyte densities should provide more reliable sample data. I have expressed the data in figure 82 in a manner similar to the data from Myers *et al.* in figure 81. The broad trend is similar: there is a significant increase in oligodendrocyte density in the diseased individuals ($p<0.005$). However, in contrast to the suggestion from Myers *et al.* this increase is not congenital. It does occur before the onset of overt symptoms, before eight weeks ($p<0.05$), but is not apparent at six weeks or younger. If the human data were to include HD-carrier youths in its sample, the picture may be identical.

There remains, however, the possibility that the increases in oligodendrocyte density occur not as a result of oligodendrocyte proliferation but rather as a result of cell shrinkage. As previously mentioned, a comparison of striatal cross-sectional area would not yield a reliable result; however, to address the question of neuronal shrinkage affecting density, one can study the corpus callosum. Given that there are no neuronal cell bodies within the corpus callosum the effect of any neuronal

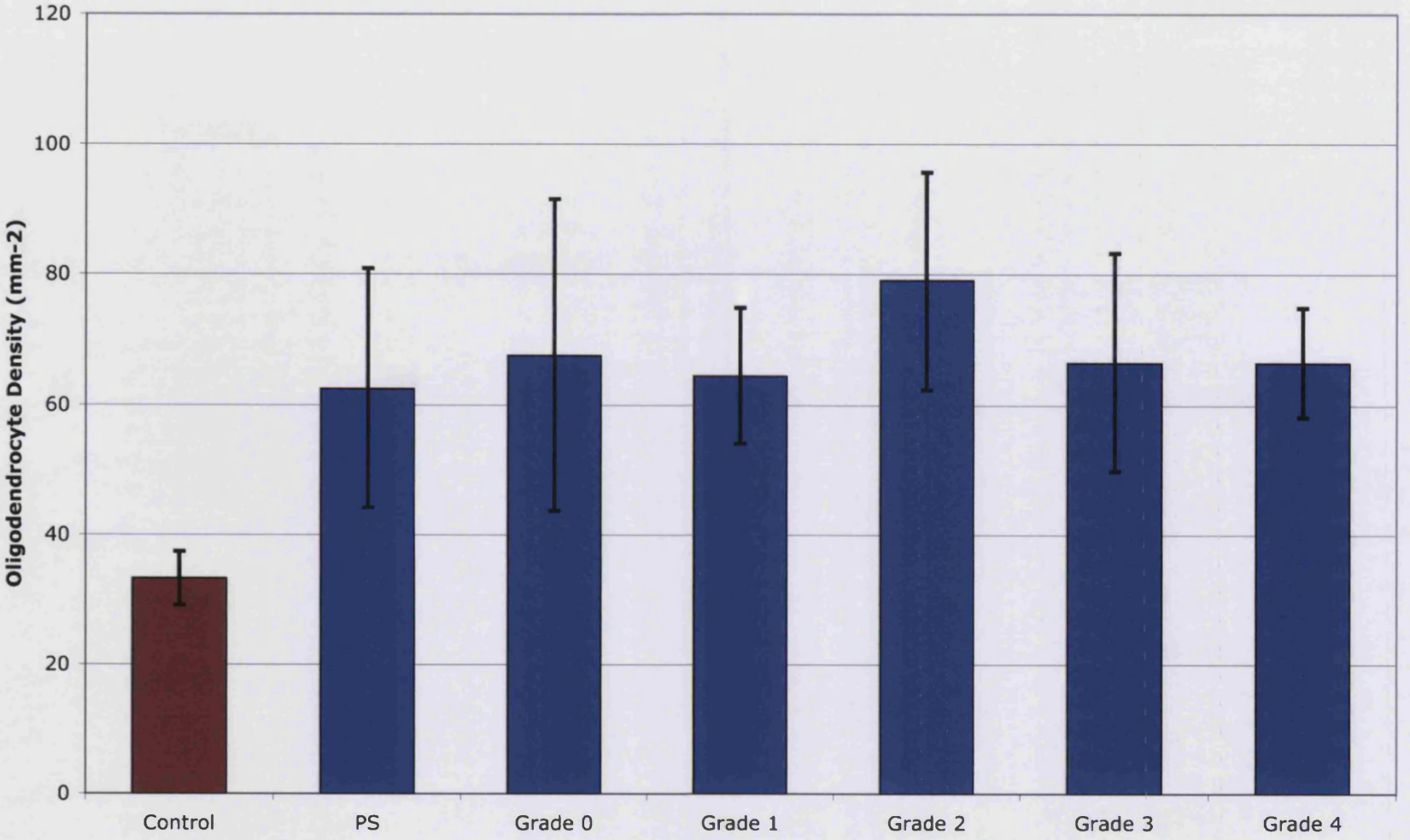

Figure 81 Density of oligodendrocytes within the striatum of human HD patients throughout disease progression compared to otherwise healthy individuals. A significant increase in density is seen at all stages of the human disease.

Redrawn from data published by Myers *et al.* (1991)

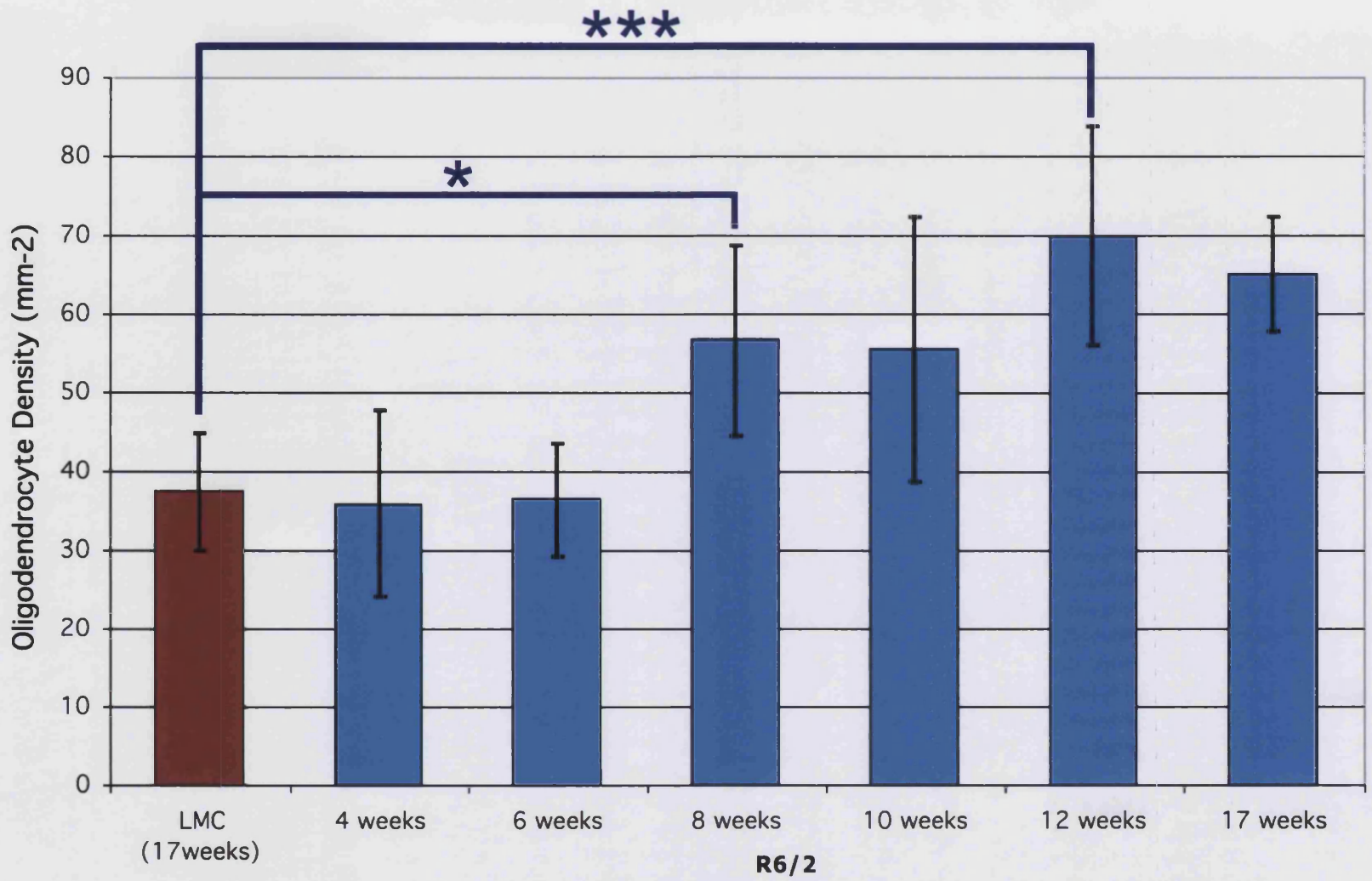

Figure 82 Density of oligodendrocytes within the striatum of the R6/2 mouse model throughout disease progression compared to littermate control mice of 17 weeks of age. A significant increase in density is seen at 8 weeks (* $p<0.05$). This increase becomes more significant as the disease progresses (*** $p<0.01$).
Students t-test (n=7); error bars = ± 1 standard error.

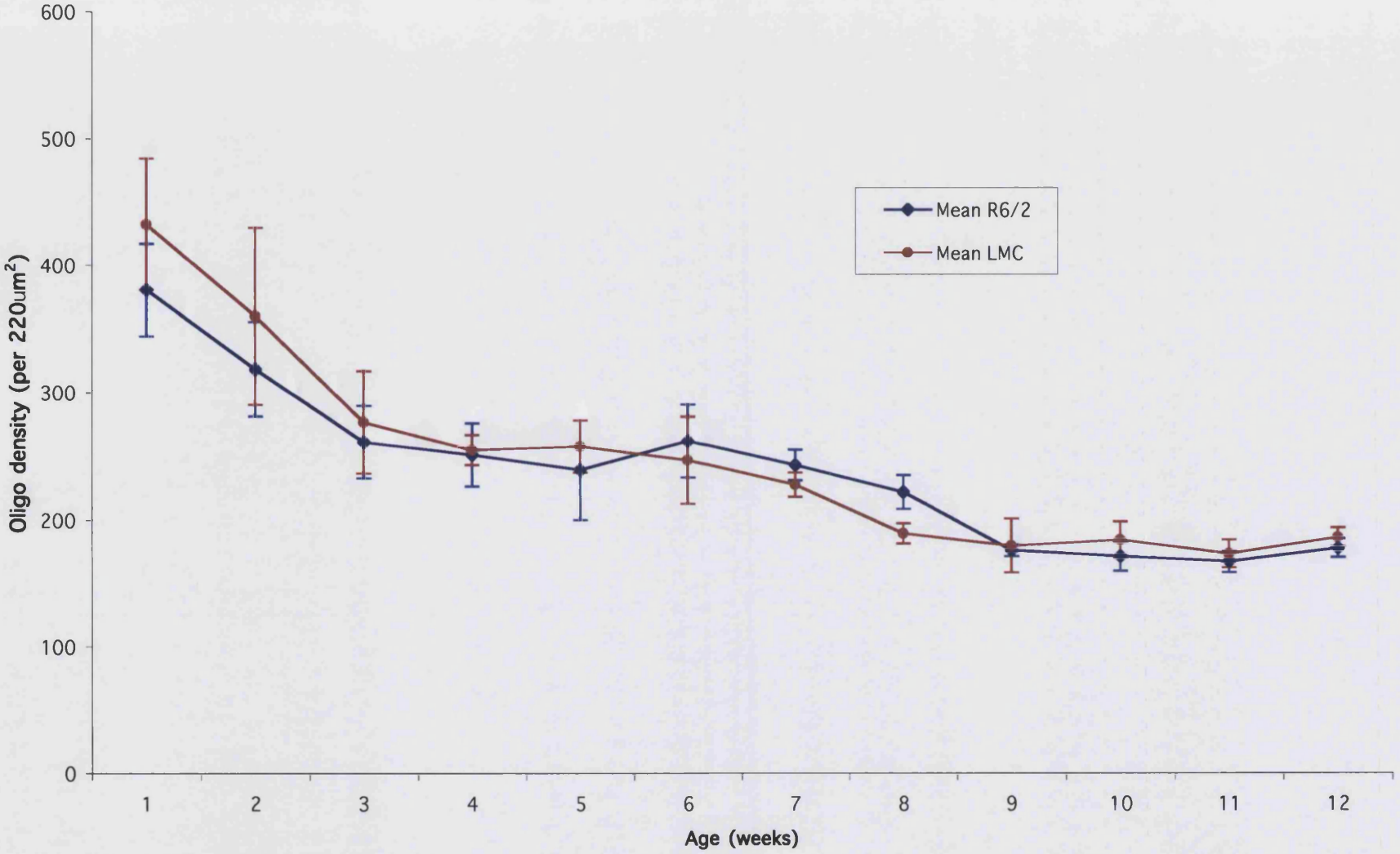

Figure 83 Density of oligodendrocytes within the corpus callosum of R6/2 and littermate control mice from 1 week to 12 weeks of age. There is no statistical difference between these densities. ($p>0.05$, $n=2$; error bars = ± 1 std err)

shrinkage should be negligible. Furthermore, given that the only cell bodies present in the corpus callosum are glial, it is even easier to count cell number. Using the OpenLab software, I counted thionin-stained cell nuclei within the corpus callosa of R6/2 and LMC mice from one week of age to twelve weeks of age (figure 83). The results indicate that there is no significant effect on oligodendrocytes in the R6/2 mouse. Indeed, density decreases as the mice age suggesting that as the size of the white matter increases, oligodendrocytes do not proliferate in exact proportion.

It has been reported that R6/2 exhibit a reduced growth; indeed, the average corpus callosum cross-sectional areas was smaller in the R6/2 mice compared to their littermates. Therefore, we would expect density values to be higher if the same number of oligodendrocytes were contained in a smaller area. Whilst the results show no statistical difference, if they suggest anything at all, it is that there is a decrease in oligodendrocyte numbers in the R6/2 corpus callosum.

It is very difficult to say whether the R6/2 striatal oligodendrocyte counts indicate a true increase in absolute number. Furthermore, whilst the human data of Myers *et al.* indicate an increase in oligodendrocytes even in presymptomatic HD patients, it has been noted that remarkable shrinkage can occur in patients before the onset of symptoms (de la Monte *et al.* 1988). It is therefore a distinct possibility that the reports of increases in striatal oligodendrocyte numbers, including my own work, are an artefact resulting from neuronal shrinkage.

It is interesting to read that Myers reports no significant astrocytosis until there is significant neuronal loss in the human disease. Given that there is no significant neuronal loss within the lifespan of the R6/2 mouse, if the model does indeed replicate the glial behaviour in the disease, one would not expect to see significant astrocytosis at all.

Whilst it is not possible to accurately identify any increases in glial numbers in the R6/2 model, it is evident that there is some form of glial response to the degenerating neurons; glial cells are seen juxtaposed to dying cells and 'cuffing' is seen around the blood vessels. In an attempt to identify these neurons which contact degenerating cells I labelled 12 week R6/2 sections for the glial markers GFAP, F4/80 and NG2; identifying astrocytes, microglia and oligodendrocytes respectively. I viewed

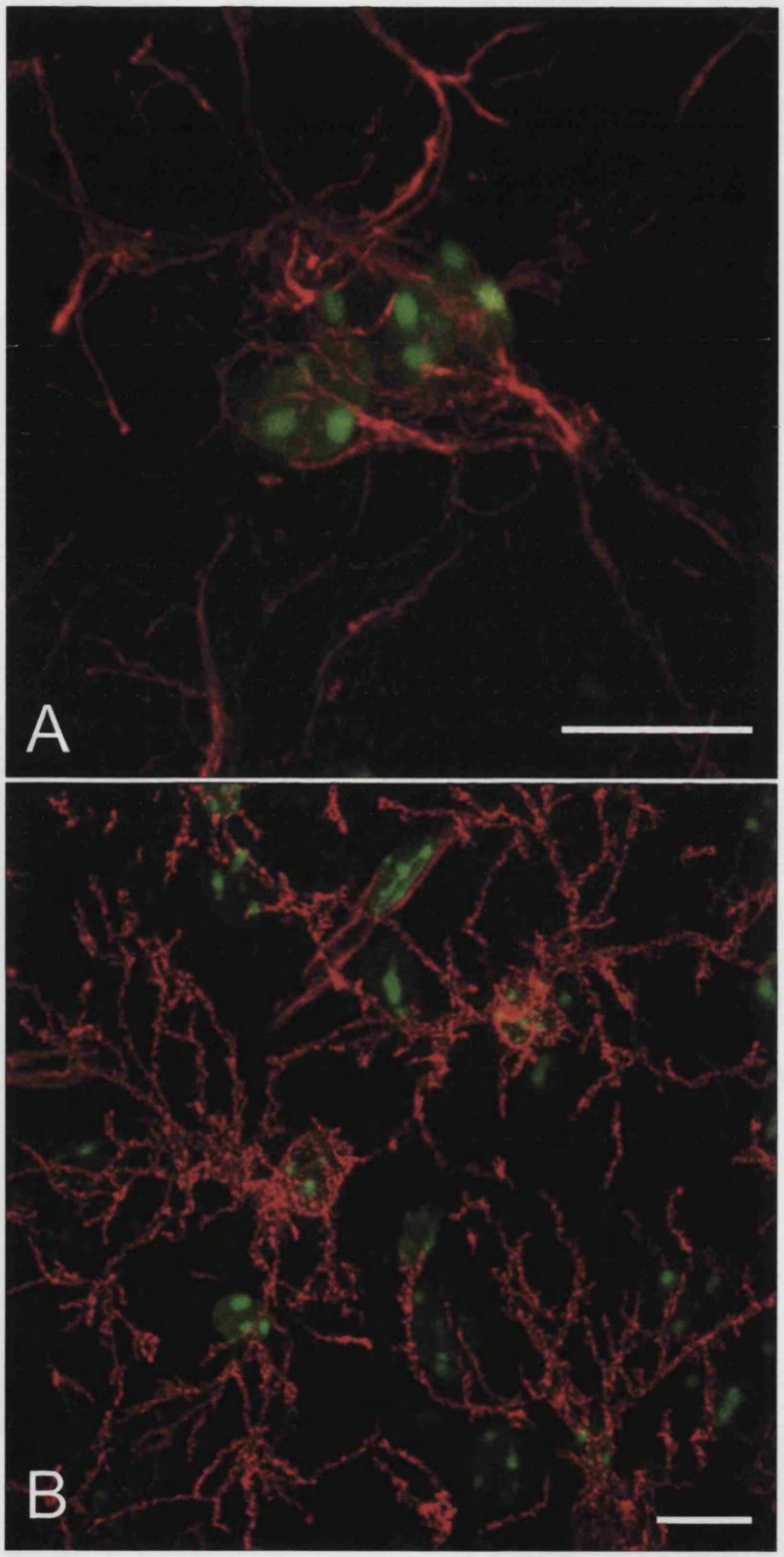

Figure 84 Confocal micrographs to illustrate the staining patterns obtained when immunolabelling for either GFAP (**A**) or NG2 (**B**). Scale bars = 10μm.

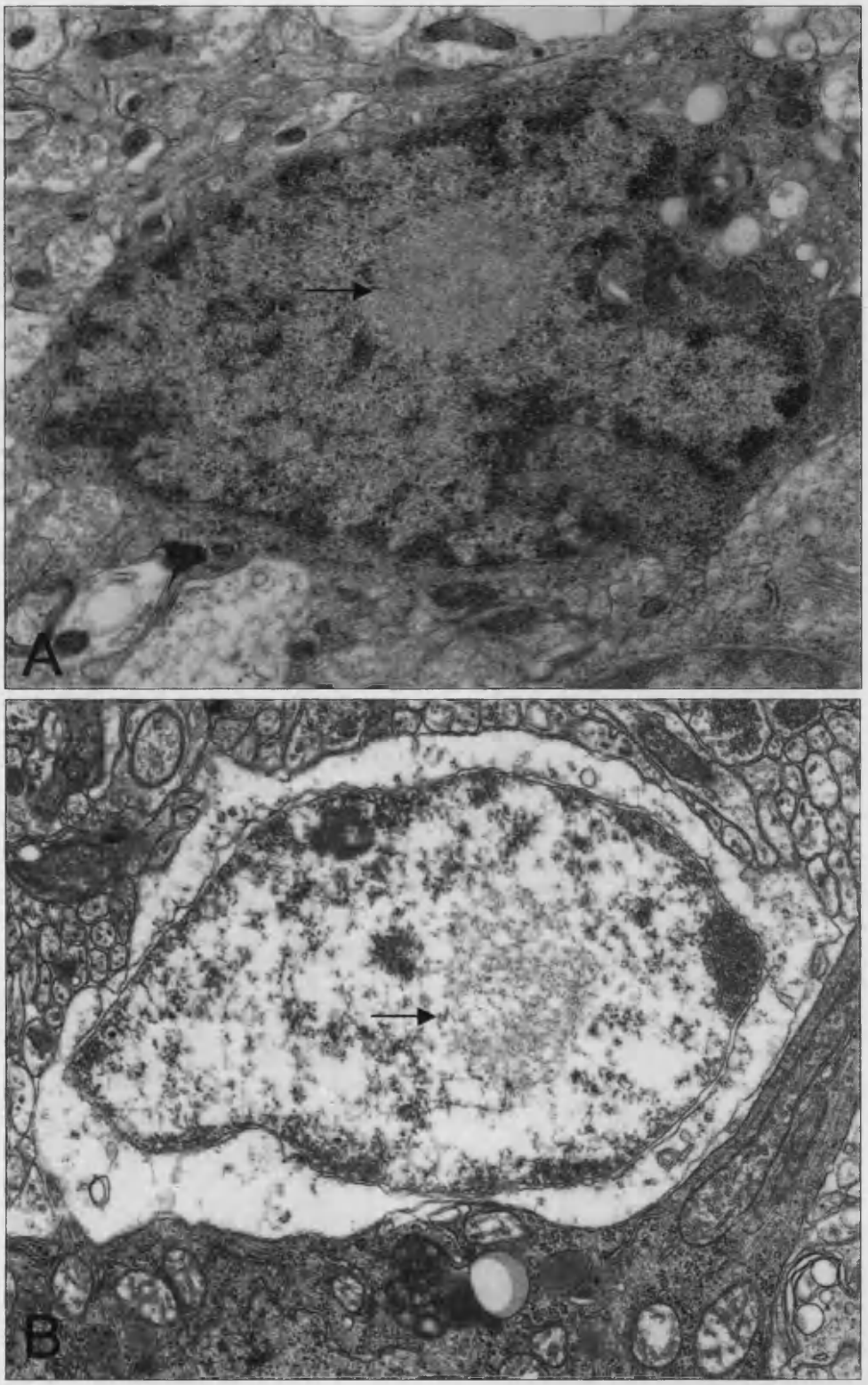

Figure 85 An oligodendrocyte (**A**) and an astrocyte (**B**) from a 17 week-old R6/2 mouse. Intranuclear inclusions are evident in both glia (arrows).

p200

Glia have NIIs in R6/2.

Not in human disease.

of dopaminergic SNC neurons. Here we have shown that the JNK3 ko provides long-lasting protection against axotomy; moreover, JNK3 ko and c-JunAA are transiently protective against 6-OHDA. These findings suggest a pro-apoptotic role of JNK3 and c-Jun in degeneration of dopaminergic neurons being in line with recent observations (Hunot et al., 2004). Moreover, c-JunAA and JNK2 revealed a non-significant tendency to improve the survival of SNC neurons following axotomy. Recently, SNC neurons were transiently protected against axotomy by *c-jun* antisense-oligonucleotides (Crocker et al., 2001), and JNK2 ko protected 7 d after MPTP induced dopaminergic death whereas later time points were not investigated (Hunot et al., 2004). We have also found that the number of dopaminergic SNC neurons in JNK1 ko was significantly enhanced compared to WT1, whereas no differences were found as published elsewhere (Hunot et al., 2004). Previously, similar numbers of facial motoneurons

these sections using confocal microscopy, such that I could also scan vertically through each section. Glial cells labelled well (figure 84), but I could not find a labelled glial cell contacting a dark nucleus indicative of a degenerating neuron. Thus, whilst it is difficult to make conclusions using such data, it suggests that those glia seen to contact degenerating neurons at the electron microscope level are neither microglia, oligodendrocytes or *mature* astrocytes. Since GFAP is present only within reactive astrocytes, there remains the possibility that the glia are astrocytic in lineage, but have yet to mature.

In undertaking these investigations an important difference between the human disease and its R6/2 model became apparent. Most evident within the corpus callosum, it can be seen that glia in the R6/2 often contain inclusions in a manner similar to the neurons. In fact at the ultrastructural level they appear similar to the NIIs (see figure 85). As illustrated, they are found both in oligodendrocytes (A) and in glia with astrocytic morphology (B). Whilst my results suggest the presence of the inclusion within the oligodendrocyte appears to affect neither its development nor its survival, there remains the possibility that its presence affects glial function. Given that glial inclusions have not been detected in the human condition, this raises the possibility that there may be a glial component to the R6/2 disease, perhaps adding to the severity of the disease phenotype.

3.2 *Degeneration in the* Hdh *Knock-In Mouse*

3.2.1 *Introduction*

AMONG the various mouse models of Huntington's disease (see 4.6), a number have involved the 'knocking-in' of the mutation that causes the human condition into the murine homologue of the IT15 gene, *Hdh* (Huntington's disease homologue). Whilst more complicated to generate, one may argue that these models recapitulate the human condition more accurately, given that the mutation is within the natural mouse gene and this gene is within the correct 'genetic context' (the random nature of the integration event(s) involved in generating transgenic mice has the potential to disrupt the normal genome).

Conversely, given that the human and mouse huntingtin proteins are only 90% similar (see 6.2), one could argue that the knock-in models replicate not the human condition, but the mouse equivalent. No mouse model is going to replicate fully the human disease simply because they are different species. Rather the question is one of the 'most appropriate' model(s).

In order to address this issue I have also studied the *Hdh* knock-in model of Dr Peggy Shelbourne in order to compare it to the R6/2 transgenic model. This *Hdh* model exists on more than one genetic background: both Black 6 and FVB mice strains, thus allowing me to also investigate any differences that may occur due to background genetics, as each strain of knock-in mouse expresses an identical mutant protein. Furthermore, a spontaneous mutation occurred in one line of Black 6 *Hdh* mice yielding an aberrant stop codon near the 3' end of intron 1. These mice express a truncated version of the mouse huntingtin containing only exon 1 with an expanded polyQ sequence, akin to the transgenic construct expressed in the R6/2 mice. Thus comparing these mice permits a comparison of the R6/2 to its knock-in equivalent (albeit with different repeat sizes).

3.2.2 Inclusion Distribution

Sections from each of the mice, *Hdh* and wild type, were immunolabelled using the htt_n antibody. Whilst each of the *Hdh* mice showed the presence of inclusions, the distribution was markedly different to that seen in the R6/2 mice. In contrast to the ubiquitous distribution seen in the R6/2, inclusions were confined to discrete areas within these mice. The primary foci for inclusions were the nucleus accumbens, olfactory tubercle and the striatum. There was no observable difference between the distribution of number of inclusions seen in either of the full-length strains, but in the striatum alone, each showed a considerably greater number of inclusions than the truncated expression black 6 strain (figures 86 and 87). Both full-length strains exhibited many mature inclusions within the striatum, and yet these are relatively rare in the truncated expression knock-in. This is rather surprising given that the work of others suggests a greater propensity for inclusion formation in models that express merely the N-terminus of huntingtin.

Each of these mice stands in stark contrast to the R6/2 where areas that were seen to possess frequent, large inclusions show no involvement at all using the knock-in approach; most noticeably all cortical regions. Furthermore, within each area that does contain inclusions, the *Hdh* mice exhibit a restricted distribution. Figure 88 contains micrographs from the striata of R6/2 and *Hdh* mice. Large inclusions are visible in both (arrowheads), and yet whereas the R6/2 shows nuclear htt_n immunoreactivity in all cells, the *Hdh* possesses cells with nuclear htt_n and large inclusions adjacent to cells with a wild-type appearance (arrows).

Referring to figure 37, within the striatum, the *Hdh* mice show profiles corresponding to all stages up to 8 weeks. At this point the mice are at the end of their natural lifespan and so cannot show more mature profiles. This would also explain why I have been unable to locate neurite inclusions in these mice. In my R6/2 analyses, neurite inclusions formed after numerous, large nuclear inclusions were evident, thus it is reasonable to assume that these mice die before neurite inclusions can form. The R6/2 mice also show mostly concomitant inclusion formation in contrast to the single-area variation seen here. Figure 88 (*Hdh*) shows that adjacent

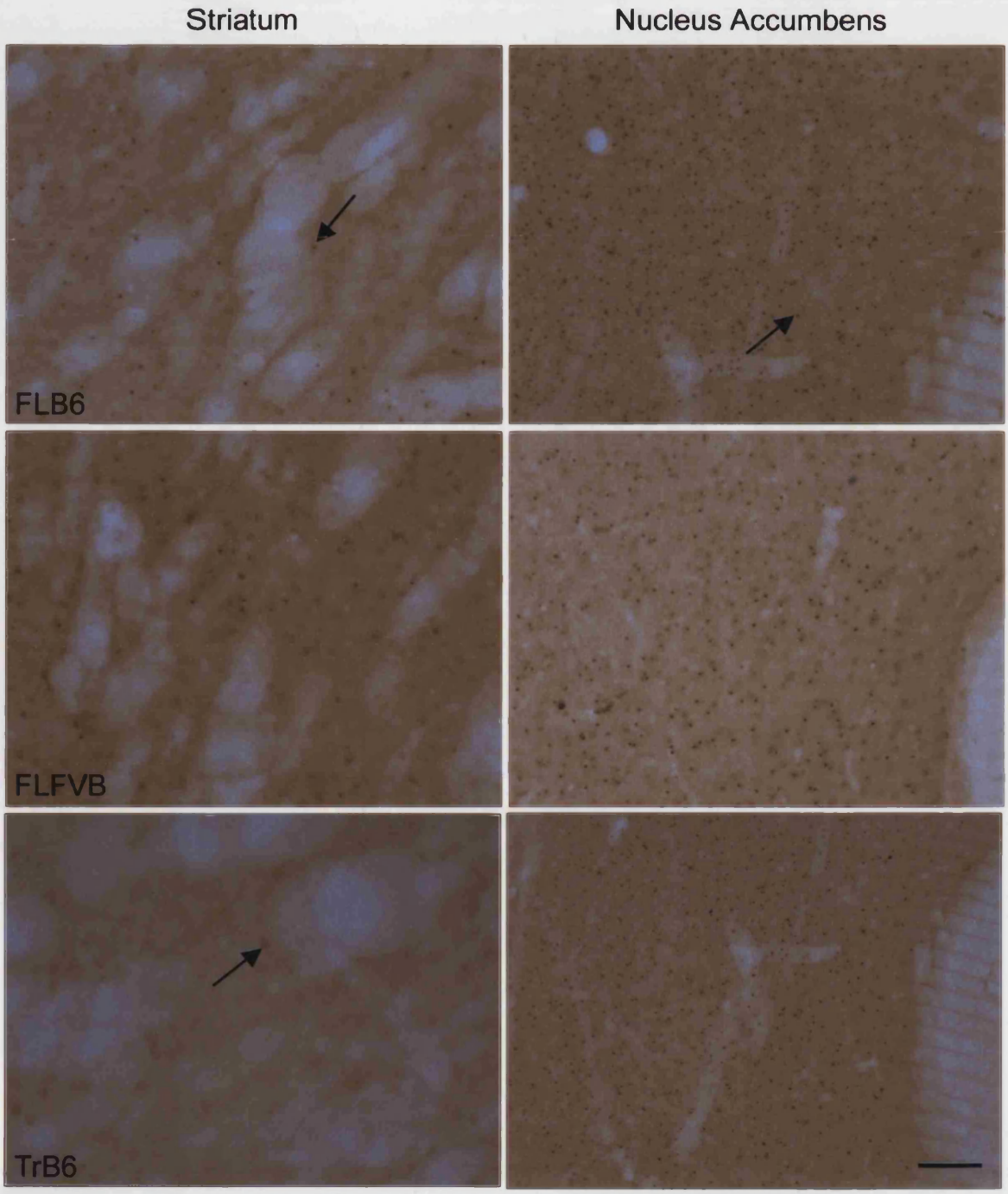

Figure 86 N-terminal huntingtin immunolabelling in the striatum and nucleus accumbens of full-length *Hdh* black 6 (FLB6), full-length *Hdh* FVB (FLFVB) and truncated *Hdh* black 6 (TrB6) mice. Inclusions (arrows) are more prevalent in the nucleus accumbens of all animals. Within the striatum, the truncated-expression black 6 mouse shows the fewest inclusions.
Scale bar = approximately 100μm

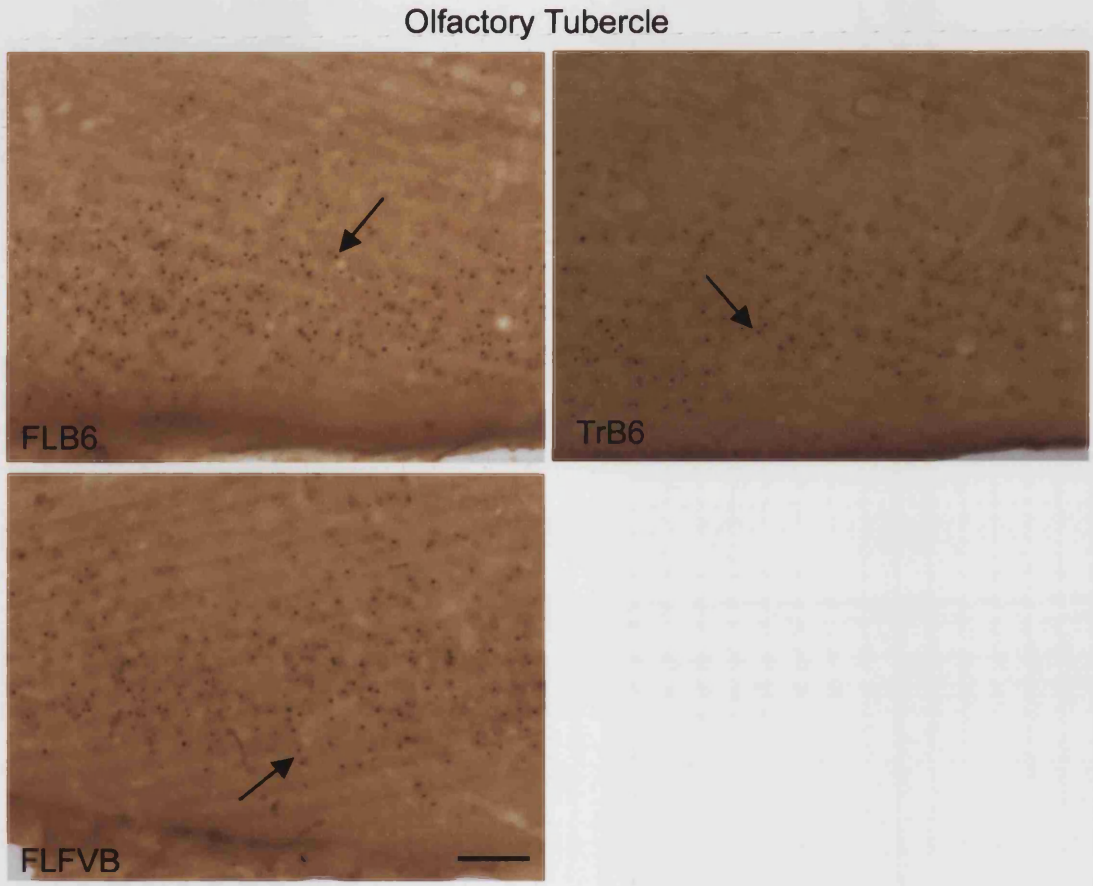

Figure 87 N-terminal huntingtin immunolabelling in the olfactory tubercle of full-length *Hdh* black 6 (FLB6), full-length *Hdh* FVB (FLFVB) and truncated *Hdh* black 6 (TrB6) mice. Inclusions are present throughout the region (arrows) at comparable frequencies in each animal. Scale bar = approximately 75µm

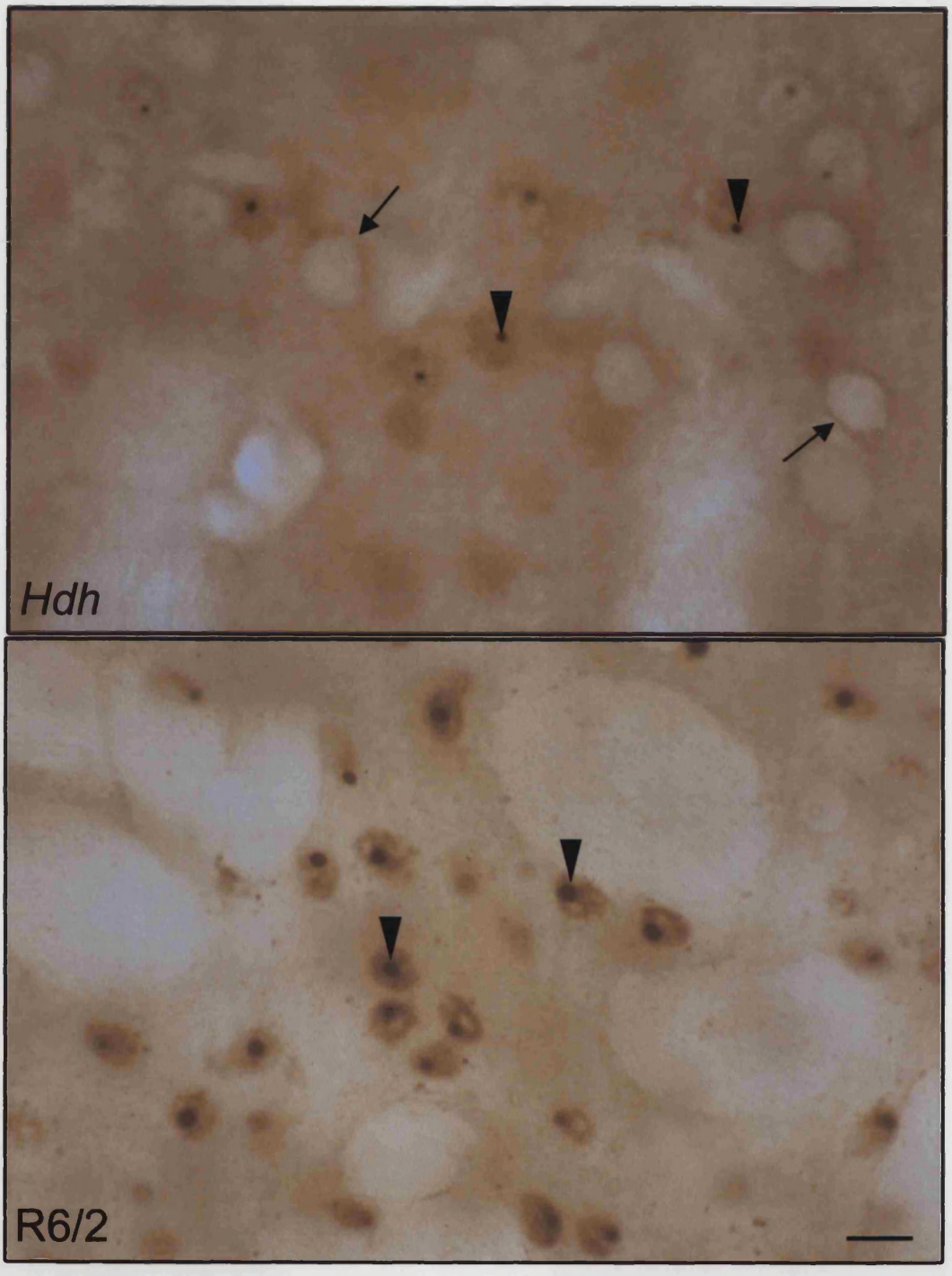

Figure 88 Striatal sections from a 29 month-old full-length *Hdh* mouse and a 12 week-old R6/2 mouse immunolabelled for N-terminal huntingtin. Inclusions (arrowheads) are smaller in the *Hdh*. The R6/2 also shows nuclear accumulation of htt in all cells, whereas the *Hdh* shows many neurons with purely cytoplasmic labelling (arrows). Scale bar = 10μm

cells can exhibit profiles at opposite ends of the inclusion spectrum. This limited variation, together with the limited distribution in the brain as a whole, may correspond to the selectivity seen in HD.

3.2.3 Patterns of Degeneration

As with the R6/2 mice, the presence of degeneration was assessed using semi-thin toludine-blue stained sections. Interestingly, considerable amounts of degeneration were observed in many areas. Given that these mice are relatively asymptomatic, exhibiting only minor behavioural alterations, the amounts of degeneration seen were truly surprising. However, the most startling observation was found in the controls. Both black 6 and FVB wild-type mice showed comparable levels of degeneration to their littermates expressing mutant huntingtin.

Sections throughout each of the brains were taken and the distribution of dark profiles noted. As reported below, variation along the anterior-posterior (A-P) axis was found for each mouse at each age (thus making quantitative analyses difficult); but for an illustrative comparison, sections from comparable regions in mice approximately 128 weeks old[♦] are presented in figures 89 to 100. As seen in the R6/2 mice, the cingulate cortex showed the greatest number of degenerating cells in the *Hdh* mice (figure 89), with the majority of cells in each layer of this region exhibiting a darkened appearance (arrows). Between the controls, degenerating cells are found more frequently in the FVB wild-type; an interesting result as this mouse is nearly two months' younger. In either case, degenerating cells within the cingulate cortices of the controls are considerably fewer than any of the knock-ins. Thus it appears degeneration in the cingulate cortex can be ascribed to the *Hdh* mutation.

The secondary motor cortex (at this A-P position) shows mild degeneration in each mouse, with no substantial differences between each of the mice (figure 90);

[♦] All black 6 mice in this comparison were 29 months and 21 days-old, the oldest surviving *Hdh* FVB mouse was 29 months and 18 days-old. Unfortunately, the only extant wild type FVB was 28 months-old exactly.

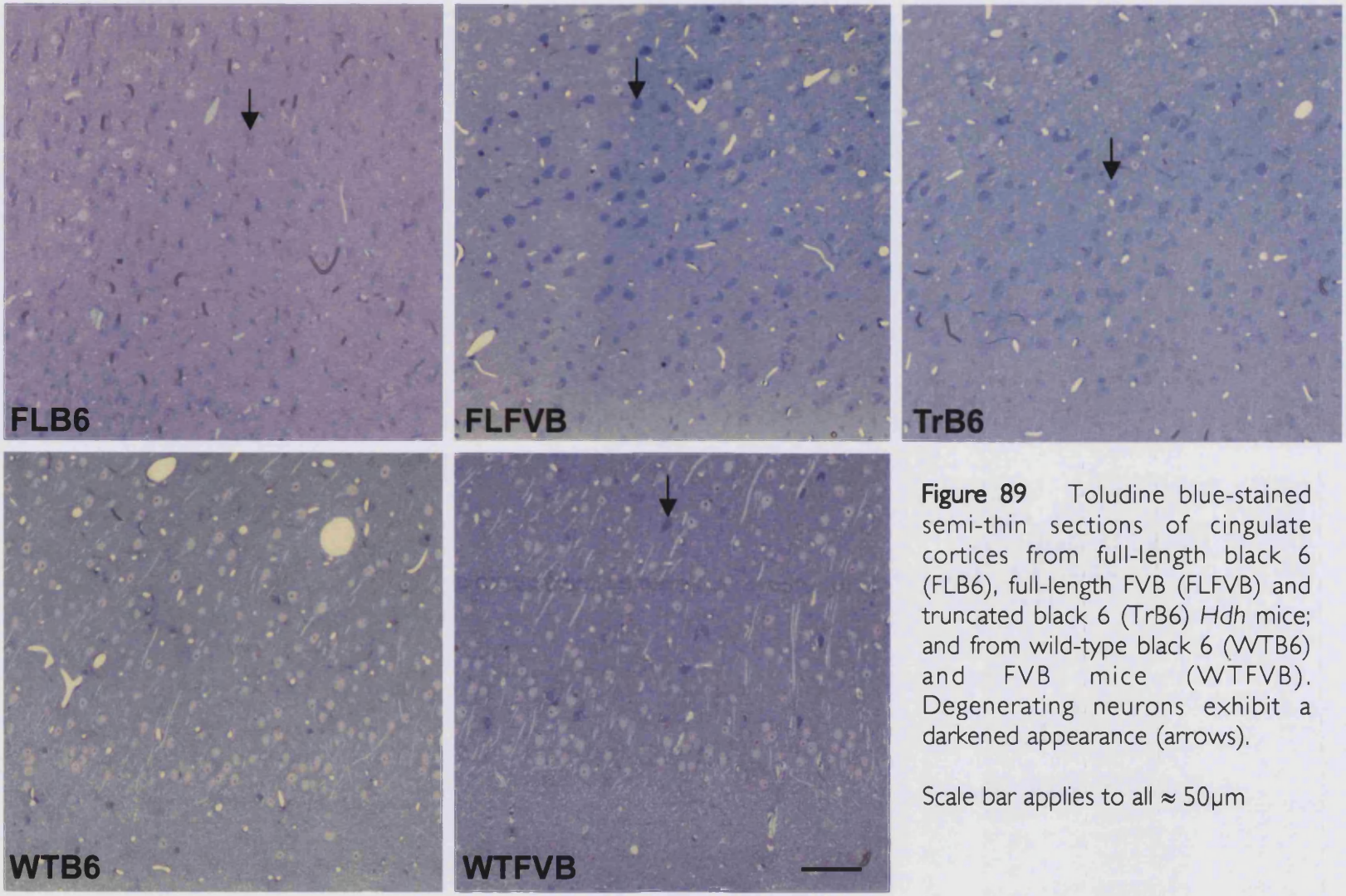

Figure 89 Toludine blue-stained semi-thin sections of cingulate cortices from full-length black 6 (FLB6), full-length FVB (FLFVB) and truncated black 6 (TrB6) *Hdh* mice; and from wild-type black 6 (WTB6) and FVB mice (WTFVB). Degenerating neurons exhibit a darkened appearance (arrows).

Scale bar applies to all ≈ 50μm

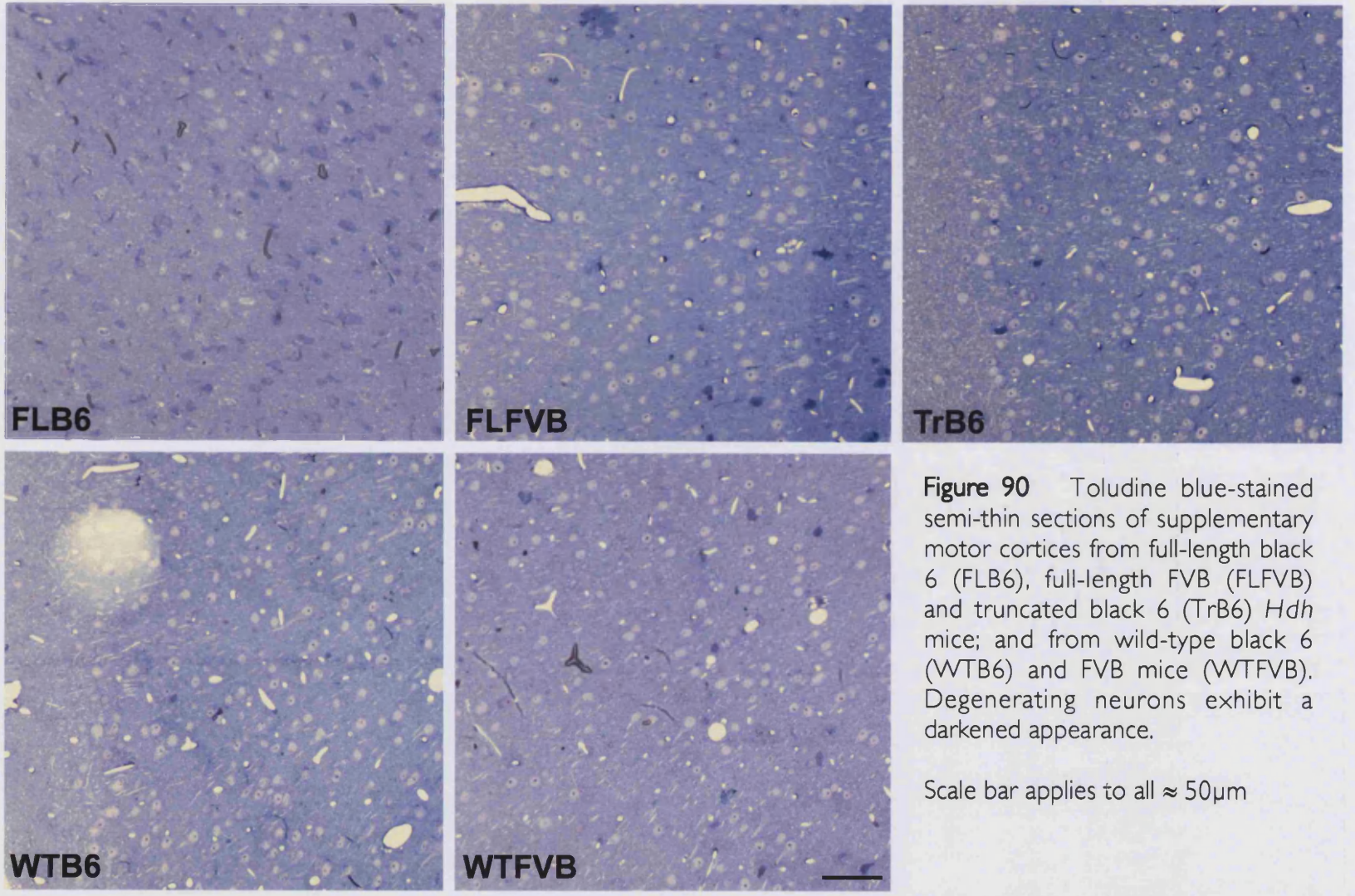

Figure 90 Toludine blue-stained semi-thin sections of supplementary motor cortices from full-length black 6 (FLB6), full-length FVB (FLFVB) and truncated black 6 (TrB6) *Hdh* mice; and from wild-type black 6 (WTB6) and FVB mice (WTFVB). Degenerating neurons exhibit a darkened appearance.

Scale bar applies to all ≈ 50μm

whereas the primary motor cortex shows degeneration in each of the *Hdh* mice with few observable changes in the controls (figure 91). Therefore it would seem that degeneration in the primary motor cortex is also attributable to the mutation.

The situation is reversed in the somatosensory cortex (figure 92) where each of the *Hdh* mice is spared degeneration in contrast to the controls, which possess numerous darkened cells at various stages of degeneration. It seems reasonable to assume that mutant huntingtin would act as a toxic stimulus over and above the degenerative effects seen with age. It is unlikely that there is an unknown beneficial effect of the mutation, delaying age-related changes, thus this situation is rather puzzling. Given the variation along the anterior-posterior axis it is likely that this situation arises as a result of comparing slightly difference areas. In most regions, this variation occurs gradually as one moves through the brain, but in the somatosensory cortex there appears to be a very defined, focal region of degeneration. Thus, whilst these sections are as close as possible, and provide a good means of contrast for most areas, they yield a misleading picture for the somatosensory cortex.

As one moves out of this area into the insular cortex (figure 93), the contrast between controls and *Hdh* mice abruptly disappears. Mild degeneration is seen in each brain, with darkened profiles most frequent in each of the full-length knock-ins. Similarly, within the pyriform cortex (figure 94) the truncated-expression black 6 mouse possesses fewer darkened profiles that either of the full-length *Hdh* mice, and a comparable number to the wild type black 6. Once again, the wild-type FVB mouse, whilst younger, exhibits a greater degree of degeneration. The preoptic area, along the entire of the anterior-posterior axis, exhibits consistently high levels of degeneration (figure 95).

The striatum is the focus of degeneration in the human condition, and it has been shown that htt_n accumulates in the nuclei of striatal neurons in each *Hdh* mouse, with large inclusions found in the full-length mice. However, striatal degeneration remains relatively rare in the mouse models (figure 96). Dark profiles are found within the striata of all mice (arrows) at comparable frequency; yet, as with the R6/2 mice, the cortex has considerably greater levels of degeneration.

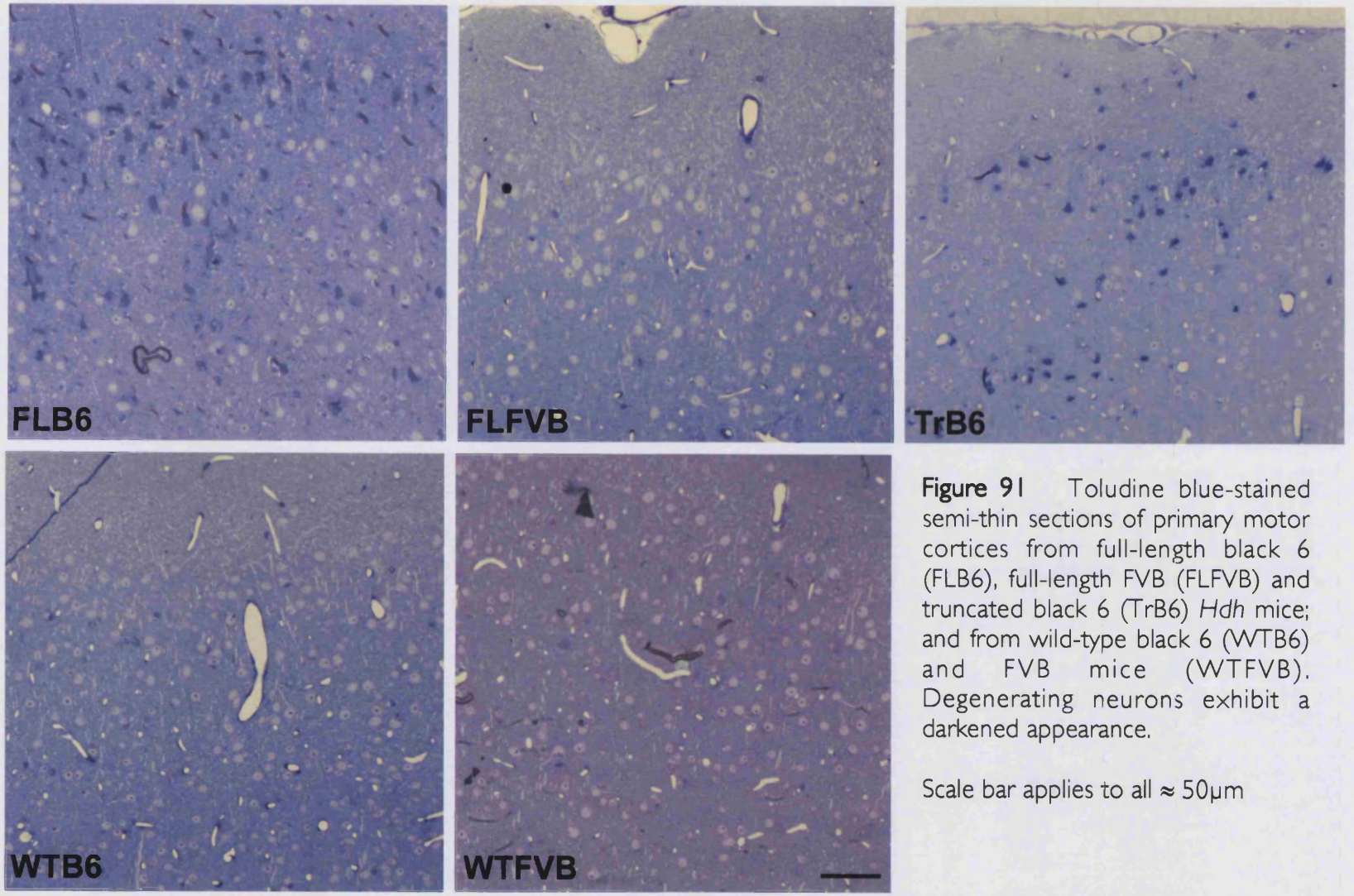

Figure 91 Toludine blue-stained semi-thin sections of primary motor cortices from full-length black 6 (FLB6), full-length FVB (FLFVB) and truncated black 6 (TrB6) *Hdh* mice; and from wild-type black 6 (WTB6) and FVB mice (WTFVB). Degenerating neurons exhibit a darkened appearance.

Scale bar applies to all ≈ 50μm

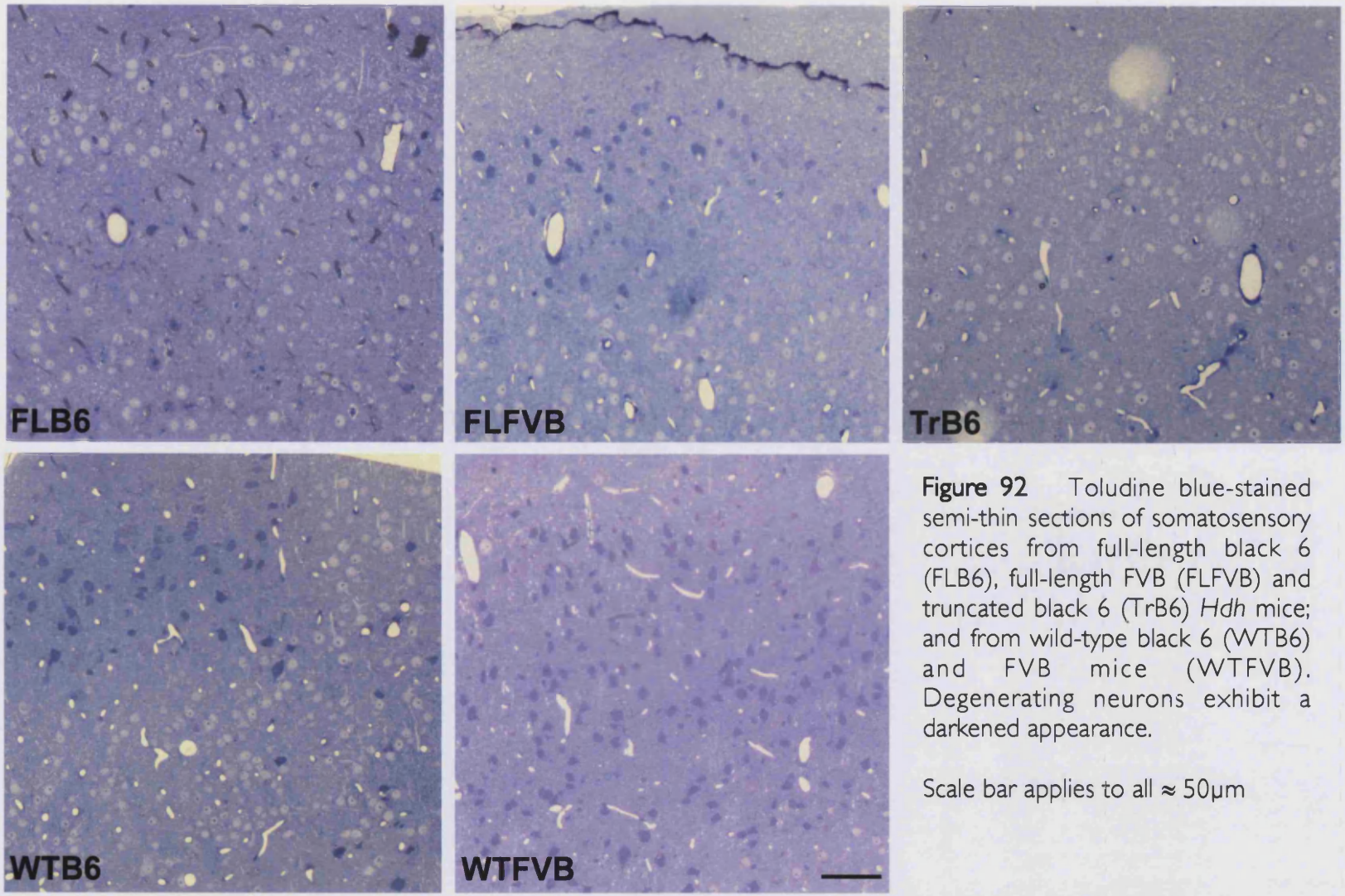

Figure 92 Toludine blue-stained semi-thin sections of somatosensory cortices from full-length black 6 (FLB6), full-length FVB (FLFVB) and truncated black 6 (TrB6) *Hdh* mice; and from wild-type black 6 (WTB6) and FVB mice (WTFVB). Degenerating neurons exhibit a darkened appearance.

Scale bar applies to all ≈ 50μm

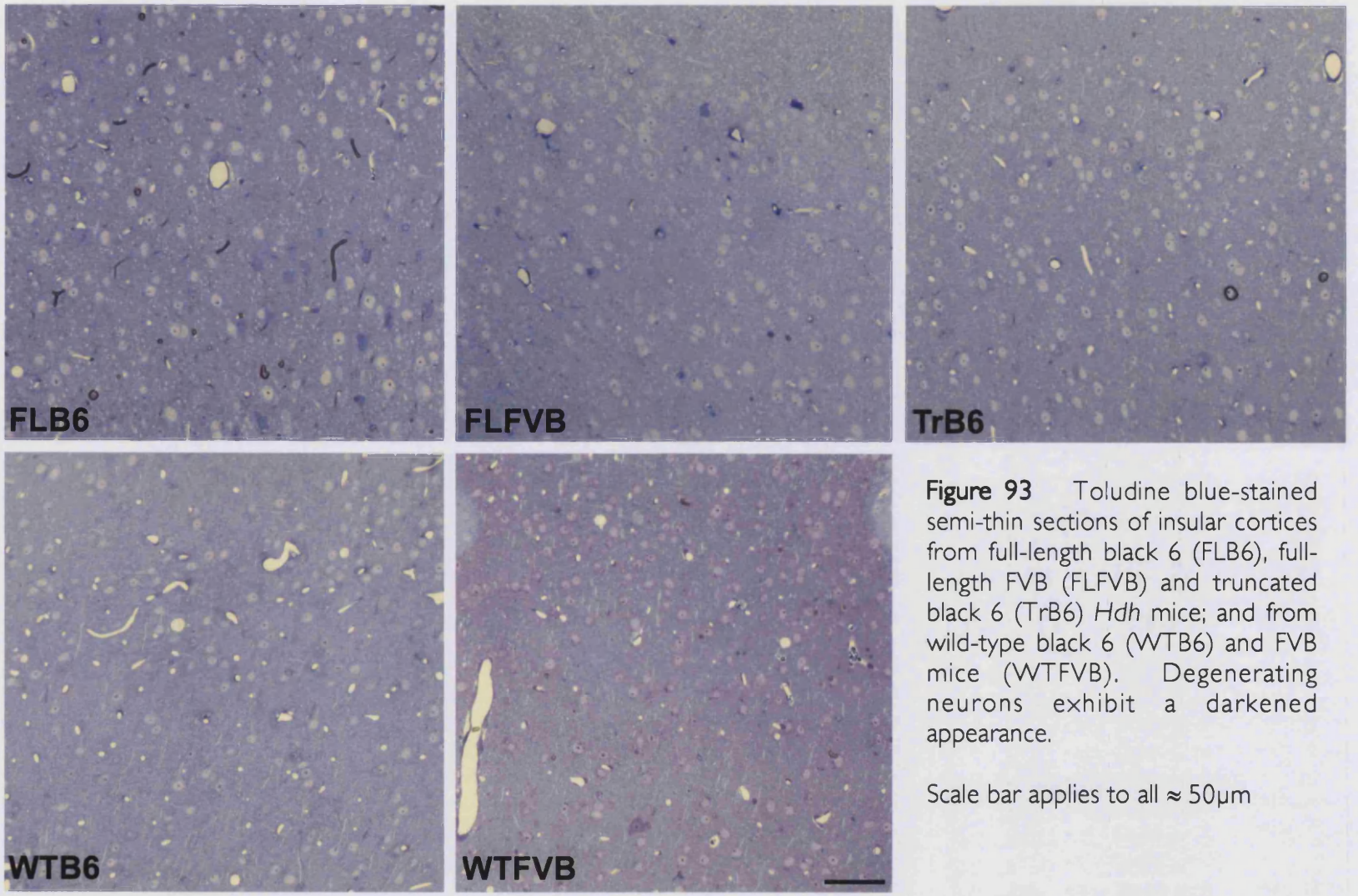

Figure 93 Toludine blue-stained semi-thin sections of insular cortices from full-length black 6 (FLB6), full-length FVB (FLFVB) and truncated black 6 (TrB6) *Hdh* mice; and from wild-type black 6 (WTB6) and FVB mice (WTFVB). Degenerating neurons exhibit a darkened appearance.

Scale bar applies to all ≈ 50μm

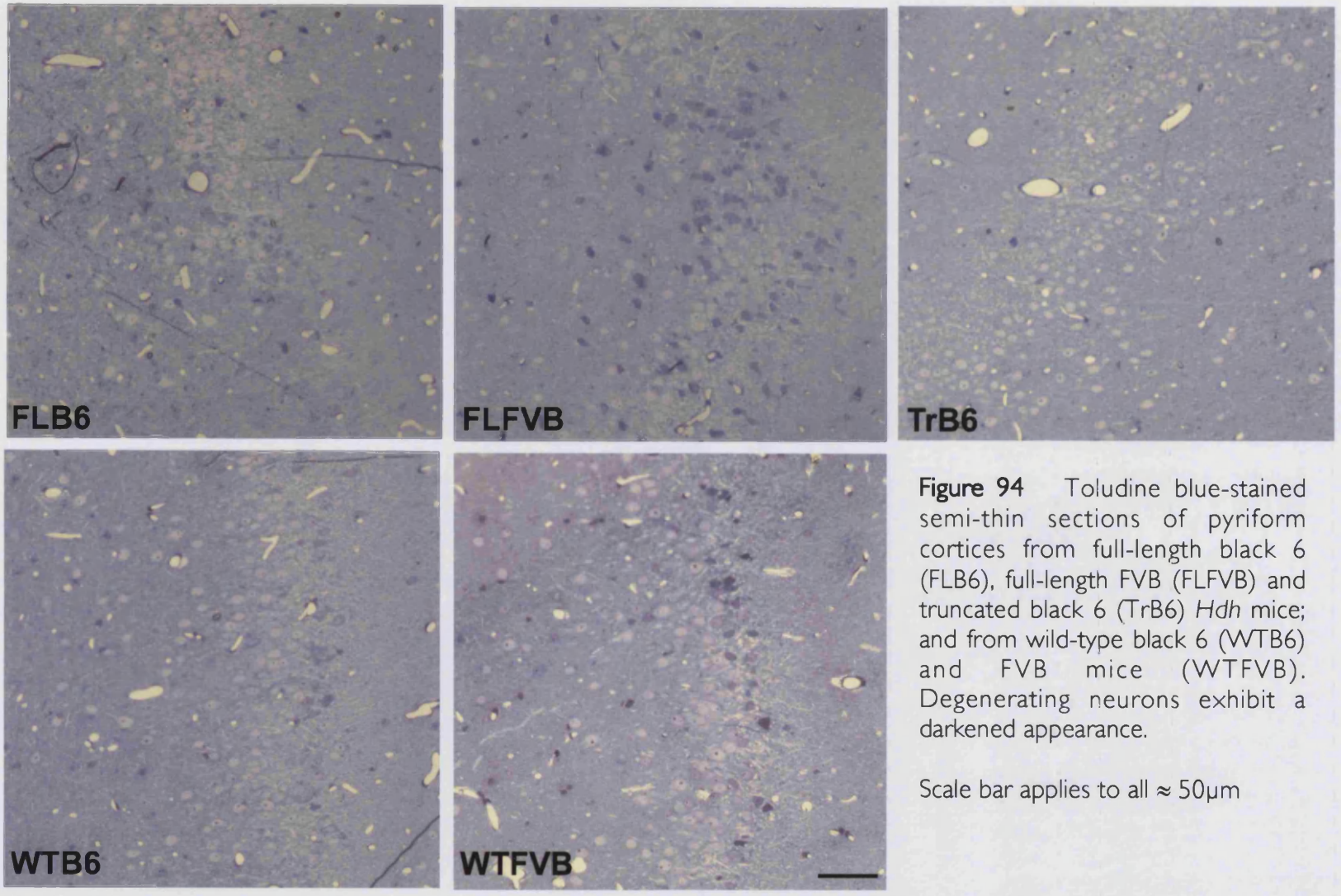

Figure 94 Toludine blue-stained semi-thin sections of pyriform cortices from full-length black 6 (FLB6), full-length FVB (FLFVB) and truncated black 6 (TrB6) *Hdh* mice; and from wild-type black 6 (WTB6) and FVB mice (WTFVB). Degenerating neurons exhibit a darkened appearance.

Scale bar applies to all ≈ 50μm

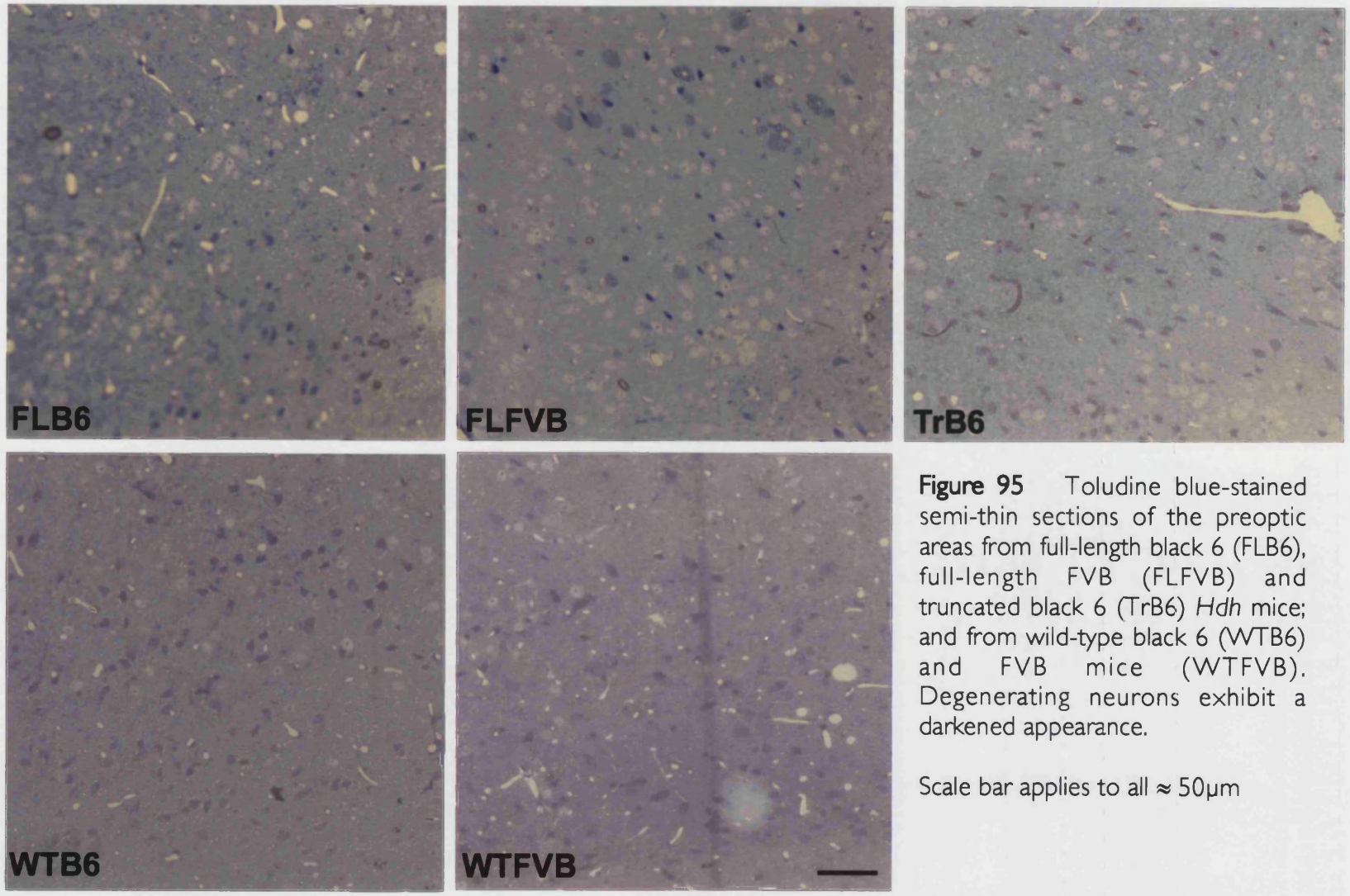

Figure 95 Toludine blue-stained semi-thin sections of the preoptic areas from full-length black 6 (FLB6), full-length FVB (FLFVB) and truncated black 6 (TrB6) *Hdh* mice; and from wild-type black 6 (WTB6) and FVB mice (WTFVB). Degenerating neurons exhibit a darkened appearance.

Scale bar applies to all ≈ 50μm

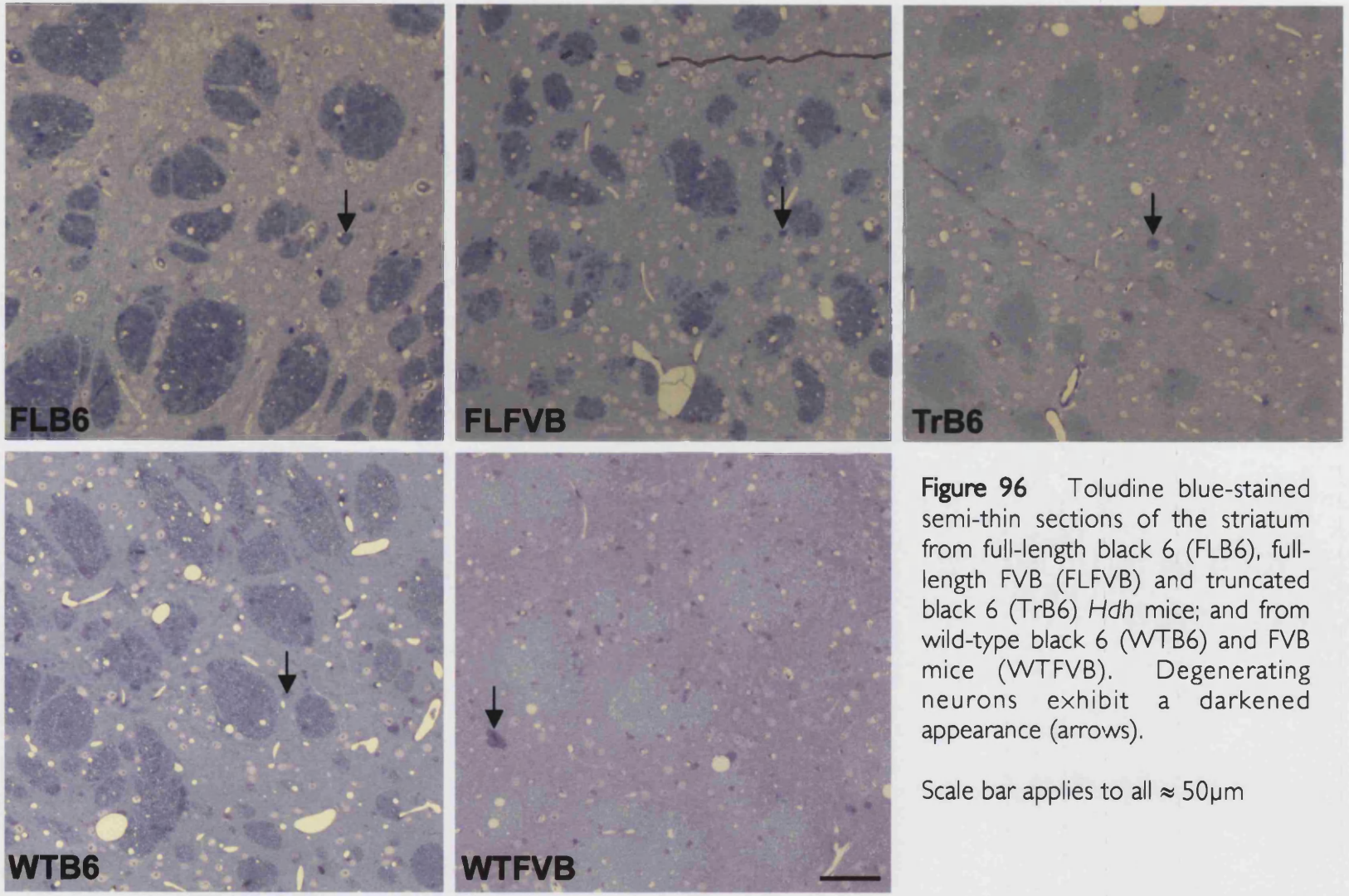

Figure 96 Toludine blue-stained semi-thin sections of the striatum from full-length black 6 (FLB6), full-length FVB (FLFVB) and truncated black 6 (TrB6) *Hdh* mice; and from wild-type black 6 (WTB6) and FVB mice (WTFVB). Degenerating neurons exhibit a darkened appearance (arrows).

Scale bar applies to all ≈ 50μm

In the R6/2 model, the hippocampus is devoid of degeneration in spite of its possessing some of the largest inclusions. In contrast, the hippocampi in the *Hdh* mice show numerous degenerating neurons with a complete lack of nuclear huntingtin. Degeneration is rare in the CA3 region (figure 99), and infrequent among the CA1 neurons (figure 97), yet the CA2 field (figure 98) exhibits frequent darkened neurons. The wild-type mice show similar levels of degeneration, therefore this degeneration cannot be attributed to the disease process, but it is interesting to note such focal and substantial degeneration.

Also interesting to note is the degeneration seen within the cerebella of these mice (figure 100). Within each mouse, knock-in or wild-type, nearly every Purkinje cell shows signs of degeneration (arrows). Given that these mice are phenotypically normal, and show no impairment on testing of motor function, one must assume that the cerebellum is perfectly functional in spite of the clear degeneration seen in the vast majority of Purkinje cells and their processes (arrowheads).

3.2.4 The Ultrastructural Appearance of Degeneration

It has been shown at the semi-thin section level that darkened profiles exist in both the *Hdh* knock-in mice and their littermate controls. The ultastructural study of these mice thus now extends from a comparison of the knock-ins and the transgene to include a comparison of the degeneration seen in all HD model mice to that seen in the aged wild-type mice.

When ultra-thin sections are viewed under the electron microscope a greater degree of pathologic change is revealed than was apparent at the semi-thin level. In the R6/2 mouse the condensation of nucleoplasm and cytoplasm occurs concomitantly (see figure 52). In contrast, it appears the darkening of the *Hdh* neurons occurs first in the cytoplasm, with a delayed onset of nucleoplasmic condensation. Figure 101 shows a section through the striatum of a full-length *Hdh* expressing black 6 mouse at 29 months of age. In the centre of the figure are condensed neurons, which would be clearly identifiable as degenerating using the

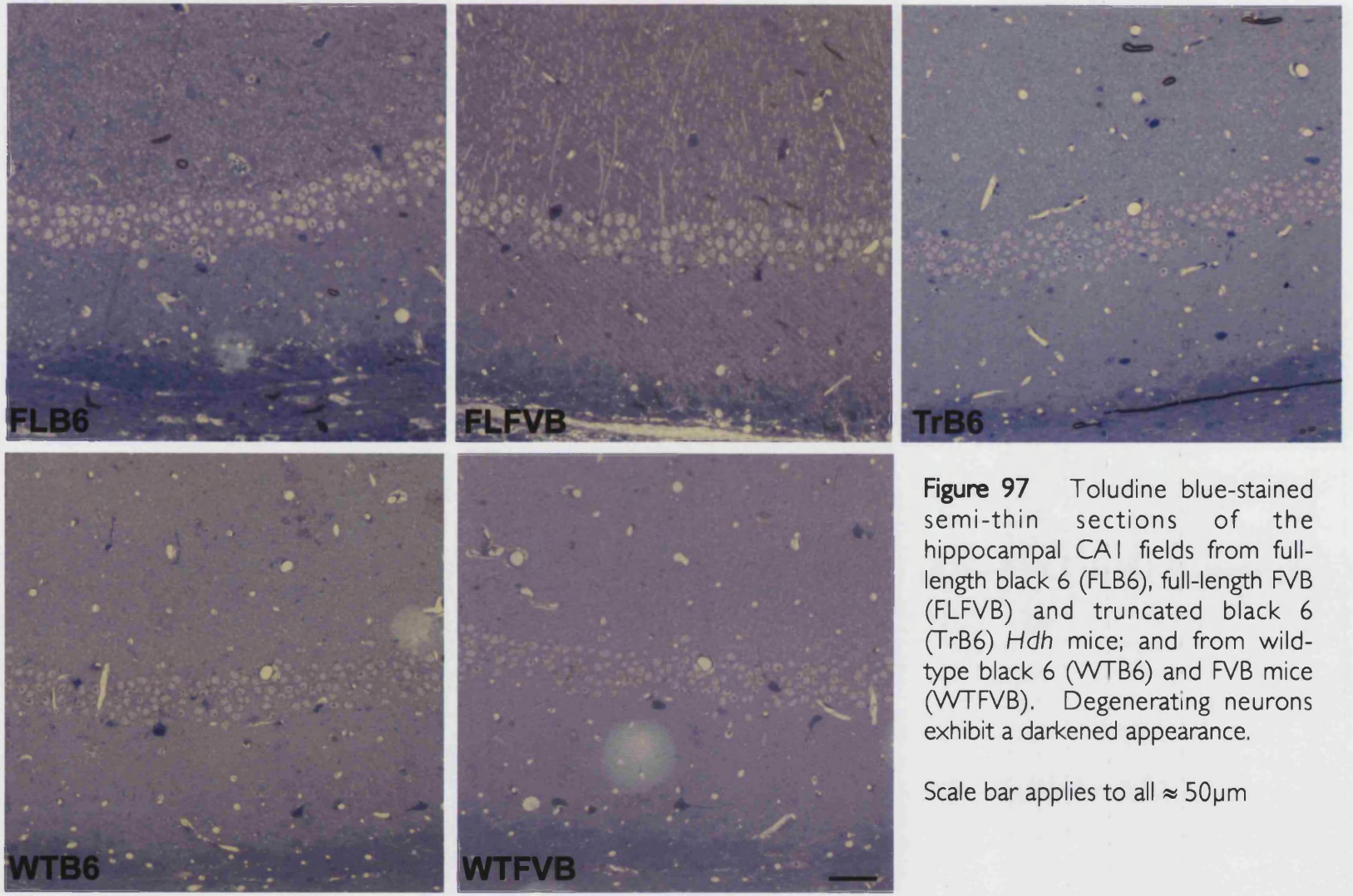

Figure 97 Toludine blue-stained semi-thin sections of the hippocampal CA1 fields from full-length black 6 (FLB6), full-length FVB (FLFVB) and truncated black 6 (TrB6) *Hdh* mice; and from wild-type black 6 (WTB6) and FVB mice (WTFVB). Degenerating neurons exhibit a darkened appearance.

Scale bar applies to all ≈ 50μm

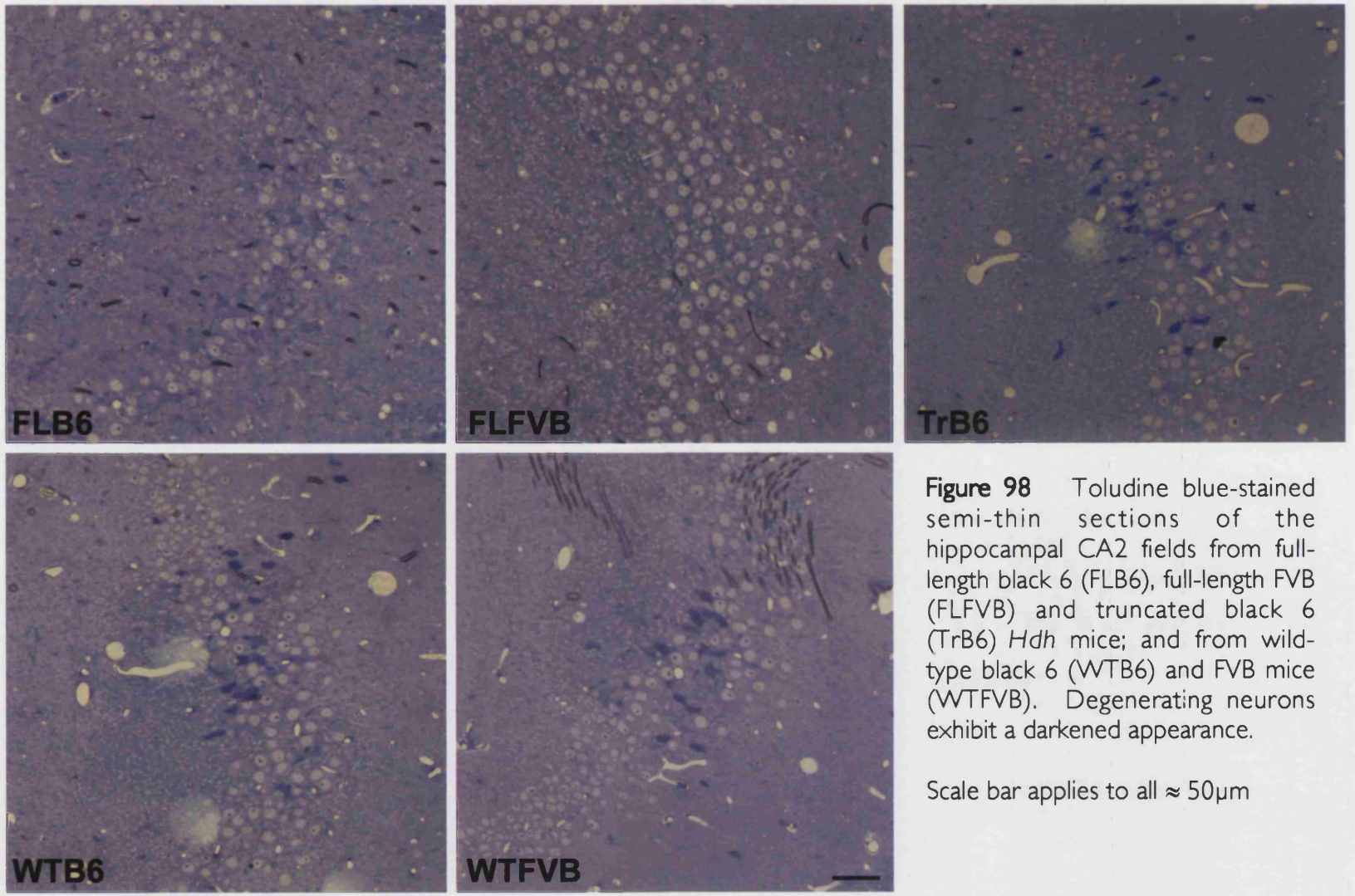

Figure 98 Toludine blue-stained semi-thin sections of the hippocampal CA2 fields from full-length black 6 (FLB6), full-length FVB (FLFVB) and truncated black 6 (TrB6) *Hdh* mice; and from wild-type black 6 (WTB6) and FVB mice (WTFVB). Degenerating neurons exhibit a darkened appearance.

Scale bar applies to all ≈ 50μm

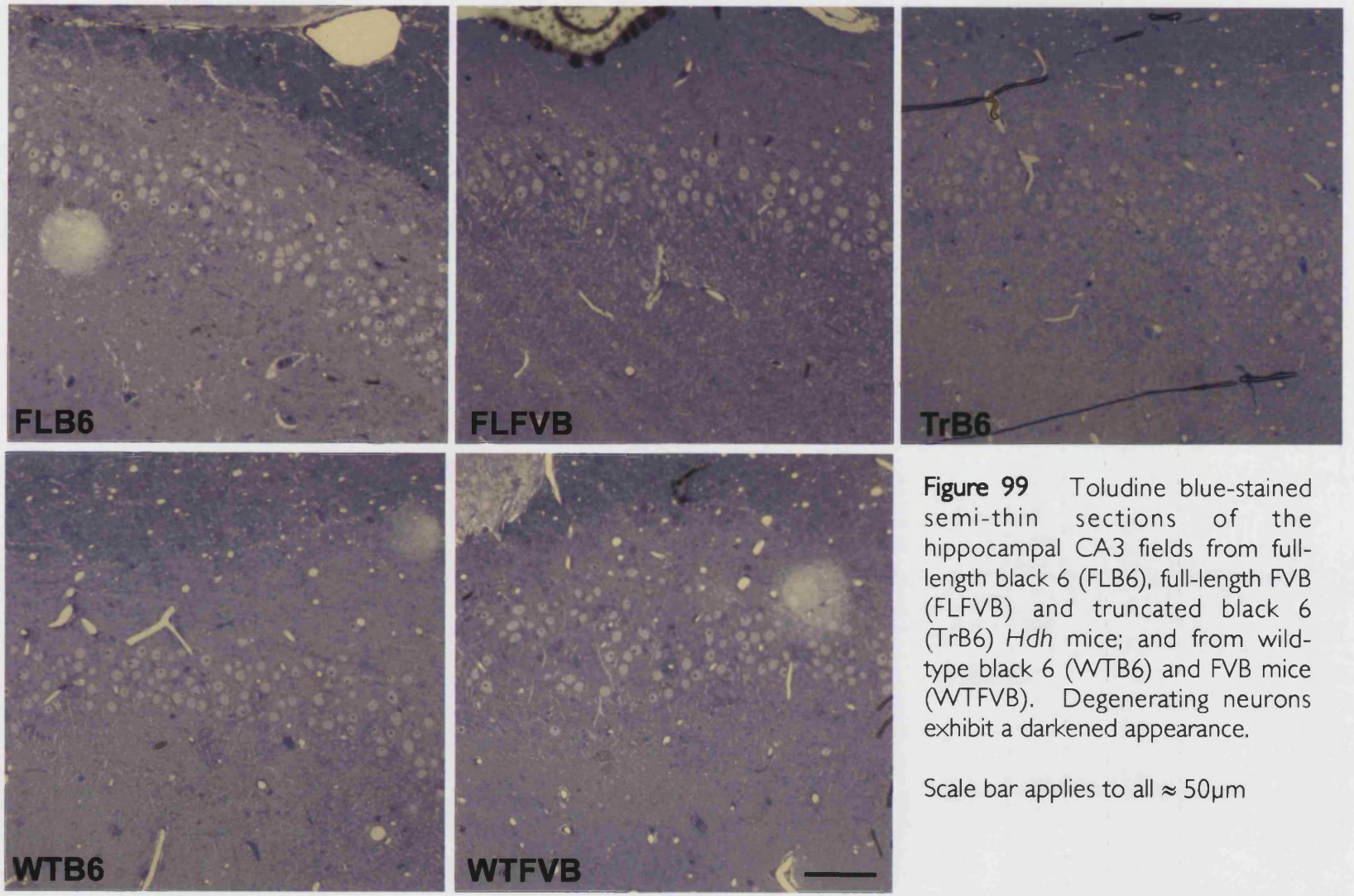

Figure 99 Toludine blue-stained semi-thin sections of the hippocampal CA3 fields from full-length black 6 (FLB6), full-length FVB (FLFVB) and truncated black 6 (TrB6) *Hdh* mice; and from wild-type black 6 (WTB6) and FVB mice (WTFVB). Degenerating neurons exhibit a darkened appearance.

Scale bar applies to all ≈ 50μm

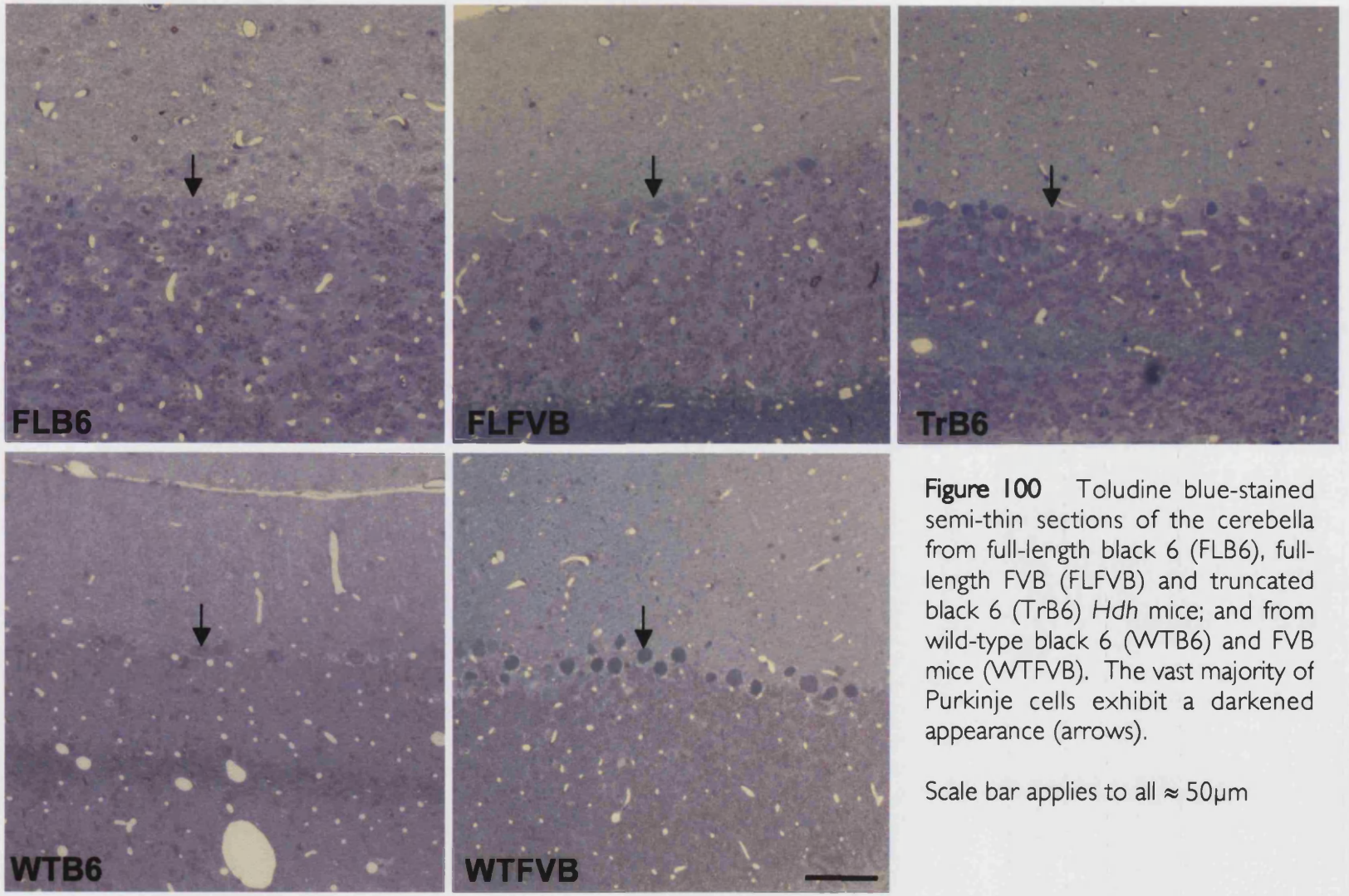

Figure 100 Toludine blue-stained semi-thin sections of the cerebella from full-length black 6 (FLB6), full-length FVB (FLFVB) and truncated black 6 (TrB6) *Hdh* mice; and from wild-type black 6 (WTB6) and FVB mice (WTFVB). The vast majority of Purkinje cells exhibit a darkened appearance (arrows).

Scale bar applies to all ≈ 50μm

toludine blue semi-thin method (arrows). However, the remaining neurons in this section all show signs of cytoplasmic condensation (arrowheads) whilst maintaining a healthy nuclear appearance. They may not be registered as degenerating in the semi-thin sections.

Perhaps one of the most important features to note, conspicuous in figure 101 by its absence, is the intranuclear inclusion. It has been shown that inclusions, whilst relatively rare compared to the R6/2, are found throughout the full-length *Hdh* striatum when immunostained for N-terminal huntingtin. However, whilst the inclusion is clearly identifiable as a structural element in the R6/2, they are rarely identifiable in the *Hdh* mice. In viewing hundreds of EM sections from *Hdh* mice, I have found fewer than ten obvious structural correlates; and only in those mice expressing full-length *Hdh*. They are more likely to be identified in cells at the later stages of degeneration as the condensation of the nucleoplasm increases contrast between itself and the inclusion; as illustrated in figure 102 (arrow).

They can be revealed in neurons at earlier stages of degeneration by immunolabelling. Figure 103 contains a neuron from a full-length black 6 *Hdh* mouse immunolabelled for N-terminal huntingtin and stained with DAB. This reveals a clear intranuclear inclusion (arrow) as well as pan-neuronal staining. Such inclusions are hard to identify without staining, as they do not possess the distinct structure of the R6/2 inclusions. There are areas of nucleoplasm that possess slightly different textures, and N-terminal huntingtin immunogold labelling confirms that these are accumulations of huntingtin (figure 104), yet in uncondensed cells these are difficult to identify.

Figure 102 also illustrates an ultrastructural feature of degeneration apparently limited to the FVB background: chromatin condensation. Within the condensed nucleoplasm of the FVB *Hdh* mouse, one can clearly identify areas of condensed chromatin (arrowheads), a certain amount of which has marginated to the nuclear membrane – a characteristic of apoptosis – yet in none of the neurons observed does this chromatin coalesce to form the bodies seen during apoptosis (see figures 45, 46 & 48). Figure 105 contains examples of striatal neurons in comparable stages of degeneration from each of the *Hdh* mice. Both the nucleoplasm and the cytoplasm show considerable condensation, and there are dark foci within the nuclei, which may

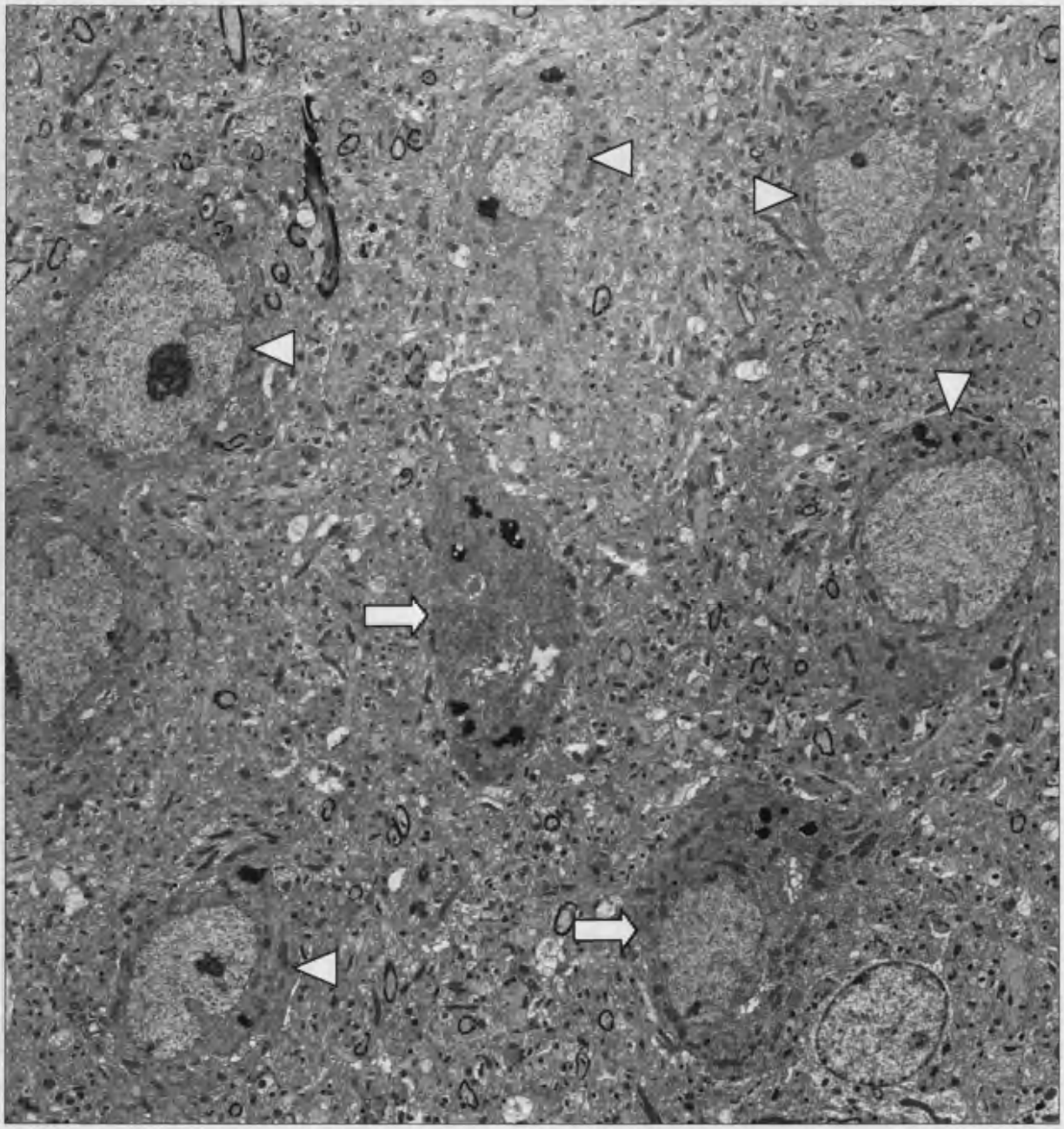

Figure 101 Electron micrograph of a cortical section from a full-length black 6 *Hdh* mouse at 29 months of age. Note the numerous dark cells (arrows), with cytoplasmic condensation occurring more rapidly than nucleoplasmic condensation (arrowheads).

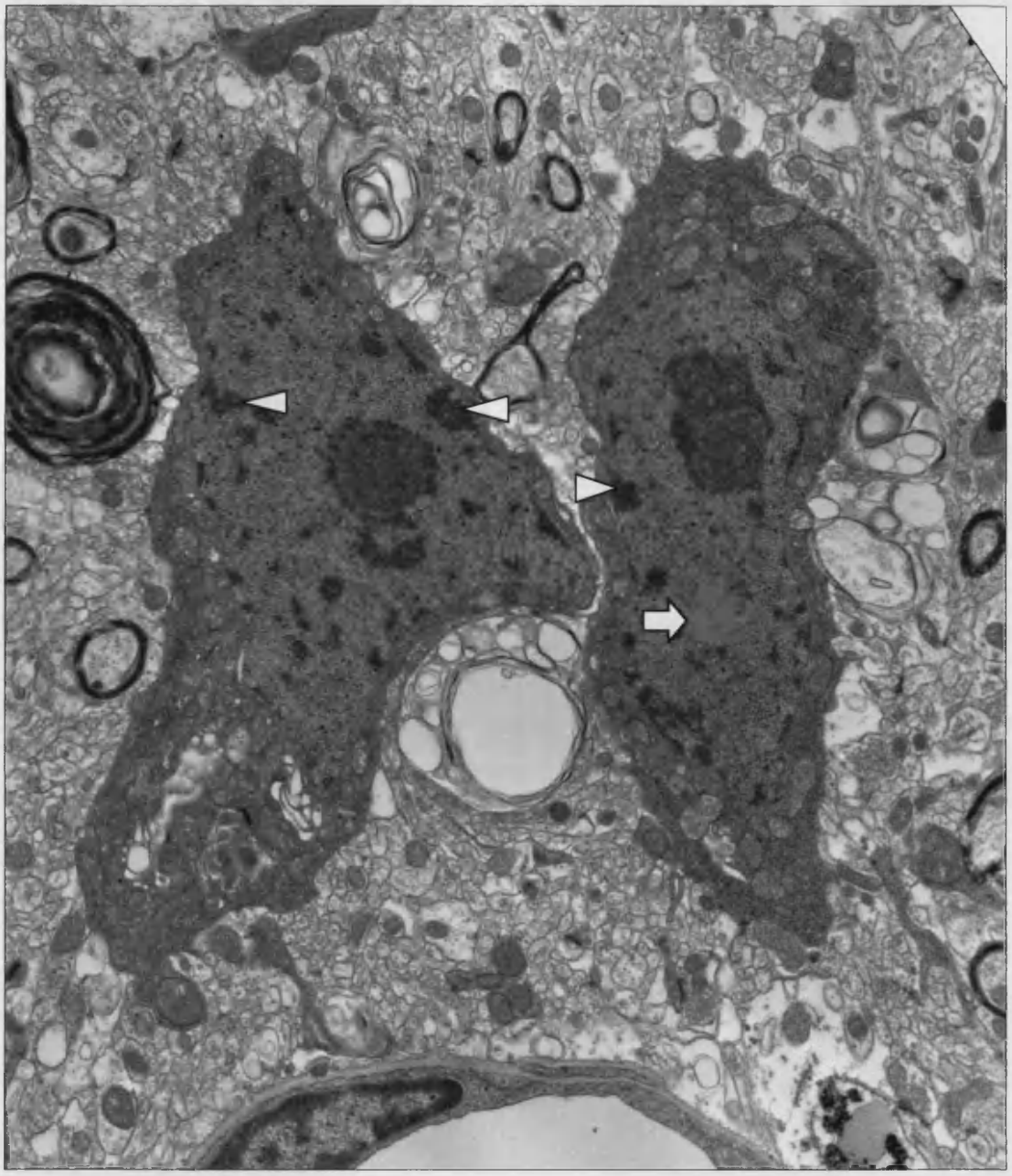

Figure 102 Electron micrograph of degenerating striatal neurons from a full-length FVB *Hdh* mouse at 27.5 months of age. Note the mild condensation of the chromatin (arrowheads) and the nuclear inclusion (arrow).

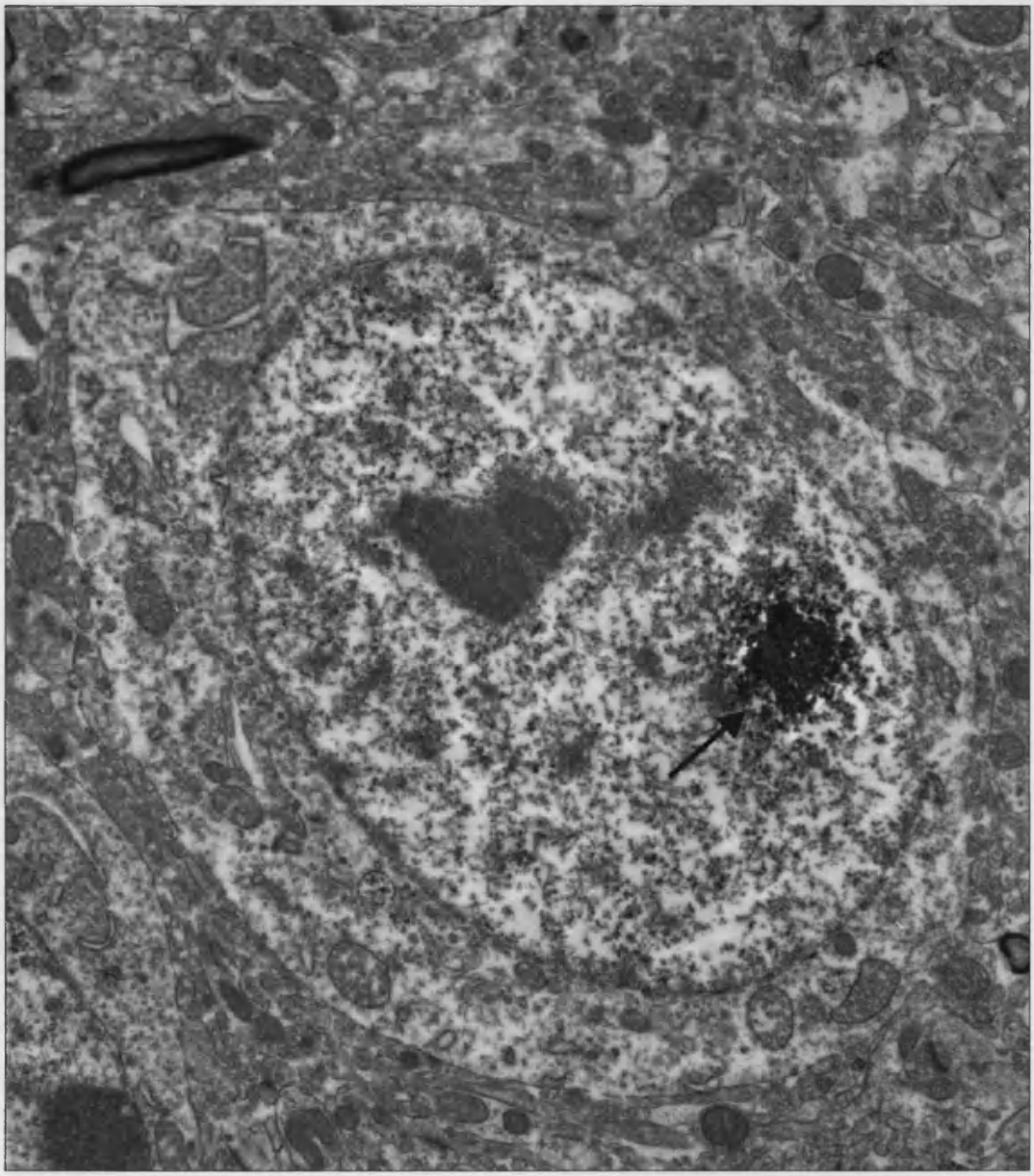

Figure 103 Electron micrograph of a striatal neuron from a full-length black 6 *Hdh* mouse; immunolabelled for N-terminal huntingtin. revealed using ABC/DAB. An intranuclear inclusion is revealed by staining (arrow).

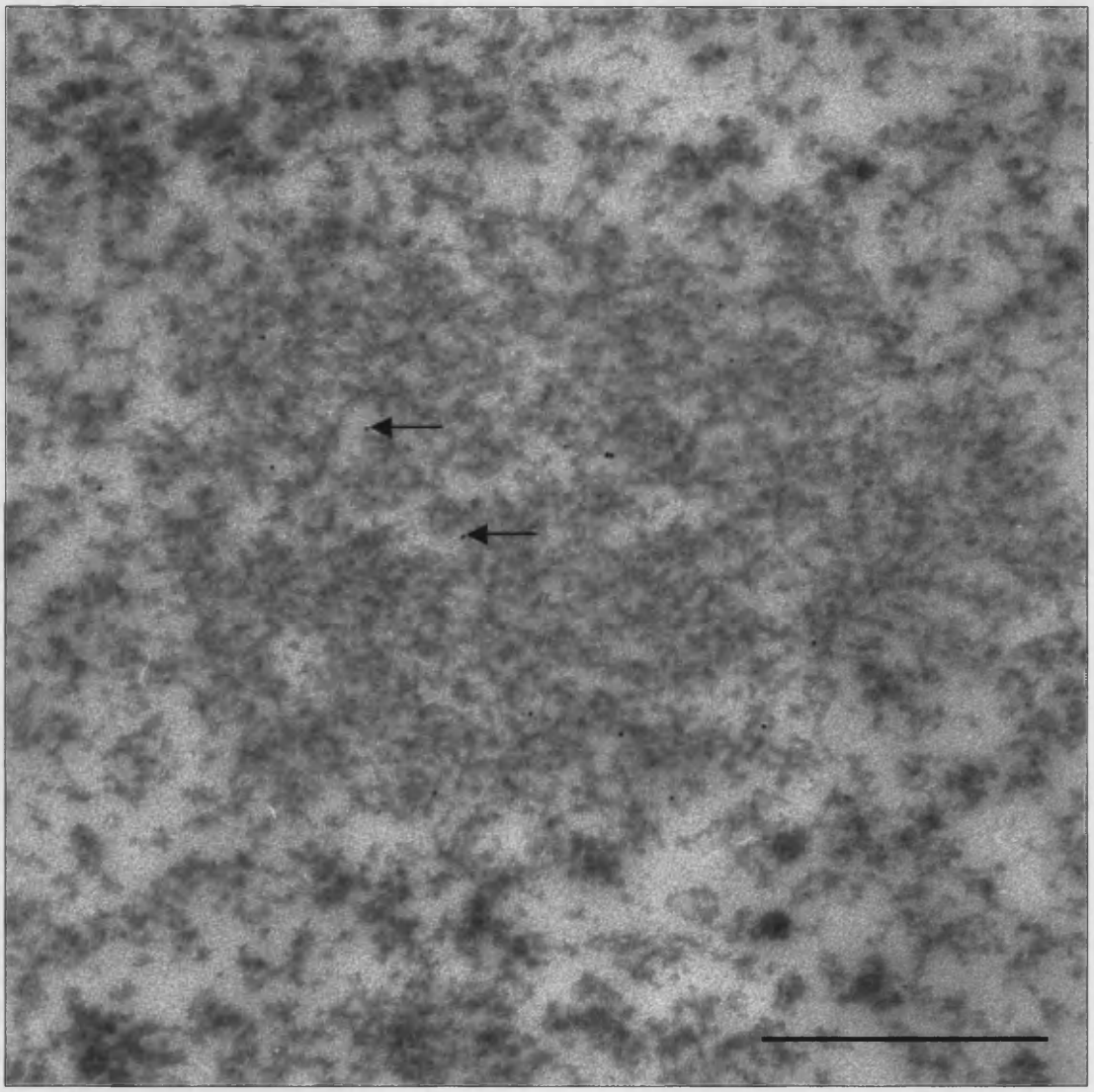

Figure 104 Neuronal Intranuclear Inclusion from the striatum of a full-length htt-expressing black 6 *Hdh* mouse, immunogold-labelled for N-terminal huntingtin. A structural correlate is visible and labels (gold particles) for N-terminal htt (arrows). Scale bar ≈ 500nm

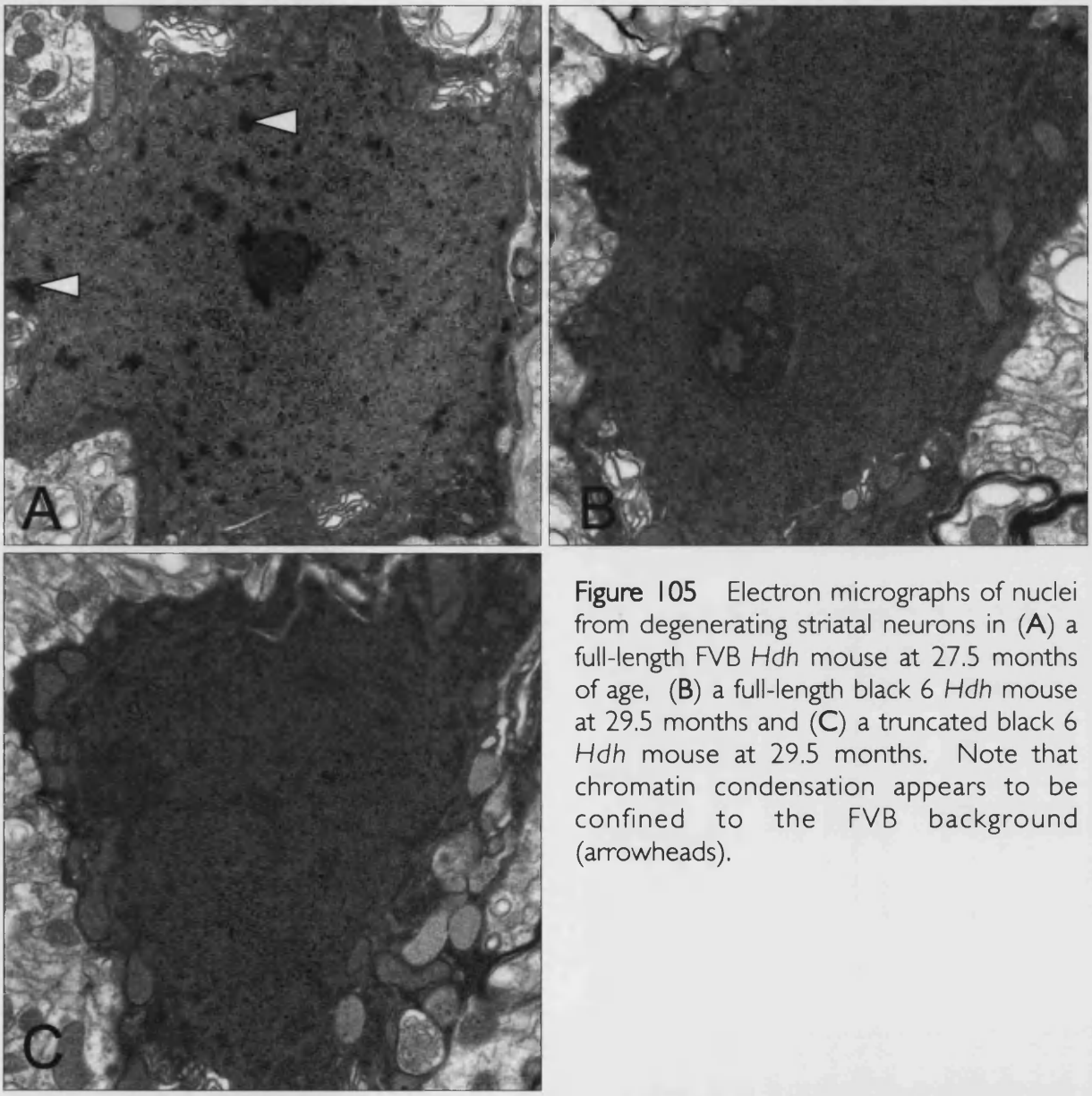

Figure 105 Electron micrographs of nuclei from degenerating striatal neurons in (**A**) a full-length FVB *Hdh* mouse at 27.5 months of age, (**B**) a full-length black 6 *Hdh* mouse at 29.5 months and (**C**) a truncated black 6 *Hdh* mouse at 29.5 months. Note that chromatin condensation appears to be confined to the FVB background (arrowheads).

be regions of chromatin, but only in the FVB background does one find the patchy accumulations.

The *Hdh* mice share many features with the R6/2 degeneration. There is clear dilation of the endoplasmic reticulum and golgi apparatus in all *Hdh* mice, as illustrated in figures 106 and 107: striatal neurons from each mouse type (arrowheads). The preservation of other structures, most notably the myelin, indicates that this dilation is not a procedural artefact. There is also dilation of the mitochondria, concomitant with loss of internal structure. Figure 108, a degenerating neuron in the FVB *Hdh* mouse, illustrates these changes. In the face of well-preserved myelin and non-native mitochondria (solid arrowheads), the golgi apparatus (solid arrows) and mitochondria (open arrowheads) within the degenerating neuron are clearly dilated. Whether as a consequence of dilation or an independent event, the cristae within the mitochondria lose their regular layered arrangement and adopt an erratic appearance.

Figure 108 also illustrates one of the more obvious features seen in these neurons, the accumulation of lipofuscin (yellow arrowheads), and evidence of autophagic activity (open arrow). Lipofuscin is also seen to accumulate in the R6/2 but to a lesser degree. Of course, one might expect greater deposits of the 'aging pigment' in mice two years' older, but these deposits are more common in the *Hdh* degenerating neurons than in otherwise healthy cells. The breakdown product is membrane-bound (figure 109) and is seen to accumulate preferentially in one locus (figure 110). This apparent preferential localisation occurs due to the fact that the large deposits (arrows) result from the continuous addition of smaller lysosomes (arrowheads), their products processed to form the mature material.

Autophagic activity is evident to varying degrees amongst the degenerating neurons in the *Hdh* mice. Figure 111 contains a section of degenerating neuron from a truncated-*Hdh* expressing mouse. Similar to the events seen in the R6/2, autophagic activity appears to be highest in the vicinity of the expanded golgi, supporting the suggestion that autophagic vacuoles are formed from budding of the endoplasmic reticulum and/or golgi (arrow). Autophagic vacuoles (AV) vary greatly in size and many of the smaller double-membrane structures seen may be AVs, certainly the larger multilamellar structures are autophagic in nature, as are those which sequester

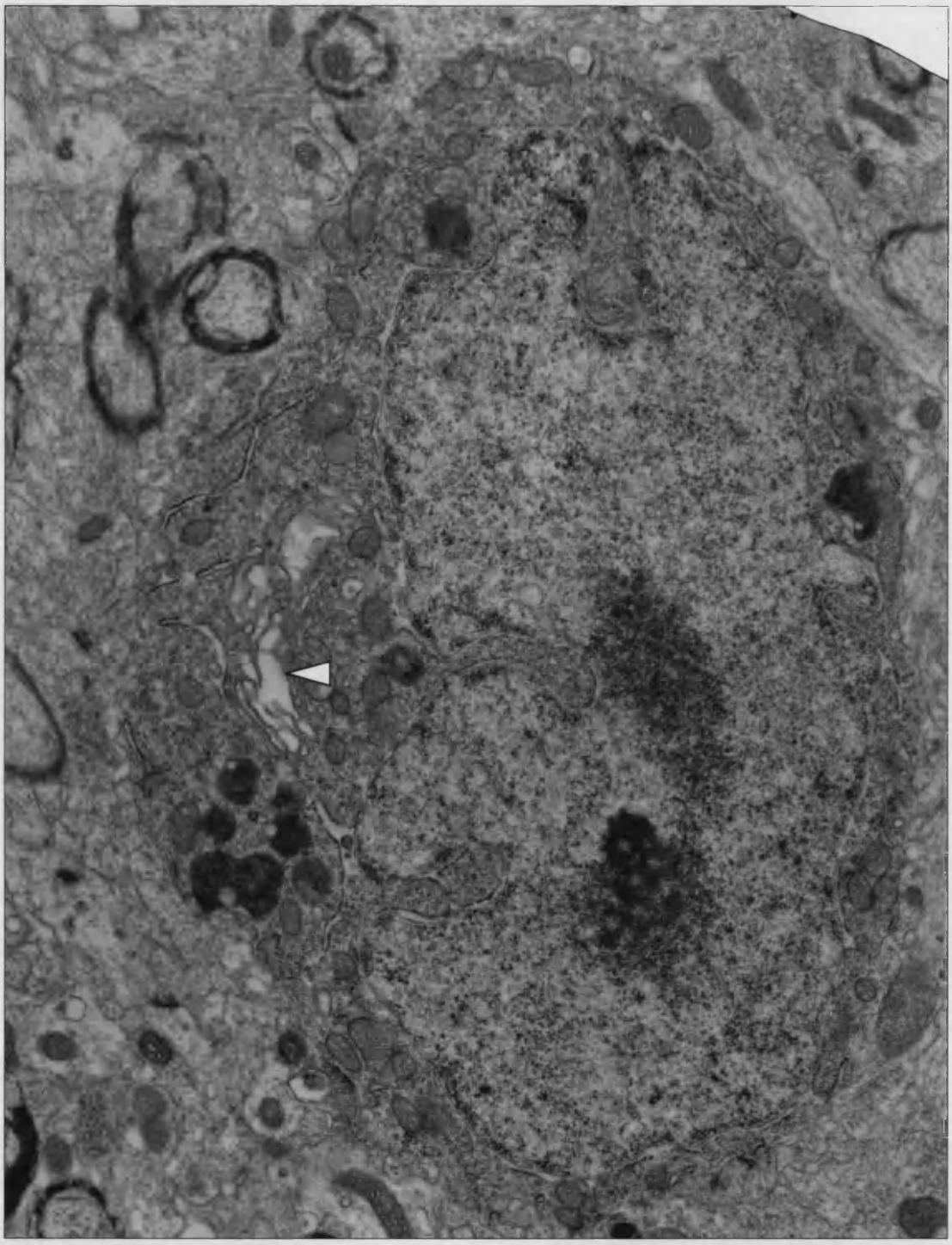

Figure 106 Electron micrograph of striatal degeneration in a full-length black 6 *Hdh* mouse at 29 months of age. Note the dilation of the endoplasmic reticulum / Golgi apparatus (arrowhead).

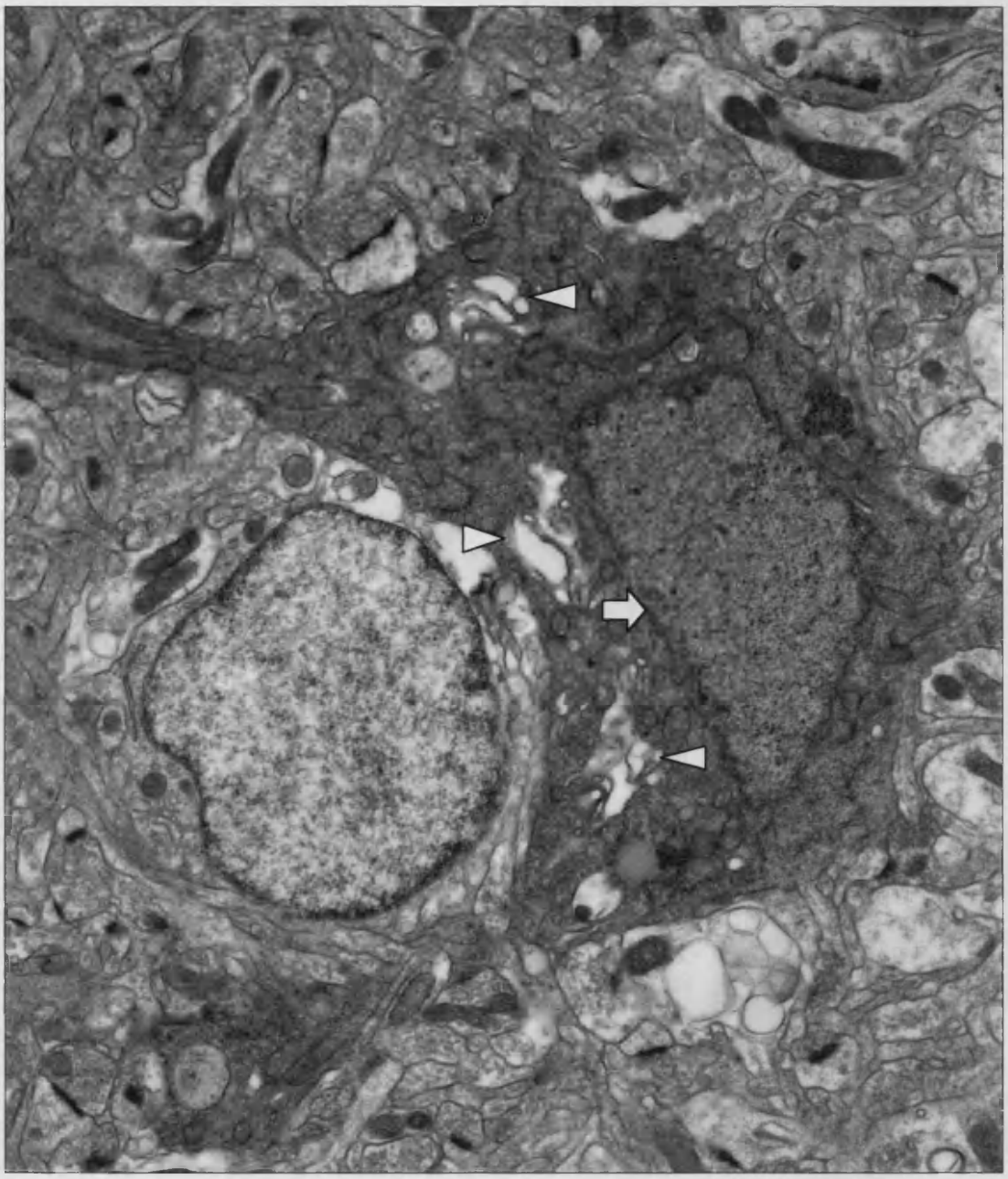

Figure 107 Electron micrograph of a degenerating striatal neuron from a truncated-expression black 6 *Hdh* mouse at 24 months of age. Note the dilation of organelles (arrowheads) within condensed cytoplasm. Also note that whilst the nuclear membrane has adopted a slightly 'ruffled' appearance (arrow), the nucleus remains relatively unaffected.

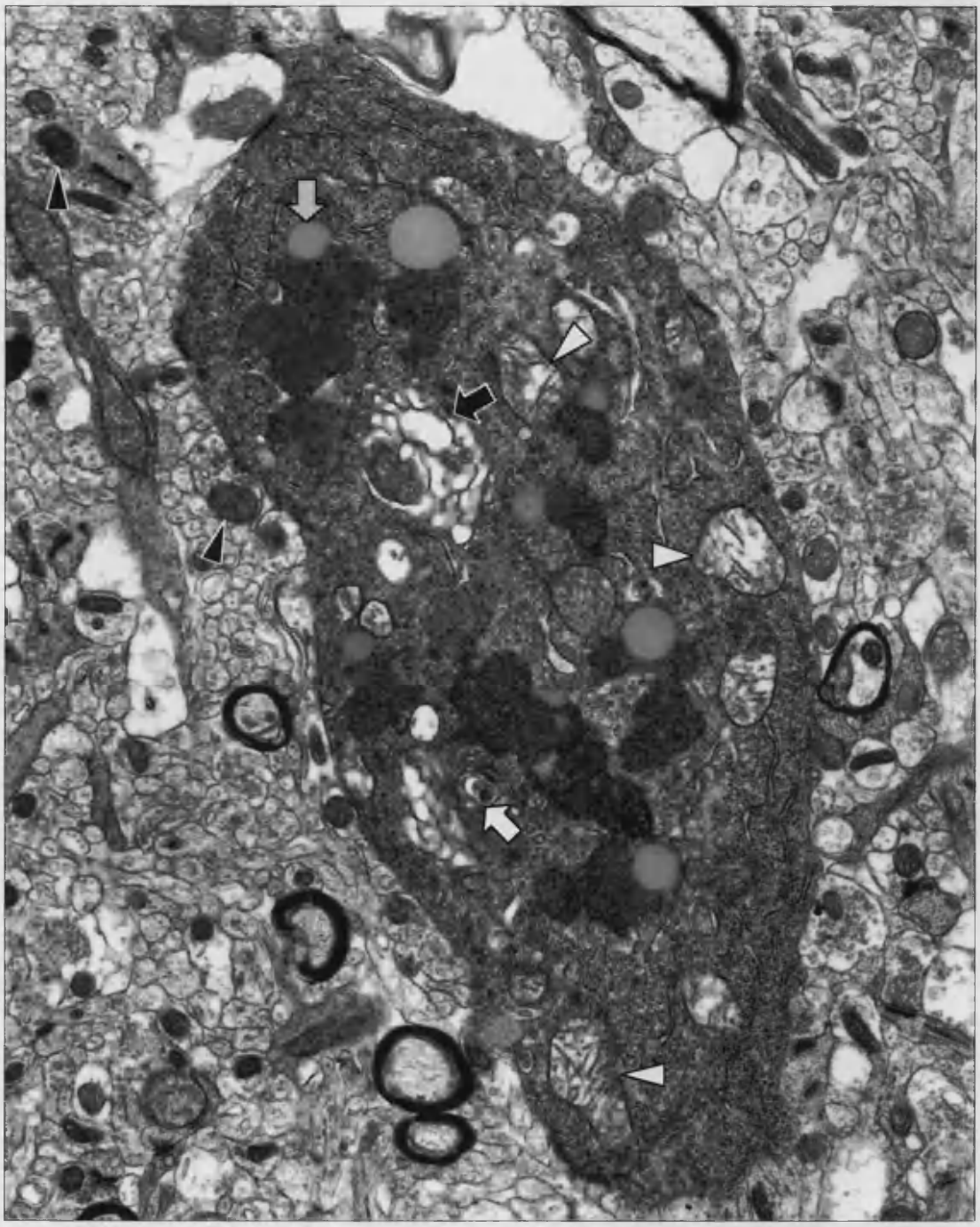

Figure 108 Electron micrograph of a degenerating cortical neuron from a full-length FVB *Hdh* mouse at 27.5 months of age. Note the dilation of motichondria and loss of internal structure (open arrowheads). Dilation is most marked when compared to unaffected mitochondria in the neuropil (solid arrowheads). Also note the dilation of the Golgi and ER (solid arrow), together with the formation of autophagic vacuoles (open arrow) and accumulation of lipofuscin (yellow arrow)

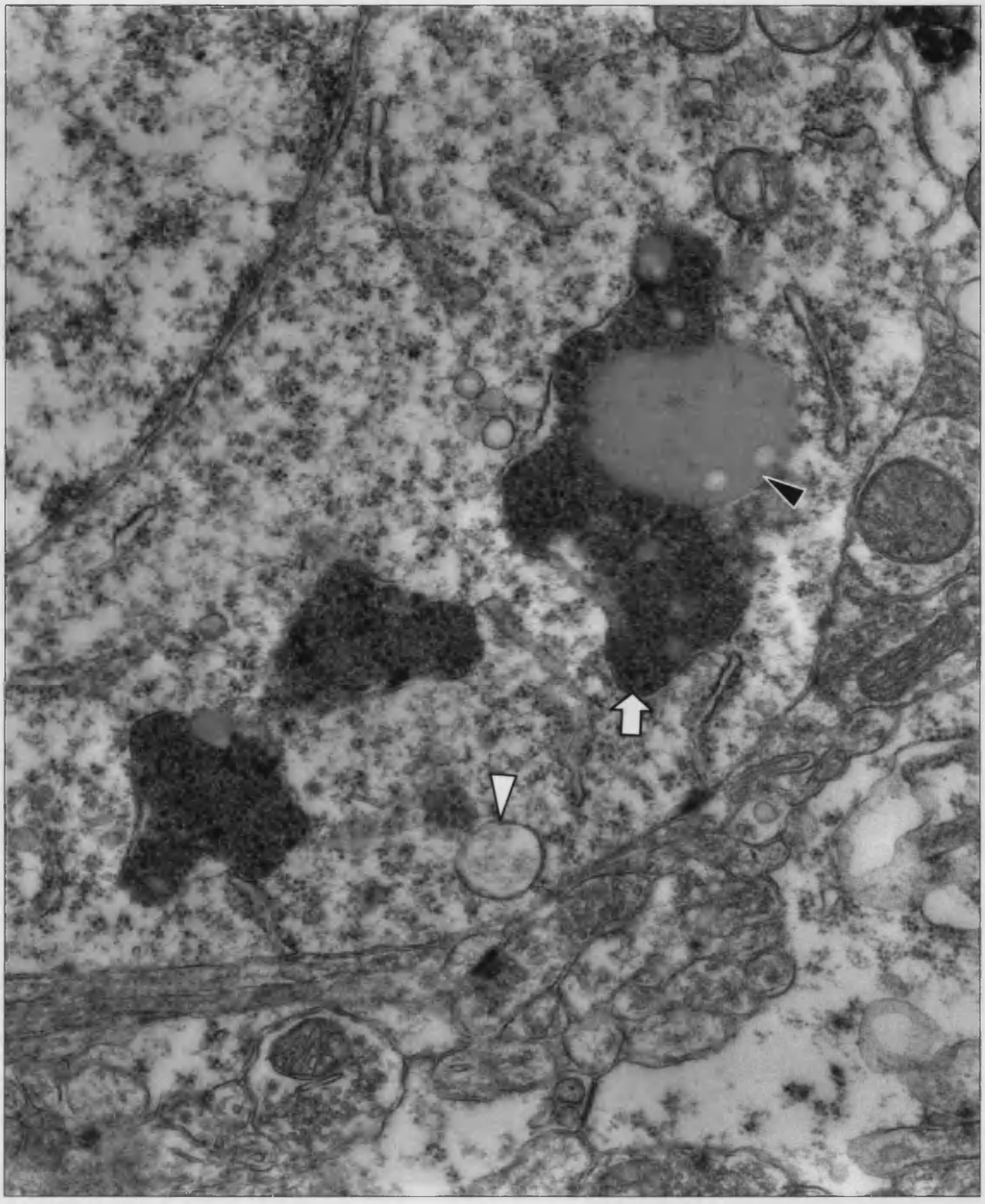

Figure 109 High-magnification electron micrograph of a striatal neuron from a full-length FVB *Hdh* mouse at 27.5 months of age. Autophagic activity is indicated by the presence of double membrane-bound autophagic vacuoles (open arrowhead) and accumulation of breakdown products, both membranous (arrow) and proteinaceous (solid arrowhead).

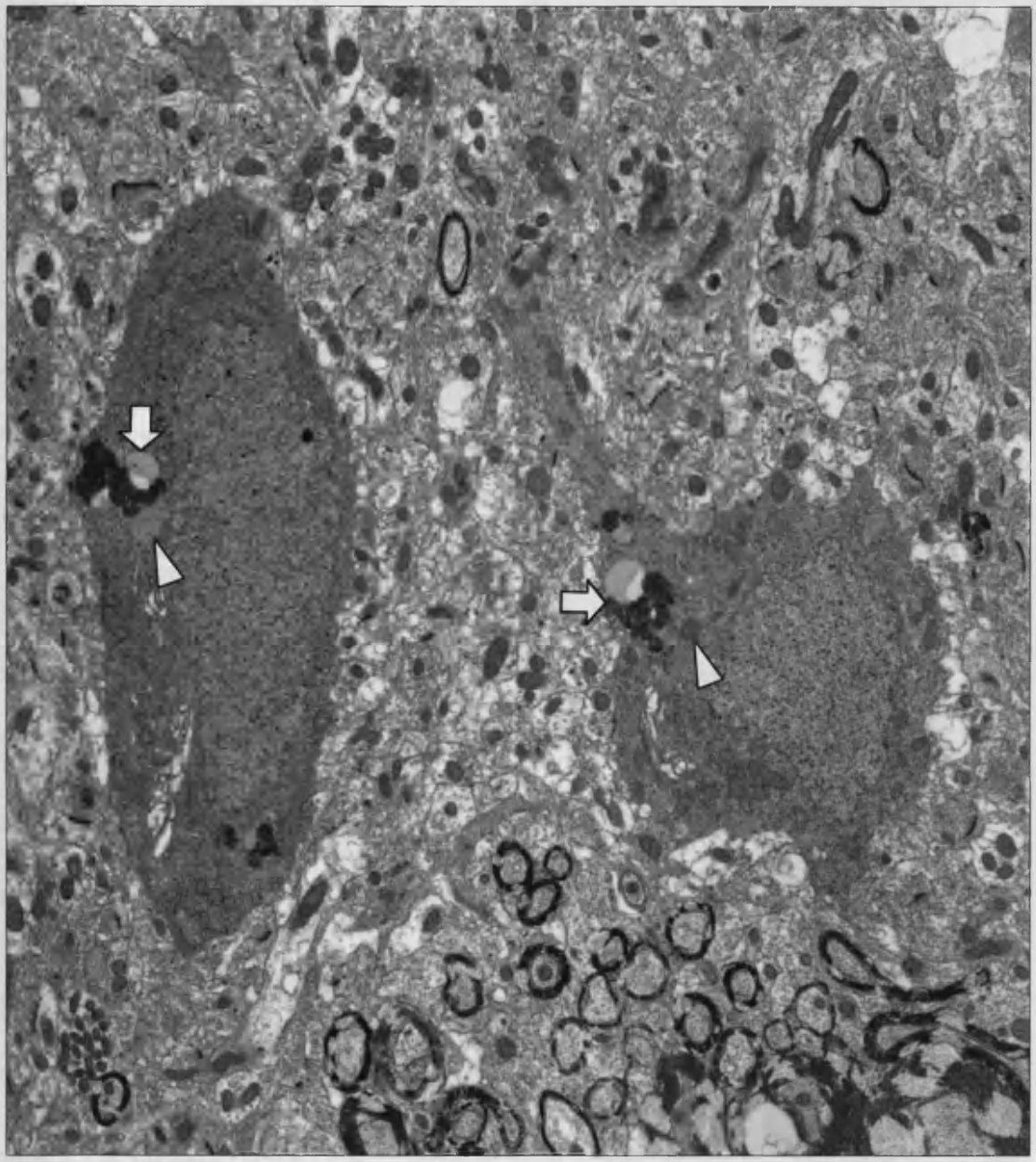

Figure 110 Electron micrograph of degenerating striatal neurons in a 29 month-old full-length black 6 *Hdh* mouse. Both neurons show a darkened appearance and accumulation of lipofuscin (arrow) through the continual addition of lysosomal material (arrowheads)

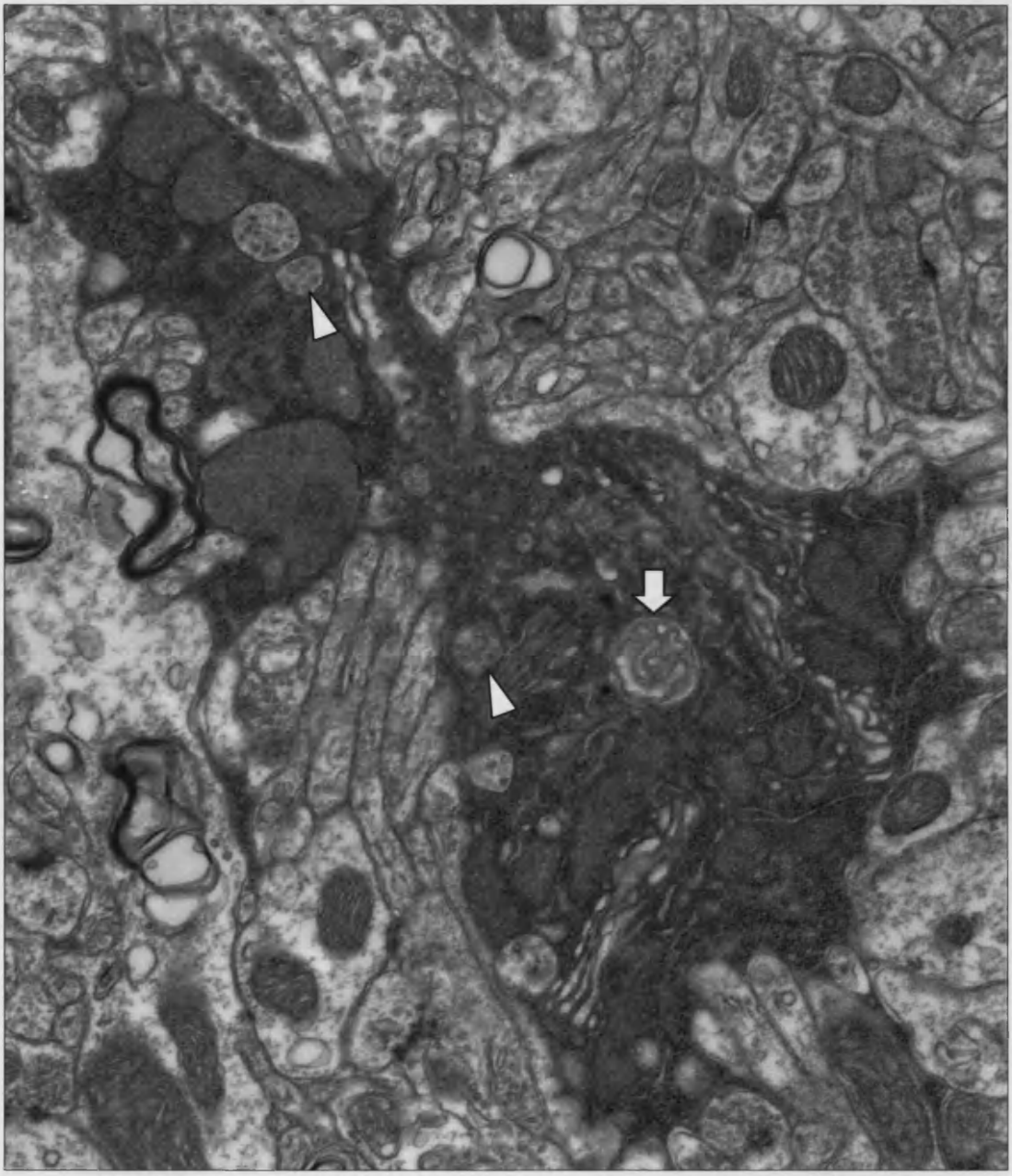

Figure 111 Electron micrograph of a process from a degenerating striatal neuron in a 29 month-old full-length black 6 *Hdh* mouse. Note the presence of multivesicular bodies (arrowheads) and autophagic vacuoles (arrow).

entire organelles (see figure 112) – indeed, autophagic processing appears to be the only means by which whole organelle turnover can be achieved. It is the processing of this cytolsolic material within the multivesicular bodies & autophagic vacuoles, and the continual fusion of these bodies, that yields the product that accumulates with age (figure 113). The level of autophagic activity appears to be far greater than that seen in the R6/2; so much so that in the *Hdh* mice, late-stage degenerating cells can appear 'foamy' as they contain so many AVs, MVBs and engorged lysosomes (figure 114). This may simply be a result of the advanced age of the knock-in mice, however, there are differences that appear to be unique to the *Hdh* mice. In particular, the presence of 'fingerprint membrane whorls' within neuronal cell bodies.

When autophagy is occurring rapidly, or the lysosomal processing pathway is impaired, such as in neuronal ceroid lipofuscinosis (Batten's) disease, membrane whorls are seen to accumulate. Membrane, presumably from the autophagic vacuoles and ingested organelles, forms electron-dense multilamellar bodies, as illustrated in figure 115 (arrow). Within striatal or cortical neurons these are visible more frequently in the degenerating cells of the FVB *Hdh* mouse. However, the greatest amount of autophagy is found in the Purkinje cells of the cerebellum.

It was shown in *3.2.3* that in each mouse, the vast majority of Purkinje cells show signs of degeneration. At the semi-thin level these cells exhibited a similar profile to those seen in other brain areas, but when viewed at the EM level a striking difference is noted. Figure 116 shows two degenerating Purkinje cells from an FVB *Hdh* mouse. The lower cell shows signs of autophagy within the cytoplasm (arrowheads), but the upper cell, sectioned off-centre, shows a remarkable amount of autophagic breakdown (arrows). Figure 117 is a higher power micrograph of the cell in the previous figure. One can see numerous multi-lamellar autophagic vacuoles (open arrows), some of which contain entire mitochondria (solid arrowhead); and a fingerprint whorl in the process of forming (solid arrow). In spite of the severity of autophagic breakdown, perhaps because of it, the cell appears relatively uncondensed; and the majority of mitochondria appear undilated and structurally sound. It appears there is an inverse correlation in the Purkinje cells between degree of autophagic activity and cell density. Figure 118 contains a second example of a Purkinje cell with

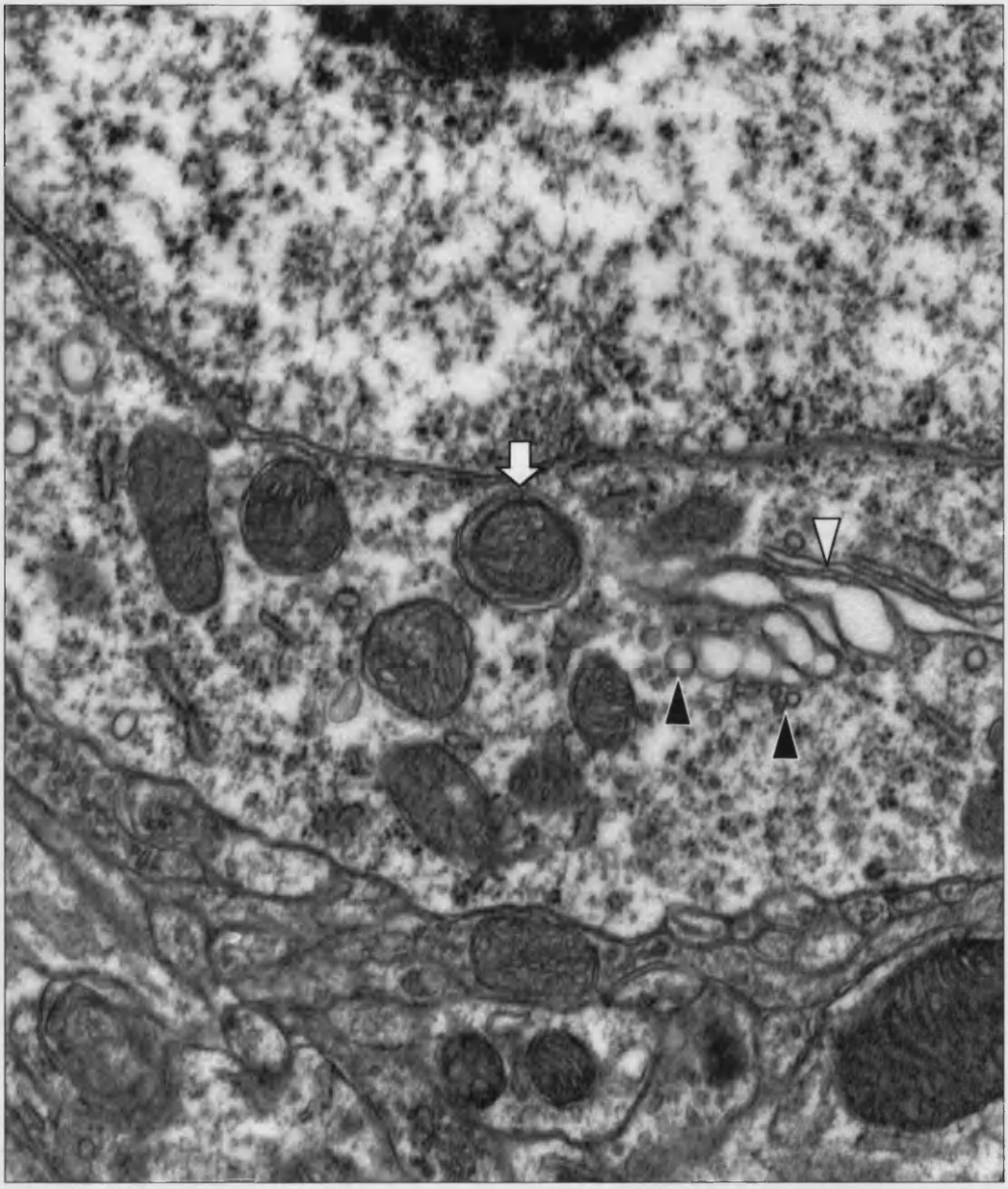

Figure 112 High-magnification electron micrograph of part of a degenerating striatal neuron in a 24 month-old truncated black 6 *Hdh* mouse. Note the dilation of the endoplasmic reticulum/Golgi (open arrowhead), from which form numerous endosomes (solid arrowheads). Note also the sequestration of an entire mitochondrion within an autophagic vacuole (arrow).

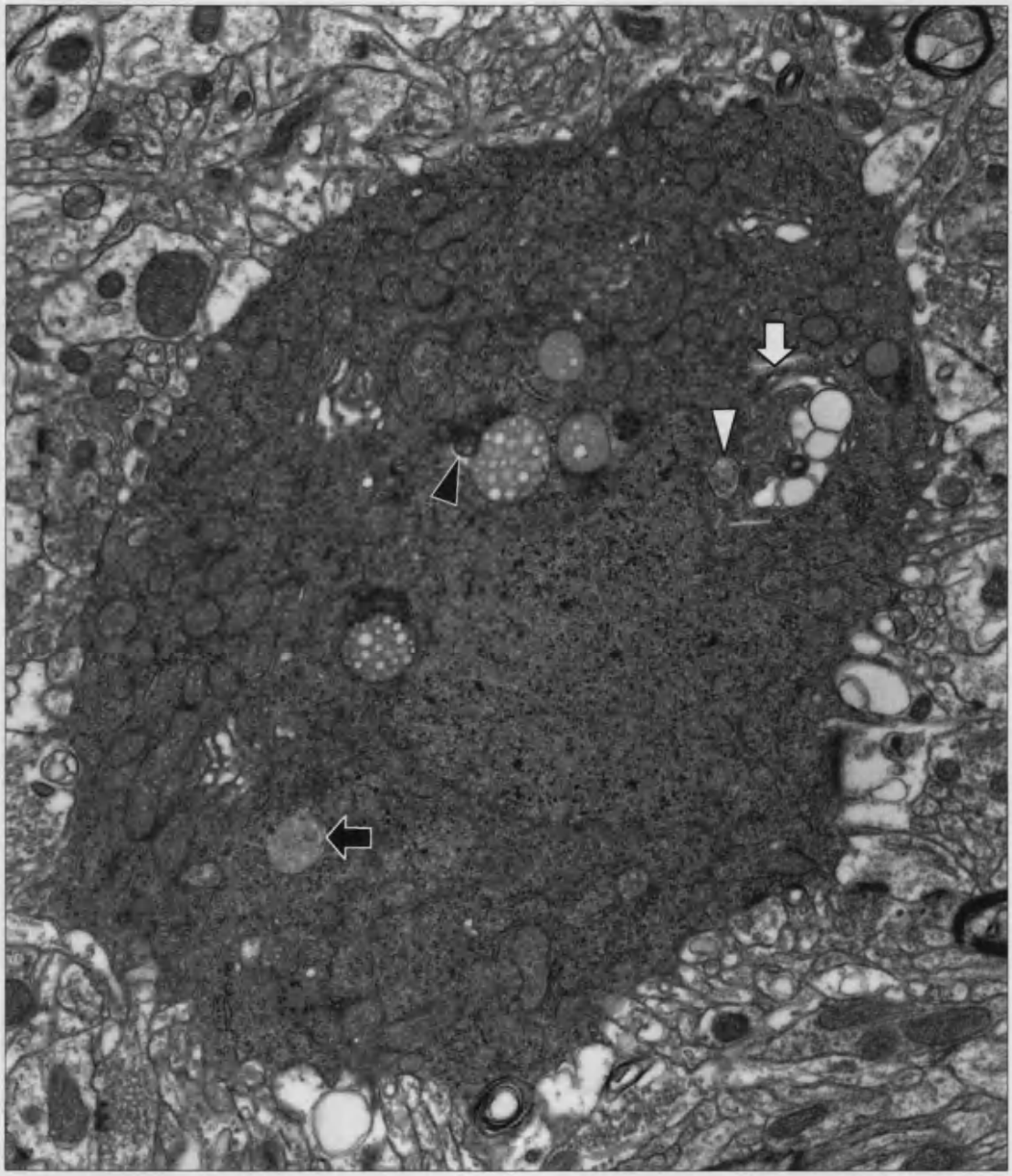

Figure 113 Electron micrograph of a degenerating striatal neuron in a 24 month-old truncated black 6 *Hdh* mouse. Note the presence of multivesicular bodies (open arrowhead), which may form from the ER shown to be dilated and forming vesicles (open arrow). Note also the mature lysosome (solid arrow) and the accumulation of material by fusing of smaller to larger lysosomes (solid arrowhead).

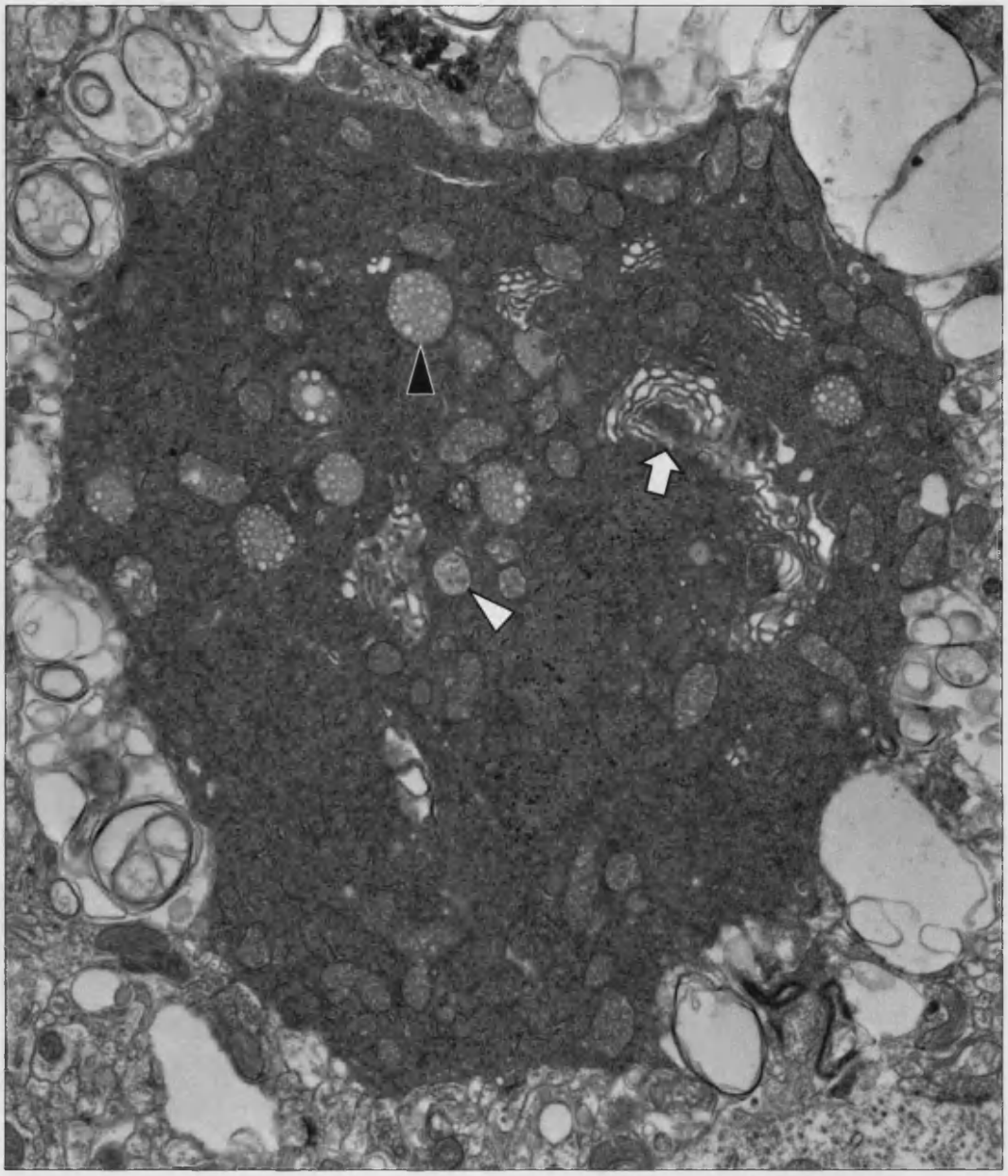

Figure 114 Electron micrograph of a degenerating striatal neuron in a 27.5 month-old full-length FVB *Hdh* mouse. The dilation of ER (arrow) and degree of lysosomal activity (arrowheads) can produce a 'foamy' appearance to some degenerating neurons.

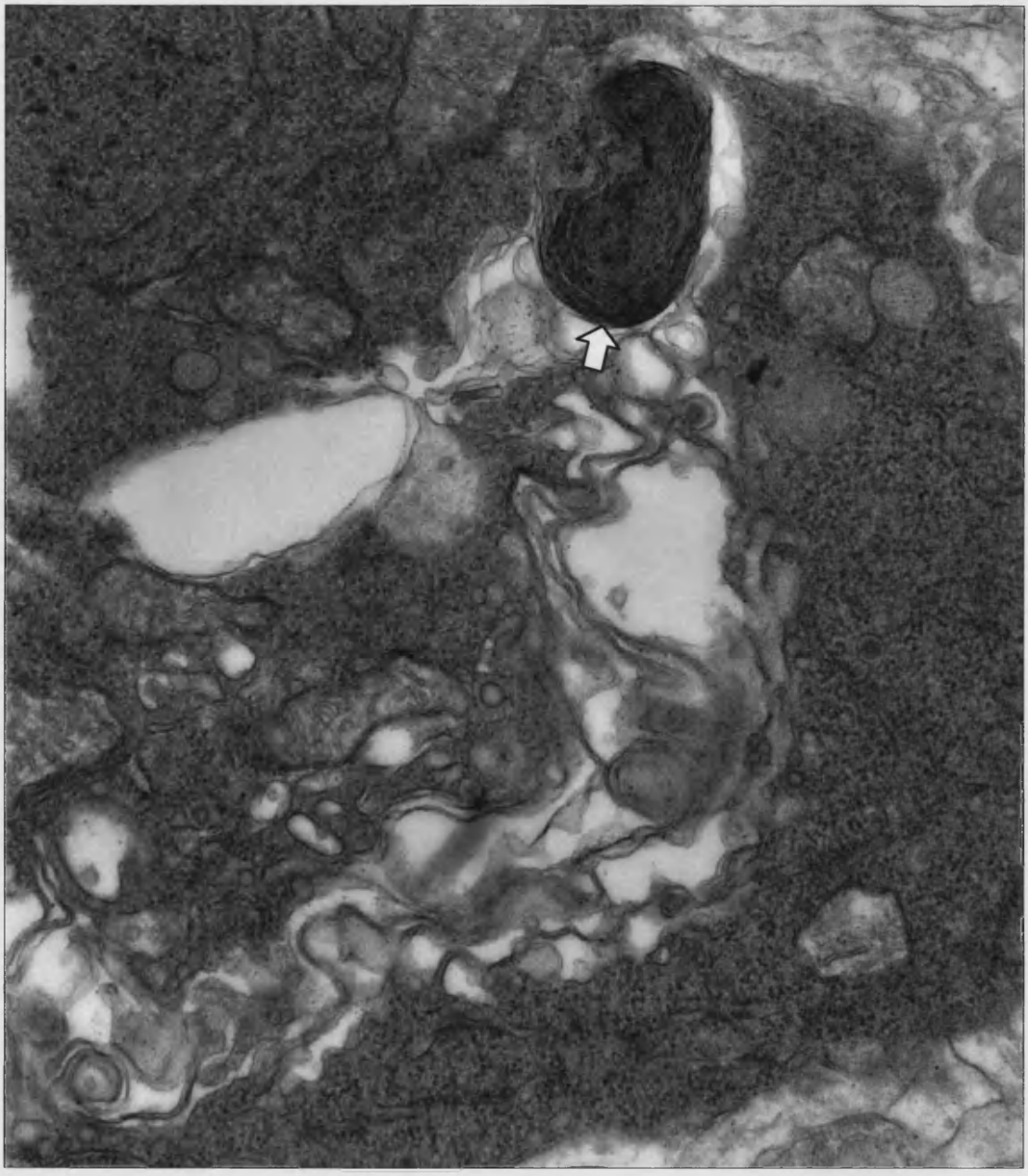

Figure 115 High magnification of an electron micrograph of a degenerating striatal neuron in a 27.5 month-old full-length FVB *Hdh* mouse. Dilated, vacuolating endoplasmic reticulum and the accumulation of membrane, producing an autophagic membrane whorl (arrow).

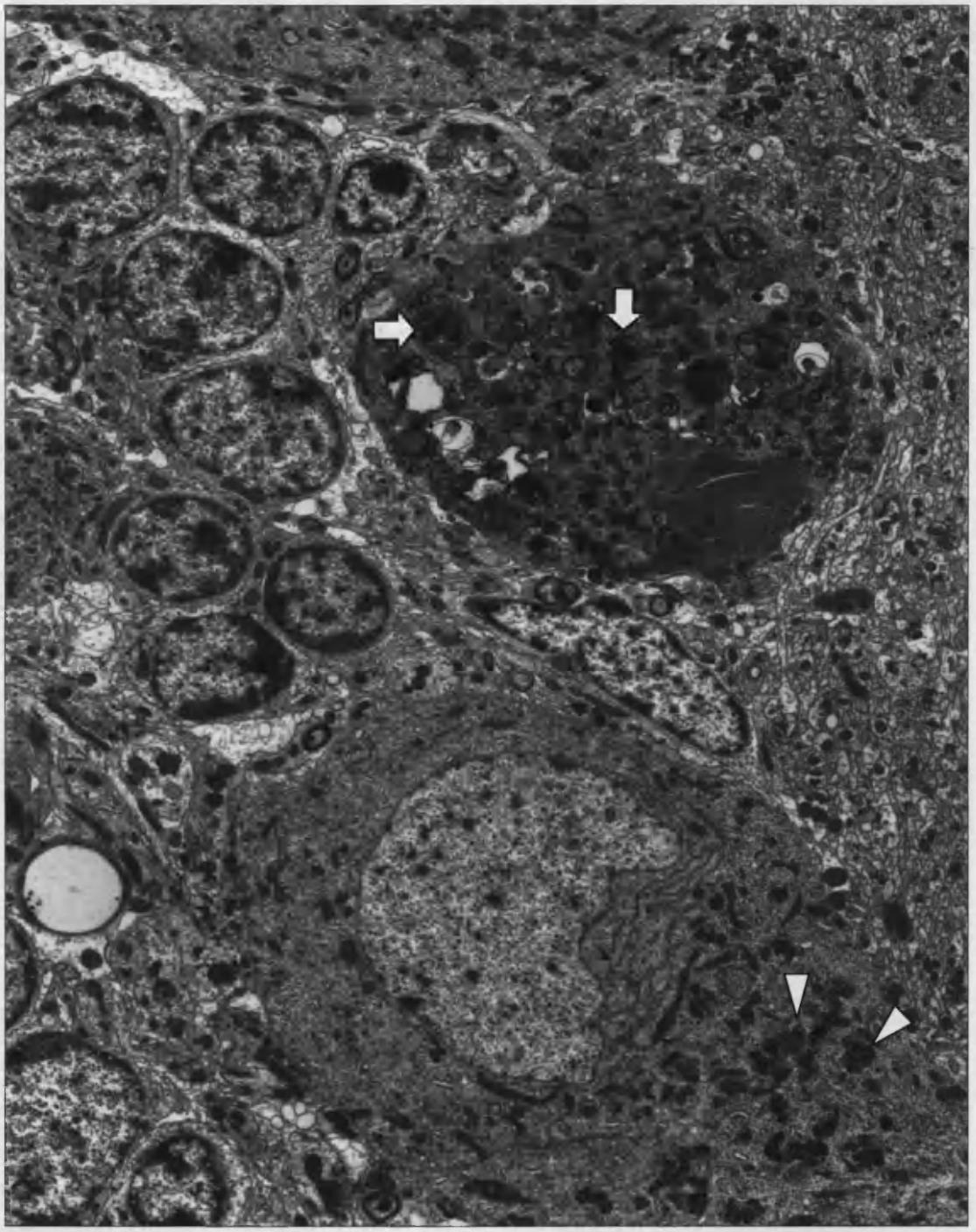

Figure 116 Electron micrograph of degenerating Purkinje cells in the cerebellum of a 29 month-old full-length black 6 *Hdh* mouse. All Purkinje cells show a marked accumulation of lipofuscin (arrowheads), but some show intense autophagic activity with numerous membrane whorls (arrows).

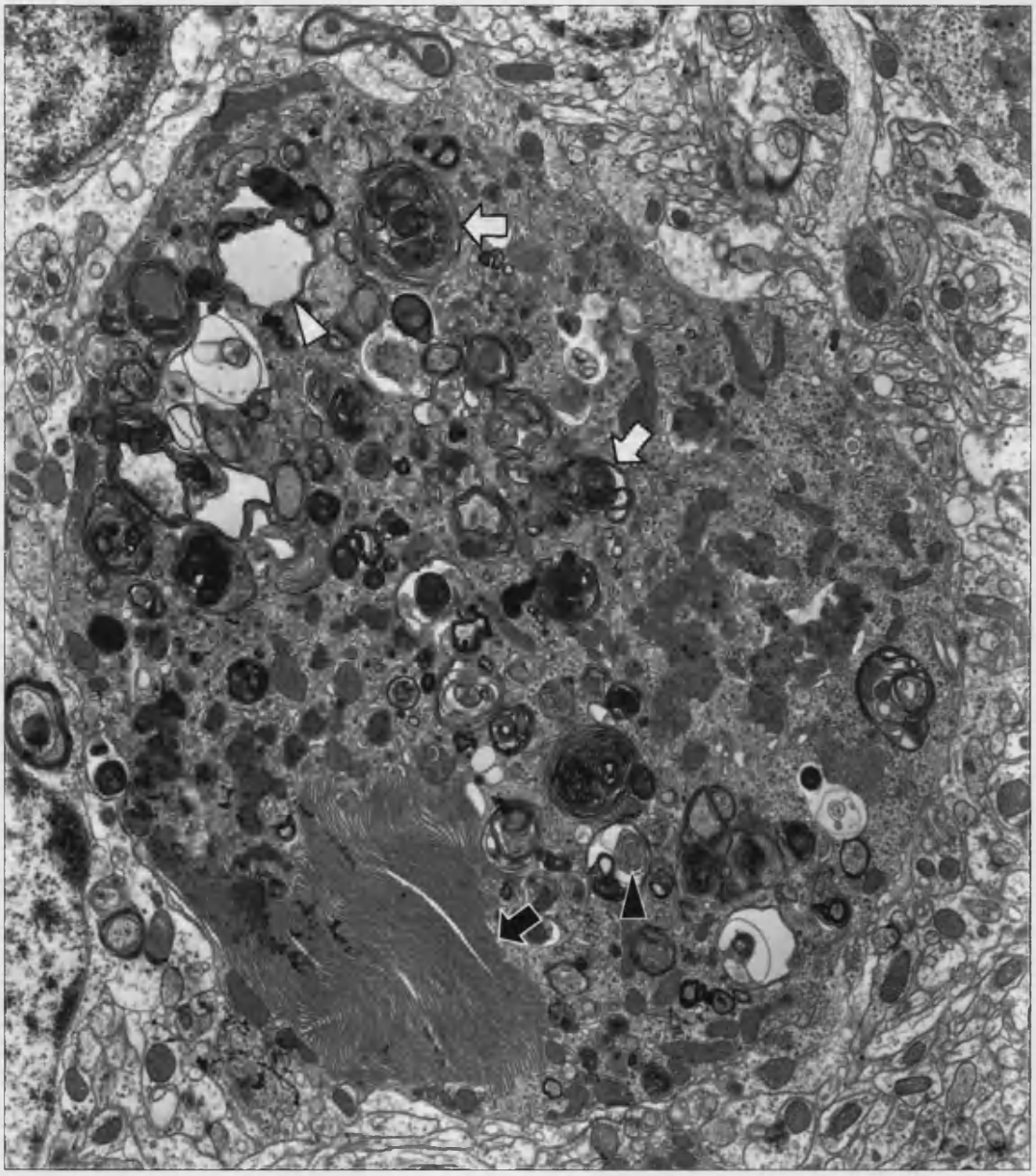

Figure 117 Electron micrograph of a degenerating Purkinje cell in the cerebellum of a 29 month-old full length black 6 *Hdh* mouse. Note the remarkable accumulation of membrane creating a 'fingerprint' membrane whorl (solid arrow); and the numerous multilamellar autophagic vacuoles (open arrows), which often contain entire mitochondria (solid arrowhead). Note also the extreme vacuolation (open arrowhead).

high levels of late-stage autophagic activity, further illustrating the lack of condensation in the cytoplasm; but this section also includes part of the nucleus, which appears normal. In contrast, figure 119 contains a Purkinje cell that, whilst showing evidence of autophagy – autophagic vacuole formation (solid arrows), multivesicular bodies (solid arrowheads) and engorged lysosomes (open arrows) – it is to a lesser degree. The cytoplasm and nucleoplasm of this cell have condensed and darked; likewise, other degenerative changes seen in cortical and striatal cells are evident, including dilation and loss of mitochondrial structure (yellow arrowhead) and condensation of chromatin (open arrowheads)[♦].

In addition to the Purkinje cells of the cerebellum, the presence of such numerous multi-lamellar autophagic vacuoles is also seen in cell processes. As observed in the R6/2 mice (see figure 68), within axons, autophagic breakdown dominates. Figure 120 contains a myelinated fibre in a full-length *Hdh* black 6 mouse, illustrating the presence of condensing autophagic vauoles (arrows), and the sequestration of entire mitochondria (arrowheads). From my work on the R6/2 mice, I had speculated that autophagic breakdown of processes may occur when neurite aggregates block transport to and/or from the soma. As I have not observed neurite inclusions in these mice, this is therefore unlikely. Rather, it appears that a separate programme exists for the degradation of processes.

Figure 121 illustrates an interesting side-point. In the R6/2 mice, the Cajal body was seen to relocate to the nuclear inclusion. Whilst the inclusions are not easily identifiable by structure in the *Hdh* mice, it is certain that in at least in a percentage of the striatal neurons they are present. The neuron in figure 121 is striatal in origin and may or may not contain an inclusion. Figure 122 is a high power image of the same cell, showing more clearly the presence of the nucleolus and its associated Cajal body (arrow). It is tempting to believe that the unidentified body (arrowhead) is part of an inclusion, but this is speculative. However, what can be said is that the Cajal body in this neuron remains associated with the nucleolus; if this cell does indeed contain an inclusion it would be an interesting difference between transgenic and knock-in models if the Cajal body failed to relocate.

[♦] Expected in this example as this Purkinje cell is from and FVB *Hdh* mouse.

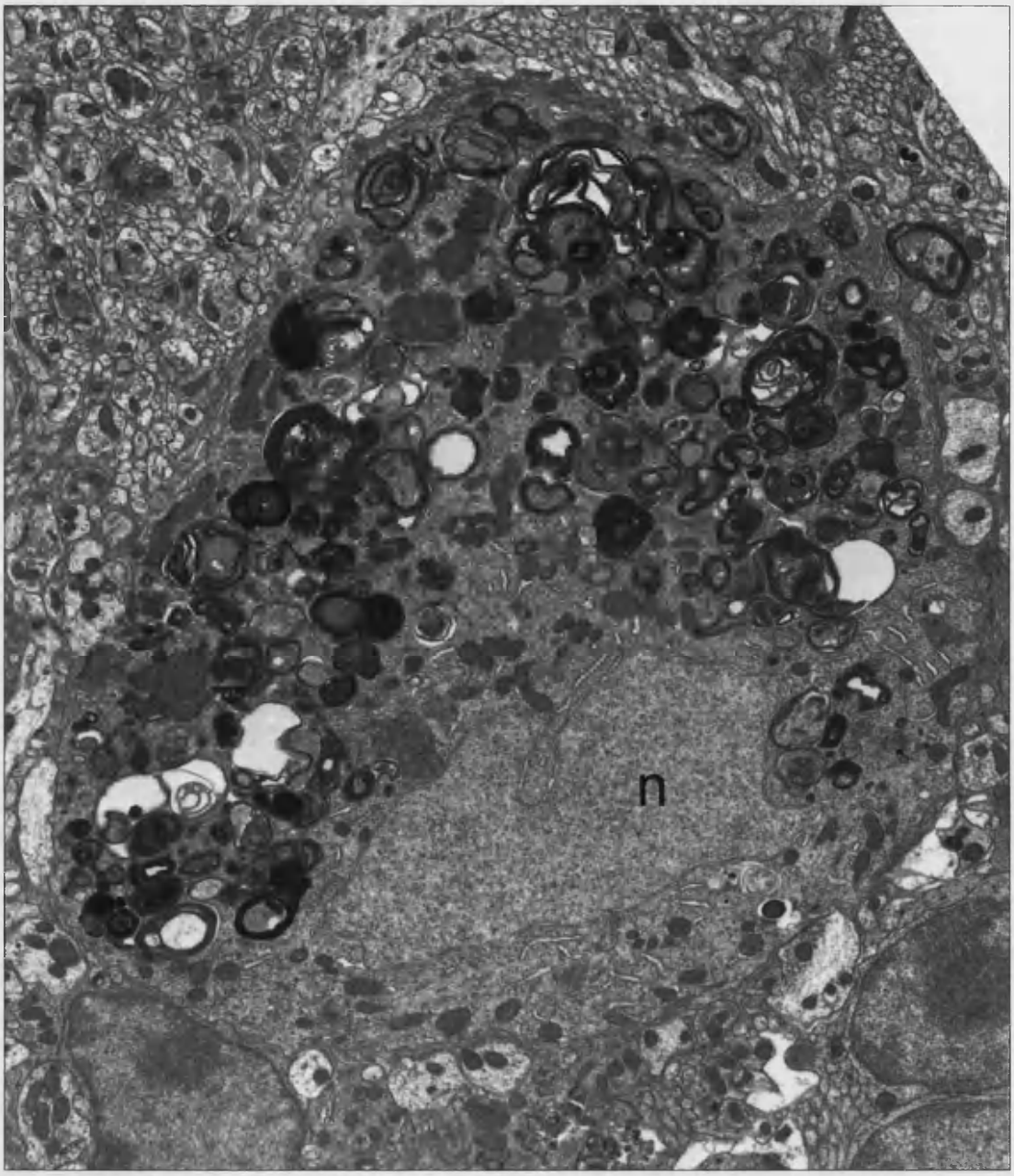

Figure 118 Electron micrograph of a degenerating Purkinje cell in the cerebellum of a 29 month-old full length black 6 *Hdh* mouse. Intense autophagic activity is once again present, but the neuronal nucleus (**n**) retains a healthy appearance.

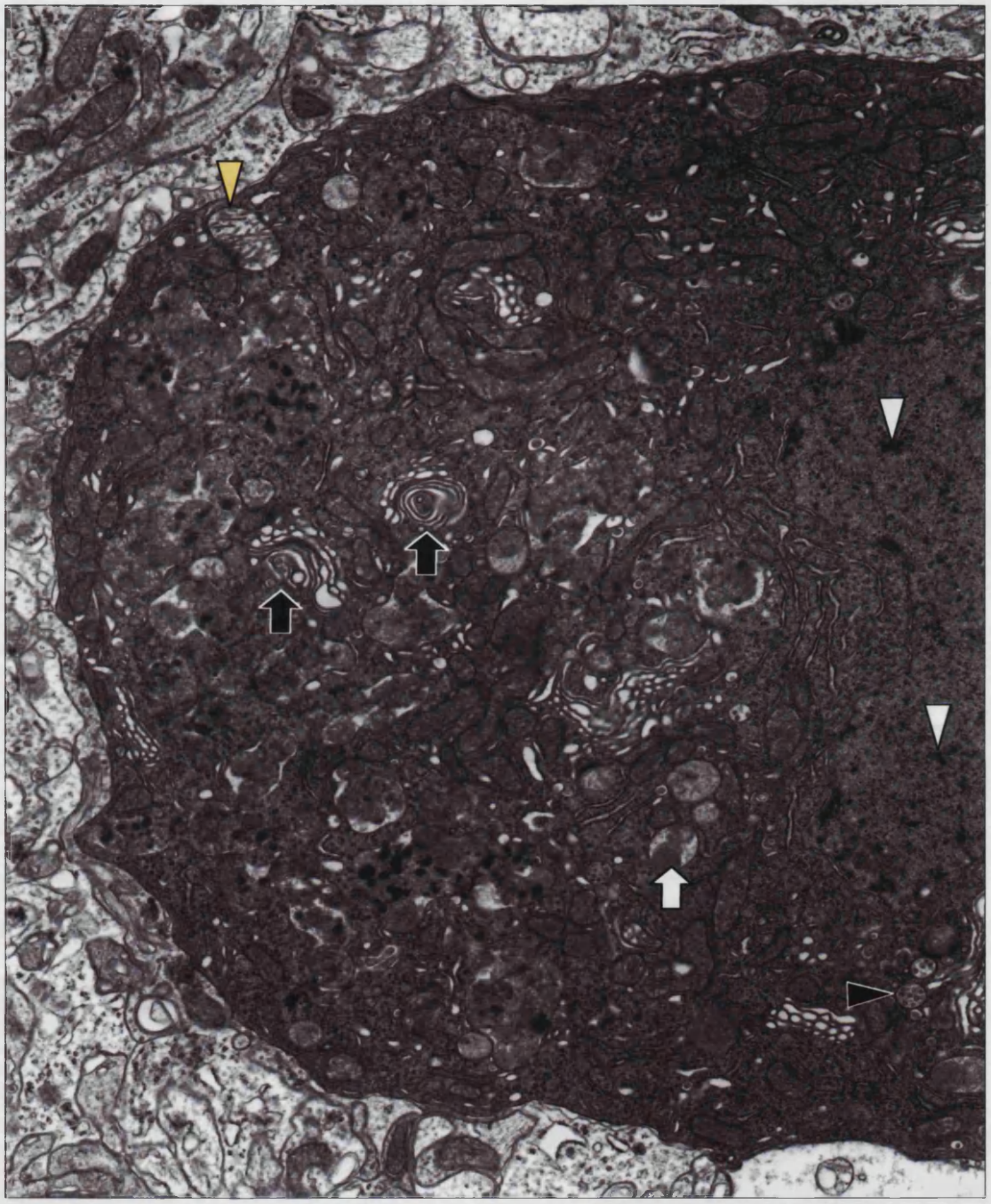

Figure 119 Electron micrograph of a degenerating Purkinje cell in the cerebellum of a 27.5 month-old full length FVB *Hdh* mouse. Autophagy can be seen in the form of multivesicular bodies (solid arrowheads), mature lysosomes (open arrow), and the formation of multilamellar autophagic vacuoles (solid arrows). This Purkinje cell shows nuclear condensation with signs of condensation of chromatin (open arrowheads).

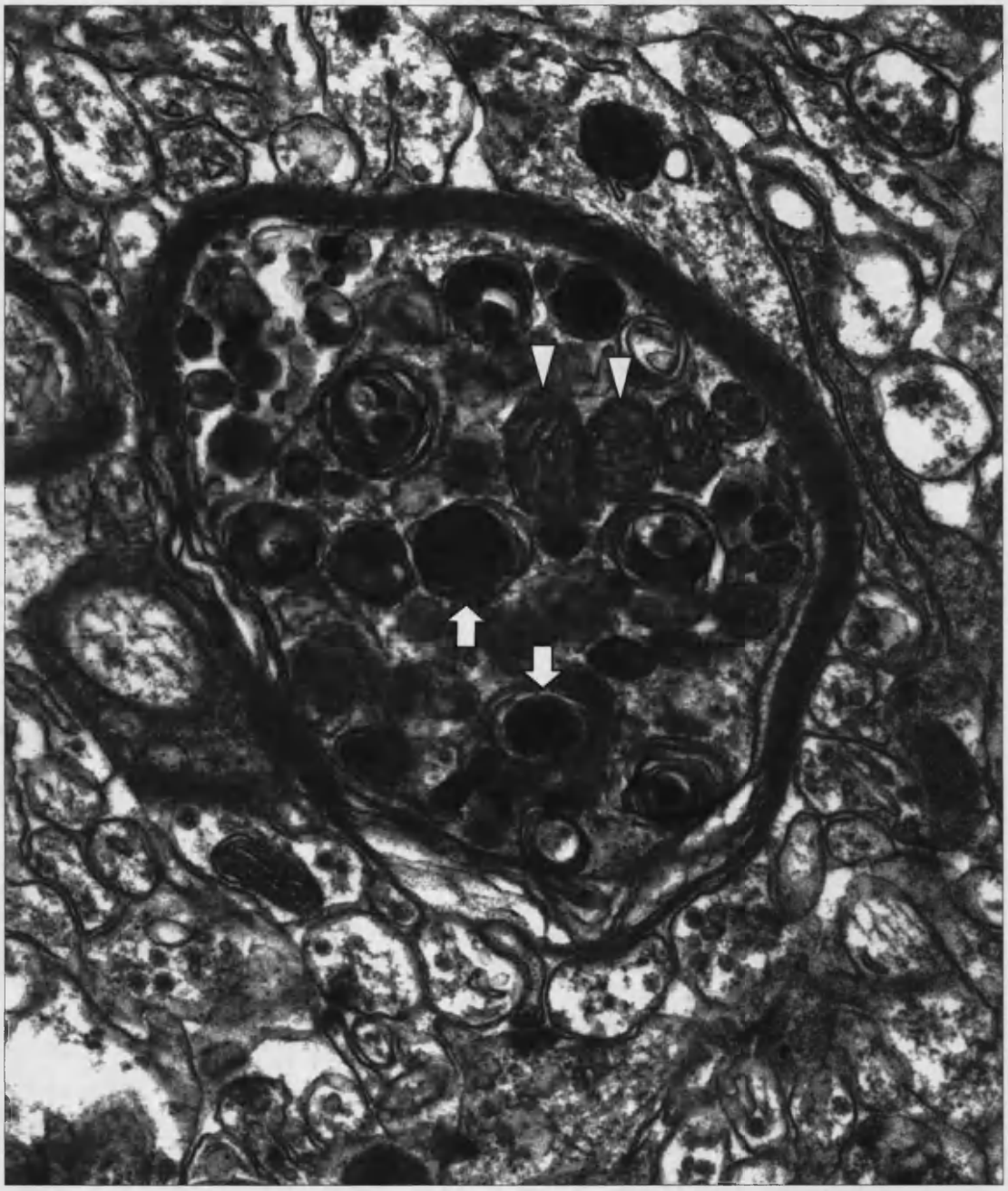

Figure 120 Electron micrograph of a degenerating axon in a 27.5 month-old full length FVB *Hdh* mouse. The axon is filled with autophagic vacuole 'whorls' (arrows), yet the mitochondria appear healthy (arrowheads).

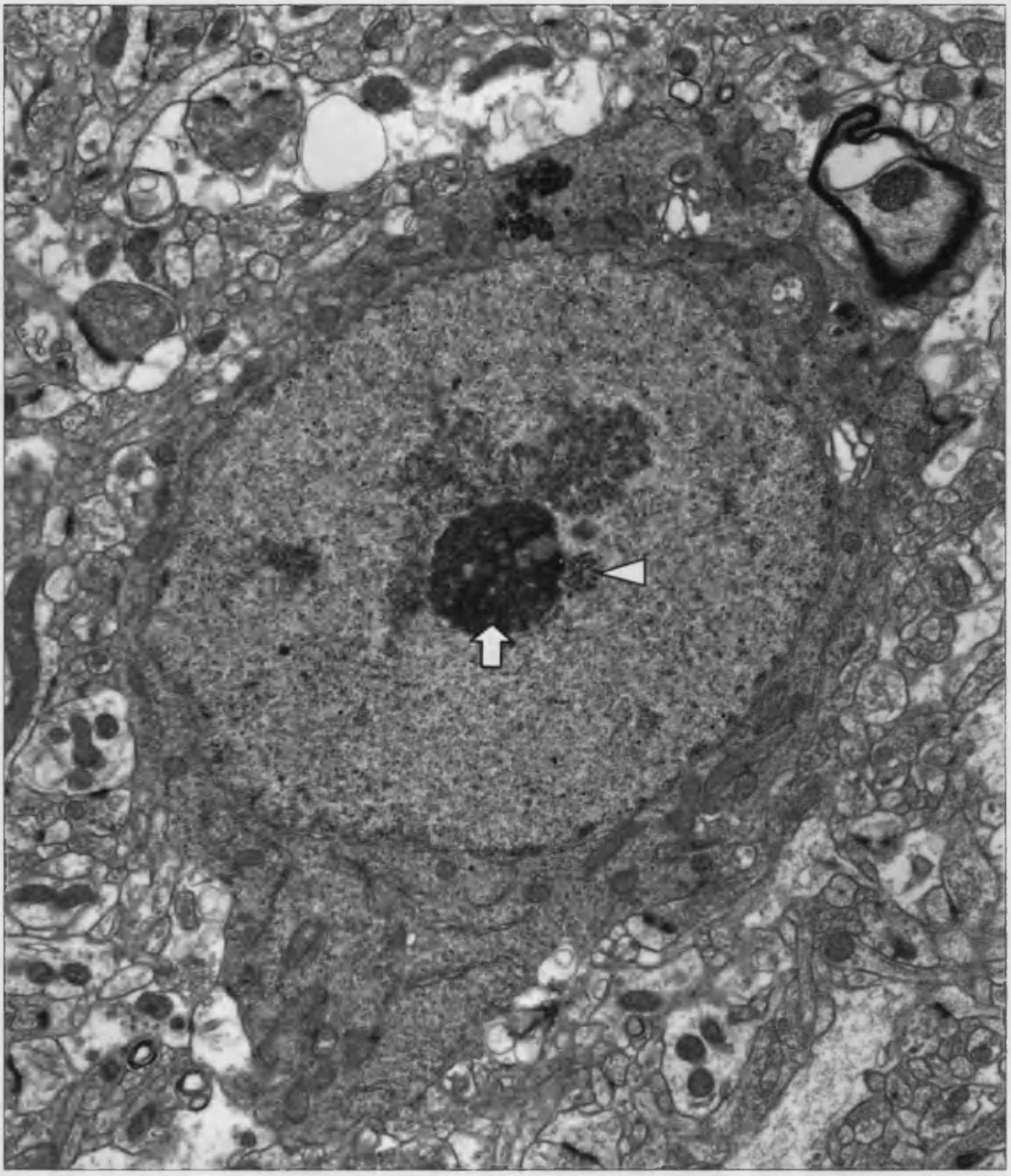

Figure 121 Electron micrograph of a degenerating neuron in a 29 month-old full length black 6 *Hdh* mouse. The Cajal body (arrowhead) remains associated with the nucleolus (arrow).

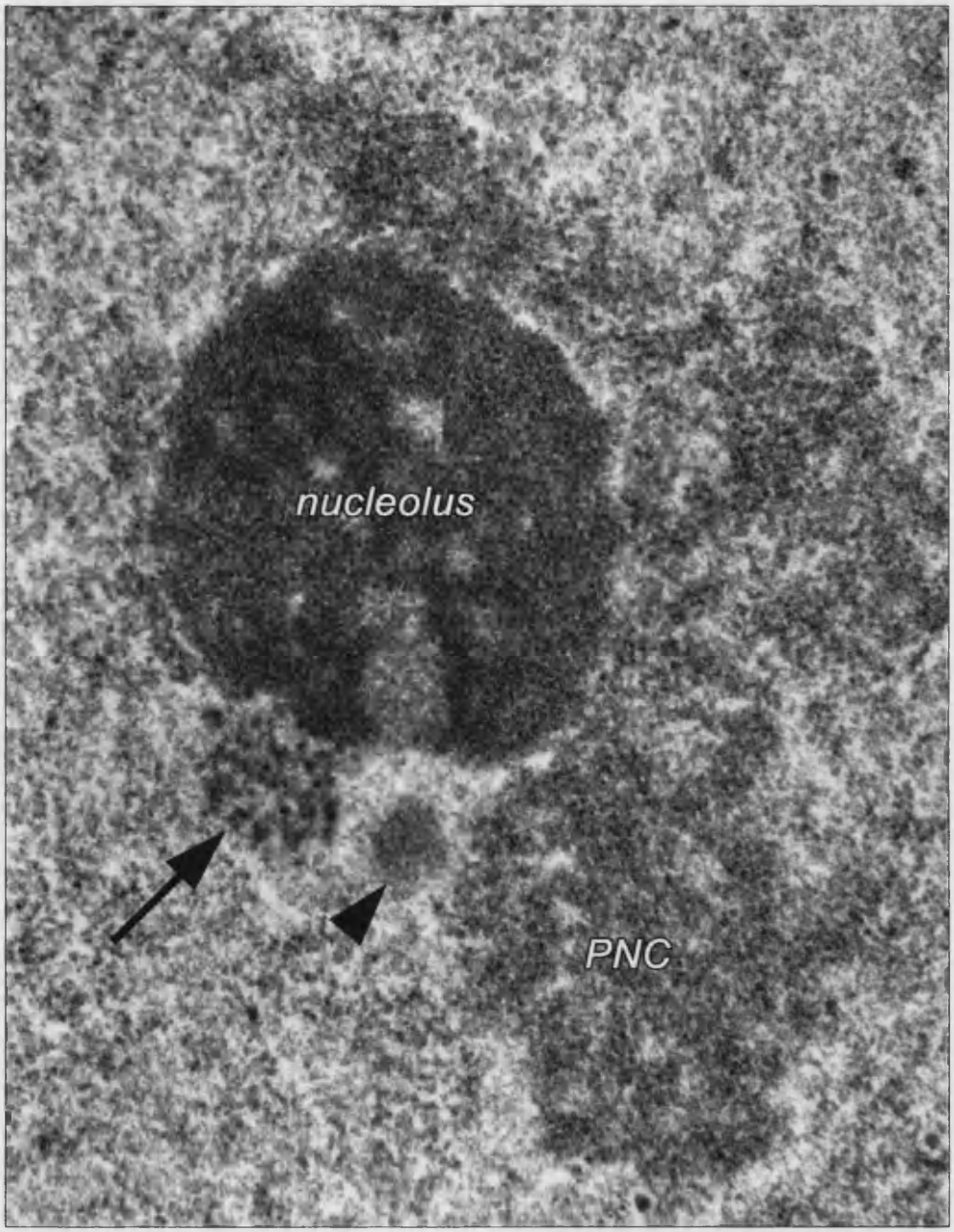

Figure 122 Section from full-length black 6 *Hdh* striatum showing nucleolus and perinucleolar cap (labelled). It is tempting to assume that the unidentified body (arrowhead) is part of an inclusion. However, whatever the nature of this structure, the Cajal bodies of *Hdh* neurons show normal nucleolar association (arrow).

3.2.5 Degeneration in Aged Wild Type Mice

Perhaps the most interesting result obtained for this thesis stems from work on the littermate controls. The nature of the *Hdh* mice is such that degeneration is not evident until the mice are older than two years of age: the last days of the mouse lifespan. Wild-type littermate mice have, of course, been used in this study to control for effects outside those of the *Hdh* mutation. Two batches of mice have been used to obtain the data presented here. The first consisted of mice ranging from 23 to 29 months of age. In these mice the *Hdh* animals showed variable levels of degeneration, predominantly in the cortex, but also in the striatum. The littermate controls (27.6 months FVB; 29 & 29.2 months black 6) showed heavy accumulations of lipofuscin (expected with age) but no other obvious changes. However, the second set of mice ranged from 28 to almost 30 months of age. In these, the *Hdh* showed far greater levels of degeneration and, interestingly, pathology was also evident in the wild type controls. Detailed ultrastructural analyses were therefore carried out on the wild type mice to identify similarities and differences between these mice and their mutant siblings.

Initial ultrastructural analysis was carried out on the 29 months and 21 day-old black 6 wild-type and it was found that the degenerating neurons are strikingly similar to those seen in each of the *Hdh* siblings; and to the degeneration seen in the R6/2. Figure 123 is a section through the cortex of this mouse. A healthy neuron is visible at the bottom of the section (arrow), highlighting the degree of condensation seen in the degenerating neurons (arrowhead). Both the cytoplasm and nucleoplasm have condensed in the degenerating cells and as a result they have adopted the 'scalloped' or 'ruffled' appearance seen in the *Hdh* and R6/2 mice. In contrast to the degeneration of the *Hdh* mice, where cytoplasmic condensation generally appears to slightly precede nuclear condensation, the condensation of wild type cytoplasm and nucleoplasm occurs concomitantly. Figure 124 contains a higher magnification micrograph of a cortical neuron; whilst the nucleus is still easily discernible (arrow), it is of similar electron-density to the cytoplasm (arrowhead).

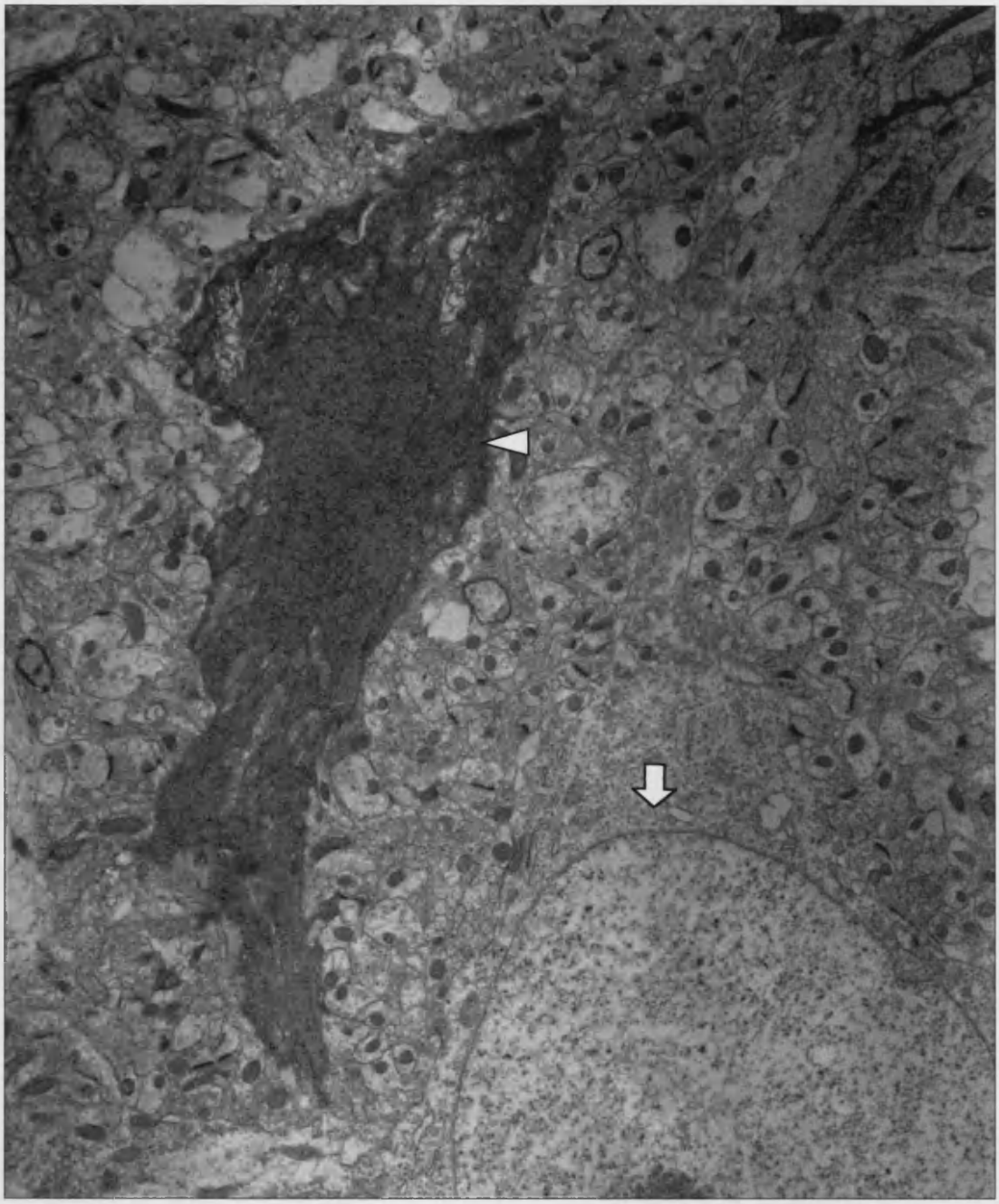

Figure 123 Electron micrograph of neurons in the cortex of a 29 month-old wild-type black 6 mouse. A neuron in an advanced stage of degeneration (arrowhead) can be compared to an adjacent healthy neuron (arrow)

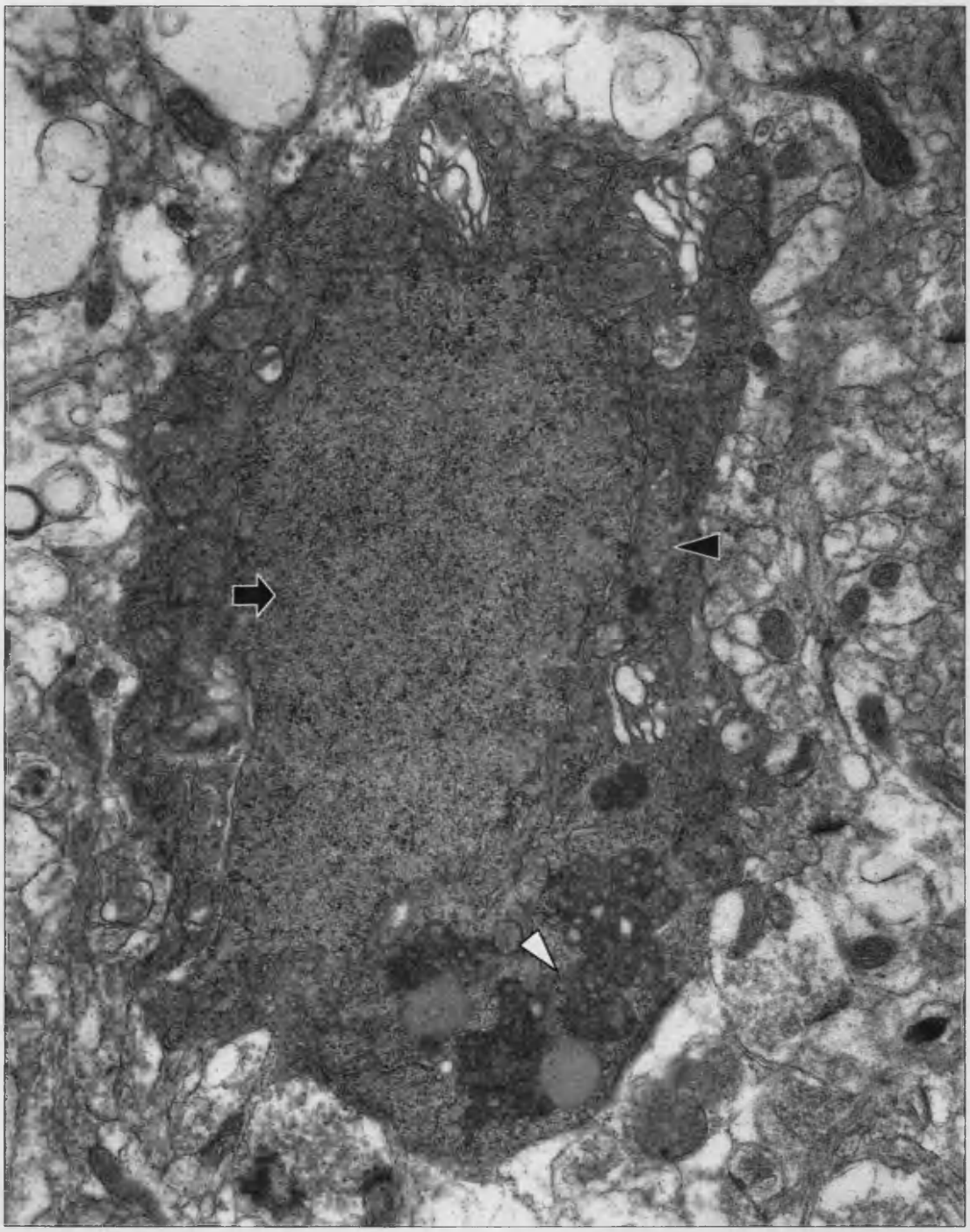

Figure 124 Electron micrograph of a degenerating cortical neuron from a 29 month-old wild-type black 6 mouse. Cytoplasm (solid arrowhead) and nucleoplasm (arrow) exhibit similar levels of condensation. Note also the large accumulation of lipofuscin (open arrowhead).

Figure 124 also illustrates the large amounts of lipofuscin found within the degenerating control neurons (open arrowhead). Whilst lipofuscin is present within the vast majority of neurons of this age, there does appear to be a greater amount in neurons undergoing degeneration. However, this may in fact be a misleading observation. Figure 125 contains an otherwise healthy striatal neuron from a wild-type mouse. The lipofuscin appears to be less than that seen in figure 124, but the condensation of this cell, together with the tendency for lipofuscin to agglomerate, would most likely yield a cell with a profile similar to that of figure 124.

A further similarity is represented in figure 126: dilation of the golgi and endoplasmic reticulum (arrows). As with the R6/2 and *Hdh* mice, the dilation is most apparent in the later stages of degeneration, but this may also be a consequence of condensation. Whatever the timing of the event, the dilation certainly occurs to varying degrees in all mice. The dilation appears to be greater in the *Hdh* mice when compared to the R6/2, but similar to the wild-type mice. Therefore, any differences in the effect are most likely to be dependent on the ages of the animals.

There is also evidence of loss of mitochondrial integrity. Figure 126 contains degenerating mitochondria (solid arrowheads), which can be compared to healthy mitochondria (open arrowheads) in the neuopil. Mitochondrial dilation is certainly apparent, but it is hardest to identify in these mice as it is less severe. There is also a loss of internal structure, though, once again, not as sever as that seen in the knock-ins or R6/2s. Given that the endoplasmic reticulum and golgi dilate to levels comparable to those seen in the *Hdh* mice and yet the mitochondria in the age-matched black 6 do not, it is reasonable to assume that mitochondrial dilation, whilst 'natural' in mice of this age, is exacerbated by the presence of mutant huntingtin.

There is evidence of autophagic activity within the degenerating cortex and striatum, suggested by the presence of multivesicular bodies and autophagic vacuoles (figure 127) however it does not appear to reach the levels observed in the *Hdh* mice; the exception being the Purkinje cells of the cerebellum. As with the knock-ins, the Purkinje cells exhibit autophagic activity ranging from large numbers of multivesicular bodies and lysosomes (figure 128) to the filling of a cell with autophagic profiles suggesting a complete deconstruction (figure 129). It is therefore probably that the

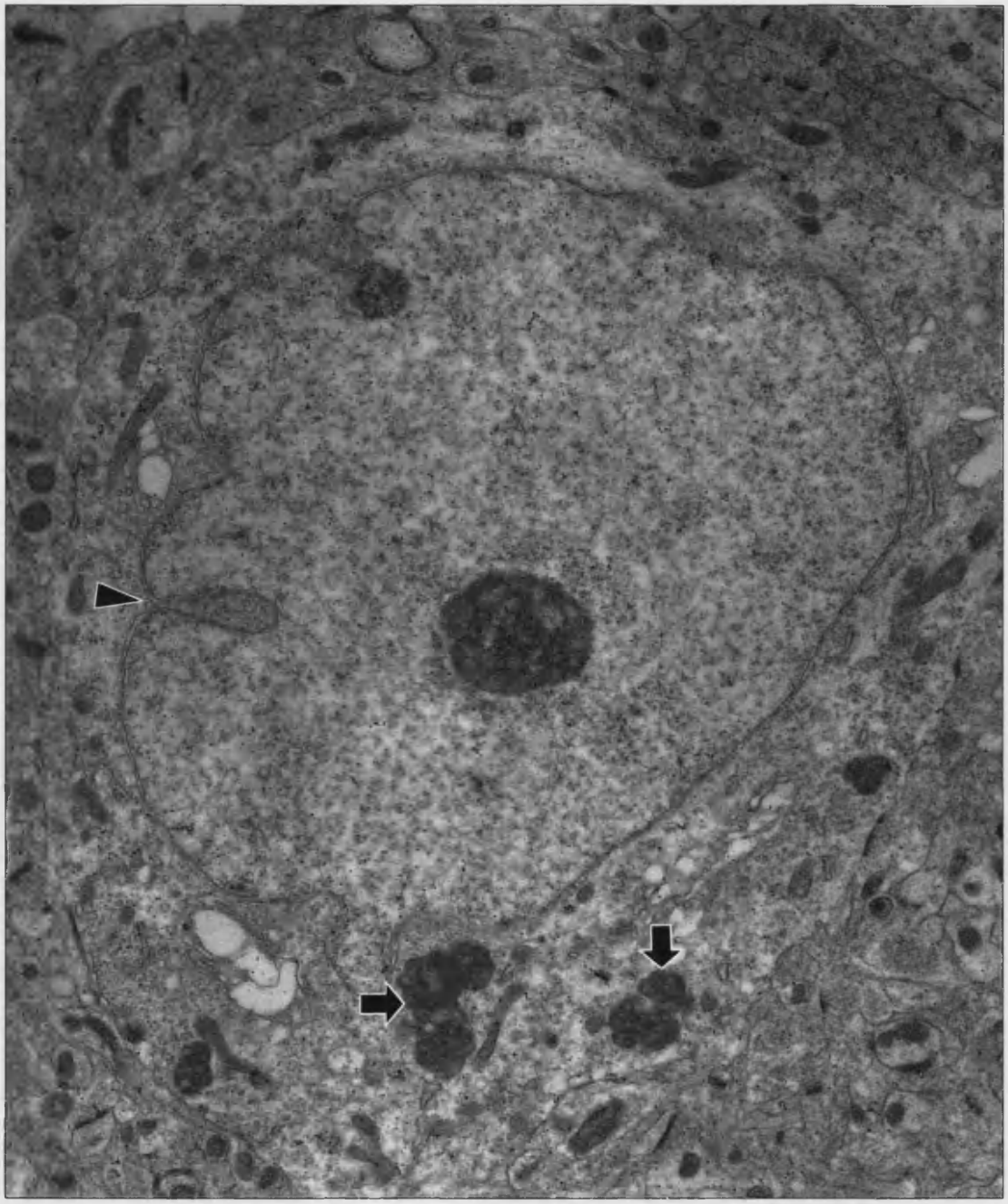

Figure 125 Electron micrograph of a striatal neuron from a 29 month-old wild-type black 6 mouse. This neuron shows a relatively healthy profile with the exception of mild invagination of the nuclear membrane (arrowhead) and accumulation of lipofuscin (arrows)

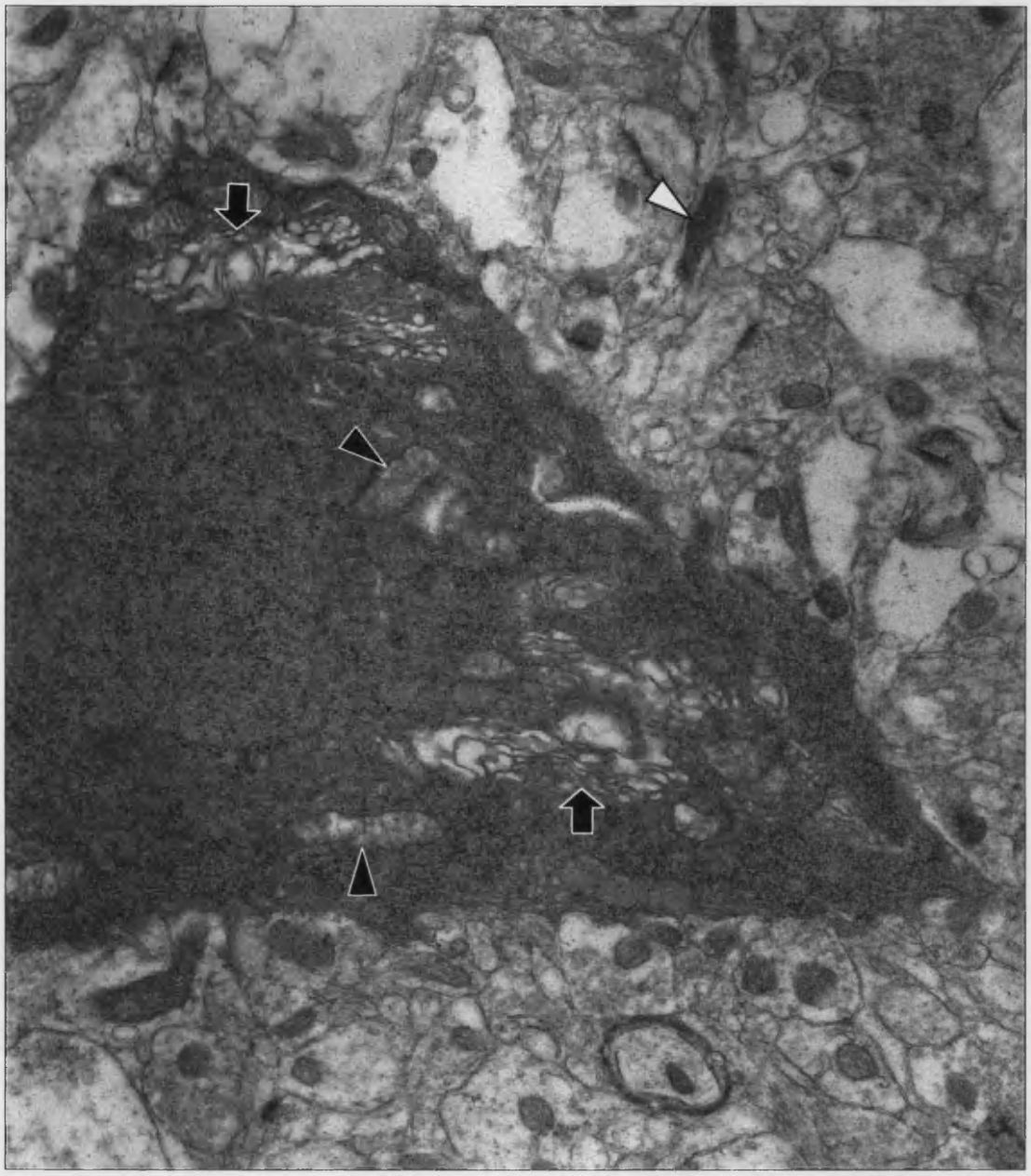

Figure 126 Electron micrograph of a section of degenerating cortical neuron from a 29 month-old wild-type black 6 mouse. Note the dilation of endoplasmic reticulum/Golgi (arrows) and the dilation of mitochondria (solid arrowheads), which can be compared to healthy mitochindria in the neuropil (open arrowhead).

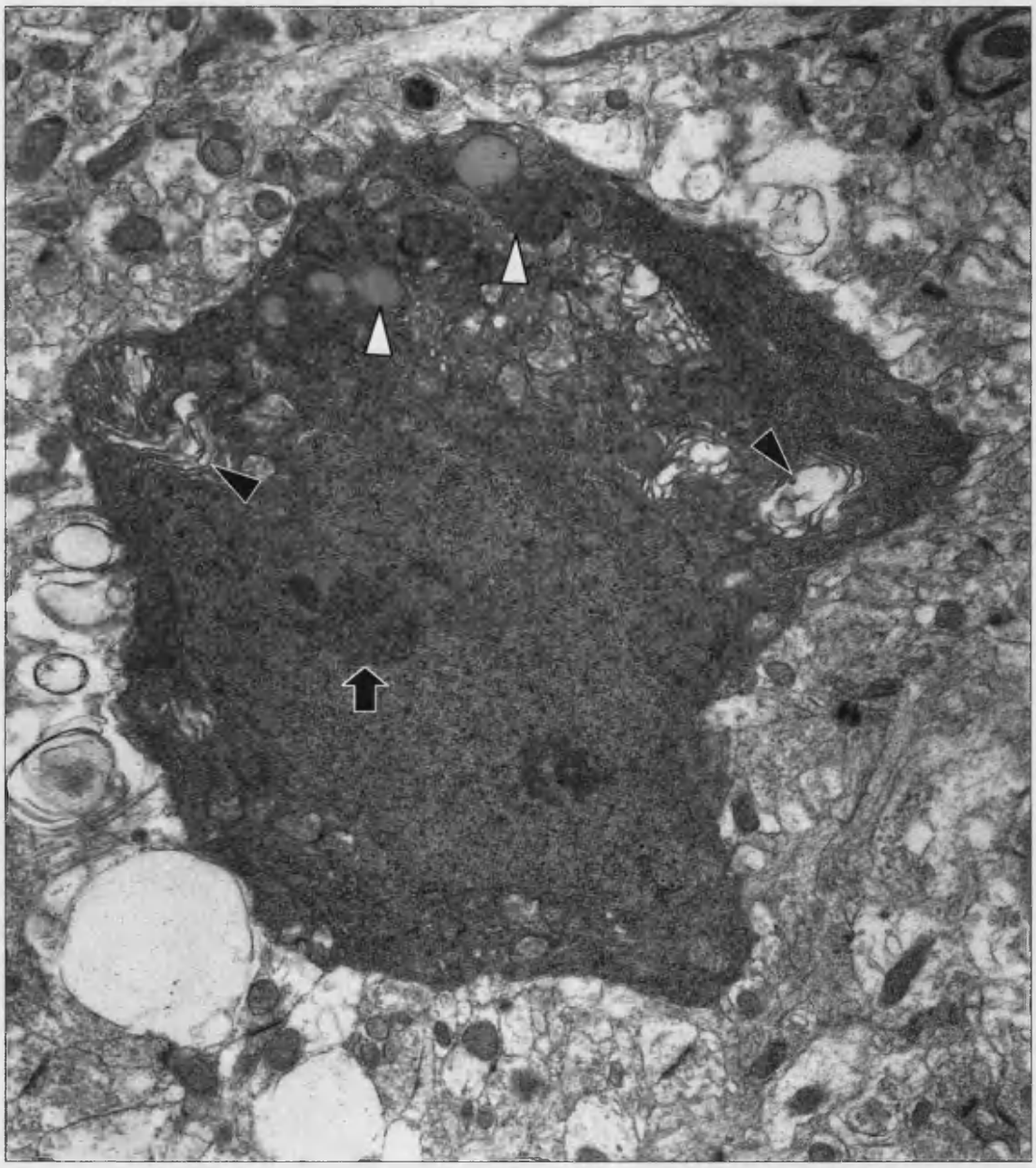

Figure 127 Electron micrograph of a degenerating cortical neuron from a 29 month-old wild-type black 6 mouse. In spite of the dilated organelles (solid arrowheads) and accumulation of lipofuscin (open arrowheads), the nucleus and nucleolus (arrow) remain intact.

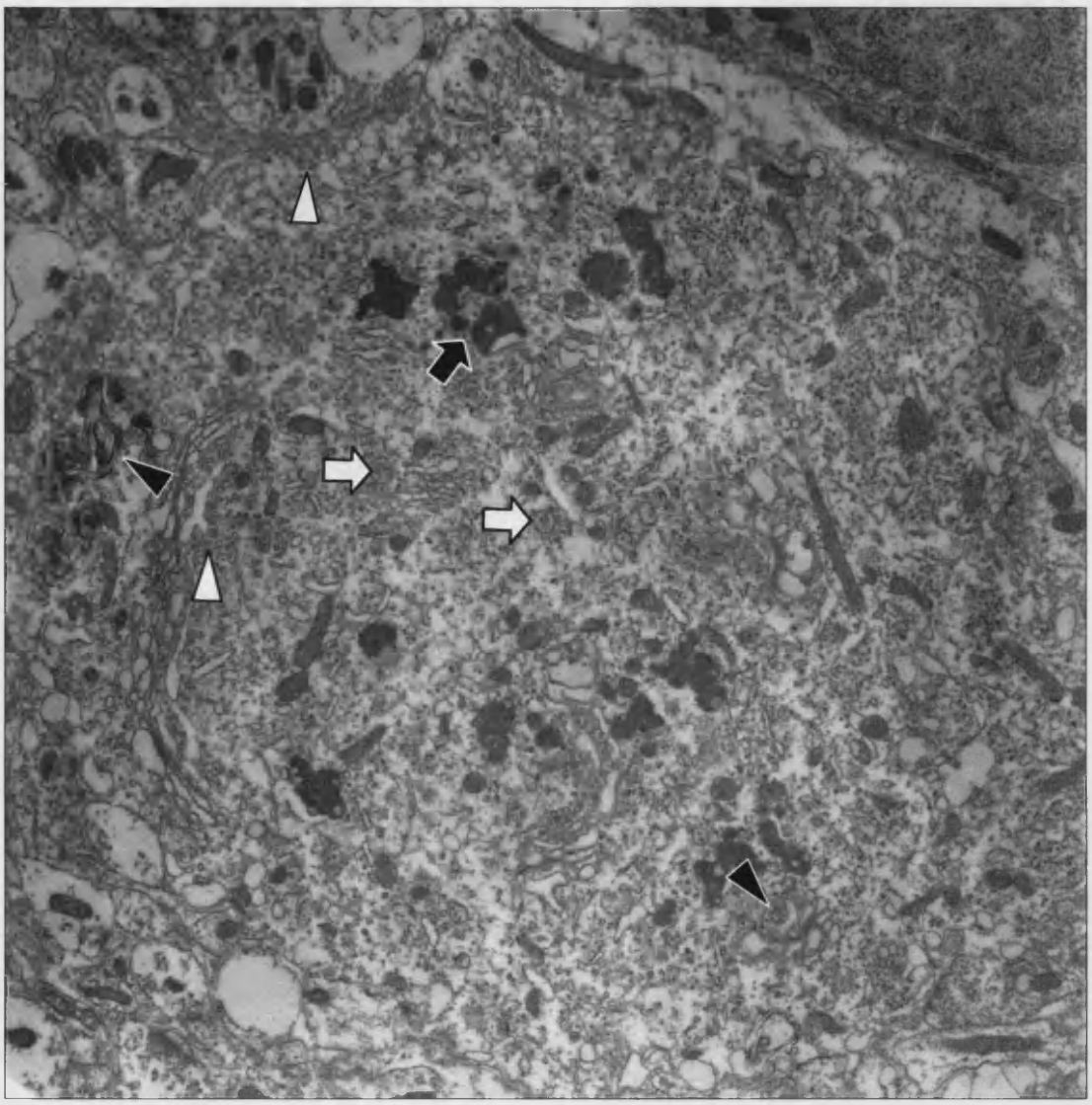

Figure 128 Electron micrograph of a cerebellar Purkinje neuron from a 29 month-old wild-type black 6 mouse. Autophagic activity is indicated by the dilation and vacuolation of the Golgi/ER (open arrowheads), the formation of multivesicular bodies (open arrows), autophagic vacuoles (solid arrowheads) and accumulation of lipofuscin (solid arrows).

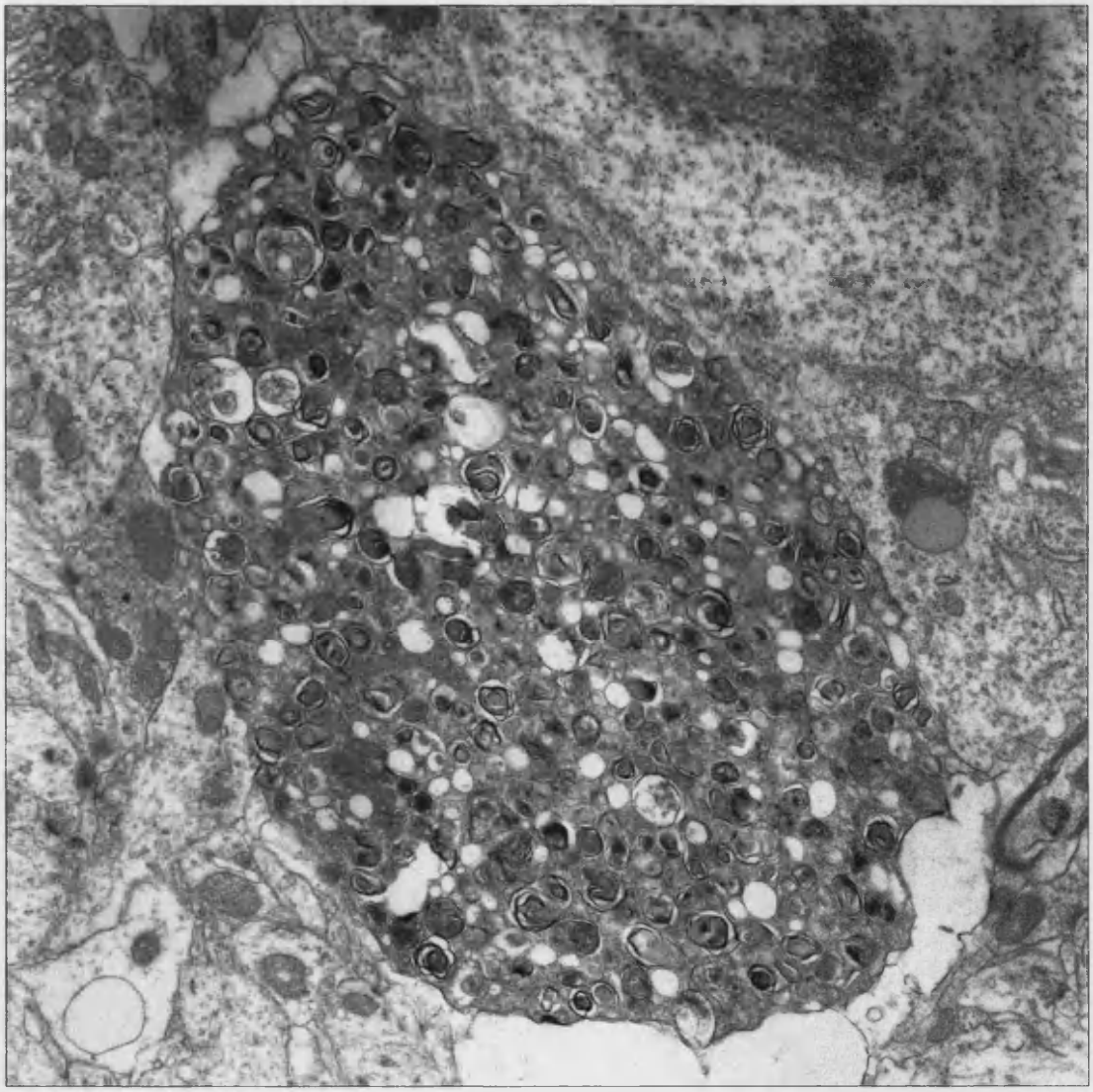

Figure 129 Electron micrograph of a cerebellar Purkinje cell from a 29 month-old wild-type black 6 mouse. The neuron appears to be undergoing autophagic breakdown.

Purkinje cell degeneration seen within each of these mice reflects merely a process associated with age. Indeed, section *3.2.3* showed comparable levels of degeneration in each mouse. Perhaps the high levels of autophagy within this cell type reflects the amount of membrane associated with the cell. As discussed in *4.5* neuronal processes are seen to be 'pruned back' in HD, if the products of dendritic breakdown are transported to the soma it may explain the appearances of cells such as that shown in figure 129.

Analysis of the FVB wild-type yielded similar results, which in itself is rather surprising as the oldest surviving FVB wild-type mouse was 28 months old, and is being compared to mice of 29 months and 20 days (±2 days). The degenerating neurons also exhibit condensation of cytoplasm and nucleoplasm at comparable rates, with many cells in a single area undergoing apparently simultaneous degeneration (figure 130). Furthermore, each wild-type background shows comparable dilation of the golgi and endoplasmic reticulum, the wild-type FVB shows a greater accumulation of lipofuscin. Figure 131 contains a degenerating and relatively healthy neuron; dense deposits of lipofuscin are evident in both (arrows). The accumulation is greater than that seen in the black 6 in healthy as well as dark cells. Figure 132 is a section of degenerating cortical neuron in which remarkable levels of all stages of autophagy are evident: the fomation of autophagic vacuoles (open arrows), multivesicular bodies (solid arrowheads) and lysosomes filled with product at varying stages of processing (open arrowhead). Furthermore, many of the mitochindria appear dilated (figure 133, solid arrowheads) when compared to healthy examples (open arrowheads), but the internal structure is generally better preserved in the wild-type degenerating neurons that in the dark cells of the *Hdh* or R6/2 mice.

Comparison of toludine blue-stained semi-thin sections has revealed similar levels of degeneration in the black 6 and FVB wild-type mice, is spite of the FVB mice being seven weeks younger. Furthermore, EM analysis has revealed that whilst very similar overall, the levels of autophagy and lipofuscin build up are apparently higher in the younger FVB background. This may be indicative of a general state of health in the FVB background. This strain may be more sensitive to stress, including simply age-related stress. The variation in dark cell distribution combined with the small number

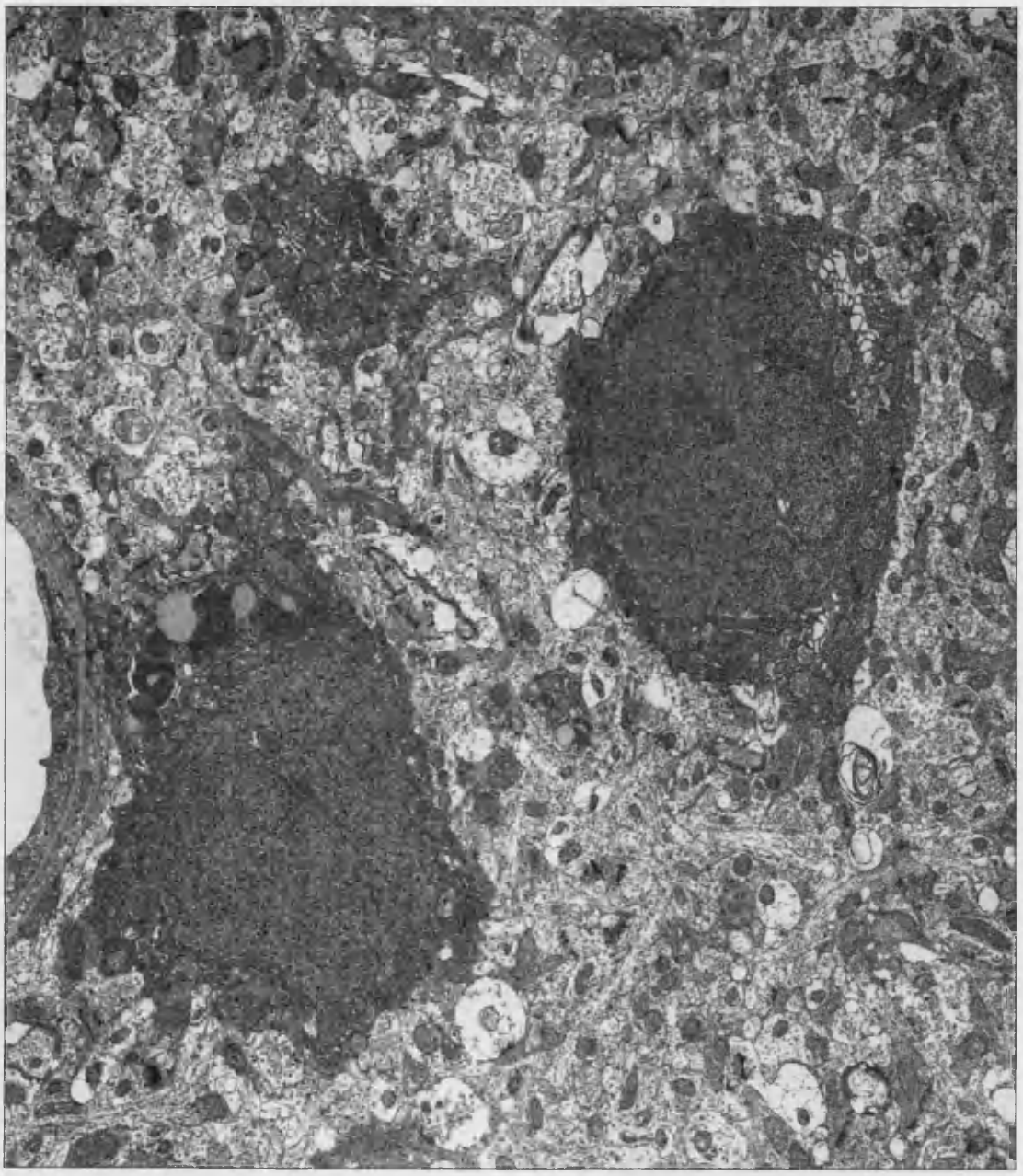

Figure 130 Degenerating neurons in the striatum of a 28 month-old wild-type FVB mouse.

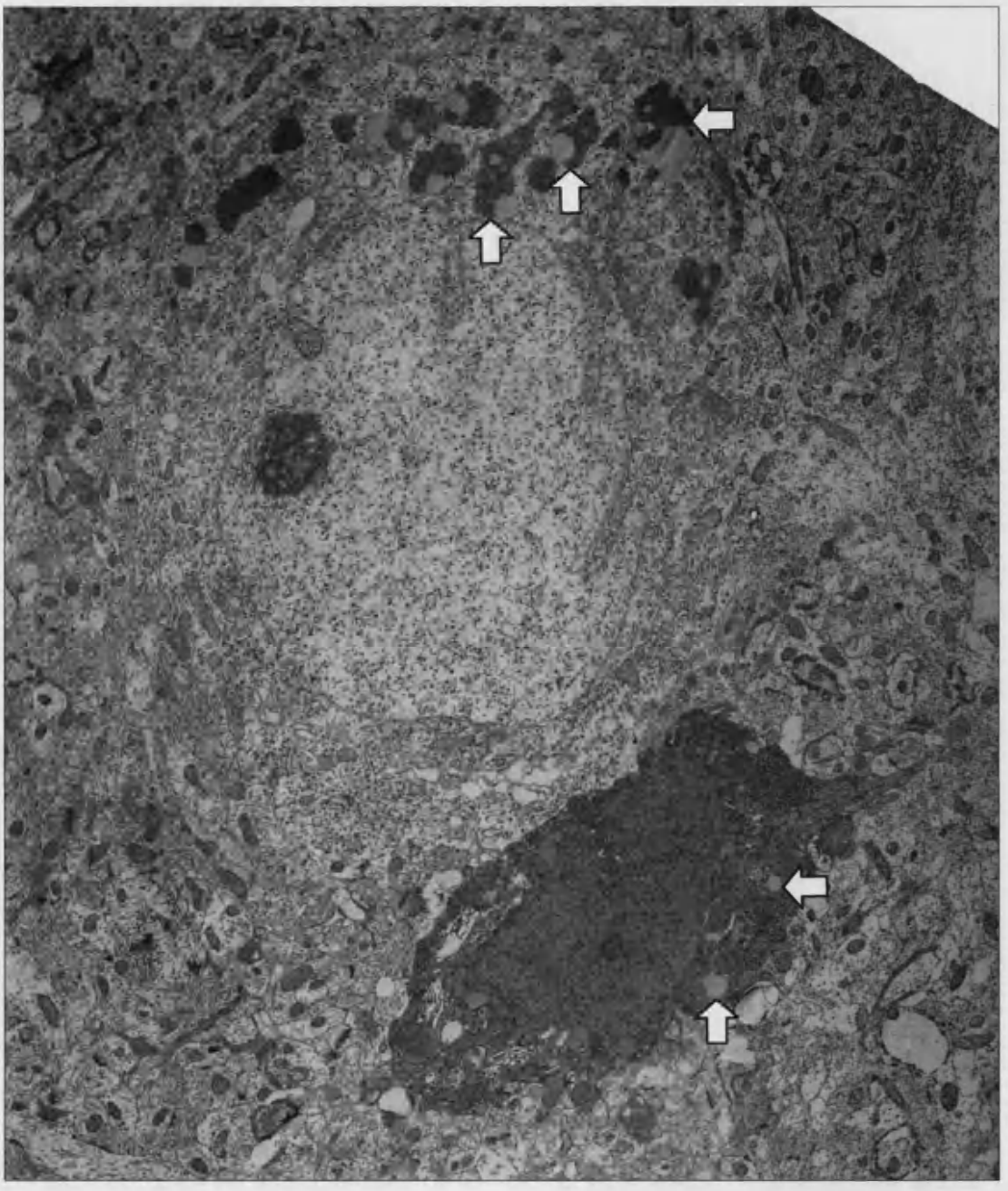

Figure 131 Degenerating neurons in the striatum of a 28 month-old wild-type FVB mouse. Note the degree of condensation in the dark neuron. Also note the high levels of lipofuscin (arrows) in both dark and 'healthy' neurons.

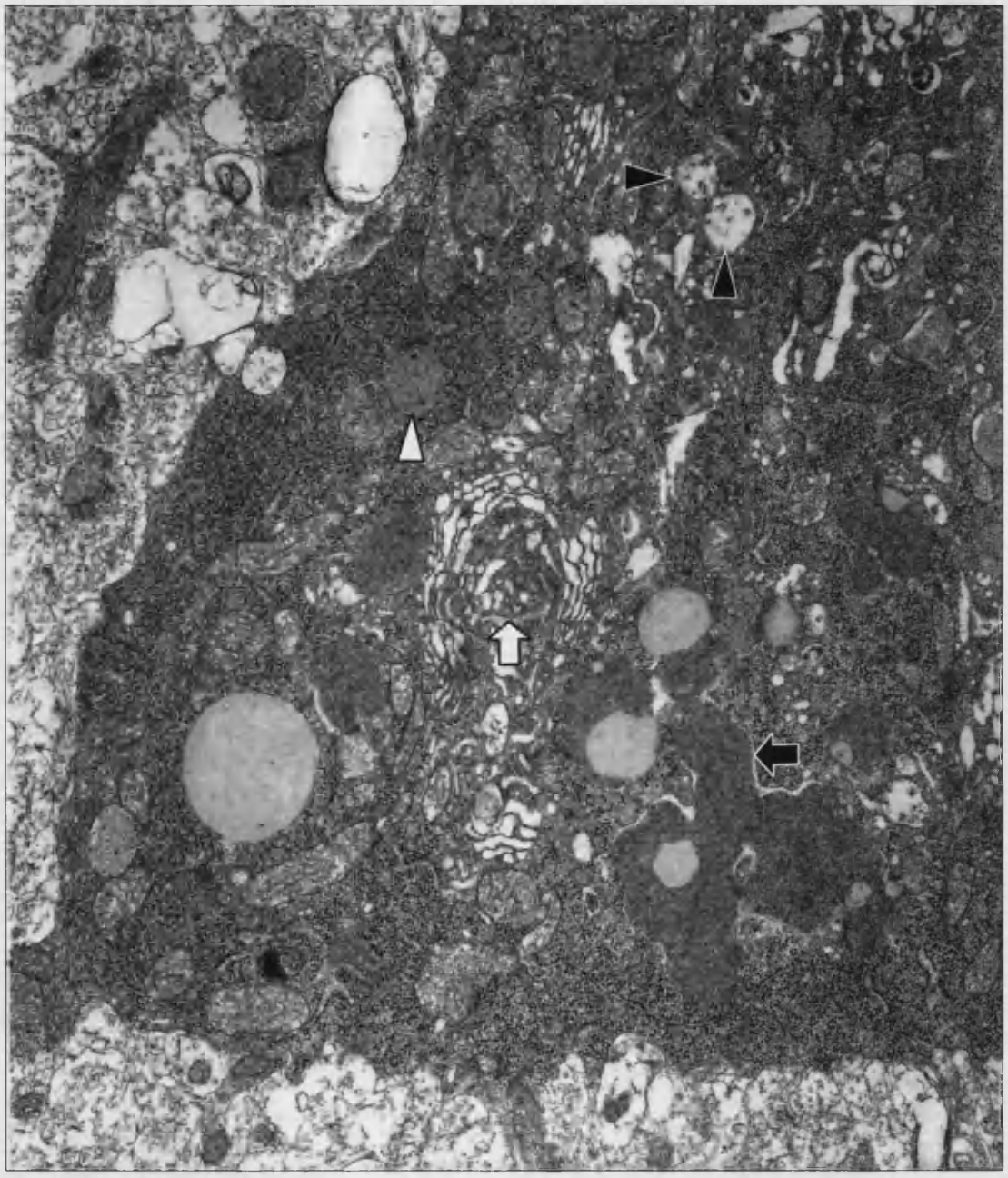

Figure 132 High-magnification electron micrograph of a degenerating neuron in the striatum of a 28 month-old wild-type FVB mouse. Widespread autophagy is evidenced by the presence of multivesicular bodies (solid arrowheads), mature lysosomes (open arrowheads), dilation and vacuolation of the ER/Golgi (open arrow), and accumulation of lipofuscin (solid arrow).

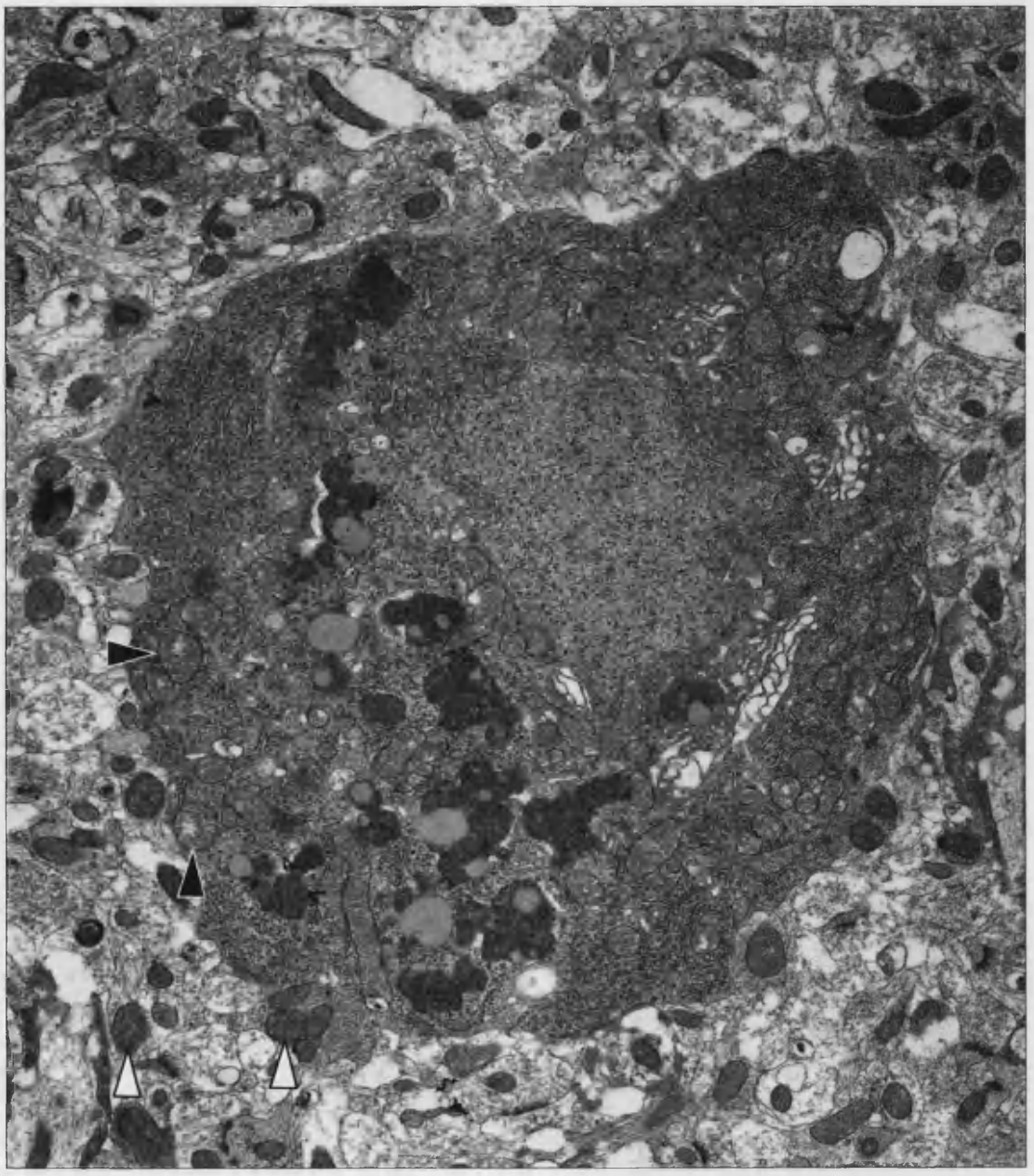

Figure 133 Electron micrograph of a degenerating neuron in the striatum of a 28 month-old wild-type FVB mouse. Concomitant with widespread autophagy, mitochondria appear dilated (solid arrowheads) – most noticeable on comparison to mitochondria in the neuropil (open arrowheads).

of mice that have been made available to me, make a quantitative analysis on levels of degeneration difficult. It appears that there is no difference whether the *Hdh* mutation is expressed on a black 6 or FVB genetic background, but this is based on qualitative observation alone. Given that the younger wild-type FVB shows comparable pathologic change, it may be that the FVB is indeed more susceptible, which could have implications for the observations of other mouse models.

3.2.6 The Biochemical Profile of Degeneration

Whilst there are no inclusions within the cortices of any of these mice, it is the cortex that shows the largest degree of degeneration. It is unlikely that this is due entirely to the disease these mice seek to model, although it does appear to modify the 'natural' degeneration seen. Whilst all areas of the brain have been analysed, the sections presented herein are from the mid-cingulate cortices of each of the mice. This area shows modification by expression of the expanded mouse huntingtin, in that the *Hdh* mice undergo greater degeneration in the cingulate that littermate controls, particularly the anterior cingulate, although this is unlikely to be a primary event. Nevertheless, by the mid-cingulate sections all mouse types show cells undergoing degeneration morphologically very similar to those seen in the R6/2 and striata of the *Hdh*, thus the molecular events underlying one should underlie the other.

Using the same antibodies used for similar studies on the R6/2 mice, the involvement of the apoptotic machinery in neurodegeneration was investigated. Positive controls were not sought as these antibodies have been shown to be successful in identifying apoptotic activation.

The results obtained were similar to those for the R6/2 degeneration. Each antibody produced identical staining patterns in each mouse type and in each area, whether or not degeneration had been shown to occur in the semi-thin analyses. Figures 134 to 139 illustrate the staining obtained with several antibodies for each mouse. I will not labour the observations as descriptions have been given for the R6/2 staining patterns. In short: once again, distinctive staining patterns are obtained for

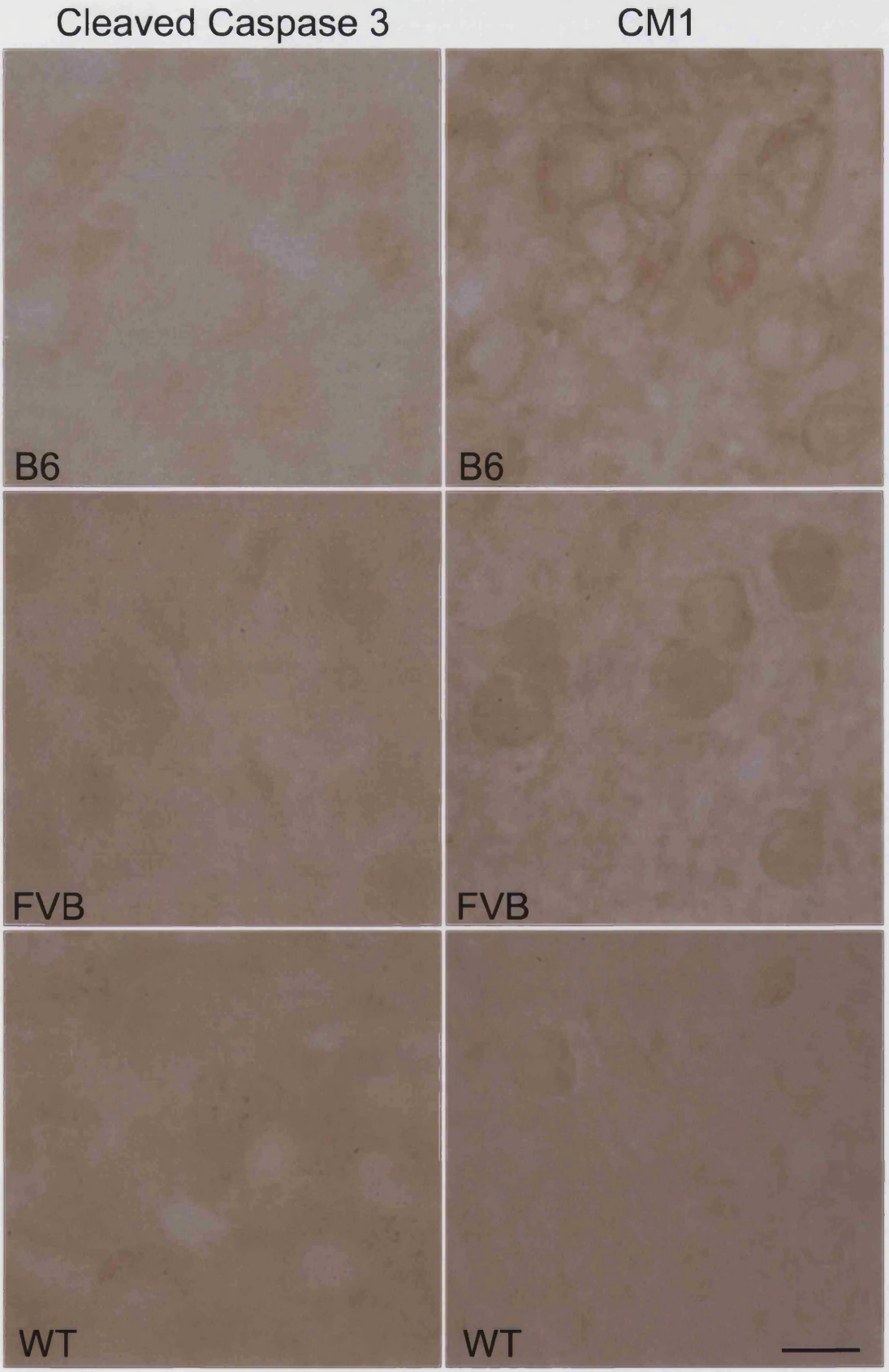

Figure 134 Sections from the anterior cingulate cortices of full-length *Hdh* black 6 (B6), FVB (FVB) and wild-type black 6 (WT) mice, each 29 months, 21 days' old, immunolabelled for activated caspase-3. Scale bar (~10μm) applies to all.

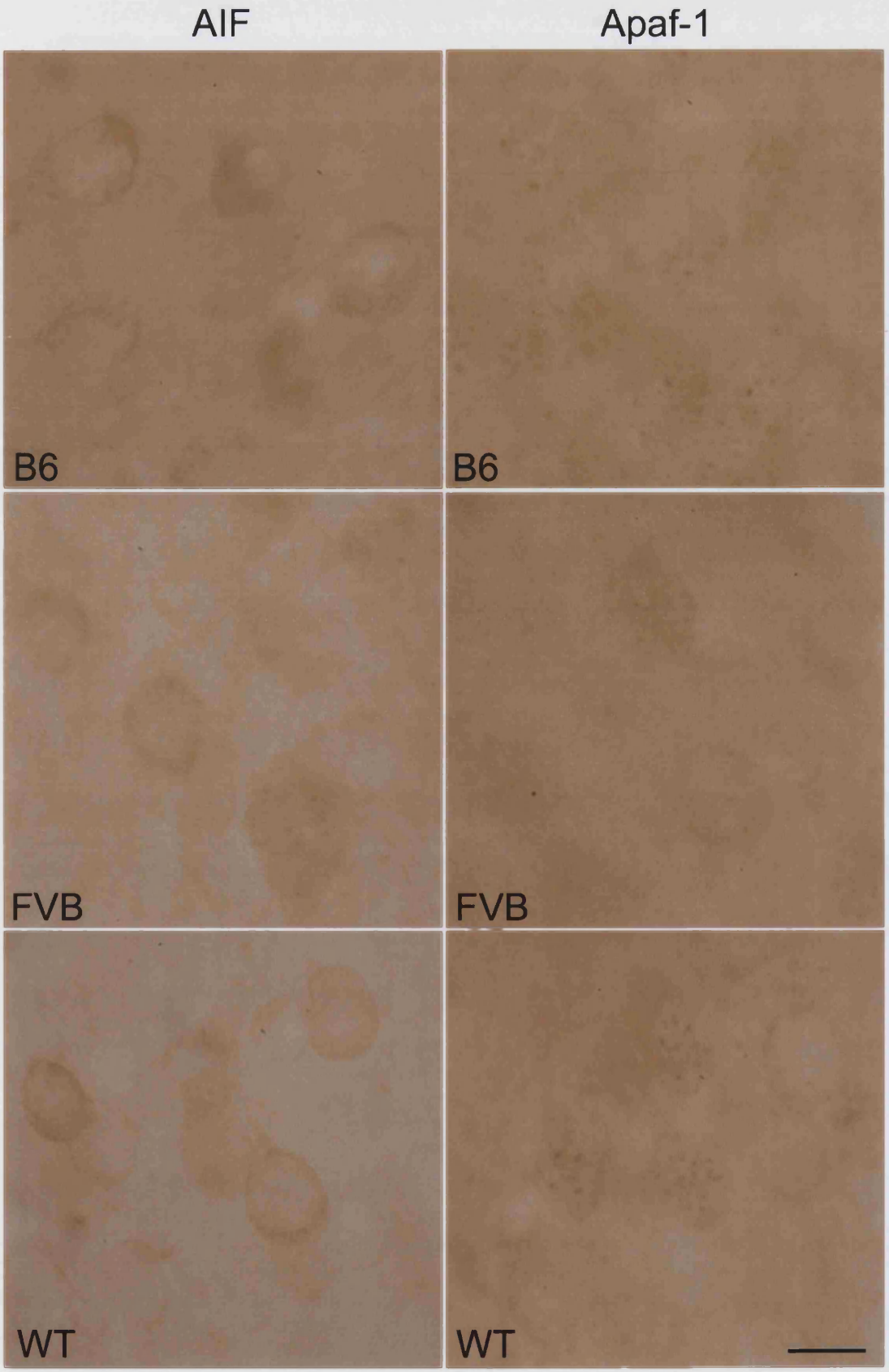

Figure 135 Sections from the anterior cingulate cortices of full-length *Hdh* black 6 (B6), FVB (FVB) and wild-type black 6 (WT) mice, each 29 months, 21 days' old, immunolabelled for AIF and Apaf-1. Scale bar (~10μm) applies to all.

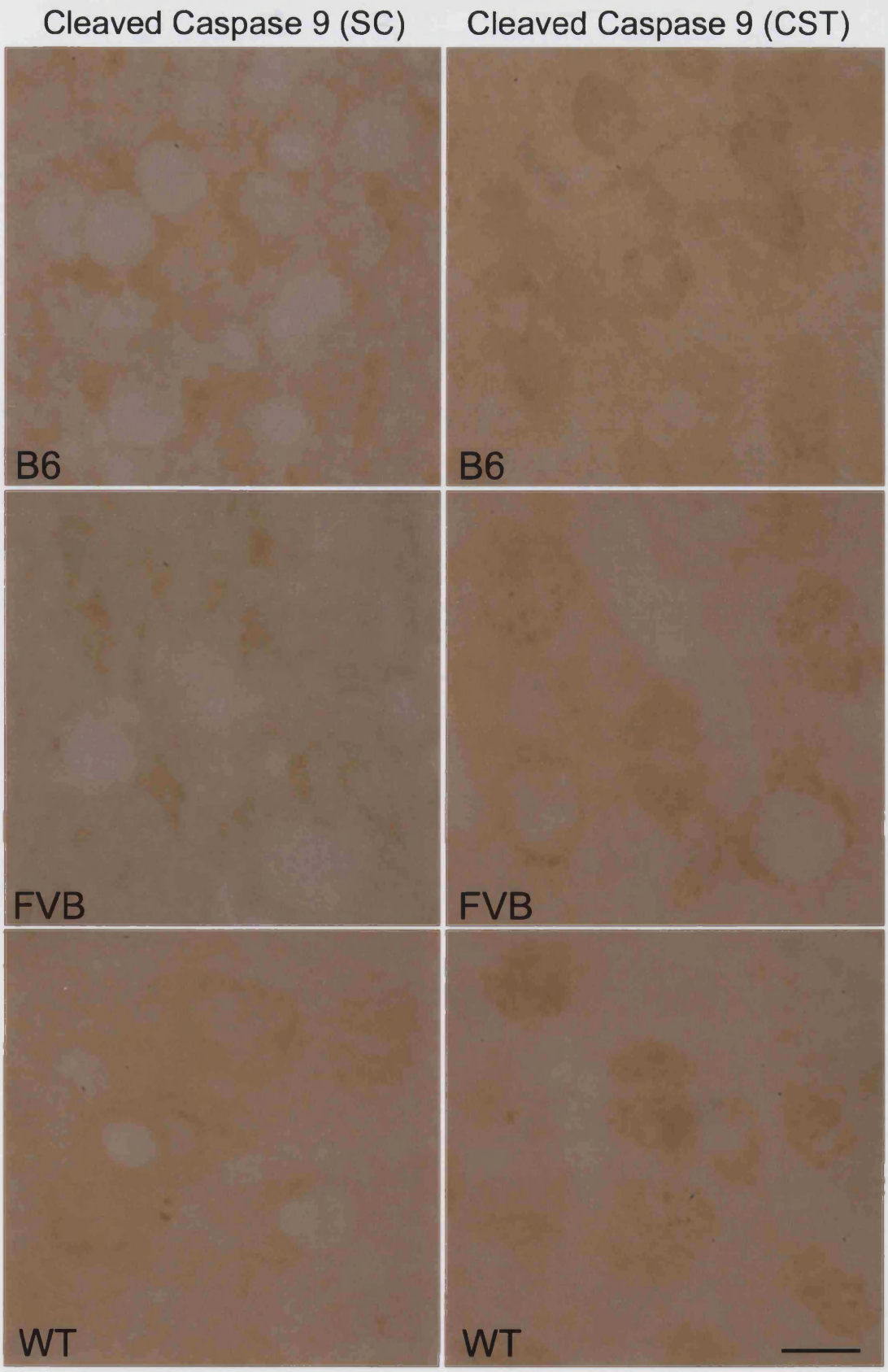

Figure 136 Sections from the anterior cingulate cortices of full-length *Hdh* black 6 (B6), FVB (FVB) and wild-type black 6 (WT) mice, each 29 months, 21 days' old, immunolabelled for activated caspase-9. Scale bar (~10μm) applies to all.

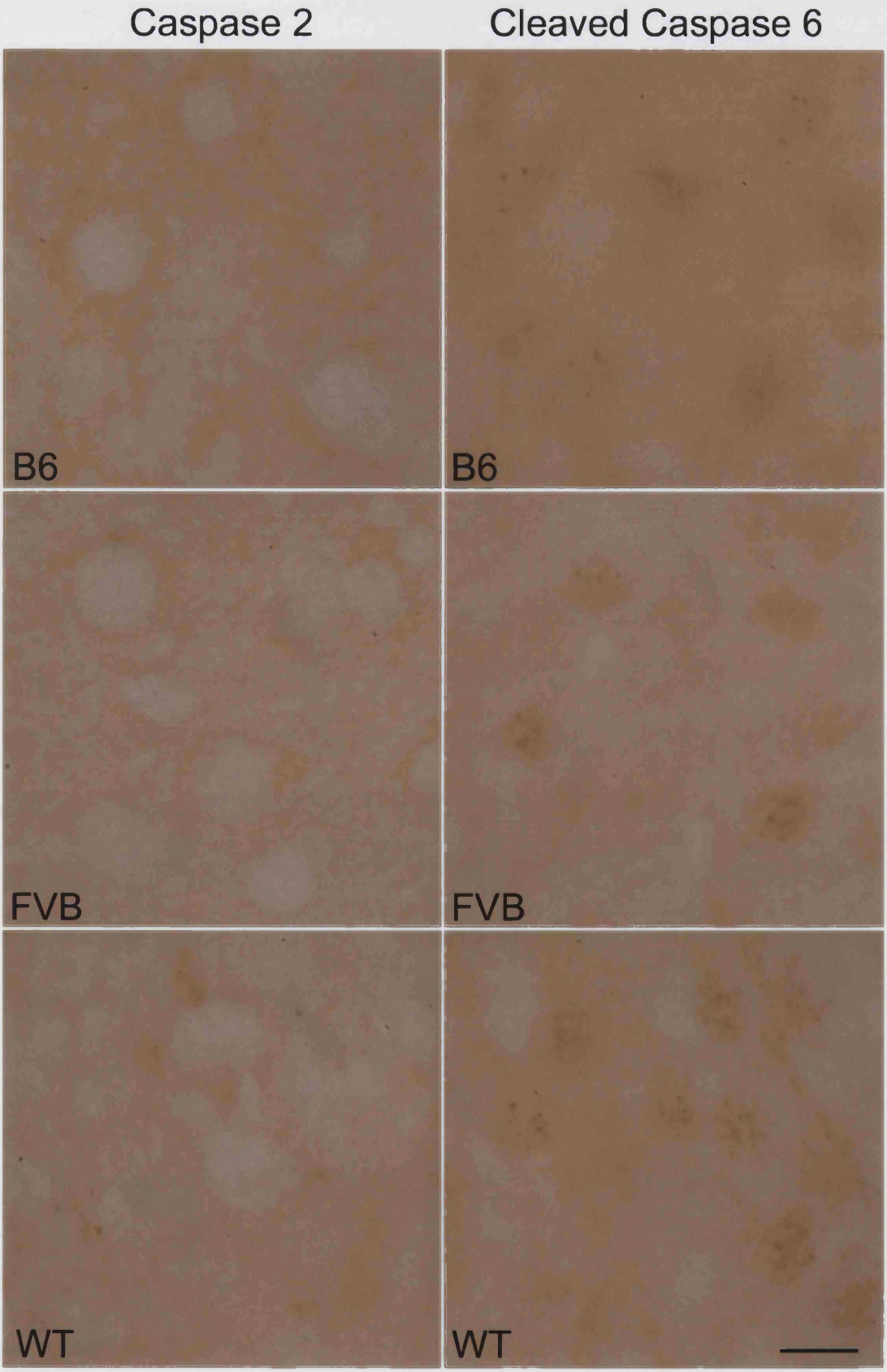

Figure 137 Sections from the ant. cingulate cortices of full-length *Hdh* black 6 (B6), FVB (FVB) & wild-type black 6 (WT) mice, each 29 months, 21 days' old, labelled for caspase-2 and cleaved caspase-6. Scale bar (~10μm) applies to all.

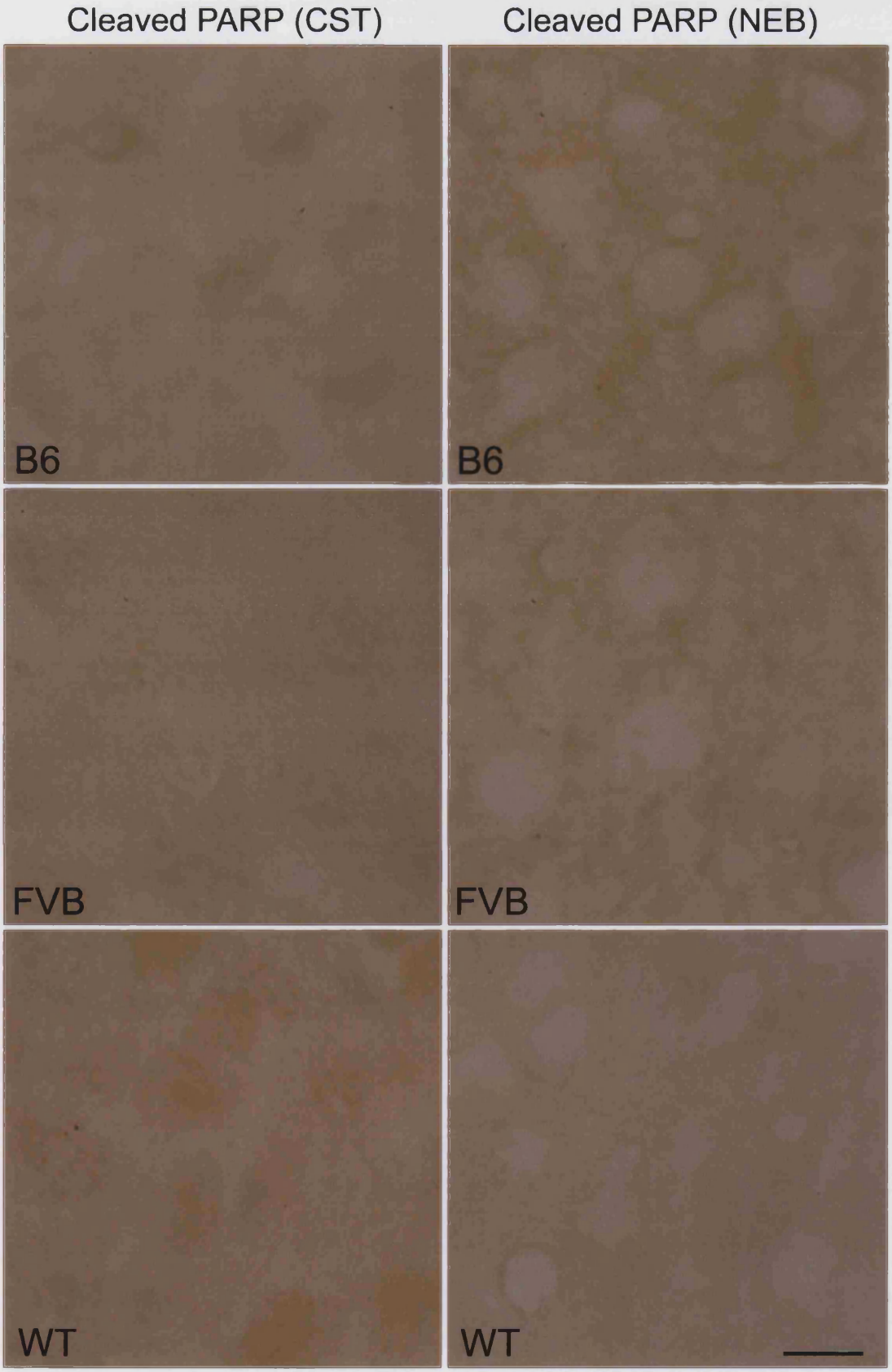

Figure 138 Sections from the anterior cingulate cortices of full-length *Hdh* black 6 (B6), FVB (FVB) and wild-type black 6 (WT) mice, each 29 months, 21 days' old, immunolabelled for cleaved PARP. Scale bar (~10μm) applies to all.

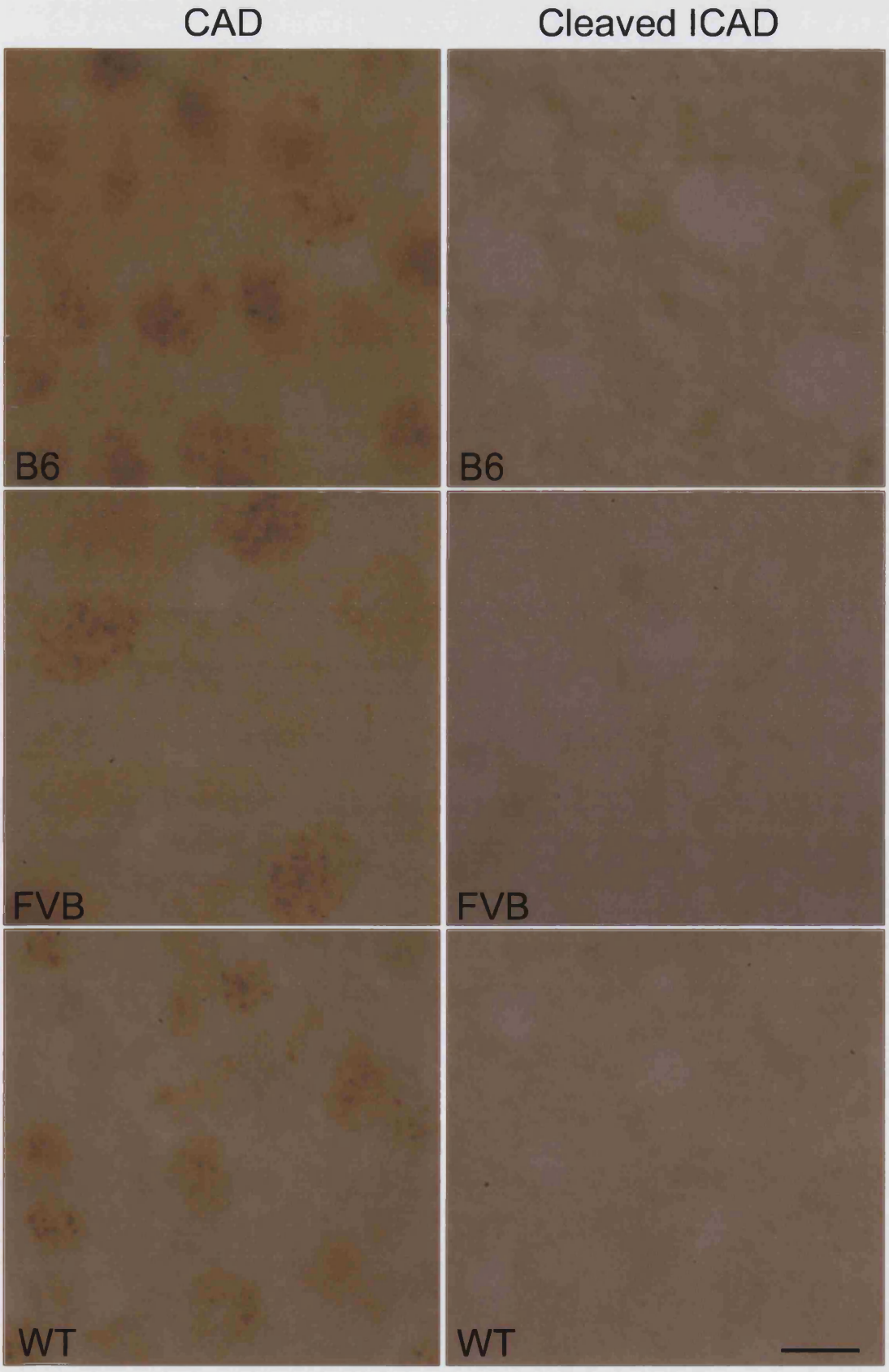

Figure 139 Sections from the anterior cingulate cortices of full-length *Hdh* black 6 (B6), FVB (FVB) and wild-type black 6 (WT) mice, each 29 months, 21 days' old, immunolabelled for CAD and cleaved ICAD. Scale bar (~10μm) applies to all.

some antibodies, and, interestingly, variation exists when different companies have made antibodies to the same protein. For example, figure 136 highlights the differences in staining pattern between the *Santa Cruz* antibody for activated caspase-9 and the *Cell Signalling Technologies* antibody for the same. However, importantly, the staining patterns are identical from mouse to mouse, including those obtained in the R6/2 analyses. Thus, as with the R6/2, it appears that the apoptotic machinery is not active in those cells undergoing dark cell degeneration.

Discussion

THE field of Huntington's disease research is fraught with numerous contradictory reports. There is also so much we still do not understand that it is difficult to draw conclusions about what factors underlie the disease process, and which may be therapeutic targets.

In order than I might explain my observations, and defend them in light of the wealth of evidence which appears to contradict my findings, I begin this chapter with a more detailed discussion on the evidence presented for the involvement of apoptosis and its factors in the pathology of Huntington's disease. I then introduce the process of autophagy and discuss the reports of its involvement in HD.

In light of these discussions, I evaluate my own results on degeneration in the HD models. I then discuss my observations of inclusions within the different models, and how these observations relate to the disease process and to the reports of others.

I am then left to summarise the hypotheses that may explain some of the questions that remain unanswered; most importantly, 'how does the accumulation of mutant huntingtin cause such a powerful phenotype?'

Finally, I summarise the other major mouse models of Huntington's disease and the differences between them; and evaluate the relevance of such models to the human disease they seek to replicate.

4.1 Apoptosis

4.1.1 From Factor to Fact

AN introduction to the basic biology of apoptosis has been presented in section *1.7*, together with a brief summary on why apoptosis is believed to underlie the degeneration in Huntington's disease in section *1.8*. Each paper that claims proof for apoptosis underlying the cell death of Huntington's disease often reports the involvement of one or two factors. It is surprising that so many make the leap from identifying the possible involvement of one factor to stating that apoptosis as a complex multifactor process is active and all-central to the disease process. Apoptosis is certainly a hot topic, hence the exponential increase in publications shown in figure 14, and as a result there seems to be a need for researchers to extrapolate beyond the bounds of logic such that they might add weight to their papers; as well as making them 'fashionable'.

Nevertheless, there is no consensus as to which molecular events define apoptosis. This in itself negates any logical debate on the topic. The original definition of apoptosis was based solely on morphological criteria (Kerr *et al.* 1972). Each biochemical action that has subsequently been identified has not been objectively weighted as a criterion and as such there can be no objective determination as to its level of importance when observed in other phenomena. There does appear to be a tacit agreement that those events that occur in the central arms of apoptosis, as opposed to the peripheral events, are more important. As described in *1.7* there are numerous inhibitors acting to suppress spontaneous activation of apoptotic cell death; as a result it is not unreasonable to ascribe more weight to those events further along the branches given that many 'checks' have to be passed before these stages can be reached.

There is one further point that is often missed in weighing up the importance of one's apoptotic observation, which is also at the very heart of the phenomenon: apoptosis is a self-propagating process. Some papers report effects that are, or can

be, merely secondary phenomena produced as a result of the activation by other apoptotic players; both through forward and back-propagation. Furthermore, one most also take into account that apoptosis seems to vary from cell type to cell type. The processes seen in cultured, transformed cells may not apply to fully differentiated adult neurons.

In light of these caveats the literature needs careful reviewing.

4.1.2 Caspases

The most powerful weapons in the apoptosis arsenal are the caspases and it is therefore these that have received the most attention in the studies on cell death.

The involvement of caspases in the disease process is suggested most directly by the observation that huntingtin is itself a substrate for cleavage by caspases (Goldberg *et al.* 1996). The relevance of this to the disease is not entirely clear. As described in *1.7* inactive caspases show mild activities, but in order for large-scale cleavage to occur the enzyme has to be active. For caspase-3 to be active, apoptosis probably has to be active. Cheryl Wellington has adapted her work into the *toxic fragment hypothesis* (see 1.6.3) based on two notions: that accumulation of the n-terminal fragement of mutant htt activates caspase, and that activated caspases cleave mutant htt (Wellington *et al.* 2000). This explains neither what underlies the initial cleavage events nor how the accumulation of mutant n-terminal htt causes caspase activation. The initial cleavage even may result from the low level of tonic activity in pro-caspases, but given the amount of accumulation seen *in vivo* before pathologic changes are evident, if, as the hypothesis suggests, accumulation of mutant htt activates caspase, such cells would no doubt have activated caspase contributing to further deposition. Work on mice has found caspase cleavage of huntingtin long before the onset of any signs of pathology (Wellington *et al.* 2002), bearing in mind the self-propagating nature of the caspase cascade, such a cell would not be devoid of pathological change for such an extended period. The same group has subsequently found evidence of caspase cleavage of huntingtin human tissue, of both expanded and

wild-type protein, but, importantly, in non-HD individuals as well as those with the disease (Kim *et al.* 2001). They reconcile this with earlier work by stating that whilst caspase cleavage of huntingtin is a normal event occurring even in non-HD individuals, in the case of disease patients such cleavage would generate the toxic fragment inducing further caspase activation. Subsequent work on mice has found caspase cleavage of huntingtin long before the onest of any disease symptoms (Wellington *et al.* 2002). This still leaves unanswered perhaps the most important factor in a model of apoptotic cell death in HD: how does accumulation of mutant htt activate caspases?

Caspase cleavage of mutant huntingtin may indeed contribute to accumulation of the protein, but only significantly once the cell is in its death throes. At this stage the importance of caspase cleavage of huntingtin to the disease process is negligible.

Caspases have been further implicated in the disease process through their detection in inclusions. One group reported the recruitment and subsequent activation of caspase-8 to aggregates in cultured neurons expressing GFP-tagged mutant ataxin 3 (Sanchez *et al.* 1999). Inhibition of caspase-8 with CrmA or the prevention of recruitment via the expression of a dominant-negative form of FADD (see 1.7.5) increased cell survival; as did expression of the construct in caspase-8-lacking Jurkat cells. To support a role for caspase-8 *in vivo* they report the finding of activated caspase-8 by western blot in tissue form affected areas in human HD patients. Within the report they state '...we provide *preliminary* evidence for the contribution of caspase-8 ... *in vivo*' (*ibid.*, italics added). Given the importance of such a finding in the human condition, it is probably of significance that they have not published anything further on caspase-8, nor have their results been replicated. Furthermore, they suggest activation of caspase-8 occurs by induced proximity (see 1.7.5). It has been demonstrated by a number of groups that the presence of inclusions rarely correlates with cell death (see 1.6.2), undermining their hypothesis that it is the aggregate that recruits and activates the caspase.

The activation of caspase-8 as a secondary phenomenon has been suggested to occur in the disease through the loss of binding of normal huntingtin to HIP1, as described in *1.6.4*. This work has been reproduced and seems reliable; free HIP1 contains a DED and is thus able to induce apoptosis. However, given the dominant

nature of the disease and the almost digital threshold for manifestation, I find it unlikely that this underlies cell death. The loss of HIP1-huntingtin association occurs proportionally to polyQ length, there is no sudden loss of binding. Furthermore, it has long been established that there is no greater severity of disease in homozygotes, if liberation of HIP1 is the cause of cell death one would expect homozygotes to show twice as much death. The greater number of free DEDs in the form of HIP1 in HD patients may increase susceptibility to apoptosis contributing in some form to the death seen in the human disease, but I do not believe it is the underlying cause.

The addition of caspase inhibitors to other model systems has also been cited in support of their involvement in the disease process. By overexpressing wild-type or mutant huntingtin in clonal striatal cells Kim *et al.* (1999) found cell death induced by either, but to a greater degree in those expressing mutant huntingtin. The addition of the caspase-1 and caspase-3 inhibitor Z-VAD-FMK increased cell survival. The addition of Z-DEVD-FMK, which inhibits only caspase-3, did not affect survival. This implies that caspase-1 is involved in the disease process. In support of this *in vivo*, the crossing of R6/2 mice with dominant negative caspase-1 mutants delays the onest of motor symptoms and prolongs mouse survival (Ona *et al.* 1999). It is suggested that the presence of intranuclear huntingtin increases expression of caspase-1 leading to its activation (Li *et al.* 2000). The administration of minocycline, which inhibits both caspase-1 and caspase-3, has been found to prolong the life of R6/2 mice (Chen *et al.* 2000). In contrast, the work of Ivelisse Sanchez cited previously suggests that caspase-1 is not involved. CrmA was used to inhibit caspase-8, but at similar concentration it is also an inhibitor of caspase-1 (Zhou *et al.* 1997). Thus, to support her suggestion that caspase-8 is the crucial factor she also expressed mutant ataxin-3 in caspase 1-negative cells. She reports no effect on toxicity of the Q79 expression (Sanchez *et al.* 1999), contradicting the reports implicating caspase-1 as a crucial player. Interestingly, she also found no effect in MCF7 cells, which do not possess the caspase-3 (Janicke *et al.* 1998), thereby casting doubt on the second target of minocycline.

4.1.3 Life in the Balance

The Wellington study mentioned in the previous section documented reduced toxicity in cells transfected with the caspase-resistant huntingtin, implying that caspase cleavage of huntingtin generates fragments which accumulate and induce apoptotic cell death (Wellington *et al.* 2000). However, the expression of mutant huntingtin alone was not sufficient to induce measurable levels of cell death; rather, all cultures were exposed to tamoxifen, a known inducer of apoptosis, and cells containing caspase-cleaved huntingtin were more affected. This is an important feature in many of the studies on the toxicity of huntingtin. Often studies that show increased apoptosis in a system actually show increased *sensitivity* to external induction of apoptosis.

As should be evident from section *1.7* there are a plethora of interacting proteins regulating apoptosis. In other words, there are continual pressures in each direction; a delicate balance between pro-life and pro-death drives. In each cell type, in each stage of its life, these drives may be differently weighted. For example, to demonstrate the efficacy of the antibodies used in the work for this thesis, x-irradiation was used to induce apoptosis in recently divided cells; utilising the fact that cells still in the cell cycle are more likely to initiate apoptosis in response to damaging stimuli. If proximity to the cell cycle directly affects the weighting of a cell's life and death drives, then one is also forced to question the validity of work comparing adult neurons to cultured cells, many of which are used precisely because they are permanently in the cell cycle. Mutant huntingtin may indeed act as a mild pro-apoptotic stimulus, but this appears to be countered by the cells many anti-apoptotic factors. Tipping the balance in favour of death, physically, chemically or even as a course of aging, will have varying results depending on the affected cell and the strength of its anti-apoptotic drives.

The concept I describe as a balance of drives, tipped towards death by mutant huntingtin, led some groups to examine the incidence of cancers among HD patients. If huntingtin predisposes cells to apoptosis, there should be fewer cases than among otherwise healthy individuals. The results have confused the issue further. One group reported a lower incidence of cancers of most major tissues in Danish HD patients

(Sorensen and Fenger 1992; Sorensen *et al.* 1999) whilst others have suggested increased cases of cancers (Ferluga 1989). Further support for increased pro-apoptotic weighting comes from another study that showed increased susceptibility in HD patient-derived lymphocytes to apoptosis induced by UVB-irradiation (Jakab *et al.* 2001).

The HD mutation may increase susceptibility to the induction of apoptosis by other harmful stimuli, but in such cases cell death is largely dependent on the nature of the toxic stimulus, not its accomplice.

4.1.4 Studying Cell Death

The brief review presented here shows how the field of cell death in the polyglutamine diseases is full of contradictory evidence. Some studies report one factor active in the death process, others will report that the same factor has no effect at all; as illustrated by the work on caspase-1. The majority of these conflicting studies use a variety of models and constructs, and it is my belief that this is the source of the confusion.

Further confusion has arisen due the ever-present desire to ascribe a name to an event. As mentioned, we have no biochemical definition of what apoptosis is, and yet many will apply the term to events which posses an active element of the process. Caspases are the central executioners of the apoptotic death programme, and the presence of any activated caspase seems sufficient for some to apply the term apoptosis; yet caspases have also been shown to be involved in 'house-keeping' activities such as altering synaptic plasticity (Chan and Mattson 1999).

Increasingly, it is becoming clear that there are many variations on the theme of cell death. *Abortosis*, *aposklesis*, *paraptosis* and *dark cell degeneration* all stem from different reports of non-apoptotic, non-necrotic cell death (see Graeber and Moran (2002) *for review*). Whilst these neologisms have yet to become defined commonplace terms, they are indicative of a field that is not 'black and white'. In spite

of this, Robert M. Friedlander, head of the Neuroapoptosis Laboratory, Harvard Medical School, opens his 2003 review of apoptosis in neurodegenerative disease with *'Cell death occurs by necrosis or apoptosis'*.

As mentioned previously, the nature of some cells may negate some of the conclusions drawn; cells closer to the cell cycle are more sensitive to harmful stimuli. Furthermore, the mode of cell death may depend on cell type. As an extreme example, human erythrocytes, which do not contain a nucleus, do not undergo apoptosis when stimulated to do so (Weil *et al.* 1996). Mouse sperm and chicken erythrocytes do contain a nucleus, but it is transcriptionally inactive. In these cells – the former of which dies spontaneously in culture, the latter induced – the death process does not appear to involve caspases (Weil *et al.* 1998). Whilst this may be due to a protein synthesis requirement for apoptosis to occur, it also suggests discrete cell death can occur in the complete absence of caspase activation. It also highlights the importance of cell type in studying cell death. Furthermore, whilst the study found no caspase activation in mature erythrocytes, activated caspases were occasionally detectable in immature erythrocytes; highlighting also the importance of the developmental maturity of the cell.

There is also the need for careful control when conducting cell culture experiments. The degree of interventional control over the experimental process, the main advantage of such work, permits the careful adjusting of conditions, but may lead to misleading results and conclusions. For example, Hackam *et al.* (1998) found that expression of wild-type huntingtin N-terminus also reduces cell viability. Likewise, Kim *et al.* (1999) report clonal striatal cells with apoptotic morphology even in control cells expressing only wild-type huntingtin. Experimental conditions may thus end up showing a stark contrast between mutant and wild-type huntingtin purely due to the nature of the experimental set up. Cell culture experiments must therefore be conducted carefully, and the relevance to the clinical situation closely monitored. A situation also true of other *in vitro* work. The work of Bucciantini *et al.* (2002) suggests that 'any' protein can form amyloid-like fibres, however, the conditions required to induce such fibrilisation are often markedly unphysiological. Rather than proving proteins readily forms such fibres *in vivo*, I rather believe it proves this unlikely.

4.2 Autophagy

4.2.1 Degradation of Cell Contents

WITHIN a cell the balance between formation and degradation of proteins and organelles has to be tightly maintained. This balance must also be alterable, to respond to demands of growth and development. There exist two broad categories of process by which this occurs, *lysosomal* and *non-lysosomal*.

The non-lysosomal process has been described in section *1.5.2*: the ubiquitin-proteasome system (UPS). To reiterate: this involves the highly selective tagging of target proteins with ubiquitin, followed by controlled hydrolysis via the proteasome. The UPS has long been implicated in the Huntington's disease process; its components co-localising with the NII, suggesting an attempt by the cell to specifically degrade the abnormal huntingtin. Indeed, given the accumulations seen in HD are of the N-terminal region alone, one may assume that the UPS successfully degrades the C-terminal portion. However, there is increasing evidence for involvement of the second process: lysosomal degradation or *autophagy*.

The lysosomal processes are most noted for their degradation of extracellular proteins via endocytosis or pinocytosis. Extracellular contents are taken-up into isolated endosomes, which are then targeted by lysosomes, which in turn release an array of hydrolases into the endosome. Likewise, as mentioned in *1.7.8*, phagocytes degrade ingested apoptotic bodies by fusing lysosomes with phagosomes, resulting in degradation of the entire phagosome content. In this way, the lysosomal processes act on a wide range of targets, degrading them in a bulk fashion. However, the action of the lysosome is not limited to the contents of the endosome. Rather, the lysosome acts also to degrade 'self' components. Indeed, lysosomal degradation is the sole means of turnover of whole organelles such as the mitochondria. This degradation of the cell's own contents is known as *autophagy*.

4.2.2 Autophagy

Autophagy is further divided into three processes: *macroautophagy, microautophagy* and *chaperone-mediated autophagy.*

Macroautophagy is the major inducible form of autophagy. It is a highly conserved mechanism involved in the bulk turnover of cell components. It was first described as a response to starvation, as one of the primary functions of autophagy is to produce free amino acids from the breakdown of non-essential proteins when amino acid levels fall (Mortimore and Poso 1986). It is also regulated by a large number of factors linked to nutrition and growth, including glucagon (Hopgood *et al.* 1980), insulin (Blommaart *et al.* 1997) and growth factors (Ballard *et al.* 1980) via a number of second messengers (Codogno *et al.* 1997). Further to this, macroautophagy also plays a role in the turnover of cell constituents under normal conditions. Generally, the two processes – starvation induced and normal turnover – are distinguished according to their associated vesicular bodies. Under starvation conditions, *autophagosomes* or *autophagic vacuoles* (AVs) are seen, which are between 8 and 200 times greater in volume than the *CVT* (cytosol to vacuole targeting) *vesicles* seen under conditions of normal turnover (Baba *et al.* 1997).

The first ultrastructural signs of macroautophagy appear as the sequestration of portions of the cytoplasm within double membrane-bound structures termed endosomes, autophagosomes or autophagic vacuoles. The nature of the autophagic vacuole varies greatly from species to species and from cell to cell. The majority of the work on autophagy has been conducted using yeast, and so the 'traditional' picture may, more or less, be limited to yeast cells. In mammals, whilst the traditional double membrane-bound autophagic vacuoles are seen, some cells also form multilamellar bodies. The source of the sequestering membrane remains under debate, but in mammalian cells it is believed to be the endoplasmic reticulum. Certainly, in this study autophagic activity is seen most frequently in areas of high ER/golgi density. Once the AV is fully formed, and its contents isolated from the cytosol, it docks and fuses with a lysosome – a process dependent on microtubule function. After fusion, the outer membrane of the AV is incorporated into the lysosomal membrane thereby releasing

a now single membrane-bound autophagic body into the lumen of the lysosome, which is readily broken down by the lysosomal hydrolases.

Microautophagy, active under basal conditions, involves the internalisation of cytosol directly into the lysosome. The situation is akin to that of endocytosis, in that invaginations form in the lysosomal membrane, which bud off into the lumen forming *multivesicular bodies* (Ahlberg *et al.* 1982; Dice *et al.* 1987). The process was initially thought to be non-selective, however there is now evidence to suggest that there is a preferential degradation of specific substrates (Luiken *et al.* 1992; Yokota *et al.* 1993; Yuan *et al.* 1997).

Substrate specificity is even more restricted in the third class: chaperone-mediated autophagy. This also occurs during periods of starvation, as a secondary response to macroautophagy, and involves the elimination of proteins possessing a particular amino acid sequence (KFERQ-related) (Dice *et al.* 1990). This sequence is recognised by the cytosolic form of the chaperone (see 1.5.1) *hsc73* (Terlecky and Dice 1993), which, on binding to the target sequence, is recognised by the lysosomal membrane receptor *lpg-96/lamp-2a* and the chaperone/protein complex is internalised (Cuervo and Dice 1996). Estimates suggest almost 30% of cytosolic proteins contain this sequence (or related); therefore a restricted but varied set of target proteins is degraded during starvation by chaperone-mediated autophagy (Dice 1992).

For detailed reviews of the molecular mechanisms underlying autophagy see Stromhaug & Klionsky (2001) and Reggiori & Klionsky (2002).

4.2.3 Autophagy and Cell Death

Lysosomal involvement was described in the seminal apoptosis paper, but the role was limited to the breakdown of phagocytosed apoptotic bodies (Kerr *et al.* 1972). It was long believed that autophagic cell death constituted a class of death programme distinct from that of apoptosis. There were many cases of cells being removed by

autophagy, most dramatically during insect metamorphosis, but also in vertebrates the process was shown to be a prominent feature of organ morphogenesis, the shaping of extremities and cavity formation (Beaulaton and Lockshin 1982; Schweichel and Merker 1973). As cells can be completely degraded by autophagy alone: autophagic cell death is a complete process that can act independently of apoptosis.

The features of autophagic cell death first appear in the cytoplasm with a degradation of its components resulting in a loss of electrondensity. The number of mitochondria declines, but those that remain appear to be structurally (and functionally) intact. The bulk of the cytoplasm is removed before the nucleus begins to collapse (Beaulaton and Lockshin 1982; Clarke 1990; Schweichel and Merker 1973). All steps of macroautophagy are ATP-dependent and require an intact cytoskeleton (and proper acidification) for vesicle transport (Blommaart *et al.* 1997; Klionsky and Emr 2000).

In terms on the machinery involved, a number of studies suggest that the death process can pass to completion independently of caspases (Borner and Monney 1999; Quignon *et al.* 1998). Given that most features one would define as 'classically apoptotic' are believed to be dependent on the action of caspases (Hengartner 2000), it is feasible that the molecular machinery of autophagic cell death remains completely distinct from that of apoptotic cell death.

However, several studies have reported considerable overlap between these two processes and it seems both can occur simultaneously, sharing much of the same molecular machinery and with interplay between these two different paths of cell death (Bursch 2001; Bursch *et al.* 2000a; Bursch *et al.* 2000b; Terwel and van de Berg 2000; Uchiyama 2001).

Opinion now is of a continuous spectrum between purely apoptotic cell death and purely autophagic cell death. Xue, Fletcher and Tolkovsky (Xue *et al.* 1999) studied the effects of apoptotic stimuli on cultured sympathetic neurons; they found that withdrawal of NGF from the growth medium, traditionally used to induce apoptosis, produced autophagic morphology (autophagic vacuoles, organelle engulfment and membrane whorls), initially in the absence of any observable nuclear changes. As the cells persist in NGF-negative growth media (>16hr), nuclear

morphology begins to alter and apoptotic changes, including caspase-3 activation, begin to appear. This situation is also seen using apoptotic inducers, such as araC; also, the presence of autophagic profiles correlates with increased sensitivity to araC-induces apoptosis. Application of the caspase-inhibitor BAF does not eliminate the autophagic death pathway but does reduce autophagic activity slightly, suggesting that whilst autophagy can proceed in the absence of apoptotic activation, it is enhanced by it. Furthermore, both apoptotic and autophagic death can be blocked using the compound 3-MA; which is not a caspase inhibitor, rather it appears to act upstream of both caspase activation and autophagosome formation, suggesting a common activation mechanism for both pathways.

It appears, therefore, that autophagic activity can be triggered by apoptotic signals (probably due to a common signalling factor) and that autophagy directly affects the execution of apoptosis. When the two processes co-activate, the onset of autophagy appears to occur prior to the initiation of apoptosis. Whilst (Xue *et al.* 1999) suggest that autophagic activity promotes apoptosis, another study on HT-29 cells found increased sensitivity to apoptosis following 3-MA treatment, which would suggest that autophagy delays the onset of apoptosis, perhaps by isolating mitochondria which would otherwise release cytochrome c into the cytosol (Bauvy *et al.* 2001).

The current view of the relationship between autophagy and apoptosis is illustrated in figure 140. In summary, autophagy appears before apoptosis; whether autophagy feeds forward into apoptosis or whether it is an attempt by the cell to prevent premature committal to death remains under debate. The amount of autophagic activity I have documented in this thesis, combined with an apparent lack of apoptotic activity, seems to suggest that autophagy does not feed forward into apoptosis. It is more likely that it delays (perhaps indefinitely) activation of apoptosis. Certainly, apoptosis appears to enhance autophagy in those cells in which it is seen. Given that that purpose of apoptosis is a 'tidy deconstruction' of the cell ready for phagocytosis, the advantages of an autophagic component to apoptotic cell death are obvious. One conclusion is becoming increasing clear: in contrast to earlier views, the two traditional processes of apoptotic and autophagic cell death are not distinct;

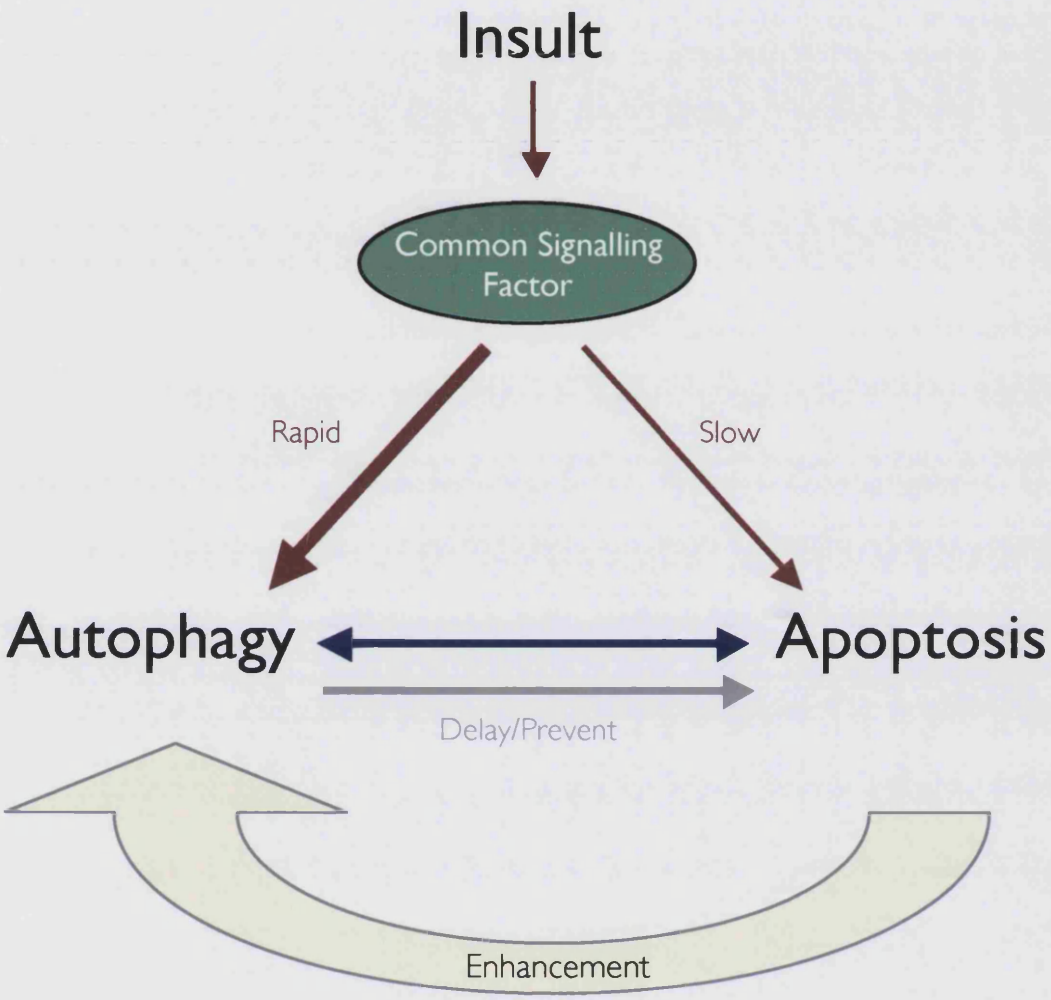

Figure 140 The relationship between autophagy and apoptosis. Each is stimulated in the face of sufficient insult, probably through the action of a common signalling factor. The activation of autophagy normally precedes the activation of apoptosis, and, depending on the strength of the insult, can prevent the activation of apoptosis. However, once apoptosis is active, it enhances autophagic activity.

though neither absolutely requires the other, they often occur in the same dying cell and appear to share some component of upstream signalling.

4.2.4 Autophagy and Huntingtin

Autophagy has been implicated in Huntington's disease as mutant huntingtin is seen to accumulate in lysosomal structures. (Sapp *et al.* 1997), documented a granular appearance of mutant huntingtin within the cytoplasm of HD neurons. When viewed at the electron microscope level these structures corresponded to multivesicular bodies. Subsequent work on cultured striatal cells has shown that mutant huntingtin accumulates in autophagosomes which internalise the lysosomal proteinase, cathepsin D in proportion to polyglutamine length, suggesting an active response by the cell, proportional to the size of the insult, to degrade the accumulating huntingtin (Kegel *et al.* 2000). Furthermore, this work has also shown that activation of the endosome-lysosome system affects the structure of the golgi, endoplasmic reticulum and mitochondria; a situation mirrored in this work in the *Hdh* and, to a lesser extent, the R6/2 mice.

It has since been demonstrated that lysosomal processing is able to successfully degrade mutant huntingtin. Following transfection of COS-7 cells with EGFP-tagged huntingtin exon 1, Ravikumar *et al.* (2002) monitored aggregate formation. In the presence of the autophagic inhibitors 3-MA (inhibiting sequestration) or BafA1 (preventing autophagosome-lysosome fusion) aggregates were more frequent and larger. Conversely, addition of the autophagy-inducer *Rapamycin* increased clearance of expanded huntingtin, resulting in fewer, smaller aggregates.

Interestingly, it has been suggested that the autophagic response of striatal neurons underlies the specificity in HD. Petersen *et al.* (2001) found no difference between survival rates of dissociated striatal neurons from wild-type and R6/2 mice. However, a single exposure to high concentrations of dopamine had a greater effect

on neurons form the transgenic animals[6]; namely the formation of structures associated with autophagy. Hence, they suggest that the presence of mutant huntingtin, together with high levels of dopamine in the striatum underlies HD regional specificity.

Superficial evidence for autophagy in the human condition has been provided by Mantle *et al.* (1995) who demonstrate an increase in the activity of the lysosomal proteinases dipeptidyl aminopeptidase II, cathepsin H and cathepsin D in sample from HD postmortem tissue.

[6] A further example of increased sensitivity to toxic stimuli, rather than an inherent toxic effect, as discussed in *4.1*

4.3 Dark Cell Degeneration

4.3.1 Apoptosis in the R6/2

IN light of these reports, the observations of this thesis must now be evaluated. I have confirmed the presence of neurons undergoing dark cell degeneration in the R6/2 mouse model. As discussed previously, there are many reports of the activation of apoptotic components in model systems, particular attention being placed on the activation of caspases. In spite of this wealth of data, I have found no evidence of activation of caspases in the R6/2. In areas known to contain dark degenerating neurons, immunohistochemistry labels cells no differently to healthy littermate control tissue. I have sought labelling for a variety of caspases, however for some, antibodies that exclusively label the activated form of the protein are not available. Given the apparent evidence for the involvement of caspase-1 in huntingtin-mediated cell death, this forced me to analyse its involvement via western blotting. However the self-propagating nature of the apoptosis machinery should mean that one should not have to study each and every caspase in order to establish an apoptotic mode of cell death. My work on the x-irradiated animals clearly shows that when apoptosis is active, not only can my methods detect it, but also that more than one marker labels the process. If I have been unable to detect caspase-3 activation, with more than one antibody, in the degenerating neurons of the R6/2 mouse, then one would not expect to see PARP cleavage and TUNEL, as is indeed the case. Thus, from my extensive, though not complete, study of the components of apoptosis in areas of known dark cell degeneration, I can reasonably conclude than that the molecular machinery of apoptosis is not active in dark neurons.

Furthermore, my thorough analyses at the level of the electron microscope reveal that dark degenerating neurons possess a unique, and consistent, ultrastructural morphology that does not resemble that of reported apoptosis. I have also used

electron microscopy to study early postnatal mouse brain and have successfully located dying cells, which do resemble the 'classical picture' of apoptosis. Thus, my ultrastructural methods are also capable of preserving the appearance of apoptotic cells; and I can easily recognise them as such.

This yields further consistency to my results. Within the same areas, of the same mouse model, I have shown the clear presence of dark degenerating cells, which do not possess an apoptotic ultrastructural morphology, and do not contain active elements of the apoptotic machinery.

Further support for a lack of apoptosis is provided by a lack of astrocytic response. Immunolabelling glia can produce highly variable, and thus unreliable, results when viewed using light microscopy. Therefore, I did not attempt to quantify astrocytes. However, as electron microscopy work has revealed glial cells often in contact with degenerating neurons I attempted to identify these cells using immunofluorescence and confocal microscopy. Whilst degenerating cells are detectable from their pyknotic appearance when stained with the nucleic acid dye DAPI, the GFAP-positive glia do not associate with such cells. There does appear to be an increased density of glia with oligodendrocyte morphology, but the significance of this is unclear. Certainly, the glial response seen during apoptosis within a neuronal cell population is not replicated in the R6/2 mice, in spite of the significant levels of degeneration.

How then to reconcile this with the observations of others? I have already questioned the transferring of observations from cultured cells onto adult neurons. My EM analysis of neonatal mice, and immunocytochemical analyses of x-irradiated pups, supports this criticism. The affected cells in each case are in close proximity to the cell cycle and show apoptosis as means of cell death. Just as x-irradiation of adult neurons proves to be a weak apoptotic stimulus, so too, huntingtin may be more likely to induce cell death in a recently divided cell in culture. Whilst these studies provide important insights into the disease, I do not believe the conclusions drawn about toxicity and cell death can be accurately projected onto the situation *in vivo*.

If one limits one's criteria for evidence to the R6/2 mouse model, the only consistently implicated factor is caspase-1. Yet, when analysed more carefully, even

this evidence proves to be flawed. In their original description of the involvement of caspase-1 in Huntington's disease, Ona *et al.* (1999) show clear improvements of phenotype when crossing the R6/2 with a caspase-1 dominant negative mouse (as described in *4.1*). Yet, crossing the R6/2 onto another background may be sufficient to reduce phenotype severity. However, the involvement of caspase-1 is further supported by the use of caspase-1 inhibitors, including minocycline. This suggests that caspase-1 inhibition does indeed improve overt phenotype, but does not prove caspase-1 activation *in vivo*, and proves the existence of apoptotic cell death even less so.

Caspase-1 activation is not shown directly in the original paper (Ona *et al.* 1999); rather, levels of converted interleukin-1ß (IL-1ß) are measured. Increases in mature IL-1ß do indeed seem to correlate with phenotype, and caspase-1 inhibition does lessen this increase, but this still fails to show direct evidence for caspase-1 activation. In subsequent work, evaluating minocycline, IL-1ß conversion is once again used a measure, but mRNA levels are also measured, and western blots performed. The results show an increase in expression of both caspase-1 and caspase-3 in the R6/2 (negated by the action of minocycline); and the generation of caspase-1 and -3 fragments of the correct molecular weight for the cleaved enzymes (Chen *et al.*, 2000). As this is the strongest evidence I sought to repeat it.

Having used antibodies to cleaved caspase-3 in my extensive immunohistochemical studies, I attempted to replicate the caspase-1 western blots. A sample blot is presented in figure 78. I consistently found the presence of the zymogen and, in the cortex, other precursor forms, but failed to find a band corresponding to the active caspase (~20kDa). This is at odds with the results of the Friedlander group. As the protein is not confined to a single, comparable band, it is not possible to accurately quantify the levels of protein; but there may be an indication of increased levels of caspase-1 in the cortex of the R6/2 mouse. If so, weight is added to the evidence of increased caspase-1 expression, but this appears to remain in the form of the inactive precursor. Whilst the area between 15 and 30 kDa appears to be clear of protein in my caspase-1 western blots, I cannot ignore the possibility that the levels of the active protein from degenerating neurons are so

dramatically lower than those of the precursors from surrounding healthy cells – which are the vast majority – that the technique would not detect them. This is why immunohistochemistry has been my weapon of choice. I have shown in my toludine blue-stained semi-thin sections that degenerating neurons in the R6/2 are relatively few and rather isolated. Using immunohistochemistry I am able to detect apoptotic activation within a single cell of a population; should it be present. Therefore, given these limitations in using western blots, I am forced to doubt the Chen *et al.* (2000) results further. The published western blot proving caspase-1 activation shows not single bands as my results do, but a 'smear' of labelled protein between the 50 and 20kDa marks. There is a break somewhere around 30kDa, but are we to assume that everything above this is the inactive form and everything below cleaved caspase-1? I have shown that the different forms of caspase-1 are easily resolvable using this technique. Further, the antibodies used by Chen *et al.* are identical to those I have used to produce clean bands from R6/2 lysates. Also, the published blot seems to indicate comparable levels of precursor and active protein (though quantification is even more difficult here as a result of the large spread of protein). Given the frequency of degenerating neurons in the R6/2 I have shown in *3.1.3*, I find it unlikely that the levels of activated caspase-1 in those cells equal levels of precursor caspase-1 in all healthy neurons and glia.

I believe the evidence for apoptotic cell death in the R6/2 model is inconclusive. The techniques I have used here allow the direct comparison of cell morphology to immunohistochemical data. Within a defined area I can easily locate degenerating neurons. I have also shown that my techniques are capable of detecting the cleavage of apoptotic proteins when it occurs; even in single cells, and yet I can find no evidence for such activation in cells known to be degenerating. Logically, it is infinitely more difficult to prove that something does not occur than to prove it does. But I believe the evidence I have presented here strongly suggests that dark cell degeneration does not involved the activation of the apoptotic machinery

4.3.2 The Nature of the Dark Neuron

One is therefore left to question the nature of the degeneration. It appears that even those cells in the most advanced stage of degeneration in the R6/2 have not initiated apoptosis. Yet something must be causing the phenotype. Is it, therefore, the dark neuron? If so, what property causes the dysfunction. An insight into this is provided by my comparisons of the R6/2 model to the *Hdh* model.

The R6/2 mouse, most probably due to the repeat size, shows a more rapid progression and more severe disease. The severity of the neuronal dysfunction is such that it kills the mouse before the large-scale cell death seen in the human condition can occur. Conversely, the progression in *Hdh* mice is so slow that the mice die naturally before onset of large-scale neuronal dysfunction. However, the insult – expanded polyglutamine within huntingtin protein – is the same for each model; thus, they most likely undergo the same pathogenic changes, albeit at differing rates. Indeed, I have shown that the appearances of the dark cells in the R6/2s and *Hdh* mice are strikingly similar.

The greatest similarity between the ultrastructural changes seen in each of the mouse type is the evidence of autophagic activity. The formation of autophagic vacuoles, multivesicular bodies and accumulation of lysosomes are observed early among the ultrastructural changes. As discussed in *4.2*, such activity has long been implicated as a response to mutant huntingtin. There is work to suggest that autophagy is successfully able to remove mutant huntingtin, and thus the observed activity may indicate an attempt by the cell to remove accumulated huntingtin that cannot be degraded via the ubiquitin proteasome system. Such a response would explain why I have observed the activity before any other consistent ultrastructural changes. Autophagy may also bring about the alterations to Golgi bodies, endoplasmic reticulum and mitochondria also seen in both mouse models. Mutant huntingtin has been shown to induce such autophagic changes *in vitro*, and the R6/2 results presented here certainly suggest the same applies *in vivo*.

~

The most notable feature in each model is the condensation, which gives the dark neuron its eponymous feature. Such condensation must be an active process, and must become increasingly energy consuming. As the cell condenses, the osmotic potential difference between cell and neuropil increases. The condensation differs slightly between the two types of HD mice. In the R6/2 condensation of cytoplasm and nucleoplasm occur, as far as I can detect, simultaneously. Whereas the *Hdh* mice tend to show cytoplasmic condensation before nuclear changes are evident. This may be of significance to the disease process. I have shown that the *Hdh* possess relatively few inclusions, and even those cells that possess some form of structural inclusion at EM show that these inclusions are not as mature as those seen in the R6/2 mice. Furthermore, figure 122 suggests that the Cajal body does not relocate to the nuclear inclusion. In the R6/2 mice, such relocation is evident before marked condensation. The nucleoli of R6/2 neurons also tend to show greater variation from the normal appearance. Thus, there is an earlier involvement of the nucleus in the R6/2 model. The degenerative process as a whole may be led by the nucleus in the R6/2. It is feasible that these changes are indicative of what may be the most important difference between the two models.

As discussed in 4.5, the behavioural phenotype of HD and the R6/2 model is likely to arise not from neuronal degeneration *per se*, but from the interaction between accumulated mutant huntingtin and cellular components, most notably, nuclear components. I have demonstrated that the nuclear accumulation of huntingtin in the *Hdh* model is confined to far fewer cells than seen in the R6/2; the formation of inclusions even fewer. Thus, it may be that the accumulation in the *Hdh* has not reached the levels required to cause significant impairment, hence the lack of significant phenotype. This might underlie the differences between the ultrastructural morphologies of the two models. As discussed in the following section, the cytoplasmic changes, and simple nuclear condensation, can be accounted for by the stimulation of autophagy. However, autophagic activity is largely confined to the cytoplasm, its effects spreading to the nucleoplasm in autophagic cell death only after the vast majority of cytoplasm has been degraded. The nuclear condensation seen in the *Hdh* model may, in some cases, bear relation to nuclear huntingtin, but as they are

seen after cytoplasmic condensation, they are more likely to occur as secondary phenomena. The active process of cytoplasmic condensation would set up an osmotic gradient, which would draw water from an otherwise healthy nucleus.

The reported effects of mutant huntingtin are described in section *4.4*. The details of the molecular events are beyond the scope of my own experimental work, but as part of my ultrastructural analyses I have reported the relocation of the Cajal body (which remains intact) to the nuclear inclusion. This is clearly a sign of the major effects mutant huntingtin has in the nucleus; effects that do not appear to be as great, or even present, in the *Hdh* mice.

Therefore, whilst the cytoplasmic changes observed may be a consequence of secondary autophagic activity (see 4.3.3), the nuclear changes may be the most important in understanding Huntington's disease.

4.3.3 Degeneration in Aged Mice

The observations of the aged wild-type mice are perhaps the most startling findings of this work. Prior to this study it has been claimed that dark cell degeneration is a novel form of cell death occurring in a variety of neurodegenerative diseases. However, section *3.2* clearly documents an extremely similar process occurring in wild-type mice. This must surely alter our perception of the degeneration seen to occur in the mouse models. I have demonstrated that the same process can occur throughout the brain as a consequence of aging alone.

The *Hdh* mice show widespread dark neurons from 26 months of age. The wild-type littermates show such cells from around 28 months of age. Therefore, it may be that mutant huntingtin accelerates the 'natural' decay of a neuron. Aging mice show accumulation of dark cell profiles in much the same way their cells show accumulation of lipofuscin. Likewise, just as the accumulation of mutant huntingtin has been shown to increase levels of lipofuscin, so too it increases the appearance of darkened profiles.

~

I have argued that individual dark cells must be metabolically functional in order to maintain structure, especially against an increased osmotic gradient. If dark cells possessed significantly impaired energy metabolism they would swell and lose structural integrity, I have clearly shown they do not. I believe the dark neurons of the wild-type aged mice, at least, must also be behaviourally functional. Using an easily identifiable cell type as an example: if almost all the Purkinje cells of a mouse are dark, as is the case in all the Shelbourne mice presented, then they cannot be significantly impaired. The loss of function of the vast majority of any animal's Purkinje cells would not render it asymptomatic. In spite of this, the Shelbourne mice have been subjected to motor testing, and there is no sign of ataxia.

How then to reconcile the ultrastructural changes seen in dark cells with the picture of an active, functional cell? Many of the ultrastructural changes I have described here are reported to occur as a consequence of an increase in autophagic activity. As mentioned in the previous section, at least the cytoplasmic changes seen to occur in the R6/2 are reconcilable with autophagy; and these changes are similar to those seen in the aged mice. The one exception appears to be the timing of the condensation events. The R6/2 neurons show apparently concomitant cytoplasmic and nucleoplasmic condensation, whereas the *Hdh* mice show cytoplasmic events preceding nuclear events. This second is, in fact, more in line with autophagy. The descriptions of autophagic cell death consistently report the degradation of cytoplasmic components before nuclear involvement (see *4.2*). Macroautophagy is active under basal conditions producing small CVT vesicles, but the larger autophagic vacuoles (and multilamellar bodies) are also present in wild-type cells during starvation conditions. Furthermore, the observation that autophagy can delay or even suppress apoptosis has led to the suggestion that it functions as an attempt by the cell to save itself. In light of this, it is reasonable to suggest that autophagic activity is part of a cellular stress response designed to prolong the life of a cell for as long as possible. If the stimulus is strong enough, or the insult protracted enough, autophagy may not be able to protect the cell. Certainly, the inhibition of autophagy can enhance cell death.

The insults of mutant huntingtin accumulation, or the stresses of old age produce a similar neuronal appearance. I have argued that the consequences of

neuronal loss are so great that mechanisms to protect the cell from summary apoptosis must have evolved. The levels of autophagy seen in dark cell degeneration may be such a response. As discussed in 4.2, autophagy has also been implicated in the human disease. The important difference between the mouse models I have studied and the human condition may be that the disease is so protracted in the human that a point is reached where autophagy can delay cell deletion no longer. In the mouse models I have studied, before such events occur to any significant degree, the mouse is either overpowered by its phenotype or has come to the end of its natural lifespan.

The important difference I have noted between the degenerative profiles of the *Hdh* & wild-type mice and those of the R6/2 is the advanced nuclear condensation in the R6/2. This, I believe, it where the most important elements lie. I have observed the relocation of the Cajal body, but this is merely a gross indicator of the numerous nuclear-led changes occurring as part of the disease.

4.3.4 Death

If the lifespan of the *Hdh* mice could be extended, or the phenotype of the R6/2 ameliorated, I believe the dark neurons would eventually die, by which I mean cell deletion. This is speculation, but I believe such a neuron cannot survive in its dysfunctional state indefinitely. I have demonstrated that autophagy has been stimulated in the mouse models. The 'common signalling factor' in figure 140 is active, therefore degeneration is underway. I have also demonstrated that those cells undergoing dark cell degeneration do not show apoptotic morphology and there is no sign of activation of the molecular machinery of apoptosis. Thus, autophagy is able to delay cell deletion; but I do not believe this could be maintained indefinitely.

4.4 Inclusions

4.4.1 Inclusions & Phenotype

THE R6/2 mice show the most severe phenotype. They also show the greatest inclusion formation, in terms of number, size and distribution. Conversely, the *Hdh* mice show limited inclusion formation and possess a relatively mild phenotype. Thus, the original postulation, based on the R6/2 mouse model, that 'formation of neuronal intranuclear inclusions underlies the neurological dysfunction' is not unreasonable (Davies *et al.* 1997).

However, the *Hdh* mice do show inclusions throughout the striatum; which are comparable to inclusions seen in the early stages of observable behavioural phenotype onset in the R6/2 mice. Is it, therefore, that inclusion formation within the striatum alone is insufficient to cause a phenotype? Human patients also exhibit cortical inclusion formation, a similarity with the R6/2 and not the *Hdh* knock-ins; therefore it may be that nuclear inclusion formation within cortical neurons underlies the behavioural phenotype. This is supported by analysis of cortico-striatal electrophysiological dysfunction (see 4.5).

It must be the case that the mutant protein causes the phenotypic change: such is the nature of genetic disorder. But whilst inclusion formation in a cell may correlate with dysfunction, it may not be the underlying cause. Whilst many of the proteins known to interact with huntingtin may be recruited to the inclusion, others also interact with soluble huntingtin. I believe there is an important distinction to be made between the inclusion being seen as the cause of neuronal dysfunction and being viewed as an indicator of mutant huntingtin load within a particular cell.

4.4.2 Inclusions & Degeneration

The R6/2 mice show the greatest number of inclusions and size thereof, with the most widespread distribution. They also show the fewest dark cell profiles. Conversely, the *Hdh* mice show the greatest number of darkened profiles, in the face of the fewest inclusions. However, whether the degeneration seen in the *Hdh* mice is due to the effects of huntingtin remains under question. As described in *4.3*, whilst all mice, control and knock-in, display comparable amounts of degeneration beyond 29 months, at 26 months of age the knock-in black 6 mouse shows moderate amounts of degeneration whilst the wild-type appears healthy. It may be that as a secondary consequence of the mutation, some cells exhibit an accelerated aging; and thus much of the degeneration seen in the knock-ins is not a direct consequence of the huntingtin mutation within those cells.

Nevertheless, even if one ignores the *Hdh* data, the degree of degeneration seen in the R6/2 mouse cannot be said to be proportional to the degree of inclusion formation. There are areas that show frequent inclusions, both nuclear and neurite, and yet have never been seen to contain degenerating cells. For example, the hippocampal CA1 neurons are seen to be among the first to develop inclusions, and go on to contain the largest of all inclusions, and yet I have failed to find a single degenerating neuron within the R6/2 hippocampus.

As described in *1.6*, there is still debate on whether the formation of the inclusion is toxic to the cell or beneficial. Certainly any inhibition of the ubiquitin-proteasome system results in increased inclusion formation, suggesting a response by the cell to degrade mutant huntingtin. Many have taken this to mean that the formation of the inclusion is an active response to deal with the mutant protein, sequestering it away. Others believe the formation of the aggregate is toxic; indeed, the Bucciantini study implies that *any* aggregate is toxic (Bucciantini *et al.* 2002). However, there is the possibility that inclusion formation is neither beneficial nor toxic; rather it occurs as a consequence of accumulation of protein that cannot be degraded. From my work on the *Hdh* mice it has become apparent that even in healthy cells of healthy animals, there is considerable accumulation of lipofuscin with age. I have come

to view the accumulation of huntingtin as a similar phenomenon. There is some other factor, or factors, which underlie the degeneration of neurons in response to mutant huntingtin. If one could identify the relevant difference between a neuron in the hippocampal CA1 field and one from the anterior cingulate cortex, one might find a therapeutic target for preventing the degeneration of the latter. Of course, whether this would save the phenotype is another matter.

4.4.3 The Formation of the Inclusion

The two leading theories for the formation of aggregates – polar zippers and tissue transglutaminase – are summarised in *1.5.5*. Recent evidence has suggested that tissue transglutaminase has no role in *in vivo* in polyglutamine aggregation, as the enzyme does not associate with aggregates nor does altering the level of the protein affect aggregation (Chun *et al.* 2001). However, the polar-zipper model has remained a favoured hypothesis. To reiterate: expanded polyglutamine repeats form stable, hydrogen bonded, paired antiparallel ß-strands. Such aggregates then precipitate out further soluble polyglutamine-containing protein, and inclusions form.

If such a mechanism of aggregation does indeed occur then one would expect the formation of regular structures. This has been demonstrated *in vitro* using a variety of huntingtin exon 1-gluthathione S-transferase fusion proteins expressed in *E. coli.* Expanded glutamine repeats cause the formation of aggregates with fibrillar morphology (Huang *et al.* 1998) reminiscent of scrapie prion rods (Prusiner 1998), ß-amyloid fibrils in Alzheimer's disease (Caputo *et al.* 1992) and α-synuclein fibres in Parkinson's disease (Conway *et al.* 1998). When viewed with electron microscopy these fibres form digested exon 1 constructs, which are 10-12nm in diameter and vary in length from 100nm to several micrometers. They also stain with Congo red showing green birefringence, indicative of the presence of ß-pleated sheets; which supports the polar-zipper model. Likewise, huntingtin aggregates prepared from

human tissue exhibit similar staining properties suggesting similar aggregation mechanisms *in vivo* (Huang *et al.* 1998).

However, such structures, like the Lewy bodies formed from α-synuclein fibres, have a readily identifiable structure when viewed at EM (figure 141). As should be apparent from the numerous examples of huntingtin inclusions presented herein, there is very little structure to the inclusions of either the R6/2 or (where visible at EM) the *Hdh* mice.

Inclusions normally present as a granular structure with a defined texture, but lacking any fibrous assembly. Fibrous elements are occasionally visible, but are rarely 10-12nm in diameter and certainly not '100nm to several micrometers' in length. As described in *3.1.7,* these elements are considerably more frequent in the neurite aggregates of the R6/2 mouse, being rarely visible in the nuclear inclusion. The situation is similar in human tissue examined. Figure 142, represents a nuclear inclusion from a human patient with approximately 100 CAG repeats. The appearance is similar to those inclusions seen in the R6/2 neuronal nuclei: a predominantly granular structure. There are some elements that may be fibrous in nature (arrowheads), but these are small and, importantly, located toward the periphery. The fibrous elements of the R6/2 neurite inclusions are also located towards the periphery. The polar-zipper model of aggregation relies upon a nucleation-dependent event: the seed for aggregation is formed by fibrilisation and further fibres are added onto this seed (Scherzinger *et al.* 1997). Thus, fibres are literally the central element to inclusion formation. If this were true, one would expect any fibrous elements to be located at the centre of inclusion and not towards the periphery.

There is clearly a vast difference between the aggregation seen *in vitro* and the inclusions seen *in vivo.* What underlies this difference? Any answer is currently speculative, but it is my opinion that this difference is the result of complexity. The inclusions formed *in vivo* are in a simple system. As mentioned previously, proteins not previously associated with aggregation can be induced to form aggregates *in vitro.* The experiments described above on huntingtin exon 1-GST fusion proteins were conducted by purifying the expressed protein from *E. coli* lysate by affinity

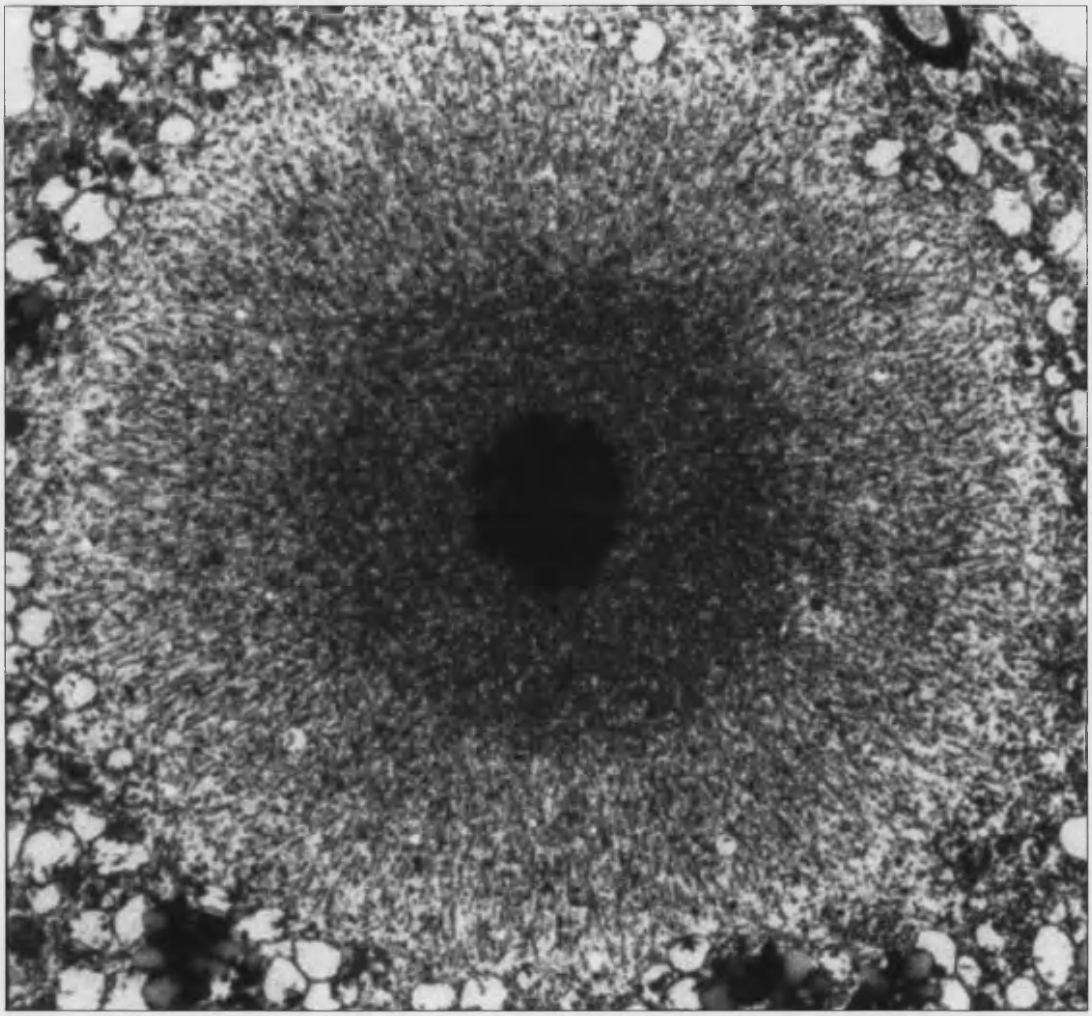

Figure 141 High-magnification electron micrograph of a Lewy Body from a patient with Parkinson's disease. The Lewy body is formed through sequential addition of fibres and as a consequence has a defined structure.

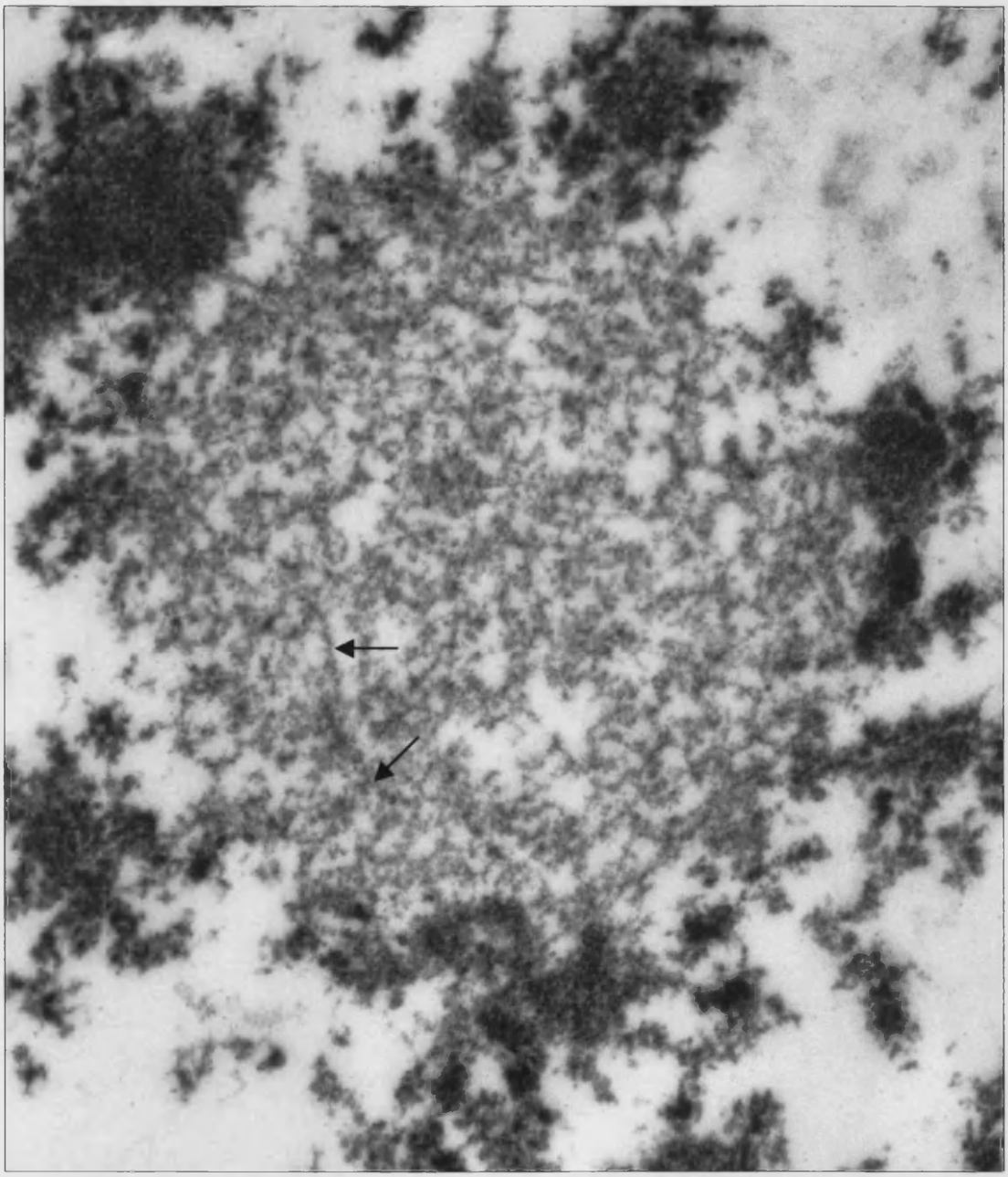

Figure 142 High-magification electron micrograph of a neuronal intranuclear inclusion from a Huntington's disease patient with approximately 100 CAG repeats (expanded allele). The structure is akin to that seen in the R6/2 mice: a granular appearance with possible fibrous elements towards the periphery (arrows).

chromatography, then digesting away the GST with trypsin. Aggregation is therefore taking place in a solution dominated by the protein in question. It is not unreasonable to assume that aggregates of Protein X are more likely to form in a concentrated solution of entirely Protein X.

Similar reasoning may explain why fibres occasionally form in neurite aggregates and very rarely in nuclear inclusions, as neurite aggregates contain fewer proteins than those of the nucleus. Colloquially, there isn't as much to get in the way of any fibrillisation that may occur. Conversely, within the nuclear inclusions there are numerous large proteins such as molecular chaperones, components of the proteasome and molecules such as the 265kDa CREB-binding protein. The situation *in vivo* is certainly not akin to that *in vitro*.

Nevertheless, inclusions do contain some fibrous elements. Notably, these are more frequent in the more mature aggregates. This further argues against a fibrillar nucleation event. It is my belief that these elements are indeed the ß-stands of the polar zipper models, which, as the *in vitro* work has shown, will form spontaneously when expanded polyglutamine-containing proteins are in sufficient concentration. However, I believe this is a secondary event to inclusion formation, occurring as a result of proximity induced by another mechanism.

4.5 Neuropathology

4.5.1 Dark Cells and Phenotype

THE R6/2 mice possess an aggressive phenotype in the face of no apparent cell death and relatively few dark cells. In contrast, the *Hdh* mice show an extremely mild phenotype and whilst there is little or no cell death, there are a considerable number of dark cells. It has also become apparent through this study that aged mice possess numerous dark neurons, and show no observable phenotype. It seems clear that in these mice, the presence of dark cells does not correlate with disease phenotype, and thus is unlikely to be the cause.

The human condition is dominated by cell loss, occurring over a protracted period, thus one cannot easily claim any correlation. Certainly, by the time the patients reach Grade 4 pathology, with up to 95% cell loss from the striatum, the patients are in the rigid akinetic stage of symptoms. Furthermore, there is a recent report of a patient with confirmed Huntington's disease (CAG 42/23) exhibiting all the choreaform symptoms, but with no observable cell loss at post-mortem (Caramins *et al.* 2003). It is likely that the initial symptoms of HD, and those one traditionally associates with the disorder, stem not from cell loss but from cell dysfunction.

In seeking a treatment for the human condition, prevention of cell loss may therefore do very little to reduce the symptoms and suffering of patients. For example, as described in *4.1*, minocycline inhibits caspase-1, and has been shown to protect against polyglutamine-induced cell death *in vitro* and prolong the life of R6/2 mice. However, subsequent analyses have revealed neither behavioural benefits nor any affect on inclusions detectable at post-mortem (Smith *et al.* 2003). Likewise, the glutamate antagonist Riluzole has been suggested as a therapeutic agent. Whilst this also increases the survival time of R6/2 mice, it has no effect on motor performance (Schiefer *et al.* 2002). Cell death is no doubt responsible for the latter, 'negative'

symptoms of HD, but the personality changes and hyperkinetic 'positive' symptoms of early HD bear no relation to neuronal loss. Thus, quests for therapies should centre on ameliorating cell dysfunction.

4.5.2 Interactions

Cell dysfunction in Huntington's disease must be a result of the mutation, most likely through perturbed or abnormal interactions with other cell components. The number of proteins with which huntingtin and/or mutant huntingtin are reported to interact is ever increasing. Furthermore, as huntingtin is found to interact with one protein, so that protein is reported to interact with numerous others. It is therefore unlikely that dysfunction arises from a simple altered interaction, rather that many interacting elements contribute to upsetting neuronal function.

The suggestion that huntingtin may be involved directly in gene transcription came soon after the cloning of the gene, as proteins with long polyglutamine or polyproline stretches often serve such roles (Gerber *et al.* 1994), such as the androgen receptor and TATA-binding protein, which themselves cause SBMA and SCA-17 when their polyQ sequences are expanded. However, wild-type huntingtin appears to be predominantly cytoplasmic and so its function is unlikely to be gene transcription.

Nevertheless, numerous alterations in gene expression have been detected in HD. Using microarray technology, Luthi-Carter *et al.* (2000) analysed the expression of over 6000 genes in the R6/2 striatum and found that between 1.2 and 1.7% percent of those genes showed altered expression in the R6/2; the majority of which were down-regulations (at a ratio of 3:1). Of particular interest to cell dysfunction and death, they report decreased expression of neural signalling molecules but no change in molecules associated with degeneration, such as glial markers. This supports the notion that cell dysfunction, in particular signalling pathways, are impaired before degeneration is evident.

Current thinking now tends towards perturbations in gene transcription occurring as a result of mutant huntingtin abnormally binding or sequestering away factors directly involved in transcription. A number of factors have been identified in nuclear inclusions, including TBP, CBP, TFIID and mSin3, each of which has a central role in transcription. mSin stabilises p53 and thus sequestration of mSin in the inclusion may result in p53 degradation and a loss of p53-dependent transcription (Boutell *et al.* 1999). Further inhibition of transcription is believed to occur through huntingtin's interaction with CBP, a crucial factor in CRE-mediated transcription. Several polyQ-containing proteins have been shown to bind CBP (McCampbell *et al.* 2000), and early down-regulation of CRE-regulated genes has been reported in both cell models of HD and the human condition (Wyttenbach *et al.* 2001). Interestingly, mutation in CBP causes Rubinstein-Taybi syndrome, a rare condition which involves severe mental retardation; supporting a causative relationship between CBP dysregulation and a neurological phenotype. Conversely, overexpression of CBP reduces mutant huntingtin toxicity in cell culture models, as does preventing CBP-huntingtin interaction (Nucifora *et al.* 2001). Another factor in CRE-mediated transcription has also been implicated in HD: $TAF_{II}130$. This cofactor in has also been located in huntingtin aggregates, and, as with CBP, overexpression restores CRE-dependent transcription (Shimohata *et al.* 2000).

Recently, it has been shown that another transcription factor, NeuroD, which is neuronal specific, interacts with HAP1, via which it may interact with huntingtin (Marcora *et al.* 2003). This is an interesting finding in that it may help to explain why mutant huntingtin predominantly affects neurons. It also serves to illustrate how the effects of mutant huntingtin may reach beyond direct interactions and recruitment, affecting transcription via numerous intermediate factors.

On a more general level, there appears to be a downregulation of transcription in various HD models due to histone deacetylation. The availability of DNA to the transcription complexed is tightly regulated by the action of histone acetyl transferases (HATs), which open up chromatin, and histone deacetylases (HDACs), which cause the tight binding of DNA to the histones. Mutant huntingtin has been reported to interact with a number of HATs (including CBP, p300 and

P/CAF), inhibiting their action and causing general transcriptional inhibition (Steffan *et al.* 2001). Such a widespread action may explain why the majority of transcription changes document by Luthi-Carter *et al.* (2000) were down-regulations. Therapeutic intervention to address the imbalance, the administration of HDAC inhibitors has shown promising preliminary results. Hockly *et al.* (2003) administered the HDAC inhibitor SAHA (suberoylanilide hydroxamic acid) to R6/2 mice and found a significant improvement in motor performance. It should be noted, however, that approximately 2mg of SAHA was administered daily via drinking water; doses greater than this proved too toxic. In their preliminary studies, Hockly *et al.* had found that doses less than 200mg injected s.c. produced no effect on histone acetylation. Therefore, it is uncertain as to whether tolerable doses of SAHA can significantly inhibit HDACs. Nevertheless, a tolerable HDAC inhibitor may one day prove to be of great therapeutic value.

4.5.3 Pathophysiology

Huntingtin has also been shown to interact with numerous proteins involved in vesicle trafficking. Indeed, the eponymous protein itself has been implicated in the role (see 1.3.2). Huntingtin-associated protein 1 (HAP1) binds the p150 subunit of dynactin (Engelender *et al.* 1997), an activator protein required for the retrograde vesicle transport along microtubules. It has been implicated in clathrin-mediated endocytosis, along with huntingtin (Velier *et al.* 1998), and huntingtin-interacting protein 1 (HIP1) (Metzler *et al.* 2001). In support of a role for HIP1 in endocytosis, the rat homologue has been shown to localise to postsynaptic spines in small vesicular structures (Okano *et al.* 2003), and it is over-expressed in certain human endothelial cell cancers, which, when replicated *in vitro*, results in altered receptor trafficking (Rao *et al.* 2003). HIP1 knock-out mice show impaired endocytosis, but, importantly, also exhibit a neurological phenotype reminiscent of some of the features of HD: tremor and ataxia

(Metzler *et al.* 2003). Given these observations, one would expect mutant huntingtin to interfere with synaptic function, and this appears to be the case.

Perturbations in electrophysiology have been reported in many of the mouse models of HD, most of the original work was conducted on hippocampal neurons. In the R6/2 mouse, basal neurotransmission across CA1 synapses in unaffected, however during intense activity a deficit becomes apparent (Murphy *et al.* 2000). Measurements of presynaptic function indicate that neurotransmitter release is impaired, but said impairment does not affect function at basal levels. This may be due to a deficit of complexin II, part of the SNARE-complex, which has been shown to be progressively lost in R6/2 mice (Morton *et al.* 2001) and PC12 cells expressing expanded huntingtin, where this loss results in decreased calcium ion-triggered exocytosis (Edwardson *et al.* 2003). In support of this loss causing the dysfunction seen, complexin II knockout mice exhibit aberrant hippocampal electrophysiology similar to that seen in the R6/2 (Takahashi *et al.* 1999).

More recent work has investigated the electrophysiology of the medium spiny striatal neurons: those directly affected in human HD. In the transgenic model of Marian DiFiglia (see 4.6), expressing a longer huntingtin N-terminal fragment with either 46 or 100 glutamine repeats, striatal neurons showed decreased responsiveness to induced cortical stimulation and to NMDA exposure. They also report the onset of behavioural phenotype occurring after striatal inclusion formation, but concomitant with nuclear accumulation of huntingtin within cortical neurons, suggesting that phenotype onset is caused either by cortical dysfunction, or by the potentiating effect of striatal and cortical dysfunction (Kegel *et al.* 2000).

In the R6/2 mice, this functional deficit has been investigated more thoroughly and more objectively. Cepeda *et al.* (2003) monitored the spontaneous excitatory post-synaptic currents (EPSCs) in striatal medium spiny neurons at three time points: presymptomatic (3-4 weeks), at onset of symptoms (5-7 weeks) and severely impaired (11-15 weeks). They report a decrease in EPSCs at 5-7 weeks, becoming more pronounced at 11-15 weeks. This supports previous data reporting that greater electrical stimulation is required to induce inward current in R6/2 striatal neurons (Klapstein *et al.* 2001). As these activities are not blocked by bicuclline or

tetrodotoxin, one can infer they are generated as a result of glutamatergic input, and therefore likely to be of cortical origin. In addition to a reduction of basal activity, they also report the appearance of isolated large synaptic inward currents in the R6/2, most pronounced in the 5-7 week animals. Interestingly, Riluzole, which decreases glutamate release (Cheramy *et al.* 1992) and has been reported to prolong the life of R6/2 mice (Schiefer *et al.* 2002), reduces the number of these large-current events. In an attempt to identify the causes of this dysfunction, Capeda *et al.* (2003) examined the distribution of synaptophysin and PSD95, key pre- and post-synaptic proteins respectively, and found significant reductions in both markers in the 11-15 week mice.

This work may indicate that complicated cortico-striatal dysfunction, with transient as well as progressive changes, may underlie the phenotype of the R6/2 and the symptoms of human HD. It may also help to explain why the Shelbourne *Hdh* mice show so little phenotypically in the face of evident pathological changes, as these mice show no nuclear huntingtin in cortical neurons.

Filling neurons with biocytin, or Golgi impregnation, allows for isolated cell morphology to be examined. Such work on the R6/2 mouse has revealed a reduction of dendritic spine density, a decreased dendritic field diameter, and a decrease in the diameter of dendritic shafts of medium spiny neurons (Klapstein *et al.* 2001). Such neurons also show numerous varicositites along the dendritic shafts, possible as the result of a 'pruning' process. In support of this, the reduction in dendritic spines is greatest the further from the cell soma. The reduction in dendritic spine density, and a decreased arborisation is likely to underlie the decreased activity seen in these neurons; and explains the loss of synaptophysin and PSD95 staining. Furthermore, this is likely to underlie the reports that R6/2 striatal neurons are more resistant to excitotoxicity (Hansson *et al.* 1999; Morton and Leavens 2000).

Such changes are not confined to the striatal medium spiny neurons, but are also found in cortical and hippocampal pyramidal neurons (Klapstein *et al.* 2001). As I have found that the cell bodies of hippocampal neurons do not show signs of dark cell degeneration in the R6/2 (see 3.1.3), the Klapstein *et al.* report serves to further highlight the lack of a causative relationship between degeneration and dysfunction.

4.6 Mouse Models and Huntington's Disease

4.6.1 Mouse Models

THERE are a growing number of models of Huntington's disease, including *C. elegans*, *Drosophila* and yeast models. However, the most evolutionary 'advanced' models, and therefore those one assumes to have the greatest relevance to the human disorder, are the mouse models[•]. For this reason they have been the most extensively studied. Tables of those mouse models which have been most extensively studied are found in figures 143 to 145.

Three broad strategies have been used to generate these mice. First, the insertion of a fragment of the human gene, containing the region associated with the disease, the polyglutamine tract, randomly into the mouse genome: truncated transgenics, such as the R6 mice. Secondly, the insertion of the full-length human gene into the mouse genome (the mouse model of Michael Hayden's research group involved the insertion of the full-length gene into a Yeast Artificial Chromosome (YAC), which is replicated in the mouse along with endogenous genetic material): full length transgenics. The final method, as used by Peggy Shelbourne, involves the elongation of the CAG repeat sequence within the mouse homologue of IT15: knock-ins.

This thesis has examined the differences between the R6/2 and Shelbourne *Hdh* mice, but further differences are brought to light when examining the full range of mice. As described in *1.5*, the cleavage of mutant huntingtin is believed to be an important event in the pathogenesis of HD, as a result one would expect those mice expressing a truncated mutant huntingtin construct to show a more rapid pathology.

[•] A rat genetic model of HD has recently been generated by von Horsten et *al.* (2003). The model was generated using truncated HD cDNA, containing 51 CAG repeats, expressed using the rat huntingtin promoter. The animals produced exhibit an adult-onset phenotype with motor & cognitive components and possess NIIs.

Model	Fragment	PolyQ	Promoter	Background	Inclusions	Phenotype	Degeneration
R6/2 (Bates)	IT15 exon 1 and 1kb upstream elements	**150Q** (now expanded to approx. 200)	Human huntingtin promoter	C57B6/CBA	Frequent, large, widespread inclusions throughout brain – NIIs and neurite inclusions – appearing first at approx. 4 weeks	Motor deficits detectable at 5-6 weeks; overt at 8 weeks, progressing to severely impaired behavioural deficits. Death at 13-15 weeks	Dark neurons found predominantly in cortex (cingulate, and motor) and in the striatum; apparent at 12 weeks. Overall brain atrophy.
N171 (Borchelt)	First 171 amino acids of IT15	**82Q** (also unaffected 44Q & 18Q)	Prion promoter	C3H/C57B6	Incusions found in striatum, cortex, hippocampus, amygdala & cerebellum; appearing at 6-8 months	Motor deficits detectable at 3 months; progressing to overt phenotype of tremors & abnormal gait. Death at 24-30 weeks.	Degenerating neurons reported within the striatum. Overall mild brain atrophy.
HD94 (Yamamoto)	Adapted exon 1	**94Q**† †interrupted sequence	BiTetO-CMV promoter Controllable expression	CBA/C57B6	Inclusions in striatum, septum, cortex and hippocampus; first at 8 weeks; reversed by turning off transgene.	Motor deficits detectable at 2.5 months; tremor and abnormal gait at 4.5 months. Normal lifespan.	Astrocytic response but no neuronal degeneration reported. Overall brain atrophy.

Figure 143 Transgenic mouse models of Huntington's disease expressing a fragment of the huntingtin gene.

Model	PolyQ	Promoter	Background	Inclusions	Phenotype	Degeneration
3kb N-terminal fragment (DiFiglia)	**100Q**	Rat neuron specific enoclase	SJL/C57B6	Inclusions reported, both NII and neurite	Onset of symptoms (clasping phenotype) at 3-4 months; hyperactivity to end-stage hypoactivity.	Cell loss (20%) reported in some animals. Overall brain atrophy also only in certain animals.
HD89 (Tagle)	**89Q**	CMV	FVB/N	Very few inclusions	Onset of symptoms (clasping phenotype) at 4 months; hyperactivity followed by end-stage hypoactivity. Death at 18-20 months for heterozygotes (homozygotes 12-15 months)	Neuronal loss reported in the striatum, cortex, hippocampus and thalamus. Gliosis also reported.
YAC72 (Hayden)	**72Q**	HD gene, including promoter, inserted into yeast artificial chromosome	FVB/N	Inclusions only in striatum	Onset of symptoms (clasping phenotype) at 3 months; hyperactivity and circling behaviour. Age at death not reported (greater than 12 months)	Dark neurons in the striatum. No evidence of cell loss.

Figure 144 Transgenic mouse models of Huntington's disease expressing truncated huntingtin (continued) or full-length human huntingtin.

Hdh Model	PolyQ	Background	Inclusions	Phenotype	Degeneration
Shelbourne	**72Q** **80Q**	FVB C57B6	Late inclusions (>18 months), predominantly in striatum, nucleus accumbens and olfactory tubercle.	No motor deficits, but behavioural phenotype (aggressiveness) reported.	Age-related degeneration in oldest mice. No cell loss.
Zeitlin	**71Q** **94Q**	C57B6	Inclusions only found in 94Q mice at late stage (>18 months); nuclear microaggregates found earlier (6 months)	Behavioural phenotype (aggressiveness) reported. Mild hyperkinesias also reported in 94Q.	No cell loss or degeneration, but dysfunction (swelling in response to NMDA) reported. Striatal cell shrinkage.
MacDonald	**111Q** **92Q**	129/CD1	Striatal nuclear inclusions at 10 months in 111Q and 12 months in 92Q	Phenotype apparently unaffected; normal lifespan	No cell loss
Detloff	**150Q**	129/Ola × C57B6/6J	Striatal nuclear inclusions evident at 10 months	Motor deficits detectable at 15-40 weeks	No cell loss

Figure 145 Knock-in mouse models of Huntington's disease.

This is certainly true when comparing the truncated transgenics to the knock-ins, which show few, late-stage inclusions and no neuronal degeneration until the last days of the mouse lifespan. However, the comparison of transgenic mice expressing just exon 1 (or the first 171 amino acids) of huntingtin to those expressing the full-length protein yields interesting results. All truncated-expression mice show similar phenotypes to the R6/2, occurring at different rates presumably due to differences in polyQ length, and frequent inclusions but show no cell loss. Conversely, transgenic mice expressing the full-length mutant protein (reportedly) show cell loss in the striatum, extending to (in the case of the Tagle mice, with the greater polyQ length) cortex, hippocampus and thalamus. Whilst showing similar initial phenotypes to the truncated transgenics, they show very few inclusions, limited to the striatum. This further undermines the notion that the formation of inclusions induces, or even correlates with, cell death. The mice of Marian DiFiglia provide an interesting 'halfway' between the two extremes of transgenic modelling, for her group have generated transgenic mice expressing mutant huntingtin that whilst truncated, is considerably longer than the proteins of the other truncated transgenics: one third of the complete sequence as opposed to one sixty-seventh (Laforet *et al.* 2001). This mouse shows features of the other truncated transgenic mice – frequent inclusions, both nuclear and neuritic, and a progressive motor phenotype – but also the cell loss (in some animals) associated with the full-length protein models.

These observations suggest that whilst truncation of the mutant protein accelerates inclusion formation, it prevents against cell loss. These may be inextricably linked, supporting the notion that the formation of the inclusion reduces toxicity.

There is an important factor that cannot easily be controlled for: expression level. The promoters used to express the construct in each of the transgenic mice are included in the figures. Each differs in some way. Whilst the R6/2 and the YAC72 models each make use of the human IT15 promoter, one cannot be certain that the nature of the YAC does not interfere with expression. Furthermore, the HD94 and HD89 models each make use of the cytomegalovirus promoter, but this has been adapted in the HD94 for the very purpose of altering its native properties. The methods used to attempt to quantify levels of expression in each of the models vary,

even down to the question of whether to quantify protein of RNA. As stability of mRNA and translation rates may vary within each mouse, and the important molecule is the protein, it would seem wisest to quantify levels of mature huntingtin. However, the very nature of the mutant protein makes this a difficult task: the longer the polyglutamine length, the greater the tendency for aggregation. As huntingtin aggregates are resistant to being broken apart they are unlikely to travel well through electrophoretic gels, thus western blot-based quantifications may yield only information on soluble or oligomeric huntingtin. As an aside, this may bear some relevance to work reporting that increasing polyglutamine length causes decreasing expression levels (Persichetti *et al.* 1995; Trottier *et al.* 1995).

As a result, any comparison of expression levels based on the available data would be tenuous, particularly as the degree of aggregation and inclusion formation varies among mice. However, there are some points that need mentioning. The mice of Danio Tagle were generated using full-length HD cDNA inserted not into a YAC but directly into the mouse genome. They may thus be considered the most faithful transgenic model. Indeed, they develop a complex motor and cognitive phenotype akin to many of the other mice, but, importantly, they also progress to a hypokinetic stage before death, thereby mimicking the complete range of symptoms seen in the human condition. These mice also substantial neuronal loss, particularly in those mice sacrificed after entering the hypokinetic stage (Reddy *et al.* 1998). This model therefore seems to replicate the human condition in all aspects. The levels of mutant huntingtin protein in these mice, examined by western blotting and therefore prone to underestimation depending on aggregation, has been estimated at up to 5 times the levels of endogenous wild-type huntingtin. Is it, therefore, protein load that kills the neurons of these mice?

This makes the DiFiglia 3kb fragment mice even more interesting. As described previously, these mice show frequent inclusions; exhibit a progressive phenotype, from hyperactivity through to hypoactivity; and lose neurons. Yet, whilst the results are variable, the mutant protein appears to be expressed at levels below that of endogenous protein (Laforet *et al.* 2001).

~

The knock-in mice are all under as equivalent promoter: the *Hdh* promoter. Each model has been reported to have protein expression levels close to endogenous. At this level of expression, even with the 111 repeats in the Marcy MacDonald mouse, there is very little effect. Inclusions are evident only in animals well into adult-hood. The fact that there is little in the way of detectable phenotype suggests that cells have yet to enter the period of dysfunction that precedes detectable cell degeneration. The degeneration in the *Hdh* mice presented herein appears to occur primarily as a result of senescence modified by the disease process. Thus, expression of even greatly expanded huntingtin driven by the endogenous mouse promoter is not sufficient to propel the mouse through the full range of the human condition.

The remaining question here concerns the truncated transgenic mice. Why do the R6/2 and N171 mice show degenerating neurons when levels of mutant protein are reported to be below those of wild-type? Yu *et al.* (2003) compared the degeneration of these mice and also of the Detloff *Hdh*150 knock-in mouse and reported activated caspase-3 only in the N171 mouse. To investigate this further they transfected human embryonic kidney (HEK) cells with a variety of constructs, varying the length of either polyQ or non-polyQ regions. As expected, they find increasing the polyQ length results in greater caspase activation. However, they also find that increasing the length of protein beyond the exon1 boundary *increased* toxicity, peaking at around 208 amino acids at which point further expansion towards the C-terminus decreases toxicity (the constructs used of lesser and greater size than the 208 construct involved the first 63 [exon 1] and 508 amino acids of huntingtin; therefore the peak lies anywhere between these two points). Whilst the relevance of caspase-3 activation in a HEK model is questionable, the fact remains that in a single model system there appears to be a context-dependent toxicity. This translates well onto the mouse models as it could explain the peculiarity of the DiFiglia 3kb fragment mice, and also why the N171 mice show severe phenotype and darkened striatal neurons whilst having only 82 repeats in a protein estimated to be expressed at 10-20% that of endogenous (the lowest expressing model of all).

~

We can therefore derive the three most important factors required to cause maximal neuronal dysfunction and death, which, we have established, is unrelated to inclusion formation.

1) Polyglutamine length
2) Non-polyQ protein length
3) Promoter: Expression Level

The transgenic mouse exhibiting the greatest neuronal toxicity would thus use the CMV promoter to express the first 200 amino acids of huntingtin, which would contain 90-150 glutamines. Of course, neuronal toxicity and the 'positive' symptoms of HD are not causatively linked, therefore such a mouse might possess a phenotype more severe than the R6/2 mouse and, likewise, die prematurely before neurons are lost. Thus, such a mouse may not be the 'best' mouse.

4.6.2 Mouse Models and the Human Disease

The 'gold standard' against which all of these models must be judged is, of course, the human condition. Human HD shows slow accumulation of huntingtin and late onset of disease symptoms. It is also shows substantial cell death. The two combine to produce a behavioural phenotype progressing from personality changes and cognitive impairment, through hyperkinesia and chorea, to hypokinesia and akinesia. The latter, 'negative' symptoms corresponding to cell loss. In these respects none of the mice accurately reproduce the human condition.

The *Hdh* knock-in mice fail to significantly reproduce the disease characteristics. The Shelbourne model shows minor behavioural abnormalities – increased aggressive behaviour – a phenomenon shared with the Zeitlin mice, of which the 94Q model also exhibits mild hyperkinesia. Interestingly, the MacDonald and Detloff mice are of similar nature, yet whilst the MacDonald mice are

phenotypically unaffected, there are reports of motor deficits in the Detloff mice. In none of these models is cell loss reported, and dark neurons are infrequent.

The transgenic mice expressing the smaller N-terminal fragments exhibit the majority of the symptomatic behavioural alterations seen in the human, including motor deficits, hyperkinesia, tremors and abnormal gait. However, in spite of the early onset of symptoms and rapid disease progression, these mice show no cell loss. Hence, they do not progress to the hypokinetic stage of the phenotype.

The mice that appear to replicate the human disease most fully are those presented in figure 144. These mice express either full-length huntingtin or a large N-terminal fragment. Yet, as mentioned previously, it is not simply a matter of fragment length. The knock-in mice studied as part of this thesis demonstrate that neither full-length nor truncated mutant huntingtin expressed under the endogenous promoter is sufficient to carry the disease phenotype beyond the initial stages. The DiFiglia mice remain an interesting mystery. The expression levels of huntingtin, or rather the first one thousand amino acids of huntingtin, are believed to be lower than endogenous and yet the disease process passes through all stages. The neuropathological investigations have yielded inconsistent results, with cell loss reported for only some of the mice. However, if there is an extra property inherent to longer N-terminal fragments, as suggested previously, then this model may lead the way to others which replicate fully the behavioural spectrum, show widespread inclusions and exhibit cell loss.

Ignoring the nature of the transgenics, the Hayden YAC mouse and the Tagle mouse are rather similar; yet whilst the Tagle mice exhibit widespread neuronal loss and a full progression of symptoms including hypoactivity, the Hayden mice progress only to the hyperactivity/dark neuron stage. Thus, it may be said that the Tagle mice are the closest to the human condition. However, in order to achieve this replication of HD, the expression level of the protein is up to five times that of the endogenous huntingtin. Is such a model an accurate recreation of the human disease?

The knock-in models show that inserting CAG repeats to extend the *Hdh* gene into the range known to pathogenic in the human condition does not necessary produce a disease phenotype in the mouse. The Detloff mouse has 150 CAG repeats

and yet whilst showing inclusion formation a third of the way through its lifespan there is only a minor detectable phenotype. Such an expansion in the human would kill the individual before adulthood. Therefore, in order to replicate human HD within the lifespan of the mouse the disease process has to be accelerated. Truncation of the mutant protein combined with repeat lengths known to cause juvenile HD accelerates the onset of symptoms, but in the case of the R6/2 and N171 mice it may be that the phenotype is accelerated to such a level that the complications arising from dysfunction kill the mice before cell death can occur. In the case of the DiFiglia mice, the juvenile HD-causing repeat length is contained within one third of the huntingtin protein. This appears to accelerate the disease process such that phenotypes are observable within the lifespan of the mouse, yet allows it to progress to completion in some animals. The Tagle mice bring about acceleration by increasing the amount of mutant protein produced. This appears to produce the most faithful replication of the human disease.

However, the human condition also shows numerous inclusions. The Tagle mice show very few. As the relevance of each of the components – huntingtin accumulation, inclusion formation, neuronal darkening, and cell death – to human HD has yet to be conclusively weighted, the true value of the Tagle model, and the values of the others are open to debate. What this does serve to illustrate, is that even the most faithful model cannot replicate all of the human condition.

Conclusion

5.1 *Dysfunction, Degeneration and Death*

AT onset of this project, the thesis title was *An Ultrastructural Analysis of Cell Death in Huntington's Disease*. However, it soon became clear that there is little to no cell deletion in the R6/2 mouse models. Thus, the title was altered to reflect the fact that this work is a study of the degenerative changes seen in those cells, which, potentially, may be deleted if the process were to continue to completion.

As the R6/2 exhibits such a powerful phenotype in the face of no apparent cell loss, one can conclude that cell death does not underlie the symptoms of the R6/2. The human condition, and some of the other mouse models, progresses to an akinetic stage, which is likely to be the result of the cell loss, but the initial 'positive' symptoms of HD and its models do not stem from cell deletion.

The 'positive' symptoms of HD must therefore result from cell dysfunction brought about by the expression of the mutant protein. The *Hdh* and aged wild-type mice show large numbers of dark degenerating neurons and yet show an extremely mild phenotype. Thus, one can conclude that cell dysfunction does not correlate with dark cell degeneration. The nature of such dysfunction is beyond the confines of this thesis, but I have speculated that, independently from dark cell degeneration, the interaction of mutant huntingtin with cell components underlies this dysfunction.

One is therefore left with the question of the nature of the dark neuron. In the mouse models I have studied, including the aged wild-type controls, neurons persist in a darkened, degenerative state; and, given the lack of a severe phenotype, must be (largely, at least) functionally intact. I have also provided evidence for a lack of activation of the machinery of apoptosis during dark cell degeneration, which may explain how such persistence can occur. The dark neuron may therefore be degeneration, but not dying.

Such persistent 'dark degeneration' may be unique to neurons. It seems clear that there is a vast difference between dividing cells in culture and post-mitotic neurons, particularly in susceptibility to apoptotic stimuli. This appears to be a logical

state of affairs. A cycling cell has not terminally differentiated and, therefore, is unlikely to have taken on its functional role. An adult CNS neuron has developed countless synaptic connections via intensely reticulated dendritic arbours, and grown axons many times the length of its own cell body. The consequences of losing the former cell are far outweighed by the consequences of losing the latter. Applying evolutionary principles, it is likely that a mechanism has evolved to protect neurons from summary apoptosis. Such a system will be negated in a neuron that is severely compromised (ischaemic or overpowered by calcium ion influx, for examples) but in the case of Huntington's disease, the insult is slow and protracted. So much so, that a cell can apparently survive for decades in the face of the accumulating insult.

The upregulation of autophagy has been shown in response to various stressful stimuli, including transfection with huntingtin. It has been demonstrated that autophagy can delay or even suppress the activation of apoptosis. Given the large-scale activation of autophagy seen in the mice I have studied, this may help to explain how dark neurons can persist for so long without undergoing apoptosis.

Autophagy has also been shown to successfully degrade mutant huntingtin. It is unlikely that this is a directed response, rather, in times of stress, autophagy is induced to non-specifically degrade cellular constituents, liberating raw materials for the construction of more essential components. This may also be true for the dendritic remodelling shown to occur. As part of a stress response, dendritic arbours may be retracted, though this does seem contrary to the hypothesis that such mechanisms would act to protect a neuron precisely because it is so highly differentiated.

However, such protective mechanisms may produce a 'double-edged' result in the human condition. I have argued that the 'positive' symptoms of Huntington's disease are produced by cell dysfunction and that cell loss yields the 'negative' symptoms. The persistence of the dark dysfunction neuron prolongs the 'positive' phase. Of course, whether a dead neuron is better than a dysfunctional neuron is a moot point. Certainly for the relatives of HD patients, the positive symptoms are more disturbing; but once a neuron is dead there is no return.

5.2 *The Relevance of Models*

ONE must not lose sight of the reason for generating each mouse model: to understand the human condition such that effective therapies might be developed. Mouse models have already provided great insights into the mechanisms behind Huntington's disease. Furthermore, insights into HD often apply to the other polyglutamine disorders, and vice versa,

Huntington's disease is a multifaceted, prolonged disorder with changes ranging from genetic alterations through to dendritic pruning and cell loss. In evaluating the mouse models I sought the 'best' model using complete replication of the human disease as my criterion. But is it necessary to replicate the full progress of the human disease in order to understand one element? Is it even wise?

I have, reluctantly, been forced to conclude that neither the R6/2 not the Shelbourne knock-in mice are wise choices for studying cell death. The Tagle or DiFiglia mice seem more suited to such studies as they (reportedly) show the greatest cell loss. But that does not mean that these are the best models for studying every element of HD. The work of Peggy Shelbourne is centred on the somatic instability of the HD mutation (see 1.3.4). The expansion of genomic CAG repeat sequences within somatic cells is perhaps the first step in the disease process. It may also underlie the cell selectivity seen HD. It is likely that such processes depend on genetic context, thus such investigation in the Hayden YAC mouse would probably be meaningless. Likewise, the Tagle mice express mutant huntingtin from the CMV promoter at up to 500% that of normal huntingtin. This level of expression may affect the somatic expansion events. Thus, whilst they show only the first stages of the disease before the effects of old age take over, the Shelbourne mice are perfect for the work of Dr Shelbourne.

Likewise, I have criticised the R6/2 model for showing no detectable cell loss. But the very fact that so many neurons are 'stuck' in the dysfunctional phase, yielding the severe phenotype, means this model is perfect for one studying dysfunction. Furthermore, the R6/2 is an excellent candidate for the testing of therapeutic

compounds that are hoped to restore function in human patients, and is indeed widely used for such purposes (though this is primarily due to the low cost of housing a mouse that will develop a phenotype within weeks rather than months).

However, the R6/2 also provides an insight that cannot be ignored when developing therapeutics. In the previous section I questioned the benefits of prolonging the life of a dysfunctional neuron. The R6/2 shows more widespread nuclear accumulation of mutant huntingtin than that seen in the human condition, but that aside, the model has confirmed that the greater the number of dysfunctional neurons in the brain at any one time, the greater the overall phenotype. Preventing the death of dysfunctional neurons in the human condition would lead to an accumulation of such cells. This may well exacerbate the phenotype.

In spite of this, work continues on various model systems to find compounds that prevent cell death. Inhibitors of almost all caspases have been used on model systems. This work provides important insights into the mechanisms of cell death, but one is forced to question the authors of such papers ending with a sentence along the lines of: 'This may provide a basis for therapy in Huntington's disease'. Human therapy should indeed always be the goal in working on mouse models of disease, but the prevention of cell death is far beyond the therapeutic window in HD. Yet, clinical trials are underway on such compounds. Prevention of cell death may be beneficial if the elements underlying dysfunction can also be inhibited. Perhaps the eventual treatment for HD will be a cocktail of drugs designed to prevent cell death, increase histone acetylation & restore inhibited transcriptional pathways, and sustain dendritic morphology. The question then is 'how would such interference in fundamental biological processes affect the rest of the body'?

5.3 *Future Directions*

WHILST this thesis has provided insights into the nature of the dark cells seen to accumulate in Huntington's disease and its mouse models, it has left unanswered some of the questions it sought to address. The process by which cells are deleted in human HD may indeed be apoptotic. I have argued that the autophagy seen in all mouse models I have studied may allow the cell to persist in spite of the insult of nuclear, mutant huntingtin. However, dark neurons may eventually become overwhelmed and autophagy can no longer delay the initiation of apoptosis. It seems clear from the human condition, that a point is reached whereupon the dark cell, which has struggled to survive in the face of mutant huntingtin accumulation, commits to death. The nature of that point, and the processes leading to deletion of the cell remain to be confirmed. Studies such as those presented here should be carried out on mice were there is clear cell death, such as the Tagle mice.

I suggested in *5.1* that the dendritic remodelling seen in the transgenic mice may also be part of the general 'insult' response in neurons. This would be relatively simple to investigate. Golgi impregnations of neurons in aged wild-type would reveal such changes; however, by definition, age-matched controls would not be available. Nevertheless, there may be a correlation between loss of dendritic arborisation, cell somal condensation and autophagy. If so this would suggest that the changes seen in the HD mice are a result of a general response to insult, throwing up more questions concerning the specificity of HD pathology. However, if cells showing age-induced dark cell degeneration possess healthy processes, one can be certain that the dendritic changes in the HD mice occur as a direct result of the huntingtin mutation, and are therefore certainly behind much of the dysfunction, and thus phenotype of Huntington's disease.

I have also suggested that the only real distinguishing element between the ultrastructural changes of the R6/2 and those of the *Hdh* or aged mice is the involvement of the nucleus. Whilst the R6/2s show similar cytoplasmic events to the

Hdh and aged wild-type mice, they also exhibit a nuclear-based pathology, which, I believe, is central to the neuropathology of HD. My investigations of nuclear changes have been limited to those visible with osmium-uranyl-lead staining at EM, which, fortunately, includes the position of the Cajal body. However, there is an ever-growing number of other 'bodies' within the nucleus, it is certainly not the homogenous structure it was once believed to be (see Spector, 2001 *for review*). Each of these bodies, as well as each of the countless free proteins within the nucleus may be affected in Huntington's disease. Such interactions have already been shown to dramatically affect models of HD, and, I believe, it is in the nucleus that the most important elements are to be found. To that end, investigations are already underway and should provide interesting results.

Appendices

6.1 *Transcript of 'On Chorea' by George Huntington*

CHOREA is essentially a disease of the nervous system. The name "chorea" is given to the disease on account of the dancing propensities of those who are affected by it, and it is a very appropriate designation. The disease, as it is commonly seen, is by no means a dangerous or serious affection, however distressing it may be to the one suffering from it, or to his friends. Its most marked and characteristic feature is a clonic spasm affecting the voluntary muscles. There is no loss of sense or of volition attending these contractions, as there is in epilepsy; the will is there, but its power to perform is deficient, the desired movements are after a manner performed, but there seems to exist some hidden power, something that is playing tricks, as it were, upon the will, and in a measure thwarting and perverting its designs; and after the will has ceased to exert its power in any given direction, taking things into its own hands, and keeping the poor victim in a continual jigger as long as he remains awake, generally, though not always, granting a respite during sleep. The disease commonly begins by slight twitchings in the muscles of the face, which gradually increase in violence and variety. The eyelids are kept winking, the brows are corrugated, and then elevated, the nose is screwed first to the one side and then to the other, and the mouth is drawn in various directions, giving the patient the most ludicrous appearance imaginable. The upper extremities may be the first affected, or both simultaneously. All the voluntary muscles are liable to be affected, those of the face rarely being exempted.

If the patient attempts to protrude the tongue it is accomplished with a great deal of diffculty and uncertainty. The hands are kept rolling—first the palms upward, and then the backs. The shoulders are shrugged, and the feet and legs kept in perpetual motion; the toes are turned in, and then everted; one foot is thrown across the other, and then suddenly withdrawn, and, in short, every conceivable attitude and expression is assumed, and so varied and irregular are the motions gone through with, that a complete description of them would be impossible. Sometimes the muscles of the lower extremities are not affected, and I believe they never are alone involved. In cases of death from chorea, all the muscles of the body seem to have been affected, and the time required for recovery and degree of success in treatment seem to depend greatly upon the amount of muscular involvement. Romberg refers to two cases in which the muscles of respiration were affected.

The disease is generally confined to childhood, being most frequent between the ages of eight and fourteen years, and occurring oftener in girls than in boys. Dufosse and Rufz refer to 429 cases; 130 occurring in boys and 299 in girls. Watson mentions a collection of 1,029 cases, of whom 733 were females, giving a proportion of nearly 5 to 2. Dr. Watson also remarks upon the disease being most frequent among children of dark complexion, while the two authorities just alluded to, Dufosse and Rufz, give as their opinion that it is most frequent in children of light hair. In every case visiting the clinics at the College of Physicians and Surgeons of New York, and of which I have the notes, the subjects were of dark complexion. Temperature is said to exert an influence over the disease, it being according to some authors, most frequent

during the winter months, and scarcely known in the tropics. Its mean duration is from thirty to sixty days, and although it is chiefly confined to children is not entirely so. Spontaneous terminations frequently occur upon the establishment of the menses in girls and of puberty in boys. There appears to be in certain cases of unusual severity or long continuance a degree of fatuity established, but it is usually recovered from upon the subsidence of the disease.

According to Rilliet and Barthez, as quoted by Dr. Condie in his work on diseases of children: "Patients laboring under chorea, being attacked by measles, scarlatina, variola, or other acute febrile disease of childhood, the chorea will generally be diminished in intensity or entirely removed."

They state that "out of nineteen cases nine were attacked with other diseases, and eight were evidently influenced by them." M. Rufz, denies that concurrent diseases exert any influence upon the severity or duration of chorea. There is generally constipation with disordered stomach and appetite, it sometimes being defective and at others ravenous. Pain is not a common attendant upon the disease, although headache may frequently be present and sometimes tenderness along the course of the spinal cord, which is increased by pressure. "Epilepsy and hemiplegia," remarks Dr. Condie, "are not uncommon results of chorea," and in many cases falling under his notice the patients had died of tubercular meningitis. Dr. Todd states that "paralysis of a limb which has been affected by chorea is not uncommon." He also states that the sounds of the heart are often changed in chorea; a bellows sound is frequently observed, and is either aortic, systolic, dependent upon anemia, or much more frequently mitral, systolic or regurgitant.

Rheumatism and rheumatic pericarditis, have been shown by Dr. Copland to be frequent accompaniments to chorea. M. Lee, Begbei, Naim, Kirkes, Trousseau, and others point out its frequent occurrence in connection with pericardial inflammation, and internal and external rheumatism. Trousseau says that examinations into the condition of the heart, and inquiry as regards rheumatism, should always be instituted.

As regards the pathology of chorea, very little satisfactory information has been gained, and indeed in a large number of persons who have died of chorea, and upon whom autopsies have been performed, in the hope of illuminating this dark subject, no morbid changes have been found of a nature to lead to the supposition that they were in any way connected with the disease, while lesions discovered in others, such as inflammation of portions of the brain, turgescence of its vessels, with effusion of serum; hypertrophy and injection of the brain and spinal cord; turgescence of the vessels of the brain and spinal cord, with several bony plates half way up the spine upon the piamater; a concretion in the left hemisphere of the brain; a tumor pressing upon the tubercular quadrigemina, with inflammation and sanguineous effusion; ecchymosis of the membranes, and a pulpy condition of the spinal cord, and an abscess within the cerebellum, as reported by Clutterbuck, Serrs, Cox, Patterson, Roser, Willan, Copland, Monad, Hutten, Beight, Brown, Keir and Schrode, these might, I say, have exerted and doubtless did exert powerful influences over the cases in which they occurred.

The most probable theory, and one which I believe is most generally accepted at the present day is, that the disease depends upon some functional derangement in the cerebellum. Modern physiologists pretty generally agree upon the opinion first

advanced by Flourens, that the function of the cerebellum is to direct, govern and coordinate the movements of the muscular system. This being the case, then, the irregular ungoverned movements of the muscles in chorea would most decidedly and emphatically point to the cerebellum as the seat of the difficulty. Undoubtedly, the abscess of the cerebellum discovered by Schrode was the exciting cause in that instance. But even if we take it for granted that we have discovered the sedes morbi we are still left in ignorance in regard to the nature of the derangement. And there we must leave the interesting subject of the pathology of this disease, and trust that the science, which has accomplished such wonders, through the never-tiring devotion of its votaries, may yet "overturn and overturn, and overturn it," until it is laid open to the light of day.

The causes predisposing to chorea are various: Improper and indigestible articles of diet, confinement in illy ventilated apartments, with want of proper exercise; disordered digestion, etc. While the exciting causes are irritation from dentition, irritation in the stomach and alimentary canal; by worms, retained faeces, etc., anger, fright, rheumatism and injuries to the head. It is, also, singular as it appears, sometimes the result of mitation.

Some authors mention the disease as occurring epidemically in schools, and in one instance among a religious sect in Kentucky and Tennessee. The disease sometimes assumes a character different from ordinary chorea, and a number of cases of this kind are alluded to by Watson. Some keep beating measured time as if they were marching to music, others are seized with an irresistible propensity to roll over and over; others to stand on their heads, others to walk forward or backward, sometimes rapidly and in one direction, until exhausted or checked by some obstacle.

The treatment of chorea now most generally adopted is by purgatives, tonics, counter-irritants, and anti-spasmodics. The first indication is, if possible, to remove the exciting cause and it will probably be different in each individual case. Bleeding used to be employed, and it is said with good results, but it is rarely used at present, except in cases when there is much pain in the head, or along the spine, when it may be taken moderately by cups or leeches.

Purgatives should be used to unload the intestines, and the bowels should be kept open, and in a condition as near normal as possible, not allowing a day to pass without a full and free evacuation. In the early stages the mild cathartics may be employed, as the fluid extract taraxacum and senna, calomel combined with rhubarb or jalap, and followed by castor oil.

The pil. comp. cath., or ol. ric., may be required when constipation is resisting, and the bowels are in a torpid state. Spts. turpentine is highly recommended by some, either by itself, or in combination with castor oil, tr. senna, etc.

Tartarized antimony has been recommended by some in as large doses as can be borne by the stomach. In the British and Foreign Medical and Surgical Review for January, 1858, two cases are reported as being successfully treated by it. In the first case the chorea had lasted a month and was increasing in intensity. Large doses of tart. emetic were given on two successive days, and thirty hours after its first administration, all choreic movements had ceased. The chorea reappeared under a severe fit of passion, but again yielded to tartar emetic. In the second case the chorea was at first general, but immediately became partial. It resisted tonic and other

treatment for six months, but yielded to tartar emetic in twenty-eight hours. Counter-irritation is often employed, either by blisters along the spine, pustulation by croton oil, or by friction with tartar emetic ointment, this last method being considered by some good authorities as preferable. The most essential part of the treatment consists in the administration of tonics, nearly all of which, both vegetable and mineral are found serviceable. Of the vegetable tonics, the best are the different preparations of bark, and the salts of quinia. Of the minerals, the chalybeates, arsenic and zinc, are undoubtedly the most valuable. Iron may be given in form of sesquioxide, proto carbonate or sulphate, and, indeed, will be found useful in any of its forms.

The proto-carbonate of iron, gr. v.–vii., given in syrup, will often be found very useful. The zinci sulph. has a great deal of testimony in its favor; the disease yielding to it when many other medicaments have failed. Its use is generally begun in small doses, say one grain, and gradually increasing a grain at a time until the stomach will bear twelve or fifteen grains. The effects produced in individual cases must guide the practitioner, and if one tonic fails, another must be substituted and persevered in as long as any benefit accrues from its use, and so on throughout the whole catalogue, if necessary. Cimicifuga, nux vomica and iodine have been used with marked su[c]cess by some, and are highly recommended by them. Opium, belladonna, hyoscyamus, stramonium, etc., are often serviceable in quieting muscular action and producing sleep, and the same may be said in favor of chloral hydrate and chloroform, the latter being used in event of failure of the other remedies. These drugs can be considered, however, only as adjuvants to the tonics. In conjunction with these means the cold bath or sea-bathing, plenty of exercise in the open air, and a strict attention to diet will in most cases prove successful.

Electricity applied along the spine has proven in the hands of some a powerful curative agent in chorea. It should never be applied directly to affected parts, as the disease is thereby aggravated, rather than relieved, and it should not be continued after the patient is convalescent. The diet should be nourishing and easy of digestion, the food to consist of such articles as beef extract, milk, eggs, etc., the condition of each patient indicating the kind and quantity of food to be given. Gymnastic exercise is often of much good and is employed by some as the sole means of cure. After recovery care should be taken to remove all exciting causes; the bowels are to be kept free and in a soluble condition, and in short, all irritation to both mind and body are to be removed as far as it is possible to do so.

And now I wish to draw your attention more particularly to a form of the disease which exists, so far as I know, almost exclusively on the east end of Long Island. It is peculiar in itself and seems to obey certain fixed laws. In the first place, let me remark that chorea, as it is commonly known to the profession, and a description of which I have already given, is of exceedingly rare occurrence there. I do not remember a single instance occurring in my father's practice, and I have often heard him say that it was a rare disease and seldom met with by him.

The hereditary chorea, as I shall call it, is confined to certain and fortunately a few families, and has been transmitted to them, an heirloom from generations away back in the dim past. It is spoken of by those in whose veins the seeds of the disease are known to exist, with a kind of horror, and not at all alluded to except through dire necessity, when it is mentioned as "that disorder." It is attended generally by all the

symptoms of common chorea, only in an aggravated degree, hardly ever manifesting itself until adult or middle life, and then coming on gradually but surely, increasing by degrees, and often occupying years in its development, until the hapless sufferer is but a quivering wreck of his former self.

It is as common and is indeed, I believe, more common among men than women, while I am not aware that season or complexion has any influence in the matter. There are three marked peculiarities in this disease: 1. Its hereditary nature. 2. A tendency to insanity and suicide. 3. Its manifesting itself as a grave disease only in adult life.

1. Of its hereditary nature. When either or both the parents have shown manifestations of the disease, and more especially when these manifestations have been of a serious nature, one or more of the offspring almost invariably suffer from the disease, if they live to adult age. But if by any chance these children go through life without it, the thread is broken and the grandchildren and great-grandchildren of the original shakers may rest assured that they are free from the disease. This you will perceive differs from the general laws of so-called hereditary diseases, as for instance in phthisis, or syphilis, when one generation may enjoy entire immunity from their dread ravages, and yet in another you find them cropping out in all their hideousness. Unstable and whimsical as the disease may be in other respects, in this it is firm, it never skips a generation to again manifest itself in another; once having yielded its claims, it never regains them. In all the families, or nearly all in which the choreic taint exists, the nervous temperament greatly preponderates, and in my grandfather's and father's experience, which conjointly cover a period of 78 years, nervous excitement in a marked degree almost invariably attends upon every disease these people may suffer from, although they may not when in health be over nervous.

2. The tendency to insanity, and sometimes that form of insanity which leads to suicide, is marked. I know of several instances of suicide of people suffering from this form of chorea, or who belonged to families in which the disease existed. As the disease progresses the mind becomes more or less impaired, in many amounting to insanity, while in others mind and body both gradually fail until death relieves them of their sufferings. At present I know of two married men, whose wives are living, and who are constantly making love to some young lady, not seeming to be aware that there is any impropriety in it. They are suffering from chorea to such an extent that they can hardly walk, and would be thought, by a stranger, to be intoxicated. They are men of about 50 years of age, but never let an opportunity to flirt with a girl go past unimproved. The effect is ridiculous in the extreme.

3. Its third peculiarity is its coming on, at least as a grave disease, only in adult life. I do not know of a single case that has shown any marked signs of chorea before the age of thirty or forty years, while those who pass the fortieth year without symptoms of the disease, are seldom attacked. It begins as an ordinary chorea might begin, by the irregular and spasmodic action of certain muscles, as of the face, arms, etc. These movements gradually increase, when muscles hitherto unaffected take on the spasmodic action, until every muscle in the body becomes affected (excepting the involuntary ones), and the poor patient presents a spectacle which is anything but pleasing to witness. I have never known a recovery or even an amelioration of symptoms in this form of chorea; when once it begins it clings to the bitter end. No

treatment seems to be of any avail, and indeed nowadays its end is so well-known to the sufferer and his friends, that medical advice is seldom sought. It seems at least to be one of the incurables.

Dr. Wood, in his work on the practice of medicine, mentions the case of a man, in the Pennsylvania Hospital, suffering from aggravated chorea, which resisted all treatment. He finally left the hospital uncured. I strongly suspect that this man belonged to one of the families in which hereditary chorea existed. I know nothing of its pathology. I have drawn your attention to this form of chorea gentlemen, not that I considered it of any great practical importance to you, but merely as a medical curiosity, and as such it may have some interest.

6.2 Comparison of Human and Mouse Huntingtin

```
Human MATLEKLMKAFESLKSFQQQQQQQQQQQQQQQQQQQQQQPPPPPPPPPPPQLPQPPPQA 60
Mouse MATLEKLMKAFESLKSFQQQQQQQPPPQ-------------APPPPPPPPPPQPPQPPPQG 47
      ************************   *              .********** ******.

Human QPLLPQPQPPPPPPPPPPGPAVAEEPLHRPKKELSATKKDRVNHCLTICENIVAQSVRNS 120
Mouse Q----------PPPPPPPPLPGPAEEPLHRPKKELSATKKDRVNHCLTICENIVAQSLRNS 97
      *          ******* *. ***********************************:***

Human PEFQKLLGIAMELFLLCSDDAESDVRMVADECLNKVIKALMDSNLPRLQLELYKEIKKNG 180
Mouse PEFQKLLGIAMELFLLCSNDAESDVRMVADECLNKVIKALMDSNLPRLQLELYKEIKKNG 157
      ******************:****************************************

Human APRSLRAALWRFAELAHLVRPQKCRPYLVNLLPCLTRTSKRPEESVQETLAAAVPKIMAS 240
Mouse APRSLRAALWRFAELAHLVRPQKCRPYLVNLLPCLTRTSKRPEESVQETLAAAVPKIMAS 217
      ************************************************************

Human FGNFANDNEIKVLLKAFIANLKSSSPTIRRTAAGSAVSICQHSRRTQYFYSWLLNVLLGL 300
Mouse FGNFANDNEIKVLLKAFIANLKSSSPTVRRTAAGSAVSICQHSRRTQYFYNWLLNVLLGL 277
      ****************************:**********************.*********

Human LVPVEDEHSTLLILGVLLTLRYLVPLLQQQVKDTSLKGSFGVTRKEMEVSPSAEQLVQVY 360
Mouse LVPMEEEHSTLLILGVLLTLRCLVPLLQQQVKDTSLKGSFGVTRKEMEVSPSTEQLVQVY 337
      ***:*:**************** ******************************:********

Human ELTLHHTQHQDHNVVTGALELLQQLFRTPPPELLQTLTAVGGIGQLTAAKEESGGRSRSG 420
Mouse ELTLHHTQHQDHNVVTGALELLQQLFRTPPPELLQALTTPGGLGQLTLVQEEARGRGRSG 397
      ************************************:**: **:**** .:**: **.***

Human SIVELIAGGGSSCSPVLSRKQKGKVLLGEEEALEDDSESRSDVSSSALTASVKDEISGEL 480
Mouse SIVELLAGGGSSCSPVLSRKQKGKVLLGEEEALEDDSESRSDVSSSAFAASVKSEIGGEL 457
      *****:*************************************************.**.***

Human AASSGVSTPGSAGHDIITEQPRSQHTLQADSVDLASCDLTSSATDGDEEDILSHSSSQVS 540
Mouse AASSGVSTPGSVGHDIITEQPRSQHTLQADSVDLSGCDLTSAATDGDEEDILSHSSSQFS 517
      ***********.**********************:.*****:****************.*

Human AVPSDPAMDLNDGTQASSPISDSSQTTTEGPDSAVTPSDSSEIVLDGTDNQYLGLQIGQP 600
Mouse AVPSDPAMDLNDGTQASSPISDSSQTTTEGPDSAVTPSDSSEIVLDGADSQYLGMQIGQP 577
      ************************************************:*.****:******

Human QDEDEE-ATGILPDEASEAFRNSSMALQQAHLLKNMSHCRQPSDSSVDKFVLRDEATEPG 659
Mouse QEDDEEGAAGVLSGEVSDVFRNSSLALQQAHLLERMGHSRQPSDSSIDKYVTRDEVAEAS 637
      *::*** *:*:*..*.*:.*****:********:.*.*.*******:**:* ***.:*..

Human DQENKPCRIKGDIGQSTDDDSAPLVHCVRLLSASFLLTGGKNVLVPDRDVRVSVKALALS 719
Mouse DPESKPCRIKGDIGQPNDDDSAPLVHCVRLLSASFLLTGEKKALVPDRDVRVSVKALALS 697
      * *.***********..********************** *:.*****************

Human CVGAAVALHPESFFSKLYKVPLDTTEYPEEQYVSDILNYIDHGDPQVRGATAILCGTLIC 779
Mouse CIGAAVALHPESFFSRLYKVPLNTTESTEEQYVSDILNYIDHGDPQVRGATAILCGTLVY 757
      *:**************:*******:*** .******************************:

Human SILSRSRFHVGDWMGTIRTLTGNTFSLADCIPLLRKTLKDESSVTCKLACTAVRNCVMSL 839
Mouse SILSRSRLRVGDWLGNIRTLTGNTFSLVDCIPLLQKTLKDESSVTCKLACTAVRHCVLSL 817
      *******::*****:*.***********.******:********************:**:**

Human CSSSYSELGLQLIIDVLTLRNSSYWLVRTELLETLAEIDFRLVSFLEAKAENLHRGAHHY 899
Mouse CSSSYSDLGLQLLIDMLPLKNSSYWLVRTELLDTLAEIDFRLVSFLEAKAESLHRGAHHY 877
      ******:*****:**:*.*:************:******************.********

Human TGLLKLQERVLNNVVIHLLGDEDPRVRHVAAASLIRLVPKLFYKCDQGQADPVVAVARDQ 959
Mouse TGFLKLQERVLNNVVIYLLGDEDPRVRHVAATSLTRLVPKLFYKCDQGQADPVVAVARDQ 937
      **:**************:***************:** *************************
```

```
Human SSVYLKLLMHETQPPSHFSVSTITRIYRGYNLLPSITDVTMENNLSRVIAAVSHELITST 1019
Mouse SSVYLKLLMHETQPPSHFSVSTITRIYRGYSLLPSITDVTMENNLSRVVAAVSHELITST 997
      ********************************.****************:***********

Human TRALTFGCCEALCLLSTAFPVCIWSLGWHCGVPPLSASDESRKSCTVGMATMILTLLSSA 1079
Mouse TRALTFGCCEALCLLSAAFPVCTWSLGWHCGVPPLSASDESRKSCTVGMASMILTLLSSA 1057
      ****************:***** ****************************:*********

Human WFPLDLSAHQDALILAGNLLAASAPKSLRSSWASEEEANPAATKQEEVWPALGDRALVPM 1139
Mouse WFPLDLSAHQDALILAGNLLAASAPKSLRSSWTSEEEANSAATRQEEIWPALGDRTLVPL 1117
      **********************************:******.***:***:********:***:

Human VEQLFSHLLKVINICAHVLDDVAPGPAIKAALPSLTNPPSLSPIRRKGKEKEPGEQASVP 1199
Mouse VEQLFSHLLKVINICAHVLDDVTPGPAIKAALPSLTNPPSLSPIRRKGKEKEPGEQASTP 1177
      **********************:*************************************.*

Human LSPKKGSEASAASRQSDTSGPVTTSKSSSLGSFYHLPSYLKLHDVLKATHANYKVTLDLQ 1259
Mouse MSPKKVGEASAASRQSDTSGPVTASKSSSLGSFYHLPSYLKLHDVLKATHANYKVTLDLQ 1237
      :****  .*****************:*************************************

Human NSTEKFGGFLRSALDVLSQILELATLQDIGKCVEEILGYLKSCFSREPMMATVCVQQLLK 1319
Mouse NSTEKFGGFLRSALDVLSQILELATLQDIGKCVEEVLGYLKSCFSREPMMATVCVQQLLK 1297
      ************************************:************************

Human TLFGTNLASQFDGLSSNPSKSQGRAQRLGSSSVRPGLYHYCFMAPYTHFTQALADASLRN 1379
Mouse TLFGTNLASQFDGLSSNPSKSQCRAQRLGSSSVRPGLYHYCFMAPYTHFTQALADASLRN 1357
      ********************** ************************************

Human MVQAEQENDTSGWFDVLQKVSTQLKTNLTSVTKNRADKNAIHNHIRLFEPLVIKALKQYT 1439
Mouse MVQAEQERDASGWFDVLQKVSAQLKTNLTSVTKNRADKNAIHNHIRLFEPLVIKALKQYT 1417
      *******.*:***********:****************************************

Human TTTCVQLQKQVLDLLAQLVQLRVNYCLLDSDQVFIGFVLKQFEYIEVGQFRESEAIIPNI 1499
Mouse TTTSVQLQKQVLDLLAQLVQLRVNYCLLDSDQVFIGFVLKQFEYIEVGQFRESEAIIPNI 1477
      ***.*********************************************************

Human FFFLVLLSYERYHSKQIIGIPKIIQLCDGIMASGRKAVTHAIPALQPIVHDLFVLRGTNK 1559
Mouse FFFLVLLSYERYHSKQIIGIPKIIQLCDGIMASGRKAVTHAIPALQPIVHDLFVLRGTNK 1537
      ************************************************************

Human ADAGKELETQKEVVVSMLLRLIQYHQVLEMFILVLQQCHKENEDKWKRLSRQIADIILPM 1619
Mouse ADAGKELETQKEVVVSMLLRLIQYHQVLEMFILVLQQCHKENEDKWKRLSRQVADIILPM 1597
      ************************************************:*******

Human LAKQQMHIDSHEALGVLNTLFEILAPSSLRPVDMLLRSMFVTPNTMASVSTVQLWISGIL 1679
Mouse LAKQQMHIDSHEALGVLNTLFEILAPSSLRPVDMLLRSMFITPSTMASVSTVQLWISGIL 1657
      *****************************************:**.*****************

Human AILRVLISQSTEDIVLSRIQELSFSPYLISCTVINRLRDGDSTSTLEEHSEGKQIKNLPE 1739
Mouse AILRVLISQSTEDIVLCRIQELSFSPHLLSCPVINRLRGGGGNVTLGECSEGKQ-KSLPE 1716
      ****************.*********:*:**.******.*... ** * ***** *.***

Human ETFSRFLLQLVGILLEDIVTKQLKVEMSEQQHTFYCQELGTLLMCLIHIFKSGMFRRITA 1799
Mouse DTFSRFLLQLVGILLEDIVTKQLKVDMSEQQHTFYCQELGTLLMCLIHIFKSGMFRRITA 1776
      :*************************:************************************

Human AATRLFRSDGCGGSFYTLDSLNLRARSMITTHPALVLLWCQILLLVNHTDYRWWAEVQQT 1859
Mouse AATRLFTSDGCEGSFYTLESLNARVRSMVPTHPALVLLWCQILLLINHTDHRWWAEVQQT 1836
      ****** **** ******:*** *.***:.***************:*****:*********

Human PKRHSLSSTKLLSPQMSGEEEDSDLAAKLGMCNREIVRRGALILFCDYVCQNLHDSEHLT 1919
Mouse PKRHSLSCTKSLNPQKSGEEEDSGSAAQLGMCNREIVRRGALILFCDYVCQNLHDSEHLT 1896
      *******.** *.** *******. **:**********************************

Human WLIVNHIQDLISLSHEPPVQDFISAVHRNSAASGLFIQAIQSRCENLSTPTMLKKTLQCL 1979
Mouse WLIVNHIQDLISLSHEPPVQDFISAIHRNSAASGLFIQAIQSRCENLSTPTTLKKTLQCL 1956
      *************************:************************ ********
```

```
Human EGIHLSQSGAVLTLYVDRLLCTPFRVLARMVDILACRRVEMLLAANLQSSMAQLPMEELN 2039
Mouse EGIHLSQSGAVLTLYVDRLLGTPFRALARMVDTLACRRVEMLLAANLQSSMAQLPEEELN 2016
      ********************* ****.****** ********************** ****

Human RIQEYLQSSGLAQRHQRLYSLLDRFRLSTMQDSLSPSPPVSSHPLDGDGHVSLETVSPDK 2099
Mouse RIQEHLQNSGLAQRHQRLYSLLDRFRLSTVQDSLSPLPPVTSHPLDGDGHTSLETVSPDK 2076
      ****:**.**********************:****** ***:*********.*********

Human DWYVHLVKSQCWTRSDSALLEGAELVNRIPAEDMNAFMMNSEFNLSLLAPCLSLGMSEIS 2159
Mouse DWYLQLVRSQCWTRSDSALLEGAELVNRIPAEDMNDFMMSSEFNLSLLAPCLSLGMSEIA 2136
      ***:**:***************************** ***.******************:

Human GGQKSALFEAAREVTLARVSGTVQQLPAVHHVFQPELPAEPAAYWSKLNDLFGDAALYQS 2219
Mouse NGQKSPLFEAARGVILNRVTSVVQQLPAVHQVFQPFLPIEPTAYWNKLNDLLGDTTSYQS 2196
      .****.****** * * **:.********:**** ** **:***.*****:**:: ***

Human LPTLARALAQYLVVVSKLPSHLHLPPEKEKDIVKFVVATLEALSWHLIHEQIPLSLDLQA 2279
Mouse LTILARALAQYLVVLSKVPAHLHLPPEKEGDTVKFVVMTVEALSWHLIHEQIPLSLDLQA 2256
      *. ***********:**:*:********* * ***** *:********************

Human GLDCCCLALQLPGLWSVVSSTEFVTHACSLIYCVHFILEAVAVQPGEQLLSPERRTNTPK 2339
Mouse GLDCCCLALQVPGLWGVLSSPEYVTHACSLIHCVRFILEAIAVQPGDQLLGPESRSHTPR 2316
      **********:****.*:**.*:********:**:*****:*****:***.** *::**:

Human AISEEEEEVDPNTQNPKYITAACEMVAEMVESLQSVLALGHKRNSGVPAFLTPLLRNIII 2399
Mouse AVRKEE--VDSDIQNLSHVTSACEMVADMVESLQSVLALGHKRNSTLPSFLTAVLKNIVI 2374
      *: :**  **.: ** .:::*******:****************** :*:***.:*:**:*

Human SLARLPLVNSYTRVPPLVWKLGWSPKPGGDFGTAFPEIPVEFLQEKEVFKEFIYRINTLG 2459
Mouse SLARLPLVNSYTRVPPLVWKLGWSPKPGGDFGTVFPEIPVEFLQEKEILKEFIYRINTLG 2434
      ***********************************.************::************

Human WTSRTQFEETWATLLGVLVTQPLVMEQEESPPEEDTERTQINVLAVQAITSLVLSAMTVP 2519
Mouse WTNRTQFEETWATLLGVLVTQPLVMEQEESPPEEDTERTQIHVLAVQAITSLVLSAMTVP 2494
      **.*************************************:******************

Human VAGNPAVSCLEQQPRNKPLKALDTRFGRKLSIIRGIVEQEIQAMVSKRENIATHHLYQAW 2579
Mouse VAGNPAVSCLEQQPRNKPLKALDTRFGRKLSMIRGIVEQEIQEMVSQRENTATHHSHQAW 2554
      **********************************:********** ***:*** **** :***

Human DPVPSLSPATTGALISHEKLLLQINPERELGSMSYKLGQVSIHSVWLGNSITPLREEEWD 2639
Mouse DPVPSLLPATTGALISHDKLLLQINPEREPGNMSYKLGQVSIHSVWLGNNITPLREEEWD 2614
      ****** **********:*********** *.*****************.**********

Human EEEEEEADAPAPSSPPTSPVNSRKHRAGVDIHSCSQFLLELYSRWILPSSSARRTPAILI 2699
Mouse EEEEEESDVPAPTSPPVSPVNSRKHRAGVDIHSCSQFLLELYSRWILPSSAARRTPVILI 2674
      ******:*.***:***.**********************************:*****.***

Human SEVVRSLLVVSDLFTERNQFELMYVTLTELRRVHPSEDEILAQYLVPATCKAAAVLGMDK 2759
Mouse SEVVRSLLVVSDLFTERTQFEMMYLTLTELRRVHPSEDEILIQYLVPATCKAAAVLGMDK 2734
      *****************.***:**:**************** ******************

Human AVAEPVSRLLESTLRSSHLPSRVGALHGVLYVLECDLLDDTAKQLIPVISDYLLSNLKGI 2819
Mouse TVAEPVSRLLESTLRSSHLPSQIGALHGILYVLECDLLDDTAKQLIPVVSDYLLSNLKGI 2794
      :**********************:::*****:*********************:***********

Human AHCVNIHSQQHVLVMCATAFYLIENYPLDVGPEFSASIIQMCGVMLSGSEESTPSIIYHC 2879
Mouse AHCVNIHSQQHVLVMCATAFYLMENYPLDVGPEFSASVIQMCGVMLSGSEESTPSIIYHC 2854
      **********************:**************:**********************

Human ALRGLERLLLSEQLSRLDAESLVKLSVDRVNVHSPHRAMAALGLMLTCMYTGKEKVSPGR 2939
Mouse ALRGLERLLLSEQLSRLDTESLVKLSVDRVNVQSPHRAMAALGLMLTCMYTGKEKASPGR 2914
      ******************:*************:**********************.****

Human TSDPNPAAPDSESVIVAMERVSVLFDRIRKGFPCEARVVARILPQFLDDFFPPQDIMNKV 2999
Mouse ASDPSPATPDSESVIVAMERVSVLFDRIRKGFPCEARVVARILPQFLDDFFPPQDVMNKV 2974
      :****.**:**************************************************:****
```

```
Human IGEFLSNQQPYPQFMATVVYKVFQTLHSTGQSSMVRDWVMLSLSNFTQRAPVAMATWSLS 3059
Mouse IGEFLSNQQPYPQFMATVVYKVFQTLHSAGQSSMVRDWVMLSLSNFTQRTPVAMAMWSLS 3034
      ****************************:******************:***** ****

Human CFFVSASTSPWVAAILPHVISRMGKLEQVDVNLFCLVATDFYRHQIEEELDRRAFQSVLE 3119
Mouse CFLVSASTSPWVSAILPHVISRMGKLEQVDVNLFCLVATDFYRHQIEEEFDRRAFQSVFE 3094
      **:*********:****************************************:*********:*

Human VVAAPGSPYHRLLTCLRNVHKVTTC 3144
Mouse VVAAPGSPYHRLLACLQNVHKVTTC 3119
      *************:**:********
```

91% homology

Amino Acid Code

G	Glycine (Gly)	**W**	Tryptophan (Trp)
P	Proline (Pro)	**H**	Histidine (His)
A	Alanine (Ala)	**K**	Lysine (Lys)
V	Valine (Val)	**R**	Arginine (Arg)
L	Leucine (Leu)	**Q**	Glutamine (Gln)
I	Isoleucine (Ile)	**N**	Asparagine (Asn)
M	Methionine (Met)	**E**	Glutamic Acid (Glu)
C	Cysteine (Cys)	**D**	Aspartic Acid (Asp)
F	Phenylalanine (Phe)	**S**	Serine (Ser)
Y	Tyrosine (Tyr)	**T**	Threonine (Thr)

Amino Acid Property Code

RED	Small, hydrophobic side-chains
GREEN	Polar, hydrophilic side-chains
BLUE	Acidic side-chains
MAGENTA	Basic side-chains

Homology Analysis Code

*	exact match
:	high similarity
.	low similarity

Produced using PubMed protein database sequences and *Clustal W* (European Bioinformatics Institute).

6.3 *Primary Antibodies*

Raised Against	Raised In	Tested Species Specificity	Manufacturer
AIF	Goat	**Human**, mouse, rat	Santa Cruz
Apaf-1 (N-19)	Goat	**Human**, mouse, rat	Santa Cruz
Apaf-1	Rabbit	**Human**, mouse, rat	Santa Cruz
Bcl-2 (C-21)	Rabbit	**Human**, mouse, rat	Santa Cruz
Bcl-2 (N-19)	Rabbit	**Human**, mouse, rat	Santa Cruz
Caspase-1 p10	Rabbit	Human, **mouse**, rat	Santa Cruz
Caspase-1 p20	Rabbit	**Mouse**, rat	Santa Cruz
Caspase-2	Goat	**Mouse**	Santa Cruz
Caspase-3 (cleaved)	Rabbit	**Human**, mouse, rat	New England Biolabs
Caspase-3 (cleaved)(CM1)	Rabbit	**Human,** mouse	Idun Pharmaceuticals
Caspase-6 (cleaved)	Rabbit	**Human**, mouse, rat	Cell Signalling Technology
Caspase-7 (cleaved)	Rabbit	**Human**, mouse, rat	Cell Signalling Technology
Caspase-7 (cleaved)	Rabbit	**Human**, rat	New England Biolabs
Caspase-8	Rabbit	Human, mouse, rat	Santa Cruz
Caspase-9 (cleaved)	Rabbit	**Human,** rat	New England Biolabs
Caspase-9 (cleaved)	Rabbit	**Human**	Cell Signalling Technology
Caspase-9 p10	Rabbit	**Human**, mouse, rat	Santa Cruz
Cytochrome c (H-104)	Rabbit	**Human**, mouse, rat	Santa Cruz
Cytochrome c (Ab-5)	Mouse	**Human,** mouse, rat	NeoMarkers
DFF40 / CAD	Rabbit	Human, **mouse**, rat	Bioquote
DFF45 / ICAD (cleaved)	Rabbit	**Human,** mouse, rat	Cell Signalling Technology
PARP (cleaved)	Rabbit	**Mouse**	Cell Signalling Technology
PARP (cleaved)	Rabbit	**Human**	New England Biolabs
Huntingtin N-terminus	Goat	**Human**, mouse	Santz Cruz
Huntingtin C-terminus	Goat	**Human,** mouse	Santa Cruz
Ubiquitin	Rabbit	**Human**, mouse	DAKO
GFAP	Rabbit	**Cow,** mouse	DAKO
F4/80	Rat	**Mouse**	Serotec
NG2	Rabbit	Mouse	*Gift*

Species specificity **bold** text indicates the species of protein against which the antibody was raised.

References

7 References

Agashe, V.R. & Hartl, F.U. *Roles of molecular chaperones in cytoplasmic protein folding.* Semin Cell Dev Biol 11 15-25 (**2000**).

Ahlberg, J., Marzella, L. & Glaumann, H. *Uptake and degradation of proteins by isolated rat liver lysosomes. Suggestion of a microautophagic pathway of proteolysis.* Lab Invest 47 523-532 (**1982**).

Albin, R.L. & Tagle, D.A. *Genetics and molecular biology of Huntington's disease.* Trends Neurosci 18 11-14 (**1995**).

Albin, R.L., Young, A.B., Penney, J.B., Handelin, B., Balfour, R., Anderson, K.D., Markel, D.S., Tourtellotte, W.W. & Reiner, A. *Abnormalities of striatal projection neurons and N-methyl-D-aspartate receptors in presymptomatic Huntington's disease.* N Engl J Med 322 1293-1298 (**1990**).

Ambrose, C.M., Duyao, M.P., Barnes, G., Bates, G.P., Lin, C.S., Srinidhi, J., Baxendale, S., Hummerich, H., Lehrach, H., Altherr, M. & et al. *Structure and expression of the Huntington's disease gene: evidence against simple inactivation due to an expanded CAG repeat.* Somat Cell Mol Genet 20 27-38 (**1994**).

Auerbach, W., Hurlbert, M.S., Hilditch-Maguire, P., Wadghiri, Y.Z., Wheeler, V.C., Cohen, S.I., Joyner, A.L., MacDonald, M.E. & Turnbull, D.H. *The HD mutation causes progressive lethal neurological disease in mice expressing reduced levels of huntingtin.* Hum Mol Genet 10 2515-2523. (**2001**).

Baba, M., Osumi, M., Scott, S.V., Klionsky, D.J. & Ohsumi, Y. *Two distinct pathways for targeting proteins from the cytoplasm to the vacuole/lysosome.* J Cell Biol 139 1687-1695 (**1997**).

Ballard, F.J., Knowles, S.E., Wong, S.S., Bodner, J.B., Wood, C.M. & Gunn, J.M. *Inhibition of protein breakdown in cultured cells is a consistent response to growth factors.* FEBS Lett 114 209-212 (**1980**).

Bao, J., Sharp, A.H., Wagster, M.V., Becher, M., Schilling, G., Ross, C.A., Dawson, V.L. & Dawson, T.M. *Expansion of polyglutamine repeat in huntingtin leads to abnormal protein interactions involving calmodulin.* Proc Natl Acad Sci U S A 93 5037-5042 (**1996**).

Barker, R.A. & Rosser, A.E. *Neural transplantation therapies for Parkinson's and Huntington's diseases.* Drug Discov Today 6 575-582 (**2001**).

Barnes, G.T., Duyao, M.P., Ambrose, C.M., McNeil, S., Persichetti, F., Srinidhi, J., Gusella, J.F. & MacDonald, M.E. *Mouse Huntington's disease gene homolog (Hdh).* Somat Cell Mol Genet 20 87-97 (**1994**).

Bates, G.P. *Huntington's disease. Exploiting expression.* Nature 413 691, 693-694. (**2001**).

Bauvy, C., Gane, P., Arico, S., Codogno, P. & Ogier-Denis, E. *Autophagy delays sulindac sulfide-induced apoptosis in the human intestinal colon cancer cell line HT-29.* Exp Cell Res 268 139-149 (**2001**).

Beal, M.F., Ferrante, R.J., Swartz, K.J. & Kowall, N.W. *Chronic quinolinic acid lesions in rats closely resemble Huntington's disease.* J Neurosci 11 1649-1659 (**1991**).

Beal, M.F. & Hantraye, P. *Novel therapies in the search for a cure for Huntington's disease.* Proc Natl Acad Sci U S A 98 3-4 (**2001**).

Beaulaton, J. & Lockshin, R.A. *The relation of programmed cell death to development and reproduction: comparative studies and an attempt at classification.* Int Rev Cytol 79 215-235 (**1982**).

Becher, M.W., Kotzuk, J.A., Sharp, A.H., Davies, S.W., Bates, G.P., Price, D.L. & Ross, C.A. *Intranuclear neuronal inclusions in Huntington's disease and dentatorubral and pallidoluysian atrophy: correlation between the density of inclusions and IT15 CAG triplet repeat length.* Neurobiol Dis 4 387-397 (**1998**).

Becker, J. & Craig, E.A. *Heat-shock proteins as molecular chaperones.* Eur J Biochem 219 11-23 (**1994**).

Beere, H.M., Wolf, B.B., Cain, K., Mosser, D.D., Mahboubi, A., Kuwana, T., Tailor, P., Morimoto, R.I., Cohen, G.M. & Green, D.R. *Heat-shock protein 70 inhibits apoptosis by preventing recruitment of procaspase-9 to the Apaf-1 apoptosome.* Nat Cell Biol 2 469-475 (**2000**).

Benitez, J., Robledo, M., Ramos, C., Ayuso, C., Astarloa, R., Garcia Yebenes, J. & Brambati, B. *Somatic stability in chorionic villi samples and other Huntington fetal tissues.* Hum Genet 96 229-232 (**1995**).

Blommaart, E.F., Luiken, J.J. & Meijer, A.J. *Autophagic proteolysis: control and specificity.* Histochem J 29 365-385 (**1997**).

Borner, C. & Monney, L. *Apoptosis without caspases: an inefficient molecular guillotine?* Cell Death Differ 6 497-507 (**1999**).

Borner, C., Monney, L., Olivier, R., Rosse, T., Hacki, J. & Conus, S. *Life and death in a medieval atmosphere.* Cell Death Differ 6 201-206 (**1999**).

Botto, M., Dell'Agnola, C., Bygrave, A.E., Thompson, E.M., Cook, H.T., Petry, F., Loos, M., Pandolfi, P.P. & Walport, M.J. *Homozygous C1q deficiency causes glomerulonephritis associated with multiple apoptotic bodies.* Nat Genet 19 56-59 (**1998**).

Boutell, J.M., Thomas, P., Neal, J.W., Weston, V.J., Duce, J., Harper, P.S. & Jones, A.L. *Aberrant interactions of transcriptional repressor proteins with the Huntington's disease gene product, huntingtin.* Hum Mol Genet 8 1647-1655 (**1999**).

Boutell, J.M., Wood, J.D., Harper, P.S. & Jones, A.L. *Huntingtin interacts with cystathionine beta-synthase.* Hum Mol Genet 7 371-378 (**1998**).

Braun, B.C., Glickman, M., Kraft, R., Dahlmann, B., Kloetzel, P.M., Finley, D. & Schmidt, M. *The base of the proteasome regulatory particle exhibits chaperone-like activity.* Nat Cell Biol 1 221-226 (**1999**).

Brinkman, R.R., Mezei, M.M., Theilmann, J., Almqvist, E. & Hayden, M.R. *The likelihood of being affected with Huntington disease by a particular age, for a specific CAG size.* Am J Hum Genet 60 1202-1210 (**1997**).

Brook, J.D., McCurrach, M.E., Harley, H.G., Buckler, A.J., Church, D., Aburatani, H., Hunter, K., Stanton, V.P., Thirion, J.P., Hudson, T. & et al. *Molecular basis of myotonic dystrophy: expansion of a trinucleotide (CTG) repeat at the 3' end of a transcript encoding a protein kinase family member.* Cell 68 799-808 (**1992**).

Brorson, J.R., Marcuccilli, C.J. & Miller, R.J. *Delayed antagonism of calpain reduces excitotoxicity in cultured neurons.* Stroke 26 1259-1266; discussion 1267 (**1995**).

Bruey, J.M., Ducasse, C., Bonniaud, P., Ravagnan, L., Susin, S.A., Diaz-Latoud, C., Gurbuxani, S., Arrigo, A.P., Kroemer, G., Solary, E. & Garrido, C. *Hsp27 negatively regulates cell death by interacting with cytochrome c.* Nat Cell Biol 2 645-652 (**2000**).

Bucciantini, M., Giannoni, E., Chiti, F., Baroni, F., Formigli, L., Zurdo, J., Taddei, N., Ramponi, G., Dobson, C.M. & Stefani, M. *Inherent toxicity of aggregates implies a common mechanism for protein misfolding diseases.* Nature 416 507-511 (**2002**).

Burke, J.R., Enghild, J.J., Martin, M.E., Jou, Y.S., Myers, R.M., Roses, A.D., Vance, J.M. & Strittmatter, W.J. *Huntingtin and DRPLA proteins selectively interact with the enzyme GAPDH.* Nat Med 2 347-350 (**1996**).

Burright, E.N., Clark, H.B., Servadio, A., Matilla, T., Feddersen, R.M., Yunis, W.S., Duvick, L.A., Zoghbi, H.Y. & Orr, H.T. *SCA1 transgenic mice: a model for neurodegeneration caused by an expanded CAG trinucleotide repeat.* Cell 82 937-948 (**1995**).

Bursch, W. *The autophagosomal-lysosomal compartment in programmed cell death.* Cell Death Differ 8 569-581 (**2001**).

Bursch, W., Ellinger, A., Gerner, C., Frohwein, U. & Schulte-Hermann, R. *Programmed cell death (PCD). Apoptosis, autophagic PCD, or others?* Ann N Y Acad Sci 926 1-12 (**2000a**).

Bursch, W., Hochegger, K., Torok, L., Marian, B., Ellinger, A. & Hermann, R.S. *Autophagic and apoptotic types of programmed cell death exhibit different fates of cytoskeletal filaments.* J Cell Sci 113 (Pt 7) 1189-1198 (**2000b**).

Calabresi, P., Centonze, D., Pisani, A., Sancesario, G., Gubellini, P., Marfia, G.A. & Bernardi, G. *Striatal spiny neurons and cholinergic interneurons express differential ionotropic glutamatergic responses and vulnerability: implications for ischemia and Huntington's disease.* Ann Neurol 43 586-597 (**1998**).

Caputo, C.B., Fraser, P.E., Sobel, I.E. & Kirschner, D.A. *Amyloid-like properties of a synthetic peptide corresponding to the carboxy terminus of beta-amyloid protein precursor.* Arch Biochem Biophys 292 199-205 (**1992**).

Caramins, M., Halliday, G., McCusker, E. & Trent, R.J. *Genetically confirmed clinical Huntington's disease with no observable cell loss.* J Neurol Neurosurg Psychiatry 74 968-970 (**2003**).

Cattaneo, E., Rigamonti, D., Goffredo, D., Zuccato, C., Squitieri, F. & Sipione, S. *Loss of normal huntingtin function: new developments in Huntington's disease research.* Trends Neurosci 24 182-188 (**2001**).

Cepeda, C., Ariano, M.A., Calvert, C.R., Flores-Hernandez, J., Chandler, S.H., Leavitt, B.R., Hayden, M.R. & Levine, M.S. *NMDA receptor function in mouse models of Huntington disease.* J Neurosci Res 66 525-539. (**2001a**).

Cepeda, C., Hurst, R.S., Calvert, C.R., Hernandez-Echeagaray, E., Nguyen, O.K., Jocoy, E., Christian, L.J., Ariano, M.A. & Levine, M.S. *Transient and progressive electrophysiological alterations in the corticostriatal pathway in a mouse model of Huntington's disease.* J Neurosci 23 961-969 (**2003**).

Cepeda, C., Itri, J.N., Flores-Hernandez, J., Hurst, R.S., Calvert, C.R. & Levine, M.S. *Differential sensitivity of medium- and large-sized striatal neurons to NMDA but not kainate receptor activation in the rat.* Eur J Neurosci 14 1577-1589 (**2001b**).

Cha, J.H., Frey, A.S., Alsdorf, S.A., Kerner, J.A., Kosinski, C.M., Mangiarini, L., Penney, J.B., Jr., Davies, S.W., Bates, G.P. & Young, A.B. *Altered neurotransmitter receptor expression in transgenic mouse models of Huntington's disease.* Philos Trans R Soc Lond B Biol Sci 354 981-989. (**1999**).

Chai, J., Du, C., Wu, J.W., Kyin, S., Wang, X. & Shi, Y. *Structural and biochemical basis of apoptotic activation by Smac/DIABLO.* Nature 406 855-862 (**2000**).

Chan, E.Y., Nasir, J., Gutekunst, C.A., Coleman, S., Maclean, A., Maas, A., Metzler, M., Gertsenstein, M., Ross, C.A., Nagy, A. & Hayden, M.R. *Targeted disruption of Huntingtin-associated protein-1 (Hap1) results in postnatal death due to depressed feeding behavior.* Hum Mol Genet 11 945-959 (**2002**).

Chan, S.L. & Mattson, M.P. *Caspase and calpain substrates: roles in synaptic plasticity and cell death.* J Neurosci Res 58 167-190 (**1999**).

Chang, C.M., Yu, Y.L., Fong, K.Y., Wong, M.T., Chan, Y.W., Ng, T.H., Leung, C.M. & Chan, V. *Huntington's disease in Hong Kong Chinese: epidemiology and clinical picture.* Clin Exp Neurol 31 43-51 (**1994**).

Chen, M., Ona, V.O., Li, M., Ferrante, R.J., Fink, K.B., Zhu, S., Bian, J., Guo, L., Farrell, L.A., Hersch, S.M., Hobbs, W., Vonsattel, J.P., Cha, J.H. & Friedlander, R.M. *Minocycline inhibits caspase-1 and caspase-3 expression and delays mortality in a transgenic mouse model of Huntington disease.* Nat Med 6 797-801 (**2000**).

Cheramy, A., Barbeito, L., Godeheu, G. & Glowinski, J. *Riluzole inhibits the release of glutamate in the caudate nucleus of the cat in vivo.* Neurosci Lett 147 209-212 (**1992**).

Choi, D.W. *Glutamate neurotoxicity and diseases of the nervous system.* Neuron 1 623-634 (**1988**).

Christensen, H. & Pain, R.H. *Molten globule intermediates and protein folding.* Eur Biophys J 19 221-229 (**1991**).

Chu-LaGraff, Q., Kang, X. & Messer, A. *Expression of the Huntington's disease transgene in neural stem cell cultures from R6/2 transgenic mice.* Brain Res Bull 56 307-312. (**2001**).

Chuang, J.Z., Zhou, H., Zhu, M., Li, S.H., Li, X.J. & Sung, C.H. *Characterization of a brain-enriched chaperone, MRJ, that inhibits Huntingtin aggregation and toxicity independently.* J Biol Chem 14 14 (**2002**).

Chun, W., Lesort, M., Lee, M. & Johnson, G.V. *Mutant huntingtin aggregates do not sensitize cells to apoptotic stressors.* FEBS Lett 515 61-65 (**2002**).

Chun, W., Lesort, M., Tucholski, J., Ross, C.A. & Johnson, G.V. *Tissue transglutaminase does not contribute to the formation of mutant huntingtin aggregates.* J Cell Biol 153 25-34 (**2001**).

Clarke, P.G. *Developmental cell death: morphological diversity and multiple mechanisms.* Anat Embryol (Berl) 181 195-213 (**1990**).

Codogno, P., Ogier-Denis, E. & Houri, J.J. *Signal transduction pathways in macroautophagy.* Cell Signal 9 125-130 (**1997**).

Concannon, C.G., Gorman, A.M. & Samali, A. *On the role of Hsp27 in regulating apoptosis.* Apoptosis 8 61-70 (**2003**).

Concannon, C.G., Orrenius, S. & Samali, A. *Hsp27 inhibits cytochrome c-mediated caspase activation by sequestering both pro-caspase-3 and cytochrome c.* Gene Expr 9 195-201 (**2001**).

Conradt, B. *Cell engulfment, no sooner ced than done.* Dev Cell 1 445-447 (**2001**).

Conradt, B. *With a little help from your friends: cells don't die alone.* Nat Cell Biol 4 E139-143 (**2002**).

Conway, K.A., Harper, J.D. & Lansbury, P.T. *Accelerated in vitro fibril formation by a mutant alpha-synuclein linked to early-onset Parkinson disease.* Nat Med 4 1318-1320 (**1998**).

Conway, K.A., Lee, S.J., Rochet, J.C., Ding, T.T., Williamson, R.E. & Lansbury, P.T., Jr. *Acceleration of oligomerization, not fibrillization, is a shared property of both alpha-synuclein mutations linked to early-onset Parkinson's disease: implications for pathogenesis and therapy.* Proc Natl Acad Sci U S A 97 571-576 (**2000**).

Cooper, J.K., Schilling, G., Peters, M.F., Herring, W.J., Sharp, A.H., Kaminsky, Z., Masone, J., Khan, F.A., Delanoy, M., Borchelt, D.R., Dawson, V.L., Dawson, T.M. & Ross, C.A. *Truncated N-terminal fragments of huntingtin with expanded glutamine repeats form nuclear and cytoplasmic aggregates in cell culture.* Hum Mol Genet 7 783-790 (**1998**).

Craig, E.A., Gambill, B.D. & Nelson, R.J. *Heat shock proteins: molecular chaperones of protein biogenesis.* Microbiol Rev 57 402-414 (**1993**).

Craufurd, D., Thompson, J.C. & Snowden, J.S. *Behavioral changes in Huntington Disease.* Neuropsychiatry Neuropsychol Behav Neurol 14 219-226. (**2001**).

Critchley, M. *Great Britain and the Early History of Huntington's Chorea.* In "Huntington's Chorea" Raven Press, NY (**1973**).

Cuervo, A.M. & Dice, J.F. *A receptor for the selective uptake and degradation of proteins by lysosomes.* Science 273 501-503 (**1996**).

Cummings, C.J., Mancini, M.A., Antalffy, B., DeFranco, D.B., Orr, H.T. & Zoghbi, H.Y. *Chaperone suppression of aggregation and altered subcellular proteasome localization imply protein misfolding in SCA1.* Nat Genet 19 148-154 (**1998**).

Davies, S. & Ramsden, D.B. *Huntington's disease.* Mol Pathol 54 409-413 (**2001**).

Davies, S.W., Beardsall, K., Turmaine, M., DiFiglia, M., Aronin, N. & Bates, G.P. *Are neuronal intranuclear inclusions the common neuropathology of triplet-repeat disorders with polyglutamine-repeat expansions?* Lancet 351 131-133. (**1998**).

Davies, S.W. & Roberts, P.J. *No evidence for preservation of somatostatin-containing neurons after intrastriatal injections of quinolinic acid.* Nature 327 326-329 (**1987**).

Davies, S.W., Turmaine, M., Cozens, B.A., DiFiglia, M., Sharp, A.H., Ross, C.A., Scherzinger, E., Wanker, E.E., Mangiarini, L. & Bates, G.P. *Formation of neuronal intranuclear inclusions underlies the neurological dysfunction in mice transgenic for the HD mutation.* Cell 90 537-548. (**1997**).

Davies, S.W., Turmaine, M., Cozens, B.A., Raza, A.S., Mahal, A., Mangiarini, L. & Bates, G.P. *From neuronal inclusions to neurodegeneration: neuropathological investigation of a transgenic mouse model of Huntington's disease.* Philos Trans R Soc Lond B Biol Sci 354 981-989. (**1999**).

de la Monte, S.M., Vonsattel, J.P. & Richardson, E.P., Jr. *Morphometric demonstration of atrophic changes in the cerebral cortex, white matter, and neostriatum in Huntington's disease.* J Neuropathol Exp Neurol 47 516-525 (**1988**).

De Rooij, K.E., De Koning Gans, P.A., Roos, R.A., Van Ommen, G.J. & Den Dunnen, J.T. *Somatic expansion of the (CAG)n repeat in Huntington disease brains.* Hum Genet 95 270-274 (**1995**).

Dedeoglu, A., Kubilus, J.K., Jeitner, T.M., Matson, S.A., Bogdanov, M., Kowall, N.W., Matson, W.R., Cooper, A.J., Ratan, R.R., Beal, M.F., Hersch, S.M. & Ferrante, R.J. *Therapeutic effects of cystamine in a murine model of Huntington's disease.* J Neurosci 22 8942-8950 (**2002**).

Deveraux, Q.L. & Reed, J.C. *IAP family proteins--suppressors of apoptosis.* Genes Dev 13 239-252 (**1999**).

Dice, J.F. *Selective degradation of cytosolic proteins by lysosomes.* Ann N Y Acad Sci 674 58-64 (**1992**).

Dice, J.F., Backer, J.M., Chiang, H.L. & Goff, S.A. *Lysosomal degradation of microinjected proteins.* Biochem Soc Trans 15 824-826 (**1987**).

Dice, J.F., Terlecky, S.R., Chiang, H.L., Olson, T.S., Isenman, L.D., Short-Russell, S.R., Freundlieb, S. & Terlecky, L.J. *A selective pathway for degradation of cytosolic proteins by lysosomes.* Semin Cell Biol 1 449-455 (**1990**).

Diez-Roux, G. & Lang, R.A. *Macrophages induce apoptosis in normal cells in vivo.* Development 124 3633-3638 (**1997**).

DiFiglia, M., Sapp, E., Chase, K., Schwarz, C., Meloni, A., Young, C., Martin, E., Vonsattel, J.P., Carraway, R., Reeves, S.A. & et al. *Huntingtin is a cytoplasmic protein associated with vesicles in human and rat brain neurons.* Neuron 14 1075-1081 (**1995**).

DiFiglia, M., Sapp, E., Chase, K.O., Davies, S.W., Bates, G.P., Vonsattel, J.P. & Aronin, N. *Aggregation of huntingtin in neuronal intranuclear inclusions and dystrophic neurites in brain.* Science 277 1990-1993. (**1997**).

Ding, Q., Lewis, J.J., Strum, K.M., Dimayuga, E., Bruce-Keller, A.J., Dunn, J.C. & Keller, J.N. *Polyglutamine expansion, protein aggregation, proteasome activity, and neural survival.* J Biol Chem 277 13935-13942 (**2002**).

Dragunow, M., Faull, R.L., Lawlor, P., Beilharz, E.J., Singleton, K., Walker, E.B. & Mee, E. *In situ evidence for DNA fragmentation in Huntington's disease striatum and Alzheimer's disease temporal lobes.* Neuroreport 6 1053-1057 (**1995**).

Duan, W., Guo, Z., Jiang, H., Ware, M., Li, X.J. & Mattson, M.P. *Dietary restriction normalizes glucose metabolism and BDNF levels, slows disease progression, and increases survival in huntingtin mutant mice.* Proc Natl Acad Sci U S A (**2003**).

Duffield, J.S., Erwig, L.P., Wei, X., Liew, F.Y., Rees, A.J. & Savill, J.S. *Activated macrophages direct apoptosis and suppress mitosis of mesangial cells.* J Immunol 164 2110-2119 (**2000**).

Duisterhof, M., Trijsburg, R.W., Niermeijer, M.F., Roos, R.A. & Tibben, A. *Psychological studies in Huntington's disease: making up the balance.* J Med Genet 38 852-861. (**2001**).

Duyao, M.P., Auerbach, A.B., Ryan, A., Persichetti, F., Barnes, G.T., McNeil, S.M., Ge, P., Vonsattel, J.P., Gusella, J.F., Joyner, A.L. & et al. *Inactivation of the mouse Huntington's disease gene homolog Hdh.* Science 269 407-410 (**1995**).

Dyer, R.B. & McMurray, C.T. *Mutant protein in Huntington disease is resistant to proteolysis in affected brain.* Nat Genet 29 270-278. (**2001**).

Earnshaw, W.C., Martins, L.M. & Kaufmann, S.H. *Mammalian caspases: structure, activation, substrates, and functions during apoptosis.* Annu Rev Biochem 68 383-424 (**1999**).

Edwardson, J.M., Wang, C.T., Gong, B., Wyttenbach, A., Bai, J., Jackson, M.B., Chapman, E.R. & Morton, A.J. *Expression of mutant huntingtin blocks exocytosis in PC12 cells by depletion of complexin II.* J Biol Chem 278 30849-30853 (**2003**).

Ellerby, L.M. *Hunting for Excitement. NMDA Receptors in Huntington's Disease.* Neuron 33 841-842. (**2002**).

Elliotson, J. *St Vitus's Dance.* Lancet I 162 - 165 (**1832**).

Engelender, S., Sharp, A.H., Colomer, V., Tokito, M.K., Lanahan, A., Worley, P., Holzbaur, E.L. & Ross, C.A. *Huntingtin-associated protein 1 (HAP1) interacts with the p150Glued subunit of dynactin.* Hum Mol Genet 6 2205-2212 (**1997**).

Faber, P.W., Barnes, G.T., Srinidhi, J., Chen, J., Gusella, J.F. & MacDonald, M.E. *Huntingtin interacts with a family of WW domain proteins.* Hum Mol Genet 7 1463-1474 (**1998**).

Fadok, V.A., Bratton, D.L., Frasch, S.C., Warner, M.L. & Henson, P.M. *The role of phosphatidylserine in recognition of apoptotic cells by phagocytes.* Cell Death Differ 5 551-562 (**1998a**).

Fadok, V.A., McDonald, P.P., Bratton, D.L. & Henson, P.M. *Regulation of macrophage cytokine production by phagocytosis of apoptotic and post-apoptotic cells.* Biochem Soc Trans 26 653-656 (**1998b**).

Ferluga, J. *Possible organ and age-related epigenetic factors in Huntington's disease and colorectal carcinoma.* Med Hypotheses 29 51-54 (**1989**).

Ferrante, R.J., Gutekunst, C.A., Persichetti, F., McNeil, S.M., Kowall, N.W., Gusella, J.F., MacDonald, M.E., Beal, M.F. & Hersch, S.M. *Heterogeneous topographic and cellular distribution of huntingtin expression in the normal human neostriatum.* J Neurosci 17 3052-3063 (**1997**).

Ferrante, R.J., Kowall, N.W., Cipolloni, P.B., Storey, E. & Beal, M.F. *Excitotoxin lesions in primates as a model for Huntington's disease: histopathologic and neurochemical characterization.* Exp Neurol 119 46-71 (**1993**).

Ferrer, I., Goutan, E., Marin, C., Rey, M.J. & Ribalta, T. *Brain-derived neurotrophic factor in Huntington disease.* Brain Res 866 257-261 (**2000**).

Figueredo-Cardenas, G., Anderson, K.D., Chen, Q., Veenman, C.L. & Reiner, A. *Relative survival of striatal projection neurons and interneurons after intrastriatal injection of quinolinic acid in rats.* Exp Neurol 129 37-56 (**1994**).

Friedlander, R.M. *Apoptosis and caspases in neurodegenerative diseases.* N Engl J Med 348 1365-1375 (**2003**).

Frontali, M., Sabbadini, G., Novelletto, A., Jodice, C., Naso, F., Spadaro, M., Giunti, P., Jacopini, A.G., Veneziano, L., Mantuano, E., Malaspina, P., Ulizzi, L., Brice, A., Durr, A. & Terrenato, L. *Genetic fitness in Huntington's Disease and Spinocerebellar Ataxia 1: a population genetics model for CAG repeat expansions.* Ann Hum Genet 60 (Pt 5) 423-435 (**1996**).

Fu, Y.H., Kuhl, D.P., Pizzuti, A., Pieretti, M., Sutcliffe, J.S., Richards, S., Verkerk, A.J., Holden, J.J., Fenwick, R.G., Jr., Warren, S.T. & et al. *Variation of the CGG repeat at the fragile X site results in genetic instability: resolution of the Sherman paradox.* Cell 67 1047-1058 (**1991**).

Garcia, I., Martinou, I., Tsujimoto, Y. & Martinou, J.C. *Prevention of programmed cell death of sympathetic neurons by the bcl-2 proto-oncogene.* Science 258 302-304 (**1992**).

Gerber, H.P., Seipel, K., Georgiev, O., Hofferer, M., Hug, M., Rusconi, S. & Schaffner, W. *Transcriptional activation modulated by homopolymeric glutamine and proline stretches.* Science 263 808-811 (**1994**).

Gervais, F.G., Singaraja, R., Xanthoudakis, S., Gutekunst, C.A., Leavitt, B.R., Metzler, M., Hackam, A.S., Tam, J., Vaillancourt, J.P., Houtzager, V., Rasper, D.M., Roy, S., Hayden, M.R. & Nicholson, D.W. *Recruitment and activation of caspase-8 by the Huntingtin-interacting protein Hip-1 and a novel partner Hippi.* Nat Cell Biol 4 95-105. (**2002**).

Giovannone, B., Sabbadini, G., Di Maio, L., Calabrese, O., Castaldo, I., Frontali, M., Novelleto, A. & Squitieri, F. *Analysis of (CAG)n size heterogeneity in somatic and sperm cell DNA from intermediate and expanded Huntington disease gene carriers.* Hum Mutat 10 458-464 (**1997**).

Giuliano, P., De Cristofaro, T., Affaitati, A., Pizzulo, G.M., Feliciello, A., Criscuolo, C., De Michele, G., Filla, A., Avvedimento, E.V. & Varrone, S. *DNA damage induced by polyglutamine-expanded proteins.* Hum Mol Genet 12 2301-2309 (**2003**).

Glickman, M.H. & Ciechanover, A. *The ubiquitin-proteasome proteolytic pathway: destruction for the sake of construction.* Physiol Rev 82 373-428 (**2002**).

Goldberg, Y.P., Nicholson, D.W., Rasper, D.M., Kalchman, M.A., Koide, H.B., Graham, R.K., Bromm, M., Kazemi-Esfarjani, P., Thornberry, N.A., Vaillancourt, J.P. & Hayden, M.R. *Cleavage of huntingtin by apopain, a proapoptotic cysteine protease, is modulated by the polyglutamine tract.* Nat Genet 13 442-449 (**1996**).

Goldstein, J.C., Waterhouse, N.J., Juin, P., Evan, G.I. & Green, D.R. *The coordinate release of cytochrome c during apoptosis is rapid, complete and kinetically invariant.* Nat Cell Biol 2 156-162 (**2000**).

Gomez-Tortosa, E., MacDonald, M.E., Friend, J.C., Taylor, S.A., Weiler, L.J., Cupples, L.A., Srinidhi, J., Gusella, J.F., Bird, E.D., Vonsattel, J.P. & Myers, R.H. *Quantitative neuropathological changes in presymptomatic Huntington's disease.* Ann Neurol 49 29-34 (**2001**).

Gottfried, M., Lavine, L. & Roessmann, U. *Neuropathological findings in Wolf-Hirschhorn (4p-) syndrome.* Acta Neuropathol (Berl) 55 163-165 (**1981**).

Graeber, M.B. & Moran, L.B. *Mechanisms of cell death in neurodegenerative diseases: fashion, fiction, and facts.* Brain Pathol 12 385-390 (**2002**).

Greenamyre, J.T. & Shoulson, I. *We need something better, and we need it now: Fetal striatal transplantation in Huntington's disease?* Neurology 58 675-676. (**2002**).

Group, T.H.s.D.S. *A randomized, placebo-controlled trial of coenzyme Q10 and remacemide in Huntington's disease.* Neurology 57 397-404. (**2001**).

Guidetti, P., Charles, V., Chen, E.Y., Reddy, P.H., Kordower, J.H., Whetsell, W.O., Jr., Schwarcz, R. & Tagle, D.A. *Early degenerative changes in transgenic mice expressing mutant huntingtin involve dendritic abnormalities but no impairment of mitochondrial energy production.* Exp Neurol 169 340-350 (**2001**).

Gusella, J.F. & MacDonald, M.E. *Huntington's disease: CAG genetics expands neurobiology.* Curr Opin Neurobiol 5 656-662 (**1995**).

Gusella, J.F. & MacDonald, M.E. *Molecular genetics: unmasking polyglutamine triggers in neurodegenerative disease.* Nat Rev Neurosci 1 109-115 (**2000**).

Gusella, J.F., MacDonald, M.E., Ambrose, C.M. & Duyao, M.P. *Molecular genetics of Huntington's disease.* Arch Neurol 50 1157-1163 (**1993**).

Gusella, J.F., McNeil, S., Persichetti, F., Srinidhi, J., Novelletto, A., Bird, E., Faber, P., Vonsattel, J.P., Myers, R.H. & MacDonald, M.E. (1996). Huntington's disease. In Cold Spring Harb Symp Quant Biol: Function & Dysfunction of the Nervous System (Cold Spring Harb Lab Press), pp. 615-626.

Gusella, J.F., Wexler, N.S., Conneally, P.M., Naylor, S.L., Anderson, M.A., Tanzi, R.E., Watkins, P.C., Ottina, K., Wallace, M.R., Sakaguchi, A.Y. & et al. *A polymorphic DNA marker genetically linked to Huntington's disease.* Nature 306 234-238 (**1983**).

Gutekunst, C.A., Levey, A.I., Heilman, C.J., Whaley, W.L., Yi, H., Nash, N.R., Rees, H.D., Madden, J.J. & Hersch, S.M. *Identification and localization of huntingtin in brain and human lymphoblastoid cell lines with anti-fusion protein antibodies.* Proc Natl Acad Sci U S A 92 8710-8714 (**1995**).

Gutekunst, C.A., Li, S.H., Yi, H., Mulroy, J.S., Kuemmerle, S., Jones, R., Rye, D., Ferrante, R.J., Hersch, S.M. & Li, X.J. *Nuclear and neuropil aggregates in Huntington's disease: relationship to neuropathology.* J Neurosci 19 2522-2534 (**1999**).

Hackam, A.S., Singaraja, R., Wellington, C.L., Metzler, M., McCutcheon, K., Zhang, T., Kalchman, M. & Hayden, M.R. *The influence of huntingtin protein size on nuclear localization and cellular toxicity.* J Cell Biol 141 1097-1105 (**1998**).

Hackam, A.S., Yassa, A.S., Singaraja, R., Metzler, M., Gutekunst, C.A., Gan, L., Warby, S., Wellington, C.L., Vaillancourt, J., Chen, N., Gervais, F.G., Raymond, L., Nicholson, D.W. & Hayden, M.R. *Huntingtin interacting protein 1 induces apoptosis via a novel caspase-dependent death effector domain.* J Biol Chem 275 41299-41308 (**2000**).

Hansson, O., Nylandsted, J., Castilho, R.F., Leist, M., Jaattela, M. & Brundin, P. *Overexpression of heat shock protein 70 in R6/2 Huntington's disease mice has only modest effects on disease progression.* Brain Res 970 47-57 (**2003**).

Hansson, O., Petersen, A., Leist, M., Nicotera, P., Castilho, R.F. & Brundin, P. *Transgenic mice expressing a Huntington's disease mutation are resistant to quinolinic acid-induced striatal excitotoxicity.* Proc Natl Acad Sci U S A 96 8727-8732 (**1999**).

Hantraye, P., Riche, D., Maziere, M. & Isacson, O. *A primate model of Huntington's disease: behavioral and anatomical studies of unilateral excitotoxic lesions of the caudate-putamen in the baboon.* Exp Neurol 108 91-104 (**1990**).

Hardesty, B., Kudlicki, W., Odom, O.W., Zhang, T., McCarthy, D. & Kramer, G. *Cotranslational folding of nascent proteins on Escherichia coli ribosomes.* Biochem Cell Biol 73 1199-1207 (**1995**).

Hartley, D.M., Walsh, D.M., Ye, C.P., Diehl, T., Vasquez, S., Vassilev, P.M., Teplow, D.B. & Selkoe, D.J. *Protofibrillar intermediates of amyloid beta-protein induce acute electrophysiological changes and progressive neurotoxicity in cortical neurons.* J Neurosci 19 8876-8884 (**1999**).

Hauser, R.A., Furtado, S., Cimino, C.R., Delgado, H., Eichler, S., Schwartz, S., Scott, D., Nauert, G.M., Soety, E., Sossi, V., Holt, D.A., Sanberg, P.R., Stoessl, A.J. & Freeman, T.B. *Bilateral human fetal striatal transplantation in Huntington's disease.* Neurology 58 687-695. (**2002**).

Hengartner, M.O. *The biochemistry of apoptosis.* Nature 407 770-776 (**2000**).

Hershko, A. *Ubiquitin: roles in protein modification and breakdown.* Cell 34 11-12 (**1983**).

Hershko, A., Heller, H., Elias, S. & Ciechanover, A. *Components of ubiquitin-protein ligase system. Resolution, affinity purification, and role in protein breakdown.* J Biol Chem 258 8206-8214 (**1983**).

Ho, L.W., Brown, R., Maxwell, M., Wyttenbach, A. & Rubinsztein, D.C. *Wild type Huntingtin reduces the cellular toxicity of mutant Huntingtin in mammalian cell models of Huntington's disease.* J Med Genet 38 450-452 (**2001**).

Hockly, E., Cordery, P.M., Woodman, B., Mahal, A., van Dellen, A., Blakemore, C., Lewis, C.M., Hannan, A.J. & Bates, G.P. *Environmental enrichment slows disease progression in R6/2 Huntington's disease mice.* Ann Neurol 51 235-242. (**2002**).

Hockly, E., Richon, V.M., Woodman, B., Smith, D.L., Zhou, X., Rosa, E., Sathasivam, K., Ghazi-Noori, S., Mahal, A., Lowden, P.A., Steffan, J.S., Marsh, J.L., Thompson, L.M., Lewis, C.M., Marks, P.A. & Bates, G.P. *Suberoylanilide hydroxamic acid, a histone deacetylase inhibitor, ameliorates motor deficits in a mouse model of Huntington's disease.* Proc Natl Acad Sci U S A 100 2041-2046 (**2003**).

Hodgson, J.G., Agopyan, N., Gutekunst, C.A., Leavitt, B.R., LePiane, F., Singaraja, R., Smith, D.J., Bissada, N., McCutcheon, K., Nasir, J., Jamot, L., Li, X.J., Stevens, M.E., Rosemond, E., Roder, J.C., Phillips, A.G., Rubin, E.M., Hersch, S.M. & Hayden, M.R. *A YAC mouse model for Huntington's disease with full-length mutant huntingtin, cytoplasmic toxicity, and selective striatal neurodegeneration.* Neuron 23 181-192 (**1999**).

Hoeppner, D.J., Hengartner, M.O. & Schnabel, R. *Engulfment genes cooperate with ced-3 to promote cell death in Caenorhabditis elegans.* Nature 412 202-206 (**2001**).

Hoffner, G., Kahlem, P. & Djian, P. *Perinuclear localization of huntingtin as a consequence of its binding to microtubules through an interaction with beta-tubulin: relevance to Huntington's disease.* J Cell Sci 115 941-948. (**2002**).

Holbert, S., Denghien, I., Kiechle, T., Rosenblatt, A., Wellington, C., Hayden, M.R., Margolis, R.L., Ross, C.A., Dausset, J., Ferrante, R.J. & Neri, C. *The Gln-Ala repeat transcriptional activator CA150 interacts with huntingtin: neuropathologic and genetic evidence for a role in Huntington's disease pathogenesis.* Proc Natl Acad Sci U S A 98 1811-1816 (**2001**).

Holmes, S.E., Hearn, E.O., Ross, C.A. & Margolis, R.L. *SCA12: an unusual mutation leads to an unusual spinocerebellar ataxia.* Brain Res Bull 56 397-403 (**2001a**).

Holmes, S.E., O'Hearn, E., Rosenblatt, A., Callahan, C., Hwang, H.S., Ingersoll-Ashworth, R.G., Fleisher, A., Stevanin, G., Brice, A., Potter, N.T., Ross, C.A. & Margolis, R.L. *A repeat expansion in the gene encoding junctophilin-3 is associated with Huntington disease-like 2.* Nat Genet 29 377-378. (**2001b**).

Holzmann, C., Schmidt, T., Thiel, G., Epplen, J.T. & Riess, O. *Functional characterization of the human Huntington's disease gene promoter.* Brain Res Mol Brain Res 92 85-97 (**2001**).

Hopgood, M.F., Clark, M.G. & Ballard, F.J. *Protein degradation in hepatocyte monolayers. Effects of glucagon, adenosine 3':5'-cyclic monophosphate and insulin.* Biochem J 186 71-79 (**1980**).

Horowitz, M.J., Field, N.P., Zanko, A., Donnelly, E.F., Epstein, C. & Longo, F. *Psychological impact of news of genetic risk for Huntington disease.* Am J Med Genet 103 188-192. (**2001**).

Horvitz, H.R., Sternberg, P.W., Greenwald, I.S., Fixsen, W. & Ellis, H.M. *Mutations that affect neural cell lineages and cell fates during the development of the nematode Caenorhabditis elegans.* Cold Spring Harb Symp Quant Biol 48 Pt 2 453-463 (**1983**).

Huang, C.C., Faber, P.W., Persichetti, F., Mittal, V., Vonsattel, J.P., MacDonald, M.E. & Gusella, J.F. *Amyloid formation by mutant huntingtin: threshold, progressivity and recruitment of normal polyglutamine proteins.* Somat Cell Mol Genet 24 217-233 (**1998**).

Humbert, S., Bryson, E.A., Cordelieres, F.P., Connors, N.C., Datta, S.R., Finkbeiner, S., Greenberg, M.E. & Saudou, F. *The IGF-1/Akt pathway is neuroprotective in Huntington's disease and involves Huntingtin phosphorylation by Akt.* Dev Cell 2 831-837 (**2002**).

Huntington, G.S. *On Chorea.* Medical and Surgical Reporter 26 (**1872**).

Huntington'sDiseaseCollaborativeResearchGroup *A novel gene containing a trinucleotide repeat that is expanded and unstable on Huntington's disease chromosomes.* Cell 72 971-983 (**1993**).

Igarashi, S., Morita, H., Bennett, K.M., Tanaka, Y., Engelender, S., Peters, M.F., Cooper, J.K., Wood, J.D., Sawa, A. & Ross, C.A. *Inducible PC12 cell model of Huntington's disease shows toxicity and decreased histone acetylation.* Neuroreport 14 565-568 (**2003**).

Ii, K., Ito, H., Tanaka, K. & Hirano, A. *Immunocytochemical co-localization of the proteasome in ubiquitinated structures in neurodegenerative diseases and the elderly.* J Neuropathol Exp Neurol 56 125-131 (**1997**).

Ishiguro, H., Yamada, K., Sawada, H., Nishii, K., Ichino, N., Sawada, M., Kurosawa, Y., Matsushita, N., Kobayashi, K., Goto, J., Hashida, H., Masuda, N., Kanazawa, I. & Nagatsu, T. *Age-dependent and tissue-specific CAG repeat instability occurs in mouse knock-in for a mutant Huntington's disease gene.* J Neurosci Res 65 289-297. (**2001**).

Jacobson, M.D., Weil, M. & Raff, M.C. *Programmed cell death in animal development.* Cell 88 347-354 (**1997**).

Jakab, K., Novak, Z., Engelhardt, J.I., Kemeny, L., Kalman, J., Vecsei, L. & Rasko, I. *UVB irradiation-induced apoptosis increased in lymphocytes of Huntington's disease patients.* Neuroreport 12 1653-1656 (**2001**).

Jana, N.R., Zemskov, E.A., Wang, G. & Nukina, N. *Altered proteasomal function due to the expression of polyglutamine-expanded truncated N-terminal huntingtin induces apoptosis by caspase activation through mitochondrial cytochrome c release.* Hum Mol Genet 10 1049-1059 (**2001**).

Janicke, R.U., Ng, P., Sprengart, M.L. & Porter, A.G. *Caspase-3 is required for alpha-fodrin cleavage but dispensable for cleavage of other death substrates in apoptosis.* J Biol Chem 273 15540-15545 (**1998**).

Jenkins, J.B. & Conneally, P.M. *The paradigm of Huntington disease.* Am J Hum Genet 45 169-175 (**1989**).

Kahlem, P., Green, H. & Djian, P. *Transglutaminase action imitates Huntington's disease: selective polymerization of Huntingtin containing expanded polyglutamine.* Mol Cell 1 595-601 (**1998**).

Kalchman, M.A., Graham, R.K., Xia, G., Koide, H.B., Hodgson, J.G., Graham, K.C., Goldberg, Y.P., Gietz, R.D., Pickart, C.M. & Hayden, M.R. *Huntingtin is ubiquitinated and interacts with a specific ubiquitin-conjugating enzyme.* J Biol Chem 271 19385-19394 (**1996**).

Kalchman, M.A., Koide, H.B., McCutcheon, K., Graham, R.K., Nichol, K., Nishiyama, K., Kazemi-Esfarjani, P., Lynn, F.C., Wellington, C., Metzler, M., Goldberg, Y.P., Kanazawa, I., Gietz, R.D. & Hayden, M.R. *HIP1, a human homologue of S. cerevisiae Sla2p, interacts with membrane-associated huntingtin in the brain.* Nat Genet 16 44-53 (**1997**).

Karpuj, M.V., Becher, M.W., Springer, J.E., Chabas, D., Youssef, S., Pedotti, R., Mitchell, D. & Steinman, L. *Prolonged survival and decreased abnormal movements in transgenic model of Huntington disease, with administration of the transglutaminase inhibitor cystamine.* Nat Med 8 143-149 (**2002a**).

Karpuj, M.V., Becher, M.W. & Steinman, L. *Evidence for a role for transglutaminase in Huntington's disease and the potential therapeutic implications.* Neurochem Int 40 31-36. (**2002b**).

Karpuj, M.V., Garren, H., Slunt, H., Price, D.L., Gusella, J., Becher, M.W. & Steinman, L. *Transglutaminase aggregates huntingtin into nonamyloidogenic polymers, and its enzymatic activity increases in Huntington's disease brain nuclei.* Proc Natl Acad Sci U S A 96 7388-7393 (**1999**).

Kazantsev, A., Walker, H.A., Slepko, N., Bear, J.E., Preisinger, E., Steffan, J.S., Zhu, Y.Z., Gertler, F.B., Housman, D.E., Marsh, J.L. & Thompson, L.M. *A bivalent Huntingtin binding peptide suppresses polyglutamine aggregation and pathogenesis in Drosophila.* Nat Genet 25 25 (**2002**).

Kegel, K.B., Kim, M., Sapp, E., McIntyre, C., Castano, J.G., Aronin, N. & DiFiglia, M. *Huntingtin expression stimulates endosomal-lysosomal activity, endosome tubulation, and autophagy.* J Neurosci 20 7268-7278 (**2000**).

Kegel, K.B., Meloni, A.R., Yi, Y., Kim, Y.J., Doyle, E., Cuiffo, B.G., Sapp, E., Wang, Y., Qin, Z.H., Chen, J.D., Nevins, J.R., Aronin, N. & DiFiglia, M. *Huntingtin is present in the nucleus, interacts with the transcriptional corepressor C-terminal binding protein, and represses transcription.* J Biol Chem 277 7466-7476. (**2002**).

Kennedy, L. & Shelbourne, P.F. *Dramatic mutation instability in HD mouse striatum: does polyglutamine load contribute to cell-specific vulnerability in Huntington's disease?* Hum Mol Genet 9 2539-2544 (**2000**).

Kerr, J.F., Wyllie, A.H. & Currie, A.R. *Apoptosis: a basic biological phenomenon with wide-ranging implications in tissue kinetics.* Br J Cancer 26 239-257 (**1972**).

Khoshnan, A., Ko, J. & Patterson, P.H. *Effects of intracellular expression of anti-huntingtin antibodies of various specificities on mutant huntingtin aggregation and toxicity.* Proc Natl Acad Sci U S A 99 1002-1007. (**2002**).

Kiechle, T., Dedeoglu, A., Kubilus, J., Kowall, N.W., Beal, M.F., Friedlander, R.M., Hersch, S.M. & Ferrante, R.J. *Cytochrome C and caspase-9 expression in Huntington's disease.* Neuromolecular Med 1 183-195 (**2002**).

Kim, M., Lee, H.S., LaForet, G., McIntyre, C., Martin, E.J., Chang, P., Kim, T.W., Williams, M., Reddy, P.H., Tagle, D., Boyce, F.M., Won, L., Heller, A., Aronin, N. & DiFiglia, M. *Mutant huntingtin expression in clonal striatal cells: dissociation of inclusion formation and neuronal survival by caspase inhibition.* J Neurosci 19 964-973 (**1999**).

Kim, Y.J., Yi, Y., Sapp, E., Wang, Y., Cuiffo, B., Kegel, K.B., Qin, Z.H., Aronin, N. & DiFiglia, M. *Caspase 3-cleaved N-terminal fragments of wild-type and mutant huntingtin are present in normal and Huntington's disease brains, associate with membranes, and undergo calpain-dependent proteolysis.* Proc Natl Acad Sci U S A 98 12784-12789. (**2001**).

Kish, S.J., Lopes-Cendes, I., Guttman, M., Furukawa, Y., Pandolfo, M., Rouleau, G.A., Ross, B.M., Nance, M., Schut, L., Ang, L. & DiStefano, L. *Brain glyceraldehyde-3-phosphate dehydrogenase activity in human trinucleotide repeat disorders.* Arch Neurol 55 1299-1304 (**1998**).

Kita, H., Carmichael, J., Swartz, J., Muro, S., Wyttenbach, A., Matsubara, K., Rubinsztein, D.C. & Kato, K. *Modulation of polyglutamine-induced cell death by genes identified by expression profiling.* Hum Mol Genet 11 2279-2287 (**2002**).

Klapstein, G.J., Fisher, R.S., Zanjani, H., Cepeda, C., Jokel, E.S., Chesselet, M.F. & Levine, M.S. *Electrophysiological and morphological changes in striatal spiny neurons in R6/2 Huntington's disease transgenic mice.* J Neurophysiol 86 2667-2677. (**2001**).

Klement, I.A., Skinner, P.J., Kaytor, M.D., Yi, H., Hersch, S.M., Clark, H.B., Zoghbi, H.Y. & Orr, H.T. *Ataxin-1 nuclear localization and aggregation: role in polyglutamine-induced disease in SCA1 transgenic mice.* Cell 95 41-53 (**1998**).

Klionsky, D.J. & Emr, S.D. *Autophagy as a regulated pathway of cellular degradation.* Science 290 1717-1721 (**2000**).

Kloetzel, P.M. *Antigen processing by the proteasome.* Nat Rev Mol Cell Biol 2 179-187 (**2001**).

Knepper-Nicolai, B., Savill, J. & Brown, S.B. *Constitutive apoptosis in human neutrophils requires synergy between calpains and the proteasome downstream of caspases.* J Biol Chem 273 30530-30536 (**1998**).

Knight, S.J., Flannery, A.V., Hirst, M.C., Campbell, L., Christodoulou, Z., Phelps, S.R., Pointon, J., Middleton-Price, H.R., Barnicoat, A., Pembrey, M.E. & et al. *Trinucleotide repeat amplification and hypermethylation of a CpG island in FRAXE mental retardation.* Cell 74 127-134 (**1993**).

Kovtun, I.V., Therneau, T.M. & McMurray, C.T. *Gender of the embryo contributes to CAG instability in transgenic mice containing a Huntington's disease gene.* Hum Mol Genet 9 2767-2775 (**2000**).

Kuemmerle, S., Gutekunst, C.A., Klein, A.M., Li, X.J., Li, S.H., Beal, M.F., Hersch, S.M. & Ferrante, R.J. *Huntington aggregates may not predict neuronal death in Huntington's disease.* Ann Neurol 46 842-849 (**1999**).

Kuwana, T., Smith, J.J., Muzio, M., Dixit, V., Newmeyer, D.D. & Kornbluth, S. *Apoptosis induction by caspase-8 is amplified through the mitochondrial release of cytochrome c.* J Biol Chem 273 16589-16594 (**1998**).

Laforet, G.A., Sapp, E., Chase, K., McIntyre, C., Boyce, F.M., Campbell, M., Cadigan, B.A., Warzecki, L., Tagle, D.A., Reddy, P.H., Cepeda, C., Calvert, C.R., Jokel, E.S., Klapstein, G.J., Ariano, M.A., Levine, M.S., DiFiglia, M. & Aronin, N. *Changes in cortical and striatal neurons predict behavioral and electrophysiological abnormalities in a transgenic murine model of Huntington's disease.* J Neurosci 21 9112-9123. (**2001**).

Lambert, M.P., Barlow, A.K., Chromy, B.A., Edwards, C., Freed, R., Liosatos, M., Morgan, T.E., Rozovsky, I., Trommer, B., Viola, K.L., Wals, P., Zhang, C., Finch, C.E., Krafft, G.A. & Klein, W.L. *Diffusible, nonfibrillar ligands derived from Abeta1-42 are potent central nervous system neurotoxins.* Proc Natl Acad Sci U S A 95 6448-6453 (**1998**).

Lang, R.A. & Bishop, J.M. *Macrophages are required for cell death and tissue remodeling in the developing mouse eye.* Cell 74 453-462 (**1993**).

Leavitt, B.R., Guttman, J.A., Hodgson, J.G., Kimel, G.H., Singaraja, R., Vogl, A.W. & Hayden, M.R. *Wild-type huntingtin reduces the cellular toxicity of mutant huntingtin in vivo.* Am J Hum Genet 68 313-324 (**2001**).

Lelouard, H., Gatti, E., Cappello, F., Gresser, O., Camosseto, V. & Pierre, P. *Transient Aggregation of Ubiquitinated Proteins During Dendritic Cell Maturation.* Nature 417 177-182 (**2002**).

Lesort, M., Chun, W., Tucholski, J. & Johnson, G.V. *Does tissue transglutaminase play a role in Huntington's disease?* Neurochem Int 40 37-52. (**2002**).

Lesort, M., Lee, M., Tucholski, J. & Johnson, G.V. *Cystamine inhibits caspase activity. Implications for the treatment of polyglutamine disorders.* J Biol Chem 278 3825-3830 (**2003**).

Li, H., Li, S.H., Yu, Z.X., Shelbourne, P. & Li, X.J. *Huntingtin aggregate-associated axonal degeneration is an early pathological event in Huntington's disease mice.* J Neurosci 21 8473-8481. (**2001**).

Li, H., Wyman, T., Yu, Z.X., Li, S.H. & Li, X.J. *Abnormal association of mutant huntingtin with synaptic vesicles inhibits glutamate release.* Hum Mol Genet 12 2021-2030 (**2003**).

Li, S.H., Gutekunst, C.A., Hersch, S.M. & Li, X.J. *Association of HAP1 isoforms with a unique cytoplasmic structure.* J Neurochem 71 2178-2185 (**1998**).

Li, S.H., Lam, S., Cheng, A.L. & Li, X.J. *Intranuclear huntingtin increases the expression of caspase-1 and induces apoptosis.* Hum Mol Genet 9 2859-2867 (**2000**).

Li, S.H. & Li, X.J. *Aggregation of N-terminal huntingtin is dependent on the length of its glutamine repeats.* Hum Mol Genet 7 777-782 (**1998**).

Li, X.J., Li, S.H., Sharp, A.H., Nucifora, F.C., Jr., Schilling, G., Lanahan, A., Worley, P., Snyder, S.H. & Ross, C.A. *A huntingtin-associated protein enriched in brain with implications for pathology.* Nature 378 398-402 (**1995**).

Lievens, J.C., Woodman, B., Mahal, A. & Bates, G.P. *Abnormal phosphorylation of synapsin I predicts a neuronal transmission impairment in the R6/2 Huntington's disease transgenic mice.* Mol Cell Neurosci 20 638-648 (**2002**).

Lin, B., Rommens, J.M., Graham, R.K., Kalchman, M., MacDonald, H., Nasir, J., Delaney, A., Goldberg, Y.P. & Hayden, M.R. *Differential 3' polyadenylation of the Huntington disease gene results in two mRNA species with variable tissue expression.* Hum Mol Genet 2 1541-1545 (**1993**).

Lin, C.H., Tallaksen-Greene, S., Chien, W.M., Cearley, J.A., Jackson, W.S., Crouse, A.B., Ren, S., Li, X.J., Albin, R.L. & Detloff, P.J. *Neurological abnormalities in a knock-in mouse model of Huntington's disease.* Hum Mol Genet 10 137-144 (**2001**).

Lin, X., Cummings, C.J. & Zoghbi, H.Y. *Expanding our understanding of polyglutamine diseases through mouse models.* Neuron 24 499-502 (**1999**).

Lindblad, A.N. *To test or not to test: an ethical conflict with presymptomatic testing of individuals at 25% risk for Huntington's disorder.* Clin Genet 60 442-446. (**2001**).

Lucas, D.R. & Newhouse, J.P. *The Toxic Effect of Sodium l-glutamate on the inner layers of the retina.* Arch Opthalmol 58 193-201 (**1957**).

Luesse, H.G., Schiefer, J., Spruenken, A., Puls, C., Block, F. & Kosinski, C.M. *Evaluation of R6/2 HD transgenic mice for therapeutic studies in Huntington's disease: behavioral testing and impact of diabetes mellitus.* Behav Brain Res 126 185-195. (**2001**).

Luiken, J.J., van den Berg, M., Heikoop, J.C. & Meijer, A.J. *Autophagic degradation of peroxisomes in isolated rat hepatocytes.* FEBS Lett 304 93-97 (**1992**).

Luthi-Carter, R., Strand, A., Peters, N.L., Solano, S.M., Hollingsworth, Z.R., Menon, A.S., Frey, A.S., Spektor, B.S., Penney, E.B., Schilling, G., Ross, C.A., Borchelt, D.R., Tapscott, S.J., Young, A.B., Cha, J.H. & Olson, J.M. *Decreased expression of striatal signaling genes in a mouse model of Huntington's disease.* Hum Mol Genet 9 1259-1271 (**2000**).

Ma, L., Morton, A.J. & Nicholson, L.F. *Microglia density decreases with age in a mouse model of Huntington's disease.* Glia 43 274-280 (**2003**).

MacDonald, M.E., Barnes, G., Srinidhi, J., Duyao, M.P., Ambrose, C.M., Myers, R.H., Gray, J., Conneally, P.M., Young, A., Penney, J. & et al. *Gametic but not somatic instability of CAG repeat length in Huntington's disease.* J Med Genet 30 982-986 (**1993**).

MacDonald, M.E., Vonsattel, J.P., Shrinidhi, J., Couropmitree, N.N., Cupples, L.A., Bird, E.D., Gusella, J.F. & Myers, R.H. *Evidence for the GluR6 gene associated with younger onset age of Huntington's disease.* Neurology 53 1330-1332 (**1999**).

Maltsberger, J.T. *Even Unto the 12th Generation: Huntington's Chorea.* J Hist Med 16 1-17 (**1961**).

Mangiarini, L., Sathasivam, K., Mahal, A., Mott, R., Seller, M. & Bates, G.P. *Instability of highly expanded CAG repeats in mice transgenic for the Huntington's disease mutation.* Nat Genet 15 197-200 (**1997**).

Mangiarini, L., Sathasivam, K., Seller, M., Cozens, B., Harper, A., Hetherington, C., Lawton, M., Trottier, Y., Lehrach, H., Davies, S.W. & Bates, G.P. *Exon 1 of the HD gene with an expanded CAG repeat is sufficient to cause a progressive neurological phenotype in transgenic mice.* Cell 87 493-506. (**1996**).

Mankodi, A., Urbinati, C.R., Yuan, Q.P., Moxley, R.T., Sansone, V., Krym, M., Henderson, D., Schalling, M., Swanson, M.S. & Thornton, C.A. *Muscleblind localizes to nuclear foci of aberrant RNA in myotonic dystrophy types 1 and 2.* Hum Mol Genet 10 2165-2170 (**2001**).

Mantle, D., Falkous, G., Ishiura, S., Perry, R.H. & Perry, E.K. *Comparison of cathepsin protease activities in brain tissue from normal cases and cases with Alzheimer's disease, Lewy body dementia, Parkinson's disease and Huntington's disease.* J Neurol Sci 131 65-70 (**1995**).

Marcora, E., Gowan, K. & Lee, J.E. *Stimulation of NeuroD activity by huntingtin and huntingtin-associated proteins HAP1 and MLK2.* Proc Natl Acad Sci U S A 100 9578-9583 (**2003**).

Margolis, R.L., O'Hearn, E., Rosenblatt, A., Willour, V., Holmes, S.E., Franz, M.L., Callahan, C., Hwang, H.S., Troncoso, J.C. & Ross, C.A. *A disorder similar to Huntington's disease is associated with a novel CAG repeat expansion.* Ann Neurol 50 373-380. (**2001**).

Martin-Aparicio, E., Yamamoto, A., Hernandez, F., Hen, R., Avila, J. & Lucas, J.J. *Proteasomal-dependent aggregate reversal and absence of cell death in a conditional mouse model of Huntington's disease.* J Neurosci 21 8772-8781. (**2001**).

Martindale, D., Hackam, A., Wieczorek, A., Ellerby, L., Wellington, C., McCutcheon, K., Singaraja, R., Kazemi-Esfarjani, P., Devon, R., Kim, S.U., Bredesen, D.E., Tufaro, F. & Hayden, M.R. *Length of huntingtin and its polyglutamine tract influences localization and frequency of intracellular aggregates.* Nat Genet 18 150-154 (**1998**).

Martinou, J.C., Dubois-Dauphin, M., Staple, J.K., Rodriguez, I., Frankowski, H., Missotten, M., Albertini, P., Talabot, D., Catsicas, S., Pietra, C. & et al. *Overexpression of BCL-2 in transgenic mice protects neurons from naturally occurring cell death and experimental ischemia.* Neuron 13 1017-1030 (**1994**).

Mastroberardino, P.G., Iannicola, C., Nardacci, R., Bernassola, F., De Laurenzi, V., Melino, G., Moreno, S., Pavone, F., Oliverio, S., Fesus, L. & Piacentini, M. *'Tissue' transglutaminase ablation reduces neuronal death and prolongs survival in a mouse model of Huntington's disease.* Cell Death Differ 9 873-880 (**2002**).

Matsuura, T., Yamagata, T., Burgess, D.L., Rasmussen, A., Grewal, R.P., Watase, K., Khajavi, M., McCall, A.E., Davis, C.F., Zu, L., Achari, M., Pulst, S.M., Alonso, E., Noebels, J.L., Nelson, D.L., Zoghbi, H.Y. & Ashizawa, T. *Large expansion of the ATTCT pentanucleotide repeat in spinocerebellar ataxia type 10.* Nat Genet 26 191-194 (**2000**).

McCampbell, A., Taylor, J.P., Taye, A.A., Robitschek, J., Li, M., Walcott, J., Merry, D., Chai, Y., Paulson, H., Sobue, G. & Fischbeck, K.H. *CREB-binding protein sequestration by expanded polyglutamine.* Hum Mol Genet 9 2197-2202 (**2000**).

McMurray, C.T. *Huntington's disease. Expanding horizons for treatment.* Lancet 358 Suppl S37. (**2001a**).

McMurray, C.T. *Huntington's disease: new hope for therapeutics.* Trends Neurosci 24 S32-38. (**2001b**).

McMurray, C.T. & Kortun, I.V. *Repair in haploid male germ cells occurs late in differentiation as chromatin is condensing.* Chromosoma 111 505-508 (**2003**).

McMurray, S.E. & McMurray, C.T. *Huntington's disease. A sports star and a cook.* Lancet 358 Suppl S38. (**2001**).

McPherson, P.S. *Regulatory role of SH3 domain-mediated protein-protein interactions in synaptic vesicle endocytosis.* Cell Signal 11 229-238 (**1999**).

Meade, C.A., Deng, Y.P., Fusco, F.R., Del Mar, N., Hersch, S., Goldowitz, D. & Reiner, A. *Cellular localization and development of neuronal intranuclear inclusions in striatal and cortical neurons in R6/2 transgenic mice.* J Comp Neurol 449 241-269 (**2002**).

Menalled, L.B., Sison, J.D., Dragatsis, I., Zeitlin, S. & Chesselet, M.F. *Time course of early motor and neuropathological anomalies in a knock-in mouse model of Huntington's disease with 140 CAG repeats.* J Comp Neurol 465 11-26 (**2003**).

Mende-Mueller, L.M., Toneff, T., Hwang, S.R., Chesselet, M.F. & Hook, V.Y. *Tissue-specific proteolysis of Huntingtin (htt) in human brain: evidence of enhanced levels of N- and C-terminal htt fragments in Huntington's disease striatum.* J Neurosci 21 1830-1837 (**2001**).

Mengual, E., Arizti, P., Rodrigo, J., Gimenez-Amaya, J.M. & Castano, J.G. *Immunohistochemical distribution and electron microscopic subcellular localization of the proteasome in the rat CNS.* J Neurosci 16 6331-6341 (**1996**).

Merry, D.E. & Korsmeyer, S.J. *Bcl-2 gene family in the nervous system.* Annu Rev Neurosci 20 245-267 (**1997**).

Metzler, M., Legendre-Guillemin, V., Gan, L., Chopra, V., Kwok, A., McPherson, P.S. & Hayden, M.R. *HIP1 functions in clathrin-mediated endocytosis through binding to clathrin and adaptor protein 2.* J Biol Chem 276 39271-39276 (**2001**).

Metzler, M., Li, B., Gan, L., Georgiou, J., Gutekunst, C.A., Wang, Y., Torre, E., Devon, R.S., Oh, R., Legendre-Guillemin, V., Rich, M., Alvarez, C., Gertsenstein, M., McPherson, P.S., Nagy, A., Wang, Y.T., Roder, J.C., Raymond, L.A. & Hayden, M.R. *Disruption of the endocytic protein HIP1 results in neurological deficits and decreased AMPA receptor trafficking.* Embo J 22 3254-3266 (**2003**).

Michaelidis, T.M., Sendtner, M., Cooper, J.D., Airaksinen, M.S., Holtmann, B., Meyer, M. & Thoenen, H. *Inactivation of bcl-2 results in progressive degeneration of motoneurons, sympathetic and sensory neurons during early postnatal development.* Neuron 17 75-89 (**1996**).

Miller, J.W., Urbinati, C.R., Teng-Umnuay, P., Stenberg, M.G., Byrne, B.J., Thornton, C.A. & Swanson, M.S. *Recruitment of human muscleblind proteins to (CUG)(n) expansions associated with myotonic dystrophy.* Embo J 19 4439-4448 (**2000**).

Miyashita, T., Matsui, J., Ohtsuka, Y., Mami, U., Fujishima, S., Okamura-Oho, Y., Inoue, T. & Yamada, M. *Expression of extended polyglutamine sequentially activates initiator and effector caspases.* Biochem Biophys Res Commun 257 724-730 (**1999**).

Mizuta, I., Ohta, M., Ohta, K., Nishimura, M., Mizuta, E. & Kuno, S. *Riluzole stimulates nerve growth factor, brain-derived neurotrophic factor and glial cell line-derived neurotrophic factor synthesis in cultured mouse astrocytes.* Neurosci Lett 310 117-120 (**2001**).

Moffatt, O.D., Devitt, A., Bell, E.D., Simmons, D.L. & Gregory, C.D. *Macrophage recognition of ICAM-3 on apoptotic leukocytes.* J Immunol 162 6800-6810 (**1999**).

Montel, V., Gardrat, F., Azanza, J.L. & Raymond, J. *20S proteasome, hsp90, p97 fusion protein, PA28 activator copurifying oligomers and ATPase activities.* Biochem Mol Biol Int 47 465-472 (**1999**).

Morales, L.M., Estevez, J., Suarez, H., Villalobos, R., Chacin de Bonilla, L. & Bonilla, E. *Nutritional evaluation of Huntington disease patients.* Am J Clin Nutr 50 145-150 (**1989**).

Mortimore, G.E. & Poso, A.R. *The lysosomal pathway of intracellular proteolysis in liver: regulation by amino acids.* Adv Enzyme Regul 25 257-276 (**1986**).

Morton, A.J. & Edwardson, J.M. *Progressive depletion of complexin II in a transgenic mouse model of Huntington's disease.* J Neurochem 76 166-172 (**2001**).

Morton, A.J., Faull, R.L. & Edwardson, J.M. *Abnormalities in the synaptic vesicle fusion machinery in Huntington's disease.* Brain Res Bull 56 111-117. (**2001**).

Morton, A.J. & Leavens, W. *Mice transgenic for the human Huntington's disease mutation have reduced sensitivity to kainic acid toxicity.* Brain Res Bull 52 51-59 (**2000**).

Muchowski, P.J., Ning, K., D'Souza-Schorey, C. & Fields, S. *Requirement of an intact microtubule cytoskeleton for aggregation and inclusion body formation by a mutant huntingtin fragment.* Proc Natl Acad Sci U S A 99 727-732. (**2002**).

Murphy, K.P., Carter, R.J., Lione, L.A., Mangiarini, L., Mahal, A., Bates, G.P., Dunnett, S.B. & Morton, A.J. *Abnormal synaptic plasticity and impaired spatial cognition in mice transgenic for exon 1 of the human Huntington's disease mutation.* J Neurosci 20 5115-5123 (**2000**).

Myers, R.H., Marans, K.S. & MacDonald, M.E. (1998). Huntington's Disease. In Genetic Instabilities and Hereditary Neurological Diseases, R. D. Wells, and S. T. Warren, eds. (Academic Press), pp. 301-323.

Myers, R.H., Vonsattel, J.P., Paskevich, P.A., Kiely, D.K., Stevens, T.J., Cupples, L.A., Richardson, E.P., Jr. & Bird, E.D. *Decreased neuronal and increased oligodendroglial densities in Huntington's disease caudate nucleus.* J Neuropathol Exp Neurol 50 729-742 (**1991**).

Myers, R.H., Vonsattel, J.P., Stevens, T.J., Cupples, L.A., Richardson, E.P., Martin, J.B. & Bird, E.D. *Clinical and neuropathologic assessment of severity in Huntington's disease.* Neurology 38 341-347 (**1988**).

Nakashima, K., Watanabe, Y., Kusumi, M., Nanba, E., Maeoka, Y., Nakagawa, M., Igo, M., Irie, H., Ishino, H., Fujimoto, A., Goto, J. & Takahashi, K. *Epidemiological and genetic studies of Huntington's disease in the San-in area of Japan.* Neuroepidemiology 15 126-131 (**1996**).

Namba, R., Pazdera, T.M., Cerrone, R.L. & Minden, J.S. *Drosophila embryonic pattern repair: how embryos respond to bicoid dosage alteration.* Development 124 1393-1403 (**1997**).

Nance, M.A., Westphal, B. & Nugent, S. *Diagnosis of patients presenting to a Huntington disease (HD) clinic without a family history of HD.* Neurology 47 1578-1580 (**1996**).

Nasir, J., Floresco, S.B., O'Kusky, J.R., Diewert, V.M., Richman, J.M., Zeisler, J., Borowski, A., Marth, J.D., Phillips, A.G. & Hayden, M.R. *Targeted disruption of the Huntington's disease gene results in embryonic lethality and behavioral and morphological changes in heterozygotes.* Cell 81 811-823 (**1995**).

Nicholson, D.W. *Caspase structure, proteolytic substrates, and function during apoptotic cell death.* Cell Death Differ 6 1028-1042 (**1999**).

Nicholson, D.W. & Thornberry, N.A. *Caspases: killer proteases.* Trends Biochem Sci 22 299-306 (**1997**).

Nishitoh, H., Matsuzawa, A., Tobiume, K., Saegusa, K., Takeda, K., Inoue, K., Hori, S., Kakizuka, A. & Ichijo, H. *ASK1 is essential for endoplasmic reticulum stress-induced neuronal cell death triggered by expanded polyglutamine repeats.* Genes Dev 16 1345-1355 (**2002**).

Nucifora, F.C., Jr., Sasaki, M., Peters, M.F., Huang, H., Cooper, J.K., Yamada, M., Takahashi, H., Tsuji, S., Troncoso, J., Dawson, V.L., Dawson, T.M. & Ross, C.A. *Interference by huntingtin and atrophin-1 with cbp-mediated transcription leading to cellular toxicity.* Science 291 2423-2428 (**2001**).

Ogg, S.C. & Lamond, A.I. *Cajal bodies and coilin--moving towards function.* J Cell Biol 159 17-21 (**2002**).

Ohba, M. *Modulation of intracellular protein degradation by SSB1-SIS1 chaperon system in yeast S. cerevisiae.* FEBS Lett 409 307-311 (**1997**).

Okada, H., Suh, W.K., Jin, J., Woo, M., Du, C., Elia, A., Duncan, G.S., Wakeham, A., Itie, A., Lowe, S.W., Wang, X. & Mak, T.W. *Generation and characterization of Smac/DIABLO-deficient mice.* Mol Cell Biol 22 3509-3517 (**2002**).

Okano, A., Usuda, N., Furihata, K., Nakayama, K., Bao Tian, Q., Okamoto, T. & Suzuki, T. *Huntingtin-interacting protein-1-related protein of rat (rHIP1R) is localized in the postsynaptic regions.* Brain Res 967 210-225 (**2003**).

Olney, J.W. *Brain lesions, obesity, and other disturbances in mice treated with monosodium glutamate.* Science 164 719-721 (**1969**).

Olney, J.W., Adamo, N.J. & Ratner, A. *Monosodium glutamate effects.* Science 172 294 (**1971**).

Ona, V.O., Li, M., Vonsattel, J.P., Andrews, L.J., Khan, S.Q., Chung, W.M., Frey, A.S., Menon, A.S., Li, X.J., Stieg, P.E., Yuan, J., Penney, J.B., Young, A.B., Cha, J.H. & Friedlander, R.M. *Inhibition of caspase-1 slows disease progression in a mouse model of Huntington's disease.* Nature 399 263-267 (**1999**).

Opal, P. & Zoghbi, H.Y. *The role of chaperones in polyglutamine disease.* Trends Mol Med 8 232-236 (**2002**).

Pandey, P., Farber, R., Nakazawa, A., Kumar, S., Bharti, A., Nalin, C., Weichselbaum, R., Kufe, D. & Kharbanda, S. *Hsp27 functions as a negative regulator of cytochrome c-dependent activation of procaspase-3.* Oncogene 19 1975-1981 (**2000a**).

Pandey, P., Saleh, A., Nakazawa, A., Kumar, S., Srinivasula, S.M., Kumar, V., Weichselbaum, R., Nalin, C., Alnemri, E.S., Kufe, D. & Kharbanda, S. *Negative regulation of cytochrome c-mediated oligomerization of Apaf-1 and activation of procaspase-9 by heat shock protein 90.* Embo J 19 4310-4322 (**2000b**).

Passani, L.A., Bedford, M.T., Faber, P.W., McGinnis, K.M., Sharp, A.H., Gusella, J.F., Vonsattel, J.P. & MacDonald, M.E. *Huntingtin's WW domain partners in Huntington's disease post-mortem brain fulfill genetic criteria for direct involvement in Huntington's disease pathogenesis.* Hum Mol Genet 9 2175-2182 (**2000**).

Paulsen, J.S., Ready, R.E., Hamilton, J.M., Mega, M.S. & Cummings, J.L. *Neuropsychiatric aspects of Huntington's disease.* J Neurol Neurosurg Psychiatry 71 310-314. (**2001a**).

Paulsen, J.S., Zhao, H., Stout, J.C., Brinkman, R.R., Guttman, M., Ross, C.A., Como, P., Manning, C., Hayden, M.R. & Shoulson, I. *Clinical markers of early disease in persons near onset of Huntington's disease.* Neurology 57 658-662. (**2001b**).

Pederson, T. *The plurifunctional nucleolus.* Nucleic Acids Res 26 3871-3876 (**1998**).

Pericak-Vance, M.A. Advances Neurol 23 (**1979**).

Persichetti, F., Ambrose, C.M., Ge, P., McNeil, S.M., Srinidhi, J., Anderson, M.A., Jenkins, B., Barnes, G.T., Duyao, M.P., Kanaley, L. & et al. *Normal and expanded Huntington's disease gene alleles produce distinguishable proteins due to translation across the CAG repeat.* Mol Med 1 374-383 (**1995**).

Perutz, M.F. *Glutamine repeats and inherited neurodegenerative diseases: molecular aspects.* Curr Opin Struct Biol 6 848-858 (**1996**).

Peters, M.F. & Ross, C.A. *Isolation of a 40-kDa Huntingtin-associated protein.* J Biol Chem 276 3188-3194 (**2001**).

Peters, P.J., Ning, K., Palacios, F., Boshans, R.L., Kazantsev, A., Thompson, L.M., Woodman, B., Bates, G.P. & D'Souza-Schorey, C. *Arfaptin 2 regulates the aggregation of mutant huntingtin protein.* Nat Cell Biol 4 240-245. (**2002**).

Petersen, A., Hansson, O., Puschban, Z., Sapp, E., Romero, N., Castilho, R.F., Sulzer, D., Rice, M., DiFiglia, M., Przedborski, S. & Brundin, P. *Mice transgenic for exon 1 of the Huntington's disease gene display reduced striatal sensitivity to neurotoxicity induced by dopamine and 6-hydroxydopamine.* Eur J Neurosci 14 1425-1435. (**2001a**).

Petersen, A., Larsen, K.E., Behr, G.G., Romero, N., Przedborski, S., Brundin, P. & Sulzer, D. *Expanded CAG repeats in exon 1 of the Huntington's disease gene stimulate dopamine-mediated striatal neuron autophagy and degeneration.* Hum Mol Genet 10 1243-1254 (**2001b**).

Philips, A.V., Timchenko, L.T. & Cooper, T.A. *Disruption of splicing regulated by a CUG-binding protein in myotonic dystrophy.* Science 280 737-741 (**1998**).

Pillot, T., Drouet, B., Queille, S., Labeur, C., Vandekerchkhove, J., Rosseneu, M., Pincon-Raymond, M. & Chambaz, J. *The nonfibrillar amyloid beta-peptide induces apoptotic neuronal cell death: involvement of its C-terminal fusogenic domain.* J Neurochem 73 1626-1634 (**1999**).

Pratley, R.E., Salbe, A.D., Ravussin, E. & Caviness, J.N. *Higher sedentary energy expenditure in patients with Huntington's disease.* Ann Neurol 47 64-70 (**2000**).

Prusiner, S.B. *Prions.* Proc Natl Acad Sci U S A 95 13363-13383 (**1998**).

Ptitsyn, O.B. *How does protein synthesis give rise to the 3D-structure?* FEBS Lett 285 176-181 (**1991**).

Quignon, F., De Bels, F., Koken, M., Feunteun, J., Ameisen, J.C. & de The, H. *PML induces a novel caspase-independent death process.* Nat Genet 20 259-265 (**1998**).

Rami, A., Ferger, D. & Krieglstein, J. *Blockade of calpain proteolytic activity rescues neurons from glutamate excitotoxicity.* Neurosci Res 27 93-97 (**1997**).

Ranen, N.G., Stine, O.C., Abbott, M.H., Sherr, M., Codori, A.M., Franz, M.L., Chao, N.I., Chung, A.S., Pleasant, N., Callahan, C. & et al. *Anticipation and instability of IT-15 (CAG)n repeats in parent-offspring pairs with Huntington disease.* Am J Hum Genet 57 593-602 (**1995**).

Rao, D.S., Bradley, S.V., Kumar, P.D., Hyun, T.S., Saint-Dic, D., Oravecz-Wilson, K., Kleer, C.G. & Ross, T.S. *Altered receptor trafficking in Huntingtin Interacting Protein 1-transformed cells.* Cancer Cell 3 471-482 (**2003**).

Rasper, D.M., Vaillancourt, J.P., Hadano, S., Houtzager, V.M., Seiden, I., Keen, S.L., Tawa, P., Xanthoudakis, S., Nasir, J., Martindale, D., Koop, B.F., Peterson, E.P., Thornberry, N.A., Huang, J., MacPherson, D.P., Black, S.C., Hornung, F., Lenardo, M.J., Hayden, M.R., Roy, S. & Nicholson, D.W. *Cell death attenuation by 'Usurpin', a mammalian DED-caspase homologue that precludes caspase-8 recruitment and activation by the CD-95 (Fas, APO-1) receptor complex.* Cell Death Differ 5 271-288 (**1998**).

Rassow, J. & Pfanner, N. *Protein biogenesis: chaperones for nascent polypeptides.* Curr Biol 6 115-118 (**1996**).

Ravikumar, B., Duden, R. & Rubinsztein, D.C. *Aggregate-prone proteins with polyglutamine and polyalanine expansions are degraded by autophagy.* Hum Mol Genet 11 1107-1117 (**2002**).

Ravikumar, B., Stewart, A., Kita, H., Kato, K., Duden, R. & Rubinsztein, D.C. *Raised intracellular glucose concentrations reduce aggregation and cell death caused by mutant huntingtin exon 1 by decreasing mTOR phosphorylation and inducing autophagy.* Hum Mol Genet 12 985-994 (**2003**).

Reddien, P.W., Cameron, S. & Horvitz, H.R. *Phagocytosis promotes programmed cell death in C. elegans.* Nature 412 198-202 (**2001**).

Reddy, P.H., Williams, M., Charles, V., Garrett, L., Pike-Buchanan, L., Whetsell, W.O., Jr., Miller, G. & Tagle, D.A. *Behavioural abnormalities and selective neuronal loss in HD transgenic mice expressing mutated full-length HD cDNA.* Nat Genet 20 198-202 (**1998**).

Rega, S., Stiewe, T., Chang, D.I., Pollmeier, B., Esche, H., Bardenheuer, W., Marquitan, G. & Putzer, B.M. *Identification of the full-length huntingtin- interacting protein p231HBP/HYPB as a DNA-binding factor.* Mol Cell Neurosci 18 68-79 (**2001**).

Reggiori, F. & Klionsky, D.J. *Autophagy in the eukaryotic cell.* Eukaryot Cell 1 11-21 (**2002**).

Reilly, C.E. *Wild-type huntingtin up-regulates BDNF transcription in Huntington's disease.* J Neurol 248 920-922 (**2001**).

Reiner, A., Del Mar, N., Meade, C.A., Yang, H., Dragatsis, I., Zeitlin, S. & Goldowitz, D. *Neurons lacking huntingtin differentially colonize brain and survive in chimeric mice.* J Neurosci 21 7608-7619. (**2001**).

Reverter, D., Strobl, S., Fernandez-Catalan, C., Sorimachi, H., Suzuki, K. & Bode, W. *Structural basis for possible calcium-induced activation mechanisms of calpains.* Biol Chem 382 753-766 (**2001**).

Reynolds, N.C., Jr., Hellman, R.S., Tikofsky, R.S., Prost, R.W., Mark, L.P., Elejalde, B.R., Lebel, R., Hamsher, K.S., Swanson, S. & Benezra, E.E. *Single photon emission computerized tomography (SPECT) in detecting neurodegeneration in Huntington's disease.* Nucl Med Commun 23 13-18. (**2002**).

Rigamonti, D., Sipione, S., Goffredo, D., Zuccato, C., Fossale, E. & Cattaneo, E. *Huntingtin's neuroprotective activity occurs via inhibition of procaspase-9 processing.* J Biol Chem 276 14545-14548 (**2001**).

Rodriguez, J. & Lazebnik, Y. *Caspase-9 and APAF-1 form an active holoenzyme.* Genes Dev 13 3179-3184 (**1999**).

Roizin, L., Stellar, S. & Liu, J.C. *Neuronal nuclear-cytoplasmic changes in Huntington's chorea: electron microscope investigations.* Advances Neurol 23 95-122 (**1979**).

Rosas, H.D., Liu, A.K., Hersch, S., Glessner, M., Ferrante, R.J., Salat, D.H., van Der Kouwe, A., Jenkins, B.G., Dale, A.M. & Fischl, B. *Regional and progressive thinning of the cortical ribbon in Huntington's disease.* Neurology 58 695-701. (**2002**).

Rosser, A. & Dunnett, S. *New drugs for Huntington's disease.* Neuroreport 13 A21-22. (**2002**).

Rubinsztein, D.C., Leggo, J., Coles, R., Almqvist, E., Biancalana, V., Cassiman, J.J., Chotai, K., Connarty, M., Crauford, D., Curtis, A., Curtis, D., Davidson, M.J., Differ, A.M., Dode, C., Dodge, A., Frontali, M., Ranen, N.G., Stine, O.C., Sherr, M., Abbott, M.H., Franz, M.L., Graham, C.A., Harper, P.S., Hedreen, J.C., Hayden, M.R. & et al. *Phenotypic characterization of individuals with 30-40 CAG repeats in the Huntington disease (HD) gene reveals HD cases with 36 repeats and apparently normal elderly individuals with 36-39 repeats.* Am J Hum Genet 59 16-22 (**1996**).

Sakamoto, N., Ohshima, K., Montermini, L., Pandolfo, M. & Wells, R.D. *Sticky DNA, a self-associated complex formed at long GAA*TTC repeats in intron 1 of the frataxin gene, inhibits transcription.* J Biol Chem 276 27171-27177 (**2001**).

Samali, A., Robertson, J.D., Peterson, E., Manero, F., van Zeijl, L., Paul, C., Cotgreave, I.A., Arrigo, A.P. & Orrenius, S. *Hsp27 protects mitochondria of thermotolerant cells against apoptotic stimuli.* Cell Stress Chaperones 6 49-58 (**2001**).

Sanchez, I., Mahlke, C. & Yuan, J. *Pivotal role of oligomerization in expanded polyglutamine neurodegenerative disorders.* Nature 421 373-379 (**2003**).

Sanchez, I., Xu, C.J., Juo, P., Kakizaka, A., Blenis, J. & Yuan, J. *Caspase-8 is required for cell death induced by expanded polyglutamine repeats.* Neuron 22 623-633 (**1999**).

Sapp, E., Schwarz, C., Chase, K., Bhide, P.G., Young, A.B., Penney, J., Vonsattel, J.P., Aronin, N. & DiFiglia, M. *Huntingtin localization in brains of normal and Huntington's disease patients.* Ann Neurol 42 604-612 (**1997**).

Sathasivam, K., Hobbs, C., Mangiarini, L., Mahal, A., Turmaine, M., Doherty, P., Davies, S.W. & Bates, G.P. *Transgenic models of Huntington's disease.* Philos Trans R Soc Lond B Biol Sci 354 963-969. (**1999**).

Sathasivam, K., Woodman, B., Mahal, A., Bertaux, F., Wanker, E.E., Shima, D.T. & Bates, G.P. *Centrosome disorganization in fibroblast cultures derived from R6/2 Huntington's disease (HD) transgenic mice and HD patients.* Hum Mol Genet 10 2425-2435. (**2001**).

Satyal, S.H., Schmidt, E., Kitagawa, K., Sondheimer, N., Lindquist, S., Kramer, J.M. & Morimoto, R.I. *Polyglutamine aggregates alter protein folding homeostasis in Caenorhabditis elegans.* Proc Natl Acad Sci U S A 97 5750-5755 (**2000**).

Saudou, F., Finkbeiner, S., Devys, D. & Greenberg, M.E. *Huntingtin acts in the nucleus to induce apoptosis but death does not correlate with the formation of intranuclear inclusions.* Cell 95 55-66 (**1998**).

Savill, J. & Fadok, V. *Corpse clearance defines the meaning of cell death.* Nature 407 784-788 (**2000**).

Savkur, R.S., Philips, A.V. & Cooper, T.A. *Aberrant regulation of insulin receptor alternative splicing is associated with insulin resistance in myotonic dystrophy.* Nat Genet 29 40-47 (**2001**).

Sawa, A., Wiegand, G.W., Cooper, J., Margolis, R.L., Sharp, A.H., Lawler, J.F., Jr., Greenamyre, J.T., Snyder, S.H. & Ross, C.A. *Increased apoptosis of Huntington disease lymphoblasts associated with repeat length-dependent mitochondrial depolarization.* Nat Med 5 1194-1198 (**1999**).

Scaffidi, C., Schmitz, I., Krammer, P.H. & Peter, M.E. *The role of c-FLIP in modulation of CD95-induced apoptosis.* J Biol Chem 274 1541-1548 (**1999**).

Scherzinger, E., Lurz, R., Turmaine, M., Mangiarini, L., Hollenbach, B., Hasenbank, R., Bates, G.P., Davies, S.W., Lehrach, H. & Wanker, E.E. *Huntingtin-encoded polyglutamine expansions form amyloid-like protein aggregates in vitro and in vivo.* Cell 90 549-558 (**1997**).

Schiefer, J., Landwehrmeyer, G.B., Luesse, H.G., Sprunken, A., Puls, C., Milkereit, A., Milkereit, E. & Kosinski, C.M. *Riluzole prolongs survival time and alters nuclear inclusion formation in a transgenic mouse model of Huntington's disease.* Mov Disord 17 748-757 (**2002**).

Schubert, U., Anton, L.C., Gibbs, J., Norbury, C.C., Yewdell, J.W. & Bennink, J.R. *Rapid degradation of a large fraction of newly synthesized proteins by proteasomes.* Nature 404 770-774 (**2000**).

Schuler, M., Bossy-Wetzel, E., Goldstein, J.C., Fitzgerald, P. & Green, D.R. *p53 induces apoptosis by caspase activation through mitochondrial cytochrome c release.* J Biol Chem 275 7337-7342 (**2000**).

Schweichel, J.U. & Merker, H.J. *The morphology of various types of cell death in prenatal tissues.* Teratology 7 253-266 (**1973**).

Senatorov, V.V., Charles, V., Reddy, P.H., Tagle, D.A. & Chuang, D.M. *Overexpression and nuclear accumulation of glyceraldehyde-3-phosphate dehydrogenase in a transgenic mouse model of Huntington's disease.* Mol Cell Neurosci 22 285-297 (**2003**).

Seppi, K., Mueller, J., Bodner, T., Brandauer, E., Benke, T., Weirich-Schwaiger, H., Poewe, W. & Wenning, G.K. *Riluzole in Huntington's disease (HD): an open label study with one year follow up.* J Neurol 248 866-869 (**2001**).

Sharp, A.H., Loev, S.J., Schilling, G., Li, S.H., Li, X.J., Bao, J., Wagster, M.V., Kotzuk, J.A., Steiner, J.P., Lo, A. & et al. *Widespread expression of Huntington's disease gene (IT15) protein product.* Neuron 14 1065-1074 (**1995**).

Shelbourne, P.F., Killeen, N., Hevner, R.F., Johnston, H.M., Tecott, L., Lewandoski, M., Ennis, M., Ramirez, L., Li, Z., Iannicola, C., Littman, D.R. & Myers, R.M. *A Huntington's disease CAG expansion at the murine Hdh locus is unstable and associated with behavioural abnormalities in mice.* Hum Mol Genet 8 763-774 (**1999**).

Shi, Y. *Mechanisms of caspase activation and inhibition during apoptosis.* Mol Cell 9 459-470 (**2002**).

Shimohata, T., Nakajima, T., Yamada, M., Uchida, C., Onodera, O., Naruse, S., Kimura, T., Koide, R., Nozaki, K., Sano, Y., Ishiguro, H., Sakoe, K., Ooshima, T., Sato, A., Ikeuchi, T., Oyake, M., Sato, T., Aoyagi, Y., Hozumi, I., Nagatsu, T., Takiyama, Y., Nishizawa, M., Goto, J., Kanazawa, I., Davidson, I., Tanese, N., Takahashi, H. & Tsuji, S. *Expanded polyglutamine stretches interact with TAFII130, interfering with CREB-dependent transcription.* Nat Genet 26 29-36 (**2000**).

Sieradzan, K.A. & Mann, D.M. *The selective vulnerability of nerve cells in Huntington's disease.* Neuropathol Appl Neurobiol 27 1-21 (**2001**).

Siesling, S., Vegter-van de Vlis, M., Losekoot, M., Belfroid, R.D., Maat-Kievit, J.A., Kremer, H.P. & Roos, R.A. *Family history and DNA analysis in patients with suspected Huntington's disease.* J Neurol Neurosurg Psychiatry 69 54-59 (**2000**).

Sittler, A., Lurz, R., Lueder, G., Priller, J., Lehrach, H., Hayer-Hartl, M.K., Hartl, F.U. & Wanker, E.E. *Geldanamycin activates a heat shock response and inhibits huntingtin aggregation in a cell culture model of Huntington's disease.* Hum Mol Genet 10 1307-1315 (**2001**).

Sittler, A., Walter, S., Wedemeyer, N., Hasenbank, R., Scherzinger, E., Eickhoff, H., Bates, G.P., Lehrach, H. & Wanker, E.E. *SH3GL3 associates with the Huntingtin exon 1 protein and promotes the formation of polyGln-containing protein aggregates.* Mol Cell 2 427-436 (**1998**).

Slow, E.J., van Raamsdonk, J., Rogers, D., Coleman, S.H., Graham, R.K., Deng, Y., Oh, R., Bissada, N., Hossain, S.M., Yang, Y.Z., Li, X.J., Simpson, E.M., Gutekunst, C.A., Leavitt, B.R. & Hayden, M.R. *Selective striatal neuronal loss in a YAC128 mouse model of Huntington disease.* Hum Mol Genet 12 1555-1567 (**2003**).

Smith, D.L., Woodman, B., Mahal, A., Sathasivam, K., Ghazi-Noori, S., Lowden, P.A., Bates, G.P. & Hockly, E. *Minocycline and doxycycline are not beneficial in a model of Huntington's disease.* Ann Neurol 54 186-196 (**2003**).

Smith, M.A., Brandt, J. & Shadmehr, R. *Motor disorder in Huntington's disease begins as a dysfunction in error feedback control.* Nature 403 544-549 (**2000**).

Sorensen, S.A. & Fenger, K. *Causes of death in patients with Huntington's disease and in unaffected first degree relatives.* J Med Genet 29 911-914 (**1992**).

Sorensen, S.A., Fenger, K. & Olsen, J.H. *Significantly lower incidence of cancer among patients with Huntington disease: An apoptotic effect of an expanded polyglutamine tract?* Cancer 86 1342-1346 (**1999**).

Spector, D.L. *Nuclear domains.* J Cell Sci 114 2891-2893 (**2001**).

Springs, S.L., Diavolitsis, V.M., Goodhouse, J. & McLendon, G.L. *The kinetics of translocation of Smac/DIABLO from the mitochondria to the cytosol in HeLa cells.* J Biol Chem 277 45715-45718 (**2002**).

Squitieri, F., Cannella, M., Giallonardo, P., Maglione, V., Mariotti, C. & Hayden, M.R. *Onset and pre-onset studies to define the Huntington's disease natural history.* Brain Res Bull 56 233-238. (**2001**).

Squitieri, F., Gellera, C., Cannella, M., Mariotti, C., Cislaghi, G., Rubinsztein, D.C., Almqvist, E.W., Turner, D., Bachoud-Levi, A.C., Simpson, S.A., Delatycki, M., Maglione, V., Hayden, M.R. & Donato, S.D. *Homozygosity for CAG mutation in Huntington disease is associated with a more severe clinical course.* Brain 126 946-955 (**2003**).

Steffan, J.S., Bodai, L., Pallos, J., Poelman, M., McCampbell, A., Apostol, B.L., Kazantsev, A., Schmidt, E., Zhu, Y.Z., Greenwald, M., Kurokawa, R., Housman, D.E., Jackson, G.R., Marsh, J.L. & Thompson, L.M. *Histone deacetylase inhibitors arrest polyglutamine-dependent neurodegeneration in Drosophila.* Nature 413 739-743 (**2001**).

Stennicke, H.R., Deveraux, Q.L., Humke, E.W., Reed, J.C., Dixit, V.M. & Salvesen, G.S. *Caspase-9 can be activated without proteolytic processing.* J Biol Chem 274 8359-8362 (**1999**).

Stevanin, G., Camuzat, A., Holmes, S.E., Julien, C., Sahloul, R., Dode, C., Hahn-Barma, V., Ross, C.A., Margolis, R.L., Durr, A. & Brice, A. *CAG/CTG repeat expansions at the Huntington's disease-like 2 locus are rare in Huntington's disease patients.* Neurology 58 965-967. (**2002**).

Stevens, D.L. *The history of Huntington's chorea.* J R Coll Physicians Lond 6 271-282 (**1972**).

Stevens, D.L. *Huntington's Chorea: a Demographic, Genetic and Clinical Study.* MD Thesis, University of London (**1976**).

Stine, O.C., Pleasant, N., Franz, M.L., Abbott, M.H., Folstein, S.E. & Ross, C.A. *Correlation between the onset age of Huntington's disease and length of the trinucleotide repeat in IT-15.* Hum Mol Genet 2 1547-1549 (**1993**).

Stoy, N. & McKay, E. *Weight loss in Huntington's disease.* Ann Neurol 48 130-131 (**2000**).

Strickland, E., Hakala, K., Thomas, P.J. & DeMartino, G.N. *Recognition of misfolding proteins by PA700, the regulatory subcomplex of the 26 S proteasome.* J Biol Chem 275 5565-5572 (**2000**).

Stromhaug, P.E. & Klionsky, D.J. *Approaching the molecular mechanism of autophagy.* Traffic 2 524-531 (**2001**).

Strong, T.V., Tagle, D.A., Valdes, J.M., Elmer, L.W., Boehm, K., Swaroop, M., Kaatz, K.W., Collins, F.S. & Albin, R.L. *Widespread expression of the human and rat Huntington's disease gene in brain and nonneural tissues.* Nat Genet 5 259-265 (**1993**).

Sugars, K.L. & Rubinsztein, D.C. *Transcriptional abnormalities in Huntington disease.* Trends Genet 19 233-238 (**2003**).

Sulston, J.E. & Horvitz, H.R. *Post-embryonic cell lineages of the nematode, Caenorhabditis elegans.* Dev Biol 56 110-156 (**1977**).

Sun, Y., Savanenin, A., Reddy, P.H. & Liu, Y.F. *Polyglutamine-expanded huntingtin promotes sensitization of N-methyl-D-aspartate receptors via post-synaptic density 95.* J Biol Chem 276 24713-24718 (**2001**).

Suzuki, M., Desmond, T.J., Albin, R.L. & Frey, K.A. *Vesicular neurotransmitter transporters in Huntington's disease: initial observations and comparison with traditional synaptic markers.* Synapse 41 329-336 (**2001**).

Takahashi, S., Ujihara, H., Huang, G.Z., Yagyu, K.I., Sanbo, M., Kaba, H. & Yagi, T. *Reduced hippocampal LTP in mice lacking a presynaptic protein: complexin II.* Eur J Neurosci 11 2359-2366 (**1999**).

Tao, T. & Tartakoff, A.M. *Nuclear relocation of normal huntingtin.* Traffic 2 385-394 (**2001**).

Telenius, H., Kremer, B., Goldberg, Y.P., Theilmann, J., Andrew, S.E., Zeisler, J., Adam, S., Greenberg, C., Ives, E.J., Clarke, L.A. & et al. *Somatic and gonadal mosaicism of the Huntington disease gene CAG repeat in brain and sperm.* Nat Genet 6 409-414 (**1994**).

Terlecky, S.R. & Dice, J.F. *Polypeptide import and degradation by isolated lysosomes.* J Biol Chem 268 23490-23495 (**1993**).

Terwel, D. & van de Berg, W. *c-Jun/AP-1 (N) directed antibodies cross-react with "apoptosis-specific protein" which marks an autophagic process during neuronal apoptosis.* Neuroscience 96 445-446 (**2000**).

Thomas, L.B., Gates, D.J., Richfield, E.K., O'Brien, T.F., Schweitzer, J.B. & Steindler, D.A. *DNA end labeling (TUNEL) in Huntington's disease and other neuropathological conditions.* Exp Neurol 133 265-272 (**1995**).

Thompson, J.C., Snowden, J.S., Craufurd, D. & Neary, D. *Behavior in Huntington's Disease: Dissociating Cognition-Based and Mood- Based Changes.* J Neuropsychiatry Clin Neurosci 14 37-43. (**2002**).

Thompson, L.M. *An expanded role for wild-type huntingtin in neuronal transcription.* Nat Genet 35 13-14 (**2003**).

Thornberry, N.A., Rano, T.A., Peterson, E.P., Rasper, D.M., Timkey, T., Garcia-Calvo, M., Houtzager, V.M., Nordstrom, P.A., Roy, S., Vaillancourt, J.P., Chapman, K.T. & Nicholson, D.W. *A combinatorial approach defines specificities of members of the caspase family and granzyme B. Functional relationships established for key mediators of apoptosis.* J Biol Chem 272 17907-17911 (**1997**).

Timchenko, L.T., Miller, J.W., Timchenko, N.A., DeVore, D.R., Datar, K.V., Lin, L., Roberts, R., Caskey, C.T. & Swanson, M.S. *Identification of a (CUG)n triplet repeat RNA-binding protein and its expression in myotonic dystrophy.* Nucleic Acids Res 24 4407-4414 (**1996a**).

Timchenko, L.T., Timchenko, N.A., Caskey, C.T. & Roberts, R. *Novel proteins with binding specificity for DNA CTG repeats and RNA CUG repeats: implications for myotonic dystrophy.* Hum Mol Genet 5 115-121 (**1996b**).

Trottier, Y., Lutz, Y., Stevanin, G., Imbert, G., Devys, D., Cancel, G., Saudou, F., Weber, C., David, G., Tora, L. & et al. *Polyglutamine expansion as a pathological epitope in Huntington's disease and four dominant cerebellar ataxias.* Nature 378 403-406 (**1995**).

Turmaine, M., Raza, A., Mahal, A., Mangiarini, L., Bates, G.P. & Davies, S.W. *Nonapoptotic neurodegeneration in a transgenic mouse model of Huntington's disease.* Proc Natl Acad Sci U S A 97 8093-8097. (**2000**).

Turner, G.C. & Varshavsky, A. *Detecting and measuring cotranslational protein degradation in vivo.* Science 289 2117-2120 (**2000**).

U, M., Miyashita, T., Ohtsuka, Y., Okamura-Oho, Y., Shikama, Y. & Yamada, M. *Extended polyglutamine selectively interacts with caspase-8 and -10 in nuclear aggregates.* Cell Death Differ 8 377-386 (**2001**).

Uchiyama, Y. *Autophagic cell death and its execution by lysosomal cathepsins.* Arch Histol Cytol 64 233-246 (**2001**).

Veis, D.J., Sorenson, C.M., Shutter, J.R. & Korsmeyer, S.J. *Bcl-2-deficient mice demonstrate fulminant lymphoid apoptosis, polycystic kidneys, and hypopigmented hair.* Cell 75 229-240 (**1993**).

Velier, J., Kim, M., Schwarz, C., Kim, T.W., Sapp, E., Chase, K., Aronin, N. & DiFiglia, M. *Wild-type and mutant huntingtins function in vesicle trafficking in the secretory and endocytic pathways.* Exp Neurol 152 34-40 (**1998**).

Verhagen, A.M., Ekert, P.G., Pakusch, M., Silke, J., Connolly, L.M., Reid, G.E., Moritz, R.L., Simpson, R.J. & Vaux, D.L. *Identification of DIABLO, a mammalian protein that promotes apoptosis by binding to and antagonizing IAP proteins.* Cell 102 43-53 (**2000**).

Verkerk, A.J., Pieretti, M., Sutcliffe, J.S., Fu, Y.H., Kuhl, D.P., Pizzuti, A., Reiner, O., Richards, S., Victoria, M.F., Zhang, F.P. & et al. *Identification of a gene (FMR-1) containing a CGG repeat coincident with a breakpoint cluster region exhibiting length variation in fragile X syndrome.* Cell 65 905-914 (**1991**).

Vetter, J.M., Jehle, T., Heinemeyer, J., Franz, P., Behrens, P.F., Jackisch, R., Landwehrmeyer, G.B. & Feuerstein, T.J. *Mice transgenic for exon 1 of Huntington's disease: properties of cholinergic and dopaminergic pre-synaptic function in the striatum.* J Neurochem 85 1054-1063 (**2003**).

Visick, J.E. & Clarke, S. *Repair, refold, recycle: how bacteria can deal with spontaneous and environmental damage to proteins.* Mol Microbiol 16 835-845 (**1995**).

Volkers, W.S. Ann Hum Genet 44 (**1980**).

Voll, R.E., Herrmann, M., Roth, E.A., Stach, C., Kalden, J.R. & Girkontaite, I. *Immunosuppressive effects of apoptotic cells.* Nature 390 350-351 (**1997**).

von Horsten, S., Schmitt, I., Nguyen, H.P., Holzmann, C., Schmidt, T., Walther, T., Bader, M., Pabst, R., Kobbe, P., Krotova, J., Stiller, D., Kask, A., Vaarmann, A., Rathke-Hartlieb, S., Schulz, J.B., Grasshoff, U., Bauer, I., Vieira-Saecker, A.M., Paul, M., Jones, L., Lindenberg, K.S., Landwehrmeyer, B., Bauer, A., Li, X.J. & Riess, O. *Transgenic rat model of Huntington's disease.* Hum Mol Genet 12 617-624 (**2003**).

Vonsattel, J.P. & DiFiglia, M. *Huntington disease.* J Neuropathol Exp Neurol 57 369-384 (**1998**).

Vonsattel, J.P., Myers, R.H., Stevens, T.J., Ferrante, R.J., Bird, E.D. & Richardson, E.P., Jr. *Neuropathological classification of Huntington's disease.* J Neuropathol Exp Neurol 44 559-577 (**1985**).

Vuillaume, I., Vermersch, P., Destee, A., Petit, H. & Sablonniere, B. *Genetic polymorphisms adjacent to the CAG repeat influence clinical features at onset in Huntington's disease.* J Neurol Neurosurg Psychiatry 64 758-762 (**1998**).

Waelter, S., Boeddrich, A., Lurz, R., Scherzinger, E., Lueder, G., Lehrach, H. & Wanker, E.E. *Accumulation of mutant huntingtin fragments in aggresome-like inclusion bodies as a result of insufficient protein degradation.* Mol Biol Cell 12 1393-1407 (**2001a**).

Waelter, S., Scherzinger, E., Hasenbank, R., Nordhoff, E., Lurz, R., Goehler, H., Gauss, C., Sathasivam, K., Bates, G.P., Lehrach, H. & Wanker, E.E. *The huntingtin interacting protein HIP1 is a clathrin and alpha-adaptin- binding protein involved in receptor-mediated endocytosis.* Hum Mol Genet 10 1807-1817. (**2001b**).

Wagner, B.J. & Margolis, J.W. *Age-dependent association of isolated bovine lens multicatalytic proteinase complex (proteasome) with heat-shock protein 90, an endogenous inhibitor.* Arch Biochem Biophys 323 455-462 (**1995**).

Walsh, D.M., Hartley, D.M., Kusumoto, Y., Fezoui, Y., Condron, M.M., Lomakin, A., Benedek, G.B., Selkoe, D.J. & Teplow, D.B. *Amyloid beta-protein fibrillogenesis. Structure and biological activity of protofibrillar intermediates.* J Biol Chem 274 25945-25952 (**1999**).

Wanker, E.E., Rovira, C., Scherzinger, E., Hasenbank, R., Walter, S., Tait, D., Colicelli, J. & Lehrach, H. *HIP-I: a huntingtin interacting protein isolated by the yeast two-hybrid system.* Hum Mol Genet 6 487-495 (**1997**).

Warrick, J.M., Paulson, H.L., Gray-Board, G.L., Bui, Q.T., Fischbeck, K.H., Pittman, R.N. & Bonini, N.M. *Expanded polyglutamine protein forms nuclear inclusions and causes neural degeneration in Drosophila.* Cell 93 939-949 (**1998**).

Weil, M., Jacobson, M.D., Coles, H.S., Davies, T.J., Gardner, R.L., Raff, K.D. & Raff, M.C. *Constitutive expression of the machinery for programmed cell death.* J Cell Biol 133 1053-1059 (**1996**).

Weil, M., Jacobson, M.D. & Raff, M.C. *Are caspases involved in the death of cells with a transcriptionally inactive nucleus? Sperm and chicken erythrocytes.* J Cell Sci 111 (Pt 18) 2707-2715 (**1998**).

Wellington, C.L., Ellerby, L.M., Gutekunst, C.A., Rogers, D., Warby, S., Graham, R.K., Loubser, O., van Raamsdonk, J., Singaraja, R., Yang, Y.Z., Gafni, J., Bredesen, D., Hersch, S.M., Leavitt, B.R., Roy, S., Nicholson, D.W. & Hayden, M.R. *Caspase cleavage of mutant huntingtin precedes neurodegeneration in Huntington's disease.* J Neurosci 22 7862-7872 (**2002**).

Wellington, C.L., Leavitt, B.R. & Hayden, M.R. *Huntington disease: new insights on the role of huntingtin cleavage.* J Neural Transm Suppl 1-17 (**2000**).

Wheeler, V.C., Lebel, L.A., Vrbanac, V., Teed, A., Te Riele, H. & MacDonald, M.E. *Mismatch repair gene Msh2 modifies the timing of early disease in Hdh(Q111) striatum.* Hum Mol Genet 12 273-281 (**2003**).

White, J.K., Auerbach, W., Duyao, M.P., Vonsattel, J.P., Gusella, J.F., Joyner, A.L. & MacDonald, M.E. *Huntingtin is required for neurogenesis and is not impaired by the Huntington's disease CAG expansion.* Nat Genet 17 404-410 (**1997**).

Wyttenbach, A., Carmichael, J., Swartz, J., Furlong, R.A., Narain, Y., Rankin, J. & Rubinsztein, D.C. *Effects of heat shock, heat shock protein 40 (HDJ-2), and proteasome inhibition on protein aggregation in cellular models of Huntington's disease.* Proc Natl Acad Sci U S A 97 2898-2903 (**2000**).

Wyttenbach, A., Swartz, J., Kita, H., Thykjaer, T., Carmichael, J., Bradley, J., Brown, R., Maxwell, M., Schapira, A., Orntoft, T.F., Kato, K. & Rubinsztein, D.C. *Polyglutamine expansions cause decreased CRE-mediated transcription and early gene expression changes prior to cell death in an inducible cell model of Huntington's disease.* Hum Mol Genet 10 1829-1845. (**2001**).

Xue, L., Fletcher, G.C. & Tolkovsky, A.M. *Autophagy is activated by apoptotic signalling in sympathetic neurons: an alternative mechanism of death execution.* Mol Cell Neurosci 14 180-198 (**1999**).

Yang, W., Dunlap, J.R., Andrews, R.B. & Wetzel, R. *Aggregated polyglutamine peptides delivered to nuclei are toxic to mammalian cells.* Hum Mol Genet 11 2905-2917 (**2002**).

Yang, Y.L. & Li, X.M. *The IAP family: endogenous caspase inhibitors with multiple biological activities.* Cell Res 10 169-177 (**2000**).

Yokota, S., Himeno, M., Roth, J., Brada, D. & Kato, K. *Formation of autophagosomes during degradation of excess peroxisomes induced by di-(2-ethylhexyl)phthalate treatment. II. Immunocytochemical analysis of early and late autophagosomes.* Eur J Cell Biol 62 372-383 (**1993**).

Yu, Z.X., Li, S.H., Evans, J., Pillarisetti, A., Li, H. & Li, X.J. *Mutant huntingtin causes context-dependent neurodegeneration in mice with Huntington's disease.* J Neurosci 23 2193-2202 (**2003**).

Yuan, W., Tuttle, D.L., Shi, Y.J., Ralph, G.S. & Dunn, W.A., Jr. *Glucose-induced microautophagy in Pichia pastoris requires the alpha-subunit of phosphofructokinase.* J Cell Sci 110 (Pt 16) 1935-1945 (**1997**).

Zainelli, G.M., Ross, C.A., Troncoso, J.C. & Muma, N.A. *Transglutaminase cross-links in intranuclear inclusions in Huntington disease.* J Neuropathol Exp Neurol 62 14-24 (**2003**).

Zeron, M.M., Chen, N., Moshaver, A., Lee, A.T., Wellington, C.L., Hayden, M.R. & Raymond, L.A. *Mutant huntingtin enhances excitotoxic cell death.* Mol Cell Neurosci 17 41-53 (**2001**).

Zeron, M.M., Hansson, O., Chen, N., Wellington, C.L., Leavitt, B.R., Brundin, P., Hayden, M.R. & Raymond, L.A. *Increased Sensitivity to N-Methyl-D-Aspartate Receptor-Mediated Excitotoxicity in a Mouse Model of Huntington's Disease.* Neuron 33 849-860. (**2002**).

Zhou, H., Li, S.H. & Li, X.J. *Chaperone suppression of cellular toxicity of huntingtin is independent of polyglutamine aggregation.* J Biol Chem 276 48417-48424. (**2001**).

Zhou, Q., Snipas, S., Orth, K., Muzio, M., Dixit, V.M. & Salvesen, G.S. *Target protease specificity of the viral serpin CrmA. Analysis of five caspases.* J Biol Chem 272 7797-7800 (**1997**).

Zuccato, C., Ciammola, A., Rigamonti, D., Leavitt, B.R., Goffredo, D., Conti, L., MacDonald, M.E., Friedlander, R.M., Silani, V., Hayden, M.R., Timmusk, T., Sipione, S. & Cattaneo, E. *Loss of huntingtin-mediated BDNF gene transcription in Huntington's disease.* Science 293 493-498 (**2001**).

Zuhlke, C., Riess, O., Bockel, B., Lange, H. & Thies, U. *Mitotic stability and meiotic variability of the (CAG)n repeat in the Huntington disease gene.* Hum Mol Genet 2 2063-2067 (**1993**).

Zwickl, P., Voges, D. & Baumeister, W. *The proteasome: a macromolecular assembly designed for controlled proteolysis.* Philos Trans R Soc Lond B Biol Sci 354 1501-1511 (**1999**).

Brunhilde mounts her horse and rides into the flames.

~ Wagner, *Gotterdammerung*